



universität
wien

DISSERTATION / DOCTORAL THESIS

Titel der Dissertation /Title of the Doctoral Thesis

„Expanding LC-MS based metabolomics for the
investigation of the exposome“

verfasst von / submitted by

Dipl.-Ing. Mira Flasch, BSc

angestrebter akademischer Grad / in partial fulfilment of the requirements for the degree of
Doktorin der Naturwissenschaften (Dr. rer. nat.)

Wien, 2022 / Vienna, 2022

Studienkennzahl lt. Studienblatt /
degree programme code as it appears on the student
record sheet:

A 796 605 419

Dissertationsgebiet lt. Studienblatt /
field of study as it appears on the student record sheet:

Chemie / Chemistry

Betreut von / Supervisor:

Assoz. Prof. Dipl.-Ing. Dr. Benedikt Warth

Danksagung

An dieser Stelle möchte ich allen Personen danken, die mich bei der Anfertigung meiner Doktorarbeit unterstützt haben.

Mein besonderer Dank gilt Assoc. Prof. Dr. Benedikt Warth für die ausgezeichnete Betreuung und Unterstützung bei der Umsetzung der gesamten Arbeit. Außerdem möchte ich Univ.Prof. Dr. Doris Marko für die Möglichkeit meine Dissertation am Institut für Lebensmittelchemie und Toxikologie durchzuführen danken.

Ein herzliches Dankeschön geht auch an meine Arbeitskollegen, die mich über die Jahre begleitet haben. Weiters möchte ich mich bei meinen Kollaborationspartnern, insbesondere den Arbeitsgruppen von Univ.-Prof. Dr. Gunda Köllensperger und Univ. Prof. Dipl.-Chem. Dr. Rainer Schuhmacher danken, ohne die ich meine Projekte nicht durchführen hätte können.

Zu guter Letzt, möchte ich auch meinen Eltern und meiner restlichen Familie meinen Dank aussprechen, die mich auf meinem Weg durch das Doktorat und mein gesamtes Studium begleitet und unterschützt haben. Meinen Dank möchte ich meinem Freund Thomas ausdrücken, der mich in herausfordernden Zeiten immer wieder aufmuntert hat und Johanna für das Korrekturlesen meiner Arbeit.

Table of Contents

Danksagung.....	III
Abstract.....	VII
Zusammenfassung.....	IX
1. Structure of the thesis.....	1
2. Scope and aims.....	3
3. Key outcomes.....	5
4. Introduction.....	9
4.1. From genetic to environmental risk factors for disease.....	9
4.2. The exposome.....	10
4.3. The metabolome.....	11
4.4. Analytical approaches in exposomic and metabolomic research.....	12
4.5. Classification of environmental exposures.....	15
4.6. Biotransformation.....	18
5. Methodology.....	23
5.1. Liquid chromatography.....	23
5.2. Mass spectrometry.....	24
5.3. Current methodological challenges.....	27
6. Original works.....	31
6.1. Overview of the original research articles included in this thesis.....	31
6.2. Manuscript #1: Flasch et al. (2022b).....	33
6.3. Manuscript #2: Flasch et al. (2022c).....	125
6.4. Publication #3: Flasch et al. (2020).....	175
6.5. Publication #4: Flasch et al. (2022a).....	196
7. Conclusion and Outlook.....	221
8. References.....	223
9. Appendix.....	231
9.1. List of additional contributions to peer-reviewed publications.....	231
9.2. List of oral presentations.....	231
9.3. List of poster presentations.....	231
9.4. List of abbreviations.....	232
9.5. List of figures.....	232
9.6. Glossary.....	233
9.7. Summary of measured sequences.....	234

Abstract

Environmental exposures are determinants of health. The field of exposome research studies the totality of environmental exposures, including their biotransformation products from conception throughout life. In human biofluids, the internal chemical exposome and the body's biological response to these external stressors, belonging to the endogenous metabolome, can be measured. The structurally diverse and highly dynamic xenobiotics challenge analytical instrumentation such as liquid chromatography – high-resolution mass spectrometry (LC-HRMS). In this thesis, new exposome-scale mass spectrometric approaches were developed, thoroughly evaluated, and applied to biological samples. As a key method, an LC-HRMS approach for the joint investigation of the endogenous metabolome and the internal chemical exposome was established. A high-throughput dual-column configuration employing a reverse-phase column for measuring apolar xenobiotics and a hydrophilic interaction liquid chromatography column for observing polar metabolites was optimised and both effluents were simultaneously analysed. Urine samples from sub-Saharan Africa and Europe showcased the setup's capability to investigate the chemical exposome and metabolome simultaneously. However, a limitation of the HRMS technique was the detection of low-abundance exposures compared to tailored triple quadrupole approaches. Thus, the discrepancy in the limit of quantitation between a single column HRMS approach for xenobiotics and an established low-resolution mass spectrometric method using identical LC parameters was evaluated based on diverse compounds in solvent and urine. The unique feature of HRMS to screen for unknown molecules was also applied in independent experiments to annotate novel biotransformation products of the mycotoxin deoxynivalenol in two cancer cell lines and two endocrine-active compounds, namely the isoflavone genistein and the xenoestrogen zearalenone, in an *in vitro* model for breast cancer. By combining non-targeted, stable isotope-assisted mass spectrometry and the bioinformatics tool MetExtract II, several known and so-far unknown biotransformation products were annotated. Despite minor limitations in terms of sensitivity, the developed versatile HRMS methods are ready to be applied in exposome-wide association studies for investigating the contribution of toxic environmental exposures to disease development.

Zusammenfassung

Umwelteinflüsse sind entscheidend für die menschliche Gesundheit. Die Exposomforschung untersucht die Gesamtheit der Umweltexpositionen, inklusive ihrer Biotransformationsprodukte. In biologischem Probenmaterial wird das interne chemische Exposom und die biologische Reaktion des Körpers auf diese externen Stressfaktoren, in Form des endogenen Metaboloms, gemessen. Die strukturell vielfältigen und hochdynamischen Xenobiotika stellen eine Herausforderung für analytische Verfahren wie beispielsweise die Flüssigkeitschromatographie in Kopplung mit der hochauflösenden Massenspektrometrie (LC-HRMS) dar. In dieser Arbeit wurden neue, massenspektrometrische Methoden für die Exposomforschung entwickelt, umfassend evaluiert und auf biologische Proben angewendet. Als Schlüsselmethode wurde ein LC-HRMS-Ansatz für die simultane Analyse des endogenen Metaboloms und des internen chemischen Exposoms etabliert. Ein Zweisäulenaufbau mit einer Umkehrphasensäule zur Messung apolarer Chemikalien und einer hydrophilen Interaktionschromatographiesäule zur Detektion polarer Metaboliten mit hohem Durchsatz wurde optimiert und beide Effluente simultan analysiert. Urinproben aus Subsahara-Afrika und aus Europa zeigten, dass die entwickelte Methode in der Lage ist, das chemische Exposom und das Metabolom gleichzeitig zu erforschen. Eine Einschränkung der HRMS-Technik war jedoch die Detektion von gering konzentrierten Umweltbelastungen im Vergleich zu maßgeschneiderten Triple-Quadrupolansätzen. Daher wurden die unterschiedlichen Bestimmungsgrenzen einer HRMS-Methode mit einer Säule für apolare Fremdstoffe und einer gerichteten, niedrig auflösenden Massenspektrometriemethode mit identischen LC-Parametern anhand verschiedener Analyten in Lösungsmittel und Urin bewertet. Die Möglichkeit mit HRMS nach unbekanntem Molekülen zu suchen, wurde auch verwendet, um neue Biotransformationsprodukte zu entschlüsseln. In zwei Krebszelllinien wurde nach Metaboliten des Mykotoxins Deoxynivalenol gesucht und die Biotransformationsprodukte zweier endokrin aktiver Verbindungen, des Isoflavons Genistein und des Xenööstrogens Zearalenon, wurden in einem in-vitro-Modell für Brustkrebs untersucht. Durch die Kombination von HRMS und dem Bioinformatik-Tool MetExtract II wurden, unterstützt durch Isotopenmarkierung, mehrere bekannte und sowie bisher unbekannte Biotransformationsprodukte nachgewiesen. Trotz geringfügiger Limitierungen hinsichtlich der Sensitivität, können die entwickelten, vielseitigen LC-HRMS-Methoden in exposomweiten Assoziationsstudien zur Untersuchung chemischer Umweltfaktoren, die in die Entstehung von Krankheiten involviert sind, eingesetzt werden.

1. Structure of the thesis

This thesis is a cumulative dissertation and consists of four sections.

First, the introduction outlines the concept of the exposome, the metabolome, and analytical approaches applied in studying endogenous metabolites and xenobiotics. Then, the diversity and classification of environmental exposures focusing on endocrine active chemicals are characterised briefly. Moreover, typical biotransformation reactions, an essential contributor to the exposome's complexity, are described.

The introduction is followed by a description of the methodology for exposome and metabolome research applied in this thesis. This part focuses on liquid chromatography coupled with high-resolution mass spectrometry, a central technique in exposomics, and low-resolution triple-quadrupole instruments used as a complementary approach focusing on quantitation. Analytical challenges are also outlined in this part.

The subsequent section of this dissertation includes the resulting original works that are either published in peer-reviewed journals or are currently under review.

In the final section, the main conclusions from this thesis are summarised and discussed in the context of future analytical and environmental health research.

2. Scope and aims

The human body is permanently confronted with various exogenous chemicals affecting our health. The exposome concept comprises environmental exposures captured over the whole lifetime (Wild et al. 2009). However, for unravelling disease development, not only external stressors but also the body's response to these chemicals is highly relevant (Vermeulen et al. 2020). Biological matrices such as urine and plasma are well-suited specimens for revealing the internal chemical exposome and the endogenous metabolome to gain insights into the impact of exogenous toxicants (Dennis et al. 2017).

Environmental chemicals' vast, diverse, and dynamic nature complicates their efficient measurement (Meijer et al. 2021; Jiang et al. 2018; Vermeulen et al. 2020). The internal modification of xenobiotics further increases the complexity of exposures as vast numbers of biotransformation products are produced (Price et al. 2022). These metabolic products are an integral part of the exposome due to their potentially altered toxicological relevance compared to the native molecule (LeBlanc 2008). Exposomic studies frequently utilise LC-HRMS to decipher the exposome as this technique can analyse various small molecules, including endogenous metabolites and exogenous stressors (David et al. 2021). Nevertheless, a single approach is rarely sufficient to capture the chemical diversity of molecules relevant to the exposome. Dual-column configurations enable time-efficient measuring of chemicals with a broad chemical background (Jones 2015). Known chemicals can also be studied with low-resolution mass spectrometry in a targeted manner for accurate quantitation at trace levels (Pourchet et al. 2020). The detection of low-level exposures benefits from the excellent sensitivity of tailored, targeted assays, but an essential feature of holistic exposure research, the screening for unknown chemicals, is unique to HRMS.

This thesis addresses the development, evaluation, and application of LC-HRMS approaches for studying small molecules relevant to the exposome and metabolome. In detail, the thesis' aims are as follows:

- I. Establishment of a comprehensive untargeted **LC-HRMS workflow** for the **joint investigation of endogenous metabolites and exogenous xenobiotics** to facilitate discovering and quantifying environmental stressors and the body's biological response to them. A reverse-phase column for detecting apolar contaminants and a hydrophilic interaction liquid chromatography column for measuring polar metabolites are simultaneously combined.
- II. **Application** of the **developed workflow** to human samples comprising **urine samples** from sub-Saharan Africa and Europe to study environmental exposures and associated metabolic changes
- III. Investigation of the **discrepancy in the limit of quantitation** between **high-resolution and low-resolution mass spectrometry** and its relevance for the discovery of trace-level contaminants
- IV. Combination of **stable isotope-labelling with LC-HRMS measurements** and data evaluation by **MetExtract II** to reveal known and so-far unknown **biotransformation products of several xenobiotics** (deoxynivalenol, zearalenone, genistein) in cell models of cancer

3. Key outcomes

The key outcomes of this thesis include the following points:

- A high-throughput dual-column approach integrating two column chemistries to simultaneously analyse exogenous xenobiotics and endogenous metabolites was established and evaluated for >240 model analytes with highly diverse physico-chemical properties.
- Urine samples from a 'low exposure' region (Europe) and a 'high exposure' scenario (Sub-Saharan Africa) were investigated and partially quantified in a targeted and untargeted manner with the dual-column approach to link external stressors to metabolic changes.
- The discrepancy in the limits of quantitation of >100 model xenobiotics between a low resolution and a high-resolution mass spectrometric approach with identical LC parameters was estimated to be a factor of about nine in pure solvent and six in urine.
- The analyses of spot urine samples with both methods (HRMS, low-resolution MS) revealed about 60% fewer chemicals in HRMS scans. The slightly improved limit of quantitation of low-resolution MS eases quantitating trace-level exposures and qualified this technique as a valuable addition to HRMS in exposomics for accurate and reliable quantitation.
- An HRMS workflow combined with stable isotope labelling and data evaluation by MetExtract II was adapted to human tissue culture to facilitate the discovery of known and novel biotransformation products.
- The mycotoxin deoxynivalenol was primarily conjugated with glutathione in liver carcinoma cells (HepG2) and a colon tumour cell line (HT29). Other biotransformation products were deoxynivalenol-cysteine, deoxynivalenol-sulfates and deoxynivalenol-sulfonates. Glucuronidation activity was lacking in these models.
- In the breast cancer cell line MCF-7, the mycoestrogen zearalenone and the phytoestrogen genistein were metabolised by phase I and phase II biotransformation, such as glucuronidation and sulfation, altering the chemical's estrogenic potency.
- Novel biotransformation products were detected in cell culture by the workflow for biotransformation detection. These uncommon modifications included a conjugate of zearalenone with vitamin B6 and the conjugation of deoxynivalenol with amino acids (tyrosine, phenylalanine, (iso)leucine) and penicillin.

Part I
Introduction

4. Introduction

Omics technologies aim to comprehensively and systematically investigate, characterise, and quantify an extensive collection of biological molecules that shape a living organism's structure, function, and dynamics (Coughlin 2014). Molecules such as genes, proteins, small molecules, RNA transcripts, microbes, and environmental exposures are explored in their specific omics field (Abdel-Aziz et al. 2020). A multidimensional view of the human body with combined information from different systems levels facilitates the understanding of disease development.

4.1. From genetic to environmental risk factors for disease

The human genome was first decoded at the turn of the millennium in 2001 (Gonzaga-Jauregui et al. 2012) and with it, the study of the function and interaction of genes was established as the first omics technique, genomics. In genome-wide association studies, specific gene variants have been associated with disease development for decades identifying genetic drivers for widespread illnesses such as Alzheimer's disease, cancer, and diabetes (Waring et al. 2008; Chen et al. 2014; Hirschhorn et al. 2005; Easton et al. 2008; Witte 2010). However, environmental factors have a crucial role in disease aetiology.

Genetic and environmental factors cause phenotypic variation. The phenotype describes the entirety of observable traits and characteristics expressed in a human, including, e.g. height, body mass index, and presence or absence of disease (Patel 2017). Monozygotic twin studies estimated the genetic risk for multiple chronic illnesses to vary between 3% for leukaemia and 49% for asthma (Rappaport 2016). The association with genes was particularly weak for cancers with about 8%. In contrast, neurological and pulmonary diseases were strongly linked to genetic drivers, as about a quarter to a third of the risk for disease development was attributed to genes. In total, genes and shared exposures were estimated to be involved in only about 16% of deaths from heart diseases and several cancer types, including lung, colorectal and breast cancer (Rappaport 2016). The substantial role of the environment as a driver of illnesses was, among others, described by the Global Burden of Disease (GBD) initiative (GBD 2017). The investigation of over 80 metabolic, environmental, occupational, and behavioural risk factors in almost 200 countries revealed that about 60% of deaths worldwide were associated with these factors. Pollution alone is a significant driver of disease, e.g. in 2015, 16% of global premature deaths (around 9 million) were attributed to pollution. This is three times more than deaths related to AIDS, tuberculosis, and malaria (Landrigan et al. 2018). Specific environmental exposures were associated with numerous, widespread diseases. Parkinson's disease was several times linked to pesticides highlighting an increased occupational risk for, e.g. farmers (Elbaz et al. 2007). Adverse impacts on the nervous system were reported from heavy metals, organophosphates, organochlorinated/organobromine compounds, bisphenol A, and phthalates (Tshala-Katumbay et al. 2015) and the risk for attention deficit hyperactivity disorder (ADHD) was increased by plasticisers, phthalates, organic contaminants, lead, and cigarette smoke exposure (Nilsen et al. 2020). Tobacco smoke and diet, especially red and processed meat, elevated cancer risk (Murphy et al. 2019; Miranda-Galvis et al. 2021; de Groot et al. 2018) and environmental contaminants such as bisphenol A and phthalates altered the risk of diabetes (Ruiz et al. 2017).

Besides the type and dose of toxicants, the timing of the exposure is critical for disease aetiology. Environmental exposures might be especially harmful during critical time windows like prenatal and childhood exposures. Thus, exposures in early life have received particular attention (Wigle et al. 2008; Selevan et al. 2000; Tamayo-Uria et al. 2019). For example, obesity was associated with exposure to persistent organic pollutants, phthalates, and perfluorinated compounds during childhood (Vilcins et al. 2021).

4.2. The exposome

The term exposome was introduced by Wild (2005) as a complement to the genome. This concept was defined as the totality of environmental exposures, including lifestyle factors from conception throughout life. Later definitions also comprised the body's biological reaction to these external stressors, such as molecules originating from inflammation, oxidative stress, lipid peroxidation, infections, and the gut flora (Rappaport et al. 2010; Miller et al. 2014). However, this broad scope hinders the categorisation of exposomics within a multi-omics world due to overlapping with related areas, e.g. metabolomics (Price et al. 2022). Therefore, the exposome's initial definition, including only external factors, is favoured in this thesis. This work focuses on the internal chemical exposome, defined as the totality of internal contact of an organism with environmental chemicals, including their biotransformation products (Figure 1) (Price et al. 2022).

The internal chemical exposome is diverse and vast. Over 160 million chemicals were registered with the Chemical Abstracts Service (CAS) in 2020, and plenty more are formed by environmental processes and human biotransformation processes (Lebedev et al. 2022). About 30.000 chemicals were commercially used in the USA and Canada in 2002 (Judson et al. 2009). The European REACH registry for chemicals manufactured and imported in larger quantities contained recently even more than 150.000 pre-registered substances (Vorkamp et al. 2021). Therefore, the number of environmental chemicals of potential toxicological concern is constantly growing and the sheer dimension of chemical production and formation makes monitoring of all relevant substances almost impossible (Lebedev et al. 2022). Toxicological data for all these chemicals is limited, making prioritisation challenging (Judson et al. 2009; Vorkamp et al. 2021). Only less than half of the 5.000 most-produced substances worldwide have already been tested for their safety or toxicity (Landrigan et al. 2018). Not only synthetic chemicals but also substances of natural origin belong to the human internal exposome and impact human health (Zhang et al. 2021a; Smith et al. 2020). Plants, fungi, and bacteria produce various substances to, e.g. defend themselves from their enemies. These naturally produced molecules enter the human body via, e.g. diet (Smith et al. 2020). Therefore, food and beverages are significant sources of exogenous, natural chemicals (Zhang et al. 2021a; Smith et al. 2020). For comprehensive exposomics research, substances from natural and anthropogenic sources should be monitored as the toxicological impact of

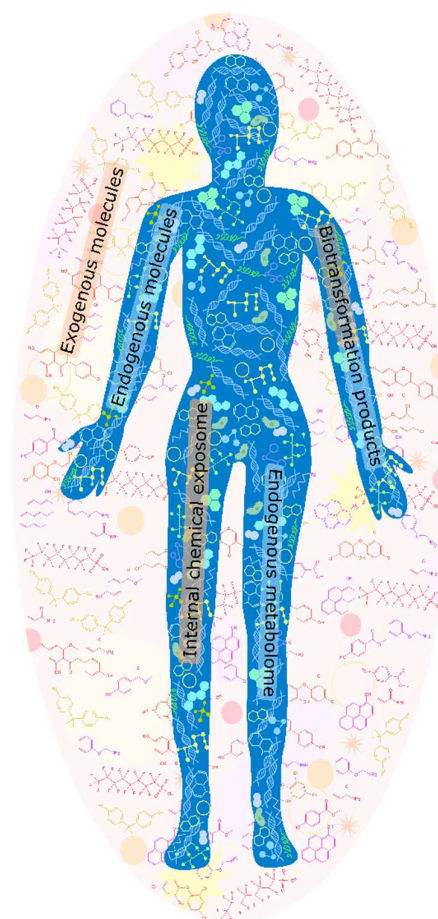


Figure 1. Schematic overview of the internal chemical exposome, including exogenous compounds and their biotransformation products, and the endogenous metabolome comprising endogenous metabolites in the body

compounds and the correlated health outcome is independent of their origin. The most potent toxins are even produced by nature (Botulinum toxin A, Ricin, Saxitoxin) (Topliss et al. 2002). Both natural and synthetic substances can have positive as well as adverse health implications depending on the actual dose (Topliss et al. 2002).

In contrast to the genome consisting of only four similar building blocks, the chemical exposome consists of many structurally diverse chemicals with a broad range of chemical properties, e.g. acidity, reactivity and physical properties, e.g. polarity. Therefore, simultaneous detection of the internal chemical exposome challenges analytical technologies (David et al. 2021). In addition, environmental exposures possess a high variability and dynamic throughout an individual's lifetime (Wild 2005), as demonstrated by Jiang et al. (2018). Thus, longitudinal sampling and sufficient sample sizes are crucial for proper experimental design in exposomics.

4.3. The metabolome

Metabolomics focuses on the quantitative and qualitative study of small molecules involved in the endogenous metabolic processes of a biological system to study pathway perturbations, metabolic flux, and regulation of biological responses (Bedia 2022; Price et al. 2022). Metabolites include endogenous low molecular weight compounds such as fatty acids, carbohydrates, nucleotides, organic compounds such as amino acids, and other products formed during biological reactions (Walker et al. 2019). In this thesis, the term metabolomics refers solely to the investigation of endogenous metabolites to differentiate the concept from exposomics. In the human metabolome database (HMDB), more than 200.000 endogenous metabolites are currently collected (Wishart et al. 2022). These compounds act as substrates, cofactors, and products in enzymatic reactions and undergo transportation, secretion, degradation, and accumulation depending on protein activity and gene expression interacting with other system levels. Thus, changes at the metabolome scale also affect other layers of systems biology (Bedia 2022). Compared to other omics levels, such as the transcriptome (set of all RNA transcripts within a biological entity) or the proteome (set of all proteins/peptides in a biological entity), the metabolome is closest to the observable cellular phenotype (Fiehn 2002). Within the metabolome, the biological response to external stressors and their impact on biological processes can be investigated to gain insights into the mechanism of disease aetiology and the effect of environmental exposures on the human body.

The concentration range of small molecules from endogenous and exogenous sources in human specimens varies tremendously. Human blood samples comprise drugs, food components, pollutants, and endogenous compounds at concentrations between 160 fM to 140 mM, spanning eleven orders of magnitude (Rappaport et al. 2014). While median blood levels of endogenous chemicals, food components, and drugs are comparable, pollutants were in the sub ng/mL range, thus about 1.000 times lower concentrated (Rappaport et al. 2014). David et al. (2021) reported a similar dynamic range of eight orders of magnitude for compounds measurable with high-resolution mass spectrometry (HRMS) coupled via electrospray ionisation (ESI) to liquid-chromatography (LC), supporting the lower concentration of pesticides and plasticisers compared to endogenous metabolites, pharmaceuticals and partly food constituents in blood.

4.4. Analytical approaches in exposomic and metabolomic research

Different analytical approaches are used in the elucidation of the internal chemical exposome. Human biomonitoring investigates exogenous chemicals and their biotransformation products in human specimens to study exposure levels in the population and support the identification of potentially harmful chemicals (Angerer et al. 2011; Bocato et al. 2019). Targeted methodology measuring only a specific subset of known chemicals is traditionally used in human biomonitoring studies. This approach relied on measuring only selected biomarkers of exposures in human matrices to estimate risk and allow informed decision-making (Vorkamp et al. 2021). Targeted analysis is typically performed with a low-resolution mass spectrometer (triple quadrupole mass spectrometer) in selected reaction monitoring (SRM) mode to gain high specificity and sensitivity (Pourchet et al. 2020). A comparison with reference standards is required to quantify and identify chemicals. Several guidelines are available to ensure the harmonisation of method performance assessment (Pourchet et al. 2020). However, targeted assays generally include only a restricted number of chemicals, e.g. in the HBM4EU project, seven substance classes and two metals were prioritised (Vorkamp et al. 2021). Targeted analysis can also be performed with high-resolution instrumentation combined with non-targeted analysis and suspect screening (Cajka et al. 2016).

Targeted methods alone are insufficient for tackling the human chemical exposome. Therefore, untargeted techniques are widely applied in exposomics. Untargeted approaches require HRMS to enable the measurement of a wide range of analytes within a specific mass range. Depending on prior information and aim untargeted approaches are divided into two strategies, suspect screening and non-targeted screening. Suspect screening is used to identify known, structurally described compounds whose presence is suspected (“known unknowns”) (Pourchet et al. 2020). This approach supports the prioritisation of analytes for further targeted in-depth studies and broadly unravels elements of complex specimens (Pourchet et al. 2020). The annotation of suspected compounds often depends on comparisons to library data and therefore, the lack of analytical standards hampers unequivocal identification and quantitation (Pourchet et al. 2020). Non-targeted screening (NTA) focuses on the discovery of unknown and new chemicals (“unknown unknowns”) without any *a priori* knowledge (Pourchet et al. 2020; Sobus et al. 2018). Despite complex data processing, NTA is the most promising method to expand the map of the human internal chemical exposome.

Technological advances in HRMS have facilitated the progress of exposomics in recent years (Niedzwiecki et al. 2019). HRMS is of high importance for measuring the exposome as this technology allows the analysis of highly diverse molecules covering a wide mass-to-charge-ratio (m/z) range between about 50 – 1200 Da in multiple matrices without the need for a specific target list beforehand (Schymanski et al. 2014b; Vermeulen et al. 2020; Warth et al. 2017). Untargeted HRMS measurements with comprehensive data extraction strategies and annotation algorithms allow the analysis of more than 20,000 signals in biological samples, including endogenous metabolites, food components, compounds formed by the microbiome, environmental contaminants, drugs, and other consumer goods (Niedzwiecki et al. 2019). The broad scope of exposomics depends on such extensive techniques as it aims to detect diverse molecules from various sources with high structural diversity. Moreover, HRMS is not limited to the study of environmental chemicals and their human biotransformation products but also captures the endogenous metabolome. Thus, HRMS also covers the biological responses of the organism to external stressors to elucidate disease development which makes it a widely-used technology in both exposomics and metabolomics (Sévin et al. 2015; Vermeulen et al. 2020; Niedzwiecki et al. 2019).

HRMS approaches with minimal sample preparation and a short chromatographic runtime allow high sample throughput while keeping costs low. However, a crucial part of the internal chemical exposome, environmental contaminants, are primarily present at only low concentrations in a biological specimen. Thus, these low abundant chemicals might benefit from more complex sample preparation and tailored mass spectrometry methods (David et al. 2021).

The currently most prominent technology for exposomics is LC coupled via electrospray ionisation (ESI) to HRMS (David et al. 2021). LC-ESI-MS covers non-volatile molecules, including their biotransformation products with a high dynamic range and versatility (Jones 2015). Various available stationary phases with different chemistry, such as reverse phase (RP), hydrophilic interaction liquid chromatography (HILIC), and normal phase columns, are available and enhance the coverage of endogenous and exogenous compounds as they retain analytes with different polarities and chemical properties (David et al. 2021). Alternative techniques are necessary to extend the measurable chemical space to more volatile, nonpolar compounds and highly polar molecules. Gas chromatography (GC)-MS complements LC-MS analysis as this technique detects volatile, nonpolar and polar chemicals, e.g. persistent organic pollutants, after derivatisation in various matrices. (Misra 2021). Capillary electrophoresis (CE)-HRMS possesses a high potential, especially in metabolomics, for highly polar compounds and ion-exchange chromatography (IC) coupled to HRMS (Zhang et al. 2021b) might allow a better analysis of small, charged, non-volatile compounds (David et al. 2021). The combination of several analytical platforms is required to comprehensively capture the internal chemical exposome with its structurally diverse chemicals from highly polar to volatile apolar molecules and consequently minimises the invisible part of the exposome.

Dual column approaches combining two columns with complementary chemistry are an opportunity to cover molecules from a broader structural spectrum while keeping analysis times short. The time advantage is generally generated by washing and re-equilibrating one column while the effluent of the other column is introduced into the mass spectrometer (Jones 2015). This approach was applied in several omics- disciplines. Schwaiger et al. (2019) consecutively measured lipids on an RP column and metabolites on a HILIC column. Lv et al. (2020) applied a dual-column approach to increase the metabolome coverage by combining RP and HILIC in succession and Soltow et al. (2013) combined an RP column with an anion exchange column to study the exposome. Instead of consecutively introducing the effluent of both columns, the flows might also be combined after the LC separation and before mass spectrometric analysis.

In genome-wide association studies, genes are associated with disease and phenotype (Patel 2017). This concept has also been transferred to the environmental exposure level. Exposome-wide association studies (ExWAS) associate environmental factors with diseases and phenotypes. In these studies, multiple environmental factors are evaluated simultaneously to prioritise compounds of interest for systematic testing and elucidate the biological effect of environmental toxicants involved in disease aetiology (David et al. 2021; Vineis et al. 2020; Orešič et al. 2020; Patel et al. 2010). However, ExWAS are still in its infant stages.

4.4.1. Matrix selection

The choice of the biological matrix is highly relevant as the exposure pattern varies depending on the investigated material. Urine and blood samples are frequently selected matrices in exposomics due to their easy obtainability (Dennis et al. 2017). Not all exposures can be detected in the same sample type. Therefore, assessing multiple matrices from the same cohort might provide the best insights into the chemical exposome. Erythrocytes (red blood cells), leukocytes (white blood cells), and thrombocytes (platelets) suspended in a fluid make up blood. Anti-coagulants such as Li-heparin, citrate, and EDTA are added to the liquid fraction of a blood sample to obtain blood plasma (Psychogios et al. 2011). The less viscous blood serum is free of clotting proteins as the supernatant of centrifuged blood is taken after clotting (Psychogios et al. 2011). Blood is in contact with the whole body and transports all sorts of molecules from all organs and tissues through the body. Therefore, altered body function can be derived from molecules in the blood. Urine is produced by the kidneys and contains water-soluble metabolic breakdown substances from the diet, drugs, environmental pollutants, eliminated endogenous compounds, and bacterial metabolites (Bouatra et al. 2013). Urine is easy to obtain in large quantities and diagnostically relevant as most xenobiotics are excreted via this biofluid (Bouatra et al. 2013).

4.4.2. Harmonisation efforts and quantitation

Introducing standard quality assurance (QA) and quality control (QC) measures is crucial for untargeted analysis. Already established approaches utilised in targeted measurements need to be expanded and adapted to be adequate for NTA and suspect screening. Suggested measures include fortified samples and internal standards with broad physico-chemical properties from sample preparation to mass spectrometric analysis to correct for extraction recovery, ion suppression, and other information loss during the sample preparation and measurement steps (Schulze et al. 2020). Moreover, the comprehensive inclusion of process blanks and pooled samples, ideally injected multiple times throughout a measurement sequence, to monitor and correct the reproducibility of the method and the replacement of manually performed steps in data processing by openly accessible algorithms improve reproducibility and transparency (Schulze et al. 2020). Caballero-Casero et al. (2021) emphasised the importance of including QA/QC measures for sample preparation, including processing blanks and fortified samples, the use of certified reference material, and a detailed description of the performed steps in standard operation protocols (SOPs) for reproducibility. The Benchmarking and Publications for Non-Targeted Analysis Working Group (BP4NTA) published efforts to harmonise NTA reporting standards (Place et al. 2021). Interlaboratory trials were advocated to evaluate the performance of NTA/suspect screening and improve comparability between laboratories (Caballero-Casero et al. 2021). In the EPA's Non-Targeted Analysis Collaborative Trial (ENTACT), ten different mixtures containing up to 365 chemicals were distributed to 25 laboratories for a blinded analysis followed by an unblinded review (Sobus et al. 2019). The blinded part revealed true positive rates ranging from 19 to 46%. After unblinding, 60% of substances were detected with LC-HRMS, but only 14% could be annotated by MS2 data, partly due to insufficient database coverage (Sobus et al. 2019).

Observed signal intensities in HRMS depend on the compound and the instrument. Consequently, each measurement would require a reference standard for each analyte of interest for quantitation. However, availability is often limited. Therefore alternative strategies need to be employed. Krue (2020) suggested using peak areas in combination with statistics, isotope dilution, radiolabelling, the use of similar compounds, or the prediction of ionisation efficiencies. Isotopically labelled standards and radio chromatography yielded the highest accuracy. In metabolomics, ¹³C-yeast has already been successfully applied to quantify an extensive range of metabolites (Wasito et al. 2021; Hermann et al. 2018). Alternatively, targeted LC-MS/MS approaches covering multiple analytes from various classes (Preindl et al. 2019; González-Domínguez et al. 2020) might aid confirmation and quantitation of analytes discovered by HRMS.

4.5. Classification of environmental exposures

The human body is confronted with various chemicals from natural and synthetic sources triggering diverse biological effects. Single chemical exposure is mostly absent under real-life conditions. On the contrary, a complex mixture of substances is present in the environment. The health impact of co-occurring compound mixtures may differ from the single pollutant's effect (Vejdovszky et al. 2017; Patel 2017). Therefore, monitoring a wide range of chemicals is highly important to understand disease aetiology. Xenobiotics refer to chemicals foreign to the human body. These chemicals are mostly synthetically produced but also naturally occurring compounds formed by other organisms such as fungi, bacteria, and plants exist (Abdelsalam et al. 2020). Harmful toxicants are primarily of xenobiotic origin, but endogenous organic or inorganic molecules involved in normal metabolism, e.g. histamine in bee venom or iron overdose in children, may also cause adverse health effects (Croom 2012). This chapter focuses on chemical classes selected as model exposures in the course of this thesis. Environmental exposures, however, comprise various other xenobiotics belonging to diverse chemical classes.

4.5.1. Endocrine disrupting chemicals

Endocrine disrupting chemicals (EDC) are a highly-relevant class of exposure. These natural or synthetic chemicals interfere with the body's endocrine system (Kabir et al. 2015). Besides the dose, the timing of exposure is essential for the effect of endocrine disruptors, and especially early life exposures might be critical even at low doses (Kabir et al. 2015). Xenoestrogens are a subcategory of EDCs and mimic the structure and functionality of a natural hormone, 17 β -estradiol, interfering with the hormone balance. The structure of xenoestrogens is diverse, but they all possess lipophilic phenolic rings and other hydrophobic components, which are also typical structural elements of steroid hormones (Watson et al. 2007) (Figure 2). The structural similarity to the female sex hormone allows these molecules to attach to the oestrogen receptors alpha and beta (Paterni et al. 2014). Oestrogen receptors occur in various tissues, e.g. central nervous system, mammary gland, placenta, and reproductive- and gastrointestinal tract and regulate the expression of specific genes (Sirotkin et al. 2014). Whereas oestrogen receptor alpha is associated with promoting cell proliferation, the beta subtype is linked to the promotion of programmed cell death (Rietjens et al. 2013).

In nature, xenoestrogens are produced by plants (phytoestrogens) and fungi (mycoestrogens) (Montes-Grajales et al. 2018). Estrogenic compounds from plants can be grouped depending on their structure into, among others, flavonoids (flavonols, flavanones), isoflavonoids (isoflavones, coumestans), lignans, and stilbenoids (Michel et al. 2013). Plants rich in phytoestrogens are soy and other legumes (genistein, daidzein, glycitein), red clover (formononetin, coumestrol), hops (isoxanthohumol, 8-prenylnaringenin), and flaxseeds (matairesinol) (Sirotkin et al. 2014). Additionally, the gut metabolome is responsible for forming further estrogenically active compounds such as enterodiol or enterolactone fromatairesinol and equol from genistein or daidzein (Wang 2002; Zhengkang et al. 2006). Phytoestrogens, especially isoflavones, possess favourable effects, e.g. prevention of menopausal problems, osteoporosis, hormone-dependent cancer types, cardiovascular-, neurodegenerative-, and immunological diseases (Sirotkin et al. 2014; Saha et al. 2020). Their primarily positive health outcome compared to other xenoestrogens might be due to their preference for binding to the potentially beneficial oestrogen receptor beta (Paterni et al. 2014). Nevertheless, adverse health effects such as breast cancer initiation and reproductive disorders have been reported (Sirotkin et al. 2014).

A common isoflavone is genistein (GEN), created by plants of the *Fabaceae* family. The antioxidative phytoestrogen might protect against diabetes, obesity, cardiovascular diseases, and certain cancer types such as breast cancer (Sharifi-Rad et al. 2021). Nevertheless, the data on breast cancer is controversial as in animal and in vitro studies, GEN shows cancer-promoting effects, especially at low levels (Kucuk 2017; Yu et al. 2021). A lowered breast cancer risk in countries with high soy intake, e.g. Asia, however, supports the beneficial effects of GEN, although the time

window of exposure, e.g. during adolescence and the dose, might be relevant for the unfolding of preventive effects (Kucuk 2017; Bhat et al. 2021).

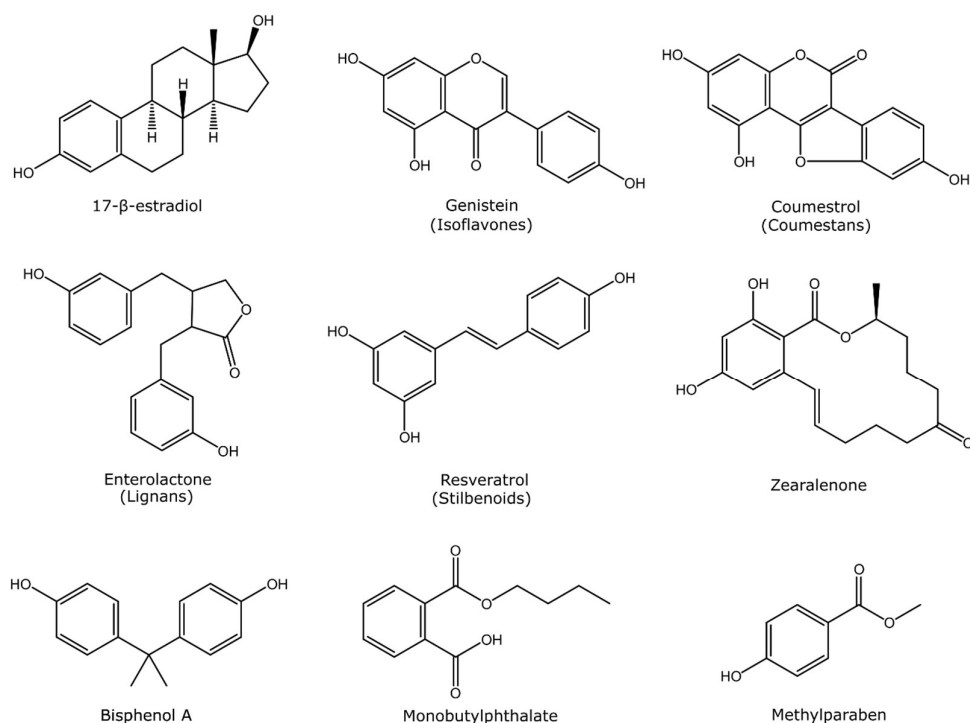


Figure 2. Chemical structures of selected xenoestrogens from natural and synthetic sources

A natural xenoestrogen associated with harmful health outcomes is the thermostable zearalenone (ZEN). This mycoestrogen is produced by *Fusarium* species and contaminates oats, maize, wheat, barley, and rice before or during storage (Rai et al. 2020). Therefore, the ingestion of contaminated foodstuff is the most prominent route of exposure. Acute toxicity of ZEN is with an oral LD50 above 2,000 mg/kg body weight in rodents low, but chronic low dose exposure might trigger an adverse health effect as the potentially carcinogenic ZEN induces cell proliferation (EFSA 2011; Rai et al. 2020). Especially in estrogen-sensitive cancers such as breast cancer, ZEN is suspected to be involved (Kowalska et al. 2016). Moreover, immunotoxicity, genotoxicity, hematotoxicity, and hepatotoxicity were also described for this xenoestrogen (Ropejko et al. 2021). However, most research has focused on animals so far. As the human body absorbs ZEN, it was detected in biofluids such as urine at levels up to 100 ng/mL in European adults (Föllmann et al. 2016) and about 800 ng/mL in African infants (Ezekiel et al. 2022). The tolerable daily intake (TDI) was defined as 0.25 µg/kg bodyweight for this mycotoxin (Mally et al. 2016).

Synthetic xenoestrogens are constituents of products such as pharmaceuticals, food preservatives, UV filters, plasticizers, pesticides, and personal care products (Paterni et al. 2017). These artificial compounds are primarily associated with harmful effects, e.g. disturbance of reproduction, breast cancer development, abnormal growth, and delays in neurodevelopment in children (Paterni et al. 2017). Well-described synthetic xenoestrogens comprise parabens, bisphenols, and phthalates.

Parabens, alkyl esters of p-hydroxybenzoic acid, are ingredients in cosmetics, pharmaceuticals, personal care products, and food due to their antimicrobial activity, which increases with chain length (Jagne et al. 2016). Breast cancer,

endometriosis, reduced sperm quality, and obesity might be associated with these weakly estrogenic compounds (Karpuzoglu et al. 2013; Jagne et al. 2016; van der Schyff et al. 2022; Nowak et al. 2021). The endocrine-disrupting potential increases with chain length. Thus, butylparaben and propylparaben are more critical than short-chain parabens (van der Schyff et al. 2022). In the EU, five branched, long-chain parabens, including benzyl paraben, were forbidden in 2014. Short-chain parabens (methyl- and ethylparaben) were limited to 0.4% of the single compound and the sum of propyl- and butylparaben was restricted to 0.19% in personal care products (Regulation 2014). Methyl- and ethylparaben and their sodium salts are the only parabens allowed as a food additive in the EU at maximum levels between 300 to 1,000 mg/kg (Gálvez-Ontiveros et al. 2021). In human biofluids, parabens were detected in the ng/mL range (van der Schyff et al. 2022; Honda et al. 2018; Sosvorova et al. 2017; Gao et al. 2020).

Bisphenols, originating from polycarbonate plastics and epoxy resins used in food/drink packaging, medical devices, and thermal papers (Bousoumah et al. 2021), impact reproduction, metabolic processes, immune system regulation, hormone-dependent tumours, and cognitive- and behavioural development (Gore et al. 2015; Cimmino et al. 2020). The most prominent representative, bisphenol A (BPA), was classified as reproductive toxicant 1B by the EU and was listed on the candidate list of substances of very high concern by the European Chemical Agency. Therefore, it was banned from baby bottles and thermal paper (Bousoumah et al. 2021). Replacement substances for BPA, such as bisphenol S (BPS) and bisphenol F (BPF), have successfully been introduced, but they are suspected to be similarly or even more harmful than BPA (Paterni et al. 2017; Thoene et al. 2020). In 2013/2014, BPA, BPS, and BPF were detected in over 95%, nearly 90% and about 66% of representative urine samples for the US-American population, respectively (Lehmlier et al. 2018). Another class of xenoestrogens used in plastics are phthalates. These plasticizers are present in plastic types such as polyvinyl chloride to boost extensibility, elasticity, and workability and are used in diverse applications, including packaging, building materials, and toys. These EDCs were associated with various adverse effects, e.g. infertility (Giuliani et al. 2020) and were widely observed in several human matrices, such as blood and urine (Mankidy et al. 2013).

4.5.2. Other toxic chemicals

Chemicals from nature not only interfere with the endocrine system but also have various other toxic properties. A large class of naturally-produced toxicants are mycotoxins, secondary fungi compounds, present on, e.g. wheat, corn, oats and rice. Toxicologically relevant toxins comprise aflatoxins, ochratoxins, trichothecenes, fumonisins, and the above-described zearalenone (Zinedine et al. 2007). A wide-spread *Fusarium* mycotoxin is the thermostable trichothecene deoxynivalenol (DON) known to trigger gastroenteritis, vomiting, diarrhoea, and ribotoxic stress in humans (Ganesan et al. 2022; Mishra et al. 2020). This mycotoxin is classified as human carcinogen group 3 by IARC (Ostry et al. 2017). Native DON and its conjugated forms were widely detected in European urine (Eriksen et al. 2021; De Santis et al. 2019; Chen et al. 2017). Plants also produce various detrimental chemicals, such as the acetylcholine imitating anisodamine and scopolamine or pyrrolizidine alkaloids, such as riddelliine, associated with hepatotoxicity (Poupko et al. 2007; Avula et al. 2015).

Synthetic chemicals from various sources also impact the human body adversely by diverse mechanisms. Major air pollutants are the potentially cancerogenic polycyclic aromatic hydrocarbons (PAH) originating from incomplete combustion of organic material. A urinary biomarker for PAHs is 1-hydroxypyrene (Hansen et al. 2008; Lawal 2017). Cancerogenic activity was also described for food-processing by-products, such as the heterocyclic amine PhIP, acrylamide (Gooderham et al. 2002), and disinfection by-products (Li et al. 2018).

4.6. Biotransformation

Once exogenous chemicals enter the human body, they might be subject to internal metabolic reactions. The role of these processes is to eliminate xenobiotics. The endogenous metabolism changes the external stressors' structure and might modify their toxicological potential (Croom 2012). Therefore, these biotransformation processes increase the exposome's chemical variety and complexity (Vermeulen et al. 2020). Biotransformation processes primarily detoxify xenobiotics, but activation is also possible (Croom 2012). Most metabolic reactions depend on enzymes, but a few reactions occur spontaneously, e.g. hydrolysis at a specific pH value (Croom 2012). In rare cases, the fate of exogenous chemicals in the body also includes elimination without any modification, e.g. hydrophilic compounds such as quaternary amines or strong carboxylic/sulfonic acid in urine and the storage for a longer time in fat or bone (Caldwell et al. 1995). The metabolism of xenobiotics, in general, begins with phase I reactions to enhance hydrophilicity and form reaction sites for subsequent steps. Phase II reactions comprise mainly conjugation reactions. Finally, transporters bring the conjugated biotransformation products out of the cell, ready to be excreted via urine or faeces (Croom 2012) (Figure 3). The final transportation step (phase III) is crucial as the natively lipophilic xenobiotics cross the lipid-rich cell membrane via passive diffusion. However, the increased polarity of their biotransformation products requires membrane proteins that actively transport them out of the cell (LeBlanc 2008). The primary site of biotransformation is the liver. However, other organs, e.g. bladder, kidney, and the gastrointestinal tract, are also involved in xenoestrogen metabolism (Beyerle et al. 2015). In case metabolic reactions activate a xenobiotic, the organ with the highest corresponding enzyme activity, mainly the liver, is the main site of toxicity (Croom 2012).

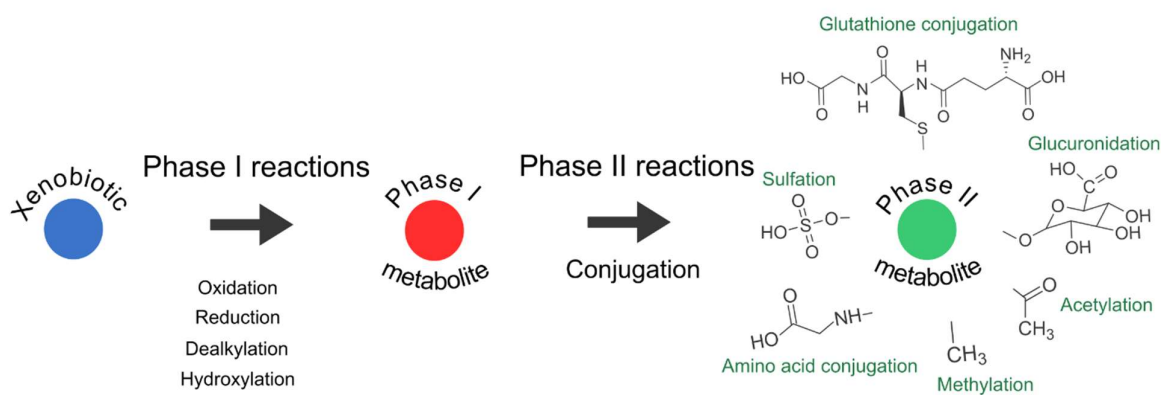


Figure 3. Simplified scheme of biotransformation processes in the human body

Oxidations, reductions, and hydrolysis are typical reactions for phase I metabolism. Cytochrome P450 (CYP) is the major enzyme involved in this phase and performs N- and O- dealkylation, aliphatic and aromatic hydroxylation, N- and S-oxidation, epoxidation, and deamination on multiple xenobiotics, e.g. PAHs and nicotine (Omiecinski et al. 2011). CYPs are crucial for eliminating toxicants, but these enzymes may activate pro-carcinogens, e.g. aflatoxin B1 and PAHs (Beyerle et al. 2015) or enhance adverse effects such as estrogenicity. The estrogenic potential of the, e.g. the mycoestrogen ZEN is affected by phase I-metabolism as the binding affinity to the oestrogen receptor is compared to the native compound, higher for the major metabolite, α -zearalenone, and lower for the reduced metabolic product, β -zearalenone (Rai et al. 2020; Ropejko et al. 2021). The CYP3 family is most abundant in liver tissue, where it metabolises 30-40% of all drugs (Zanger et al. 2013). Outside of the liver, the CYP1 family is more prominent (Stiborová et al. 2002). Other phase I enzymes include flavin-dependent monooxygenases (FMO), hydrolases, and epoxide hydrolases (Croom 2012). As showcased by the endocrine active ZEN, hydroxylation via 3 α - and 3 β -

hydroxysteroid dehydrogenases (HSD) and the reduction of a double bond (Mally et al. 2016) are further metabolic reactions.

During phase II metabolism, small endogenous substances are conjugated to xenobiotics or their phase I metabolites (LeBlanc 2008). Phase II - reactions involve, e.g. glucuronidation with glucuronic acid, sulfation with sulfate, glutathione-conjugation, amino acid conjugation, methylation, and acetylation (Croom 2012). These conjugation reactions generally result in less toxic biotransformation products. However, a few xenobiotics are activated by phase II biotransformation, e.g. arylamines by glucuronidation, 2-acetylaminofluorene by sulfation, and halogenated alkanes by glutathione conjugation (LeBlanc 2008). Glucuronidation of native substances and their phase I metabolites is the dominant detoxifying phase II reaction for most compounds, including phytoestrogens, e.g. GEN, and mycotoxins such as DON and ZEN, although sulfation has been widely described in lower quantities (Paterni et al. 2017; Al-Jaal et al. 2019). Enzymes involved in conjugation reactions are diverse, comprising UDP-glucuronyltransferases (UGTs), sulfotransferases (SULTs), N-acetyltransferases (NATs), glutathione-S-transferases (GSTs), and methyltransferases such as catechol-O-methyl transferase (COMT) (Omiecinski et al. 2011). UGTs are a vital part of phase II metabolism as these enzymes binding electron-rich nucleophilic heteroatoms to glucuronides have a high metabolic capacity and low affinity allowing the rapid conjugation of high-concentrated xenobiotics (Negishi et al. 2001). Three families of UGTs are described in humans, of which the UGT1 and UGT2 families catalyse the conjugation of steroid hormones and xenobiotics (LeBlanc 2008). The sulfate moiety for sulfation by SULTs is often obtained from 3-phosphoadenosine-5' phosphosulfate (PAPS) and alcohols, phenols, and arylamines are particularly likely to form sulfates (LeBlanc 2008). The SULT 1A family, especially SULT1A1 and SULT1A2, are involved in xenobiotic biotransformation, but also several others contribute to the biotransformation of xenobiotics, such as SULT1B1, SULT1E, SULT2A, and SULT2B. Over 30 enzymes categorised into four classes belong to the GST family and perform human glutathione conjugation (Omiecinski et al. 2011). Two NATs (NAT1 and NAT2) that catalyse acetylation are known in humans (Omiecinski et al. 2011). A minor biotransformation reaction is the conjugation of primarily xenobiotics containing a carboxylic acid group with amino acids such as glycine, glutamine, arginine, and taurine. A mitochondrial enzyme system is responsible for this metabolic reaction. Initially, acyl-CoA ligase produces a coenzyme A (CoA) derivative that transforms into an acylated amino acid conjugate and CoA (LeBlanc 2008).

Part II
Methodology

5. Methodology

Liquid chromatography-mass spectrometry (LC-MS) is a widely used analytical platform for detecting various chemicals. This approach was also applied in this thesis. The investigated sample is injected into the liquid eluent flow (mobile phase) and the different molecules in the sample are separated in the column, the stationary phase. The separated compounds then leave the column and are captured in a detector such as mass spectrometry.

5.1. Liquid chromatography

LC separates complex chemical mixtures based on the affinity and interaction of the analyte to the liquid mobile and the solid stationary phase. The time the chemicals need to elute from the column depends on their properties. Applying pressure to the column allows pumping the mobile phase through columns with a smaller particle size improving sensitivity, enhancing resolution, and reducing analysis time. However, smaller particle size increases the pressure on the system requiring pressure-stable instrumentation. Ultra-performance liquid chromatography (UPLC) generally applies columns packed with particles in the sub-2 μm range and 50-100 mm in length (Moldoveanu et al. 2013). A schematic LC system consists of a solvent reservoir, a pump, an injection valve, a column in a temperature-controlled compartment, and a detector.

Different separation modes, mainly depending on the column chemistry, are available. Common modes are reverse-phase chromatography (RP), hydrophilic interaction liquid chromatography (HILIC) and normal phase chromatography (NP). In RP, a nonpolar column such as C18- and phenyl groups bonded to silica particles and a polar solvent, commonly water with some organic solvent, are used. The variety of available column-solvent combinations for RP allows the separation of molecules with hydrophobic moieties, making it universally applicable in, e.g., exposure monitoring, pharmaceutical analysis, and analysis of proteins (Vailaya et al. 1998). The underlying separation mechanism involves partitioning, where the analyte enters the bonded phase and adsorption processes at the stationary/mobile phase interphase. Especially in longer chain stationary phases, e.g. C18, both phenomena contribute to the retention (Žuvela et al. 2019). Since the mobile phase is more polar than the stationary phase, the time from injection until elution, the retention time, increases with the hydrophobic character of the analyte, the hydrophobicity of the stationary phase and the polarity of the mobile phase (Žuvela et al. 2019). Hydrophilic interaction chromatography (HILIC) utilises a polar column with a mobile phase such as water and organics like acetonitrile. HILIC is primarily used to separate polar compounds that in RP elute with the dead volume. Typical HILIC columns are made of bare silica, silica particles modified with polar groups, or polymer-based columns. One column type is a zwitterionic sulfoalkylbetaine phase comprising strongly acidic sulfonic acid moieties and strongly basic quaternary ammonium moieties that enable ion-exchange interactions. The zwitterionic phase absorbs water due to hydrogen bonding forming a water layer that is involved in the retention of molecules (Buszewski et al. 2012). HILIC retention is proposed to be based on partitioning and might originate from the distribution of the dissolved analyte between the organic eluent and the water layer adsorbed on the hydrophilic stationary phase. With increasing hydrophilicity of the analyte, the partitioning equilibrium is moved towards the water-enriched layer of the stationary phase and the analyte is longer retained on the column (Buszewski et al. 2012). LC methods either use the same eluent composition throughout the separation (isocratic elution) or a gradient elution where the composition is changed to increasing levels of eluent with higher elution strength. In RP, the proportion of organic solvent is increased and HILIC gradients begin with an apolar organic solvent, gradually shifting to a more polar eluent. Gradient elution is the dominant approach in modern LC-MS due to reduced analysis time, higher resolution, and increased sensitivity (Snyder et al. 2010).

5.2. Mass spectrometry

Mass spectrometry (MS) is a destructive detector frequently coupled to LC to identify and quantify molecules based on their mass to charge ratio (m/z). A mass spectrometer consists of an ion source to ionise the introduced samples, followed by a mass analyser to separate the ions depending on their m/z ratio. Finally, the ions are measured and transformed into spectra displaying the m/z values' intensity at a specific retention time.

5.2.1. Ionisation

A prominent ionisation technique for biological samples is electrospray ionisation due to its easy coupling to LC and the formation of intact gas-phase ions (Page et al. 2007). This ionisation technique was also applied in the scope of this thesis. Dissolved analytes are directed at a set flow rate in the sub mL/min range via an inlet capillary to the tip of the ESI needle. A high voltage between this tip and the inlet of the MS generates a Taylor cone at the end of the capillary emitting a stream of highly charged, tiny droplets (Figure 4). The charge of the droplets is equal to the applied voltage. A coaxial N_2 sheath gas flow supports nebulisation and aids in directing the stream of droplets to the MS. Solvent evaporation supported by an increased temperature and an additional nitrogen flow reduces the droplet's size. Thus, the surface charge density is increased and destabilised. When the Coulomb repulsion exceeds the surface tension, a Coulomb explosion happens, resulting in even tinier droplets. This process is repeated until the ions are released into the gas phase and the solvent is gone (Smoluch et al. 2019).

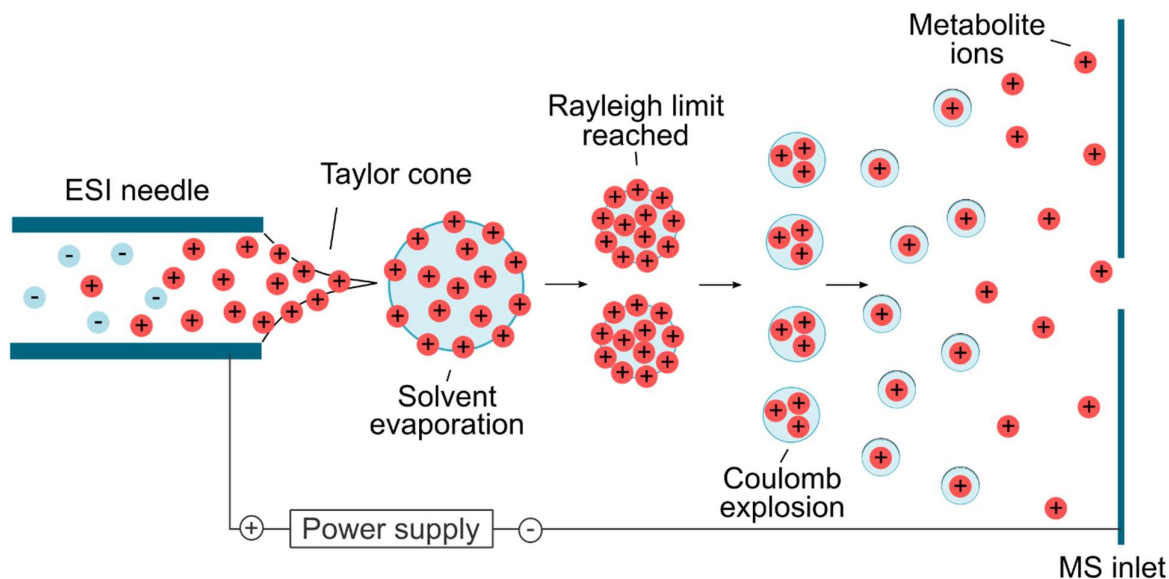


Figure 4. Scheme of the processes during electrospray ionisation (ESI)

5.2.2. Mass analysers

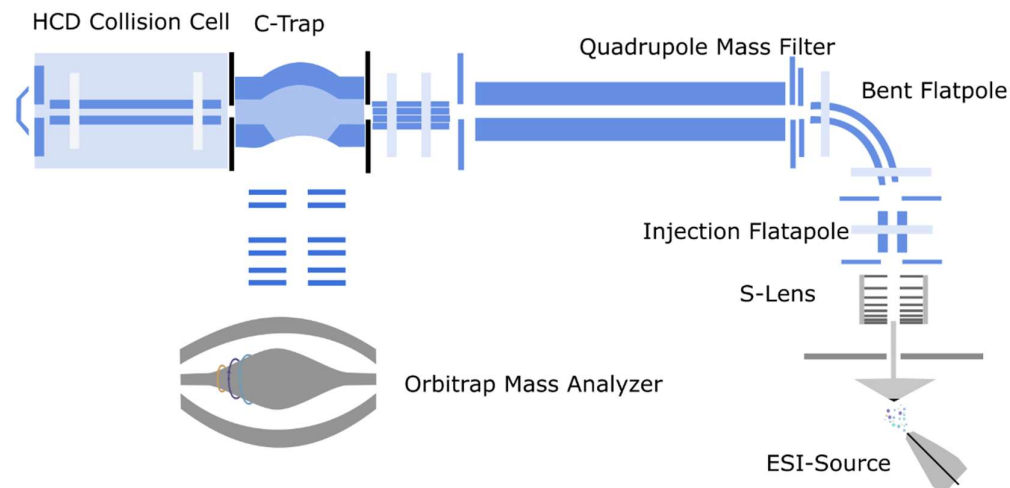
Several mass analysers are available to separate the ions based on their m/z value. High-resolution mass spectrometers rely on mass analysers such as time of flight and orbitrap, while low-mass resolution instruments work with, e.g. quadrupoles and ion traps. The improved mass resolution and mass accuracy in HRMS enables differentiation of peaks with minor m/z differences, decreasing the number of possible formulas and easing subsequent compound identification. In HRMS, the mass accuracy, describing the difference to the actual exact mass, is below 1 ppm, whereas low-resolution instruments have only a mass accuracy in the integer range. The mass resolution describes the ability to distinguish two peaks with a small m/z difference and depends on the mass. Low-resolution MS works with a unit mass resolution of about 1,000 and orbitraps reach a mass resolving power of hundreds of thousands (Geer Wallace et al. 2020). The instrumentation applied in this thesis was equipped with a quadrupole mass analyser and an orbitrap.

Ion separation in a quadrupole is based on the ion's stable oscillatory trajectories in an electric field. This type of analyser consists of four parallel cylindrical rods in the form of a square. An electric voltage is applied to rods opposite each other. A direct current (DC) voltage is used for one pair while the other two rods are operated with radio frequency (RF) voltage. The ion beam enters parallel to the rods but only ions of a specific m/z value have a stable trajectory passing through the quadrupole. The other ions are discharged after colliding with the rods. Different ions travel through the quadrupole by continuously changing the applied voltages while keeping the ratio of DC and RF constant. The ions are then transformed into a voltage pulse proportional to the number of ions in the adjacent detector. The instrument subsequently converts the voltage pulse into a signal (Smoluch et al. 2019).

In triple-quadrupole instruments, several quadrupoles are combined (Figure 5B). After the introduction into the mass spectrometer, the ion beam is focused and efficiently transferred to the Q1 section by quadrupoles (QJet, Q0). The first (Q1) and the third (Q3) filtering quadrupoles are used as mass analysers to select ions with specific m/z values. Fragmentation by collision with gas molecules occurs between Q1 and Q3 in a quadrupole used as a collision cell. Multiple reaction monitoring (MRM) is a typical measurement mode. A specific m/z value is selected in MRM as the parent ion ('precursor ion'). The ion is then fragmented in the collision cell (Q2) with optimised parameters and selected fragments ('product ions') are monitored in the third quadrupole. The multiple transitions of several analytes can be measured at once in MRM.

An orbitrap separates m/z values due to the frequency of their oscillations in an electrostatic field. This mass analyser combines an axial internal electrode shaped like a spindle and two outer electrodes shaped like barrels separated by an insulating layer. An equilibrium between the electrostatic and centrifugal forces stabilises the ions on stable orbital flight paths. Before entering the orbitrap, the ions are gathered in an ion trap, e.g. a C-Trap. The C-Trap is a linear trap filled with gas with a curved central axis and an opening towards the orbitrap. In this trap, the kinetic energy of the charged molecules is decreased by collision cooling with nitrogen. The ions are then released by ramping down the RF, followed by voltage pulses to rapidly force the ions in short packets of ions with the same m/z into the orbitrap. As the ion packets enter the orbitrap with offset from the equatorial plane, oscillation starts spontaneously. The electric field is gradually enhanced to reduce the radius of the ion cloud enabling new ion packets to arrive in the orbitrap. Once the ions of all m/z are in the orbitrap, the voltage is kept constant to enable their detection via image current. The ion's trajectories are defined by a rotation around the axial central electrode and harmonic oscillation along the z-axis. This harmonic oscillation's frequency depends on the m/z ratio and an instrument constant. The oscillating movement of the ions along the z-axis induces a current in the two divided parts of the outer electrode. This signal (image current) is then amplified and undergoes Fourier transformation to obtain the frequencies of the oscillating ions and calculate their m/z values (Smoluch et al. 2019).

A) High-resolution mass spectrometer (Orbitrap)



B) Triple quadrupole mass spectrometer

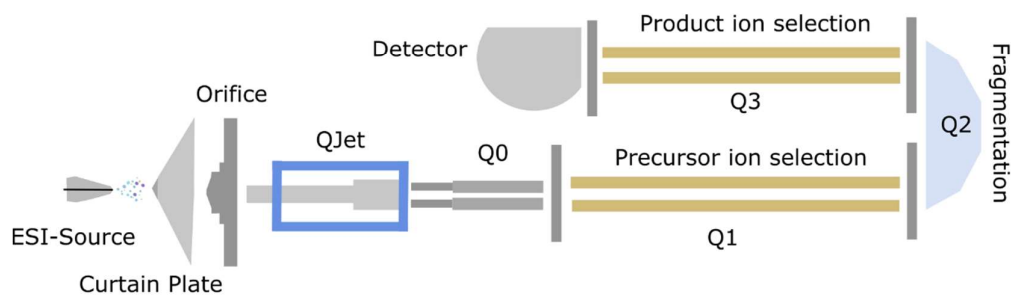


Figure 5. Schematic setup of A) an orbitrap high-resolution mass spectrometer and B) a triple quadrupole low resolution mass spectrometer

The orbitrap mass analyser is often combined with a quadrupole analyser (Figure 5A). Ions enter the mass spectrometer via a transfer capillary and the ion beam is subsequently focused by lenses, e.g. S-Lens and flatpoles such as the injection flatpole. In the bent flatpole, only ions can follow the 90° bent ion transmission device, while neutral particles are removed. The mass filtering quadrupole selects precursors and the orbitrap is used to detect full scans, where all ions pass through the quadrupole and MS/MS spectra. MS/MS spectra are produced by fragmentation in a higher-energy collision-induced dissociation chamber (HCD) filled with gas and subsequent analysis in the orbitrap.

5.3. Current methodological challenges

A specific analytical technique only captures a limited part of the internal chemical exposome. The combination of several analytical techniques minimises the invisible part of the exposome, but even if biospecimens are investigated with a multitude of instrumentations, the totality of environmental exposures might never be completely deciphered. However, HRMS coupled with separation techniques such as LC and GC still is capable of illuminating a substantial part of the internal chemical exposome.

Another issue in exposomics research is that low-concentrated environmental pollutants are often missed during analysis due to sensitivity issues and are hidden from the measurement. Comparing the limit of detection (LOD) of 30 diverse exogenous chemicals in the blood to concentration ranges of endogenous and exogenous substances in literature showcased that the LOD of LC-HRMS still struggles to reach the desired sensitivity for numerous pollutants (David et al. 2021). Thus, hidden chemicals are still a significant challenge in measuring environmental chemicals. Sensitivity issues in LC-ESI-HRMS are, among others, caused by matrix effects and the resulting ion suppression (Antignac et al. 2005). Ion suppression has multiple sources, such as the co-elution of especially high concentrated endogenous molecules (e.g. inorganic electrolytes, salts, pigments, carbohydrates, lipids, and peptides) and exogenous substances introduced during sample preparation (e.g. plastic/polymer residues, buffers, and LC stationary phases) (Antignac et al. 2005). Several mechanistic processes mainly occurring in the liquid phase are involved in the ion suppression mechanism (Antignac et al. 2005). High concentrated molecules might boost the formed droplets' viscosity and surface tension, decreasing evaporation efficiency and analytes might co-precipitate with non-volatile components. In addition, competition for the limited ionisation efficiency is proposed as a potential cause. Finally, neutralisation processes caused by interfering molecules with high basicity in the gas phase result in a loss of charge in the gas phase (Antignac et al. 2005; Truffelli et al. 2011).

HRMS datasets are vast, with more than 10,000 features with corresponding retention time, m/z value, and an area or intensity for each feature (David et al. 2021; Vermeulen et al. 2020). Advancing from feature detection to structural identification is demanding and time-consuming as exact masses, retention times, isotopic patterns, and MS2 spectra need to be compared to reference data (Schymanski et al. 2014a). The annotation procedure relies on databases such as the metabolome focused HMDB (Wishart et al. 2018) or the CompTox Chemicals Dashboard (Williams et al. 2017), which specialises in environmental exposures of toxicological relevance or the Blood Exposome Database (Barupal et al. 2019). The European Human Biomonitoring for Europe initiative (HBM4EU) collected over 70,000 structures of exposures and over 300,000 biotransformation products of these exposures in an openly accessible database, CECsreen (Meijer et al. 2021), expanding available structural information for exposures of interest.

However, even with the high mass accuracy of HRMS instrumentation below five ppm, an exact mass might be attributed to hundreds of candidates in vast, non-specialised databases such as PubChem (Kim et al. 2021). Therefore, experimental fragmentation data (MS2) is essential to prioritise potential structures. Databases containing MS2 data such as HMDB (Wishart et al. 2018), Metlin (Guijas et al. 2018) or mzcloud are available for comparing suitable candidates. However, only for a limited number of chemicals reference MS2 spectra are available in databases. From the vast pool of suspects collected in the CompTox Dashboard (875,000 compounds) and HMDB (over 140,000), only for a small proportion (below 1%) MS2 data is accessible (Oberacher et al. 2020). *In silico* fragmentation tools such as MetFrag (Ruttkies et al. 2016) and other sources (Blaženović et al. 2018) help to close the existing annotation gap. Despite immense efforts to expand and ease access to databases and the development of bioinformatics tools for *in silico* fragmentation, annotation is still a bottleneck. Therefore, a substantial part of the measured chemical exposome remains in the dark.

Part III
Original Works

6. Original works

6.1. Overview of the original research articles included in this thesis

Manuscript #1: Establishment of a dual-column approach and its application to biological samples

Mira Flasch, Veronika Fitz, Evelyn Rampler, Chibundu N. Ezekiel, Gunda Koellensperger, Benedikt Warth. '**Integrated exposomics/metabolomics for rapid exposure and effect analyses**', *ChemRxiv pre-print*, 2022

DOI: 10.26434/chemrxiv-2022-sgq04-v2

Manuscript #2: Comparing the sensitivity of high-resolution -and low-resolution mass spectrometry

Mira Flasch, Gunda Koellensperger, Benedikt Warth. '**Comparing the sensitivity of low- and high-resolution mass spectrometry for xenobiotic trace analysis: An exposome-type case study**', *ChemRxiv pre-print*, 2022

DOI: 10.26434/chemrxiv-2022-x4kk7

Publication #3: Optimisation of a high-resolution mass spectrometry workflow to investigate biotransformation products in human cell culture

Mira Flasch, Christoph Bueschl, Lydia Woelflingseder, Heidi E Schwartz-Zimmermann, Gerhard Adam, Rainer Schuhmacher, Doris Marko, Benedikt Warth. '**Stable Isotope-Assisted Metabolomics for Deciphering Xenobiotic Metabolism in Mammalian Cell Culture**', *ACS Chemical Biology*, 2020

DOI: 10.1021/acscchembio.9b01016

Publication #4: Investigating biotransformation products of xenoestrogens in human breast cancer cells

Mira Flasch, Christoph Bueschl, Giorgia Del Favero, Gerhard Adam, Rainer Schuhmacher, Doris Marko, Benedikt Warth. '**Elucidation of xenoestrogen metabolism by non-targeted, stable isotope-assisted mass spectrometry in breast cancer cells**', *Environment International*, 2022

DOI: 10.1016/j.envint.2021.106940

6.2. Manuscript #1: Flasch et al. (2022b)

Status	Submitted for publishing
Title	Integrated exposomics/metabolomics for rapid exposure and effect analyses
Authors	Mira Flasch ^{1,2} , Veronika Fitz ^{2,3} , Evelyn Rampler ³ , Chibundu N. Ezekiel ⁴ , Gunda Koellensperger ^{3,5} , Benedikt Warth ^{1,5*}
Affiliations	<p>¹University of Vienna, Faculty of Chemistry, Department of Food Chemistry and Toxicology, Währinger Straße 38-40, 1090 Vienna, Austria</p> <p>²University of Vienna, Vienna Doctoral School of Chemistry, Währinger Straße 42, 1090, Vienna, Austria</p> <p>³University of Vienna, Faculty of Chemistry, Department of Analytical Chemistry, Währinger Straße 38-40, 1090 Vienna, Austria</p> <p>⁴Department of Microbiology, Babcock University, Ilishan Remo, Ogun State, Nigeria</p> <p>⁵Exposome Austria, Research Infrastructure and National EIRENE Hub, Austria</p> <p>*Corresponding author</p>
Year	2022
Preprint server	ChemRxiv
DOI	10.26434/chemrxiv-2022-sgq04-v2
Contribution	Mira Flasch (MF) optimised the sample preparation, developed the LC-HRMS(/MS) method, evaluated and interpreted the results, and wrote the manuscript.

Integrated exposomics/metabolomics for rapid exposure and effect analyses

Mira Flasch^{1,2}, Veronika Fitz^{2,3}, Evelyn Rampler³, Chibundu N. Ezekiel⁴, Gunda Koellensperger^{3,5}, Benedikt Warth^{1,5*}

¹University of Vienna, Faculty of Chemistry, Department of Food Chemistry and Toxicology, Währinger Straße 38-40, 1090 Vienna, Austria

²University of Vienna, Vienna Doctoral School of Chemistry, Währinger Straße 42, 1090, Vienna, Austria

³University of Vienna, Faculty of Chemistry, Department of Analytical Chemistry, Währinger Straße 38-40, 1090 Vienna, Austria

⁴Department of Microbiology, Babcock University, Ilishan Remo, Ogun State, Nigeria

⁵Exposome Austria, Research Infrastructure and National EIRENE Hub, Austria

ABSTRACT: Environmental drivers of disease susceptibility, referred to as the exposome in its totality, are poorly understood. Measuring the myriad of chemicals that humans are exposed to is immensely challenging and identifying disrupted metabolic pathways is an even more complex task. Here, we present a novel technological approach for the comprehensive, rapid and integrated analysis of the endogenous human metabolome and the chemical exposome. By combining reverse-phase and hydrophilic interaction liquid chromatography and fast polarity switching, molecules with highly diverse chemical structures can be analyzed in 15 minutes with a single analytical run. Standard reference materials and authentic standards were evaluated to critically benchmark performance. Highly sensitive median limits of detection with 0.04 μM for >140 quantitatively assessed endogenous metabolites and 0.08 ng/mL for the >100 model xenobiotics were obtained. To prove the dual-column approach's applicability, real-life samples from sub-Saharan Africa (high exposure scenario) and Europe (low exposure scenario) were assessed in a targeted and non-targeted manner. Our LC-HRMS approach demonstrates the feasibility to quantitatively and simultaneously assess the endogenous metabolome and the chemical exposome for the high-throughput measurement of environmental drivers of disease.

INTRODUCTION

Since the 'exposome' first emerged as a new paradigm in environmental health describing the entity of all environmental exposures enclosing lifestyle factors throughout a human's lifespan (Wild 2005), its scope has further been expanded. In recent definitions, endogenous metabolites involved in biological responses (i.e. the endogenous metabolome) that have been triggered by external exposures are typically included (Miller et al. 2014; Rappaport et al. 2014).

Comprehensive liquid chromatography high resolution mass spectrometry (LC-HRMS)-based approaches hold the promise to more comprehensively elucidate the exposome in future exposome-wide association studies (ExWAS). A broad spectrum of small molecules with diverse chemical properties ranging from endogenous metabolites to environmental xenobiotics can be determined with this technique. External stressors including xenobiotics and environmental changes are measured at the same

time as phenotypical changes in response to these exposures. Thus, LC-HRMS is an ideal platform for developing more holistic methods to study the exposome (Vermeulen et al. 2020). Its applicability to investigate the impact of environmental toxicants on the endogenous metabolome has previously been showcased (Warth et al. 2017; Johnson et al. 2012). Metabolomics has been applied in large metabolome-wide association studies (MWAS) to investigate biological mechanisms of diseases, their diagnosis and treatment. Several studies succeeded in deriving biological effects from their data, although data interpretation remains a challenge (Garratt et al. 2018; Reinke et al. 2017; Ganna et al. 2014; Rhoades et al. 2017; Hu et al. 2021). The approach plays also an important role in biomarker discovery and personalized medicine (Jacob et al. 2019). However, the study of external stressors and complex environmental exposures is clearly less explored and constitutes the next frontier in the current era of omic-scale exposure measurement and systems toxicology.

Targeted multi-analyte methods are commonly used for human biomonitoring (HBM) of xenobiotics, although most approaches assess only a relatively limited number of different exposure markers or chemical classes (Prasain et al. 2010; Vela-Soria et al. 2011; Azzouz et al. 2016; de Oliveira et al. 2019; Kolatorova Sosvorova et al. 2017; Braun et al. 2018; Šarkanj et al. 2018). However, recent initiatives aim to expand the coverage of such multi-analyte and multi-class HBM methods to a larger range of xenobiotics as exemplified e.g. Jamnik et al. (2022) who simultaneously assessed more than eighty chemicals with known affinity to the estrogen receptor in relevant biological specimen (blood, urine and breast milk).

The vast physico-chemical diversity of xenobiotics implies also a widely varying toxicological effects of them on humans. The adverse impact of e.g. mycotoxins, a group of fungal food toxins, range from liver carcinogenicity (aflatoxins), nephrotoxicity (ochratoxin A), estrogenicity (zearalenone) to inhibition of protein synthesis and mitochondrial function (trichothecenes) (Marin et al. 2013). Xenoestrogens may have an immense impact on hormone homeostasis and endocrine disruption, especially in critical time windows, since they interfere with the endocrine system, partly even at extremely low concentrations (Xu et al. 2017; Sofie et al. 2014). Estrogenic chemicals occur for example naturally in plants (phytoestrogens) like genistein or daizein and synthetic estrogens

may be present in pharmaceuticals, insecticides and plasticizers (Paterni et al. 2017; Xu et al. 2017).

Similar to meaningful population-based metabolome research, also exposomics requires large-scale studies for exposome-wide association studies to draw reliable conclusions. The suggested mean sample size on male fertility was estimated to be 2700 men (Chung et al. 2019). Hence, high throughput methods are urgently needed as time is a limiting factor in large-scale epidemiological investigations. In the field of metabolomics, efforts to increase time efficiency are a current priority (Rampler et al. 2021; Liu et al. 2019). For example, the usefulness of a dual column approach to gain more information about the metabolome and lipidome within a short runtime was described by Schwaiger et al. (2019).

The combined and comprehensive measurement of the metabolome and the exposome is challenging as the concentrations of metabolites, drugs, food constituents and environmental contaminants span over estimated ten orders of magnitude and highly diverse classes of chemicals (Bloszies et al. 2018; Rappaport et al. 2014). Here, we present a rapid high-throughput workflow, combining the analysis of endogenous metabolites and multiple classes of xenobiotics in human urine and plasma. To cover polar compounds as well as the mostly non-polar xenobiotics, the approach utilizes a dual column approach with a reverse-phase (RP) and a hydrophilic interaction chromatography column (HILIC) being operated in parallel. To prove the power of the new method, the exposome coverage was evaluated based on more than 200 highly diverse analytes comprising endogenous metabolites and xenobiotics. The applicability to real-life samples was demonstrated by the analysis of urine samples of test sub-populations from Nigeria and Austria.

MATERIALS AND METHODS

Chemicals

A multi-analyte stock solution contained endogenous human metabolites (145 analytes) at 50 μM and xenobiotics including estrogenic compounds (106 analytes) at a concentration between 5 – 5000 ng/mL (median 100 ng/mL) and was prepared in ACN/water (50/50; v/v) (Figure S1). In the context of this paper the estrogens are evaluated together with the xenobiotic substances and mentioned accordingly. In addition, 15 different isotopically labelled standards of xenobiotics and a separate ^{13}C -labelled yeast extract (ISOtopic solutions, Vienna) were used as internal standards. A full list of all analytes is available in the Supporting Information (Table S1). A 24 h pooled urine sample obtained from a healthy female volunteer collected during one day after three days of a low xenoestrogen/polyphenol diet was chosen as model matrix in this study since urine is frequently used for assessing chemical exposure. Moreover, pooled human Li-Heparin plasma was acquired from Innovative Research (Novi, USA) as a second model matrix. Arylsulfatase/ β -glucuronidase from *Helix pomatia* was purchased from Sigma-Aldrich (Vienna, Austria). All materials were stored at -80°C prior to extraction. The concentrations of all analytes (xenoestrogens, mycotoxins and endogenous estrogens)

in the calibration standards (8 levels) are listed in the Supporting Information (Table S2). The remaining endogenous metabolites were present at concentrations between 0.001 μM - 10 μM at the same dilutions as the other analytes.

Samples

For the optimization of the eluent/column combination a solvent standard and a matrix-matched standard at a medium concentration range (Level 6; Table S2) were used. SRM1950 (Metabolites in Frozen Human Plasma) and SRM3672 (Organic Contaminants in Smoker's Urine) were purchased from the National Institute of Standards & Technology (NIST, Gaithersburg, USA). In addition, 24 h urine samples from a food intervention study performed in 2021 with four different individuals (2 female and 2 male) collected at three different timepoints (3 different days) were tested. For details kindly refer to Oesterle et al. (2022). Furthermore, urine samples from Nigerian women sampled in 2016 were investigated. This longitudinal sample set was already analyzed before on biomarkers of mycotoxin exposure (Braun et al. 2022), therefore not all samples from the original study were available due to limited sample volumes. The sample set included 77 spot urine specimens from four timepoints (morning and evening over two days) of 23 mothers. All samples were stored at -80°C until analysis.

Sample preparation

During the whole sample preparation procedure, the samples were kept on ice. At first 200 μL urine were mixed with 20 μL internal standard mix (Table S3) and 20 μL of the ^{13}C -labelled yeast metabolite extract. For the experiment to determine the best solvent/column combination no internal standard was used, therefore only 40 μL H₂O were used instead of the internal standard mix. The samples were then vortexed. Afterwards, the samples were mixed with 760 μL of extraction solvent (ACN:MeOH (1:1, v:v)). After thoroughly vortexing and sonication on ice (10 min), the samples were put on -20°C for 2 h and centrifuged at 18,000 x g and 4°C (10 min) and 960 μL of the supernatant was transferred to a new tube. Then, the samples were evaporated in a vacuum concentrator (Labconco). The residues were reconstituted in 192 μL solvent (ACN/ water, 50:50, v:v), vortexed and centrifuged at 4°C for 10 min. Finally, the supernatants were transferred to HPLC vials and stored at -80°C until analysis. Moreover, matrix matched calibration standards for urine and plasma were prepared by reconstituting matrix extracted according to the sample preparation protocol with respective solvent standard solutions. SRM3672 was additionally treated with a β -glucuronidase/arylsulfatase enzymes from *Helix pomatia* for 12 h at 37°C prior to extraction as the NIST certified reference values are given for deconjugated samples. This additional step was not performed for the other samples because the heat treatment would have disturbed measurements of endogenous metabolites. A non-deconjugated sample was prepared for the SRM material for comparison as well.

Quality control measures

As quality control samples, SRM 1950 in one to ten dilution and a solvent QC comprising all target analytes at 1 μM (metabolites) and

approximately 100 ng/mL (xenobiotics) were analyzed throughout the sequence. Moreover, separate pooled urine samples from the measured Nigerian and Austrian were repeatedly injected with a maximum of nine samples between the injection of the pooled urine samples to check the instrument performance. Solvent blanks (pure reconstitution solvent) and system blanks (200 μ L water extracted according to the sample preparation protocol) were measured to correct for contaminations in the system and during the sample preparation.

LC-HRMS(/MS) analysis

To optimize chromatographic separation for our highly diverse set of endogenous and exogenous analytes, a Vanquish Duo UHPLC system with two independent pumping systems and two different columns was used. Different column/eluent systems were examined. As reverse-phase column (RP), an Acquity HSS T3 (1.8 μ m, 100 x 2.1 mm) was used. For HILIC chromatography, two different hydrophilic interaction liquid chromatography columns (HILIC) were used, namely, a SeQuant[®]ZIC[®]-pHILIC (5 μ m, polymeric, 150 x 4.6 mm) and an Acquity BEH Amide (1.8 μ m, 100 x 2.1 mm) were tested. Eluent B was in all cases 100% ACN. The aqueous eluent (solvent A) was changed as stated in Table 1. The injection volume was 5 μ L for all columns and experiments.

For the RP measurements the gradient was as follows: 0 - 1 min, constant flow at 10% B; 1 - 10 min, increase to 70% B; 10 - 11 min, rise to 100% B and 13.5 - 15 min, equilibration at 10% B. A hydrophilic interaction liquid chromatography column (HILIC), SeQuant[®]ZIC[®]-pHILIC (5 μ m, polymeric, 150 x 4.6 mm) was operated with the following gradient: 0-1 min, constant flow at 75% B; 1-6 min, linear decrease to 50%; 6-7 min, drop to 30% B; 7-11 min, constant follow at 30%; 11-15 min, equilibration at 75% B. Both columns were at 40 °C and a flow rate of 0.3 mL/min was set. The Acquity BEH Amide was operated with a slightly different gradient as follows: 0-2 min, constant at 80% B; 2-8 min decrease to 40% B; 8-10 min, constant at 40% B and 10-15 min, equilibration at 80% B. Both capillaries were connected with a T-piece to mix the effluents before introduction into the ESI source of the mass

spectrometer (Figure 1A). As needle wash, 75% ACN was used for the HILIC measurement, while for the RP run H₂O:ACN:MeOH (2:1:1,v:v:v) was applied.

Measurements were conducted in fast polarity-switching full scan mode on a Q Exactive HF quadrupole-Orbitrap mass spectrometer. The settings of the ESI interface were as follows: sheath gas, 48 au; auxiliary gas, 11 au; sweep gas flow, 2 au; capillary voltage, 3.5 kV (positive), 2.8 kV (negative); capillary temperature, 260°C; auxiliary gas heater, 410°C. The scan range was from 65 to 900 m/z. For full scan only measurements the resolution was set to 60,000 with an AGC target (automatic gain control) of 1 x 10⁶ and a maximum injection time of 200 ms. The instrument was calibrated before the analysis.

Following the optimization of chromatographic conditions, the most suitable RP/HILIC combination was selected, consequently the above-mentioned parameters of combination two (Figure 1B) were applied for the sample measurement. A mixture of both effluents entered the mass spectrometer via the ESI source (Figure 1C). For analyses with data-dependent MS² a resolution of 60,000 with an AGC target of 1x10⁶ and a maximum injection time of 100 ms were chosen for the full scan. The settings for the MS² collection were the following: resolution, 30,000; AGC target, 1 x 10⁵; maximum injection time, 50 ms, loop count, 10; isolation window, 1.0 m/z; normalized collision energy, 30 eV; minimum AGC, 8x10³; dynamic exclusion, 4 s. Iterative exclusion lists were generated with IE-Omics (Koelmel et al. 2017). The urine samples from Nigeria and Austria were analyzed in randomized order.

Data Analysis

Skyline (version 20.2.0.286, (MacLean et al. 2010)) was used for targeted analysis and quantification. Internal standard correction was performed. If for the specific analyte no internal standard was included, the internal standard with the closest retention time was selected as surrogate standard for normalization (Table S7). The linear calibration curves (Table S7) were 1/x weighted. Matrix matched calibration for urine and plasma was performed and the

Table 1 Optimization design of the tested column/eluent systems for the dual approach

	Combination 1	Combination 2	Combination 3	Combination 4
RP				
Column	Acquity HSS T3			
Aqueous eluent	0.6 mM NH ₄ F in H ₂ O	0.3 mM NH ₄ F in H ₂ O	1 mM NH ₄ F in H ₂ O	0.6 mM NH ₄ F in H ₂ O
Organic eluent	ACN			
HILIC				
Column	SeQuant [®] ZIC [®] -pHILIC		Acquity BEH Amide	
Aqueous eluent	10 mM NH ₄ HCO ₃ (pH 9.2) in H ₂ O /ACN (9:1, v:v)	2 mM NH ₄ F in H ₂ O	1 mM NH ₄ F in H ₂ O	50 mM CH ₃ COONH ₄ (pH 6) in H ₂ O
Organic eluent	ACN			

corresponding calibration curves were used for quantification of xenobiotics. However, endogenous metabolites were, as expected, frequently highly abundant in the matrices, therefore solvent calibration was applied for endogenous metabolites (excluding estrogens). Limit of detections (LODs) were determined based on

the EURACHEM guideline (Ellison et al. 2012) as three-times the standard deviation of the multiple injection of a low-concentrated standard (n=6) divided by the square-root of the number of replicates. For the limit of quantification (LOQ) the tenfold standard deviation was used.

Spearman correlation was calculated for compounds positive in at least 20% of all Nigerian samples with R and plotted with the *corrplot* package (version 0.90) (Wei et al. 2017). For pathway analysis MetaboAnalyst 5.0 (Pang et al. 2021) was used. A hypergeometric test was selected as enrichment method and for topology analysis relative-betweenness centrality. The pathway library was *Homo sapiens* (KEGG).

The pooled Nigerian urine sample including MS2 data measured in negative and positive ionization mode with iterative exclusion lists (n=4) was used to screen for potential additional xenobiotics not covered by the targeted evaluation using authentic reference standards. Suspect screening was performed in R applying the

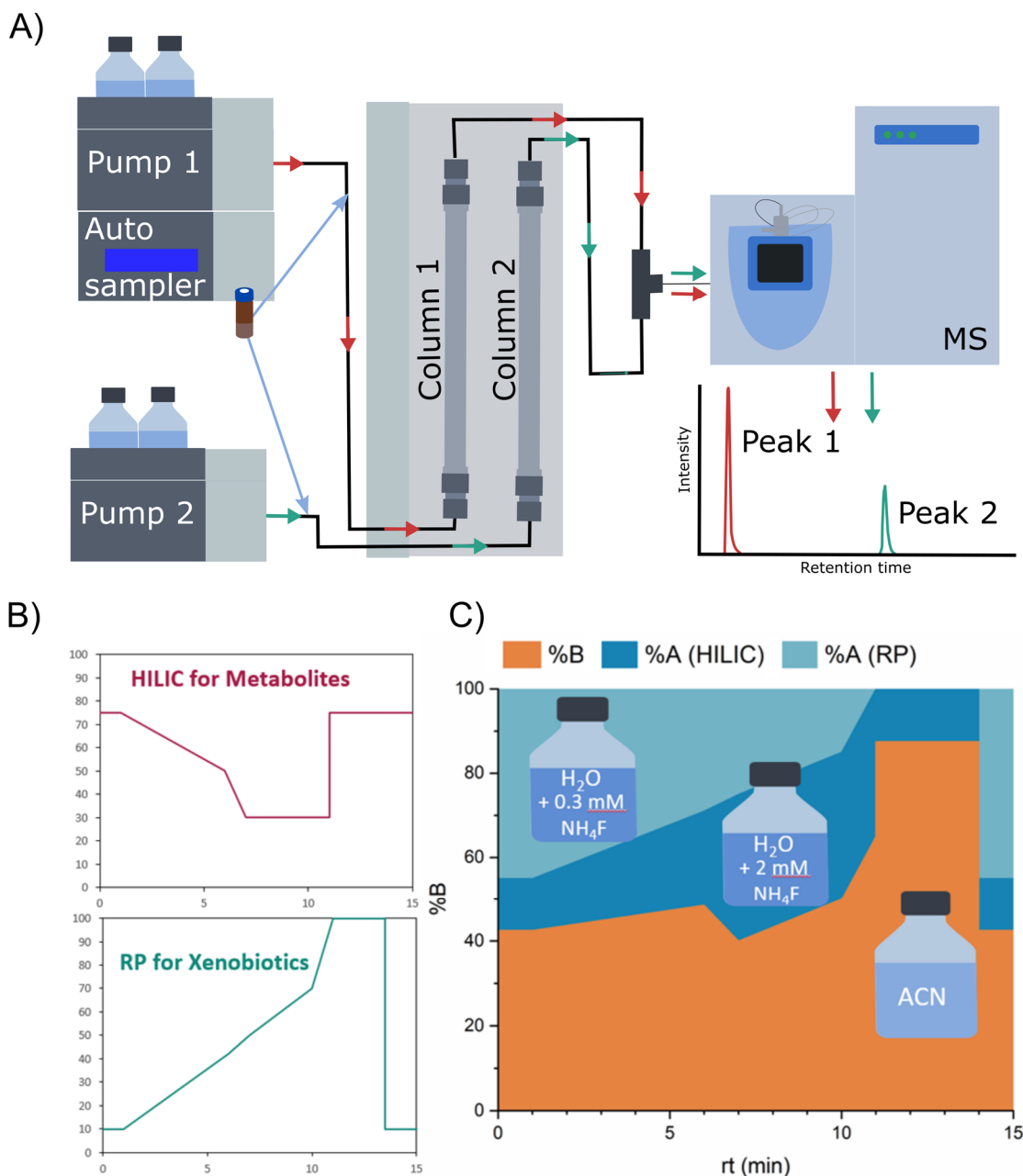


Figure 1 Dual column setup (A) LC-HRMS system comprising two separate LC-pumps and columns combined by a T-piece before entering the mass spectrometer. (B) Gradients of both individual columns. (C) Eluent composition entering the mass spectrometer after the effluents were mixed

patRoan package (Helmus et al. 2021). Solvent blanks (only in the corresponding polarity) were defined as blank measurements. The raw data files were converted to mzML-files and centroided with ProteoWizard (Chambers et al. 2012). For peak picking and grouping the “openms” algorithm was set with the following

parameters: noise threshold: 4E3, chromFWHM: 3, minFWHM: 1, maxFWHM: 30, chromSNR: 5 and mzPPM: 3. Only features with a minimum absolute feature intensity of 3E5, a minimum feature intensity above blank of 10, present in at least 60% of replicates were kept and blank analyses were removed after this step. A

suspect list from the ENTACT trial (Sobus et al. 2019) based on the EPA's ToxCast library including > 4000 substances was adopted for this experiment. Analytes which had already been included in the targeted list were removed to avoid redundancy. For the suspect screening a m/z window of 0.002 was set. MS peak list data was extracted with the mzr-algorithm (precursor m/z window: 0.5) and filtered (relative intensity threshold: 0.02, top 10 MS/MS peaks). Then molecular formulas were generated considering [M+H]⁺ and [M-H]⁻ adducts respectively and the elements C, H, N, O, P, S, Cl, Br using genform. Chemical compounds were annotated with metfrag and the comptox database. With annotateSuspects and the generated peak lists, formula and compound data the suspect screening results were refined. An identification level was assigned depending on the rank and scores (isoScore, individualMoNAScore) of formula/compound candidates roughly based on Schymanski et al. (2014). The default settings in the annotateSuspects algorithm were applied. As no retention time data was available, level one identifications were not possible. The other identification levels were: level 2a (good MS/MS library match, top ranked in compound results, individualMoNAScore ≥ 0.9, no MoNA library score for other candidates), level 3a (fair library match, individualMoNAScore ≥ 0.4), level 3b (known MS/MS match, at least three fragments match), level 3c (good in-silico MS/MS match, annotation MS/MS similarity (annSimComp) ≥ 0.7), level 3c (good formula MS/MS match, top ranked formula candidate, annSimForm ≥ 0.7, isotopic match (isoScore) ≥ 0.5, both scores at least 0.2 higher than next best ranked candidate), level 4b (good formula isotopic pattern match, top ranked formula candidate, isoScore ≥ 0.9, score at least 0.2 higher than next best ranked candidate) and level 5 (nothing of the above mentioned criteria match).

RESULTS & DISCUSSION

Establishing a dual column approach for combined exposure & effect analysis

Selection of columns and eluents

In optimization experiments different eluent-column combinations were tested for the best overall performance and compatibility. Only eluents with a basic (pH 9.2) to slightly acid pH (pH 6) were combined with NH₄F to avoid the formation of hydrofluoric acid. For a representative selection of selected compounds (25 metabolites on the HILIC column and 25 xenobiotics on the RP column) the averaged peak area (n=4-6) in a matrix-matched standard (urine) and a solvent standard both at a medium concentration level (level 6) were compared between the combinations (Figure 2 and Table S4). Peak areas were normalized to the best combination for each analyte to simplify comparison. Endogenous metabolites are naturally abundantly present in urine, therefore the peak areas in the standard-spiked urine were increased compared to the solvent standards. For xenobiotics, the observed signal was mostly decreased due to signal suppression in the urine matrix. The averaged peak areas of the selected

metabolites showed that the combination of 2 mM NH₄F/ACN on a SeQuant[®]ZIC[®]-pHILIC column (HILIC) and 0.3 mM NH₄F/ACN on an Acquity HSS T3 is favourable (highest peak area) in solvent. However, the difference to the three others is only minor with combination 2 reaching about 85% of the average peak area of combination 1. In urine, the average peak area of combination 4, which uses an Acquity BEH amide column instead of a SeQuant ZIC-pHILIC column, is only about half of the others. Except for combination 4, all eluent-column combinations performed similar, but with combination 2 and 3, both using NH₄F as additive, up to four metabolites (choline, phosphocreatinine, citric acid, 3-methylcytidine) were not detectable at the chosen concentration level, therefore the SeQuant ZIC pHILIC column with a basic NH₄CO₃ buffer based on Schwaiger et al. (2019) seemed to be the best choice regarding endogenous metabolites excluding estrogen hormones. When xenobiotics and endogenous estrogens were investigated, however the additive NH₄F clearly outperformed the basic buffer. The average peak area in urine and solvent of this group nearly doubled when NH₄F was used. Since xenobiotics are generally less concentrated than metabolites in real-life samples, we decided to use this additive to boost their sensitivity and finally selected the combination with 2 mM NH₄F as aqueous HILIC eluent and 0.3 mM NH₄F as aqueous RP column due to a better overall performance.

Long term stability of LC-MS setup

A solvent QC sample containing endogenous metabolites at 1 μM and xenobiotics at approximately 100 ng/mL was injected throughout the sequence (n=11) spanning over a period of 40 h. Only the most abundant ion species was considered. For endogenous metabolites the peak from the HILIC column and for xenobiotics the peak from the RP column was evaluated. At the chosen concentration level, 113 out of the 146 metabolites (77%) retained with a retention time bigger than 1 min on the HILIC column and 104 out of the 106 xenobiotics (98%) with retention on the RP column (retention time > 0.8 min) were detectable. Four analytes were not detectable even at higher levels, therefore the best ionization mode remains unclear. The relative standard deviation (RSD) was calculated for the peak area and the retention of all detectable molecules at this level (Figure 3A and 3B). The median RSD of the area was 21.7% and 31% in negative and positive ionisation mode, respectively. The difference between peaks from the HILIC and RP separation was minor, but in positive ionisation mode the relative standard deviation was bigger. Regarding retention time the median RSD was 0.4% for negative mode and 0.7% for positive mode. The xenobiotics' retention times were more stable with a median of 0.3% compared to 1.3% for the endogenous metabolites.

The recoveries ranged in solvent between 83% and 123% with an average of 104% for xenobiotics and 81% and 119% with an average

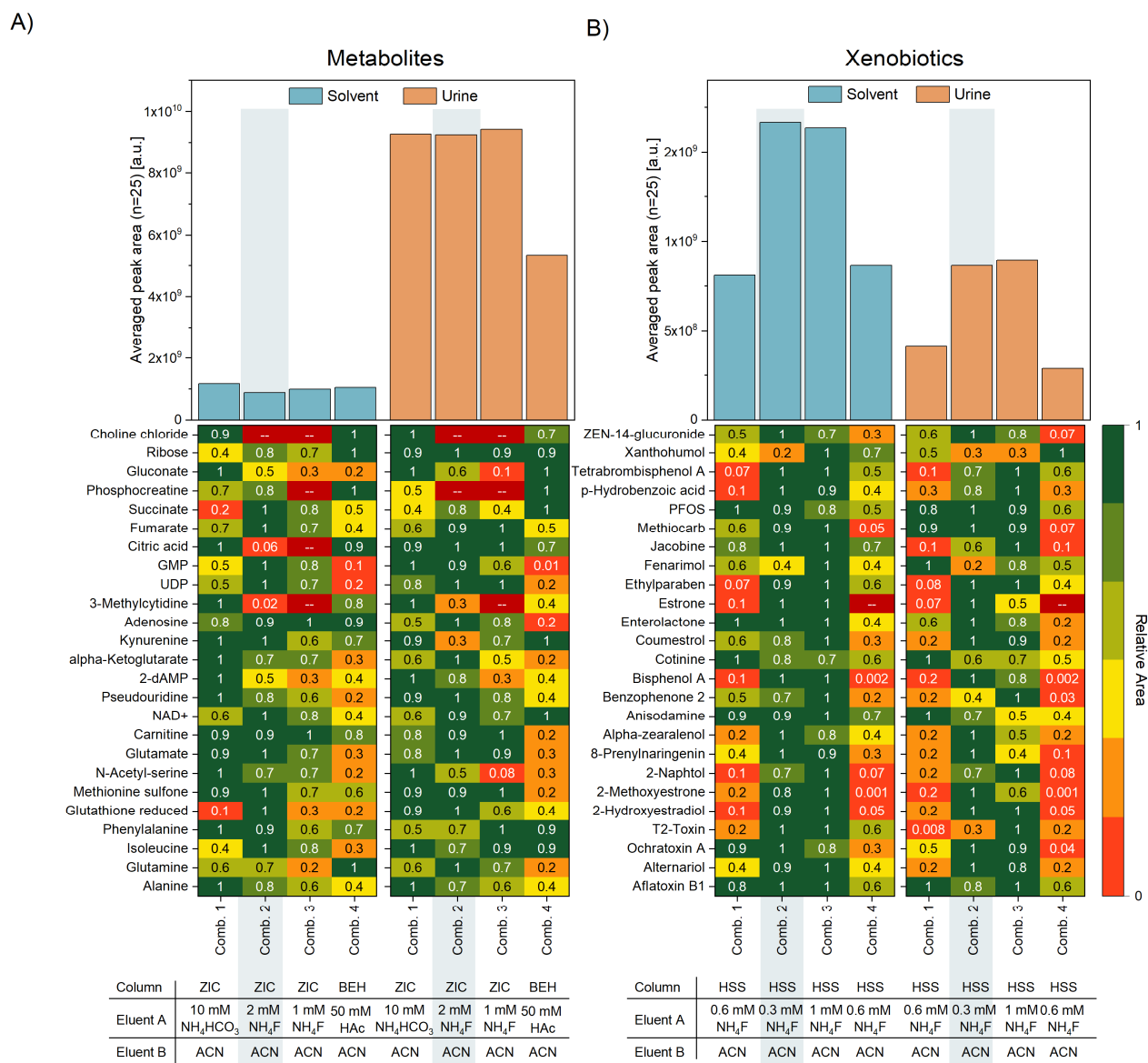


Figure 2 Comparison of the average peak areas of selected, representative endogenous metabolites (A) and xenobiotics including estrogen hormones (B) in solvent and urine including a detailed overview of the averaged peak areas (n=4-6) relative to the highest peak area of the individual molecule. The best combination is shaded in grey. Different columns, namely Acquity HSS T3 (HSS), SeQuant[®]ZIC[®]-pHILIC (ZIC), Acquity BEH Amide (BEH), and eluents, namely 0.3/0.6 /1/2 NH₄F in H₂O (0.3/0.6/1/2 mM NH₄F), 10 mM NH₄HCO₃ (pH 9.2) in H₂O/ACN (9:1, v:v) (10 mM NH₄HCO₃), 50 mM CH₃COONH₄ (pH 6) in H₂O (50 mM HAC) were tested

of 101% for endogenous metabolites (Table S19/Table S20). Furthermore, the extraction recoveries were evaluated in spiked urine and plasma samples. The median recovery of xenobiotics was 97% in urine and 103% in plasma whereas for metabolites these figures were determined to be 97% and 99%, respectively. Only 10% of the analytes in urine and 14% in plasma, had a recovery below 80%. The recoveries were above 120% for about 1% of compounds in urine and 3% in plasma. Several analytes, especially endogenous metabolites, were already present in high quantities

in the non-fortified urine and plasma, hence the extraction recovery was not estimated for all compounds.

Pooled quality control samples of both sample sets were measured several times throughout the measurement (Figure S2). The relative standard deviation of the retention time and the normalised peak area was calculated for highly diverse analytes. This included Bisphenol A (BPA), daidzein, enterodiol, glycitein, methylparaben and triclosan in the pooled urine of the Nigerian samples (n=9) and BPA, daidzein, nonylphenol and p-

hydroxybenzoic acid in the pooled urine of the Austrian samples (n=5). In addition, four metabolites (tryptophan, uracil, fumaric acid, gluconate) were investigated. The relative standard deviation of the retention time was < 1.5% for all analytes except fumaric acid (about 2.8%). The relative standard deviation of the normalised area was < 20% for all analytes except for BPA (22%), which was only at a concentration around the LOD in the Austrian pooled urine sample. The variation tended to be lower if the corresponding ¹³C-labelled compound was available for compound-specific internal

standardization (e.g. for methylparaben) as compared to surrogate internal standardization.

Quantification of reference material

The limits of detection for the xenobiotics ranged from 0.01 to 5.7 ng/mL with a median of 0.08 ng/mL in solvent (Table S5, Figure 4C). In matrix the median LOD increased to 0.7 (urine, Figure 4A) and 0.5 (plasma, Figure 4B) most likely due to matrix effects and matrix interferences. Phytoestrogens like daidzein

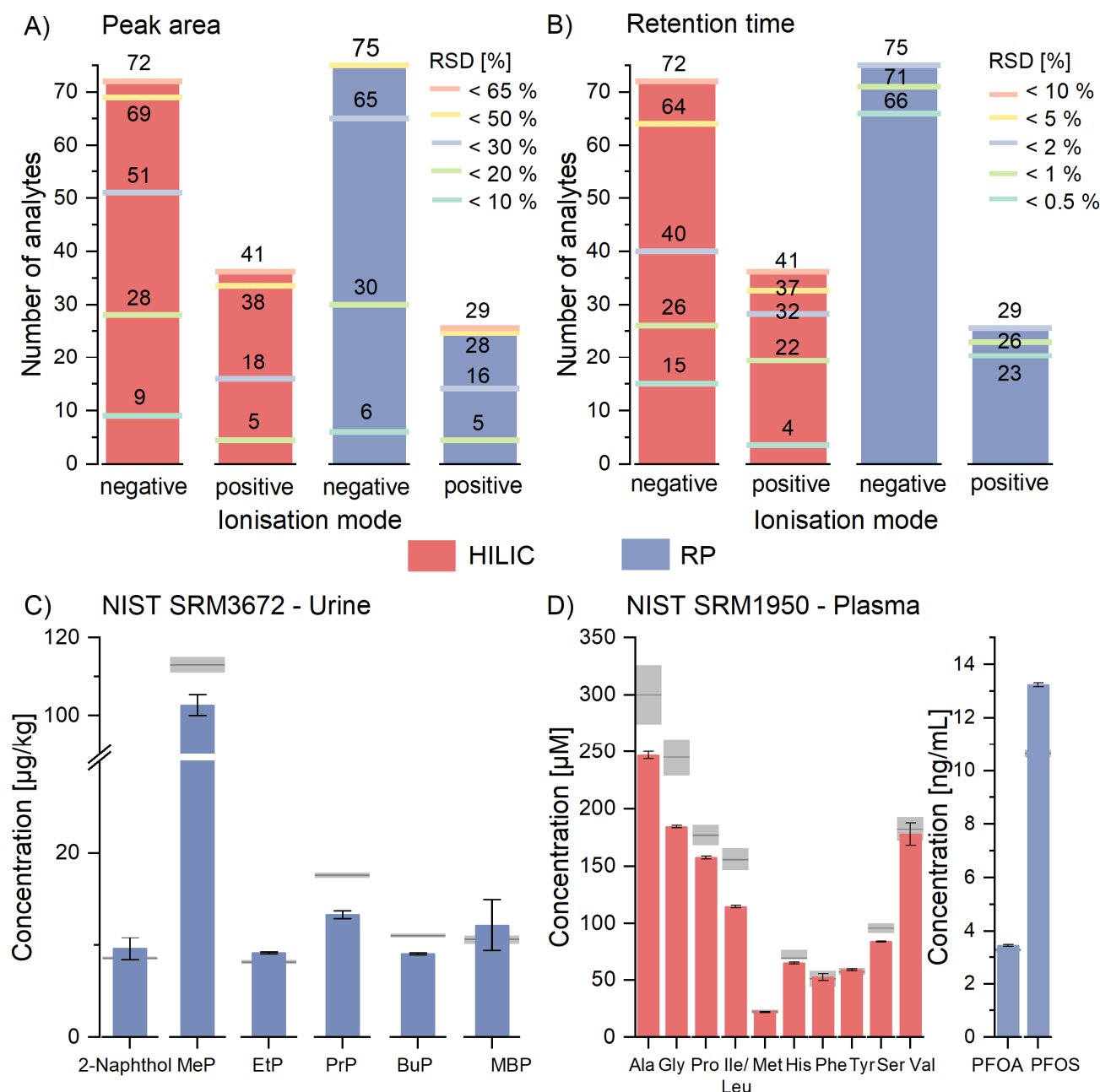


Figure 3 Repeatability and accuracy reported as the number of analytes within a certain relative standard deviation of A) peak area and B) retention time. The lines mark the thresholds and the labels indicated how many analytes fall below a respective RSD percentage. Only the most abundant ion species was considered on the respective column. C) Analytes reported in SRM3672 and D) in SRM1950 with the grey line indicating the certified reference value and the expanded uncertainty according to the certificate of analysis

and genistein and personal care product ingredients e.g., parabens exhibited the lowest LODs. The LODs were for most xenobiotics sufficient to detect them in averagely contaminated samples considering concentration levels from published human biomonitoring studies. For example, published paraben levels in urine exceed 100 ng/mL for methylparaben and 20 ng/mL for propylparaben in several human biomonitoring studies (Wei et al. 2021), which is more than 100-times the LOD value of the reported method. The analysis of bisphenol levels in U.S. urine samples showed levels of 0.4 -2 ng/mL BPA, 0.15-0.5 ng/mL BPF and <0.1-0.25 ng/mL BPS (Ye et al. 2015), making the detection of BPS and BPF difficult, but BPA was detected at a concentration above our method's LOD. Mycotoxins were reported to be present in Nigerian urine samples at an average concentration of 0.75 ng/mL (ZEN) and 0.06 ng/mL (AOH) (Šarkanj et al. 2018). The average levels of these mycotoxin were just slightly above our calculated LOD. However, these toxins would be detectable in medium to highly contaminated samples. For triclosan mean concentrations of 28.6 ng/mL were detected in urine from the USA, Greece, and Asian countries (Iyer et al. 2018). In Israeli urine the mean detected concentration was 28.9 ng/mL for monobutyl phthalate, 12 ng/mL for MEHP, 0.17 ng/mL for 1-OH pyrene, 26.9 ng/mL for genistein and 66.8 ng/mL for daidzein (Berman et al. 2013). Besides 1-OH-pyrene, the pesticide triclosan, plasticizers and phytoestrogens were reported in concentration ranges covered with our approach. The linear dynamic range was highly variable and depended on the molecule (Table S19). About 10% of the xenobiotics had a linear range spanning five orders of magnitude. Half of them covered a range of four, and approximately a third a range of three orders of magnitude in solvent. Matrix-matching resulted typically in a reduction of the dynamic range of about one order of magnitude due to matrix effects as the LOD of the xenobiotics in matrix was generally lower.

The solvent LOD of endogenous metabolites ranged from 0.001 μM to 6.6 μM with a median of 0.04 μM (Table S6, Figure 4D). The LOD values were estimated for 134 analytes including several jointly evaluated isomers. The LOD of several endogenous metabolites was not estimated in the human matrices due to their high natural abundance. About one third of all compounds showed LODs < 0.01 μM and about two thirds < 0.1 μM allowing for the straight-forward (semi-) quantitative assessment of the metabolome in most biological systems. The reference standards spanned five orders of magnitude from 0.001 μM to 10 μM . However, most metabolites were not detectable at the lower calibration level (0.001 μM – 0.01 μM) limiting the linear dynamic range to four (45%), three (29%) or even less (8%) orders of magnitude (Table S20).

Limitations

Out of the 146 endogenous metabolites present in the standard mix, five (1-methylnicotinamide, thiamine, choline, spermine and

spermidine) were not detectable even at the highest concentration level (10 μM). Isomers were not separated in some cases. These included 2-/3-phosphoglyceric acid, citric /isocitric acid, homoserine/threonine and isoguanosine/guanosine. The hexoses fructose, galactose, mannose, glucose and inositol were not distinguishable as well as their phosphates (fructose-6-phosphate, glucose-1-phosphate and glucose-6-phosphate) as they were co-eluting and therefore the peaks were not baseline separated. Pentose-phosphates, ribose-5-phosphate and ribulose-5-phosphate were not baseline separated, too. For arginine and palmitic acid no satisfactory linear regression was possible most likely due to severe carry-over effects.

Six analytes for which certified reference values are available in SRM3672 (Organic Contaminants in Smoker's Urine) were detected and quantified (Table S13). As the values stated in the certificate were total analyte concentrations after hydrolysis, β -glucuronidase/arylsulfatase-treated reference urine was analyzed. The relative error compared to the reference value was < 20% for all of these (Figure 3C). 1-OH-pyrene and MEHP were not detected, although they are present in the smokers' urine due to their low concentration below the method's quantification limits. Besides several amino acids, PFOA and PFOS were quantified in SRM1950 (Metabolites in Frozen Human Plasma) and compared to the certificate (Figure 3D, Table S14). Threonine was not evaluated as it coeluted with homoserine and therefore only a combined value for both amino acids was available. Isoleucine and leucine were not baseline separated as well, but for both molecules reference values were given, therefore the sum of both concentrations was compared. The relative error was < 26% for all amino acids, whereby the recoveries were in general lower for the high abundance amino acids (glycine (75%), alanine (82%), isoleucine/leucine (74%)), possibly due to saturation effects as the values were outside of the calibration range (Figure 3D). The samples were injected undiluted to ensure a high detectability of low-concentrated xenobiotics despite possible saturation issues for the endogenous metabolites at higher concentrations. The relative errors of PFOA and PFOS were even < 5% and < 20%, respectively. In general, the determined values were in good agreement with the reference values of both SRMs especially given the extremely broad scope of the new workflow with recoveries ranging from 74% to 124% in SRM1950 and recoveries between 81% and 115% in SRM3672 (Figure 3C). These recoveries are similar to values reported in literature for SRM3672 by Karthikraj et al. (2020) (80.5% - 105%) and Zhu et al. (2021) (80 – 111%).

In the reference materials, several additional metabolites and xenobiotics were quantified (Figure S3, Table S16). In SRM3672, 18 xenobiotics and two estrogens were detected. SRM1950 was contaminated with 17 xenobiotics with nine of them being detected in both reference materials including personal care

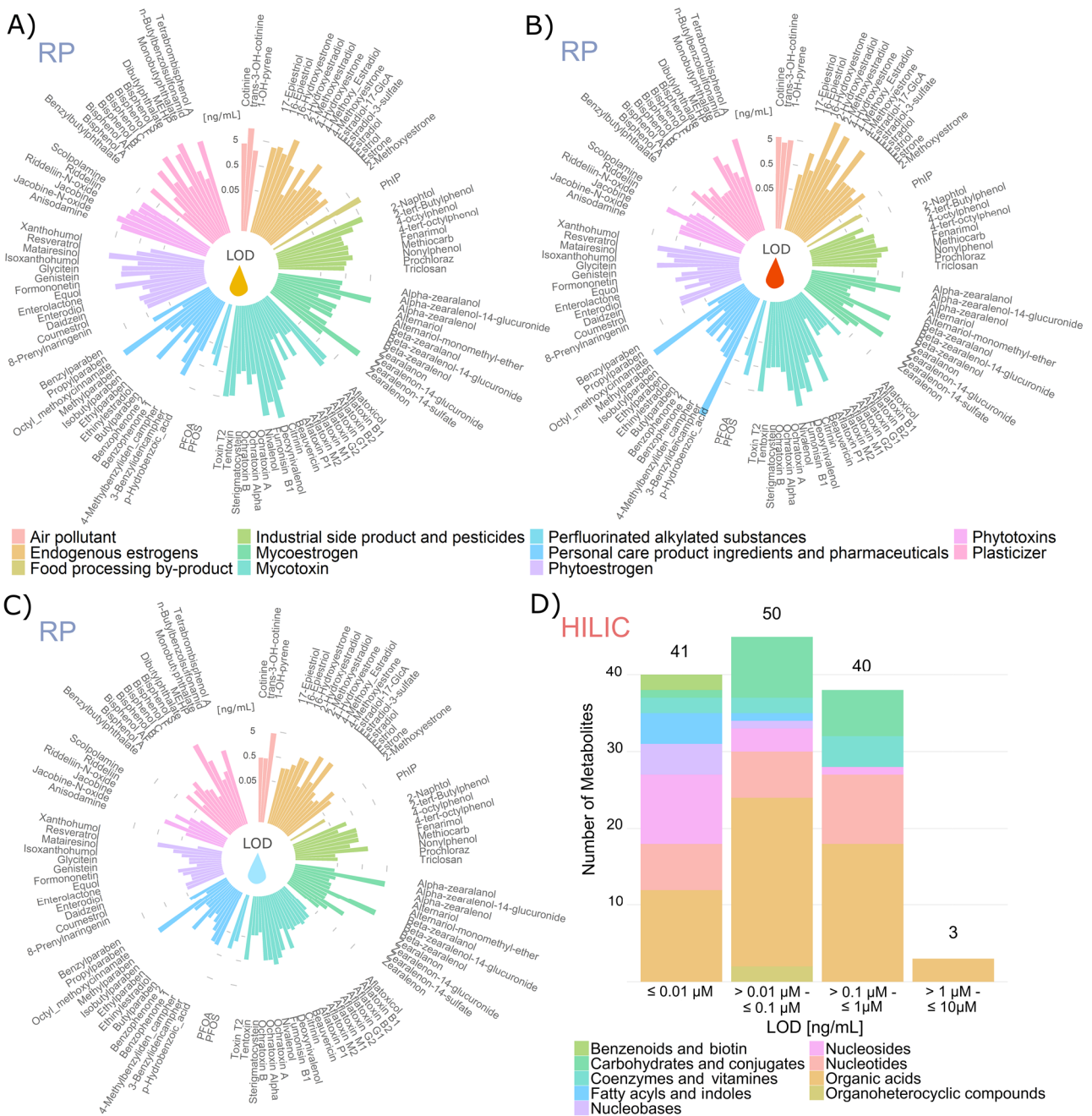


Figure 4 Limit of detection (LOD) of representative xenobiotics and estrogens in urine (A), plasma (B) and neat solvent (C) sorted by compound classification. The values were plotted on a logarithmic scale. D) Number of endogenous metabolites in a specific LOD range. The colour indicates the category to which the analytes can be classified to

product ingredients (methylparaben, propylparaben, p-hydroxybenzoic acid, benzophenone-1), phytoestrogens (genistein, daidzein), smoking markers (cotinine, trans-3-OH-cotinine) and an industrial side product (2-naphthol). In SRM3672 additional phytoestrogens (e.g. enterolactone, enterodiol, daidzein, glycitein), a plasticizer (mono butyl phthalate) and butylparaben were observed, whereas in SRM1950 scopolamine, a phytotoxin, perfluorinated substances (PFOA, PFOS), industrial side products (nonylphenol, 4-tert-octylphenol) and other plasticizers (BPS, BPA) were found. The quantified metabolome comprised 48 (SRM1950)

and 61 (SRM3672) additional compounds, respectively. Smoker's urine was not enzyme treated for the evaluation. Mainly amino acids, nucleobases and nucleosides were quantified in these samples. The concentrations ranged over four orders of magnitude for metabolites in the urine plasma reference material. When expanding to exogenic contaminants this range spanned even over six orders of magnitude. In the urine reference material concentrations were less variable covering three orders of magnitude.

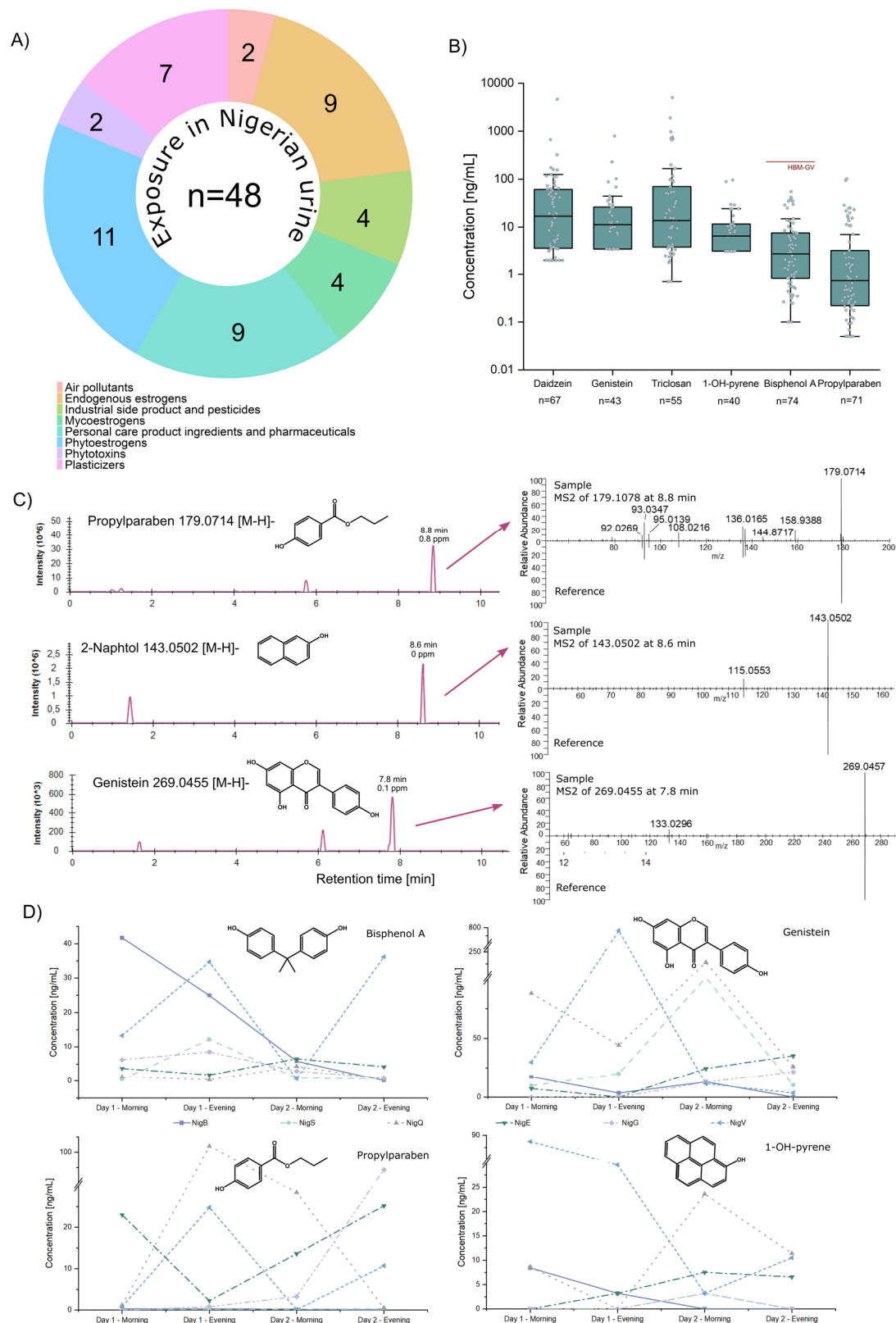


Figure 5 Detection of xenobiotics in Nigerian samples. A) Variety of observed xenobiotics and their classification. B) Individual concentrations of selected analytes that have been detected in > 50% of the samples (n=77). The human biomonitoring (HBM) guidance value (Ougier et al. 2021) was added in red. C) Extracted ion chromatograms (XICs) of selected analytes including corresponding MS2 spectra of experimental samples and authentic reference standards. D) Variation of analyte concentration in six individuals for selected xenobiotics demonstrate severe exposure dynamics and the need for longitudinal sampling design

Application in biomonitoring studies from Europe and Sub-Saharan Africa

The established analysis pipeline was applied in proof-of-principle studies of two different urine sample sets from geographically different areas, Austria and Nigeria. Both studies included several individuals (Austria (4) and Nigeria (23)), who donated samples at four different time points. In the Austrian samples 17 different xenobiotics belonging to four compound categories were identified (Figure S5A/B, Table S10). Most exposures were either personal care product ingredients or phytoestrogens. The Nigerian urine samples were contaminated with more than twice as many chemicals ($n=48$) coming from diverse sources (Figure 5A, Table S9), but personal care product ingredients and phytoestrogens were still the dominant classes. Concentrations covered five orders of magnitude from the sub-ppb to the ppm range. The Nigerian samples were contaminated with a wider diversity of chemicals including air pollutants (1-OH-pyrene), mycoestrogens (ZEN, AME) and industrial side products (2-naphthol) and higher concentration levels. In particular the maximum values were frequently 10-100-times higher compared to the Austrian samples. However, especially the Austrian dataset was small and homogenous, therefore the available data is not sufficiently representative to estimate population-wide exposure levels. The Austrian samples were considered as low-exposure scenario, whereas the Nigerian samples were regarded as high-exposure samples as often food/environmental safety regulations are lacking or not adequately enforced. Each detected xenobiotic was on average detected in 31 out of 77 Nigerian samples. Four analytes (enterolactone, BPA, nonylphenol and propylparaben) were present in > 90% of all samples (Figure 5B). In the Austrian samples, two thirds were contaminated with daidzein, 4-tert-octylphenol, BPA and propylparaben, besides the in all samples detected nonylphenol and dibutyl phthalate. MS2 spectra further supported identification (Figure 5C), although for all analytes discovered here reference standards were used for retention time confirmation. The number and level of the detected phytoestrogens was restricted due to the regulated diet with no vegetable and fruit intake except for a smoothie on day 2 before the Austrian study and on the first two study days. Approximately 70 diverse endogenous metabolites were quantified in the urine samples of both studies (Table S11, Table S12). Thirteen individuals completed the full longitudinal sampling with four timepoints. The variation over the timeframe of two days is exemplary depicted for six individuals and analytes of distinct origin including the plasticizer bisphenol A, the phytoestrogen genistein, the personal care product ingredient propylparaben and the air pollutant 1-OH-pyrene in Figure 5D. The concentrations spanned over three orders of magnitude within the sample individual. Genistein and propylparaben differed vastly between the timepoints in particular. The intraindividual variation was like the interindividual variation demonstrating the importance of longitudinal sampling for exposure assessment for several participants. The diversity and high dynamic of the exposome even within the same individual was described previously (Jiang et al. 2018) and further supports the need for time-resolved testing to capture dynamic exposure in spot urine samples or 24 h urine.

To showcase the power of our approach for investigating the impact of exogenous exposures on the endogenous metabolite, a

spearman correlation matrix was created. Various significant correlations between xenobiotics but also xenobiotics and metabolites were demonstrated (Figure S4). Mainly analytes which were detected in a multitude of samples, e.g., mono butyl phthalate, ethyl paraben, MEHP, benzophenone and enterolactone, yielded significant correlations, probably due to the higher statistical power. High correlation coefficients were observed for monobutyl phthalate and MEHP (0.72), ethyl paraben and p-hydroxybenzoic acid (0.64), benzophenone-1 and enterolactone (0.74), and propylparaben and methylparaben (0.59). MEHP and monobutyl phthalate are both urinary biomarkers of phthalate exposure with estrogenic potential (Wenzel et al. 2018). The preservatives ethyl paraben and p-hydroxybenzoic acid were likely to be an ingredient in the same type of personal care products and also methylparaben and ethyl paraben may be present in similar products. Enterolactone, a biotransformation product of plant lignans originating from e.g. flaxseeds and sesame (Axelson et al. 1982), and the urinary biotransformation product of benzophenone-3, benzophenone-1, a UV-filter used in cosmetics (Kang et al. 2019), clearly have different sources. However, both are hormonally active and have a shared mechanism concerning obesity antagonism. This was demonstrated to be associated with late on-set of puberty in girls (Wolff et al. 2015).

The link between external exposures and the ensuing disturbance of the internal metabolome is one step to elucidate disease development, which is part of the broad scope of exposome research. With our approach connections between xenobiotics and metabolites were indicated. A strong correlation between ethyl paraben and the carboxylic acids fumaric acid (0.68) and malic acid (0.67) and the amino acid alanine (0.62) were uncovered. Alanine (0.64), fumaric acid (0.63) and malic acid (0.6) were connected to benzophenone-1, too. The matrix also strongly correlated mono butyl phthalate and aspartic acid (0.66).

Phthalate exposure was associated with altered carnitine levels and changes in metabolites associated with amino acid metabolism in urine of Chinese men (Zhang et al. 2016). In our study, carnitine, propionylcarnitine and several amino acids were correlated with mono butyl phthalate, too. Pathway analysis was performed for significantly correlated metabolites with mono butyl phthalate (Figure S6). The results revealed a strong impact on the alanine, aspartate and glutamate metabolism, the arginine biosynthesis, and the citrate cycle. The pathway analysis of with ethyl paraben associated metabolites exposed similar results with arginine biosynthesis and alanine, aspartate and glutamate metabolism being the most impacted pathways (Figure S7). These two pathways were also the most affected among with benzophenone-1 correlated metabolites (Figure S8). The xenobiotics benzophenone-1, mono butyl phthalate and ethyl paraben had at least a moderate correlation (correlation coefficient between 0.5 and 0.64) among each other, therefore the disturbance in amino acid metabolism might not be triggered by a single compound but rather by a mixture of different chemicals.

Recent studies demonstrated the feasibility of exposome-wide association studies (ExWAS), e.g. extensive effect biomarker and biomarker discovery of air pollutant exposure (Tang et al. 2021) and linking metabolic profiling and exposure to perfluoroalkyl

substances (Alderete et al. 2019). However, to capture the metabolome and the chemical exposome several independent measurements were required, increasing the measurement time compared to our 15 min LC-HRMS/MS run covering both polar metabolites and the primarily apolar xenobiotics. Especially molecules with a high vapor pressure and low boiling/melting point were not accessible with LC-MS technology, therefore GC-MS would need to be integrated to further extend coverage (Ulrich et al. 2019; Hu et al. 2019). Although our fast LC-MS approach might be advantageous regarding run time, the vast concentration difference between endogenous metabolites and environmental contaminants (Bloszies et al. 2018) hamper their simultaneous measurement as several endogenous metabolites were close to the detector saturation and low abundant xenobiotics still need higher sensitivity. In particular, quantification posed a challenge, as calibration ranges were partially exceeded. Internal standard correction eased linearity issues especially at high concentrations.

Suspect screening in biological samples obtained from Nigerian women

To demonstrate the workflow's suitability for suspect and non-targeted screening/analysis (NTS/NTA), raw data from four pooled Nigerian urine samples with iterative MS2 exclusion lists were processed for suspect screening. On average 14,126 and 18,408 features were picked in each sample in negative mode and positive mode, respectively. 16,288 negative features in 4,590 groups remained after removal of features present in the blank and application of an intensity and replicate abundance filter. In positive ionization mode 21,384 features in 5,937 groups remained after filtering. Features were included if they were present in at least 3 out of 4 replicates, therefore the feature number after the application of the filter was higher than in the individual sample. For 706 (positive) and 749 (negative) peaks a match with the suspect list was found. The suspect list contained several isomers, therefore in some cases various molecules were suggested as annotation. Altogether, 1,238 different compounds, partly observed in both ionization modes, were proposed as potential annotations for the feature groups. Identification levels 1-4 were established for 52% (370) and 58% (435) in positive and negative ionization mode, respectively (Table S17 and Table S18). MS2 matches (level $\geq 3c$) were obtained for 187 (positive mode) and 190 (negative mode) feature groups. The annotation of 377 feature groups in both ionization modes with an identification level of at least 3c was successful, consequently showcasing the workflow's ability to not only detect analytes with available reference standard, but also to capture additional compounds potentially present in the samples.

CONCLUSION

The presented workflow facilitates the rapid and simultaneous exploration of complex environmental exposures and their effect on the human metabolome. Despite issues due to the wide concentration range, the quantification of several endogenous metabolites and exogenous chemicals acquired simultaneously in one short LC-MS/MS run succeeded and correlations between metabolites and chemicals were revealed. Consequently, the effect of certain exposures on the metabolome were directly derived from exposure data in a so far unique way. Combining two columns

and both ionization modes in one single datafile drastically decreased measurement time and simplified data evaluation and storage requirements. For the deciphering of the exposome hundreds to thousands of samples will be needed to be analyzed, therefore the reduced analysis time opens up for so far unseen throughput in exposome-wide association studies for drawing reliable conclusions on the impact of environmental factors on disease development.

ACKNOWLEDGMENTS

We greatly appreciate the volunteers for donating urine samples and the members of the Warth and Koellensperger labs for critical advice and feedback. We would like to thank the Mass Spectrometry Centre (MSC) of Faculty of Chemistry at the University of Vienna for technical support. This study was financed by the University of Vienna and supported by the ESFRI Research Infrastructure EIRENE.

CONFLICT OF INTEREST

The authors declare that there are no conflicts of interest.

AUTHOR INFORMATION

Corresponding Author

*benedikt.warth@univie.ac.at; +43 664 60277 70806

REFERENCES

- Alderete, T.L., R. Jin, D.I. Walker, D. Valvi, Z. Chen, D.P. Jones, C. Peng, F.D. Gilliland, K. Berhane, D.V. Conti, M.I. Goran, and L. Chatzi. 2019. 'Perfluoroalkyl substances, metabolomic profiling, and alterations in glucose homeostasis among overweight and obese Hispanic children: A proof-of-concept analysis', *Environment International*, 126: 445-53.
- Axelsson, M., J. Sjövall, B.E. Gustafsson, and K.D.R. Setchell. 1982. 'Origin of lignans in mammals and identification of a precursor from plants', *Nature*, 298: 659-60.
- Azzouz, A., A.J. Rascón, and E. Ballesteros. 2016. 'Simultaneous determination of parabens, alkylphenols, phenylphenols, bisphenol A and triclosan in human urine, blood and breast milk by continuous solid-phase extraction and gas chromatography-mass spectrometry', *Journal of Pharmaceutical and Biomedical Analysis*, 119: 16-26.
- Berman, T., R. Goldsmith, T. Göen, J. Spungen, L. Novack, H. Levine, Y. Amitai, T. Shohat, and I. Grotto. 2013. 'Urinary concentrations of environmental contaminants and phytoestrogens in adults in Israel', *Environment International*, 59: 478-84.
- Bloszies, C.S., and O. Fiehn. 2018. 'Using untargeted metabolomics for detecting exposome compounds', *Current Opinion in Toxicology*, 8: 87-92.
- Braun, D., W.A. Abia, B. Šarkanj, M. Sulyok, T. Waldhoer, A.C. Erber, R. Krska, P.C. Turner, D. Marko, C.N. Ezekiel, and B. Warth. 2022. 'Mycotoxin-mixture assessment in mother-infant pairs in Nigeria: From mothers' meal to infants' urine', *Chemosphere*, 287: 132226.
- Braun, D., C.N. Ezekiel, W.A. Abia, L. Wisgrill, G.H. Degen, P.C. Turner, D. Marko, and B. Warth. 2018. 'Monitoring Early Life Mycotoxin Exposures via LC-MS/MS Breast Milk Analysis', *Analytical Chemistry*, 90: 14569-77.
- Chambers, M.C., B. Maclean, R. Burke, D. Amodei, D.L. Ruderman, S. Neumann, L. Gatto, B. Fischer, B. Pratt, J. Egertson, K. Hoff, D. Kessner, N. Tasman, N. Shulman, B. Frewen, T.A. Baker, M.-Y. Brusniak, C. Paulse, D. Creasy, L. Flashner, K. Kani, C. Moulding, S.L. Seymour, L.M. Nuwaysir, B. Lefebvre, F. Kuhlmann, J. Roark, P. Rainer, S. Detlev, T. Hemenway, A. Huhmer, J. Langridge, B. Connolly, T. Chadick, K. Holly, J. Eckels, E.W. Deutsch, R.L. Moritz, J.E. Katz, D.B. Agus, M. MacCoss, D.L. Tabb, and P. Mallick. 2012. 'A cross-platform toolkit for mass spectrometry and proteomics', *Nature Biotechnology*, 30: 918-20.
- Chung, M.K., G.M. Buck Louis, K. Kannan, and C.J. Patel. 2019. 'Exposome-wide association study of semen quality: Systematic discovery of endocrine disrupting chemical biomarkers in fertility require large sample sizes', *Environment International*, 125: 505-14.
- de Oliveira, M.L., B.A. Rocha, V.C.d.O. Souza, and F. Barbosa. 2019. 'Determination of 17 potential endocrine-disrupting chemicals in human saliva by dispersive liquid-liquid microextraction and liquid chromatography-tandem mass spectrometry', *Talanta*, 196: 271-76.
- Ellison, S.L.R., and A. William. 2012. 'EURACHEM/CITAC Guide CG 4-Quantifying Uncertainty in Analytical Measurement', Third Edition.
- Ganna, A., S. Salihovic, J. Sundström, C.D. Broeckling, Å.K. Hedman, P.K.E. Magnusson, N.L. Pedersen, A. Larsson, A. Siegbahn, M. Zilmer, J. Prenni, J. Ärnlöv, L. Lind, T. Fall, and E. Ingelsson. 2014. 'Large-scale Metabolomic Profiling Identifies Novel Biomarkers for Incident Coronary Heart Disease', *PLoS Genetics*, 10: e1004801.

- Garratt, M., K.A. Lagerborg, Y.-M. Tsai, A. Galecki, M. Jain, and R.A. Miller. 2018. 'Male lifespan extension with 17- α estradiol is linked to a sex-specific metabolomic response modulated by gonadal hormones in mice', *Aging Cell*, 17: e12786.
- Helmus, R., T.L. ter Laak, A.P. van Wezel, P. de Voogt, and E.L. Schymanski. 2021. 'patRoom: open source software platform for environmental mass spectrometry based non-target screening', *Journal of Cheminformatics*, 13: 1.
- Hu, X., D.I. Walker, Y. Liang, M.R. Smith, M.L. Orr, B.D. Juran, C. Ma, K. Uppal, M. Koval, G.S. Martin, D.C. Neujahr, C.J. Marsit, Y.-M. Go, K.D. Pennell, G.W. Miller, K.N. Lazaridis, and D.P. Jones. 2021. 'A scalable workflow to characterize the human exposome', *Nature Communications*, 12: 5575.
- Hu, Y., B. Cai, and T. Huan. 2019. 'Enhancing Metabolome Coverage in Data-Dependent LC-MS/MS Analysis through an Integrated Feature Extraction Strategy', *Analytical Chemistry*.
- Iyer, A.P., J. Xue, M. Honda, M. Robinson, T.A. Kumosani, K. Abulnaja, and K. Kannan. 2018. 'Urinary levels of triclosan and triclocarban in several Asian countries, Greece and the USA: Association with oxidative stress', *Environmental Research*, 160: 91-96.
- Jacob, M., A.L. Lopata, M. Dasouki, and A.M. Abdel Rahman. 2019. 'Metabolomics toward personalized medicine', *Mass Spectrometry Reviews*, 38: 221-38.
- Jamnik, T., M. Flasch, D. Braun, Y. Fareed, D. Wasinger, D. Seki, D. Berry, A. Berger, L. Wisgrill, and B. Warth. 2022. 'Next-generation biomonitoring of the early-life chemical exposome in neonatal and infant development', *ChemRxiv*, Cambridge: Cambridge Open Engage.
- Jiang, C., X. Wang, X. Li, J. Inlora, T. Wang, Q. Liu, and M. Snyder. 2018. 'Dynamic Human Environmental Exposome Revealed by Longitudinal Personal Monitoring', *Cell*, 175: 277-91.e31.
- Johnson, C.H., A.D. Patterson, J.R. Idle, and F.J. Gonzalez. 2012. 'Xenobiotic Metabolomics: Major Impact on the Metabolome', *Annual Review of Pharmacology and Toxicology*, 52: 37-56.
- Kang, H., S. Kim, G. Lee, I. Lee, J.P. Lee, J. Lee, H. Park, H.-B. Moon, J. Park, S. Kim, G. Choi, and K. Choi. 2019. 'Urinary metabolites of dibutyl phthalate and benzophenone-3 are potential chemical risk factors of chronic kidney function markers among healthy women', *Environment International*, 124: 354-60.
- Karthikraj, R., S. Lee, and K. Kannan. 2020. 'Biomonitoring of exposure to bisphenols, benzophenones, triclosan, and triclocarban in pet dogs and cats', *Environmental Research*, 180: 108821.
- Koelmel, J.P., N.M. Kroeger, E.L. Gill, C.Z. Ulmer, J.A. Bowden, R.E. Patterson, R.A. Yost, and T.J. Garrett. 2017. 'Expanding lipidome coverage using LC-MS/MS data-dependent acquisition with automated exclusion list generation', *Journal of the American Society for Mass Spectrometry*, 28: 908-17.
- Kolatorova Sosvorova, L., T. Chlupacova, J. Vitku, M. Vlk, J. Heracek, L. Starka, D. Saman, M. Simkova, and R. Hampl. 2017. 'Determination of selected bisphenols, parabens and estrogens in human plasma using LC-MS/MS', *Talanta*, 174: 21-28.
- Liu, X., L. Zhou, X. Shi, and G. Xu. 2019. 'New advances in analytical methods for mass spectrometry-based large-scale metabolomics study', *TRAC Trends in Analytical Chemistry*, 121: 115665.
- MacLean, B., D.M. Tomazela, N. Shulman, M. Chambers, G.L. Finney, B. Frewen, R. Kern, D.L. Tabb, D.C. Liebler, and M.J. MacCoss. 2010. 'Skyline: an open source document editor for creating and analyzing targeted proteomics experiments', *Bioinformatics (Oxford, England)*, 26: 966-68.
- Marin, S., A.J. Ramos, G. Cano-Sancho, and V. Sanchis. 2013. 'Mycotoxins: Occurrence, toxicology, and exposure assessment', *Food and Chemical Toxicology*, 60: 218-37.
- Miller, G.W., and D.P. Jones. 2014. 'The Nature of Nurture: Refining the Definition of the Exposome', *Toxicological Sciences*, 137: 1-2.
- Ougier, E., F. Zeman, J.-P. Antignac, C. Rousselle, R. Lange, M. Kolossa-Gehring, and P. Apel. 2021. 'Human biomonitoring initiative (HBM4EU): Human biomonitoring guidance values (HBM-GVs) derived for bisphenol A', *Environment International*, 154: 106563.
- Pang, Z., J. Chong, G. Zhou, D.A. de Lima Morais, L. Chang, M. Barrette, C. Gauthier, P.-É. Jacques, S. Li, and J. Xia. 2021. 'MetaboAnalyst 5.0: narrowing the gap between raw spectra and functional insights', *Nucleic Acids Research*, 49: W388-W96.
- Paterni, I., C. Granchi, and F. Minutolo. 2017. 'Risks and benefits related to alimentary exposure to xenoestrogens', *Critical Reviews in Food Science and Nutrition*, 57: 3384-404.
- Prasain, J.K., A. Arabshahi, D.R. Moore, 2nd, G.A. Greendale, J.M. Wyss, and S. Barnes. 2010. 'Simultaneous determination of 11 phytoestrogens in human serum using a 2 min liquid chromatography/tandem mass spectrometry method', *Journal of chromatography. B, Analytical technologies in the biomedical and life sciences*, 878: 994-1002.
- Rampl, E., Y.E. Abiead, H. Schoeny, M. Ruz, F. Hildebrand, V. Fitz, and G. Koellensperger. 2021. 'Recurrent Topics in Mass Spectrometry-Based Metabolomics and Lipidomics—Standardization, Coverage, and Throughput', *Analytical Chemistry*, 93: 519-45.
- Rappaport, S.M., D.K. Barupal, D. Wishart, P. Vineis, and A. Scalbert. 2014. 'The blood exposome and its role in discovering causes of disease', *Environmental Health Perspectives*, 122: 769-74.
- Reinke, S.N., H. Gallart-Ayala, C. Gómez, A. Checa, A. Fauland, S. Naz, M.A. Kamleh, R. Djukanović, T.S.C. Hinks, and C.E. Wheelock. 2017. 'Metabolomics analysis identifies different metabolotypes of asthma severity', *European Respiratory Journal*, 49: 1601740.
- Rhoades, S.D., A. Sengupta, and A.M. Weljie. 2017. 'Time is ripe: maturation of metabolomics in chronobiology', *Current Opinion in Biotechnology*, 43: 70-76.
- Šarkanj, B., C.N. Ezekiel, P.C. Turner, W.A. Abia, M. Rychlik, R. Krska, M. Sulyok, and B. Warth. 2018. 'Ultra-sensitive, stable isotope assisted quantification of multiple urinary mycotoxin exposure biomarkers', *Analytica Chimica Acta*, 1019: 84-92.
- Schwaiger, M., H. Schoeny, Y. El Abiead, G. Hermann, E. Rampl, and G. Koellensperger. 2019. 'Merging metabolomics and lipidomics into one analytical run', *Analyst*, 144: 220-29.
- Schymanski, E.L., J. Jeon, R. Gulde, K. Fenner, M. Ruff, H.P. Singer, and J. Hollender. 2014. 'Identifying Small Molecules via High Resolution Mass Spectrometry: Communicating Confidence', *Environmental Science & Technology*, 48: 2097-98.
- Sobus, J.R., J.N. Grossman, A. Chao, R. Singh, A.J. Williams, C.M. Grulke, A.M. Richard, S.R. Newton, A.D. McEachran, and E.M. Ulrich. 2019. 'Using prepared mixtures of ToxCast chemicals to evaluate non-targeted analysis (NTA) method performance', *Analytical and Bioanalytical Chemistry*, 411: 835-51.
- Sofie, C., A. Marta, B. Julie, V. Anne Marie, P. Gitte Alsing, and H. Ulla. 2014. 'Low-dose effects of bisphenol A on early sexual development in male and female rats', *Reproduction*, 147: 477-87.
- Tang, S., T. Li, J. Fang, R. Chen, Y.e. Cha, Y. Wang, M. Zhu, Y. Zhang, Y. Chen, Y. Du, T. Yu, D.C. Thompson, K.J. Godri Pollitt, V. Vasilios, J.S. Ji, H. Kan, J.J. Zhang, and X. Shi. 2021. 'The exposome in practice: an exploratory panel study of biomarkers of air pollutant exposure in Chinese people aged 60–69 years (China BAPE Study)', *Environment International*, 157: 106866.
- Ulrich, E.M., J.R. Sobus, C.M. Grulke, A.M. Richard, S.R. Newton, M.J. Strynar, K. Mansouri, and A.J. Williams. 2019. 'EPA's non-targeted analysis collaborative trial (ENTACT): genesis, design, and initial findings', *Analytical and Bioanalytical Chemistry*, 411: 853-66.
- Vela-Soria, F., I. Jiménez-Díaz, R. Rodríguez-Gómez, A. Zafra-Gómez, O. Ballesteros, A. Navalón, J.L. Vilchez, M.F. Fernández, and N. Olea. 2011. 'Determination of benzophenones in human placental tissue samples by liquid chromatography-tandem mass spectrometry', *Talanta*, 85: 1848-55.
- Vermeulen, R., E.L. Schymanski, A.-L. Barabási, and G.W. Miller. 2020. 'The exposome and health: Where chemistry meets biology', *Science*, 367: 392-96.
- Warth, B., S. Spangler, M. Fang, C.H. Johnson, E.M. Forsberg, A. Granados, R.L. Martin, X. Domingo-Almenara, T. Huan, D. Rinehart, J.R. Montenegro-Burke, B. Hilmers, A. Aisporna, L.T. Hoang, W. Uritboonthai, H.P. Benton, S.D. Richardson, A.J. Williams, and G. Siuzdak. 2017. 'Exposome-Scale Investigations Guided by Global Metabolomics, Pathway Analysis, and Cognitive Computing', *Analytical Chemistry*, 89: 11505-13.
- Wei, F., M. Mortimer, H. Cheng, N. Sang, and L.-H. Guo. 2021. 'Parabens as chemicals of emerging concern in the environment and humans: A review', *Science of the Total Environment*, 778: 146150.
- Wei, T., and V. Simko. 2017. 'R package "corrplot": Visualization of a Correlation Matrix', Available from <https://github.com/taiyun/corrplot>.
- Wenzel, A.G., J.W. Brock, L. Cruze, R.B. Newman, E.R. Unal, B.J. Wolf, S.E. Somerville, and J.R. Kucklick. 2018. 'Prevalence and predictors of phthalate exposure in pregnant women in Charleston, SC', *Chemosphere*, 193: 394-402.
- Wild, C.P. 2005. 'Complementing the Genome with an "Exposome": The Outstanding Challenge of Environmental Exposure Measurement in Molecular Epidemiology', *Cancer Epidemiology Biomarkers & Prevention*, 14: 1847.
- Wolff, M.S., S.L. Teitelbaum, K. McGovern, S.M. Pinney, G.C. Windham, M. Galvez, A. Pajak, M. Rybak, A.M. Calafat, L.H. Kushi, and F.M. Biro. 2015. 'Environmental phenols and pubertal development in girls', *Environment International*, 84: 174-80.
- Xu, Z., J. Liu, X. Wu, B. Huang, and X. Pan. 2017. 'Nonmonotonic responses to low doses of xenoestrogens: A review', *Environmental Research*, 155: 199-207.
- Ye, X., L.-Y. Wong, J. Kramer, X. Zhou, T. Jia, and A.M. Calafat. 2015. 'Urinary Concentrations of Bisphenol A and Three Other Bisphenols in Convenience Samples of U.S. Adults during 2000–2014', *Environmental Science & Technology*, 49: 11834-39.
- Zhang, J., L. Liu, X. Wang, Q. Huang, M. Tian, and H. Shen. 2016. 'Low-Level Environmental Phthalate Exposure Associates with Urine Metabolome Alteration in a Chinese Male Cohort', *Environmental Science & Technology*, 50: 5953-60.
- Zhu, H., S. Chinthakindi, and K. Kannan. 2021. 'A method for the analysis of 121 multi-class environmental chemicals in urine by high-performance liquid chromatography-tandem mass spectrometry', *Journal of Chromatography A*, 1646: 462146.

Supporting Information

Integrated exposomics/metabolomics for rapid exposure and effect analyses

Mira Flasch^{1,2}, Veronika Fitz^{2,3}, Evelyn Rampler³, Chibundu N. Ezekiel⁴, Gunda Koellensperger^{3,5}, Benedikt Warth^{1,5*}

¹University of Vienna, Faculty of Chemistry, Department of Food Chemistry and Toxicology, Währinger Straße 38-40, 1090 Vienna, Austria

²University of Vienna, Vienna Doctoral School of Chemistry, Währinger Straße 42, 1090, Vienna, Austria

³University of Vienna, Faculty of Chemistry, Department of Analytical Chemistry, Währinger Straße 38-40, 1090 Vienna, Austria

⁴Department of Microbiology, Babcock University, Ilishan Remo, Ogun State, Nigeria

⁵Exposome Austria, Research Infrastructure and National EIRENE Hub, Austria

Table of Contents

Figure S1 Structural diversity of some of the model molecules involved in this study	3
Figure S2 Peak areas normalized to internal standard of the pooled QC sample from A) Nigerian urine and B) Austrian urine	4
Figure S3 Concentration of quantified A) xenobiotics (only analytes not described in the certificate) and B) endogenous metabolites present in SRM3672 (green) and SRM1950 (grey)	5
Figure S4 Spearman correlation matrix of analytes detected in at least 20 % of all samples.	6
Figure S5 Detection of xenobiotics in Austrian urine samples.....	7
Figure S6 Results of pathway analysis of with monobutyl phthalate correlated metabolites	8
Figure S7 Results of pathway analysis of with ethylparaben correlated metabolites	9
Figure S8 Results of pathway analysis of with benzophenone 1 correlated metabolites	10
Table S1 Summary of molecules present in the multi-analyte mixture and internal standards	11
Table S2 Analyte concentrations in the solvent multi-analyte standard	19
Table S3 Concentrations of ¹³ C-labeled analytes in the internal standard mix	24
Table S4 Average peak area of individual endogenous metabolites (analysed with the HILIC column) and xenobiotics (analysed with the RP column)	25
Table S5 Limit of detection (LOD), retention time and the detected adducts (with the most abundant one in bold)	27
Table S6 Limit of detection (LOD), retention time and the detected adducts.....	31
Table S7 Calibration parameter of analytes in all three matrices and normalization method.....	36
Table S19 Linear dynamic range of solvent standards and matrix-matched standards, recovery of solvent standards and extraction recovery of spiked matrix standards	46
Table S20 Linear dynamic range of solvent standards and matrix-matched standards, recovery of solvent standards and extraction recovery of spiked matrix standards	49

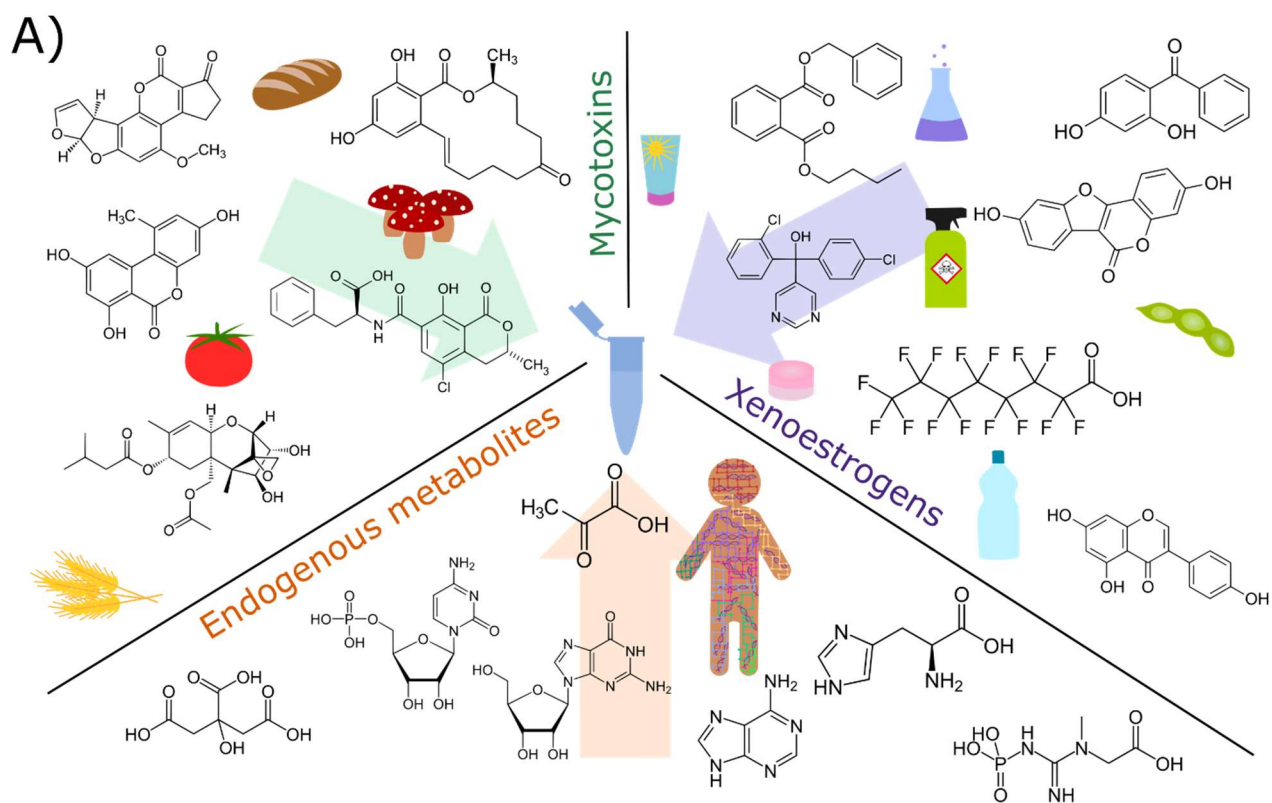


Figure S1 Structural diversity of some of the model molecules involved in this study

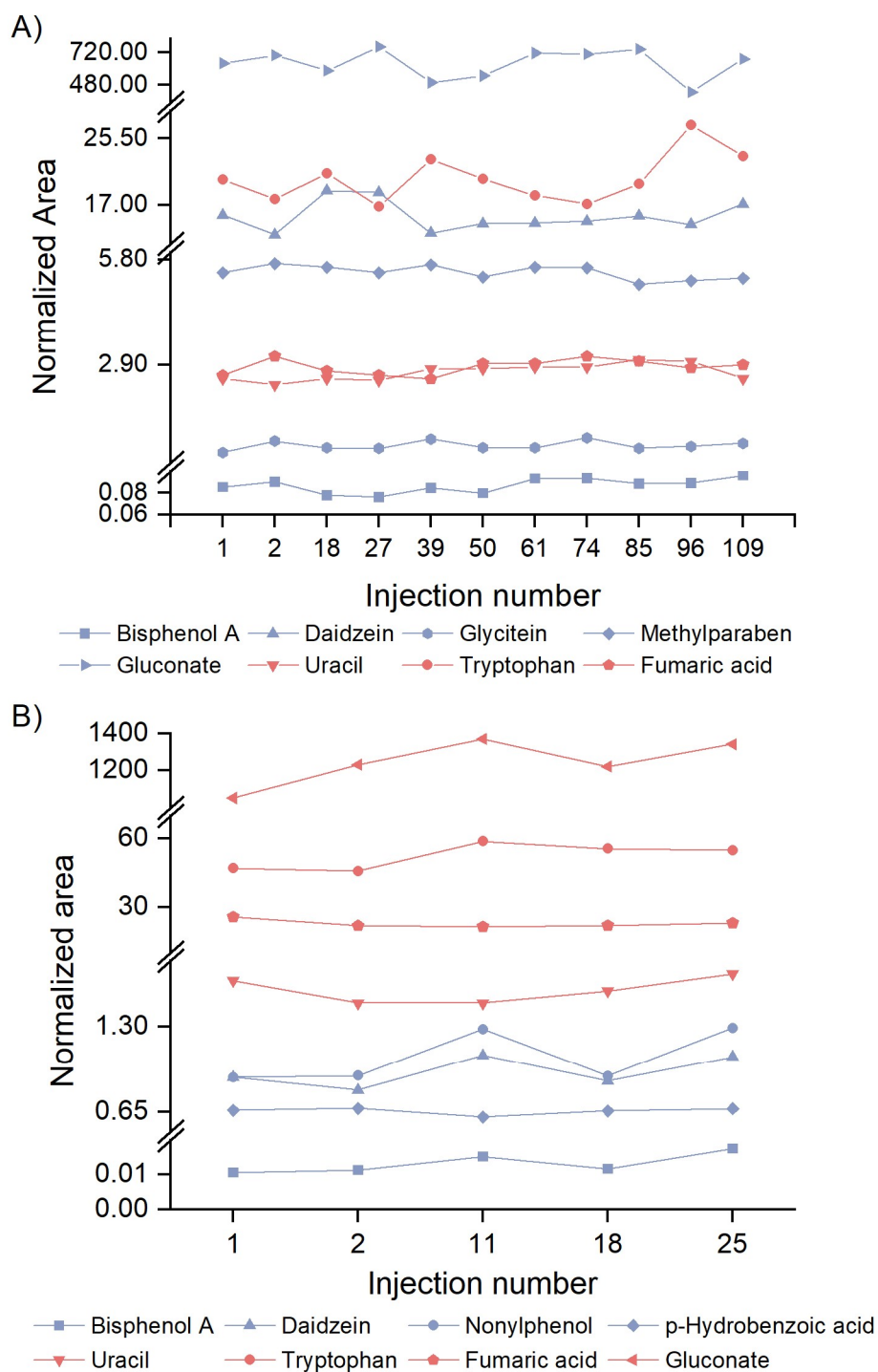


Figure S2 Peak areas normalized to internal standard of the pooled QC sample from A) Nigerian urine and B) Austrian urine over several injections within the sequence to demonstrate the high robustness and repeatability of the method

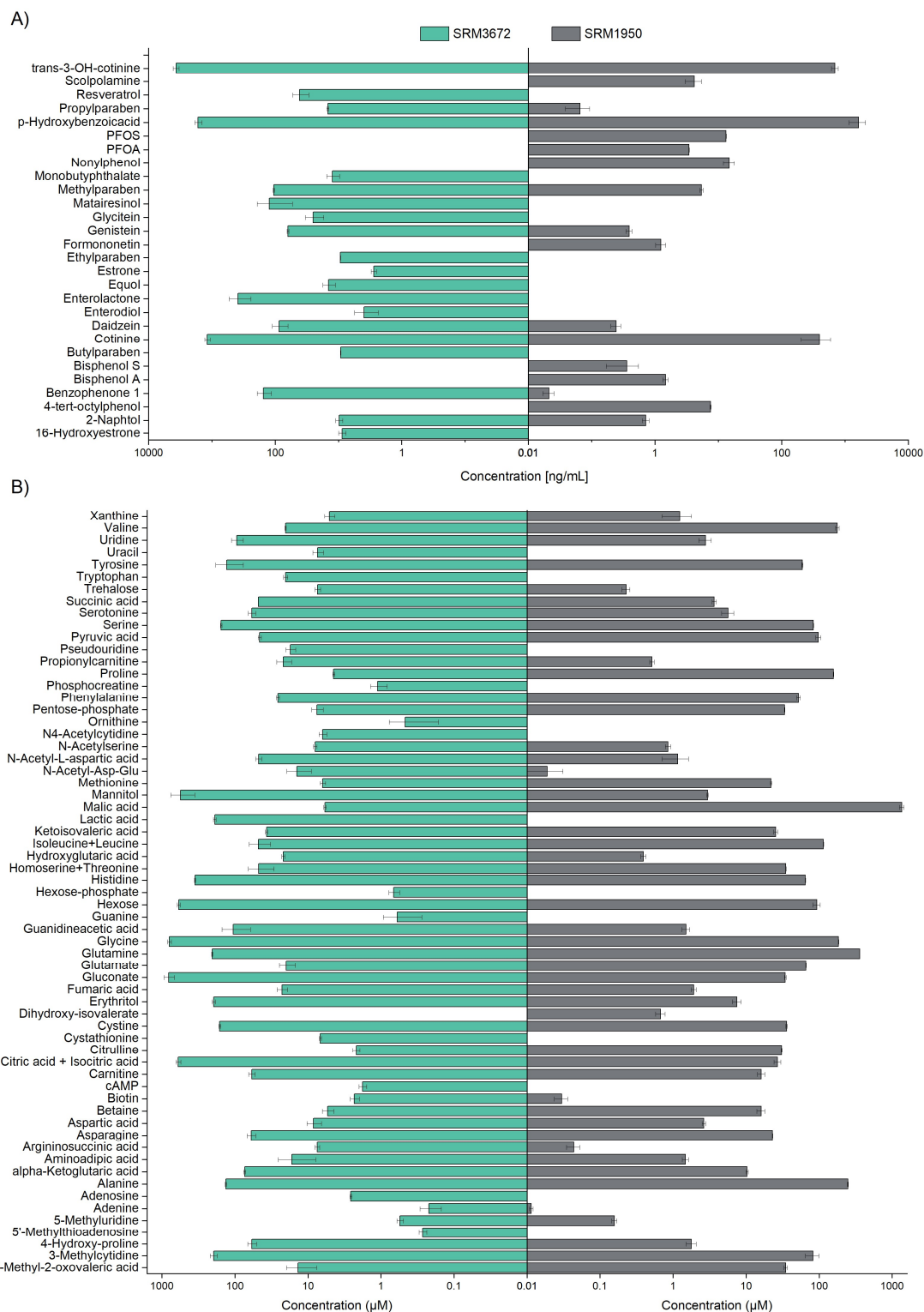


Figure S3 Concentration of quantified A) xenobiotics (only analytes not described in the certificate) and B) endogenous metabolites present in SRM3672 (green) and SRM1950 (grey)

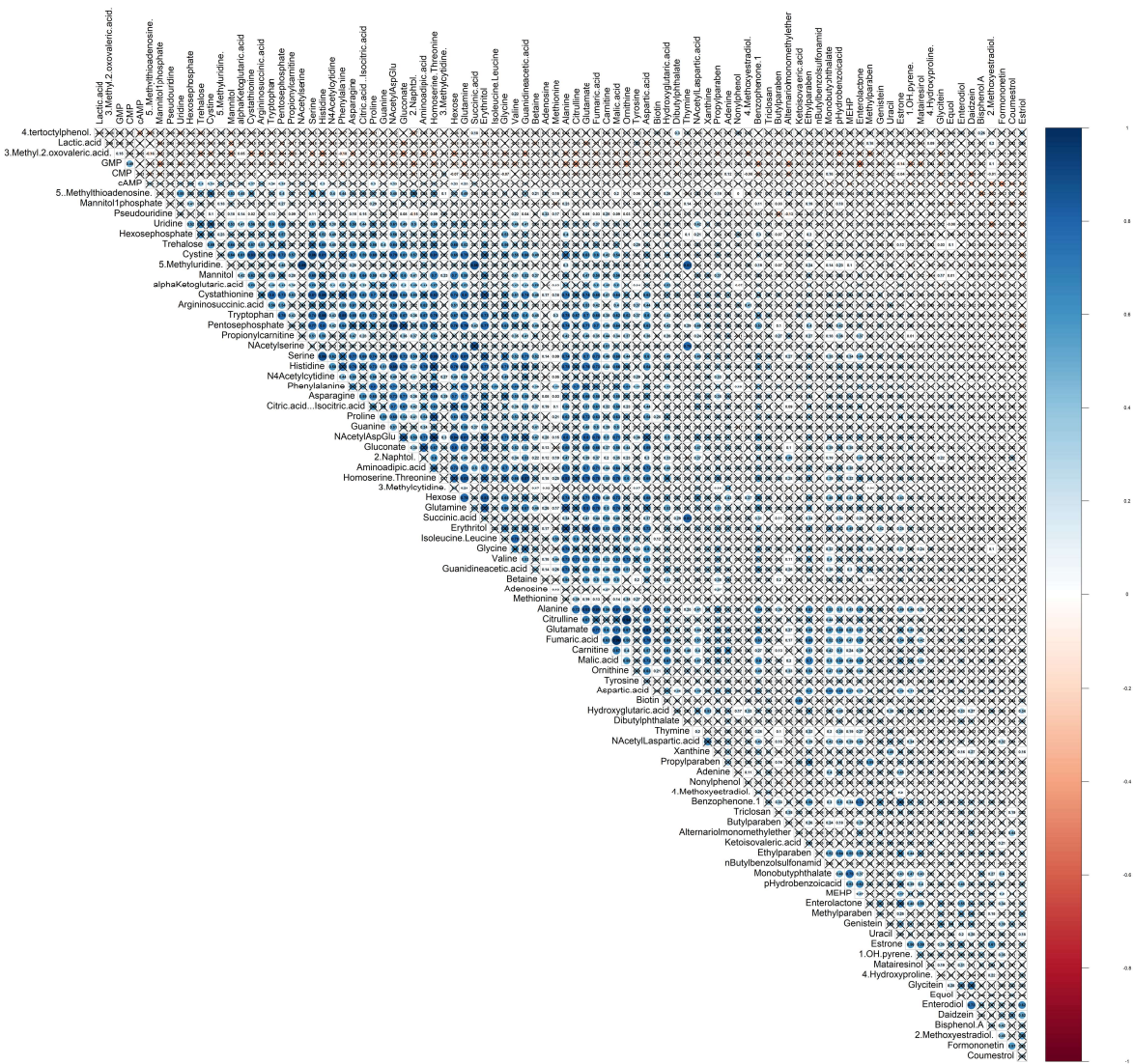
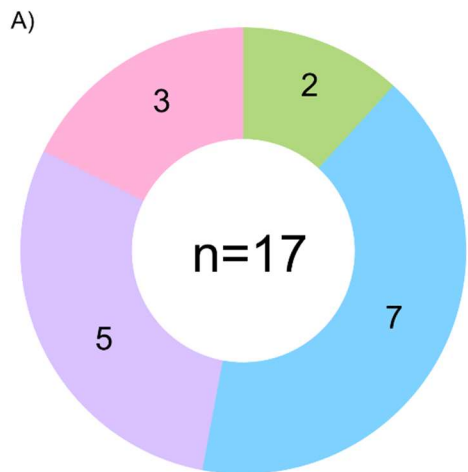


Figure S4 Spearman correlation matrix of analytes detected in at least 20 % of all samples. The significance level was tested and if higher than 0.01 the squares were crossed



■ Industrial side product and pesticides
■ Personal care product ingredients and pharmaceuticals
■ Phytoestrogens
■ Plasticizers

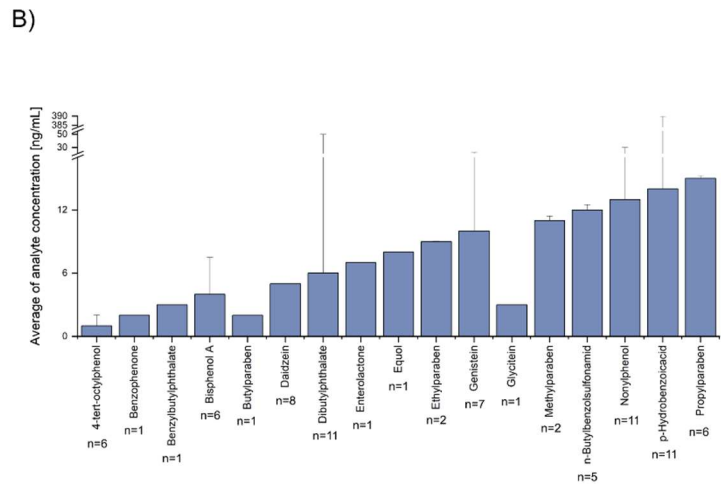
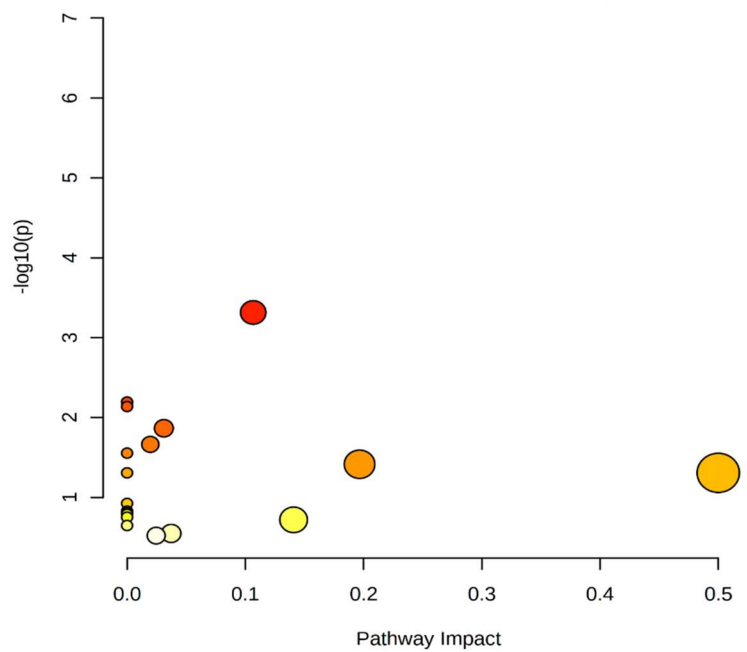
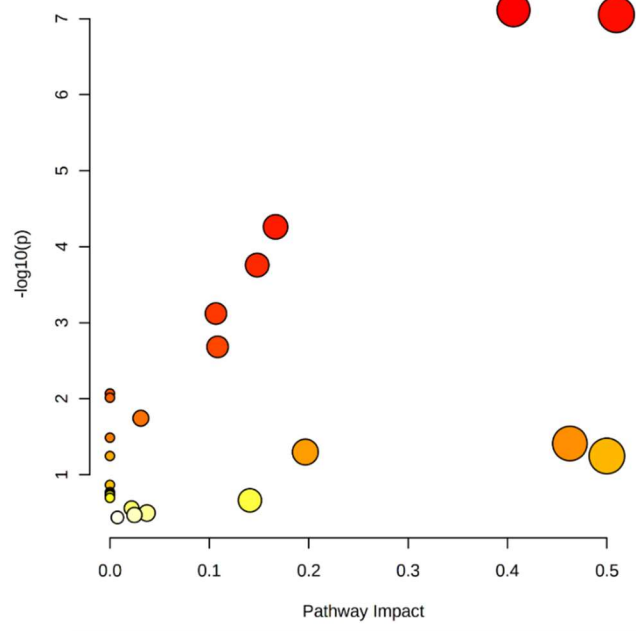


Figure S5 Detection of xenobiotics in Austrian urine samples. A) Variety of observed xenobiotics and their expected origin. B) Average concentration of in the samples detectable compounds with standard deviation



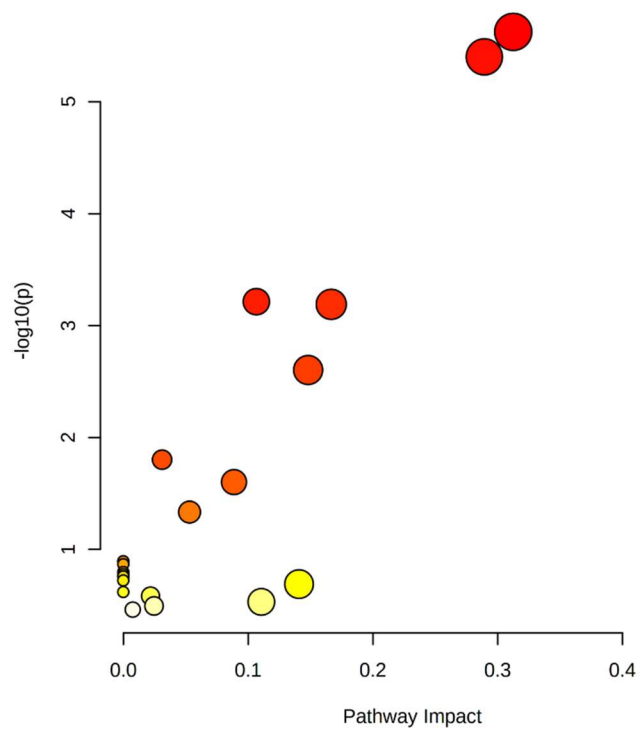
Pathway Name	Match Status	p	-log(p)	Holm p	FDR	Impact	Details
Alanine, aspartate and glutamate metabolism	6/28	3.1097E-8	7.5073	2.6121E-6	1.405E-6	0.50962	KEGG SMP SMP SMP
Arginine biosynthesis	5/14	3.3453E-8	7.4756	2.7766E-6	1.405E-6	0.40609	KEGG
Citrate cycle (TCA cycle)	3/20	4.8454E-4	3.3147	0.039733	0.013567	0.10666	KEGG SMP
Aminoacyl-tRNA biosynthesis	3/48	0.0064113	2.1931	0.51932	0.10214	0.0	KEGG

Figure S6 Results of pathway analysis of with monobutyl phthalate correlated metabolites including for multiple testing corrected p-values from MetaboAnalyst 5.0 (Pang et al. 2021)



Pathway Name	Match Status	p	-log(p)	Holm p	FDR	Impact	Details
Arginine biosynthesis	5/14	7.7299E-8	7.1118	6.4931E-6	3.7167E-6	0.40609	KEGG
Alanine, aspartate and glutamate metabolism	6/28	8.8492E-8	7.0531	7.3449E-6	3.7167E-6	0.50962	KEGG SMP SMP SMP
Aminoacyl-tRNA biosynthesis	5/48	5.4905E-5	4.2604	0.0045022	0.0015374	0.16667	KEGG
Glyoxylate and dicarboxylate metabolism	4/32	1.7451E-4	3.7582	0.014135	0.0036647	0.14815	KEGG
Citrate cycle (TCA cycle)	3/20	7.5822E-4	3.1202	0.060657	0.012738	0.10666	KEGG SMP
Glutathione metabolism	3/28	0.0020793	2.6821	0.16426	0.02911	0.10839	KEGG SMP

Figure S7 Results of pathway analysis of with ethylparaben correlated metabolites including for multiple testing corrected p-values from MetaboAnalyst 5.0 (Pang et al. 2021)



Pathway Name	Match Status	p	-log(p)	Holm p	FDR	Impact	Details
Alanine, aspartate and glutamate metabolism	5/28	2.3737E-6	5.6246	1.9939E-4	1.6677E-4	0.3125	KEGG SMP SMP SMP
Arginine biosynthesis	4/14	3.9707E-6	5.4011	3.2957E-4	1.6677E-4	0.28934	KEGG
Citrate cycle (TCA cycle)	3/20	6.1161E-4	3.2135	0.050152	0.013567	0.10666	KEGG SMP
Aminoacyl-tRNA biosynthesis	4/48	6.4607E-4	3.1897	0.052332	0.013567	0.16667	KEGG
Glyoxylate and dicarboxylate metabolism	3/32	0.0024951	2.6029	0.19961	0.041918	0.14815	KEGG

Figure S8 Results of pathway analysis of with benzophenone 1 correlated metabolites including for multiple testing corrected p-values from MetaboAnalyst 5.0 (Pang et al. 2021)

Table S1 Summary of molecules (n=251) present in the multi-analyte mixture and available internal standards (n=15)

Compound	Molecular Formula	CAS number	Classification	Abbreviation
Endogenous metabolites excluding human estrogens				
1-Methylhydantoin	C4H6N2O2	616-04-6	Organoheterocyclic compounds	Methylhydantoin
1-Methylnicotinamide	C7H8N2O	3106-60-3	Organoheterocyclic compounds	MNA
2-(Carbamoylamino)butanedioic acid (Ureidosuccinic acid)	C5H8N2O5	923-37-5	Organic acids (Amino acids)	Carbamoyl-Asp
2'-Deoxyadenosine 5'-monophosphate	C10H14N5O6P	653-63-4	Nucleotides	dAMP
2'-Deoxycytidine	C9H13N3O4	951-77-9	Nucleosides	dCdin
2-Deoxycytidine 5'-Monophosphate	C9H14N3O7P	1032-65-1	Nucleotides	dCMP
2'-Deoxyuridine	C9H12N2O5	951-78-0	Nucleosides	dUdin
2-Phosphoglycerate	C3H7O7P	2553-59-5	Carbohydrates and conjugates	2PG
3-Methyl-2-oxovaleric acid	C6H10O3	1460-34-0	Organic acids (Keto acids)	K-Ile
3-Methylcytidine	C10H15N3O5	2140-64-9	Nucleosides	Mcdin
3-Phosphoglycerate	C3H7O7P	820-11-1	Carbohydrates and conjugates	3PG
4-Hydroxy-proline	C5H9NO3	6912-67-0	Organic acids (Amino acids)	Hydroxyproline
5'-Deoxy-5'-Methylthioadenosine	C11H15N5O3S	2457-80-9	Nucleosides	5d5mtAsin
5-Methyluridine	C10H14N2O6	1463-10-1	Nucleosides	5MUdin
6-Phosphogluconate	C6H13O10P	921-62-0	Carbohydrates and conjugates	6PGA
Adenine	C5H5N5	73-24-5	Nucleobases	Ade
Adenosine	C10H13N5O4	58-61-7	Nucleosides	Asin
Adenosine 3',5'-cyclic monophosphate	C10H12N5O6P	60-92-4	Nucleotides	cAMP
Adenosine 3'-monophosphate	C10H14N5O7P	84-21-9	Nucleotides	3AMP
Adenosine 5'-monophosphate	C10H14N5O7P	61-19-8	Nucleotides	5AMP
Adenosine 5'-triphosphate	C10H16N5O13P3	56-65-5	Nucleotides	ATP
Adenosine diphosphate	C10H15N5O10P2	58-64-0	Nucleotides	ADP
Alanine	C3H7NO2	302-72-7	Organic acids (Amino acids)	Ala
alpha-Amino adipic acid	C6H11NO4	542-32-5	Organic acids (Amino acids)	AAA
alpha-Ketoglutarate	C5H6O5	328-50-7	Organic acids (Keto acids)	AKG
Arginine	C6H14N4O2	74-79-3	Organic acids (Amino acids)	Arg
Argininosuccinic acid	C10H18N4O6	2387-71-5	Organic acids (Amino acids)	Arg-Suc
Asparagine	C4H8N2O3	70-47-3	Organic acids (Amino acids)	Asn
Aspartic acid (Aspartate)	C4H7NO4	56-84-8	Organic acids (Amino acids)	Asp
Betaine	C5H11NO2	107-43-7	Organic acids (Amino acids)	Betaine
Biotin	C10H16N2O3S	58-85-5	Biotin and derivatives	Biotin
Carnitine	C7H15NO3	406-76-8	Quaternary ammonium salts	Carn
Choline chloride	C5H14NO	67-48-1	Quaternary ammonium salts	Choline

Compound	Molecular Formular	CAS number	Classification	Abbreviation
Endogenous metabolites excluding human estrogens				
cis-Aconitate	C6H6O6	585-84-2	Organic acids (Carboxylic acids)	Aco
Citrate	C6H8O7	126-44-3	Organic acids (Carboxylic acids)	Cit
Cytidine-5'-monophosphate	C9H14N3O8P	63-37-6	Nucleotides	CMP
Cysteic acid	C3H7NO5S	13100-82-8	Organic acids (Amino acids)	Cysteic acid
Cysteine	C3H7NO2S	52-90-4	Organic acids (Amino acids)	Cys
Cysteinyl-glycine	C5H10N2O3S	19246-18-5	Organic acids (Amino acids)	Cys-Gly
Cystine	C6H12N2O4S2	923-32-0	Organic acids (Amino acids)	Cyst
Cytidine	C9H13N3O5	65-46-3	Nucleosides	Cdin
Cytidine 5'-triphosphate	C9H16N3O14P3	65-47-4	Nucleotides	CTP
Cytosine	C4H5N3O	71-30-7	Nucleobases	Cyt
Deoxyguanosine triphosphate	C10H16N5O13P3	2564-35-4	Nucleotides	dGTP
Dihydroxyacetonephosphate	C3H7O6P	57-04-5	Carbohydrates and conjugates	DHAP
Dihydroxyisovalerate	C5H10O4	19451-56-0	Fatty acyls	DHIV
Erythrito	C4H10O4	149-32-6	Carbohydrates and conjugates	EryOI
Erythrose-4-phosphate	C4H9O7P	585-18-2	Carbohydrates and conjugates	E4P
Flavinadenin dinucleotide	C27H33P2N9O15	146-14-5	Coenzymes and Vitamines	FAD
Fructose	C6H12O6	6347-01-9	Carbohydrates and conjugates	Fru
Fructose-1,6-bisphosphate	C6H14O12P2	34693-23-7	Carbohydrates and conjugates	FBP
Fructose-6-phosphate	C6H13O9P	643-13-0	Carbohydrates and conjugates	F6P
Fumarate	C4H4O4	142-42-7	Organic acids (Carboxylic acids)	Fum
Galactose	C6H12O6	10257-28-0	Carbohydrates and conjugates	Gal
Gluconate	C6H12O7	526-95-4	Carbohydrates and conjugates	Glc-ON
Glucose	C6H12O6	2280-44-6	Carbohydrates and conjugates	Glc
Glucose-1-phosphate	C6H13O9P	59-56-3	Carbohydrates and conjugates	G1P
Glucose-6-phosphate	C6H13O9P	299-31-0	Carbohydrates and conjugates	G6P
Glutamate	C5H9NO4	56-86-0	Organic acids (Amino acids)	Glu
Glutamine	C5H10N2O3	56-85-9	Organic acids (Amino acids)	Gln
Glutamyl-cysteine	C8H14N2O5S	686-58-8	Organic acids (Amino acids)	Glu-Cys
Glutathione, oxidized	C20H32N6O12S2	27025-41-8	Organic acids (Amino acids)	GSSG
Glutathione, reduced	C10H17N3O6S	70-18-8	Organic acids (Amino acids)	GSH
Glycine	C2H5NO2	56-40-6	Organic acids (Amino acids)	Gly
Glyoxylic acid	C2H2O3	298-12-4	Organic acids (Carboxylic acids)	Glyoxylate
Guanosine-5'-monophosphate	C10H14N5O8P	85-32-5	Nucleotides	GMP

Compound	Molecular Formula	CAS number	Classification	Abbreviation
Endogenous metabolites excluding human estrogens				
Guanidineacetic acid	C3H7N3O2	352-97-6	Organic acids (Amino acids)	GdinAc
Guanine	C5H5N5O	73-40-5	Nucleobases	Gnin
Guanosine	C10H13N5O5	118-00-3	Nucleosides	Gsin
Guanosine 3',5'-cyclic monophosphate	C10H12N5O7P	7665-99-8	Nucleotides	cGMP
Guanosine 5'-diphosphate	C10H15N5O11P2	146-91-8	Nucleotides	GDP
Guanosine 5'-triphosphate	C10H16N5O14P3	86-01-1	Guanosine 5'-triphosphate	GTP
Histidine	C6H9N3O2	71-00-1	Organic acids (Amino acids)	His
Homocysteine	C4H9NO2S	6027-13-0	Organic acids (Amino acids)	Hcys
Homoserine	C4H9NO3	1927-25-9	Organic acids (Amino acids)	H-Ser
Hydroxyglutaric acid	C5H8O5	2889-31-8	Organic acids (Hydroxy acids)	2HG
Inosine	C10H12N4O5	58-63-9	Nucleosides	Isin
Inosine 5'-monophosphate	C10H13N4O8P	131-99-7	Nucleotides	IMP
Inositol	C6H12O6	551-72-4	Carbohydrates and conjugates	Ino
Isocitrate	C6H8O7	320-77-4	Organic acids (Carboxylic acids)	I-Cit
Isoguanosine	C10H13N5O5	1818-71-9	Nucleosides	IGsin
Isoleucine	C6H13NO2	443-79-8	Organic acids (Amino acids)	Ile
Ketoisovalerate	C5H8O3	759-05-7	Organic acids (Keto acids)	K-Val
Kynurenine	C10H12N2O3	343-65-7	Organic acids (Amino acids)	Kynurenine
Lactate	C3H6O3	113-21-3	Organic acids (Hydroxy acids)	Lac
L-Citrulline	C6H13N3O3	372-75-8	Organic acids (Amino acids)	Citrulline
L-Cystathionine	C7H14N2O4S	56-88-2	Organic acids (Amino acids)	LCT
Leucine	C6H13NO2	61-90-5	Organic acids (Amino acids)	Leu
L-Ornithine	C5H12N2O2	70-26-8	Organic acids (Amino acids)	Orn
Lysine	C6H14N2O2	56-87-1	Organic acids (Amino acids)	Lys
Malic acid (Malate)	C4H6O5	320-77-4	Organic acids (Hydroxy acids)	Mali
Mannitol	C6H14O6	69-65-8	Carbohydrates and conjugates	Man-OL
Mannitol 1-phosphate	C6H15O9P	15806-48-1	Carbohydrates and conjugates	Man-OL-1-P
Mannose	C6H12O6	530-26-7	Carbohydrates and conjugates	Man
Melatonin	C13H16N2O2	73-31-4	Indoles and derivatives	Melatonin
Methionine	C5H11NO2S	63-68-3	Organic acids (Amino acids)	Met
Methionine sulfone	C5H11NO4S	7314-32-1	Organic acids (Amino acids)	MetSulf
Mevalonic acid	C6H12O4	17817-88-8	Fatty acyls	Meva
N4-Acetylcytidine	C11H15N3O6	3768-18-1	Nucleosides	AcCdin
N-Acetyl-Asp-Glu	C11H16N2O8	3106-85-2	Organic acids (Amino acids)	Acetyl-Asp-Glu

Compound	Molecular Formular	CAS number	Classification	Abbreviation
Endogenous metabolites excluding human estrogens				
N-Acetyl-L-aspartic acid	C6H9NO5	997-55-7	Organic acids (Amino acids)	Acetyl-Asp
N-Acetyl-serine	C5H9NO4	16354-58-8	Organic acids (Amino acids)	N-Acetyl-DL-serine
NAD+	C21H27N7O14P2	53-84-9	Coenzymes and Vitamines	NAD
NADH	C21H29N7O14P2	58-68-4	Coenzymes and Vitamines	NADH
NADP+	C21H28N7O17P3	604-79-5	Coenzymes and Vitamines	NADP
NADPH	C21H30N7O17P3	53-57-6	Coenzymes and Vitamines	NADPH
Nicotinamide	C6H6N2O	98-92-0	Coenzymes and Vitamines	NAM
Octopamine	C8H11NO2	104-14-3	Benzenoids	Octopamine
Oxaloacetic acid	C4H4O5	328-42-7	Organic acids (Keto acids)	Oac
Palmitic acid	C16H32O2	57-10-3	Fatty acyls	Palm A
Phenylalanine	C9H11NO2	63-91-2	Organic acids (Amino acids)	Phe
Phosphocreatine	C4H10N3O5P	67-07-2	Organic acids (Amino acids)	P-Creatine
Proline	C5H9NO2	4305-67-3	Organic acids (Amino acids)	Pro
Propionyl-L-carnitine	C10H19NO4	17298-37-2	Fatty acyls	Prop. Carn
Pseudouridine	C9H12N2O6	1445-07-4	Nucleosides	Pudin
Pyruvate	C3H4O3	57-60-3	Organic acids (Keto acids)	Pyr
Ribose	C5H10O5	10257-32-6	Carbohydrates and conjugates	Rib
Ribose-5-phosphate	C5H11O8P	4300-28-1	Carbohydrates and conjugates	R5P
Ribulose-5-phosphate	C5H11O8P	551-85-9	Carbohydrates and conjugates	R15P
S-(Adenosyl)-methionine	C15H22N6O5S	29908-03-0	Coenzymes and Vitamines	SAM
Sarcosine	C3H7NO2	107-97-1	Organic acids (Amino acids)	Sarcosine
Sedoheptulose-7-phosphate	C7H15O10P	2646-35-7	Carbohydrates and conjugates	S7P
Seleno-methionine	C5H11NO2Se	3211-76-5	Organic acids (Amino acids)	Se-Met
Serine	C3H7NO3	56-45-1	Organic acids (Amino acids)	Ser
Serotonine	C10H12N2O	50-67-9	Indoles and derivatives	Serotonine
Spermidine	C7H19N3	124-20-9	Amines	Spermidine
Spermine	C10H26N4	71-44-3	Amines	Spermine
Succinate	C4H6O4	56-14-4	Organic acids (Carboxylic acids)	Suc
Thiamine hydrochloride	C12H17N4OS	67-03-8	Coenzymes and Vitamines	Thiamine
Threonine	C4H9NO3	72-19-5	Organic acids (Amino acids)	Thr
Thymidine	C10H14N2O5	50-89-5	Nucleosides	Tdin
Thymidine 5'-monophosphate	C10H15N2O8P	14057-65-9	Nucleotides	TMP
Thymidine 5'-triphosphate	C10H17N2O14P3	365-08-2	Nucleotides	TTP
Thymine	C5H6N2O2	65-71-4	Nucleobases	Thy

Compound	Molecular Formula	CAS number	Classification	Abbreviation
Endogenous metabolites excluding human estrogens				
Trehalose	C12H22O11	99-20-7	Carbohydrates and conjugates	Tre
Tryptophan	C11H12N2O2	73-22-3	Organic acids (Amino acids)	Trp
Tyrosine	C9H11NO3	60-18-4	Organic acids (Amino acids)	Tyr
Uridine 5'-monophosphate	C9H13N2O9P	58-97-9	Nucleotides	UMP
Uracil	C4H4N2O2	66-22-8	Nucleobases	Ura
Uridine	C9H12N2O6	58-96-8	Nucleosides	Uri
Uridine 5'-diphosphate	C9H14N2O12P2	58-98-0	Nucleotides	UDP
Uridine 5'-triphosphate	C9H15N2O15P3	63-39-8	Nucleotides	UTP
Valine	C5H11NO2	72-18-4	Organic acids (Amino acids)	Val
Xanthine	C5H4N4O2	69-89-6	Nucleobases	Xan
Xylose	C5H10O5	10257-31-5	Carbohydrates and conjugates	Xyl
Xenobiotics and human estrogens				
16-Epiestriol	C18H24O3	547-81-9	Endogenous estrogens	16EpiE3
16-Hydroxyestrone	C18H22O3	566-76-7	Endogenous estrogens	16OHE1
17-Epiestriol	C18H24O3	1228-72-4	Endogenous estrogens	17EpiE3
1-OH-pyrene	C16H10O	5315-79-7	Air pollutant	1OHPy
2-Methoxyestradiol	C19H26O3	362-07-2	Endogenous estrogens	2MeOE2
2-tert Butylphenol	C10H14O	88-18-6	Industrial side product and pesticides	2-tert-BP
2-Hydroxyestradiol	C18H24O3	362-05-0	Endogenous estrogens	2OHE2
2-Methoxyestrone	C19H24O3	362-08-3	Endogenous estrogens	2MeOE1
2-Naphtol	C10H8O	135-19-3	Industrial side product and pesticides	2Naph
3-Benzylidencampher	C17H20O	15087-24-8	Personal care product ingredients and pharmaceuticals	3-BC
4-Methoxyestradiol	C19H26O3	26788-23-8	Endogenous estrogens	4MeOE2
4-Hydroxyestrone	C18H22O3	3131-23-5	Endogenous estrogens	4OHE1
4-Methoxyestrone	C19H24O3	58562-33-7	Endogenous estrogens	MeOE1
4-Methylbenzyliden campher	C18H22O	36861-47-9	Personal care product ingredients and pharmaceuticals	4-MBC
4-Octylphenol	C14H22O	1806-26-4	Industrial side product and pesticides	4-OP
4-tert-Octylphenol	C14H22O	140-66-9	Industrial side product and pesticides	4-tert-OP
8-Prenylaringenin	C20H20O5	53846-50-7	Phytoestrogen	8-Pn
Aflatoxicol	C17H14O6	29611-03-8	Mycotoxin	AFL
Aflatoxin B1	C17H12O6	1162-65-8	Mycotoxin	AFB1
Aflatoxin B2	C17H14O6	7220-81-7	Mycotoxin	AFB2
Aflatoxin G1	C17H12O7	1165-39-5	Mycotoxin	AFG1
Aflatoxin G2	C17H14O7	7241-98-7	Mycotoxin	AFG2
Aflatoxin M1	C17H12O7	6795-23-9	Mycotoxin	AFM1
Aflatoxin M2	C17H14O7	6885-57-0	Mycotoxin	AFM2
Aflatoxin P1	C16H10O6	32215-02-4	Mycotoxin	AFP1
Aristolactam I	C17H11NO4	13395-02-3	Phytotoxin	Aristolactam
Alpha-zearalanol	C18H26O5	26538-44-3	Mycoestrogen	α-ZAL
Alpha-zearalenol	C18H24O5	36455-72-8	Mycoestrogen	α-ZEL
Alpha-zearalenol-14-glucuronide	C24H32O11	-	Mycoestrogen	α-ZEL-GlcA
Alternariol	C14H10O5	641-38-3	Mycoestrogen	Alternariol
Alternariol monomethyl ether	C15H12O5	26894-49-5	Mycoestrogen	AME
Anisodamine	C17H23NO4	55869-99-3	Phytotoxins	Anisodamine
Aristolochic acid I	C17H11NO7	313-67-7	Phytotoxins	AA
Beauvericin	C45H57N3O9	26048-05-5	Mycotoxin	BEA

Compound	Molecular Formula	CAS number	Classification	Abbreviation
Endogenous metabolites excluding human estrogens				
Benzophenone 1	C13H10O3	131-56-6	Personal care product ingredients and pharmaceuticals	Benzophenone 1
Benzophenone 2	C13H10O5	131-55-5	Personal care product ingredients and pharmaceuticals	Benzophenone 2
Benzylbutyl phthalate	C19H20O4	85-68-7	Plasticizer	Benzyl butyl phthalate
Benzylparaben	C14H12O3	94-18-8	Personal care product ingredients and pharmaceuticals	B4HB
Beta-zearalanol	C18H26O5	42422-68-4	Mycoestrogen	β-ZAL
Beta-zearalenol	C18H24O5	71030-11-0	Mycoestrogen	β-ZEL
Beta-zearalenol-14-glucuronide	C24H32O11	-	Mycoestrogen	β-ZEL-GlcA
Bisphenol A	C15H16O2	80-05-07	Plasticizer	BPA
Bisphenol AF	C15H10F6O2	1478-61-1	Plasticizer	BPAF
Bisphenol B	C14H10Cl2O2	77-40-7	Plasticizer	BPB
Bisphenol C	C16H18O2	79-97-0	Plasticizer	BPC
Bisphenol F	C13H12O2	620-92-8	Plasticizer	BPF
Bisphenol S	C12H10O4S	80-09-1	Plasticizer	BPS
Butylparaben	C11H14O3	94-26-8	Personal care product ingredients and pharmaceuticals	Butylparaben
Citrinin	C13H14O5	518-75-2	Mycotoxin	CIT
Cotinine	C10H12N2O	486-56-6	Air pollutant	Cotinine
Coumestrol	C15H8O5	479-13-0	Phytoestrogen	Coumestrol
Daidzein	C15H10O4	486-66-8	Phytoestrogen	DAI
Deoxynivalenol	C15H20O6	51481-10-8	Mycotoxin	DON
Dibutylphthalate	C16H22O4	84-74-2	Plasticizer	Dibutylphthalate
Estradiol-17-glucuronide	C24H32O8	15087-02-2	Endogenous estrogens	E2-17-GlcA
Enterodiol	C18H22O4	80226-00-2	Phytoestrogen	Enterodiol
Enterolactone	C18H18O4	78473-71-9	Phytoestrogen	Enterolactone
Equol	C15H14O3	94105-90-5	Phytoestrogen	Equol
Estradiol	C18H24O2	50-28-2	Endogenous estrogens	E2
Estradiol-3-sulfate	C18H24O5S	4999-79-5	Endogenous estrogens	E2-3-sulfate
Estriol	C18H24O3	50-27-1	Endogenous estrogens	E3
Estrone	C18H22O2	53-16-7	Endogenous estrogens	E1
Ethinylestradiol	C20H24O2	57-63-6	Personal care product ingredients and pharmaceuticals	EE
Ethylparaben	C9H10O3	120-47-8	Personal care product ingredients and pharmaceuticals	Ethylparaben
Fenarimol	C17H12Cl2N2O	60168-88-9	Industrial side product and pesticides	Fenarimol
Formononetin	C16H12O4	485-72-3	Phytoestrogen	Formononetin
Genistein	C15H10O5	446-72-0	Phytoestrogen	GEN
Glycitein	C16H12O5	40957-83-3	Phytoestrogen	Glycitein
Isobutylparaben	C11H14O3	4247-02-3	Personal care product ingredients and pharmaceuticals	Isobutylparaben
Isoxanthohumol	C21H22O5	70872-29-6	Phytoestrogen	Isoxanthohumol
Jacobine	C18H25NO6	6870-67-3	Phytotoxins	Jacobine
Jacobine-N-oxide	C18H25NO7	38710-25-7	Phytotoxins	Jacobine-N-oxide
Matairesinol	C20H22O6	580-72-3	Phytoestrogen	Matairesinol
Mono-2-ethylhexyl phthalate	C16H21O4	4376-20-9	Plasticizer	MEHP
Methiocarb	C11H15NO2S	2032-65-7	Industrial side product and pesticides	Methiocarb

Compound	Molecular Formular	CAS number	Classification	Abbreviation
Endogenous metabolites excluding human estrogens				
Methylparaben	C8H8O3	99-76-3	Personal care product ingredients and pharmaceuticals	Methylparaben
Monobutyl phthalate	C12H14O4	131-70-4	Plasticizer	MBP
n-Butylbenzolsulfonamid	C10H15NO2S	3622-84-2	Plasticizer	n-Butylbenzolsulfonamid
Nivalenol	C15H20O7	23282-20-4	Mycotoxin	NIV
Nonylphenol	C15H24O	84852-15-3	Mycotoxin	Nonylphenol
Ochratoxin A	C20OH18NO6	303-47-9	Mycotoxin	OTA
Ochratoxin Alpha	C11H10O5	19165-63-0	Mycotoxin	Ot α
Ochratoxin B	C11OH9O5	4825-86-9	Mycotoxin	OTB
Octyl methoxycinnamate	C18H26O3	5466-77-3	Personal care product ingredients and pharmaceuticals	OMC
Perfluorooctanoic acid	C8HF15O2	335-67-1	Perfluorinated alkylated substances	PFOA
Perfluorooctanesulfonic acid	C8HF17O3S	1763-23-1	Perfluorinated alkylated substances	PFOS
PhIP	C13H12N4	105650-23-5	Food processing by-products	PhIP
p-Hydrobenzoic acid	C7H6O3	99-96-7	Personal care product ingredients and pharmaceuticals	pOHBA
Prochloraz	C15H16Cl3N3O2	67747-09-5	Industrial side product and pesticides	Prochloraz
Propylparaben	C10H12O3	94-13-3	Personal care product ingredients and pharmaceuticals	Propylparaben
Resveratrol	C14H12O3	501-36-0	Phytoestrogen	Resveratrol
Riddeliin	C18H23NO6	23246-96-0	Phytotoxins	Riddeliin
Riddeliin-N-oxide	C18H23NO7	75056-11-0	Phytotoxins	Riddeliin-N-oxide
Scopolamine	C17H21NO4	51-34-3	Phytotoxins	Scopolamine
Sterigmatocystein	C18H12O6	10048-13-2	Mycotoxin	Sterigmatocystein
Tentoxin	C22H30N4O4	28540-82-1	Mycotoxin	Tentoxin
Tetrabrombispfenol A	Br4C15H12O2	79-94-7	Plasticizer	TBPA
HT-2 Toxin	C22H32O8	26934-87-2	Mycotoxin	HT2
T-2 Toxin	C24H34O9	21259-20-1	Mycotoxin	T2
Trans-3-hydroxy-cotinine	C10H12N2O2	34834-67-8	Air pollutant	trans-3-OH-cotinine
Triclosan	C12H7Cl3O2	3380-34-5	Industrial side product and pesticides	Triclosan
Xanthohumol	C21H22O5	569-83-5	Phytoestrogen	Xanthohumol
Zearalanone	C18H22O5	5975-78-0	Mycoestrogen	ZAN
Zearalenone	C18H24O5	17924-92-4	Mycoestrogen	ZEN
Zearalenone-14-glucuronide	C24H30O11	-	Mycoestrogen	ZEN-14-GlcA
Zearalenone-14-sulfate	C18H22O8S	-	Mycoestrogen	ZEN-14-sulfate
Internal standards				
¹³ C ₁₂ -Bisphenol A		263261-85-0		
¹³ C ₁₈ - Zearalenone				
¹³ C ₄ -Monobutyl phthalate				
¹³ C ₄ -MEHP				
¹³ C ₃ -Estradiol		1261254-48-1		
¹³ C ₆ -4-tert-octylphenol		1173020-24-0		
¹³ C ₆ -Butylparaben				
¹³ C ₆ -Ethylparaben				
¹³ C ₆ -Methylparaben				
¹³ C ₆ -p-Hydroxybenzoic acid		267399-29-5		
¹³ C ₆ -Propylparaben				

Compound	Molecular Formular	CAS number	Classification	Abbreviation
Endogenous metabolites excluding human estrogens				
¹³ C ₈ -PFOA				
¹³ C ₈ -PFOS				
¹³ C ₁₅ -Deoxynivalenol				
¹³ C ₁₇ -Aflatoxin M1				

Table S2 Analyte concentrations in the solvent multi-analyte standard. The same concentration levels were used for the preparation of the corresponding matrix-matched standard.

Compound	Concentration [ng/mL]							
	Std 1	Std 2	Std 3	Std 4	Std 5	Std 6	Std 7	Std 8
	Endogenous metabolites							
	0.001 μM	0.01 μM	0.03 μM	0.1 μM	0.3 μM	1 μM	3 μM	10 μM
1-Methylhydantoin	0.1	1.1	3.4	11.4	34.2	114.1	342.3	1141
1-Methylnicotinamide	0.1	1.4	4.1	13.7	41.1	137.2	411.5	1371.6
2-(Carbamoylamino)butanedioic acid	0.2	1.8	5.3	17.6	52.8	176.1	528.4	1761.3
2'-Deoxyadenosine 5'-monophosphate	0.3	3.3	9.9	33.1	99.4	331.2	993.7	3312.2
2'-Deoxycytidine	0.2	2.3	6.8	22.7	68.2	227.2	681.7	2272.2
2-Deoxycytidine 5'-Monophosphate	0.3	3.1	9.2	30.7	92.2	307.2	921.6	3072
2'-Deoxyuridine	0.2	2.3	6.8	22.8	68.5	228.2	684.6	2282
2-Phosphoglyceric acid	0.2	1.9	5.6	18.6	55.8	186.1	558.2	1860.6
3'AMP	0.3	3.5	10.4	34.7	104.2	347.2	1041.7	3472.2
3-Methyl-2-oxovaleric acid	0.1	1.3	3.9	13	39.0	130.1	390.4	1301.39
3-Methylcytidine	0.3	2.6	7.7	25.7	77.2	257.2	771.7	2572.4
3-Phosphoglycerate	0.2	1.9	5.6	18.6	55.8	186.1	558.2	1860.6
4-Hydroxy-proline	0.1	1.3	3.9	13.1	39.3	131.1	393.4	1311.3
5'-Deoxy-5'-Methylthioadenosine	0.3	3	8.9	29.7	89.2	297.3	892.0	2973.4
5-Methyluridine	0.3	2.6	7.7	25.8	77.5	258.2	774.7	2582.3
6-Phosphogluconate	0.3	2.8	8.3	27.6	82.8	276.1	828.4	2761.4
Adenine	0.1	1.4	4.1	13.5	40.5	135.1	405.4	1351.3
Adenosine	0.3	2.7	8	26.7	80.2	267.2	801.7	2672.4
Adenosine 3',5'-cyclic monophosphate	0.3	3.3	9.9	32.9	98.8	329.2	987.6	3292.1
Adenosine 5'-triphosphate	0.5	5.1	15.2	50.7	152.2	507.2	1521.5	5071.8
Adenosine diphosphate	0.4	4.3	12.8	42.7	128.2	427.2	1281.6	4272
Alanine	0.1	0.9	2.7	8.9	26.7	89.1	267.3	890.9
alpha-Aminoadipic acid	0.2	1.6	4.8	16.1	48.3	161.2	483.5	1611.6
alpha-Ketoglutarate	0.1	1.5	4.4	14.6	43.8	146.1	438.3	1461
5'AMP	0.3	3.5	10.4	34.7	104.2	347.2	1041.7	3472.2
Arginine	0.2	1.7	5.2	17.4	52.3	174.2	522.6	1742
Argininosuccinic acid	0.3	2.9	8.7	29	87.1	290.3	870.8	2902.7
Asparagine	0.1	1.3	4	13.2	39.6	132.1	396.4	1321.2
Aspartate	0.1	1.3	4	13.3	39.9	133.1	399.3	1331
Betaine	0.1	1.2	3.5	11.7	35.1	117.2	351.5	1171.5
Biotin	0.2	2.4	7.3	24.4	73.3	244.3	732.9	2443.1
Carnitine	0.2	1.6	4.8	16.1	48.4	161.2	483.6	1612
Choline chloride	0.1	1	3.1	10.4	31.3	104.2	312.5	1041.7
cis-Aconitate	0.2	1.7	5.2	17.4	52.2	174.1	522.3	1741.1
Citrate	0.2	1.9	5.8	19.2	57.6	192.1	576.4	1921.2
CMP	0.3	3.2	9.7	32.3	97.0	323.2	969.6	3232
Cysteic acid	0.2	1.7	5.1	16.9	50.7	169.2	507.5	1691.6
Cysteine	0.1	1.2	3.6	12.1	36.3	121.2	363.5	1211.6
Cysteinyl-glycine	0.2	1.8	5.3	17.8	53.5	178.2	534.6	1782.1
Cystine	0.2	2.4	7.2	24	72.1	240.3	720.9	2403
Cytidine	0.2	2.4	7.3	24.3	73.0	243.2	729.7	2432.2
Cytidine 5'-triphosphate	0.5	4.8	14.5	48.3	144.9	483.2	1449.5	4831.6
Cytosine	0.1	1.1	3.3	11.1	33.3	111.1	333.3	1111
Deoxyguanosine triphosphate	0.5	5.1	15.2	50.7	152.2	507.2	1521.5	5071.8
Dihydroxyacetonephosphate	0.2	1.7	5.1	17	51.0	170.1	510.2	1700.6
Dihydroxyisovalerate	0.1	1.3	4	13.4	40.2	134.1	402.4	1341.3
Erythritol	0.1	1.2	3.7	12.2	36.6	122.1	366.4	1221.2
Erythrose-4-phosphate	0.2	2	6	20	60.0	200.1	600.2	2000.8

Compound	Concentration [ng/mL]							
	Std 1	Std 2	Std 3	Std 4	Std 5	Std 6	Std 7	Std 8
Endogenous metabolites								
Flavinadenin dinucleotide	0.8	7.9	23.6	78.6	235.7	785.5	2356.5	7855
Fructose	0.2	1.8	5.4	18	54.0	180.2	540.4	1801.6
Fructose-1,6-bisphosphate	0.3	3.4	10.2	34	102.0	340.1	1020.4	3401.2
Fructose-6-phosphate	0.3	2.6	7.8	26	78.0	260.1	780.4	2601.4
Fumarate	0.1	1.2	3.5	11.6	34.8	116.1	348.2	1160.7
Galactose	0.2	1.8	5.4	18.0	54.0	180.2	540.5	1801.6
Gluconate	0.2	2	5.9	19.6	58.8	196.2	588.5	1961.6
Glucose	0.2	1.8	5.4	18.0	54.0	180.16	540.5	1801.6
Glucose-1-phosphate	0.3	2.6	7.8	26	78.0	260.1	780.4	2601.4
Glucose-6-phosphate	0.3	2.6	7.8	26	78.0	260.1	780.4	2601.4
Glutamate	0.1	1.5	4.4	14.7	44.1	147.1	441.4	1471.3
Glutamine	0.1	1.5	4.4	14.6	43.8	146.1	438.4	1461.4
Glutamyl-cysteine	0.3	2.5	7.5	25	75.1	250.3	750.8	2502.7
Glutathione, oxidized	0.6	6.1	18.4	61.3	183.8	612.6	1837.8	6126
Glutathione, reduced	0.3	3.1	9.2	30.7	92.2	307.3	922.0	3073.3
Glycine	0.1	0.8	2.3	7.5	22.5	75.1	225.2	750.7
Glyoxylic acid	0.1	0.7	2.2	7.4	22.2	74.0	222.1	740.4
GMP	0.4	3.6	10.9	36.3	109.0	363.2	1089.7	3632.2
Guanidineacetic acid	0.1	1.2	3.5	11.7	35.1	117.1	351.3	1171.1
Guanine	0.2	1.5	4.5	15.1	45.3	151.1	453.4	1511.3
Guanosine	0.3	2.8	8.5	28.3	85.0	283.2	849.7	2832.4
Guanosine 3',5'-cyclic monophosphate	0.3	3.5	10.4	34.5	103.6	345.2	1035.6	3452.1
Guanosine 5'-diphosphate	0.4	4.4	13.3	44.3	133.0	443.2	1329.6	4432
Guanosine 5'-triphosphate	0.5	5.2	15.7	52.3	157.0	523.2	1569.5	5231.8
Histidine	0.2	1.6	4.7	15.5	46.5	155.2	465.5	1551.5
Homocysteine	0.1	1.4	4.1	13.5	40.6	135.2	405.6	1351.9
Homoserine	0.1	1.2	3.6	11.9	35.7	119.1	357.4	1191.2
Hydroxyglutaric acid	0.1	1.5	4.4	14.8	44.4	148.1	444.3	1481.1
Inosine	0.3	2.7	8	26.8	80.5	268.2	804.7	2682.3
Inosine 5'-monophosphate	0.3	3.5	10.4	34.8	104.5	348.2	1044.6	3482.1
Inositol	0.2	1.8	5.4	18.0	54.0	180.2	540.5	1801.6
Isocitrate	0.2	1.9	5.8	19.2	57.6	192.1	576.4	1921.2
Isoguanosine	0.3	2.8	8.5	28.3	85.0	283.2	849.7	2832.4
Isoleucine	0.1	1.3	3.9	13.1	39.4	131.2	393.5	1311.7
Ketoisovalerate	0.3	2.8	8.3	27.5	82.6	275.5	826.5	2754.9
Kynurenine	0.2	2.1	6.2	20.8	62.5	208.2	624.6	2082.1
Lactate	0.1	0.9	2.7	9	27.0	90.1	270.2	900.8
L-Citrulline	0.2	1.8	5.3	17.5	52.6	175.2	525.6	1751.9
L-Cystathionine	0.2	2.2	6.7	22.2	66.7	222.3	666.8	2222.6
Leucine	0.1	1.3	3.9	13.1	39.4	131.2	393.5	1311.7
L-Ornithine	0.1	1.3	4	13.2	39.6	132.2	396.5	1321.6
Lysine	0.1	1.5	4.4	14.6	43.9	146.2	438.6	1461.9
Malate	0.1	1.3	4	13.4	40.2	134.1	402.3	1340.9
Mannitol	0.2	1.8	5.5	18.2	54.7	182.2	546.5	1821.7
Mannitol 1-phosphate	0.3	2.6	7.9	26.2	78.6	262.2	786.5	2621.5
Mannose	0.2	1.8	5.4	18.0	54.0	180.2	540.5	1801.6
Melatonin	0.2	2.3	7	23.2	69.7	232.3	696.8	2322.8
Methionine	0.1	1.5	4.5	14.9	44.8	149.2	447.6	1492.1
Methionine sulfone	0.2	1.8	5.4	18.1	54.4	181.2	543.6	1812.1
Mevalonic acid	0.1	1.5	4.4	14.8	44.4	148.2	444.5	1481.6
N4-Acetylcytidine	0.3	2.9	8.6	28.5	85.6	285.3	855.8	2852.5
N-Acetyl-Asp-Glu	0.3	3	9.1	30.4	91.3	304.3	912.8	3042.5
N-Acetyl-L-aspartic acid	0.2	1.8	5.3	17.5	52.5	175.1	525.4	1751.4
N-Acetyl-serine	0.1	1.5	4.4	14.7	44.1	147.1	441.4	1471.3
NAD+	0.7	6.6	19.9	66.3	199.0	663.4	1990.2	6634
NADH	0.7	6.7	20	66.5	199.6	665.4	1996.2	6654

Compound	Concentration [ng/mL]							
	Std 1	Std 2	Std 3	Std 4	Std 5	Std 6	Std 7	Std 8
Endogenous metabolites								
NADP+	0.7	7.4	22.3	74.4	223.3	744.4	2233.2	7444
NADPH	0.7	7.5	22.4	74.5	223.6	745.4	2236.2	7454
Nicotinamide	0.1	1.2	3.7	12.2	36.6	122.1	366.4	1221.2
Octopamine	0.2	1.5	4.6	15.3	46.0	153.2	459.5	1531.8
Oxaloacetic acid	0.1	1.3	4	13.2	39.6	132.1	396.2	1320.7
Palmitic acid	0.3	2.6	7.7	25.6	76.9	256.4	769.3	2564.2
Phenylalanine	0.2	1.7	5	16.5	49.6	165.2	495.6	1651.9
Phosphocreatine	0.2	2.1	6.3	21.1	63.3	211.1	633.3	2111.1
Proline	0.1	1.2	3.5	11.5	34.5	115.1	345.4	1151.3
Propionyl-L-carnitine	0.2	2.2	6.5	21.7	65.2	217.3	651.8	2172.6
Pseudouridine	0.2	2.4	7.3	24.4	73.3	244.2	732.6	2442
Pyruvate	0.1	0.9	2.6	8.8	26.4	88.1	264.2	880.6
Ribose	0.2	1.5	4.5	15	45.0	150.1	450.4	1501.3
Ribose-5-phosphate	0.2	2.3	6.9	23	69.0	230.1	690.3	2301.1
Ribulose-5-phosphate	0.2	2.3	6.9	23	69.0	230.1	690.3	2301.1
S-(Adenosyl)-methionine	0.4	3.8	11.5	38.4	115.3	384.4	1153.2	3844.1
Sarcosine	0.1	0.9	2.7	8.9	26.7	89.1	267.3	890.9
Sedoheptulose-7-phosphate	0.3	2.9	8.7	29	87.0	290.2	870.5	2901.6
Seleno-methionine	0.2	2	5.9	19.6	58.8	196.1	588.4	1961.2
Serine	0.1	1.1	3.2	10.5	31.5	105.1	315.3	1050.9
Serotonine	0.2	1.8	5.3	17.6	52.9	176.2	528.6	1762.1
Spermidine	0.1	1.5	4.4	14.5	43.6	145.3	435.8	1452.5
Spermine	0.2	2	6.1	20.2	60.7	202.3	607.0	2023.4
Succinate	0.1	1.2	3.5	11.8	35.4	118.1	354.3	1180.9
Thiamine hydrochloride	0.3	2.7	8	26.5	79.6	265.4	796.1	2653.6
Threonine	0.1	1.2	3.6	11.9	35.7	119.1	357.4	1191.2
Thymidine	0.2	2.4	7.3	24.2	72.7	242.2	726.7	2422.3
Thymidine 5'-monophosphate	0.3	3.2	9.6	32.1	96.4	321.2	963.6	3212
Thymine	0.1	1.3	3.8	12.6	37.8	126.1	378.3	1261.1
Trehalose	0.3	3.4	10.3	34.2	102.7	342.3	1026.9	3423
Tryptophan	0.01	0.1	0.3	1	3.0	10.0	30.0	100
TTP (Thymidinetriphosphate)	0.2	2	6.1	20.4	61.3	204.2	612.7	2042.2
Tyrosine	0.5	4.8	14.5	48.2	144.7	482.2	1446.5	4821.7
UMP	0.3	3.2	9.7	32.4	97.3	324.2	972.5	3241.8
Uracil	0.1	1.1	3.4	11.2	33.6	112.1	336.3	1120.9
Uridine	0.2	2.4	7.3	24.4	73.3	244.2	732.6	2442
Uridine 5'-diphosphate	0.4	4	12.1	40.4	121.2	404.2	1212.5	4041.6
Uridine 5'-triphosphate	0.5	4.8	14.5	48.4	145.2	484.1	1452.4	4841.4
Valine	0.1	1.2	3.5	11.7	35.1	117.2	351.5	1171.5
Xanthine	0.2	1.5	4.6	15.2	45.6	152.1	456.3	1521.1
Xylose	0.2	1.5	4.5	15	45.0	150.1	450.4	1501.3
Xenobiotics								
16-Epiestriol	0.05	0.5	1.5	5	15.0	50.0	150.0	500
16-Hydroxyestrone	0.01	0.1	0.3	1	3.0	10.0	30.0	100
17-Epiestriol	0.05	0.5	1.5	5	15.0	50.0	150.0	500
1-OH-pyrene	0.01	0.1	0.3	1	3.0	10.0	30.0	100
2 Methoxyestradiol	0.03	0.3	0.9	3	9.0	30.0	90.0	300
2 tert Butylphenol	0.2	2	6	20	60.0	200.0	600.0	2000
2-Hydroxyestradiol	0.1	1	3	10	30.0	100.0	300.0	1000
2-Methoxyestrone	0.03	0.3	0.9	3	9.0	30.0	90.0	300
2-Naphtol	0.05	0.5	1.5	5	15.0	50.0	150.0	500
3-Benzylidenecampher	0.5	5	15	50	150.0	500.0	1500.0	5000
4 Methoxyestradiol	0.01	0.1	0.2	0.5	1.5	5.0	15.0	50
4-Hydroxyestrone	0.05	0.5	1.5	5	15.0	50.0	150.0	500
4-Methoxyestrone	0.01	0.1	0.2	0.5	1.5	5.0	15.0	50
4-Methylbenzyliden campher	0.2	2	6	20	60.0	200.0	600.0	2000
4-octylphenol	0.1	1	3	10	30.0	100.0	300.0	1000

Compound	Concentration [ng/mL]							
	Std 1	Std 2	Std 3	Std 4	Std 5	Std 6	Std 7	Std 8
Endogenous metabolites								
4-tert-octylphenol	0.1	1	3	10	30.0	100.0	300.0	1000
8-Prenylnaringenin	0.001	0.01	0.03	0.1	0.3	1.0	3.0	10
Aflatoxicol	0.01	0.1	0.2	0.5	1.5	5.0	15.0	50
Aflatoxin B1	0.01	0.1	0.3	1	3.0	10.0	30.0	100
Aflatoxin B2	0.01	0.1	0.3	1	3.0	10.0	30.0	100
Aflatoxin G1	0.01	0.1	0.3	1	3.0	10.0	30.0	100
Aflatoxin G2	0.01	0.1	0.3	1	3.0	10.0	30.1	100.3
Aflatoxin M1	0.01	0.1	0.3	1	3.0	10.0	30.0	100
Aflatoxin M2	0.01	0.1	0.3	1	3.0	10.0	30.1	100.3
Aflatoxin P1	0.01	0.1	0.3	1	3.0	10.0	30.0	100
Aristolactam I	0.01	0.1	0.3	1	3.0	10.0	30.0	100
Alpha-zearalanol	0.01	0.1	0.3	1	3.0	10.0	30.0	100
Alpha-zearalenol	0.01	0.1	0.3	1	3.0	10.0	30.0	100
Alpha-zearalenol-14-glucuronide	0.01	0.1	0.3	1	3.0	10.0	30.0	100
Alternariol	0.01	0.1	0.3	1	3.0	10.0	30.0	100
Alternariol monomethyl ether	0.01	0.1	0.3	1	3.0	10.0	30.0	100
Anisodamine	0.01	0.1	0.3	1	3.0	10.0	30.0	100
Aristolochic acid I	0.01	0.1	0.3	1	3.0	10.0	30.0	100
Beauvericin	0.01	0.1	0.2	0.5	1.5	5.0	15.0	50
Benzophenone 1	0.001	0.01	0.03	0.1	0.3	1.0	3.0	10
Benzophenone 2	0.01	0.1	0.2	0.5	1.5	5.0	15.0	50
Benzylbutyl phthalate	0.05	0.5	1.5	5	15.0	50.0	150.0	500
Benzylparaben (B4HB)	0.001	0.01	0.02	0.1	0.2	0.5	1.5	5
Beta-zearalanol	0.01	0.1	0.3	1	3.0	10.0	30.0	100
Beta-zearalenol	0.01	0.1	0.3	1	3.0	10.0	30.0	100
Beta-zearalenol-14-glucuronide	0.01	0.1	0.3	1	3.0	10.0	30.0	100
Bisphenol A	0.01	0.1	0.3	1	3.0	10.0	30.0	100
Bisphenol AF	0.01	0.1	0.2	0.5	1.5	5.0	15.0	50
Bisphenol B	0.01	0.1	0.3	1	3.0	10.0	30.0	100
Bisphenol C	0.02	0.2	0.6	2	6.0	20.0	60.0	200
Bisphenol F	0.02	0.2	0.6	2	6.0	20.0	60.0	200
Bisphenol S	0.001	0.01	0.03	0.1	0.3	1.0	3.0	10
Butylparaben	0.01	0.1	0.2	0.5	1.5	5.0	15.0	50
Citrinin	0.01	0.1	0.3	1	3.0	10.0	30.0	100
Cotinine	0.01	0.1	0.3	1	3.0	10.0	30.0	100
Coumestrol	0.01	0.1	0.3	1	3.0	10.0	30.0	100
Daidzein	0.01	0.1	0.2	0.5	1.5	5.0	15.0	50
Deoxynivalenol	0.01	0.1	0.3	1	3.0	10.0	30.0	100
Dibutylphthalate	0.1	1	3	10	30.0	100.0	300.0	1000
E2-17-GlcA	0.05	0.5	1.5	5	15.0	50.0	150.0	500
Enterodiol	0.01	0.1	0.2	0.5	1.5	5.0	15.0	50
Enterolactone	0.01	0.1	0.3	1	3.0	10.0	30.0	100
Equol	0.01	0.1	0.3	1	3.0	10.0	30.0	100
Estradiol	0.02	0.2	0.6	2	6.0	20.0	60.0	200
Estradiol-3-sulfate	0.02	0.2	0.6	2	6.0	20.0	60.0	200
Estriol	0.02	0.2	0.6	2	6.0	20.0	60.0	200
Estrone	0.01	0.1	0.3	1	3.0	10.0	30.0	100
Ethinylestradiol	0.05	0.5	1.5	5	15.0	50.0	150.0	500
Ethylparaben	0.01	0.1	0.2	0.5	1.5	5.0	15.0	50
Fenarimol	0	0	0	0.1	0.2	0.5	1.5	5
Formononetin	0.01	0.1	0.2	0.5	1.5	5.0	15.0	50
Genistein	0.01	0.1	0.2	0.5	1.5	5.0	15.0	50
Glycitein	0.01	0.1	0.2	0.5	1.5	5.0	15.0	50
Isobutylparaben	0.01	0.1	0.2	0.5	1.5	5.0	15.0	50
Isoxanthohumol	0	0	0	0.1	0.2	0.5	1.5	5
Jacobine	0.01	0.1	0.3	1	3.0	10.0	30.0	100
Jacobine-N-oxide	0.01	0.1	0.3	1	3.0	10.0	30.0	100

Compound	Concentration [ng/mL]							
	Std 1	Std 2	Std 3	Std 4	Std 5	Std 6	Std 7	Std 8
Endogenous metabolites								
Matairesinol	0.02	0.2	0.6	2	6.0	20.0	60.0	200
MEHP	0.02	0.2	0.6	2	6.0	20.0	60.0	200
Methiocarb	0.03	0.3	0.9	3	9.0	30.0	90.0	300
Methylparaben	0.01	0.1	0.3	1	3.0	10.0	30.0	100
Monobutyl phthalate	0.02	0.2	0.6	2	6.0	20.0	60.0	200
n Butylbenzolsulfonamid	0.02	0.2	0.6	2	6.0	20.0	60.0	200
Nivalenol	0.01	0.1	0.3	1	3.0	10.0	30.0	100
Nonylphenol	0.05	0.5	1.5	5	15.0	50.0	150.0	500
Ochratoxin A	0.01	0.1	0.3	1	3.0	10.0	30.0	100
Ochratoxin Alpha	0.01	0.1	0.3	1	3.0	10.0	30.0	100
Ochratoxin B	0.01	0.1	0.3	1	3.0	10.0	30.0	100
Octyl methoxycinnamate	0.5	5	15	50	150.0	500.0	1500.0	5000
Perfluorooctanoic acid (PFOA)	0.01	0.1	0.2	0.5	1.5	5.0	15.0	50
PFOS	0.03	0.3	0.9	3	9.0	30.0	90.0	300
PhIP	0.01	0.1	0.3	1	3.0	10.0	30.0	100
p-Hydrobenzoic acid	0.3	3	9	30	90.0	300.0	900.0	3000
Prochloraz	0	0	0	0.1	0.3	1.0	3.0	10
Propylparaben	0.01	0.1	0.2	0.5	1.5	5.0	15.0	50
Resveratrol	0.05	0.5	1.5	5	15.0	50.0	150.0	500
Riddeliin	0.08	0.8	2.4	8	24.0	80.0	240.0	800
Riddeliin-N-oxide	0.08	0.8	2.4	8	24.0	80.0	240.0	800
Scopolamine	0.01	0.1	0.2	0.5	1.5	5.0	15.0	50
Sterigmatocystein	0.01	0.1	0.3	1	3.0	10.0	30.0	100
Tentoxin	0.01	0.1	0.3	1	3.0	10.0	30.0	100
Tetrabromobisphenol A	0.02	0.2	0.6	2	6.0	20.0	60.0	200
Toxin HT 2	0.01	0.1	0.3	1	3.0	10.0	30.0	100
Toxin T2	0.01	0.1	0.3	1	3.0	10.0	30.0	100
trans-3-OH-cotinine	0.08	0.8	2.4	8	24.0	80.0	240.0	800
Triclosan	0.01	0.1	0.3	1	3.0	10.0	30.0	100
Xanthohumol	0.01	0.1	0.2	0.5	1.5	5.0	15.0	50
Zearalanone	0.01	0.1	0.3	1	3.0	10.0	30.0	100
Zearalenone	0.01	0.1	0.3	1	3.0	10.0	30.0	100
Zearalenone-14-glucuronide	0.01	0.1	0.3	1	3.0	10.0	30.0	100
Zearalenone-14-sulfate	0.01	0.1	0.3	1	3.0	10.0	30.0	100

Table S3 Concentrations of ¹³C-labeled analytes in the internal standard mix

Compound	Concentration [ng/mL]
¹³ C ₁₂ -Bisphenol A	100
¹³ C ₁₈ - Zearalenone	200
¹³ C ₄ -Monobutyl phthalate	800
¹³ C ₄ -MEHP	800
¹³ C ₃ -Estradiol	400
¹³ C ₆ -4-tert-octylphenol	500
¹³ C ₆ -Butylparaben	100
¹³ C ₆ -Ethylparaben	100
¹³ C ₆ -Methylparaben	100
¹³ C ₆ -p-Hydroxybenzoic acid	8000
¹³ C ₆ -Propylparaben	100
¹³ C ₈ -PFOA	100
¹³ C ₈ -PFOS	100
¹³ C ₁₅ -Deoxynivalenol	400
¹³ C ₁₇ -Aflatoxin M1	20

Table S4 Average peak area of individual endogenous metabolites (analysed with the HILIC column) and xenobiotics (analysed with the RP column) measured with different eluent/column combinations. The average peak area over all analytes was calculated for each combination for the selection of the best column/eluent combination. The highest value is highlighted in bold.

	Average Area							
	Comb.1	Comb.2	Comb.3	Comb.5	Comb.1	Comb.2	Comb.3	Comb.5
	Solvent				Urine			
Endogenous metabolites (HILIC)								
Alanine	2.59E+0 8	2.16E+0 8	1.54E+0 8	1.10E+0 8	6.34E+0 9	4.33E+0 9	3.78E+0 9	2.30E+0 9
Glutamine	3.65E+0 8	4.22E+0 8	1.38E+0 8	6.33E+0 8	4.16E+0 9	6.42E+0 9	4.79E+0 9	1.56E+0 9
Isoleucine	1.73E+0 8	4.47E+0 8	3.60E+0 8	1.21E+0 8	1.26E+0 9	9.00E+0 8	1.17E+0 9	1.18E+0 9
Phenylalanine	3.81E+0 8	3.41E+0 8	2.40E+0 8	2.70E+0 8	9.70E+0 8	1.27E+0 9	1.91E+0 9	1.76E+0 9
Glutathione reduced	2.38E+0 5	1.89E+0 6	5.89E+0 5	3.46E+0 5	1.12E+0 7	1.26E+0 7	7.69E+0 6	5.26E+0 6
Methionine sulfone	1.37E+0 8	1.61E+0 8	1.06E+0 8	1.00E+0 8	1.71E+0 8	1.71E+0 8	1.93E+0 8	3.66E+0 7
N-Acetyl-serine	3.96E+0 8	2.80E+0 8	2.70E+0 8	9.45E+0 7	1.41E+0 9	7.23E+0 8	1.13E+0 8	4.31E+0 8
Glutamate	4.81E+0 7	5.51E+0 7	3.95E+0 7	1.65E+0 7	1.48E+0 8	1.83E+0 8	1.58E+0 8	5.73E+0 7
Carnitine	1.28E+1 0	1.31E+1 0	1.41E+1 0	1.11E+1 0	8.48E+1 0	9.68E+1 0	1.02E+1 1	2.08E+1 0
NAD+	5.72E+0 7	9.38E+0 7	7.07E+0 7	4.14E+0 7	1.84E+0 7	2.67E+0 7	2.15E+0 7	2.92E+0 7
Pseudouridine	3.23E+0 8	2.64E+0 8	1.82E+0 8	5.96E+0 7	4.86E+0 9	5.43E+0 9	4.47E+0 9	2.12E+0 9
2-dAMP	4.77E+0 8	2.25E+0 8	1.24E+0 8	2.09E+0 8	1.15E+0 8	9.32E+0 7	3.73E+0 7	4.20E+0 7
alpha-Ketoglutarate	1.20E+0 8	8.26E+0 7	8.99E+0 7	4.11E+0 7	3.23E+0 9	5.80E+0 9	2.79E+0 9	1.11E+0 9
Kynurenine	3.23E+0 8	3.23E+0 8	1.80E+0 8	2.39E+0 8	1.63E+0 8	4.87E+0 7	1.32E+0 8	1.83E+0 8
Adenosine	3.19E+0 9	3.94E+0 9	4.21E+0 9	3.82E+0 9	6.27E+0 8	1.22E+0 9	9.70E+0 8	1.88E+0 8
3-Methylcytidine	4.25E+0 9	6.64E+0 7	n.d.	3.42E+0 9	9.14E+0 8	2.51E+0 8	n.d.	3.38E+0 8
UDP	3.56E+0 7	6.50E+0 7	4.59E+0 7	1.04E+0 7	2.48E+0 7	3.05E+0 7	3.03E+0 7	6.71E+0 6
GMP	3.23E+0 7	7.13E+0 7	5.38E+0 7	9.55E+0 6	3.11E+0 7	2.74E+0 7	1.98E+0 7	3.52E+0 5
Citric acid	7.15E+0 8	4.42E+0 7	n.d.	6.22E+0 8	6.87E+1 0	7.80E+1 0	8.04E+1 0	5.57E+1 0
Fumarate	1.02E+0 8	1.55E+0 8	1.12E+0 8	6.63E+0 7	1.84E+0 8	3.06E+0 8	3.32E+0 8	1.63E+0 8
Succinate	6.88E+0 7	4.03E+0 8	3.09E+0 8	1.82E+0 8	5.06E+0 8	1.16E+0 9	5.94E+0 8	1.43E+0 9
Phosphocreatine	2.21E+0 7	2.78E+0 7	n.d.	3.38E+0 7	2.31E+0 7	n.d.	n.d.	4.97E+0 7
Gluconate	5.27E+0 8	2.52E+0 8	1.55E+0 8	1.24E+0 8	1.33E+1 0	8.36E+0 9	1.83E+0 9	1.38E+1 0
Ribose	2.27E+0 6	4.47E+0 6	3.74E+0 6	5.68E+0 6	1.16E+0 9	1.23E+0 9	1.17E+0 9	1.12E+0 9

	4.42E+0			4.69E+0	3.87E+1			2.85E+1
Choline chloride	9	n.d.	n.d.	9	0	n.d.	n.d.	0
Average	1.17E+0	8.78E+0	9.95E+0	1.04E+0	9.27E+0	9.25E+0	9.42E+0	5.32E+0
	9	8	8	9	9	9	9	9

Xenobiotics (RP)

Aflatoxin_B1	4.33E+0	5.04E+0	5.16E+0	3.00E+0	3.56E+0	2.88E+0	3.45E+0	2.11E+0
	8	8	8	8	8	8	8	8
Alternariol	2.97E+0	6.21E+0	6.72E+0	2.42E+0	1.69E+0	7.55E+0	6.30E+0	1.68E+0
	8	8	8	8	8	8	8	8
Ochratoxin A	1.08E+0	1.26E+0	1.03E+0	3.42E+0	4.41E+0	9.40E+0	8.64E+0	4.20E+0
	7	7	7	6	6	6	6	5
Toxin T2	1.31E+0	5.53E+0	5.54E+0	3.27E+0	3.87E+0	1.23E+0	4.84E+0	8.85E+0
	6	6	6	6	5	7	7	6
2-Hydroxyestradiol	2.51E+0	1.50E+0	1.74E+0	7.93E+0	3.22E+0	1.78E+0	1.77E+0	9.44E+0
	8	9	9	7	8	9	9	7
2-Methoxyestrone	6.34E+0	2.57E+0	3.08E+0	1.72E+0	8.48E+0	5.14E+0	2.98E+0	3.26E+0
	7	8	8	5	7	8	8	5
2-Naphtol	1.82E+0	9.22E+0	1.32E+0	9.61E+0	2.64E+0	1.07E+0	1.44E+0	1.12E+0
	8	8	9	7	8	9	9	8
8-Prenylnaringenin	3.04E+0	7.85E+0	7.22E+0	2.46E+0	2.70E+0	1.55E+0	6.89E+0	2.15E+0
	7	7	7	7	7	8	7	7
Alpha-zearalenol	4.16E+0	1.81E+0	1.47E+0	6.44E+0	4.11E+0	2.42E+0	1.31E+0	5.45E+0
	8	9	9	8	8	9	9	8
Anisodamine	3.55E+0	3.72E+0	4.06E+0	2.94E+0	1.36E+0	9.82E+0	6.76E+0	5.59E+0
	9	9	9	9	9	8	8	8
Benzophenone 2	3.06E+0	3.89E+0	5.77E+0	1.35E+0	8.87E+0	1.96E+0	4.41E+0	1.19E+0
	8	8	8	8	7	8	8	7
Bisphenol_A	2.82E+0	2.52E+0	2.51E+0	4.23E+0	3.32E+0	2.16E+0	1.79E+0	4.71E+0
	7	8	8	5	7	8	8	5
Cotinine	5.52E+0	4.35E+0	4.09E+0	3.44E+0	1.98E+0	1.16E+0	1.29E+0	9.20E+0
	9	9	9	9	9	9	9	8
Coumestrol	5.88E+0	8.24E+0	1.04E+0	3.23E+0	2.57E+0	1.27E+0	1.14E+0	2.18E+0
	8	8	9	8	8	9	9	8
Enterolactone	5.19E+0	5.14E+0	4.97E+0	1.99E+0	4.03E+0	6.57E+0	5.03E+0	1.57E+0
	8	8	8	8	8	8	8	8
Estrone	2.44E+0	1.99E+0	1.95E+0	n.d.	2.85E+0	4.34E+0	2.04E+0	n.d.
	7	8	8	n.d.	7	8	8	n.d.
Ethylparaben	3.67E+0	4.78E+0	5.17E+0	3.12E+0	4.46E+0	5.46E+0	5.42E+0	2.45E+0
	7	8	8	8	7	8	8	8
Fenarimol	3.22E+0	1.97E+0	5.35E+0	2.03E+0	3.13E+0	6.50E+0	2.60E+0	1.62E+0
	7	7	7	7	7	6	7	7
Jacobine	2.52E+0	3.17E+0	3.31E+0	2.33E+0	2.45E+0	1.06E+0	1.69E+0	2.22E+0
	9	9	9	9	8	9	9	8
Methiocarb	2.71E+0	3.96E+0	4.20E+0	2.19E+0	2.63E+0	2.92E+0	2.74E+0	1.98E+0
	8	8	8	7	8	8	8	7
PFOS	2.37E+0	2.11E+0	1.93E+0	1.22E+0	1.01E+0	1.20E+0	1.12E+0	7.42E+0
	9	9	9	9	9	9	9	8
p-Hydrobenzoic acid	2.52E+0	1.94E+1	1.71E+1	7.92E+0	2.59E+0	6.37E+0	8.13E+0	2.16E+0
	9	0	0	9	9	9	9	9
Tetrabrombisphenol A	1.87E+0	2.70E+0	2.70E+0	1.47E+0	2.34E+0	1.67E+0	2.29E+0	1.29E+0
	6	7	7	7	6	7	7	7
Xanthohumol	2.44E+0	1.46E+0	6.62E+0	4.60E+0	2.23E+0	1.26E+0	1.29E+0	4.12E+0
	8	8	8	8	8	8	8	8
Zearalenon-14-glucuronide	1.40E+0	2.70E+0	2.01E+0	6.80E+0	1.09E+0	1.94E+0	1.58E+0	1.45E+0
	7	7	7	6	7	7	7	6
Average	8.09E+0	1.67E+0	1.63E+0	8.63E+0	4.09E+0	8.63E+0	8.92E+0	2.86E+0
	8	9	9	8	8	8	8	8

Table S5 Limit of detection (LOD), retention time and the detected adducts (with the most abundant one in bold) in solvent and two complex biological matrices (urine and plasma) for the xenobiotics and human estrogens measured on the reverse phase column

Compound	Neutral exact mass [m/z]	Species	Retention time [min]			LOD [$\mu\text{g/L}$]		
			Solvent	Plasma	Urine	Solvent	Plasma	Urine
1-OH-pyrene	218.0732	[M-H]⁻ [M+H] ⁺	11.3	11.3	7.5	4.13	4.57	1.89
16-Epiestriol	288.1725	[M-H]⁻	7.5	7.5	7.6	0.21	2.08	4.19
16-Hydroxyestrone	286.1569	[M-H]⁻	7.6	7.6	7.8	0.36	0.45	2.61
17-Epiestriol	288.1725	[M-H]⁻	7.8	7.7	11.3	0.20	0.23	3.40
2-Hydroxyestradiol	288.1725	[M-H]⁻	8.2	8.5	9.7	0.88	70.8	12.8
2-Methoxyestrone	300.1725	[M-H]⁻ [M+H] ⁺	10.4	10.4	11.0	0.16	1.36	0.79
2-Naphtol	302.1882	[M-H]⁻	8.7	8.6	8.2	0.21	0.23	5.42
2-Methoxyestradiol	150.1045	[M-H]⁻	9.7	9.7	10.4	0.83	2.20	1.22
2-tert-Butylphenol	240.1514	[M-H]⁻	11.0	11.0	8.6	0.08	0.09	1.73
3-Benzylidencampher	144.0575	[M+H]⁺	12.5	12.5	12.5	0.20	0.59	2.33
4-Hydroxyestrone	302.1882	[M-H]⁻	9.0	7.6	9.0	0.07	31.50	0.08
4-Methoxyestradiol	286.1569	[M-H]⁻	9.4	9.4	9.4	2.17	2.39	1.53
4-Methoxyestrone	300.1725	[M-H]⁻ [M+H] ⁺	10.2	10.2	10.2	0.18	0.19	0.22
4-Methylbenzylidencampher	254.1671	[M+H]⁺	12.7	12.7	12.7	0.08	0.45	0.81
4-octylphenol	206.1671	[M-H]⁻	12.7	12.7	12.7	0.42	0.50	0.50
4-tert-octylphenol	206.1671	[M-H]⁻	12.3	12.3	12.3	0.41	0.46	0.53
8-Prenylnaringenin	340.1311	[M-H]⁻ [M+H] ⁺	10.0	10.0	10.0	0.04	0.46	0.36
Aflatoxicol	296.0685	[M+H]⁺	8.1	8.1	8.1	0.02	0.22	2.64
Aflatoxin B1	312.0634	[M+H]⁺ , [M-H] ⁻	7.8	7.8	7.8	0.04	0.05	3.52
Aflatoxin B2	314.0790	[M+H]⁺ , [M-H] ⁻	7.4	7.4	7.4	0.04	0.05	0.05
Aflatoxin G1	328.0583	[M+H]⁺ , [M-H] ⁻	7.4	7.4	7.4	0.05	0.05	0.05
Aflatoxin G2	330.0740	[M+H]⁺ , [M-H] ⁻	6.9	6.9	6.9	0.004	0.07	0.39
Aflatoxin M1	328.0583	[M+H]⁺ , [M-H] ⁻	6.5	6.4	6.4	0.004	0.01	0.03
Aflatoxin M2	330.0740	[M+H]⁺ , [M-H] ⁻	6.1	6.0	6.0	0.05	0.47	0.38
Aflatoxin P1	298.0477	[M-H]⁻ [M+H] ⁺	6.2	4.3	6.2	0.04	4.50	0.04
Alpha-zearalanol	322.1780	[M-H]⁻ [M+H] ⁺	9.1	9.1	9.1	0.04	0.43	0.39
Alpha-zearalenol-14-glucuronide	320.1624	[M-H]⁻ [M+H] ⁺	5.2	4.7	9.3	4.96	4.91	0.34
Alpha-zearalenol	496.1945	[M-H]⁻ [M+H] ⁺	9.3	9.3	5.2	0.05	0.50	7.02

Alternariol	258.0528	[M-H] ⁻ , [M+H] ⁺	8.2	7.2	8.1	0.03	0.05	0.45
Alternariol monomethylether	272.0685	[M-H] ⁻ , [M+H] ⁺	10.2	10.2	10.2	0.04	0.04	0.06
Anisodamine	305.1627	[M+H] ⁺	4.1	5.4	4.2	0.04	0.47	3.98
Beauvericin	783.4095	[M+NH4] ⁺	13.6	13.6	13.6	0.23	0.26	1.89
Benzophenone 1	214.0630	[M-H] ⁻ , [M+H] ⁺	9.4	9.3	9.4	0.04	0.05	0.04
Benzophenone 2	246.0528	[M-H] ⁻	7.1	5.6	7.1	0.02	0.25	0.17
Benzylbutylphthalate	312.1362	[M+H] ⁺	12.4	12.4	12.4	0.22	1.11	1.93
Benzylparaben	228.0786	[M-H] ⁻	9.9	9.9	9.9	0.05	0.05	0.38
Beta-zearalanol	322.1780	[M-H] ⁻ , [M+H] ⁺	8.5	8.5	8.5	0.04	0.06	0.40
Beta-zearalenol-14-glucuronide	320.1624	[M-H] ⁻ , [M+H] ⁺	4.8	4.1	8.6	4.92	4.40	0.32
Beta-zearalenol	496.1945	[M-H] ⁻ , [M+H] ⁺	8.6	8.6	4.7	0.04	0.12	44.37
Bisphenol A	228.1150	[M-H] ⁻	8.9	8.9	8.9	0.04	0.44	0.05
Bisphenol AF	336.0585	[M-H] ⁻	10.2	10.1	10.2	0.18	0.22	0.25
Bisphenol B	242.1307	[M-H] ⁻	9.6	9.6	9.6	0.34	0.45	3.94
Bisphenol C	256.1463	[M-H] ⁻	10.3	10.2	10.3	0.10	0.12	0.70
Bisphenol F	200.0837	[M-H] ⁻	7.8	7.8	7.8	0.08	0.13	8.19
Bisphenol S	250.0300	[M-H] ⁻	6.3	5.8	6.2	0.03	0.13	0.24
Butylparaben	194.0943	[M-H] ⁻	9.9	9.8	9.8	0.04	0.05	0.03
Citrinin	250.0841	[M+H] ⁺ , [M-H] ⁻	5.2	4.6	5.2	0.03	0.47	3.99
Cotinine	176.0950	[M+H] ⁺	3.6	3.5	3.5	0.40	5.79	3.37
Coumestrol	268.0372	[M-H] ⁻ , [M+H] ⁺	7.9	7.2	7.9	0.04	0.44	0.42
Daidzein	254.0579	[M-H] ⁻ , [M+H] ⁺	6.8	5.8	6.8	0.02	0.02	0.57
Deoxynivalenol	296.1260	[M-H] ⁻ , [M+H] ⁺	2.8	3.3	3.4	0.21	6.96	48.24
Dibutylphthalate	278.1518	[M+H] ⁺	12.5	12.5	12.5	5.74	3.82	5.51
E2-17-GlcA	448.2097	[M-H] ⁻	5.2	4.6	5.1	2.25	23.23	5.20
Enterodiol	302.1518	[M-H] ⁻	6.8	6.8	6.8	0.02	0.21	0.19
Enterolactone	298.1205	[M-H] ⁻ , [M+H] ⁺	8.1	8.1	8.1	0.04	0.05	0.34
Equol	242.0943	[M-H] ⁻ , [M+H] ⁺	8.0	7.9	7.9	0.06	0.43	4.00
Estradiol-3-sulfate	272.1776	[M-H] ⁻	6.2	5.8	9.2	0.10	0.84	0.63
Estradiol	278.1518	[M-H] ⁻	9.2	9.2	6.2	0.05	0.85	0.73
Estriol	352.1344	[M-H] ⁻	6.5	6.5	6.5	0.07	0.98	0.88
Estrone	288.1725	[M-H] ⁻	9.9	9.9	9.9	0.34	0.45	0.41
Ethinylestradiol	270.1620	[M-H] ⁻	9.7	9.7	9.7	0.23	0.26	2.50
Ethylparaben	296.1776	[M-H] ⁻	7.7	7.5	7.6	0.02	0.26	0.07
Fenarimol	330.0327	[M+H] ⁺ , [M-H] ⁻	10.5	10.4	10.5	0.41	0.48	0.73

Formononetin	268.0736	[M+H] ⁺ , [M-H] ⁻	8.8	8.7	8.7	0.01	0.23	0.15
Fumonisin B1	721.3885	[M+H] ⁺ , [M-H] ⁻	6.1	4.3	6.1	0.39	4.47	9.62
Genistein	270.0528	[M-H] ⁻ , [M+H] ⁺	7.9	7.1	7.9	0.02	0.05	2.10
Glycitein	284.0685	[M-H] ⁻ , [M+H] ⁺	6.9	6.0	6.9	0.02	2.22	1.93
Isobutylparaben	194.0943	[M-H] ⁻	9.8	9.8	9.8	0.02	0.02	0.19
Isoxanthohumol	354.1467	[M-H] ⁻ , [M+H] ⁺	8.7	8.8	8.8	0.04	0.45	0.45
Jacobine-N-oxide	351.1682	[M+H] ⁺ , [M-H] ⁻	3.7	3.6	4.2	0.38	0.49	7.30
Jacobine	367.1631	[M+H] ⁺	4.6	4.2	3.6	0.04	0.33	3.68
Matairesinol	358.1416	[M-H] ⁻ , [M+H] ⁺	8.0	7.9	8.0	0.09	0.90	6.69
MEHP	278.1518	[M-H] ⁻ , [M+H] ⁺	9.1	9.1	9.1	0.82	1.27	11.76
Methiocarb	225.0823	[M+H] ⁺	10.2	10.2	10.2	0.17	1.36	0.70
Methylparaben	152.0473	[M-H] ⁻	6.5	5.6	6.5	0.06	0.12	0.24
Mono_buty_phthalate	222.0892	[M-H] ⁻ , [M+H] ⁺	5.2	3.8	5.2	0.10	0.45	0.59
n-Butylbenzolsulfonamid	213.0823	[M-H] ⁻ , [M+H] ⁺	9.5	9.5	9.5	0.19	0.24	0.23
Nivalenol	312.1209	[M-H] ⁻ , [M+H] ⁺	1.4	1.8		0.67	21.21	>30.00
Nonylphenol	220.1827	[M-H] ⁻	12.7	12.7	12.7	0.87	0.70	0.97
Ochratoxin A	403.0823	[M-H] ⁻ , [M+H] ⁺	7.0	5.9	7.1	0.41	4.50	0.58
Ochratoxin Alpha	369.1212	[M-H] ⁻ , [M+H] ⁺	4.9	4.2	4.9	0.41	0.73	1.43
Ochratoxin B	256.0139	[M-H] ⁻ , [M+H] ⁺	6.1	5.0	6.0	0.03	0.46	0.41
Octylmethoxycinnamate	290.1882	[M+H] ⁺	13.1	13.1	13.1	2.83	38.78	18.89
p-Hydrobenzoic_acid	138.0317	[M-H] ⁻	1.8	1.7	8.1	0.23	0.2	0.15
PFOA	413.9737	[M-H] ⁻	8.1	7.9	9.6	0.20	0.23	0.13
PFOS	499.9375	[M-H] ⁻	9.6	9.4	6.8	0.09	1.36	0.34
PhIP	224.1062	[M+H] ⁺ , [M-H] ⁻	6.8	6.8	1.8	0.04	0.38	10.33
Prochloraz	375.0308	[M+H] ⁺	11.7	11.7	11.7	0.04	0.46	0.52
Propylparaben	180.0786	[M-H] ⁻ , [M+H] ⁺	8.9	8.8	8.9	0.01	0.02	0.02
Resveratrol	228.0786	[M-H] ⁻ , [M+H] ⁺	6.6	6.5	6.6	0.41	2.36	0.55
Riddeliin-N-oxide	349.1525	[M+H] ⁺ , [M-H] ⁻	3.6	3.5	4.1	0.19	3.18	3.24
Riddeliin	365.1475	[M+H] ⁺ , [M-H] ⁻	3.9	4.6	3.5	0.05	0.38	1.75
Scolpolamine	303.1471	[M+H] ⁺ , [M-H] ⁻	4.6	4.6	4.4	0.02	0.23	1.77
Sterigmatocystein	324.0634	[M+H] ⁺ , [M-H] ⁻	10.8	10.8	10.8	0.04	0.46	0.53

Tentoxin	414.2267	[M+H] ⁺ , [M-H] ⁻	8.3	8.2	8.3	0.04	0.50	4.06
Tetrabrombisphenol A	539.7571	[M-H] ⁻	12.2	12.2	12.2	1.27	8.50	7.32
Toxin T2	466.2203	[M+H] ⁺	9.8	9.8	9.8	0.40	4.81	4.55
trans-3-OH-cotinine	192.0899	[M+H] ⁺	2.0	2.0	2.0	0.38	3.51	14.01
Triclosan	287.9512	[M-H] ⁻	12.2	12.2	12.2	0.05	0.43	0.43
Xanthohumol	354.1467	[M-H] ⁻ , [M+H] ⁺	11.6	11.6	11.5	0.01	0.20	0.16
Zearalanone	318.1467	[M-H] ⁻ , [M+H] ⁺	10.2	10.2	10.2	0.04	0.05	0.05
Zearalenone-14- glucuronide	320.1624	[M-H] ⁻	5.7	5.2	5.7	0.39	5.01	0.36
Zearalenone-14-sulfate	494.1788	[M-H] ⁻	6.9	6.6	6.9	0.08	0.44	21.05
Zearalenone	398.1035	[M-H] ⁻ , [M+H] ⁺	10.3	10.3	10.3	0.04	0.21	0.42

Table S6 Limit of detection (LOD), retention time and the detected adducts with the most abundant one in bold in solvent and two matrices (urine and plasma) for endogenous metabolites on the HILIC column. Not detected compounds are marked with n.d. (not detected) and bg indicates analytes where the background signal was too high for LOD determination

Compound	Neutral exact mass [m/z]	Species	Retention time [min]			LOD [μ M]		
			Solvent	Urine	Plasma	Solvent	Urine	Plasma
1-Methylhydantoin	114.0429	[M-H]⁻	5.2	5.2	5.2	0.09	bg	3
1-Methylnicotinamide	136.0637		Not detected					
2-(Carbamoylamino)butanedioic acid	176.0433	[M-H]⁻ ; [M+H]⁺	3.9	4.3	4.9	0.2	1	0.3
2'-Deoxyadenosine 5'-monophosphate	331.0682	[M+H]⁺ ; [M-H]⁻	2	2.1	2.6	0.003	0.4	0.05
2'-Deoxycytidine	227.0906	[M-H]⁻ ; [M+H]⁺	2.7	2.7	2.7	0.004	0.3	0.4
2-Deoxycytidine 5'-Monophosphate	307.0569	[M-H]⁻ ; [M+H]⁺	3.3	4	4.6	0.01	0.3	0.3
2'-Deoxyuridine	228.0746	[M-H]⁻ ; [M+H]⁺	2	2	2	0.01	0.03	0.03
2-Phosphoglyceric acid + 3-Phosphoglyceric acid	185.9929	[M-H]⁻ ; [M+H]⁺		8.0-8.7		0.03	0.3	0.3
3'AMP	347.0631	[M+H]⁺ ; [M-H]⁻	2.1	2.2	4.2*	0.01	3	0.3
3-Methyl-2-oxovaleric acid	130.0630	[M-H]⁻	1.1	1.2	1.1	0.02	0.08	bg
3-Methylcytidine	257.1012	[M-H]⁻ ; [M+H]⁺	2.4	2.2	2.1	1	bg	1
4-Hydroxy-proline	131.0582	[M-H]⁻ ; [M+H]⁺	4.4	4.4	4.3	0.05	0.2	0.05
5'AMP	347.0631	[M+H]⁺ ; [M-H]⁻	2.5	2.6	4.2*	0.01	0.3	0.03
5'-Deoxy-5'-Methylthioadenosine	297.0896	[M+H]⁺ ; [M-H]⁻	1.6	1.6	1.6	0.004	0.004	0.005
5-Methyluridine	258.0852	[M-H]⁻ ; [M+H]⁺	2	2	2	0.004	0.04	0.05
6-Phosphogluconate	276.0246	[M-H]⁻ ; [M+H]⁺	8.5-8.7	8-8.4	7.5-8.2	0.1	0.3	0.3
Adenine	135.0545	[M+H]⁺ ; [M-H]⁻	2.3	2.3	2.3	0.004	0.01	0.004
Adenosine	267.0968	[M+H]⁺ ; [M-H]⁻	2.1	2.2	2.1	0.004	0.01	0.006
Adenosine 3',5'-cyclic monophosphate	329.0525	[M-H]⁻ ; [M+H]⁺	1.9	1.9	1.9	0.004	0.3	0.05
Adenosine 5'-triphosphate	506.9957	[M+H]⁺ ; [M-H]⁻	9.0-9.4	8.9-9.1	n.d.	0.3	0.3	n.d.
Adenosine diphosphate	427.0294	[M-H]⁻ ; [M+H]⁺	8.7-9	8.5-8.7	8.3-8.6	0.3	0.5	0.3
Alanine	89.0477	[M+H]⁺ ; [M-H]⁻	4.6	4.5	4.7	0.4	bg	bg
alpha-Amino adipic acid	161.0688	[M+H]⁺ ; [M-H]⁻	4	4	4.8	0.04	bg	bg
alpha-Ketoglutarate	146.0215	[M-H]⁻	2.8	2.9	3.3	0.04	bg	bg
Arginine	174.1117	[M-H]⁻ ; [M+H]⁺	No calibration possible					
Argininosuccinic acid	290.1226	[M+H]⁺ ; [M-H]⁻	5	5.2	5.2	0.004	0.2	0.02
Asparagine	132.0535	[M-H]⁻ ; [M+H]⁺	5.1	5.2	5.2	0.04	bg	0.2

Compound	Neutral exact mass [m/z]	Species	Retention time [min]			LOD [μ M]		
			Solvent	Urine	Plasma	Solvent	Urine	Plasma
Aspartate	133.0375	[M-H] ⁻ , [M+H] ⁺	4.1	4.2	4.8	0.04	0.3	0.4
Betaine	117.0790	[M+H] ⁺ , [M-H] ⁻	2.8	2.7	2.8	0.04	bg	bg
Biotin	244.0882	[M+H] ⁺ , [M-H] ⁻	1.5	1.4	1.3	0.002	0.03	0.02
Carnitine	161.1052	[M+H] ⁺	4.1	4.1	4	0.03	bg	bg
Choline chloride	104.1075		Not detected					
cis-Aconitate	174.0164	[M-H] ⁻	3.2-3.4	3.3-3.5	5-5.1	0.04	bg	bg
Citrate + Isocitrate	192.0270	[M-H] ⁻	8.0-8.9	4.9-5	7.2-8.2**	1	bg	1
CMP	323.0519	[M-H] ⁻ , [M+H] ⁺	4.2	4.2	4.8	0.04	0.3	0.2
Cysteic acid	169.0045	[M-H] ⁻ , [M+H] ⁺	3.9-4.1	4.3	4.8	0.01	0.03	0.1
Cysteine	121.0197	[M-H] ⁻ , [M+H] ⁺	6.2	n.d.	n.d.	1	bg	bg
Cysteinyl-glycine	178.0412	[M-H] ⁻ , [M+H] ⁺	5.7	5.7	5.7	6	bg	bg
Cystine	240.0238	[M+H] ⁺ , [M-H] ⁻	6.4	6.4	6.4	0.4	bg	bg
Cytidine	243.0855	[M+H] ⁺ , [M-H] ⁻	3.4	3.3	3.3	0.03	0.03	0.1
Cytidine 5'-triphosphate	482.9845	[M+H] ⁺ , [M-H] ⁻	8.7	8.8	n.d.	0.4	2	n.d.
Cytosine	111.0433	[M+H] ⁺ , [M-H] ⁻	3.4	3.3	3.3	0.01	1	0.1
Deoxyguanosine triphosphate	506.9957	[M+H] ⁺ , [M-H] ⁻	9.1	9.1	n.d.	0.3	1	n.d.
Dihydroxyacetonephosphate	169.9980	[M-H] ⁻ , [M+H] ⁺	3.6	3.9	4.8	0.4	0.4	2.5
Dihydroxyisovalerate	134.0579	[M-H] ⁻	1.3	1.4	1.3	0.03	0.03	0.03
Erythritol	122.0579	[M-H] ⁻	3.1	3.1	3.1	0.04	bg	0.4
Erythrose-4-phosphate	200.0086	[M-H] ⁻	3.6-4.6	4-4.9	5.1-5.2	0.4	bg	1.7
Flavinadenin dinucleotide	785.1571	[M+H] ⁺ , [M-H] ⁻	1.8	2.2	2.2	0.4	0.4	0.5
Hexose (Fructose, Galactose, Mannose, Glucose, Inositol)	180.0634	[M-H] ⁻	5.5	5.4	5.5	0.5	bg	bg
Fructose-1,6-bisphosphate	339.9961	[M-H] ⁻ , [M+H] ⁺	9	8.6	n.d.	0.3	1	n.d.
Hexose-6-phosphate (Fructose-6-phosphate, Glucose-1-phosphate, Glucose-6-phosphate)	260.0297	[M-H] ⁻ , [M+H] ⁺	4.5-5	4.9-5	5.1-5.2	0.04	0.01	0.04
Fumarate	116.0110	[M-H] ⁻	4.3	4.4	5	0.4	0.6	0.04
Gluconate	196.0583	[M-H] ⁻	3.1-3.4	4	4.7	0.04	bg	0.5
Glutamate	147.0532	[M-H] ⁻ , [M+H] ⁺	4	4.1	4.8	0.4	0.4	bg
Glutamine	146.0691	[M+H] ⁺ , [M-H] ⁻	4.9	4.9	4.9	0.04	bg	bg
Glutamyl-cysteine	250.0623	[M+H] ⁺ , [M-H] ⁻	3.1	3.2	5.5	0.4	bg	bg
Glutathione, oxidized	612.1519	[M+H] ⁺ , [M-H] ⁻	5.3	5.3	5.5	0.4	1	0.5
Glutathione, reduced	307.0838	[M-H] ⁻ , [M+H] ⁺	3.1-3.7	3.3-4	5.4	0.5	0.5	1
Glycine	75.0320	[M-H] ⁻ , [M+H] ⁺	5.1	5.1	5.1	0.4	bg	bg

Compound	Neutral exact mass [m/z]	Species	Retention time [min]			LOD [μ M]		
			Solvent	Urine	Plasma	Solvent	Urine	Plasma
Glyoxylic acid	74.0004		Not detected					
GMP	363.0580	[M-H] ⁻ , [M+H] ⁺	4.7	5	5.1	0.04	0.4	0.05
Guanidineacetic acid	117.0538	[M+H] ⁺ , [M-H] ⁻	4.8	5	5	0.4	bg	0.4
Guanine	151.0494	[M+H] ⁺ , [M-H] ⁻	3.5	3.5	3.4	0.004	0.01	0.01
Guanosine + Isoguanosine	283.0917	[M+H] ⁺ , [M-H] ⁻	3.6-3.8	3.6-3.8	3.6-3.8	0.01	0.30	0.01
Guanosine 3',5'-cyclic monophosphate	345.0474	[M+H] ⁺ , [M-H] ⁻	2.6	2.6	2.6	0.004	0.3	0.5
Guanosine 5'-diphosphate	443.0243	[M-H] ⁻ , [M+H] ⁺	8.8-9.0	8.5-8.8	8.8	0.3	0.3	30
Guanosine 5'-triphosphate	522.9907	[M+H] ⁺ , [M-H] ⁻	8.7	8.7	n.d.	0.4	1.6	n.d.
Histidine	155.0695	[M+H] ⁺ , [M-H] ⁻	7.6	6.9	7.1	0.05	bg	bg
Homocysteine	135.0354	[M+H] ⁺ , [M-H] ⁻	4.2-5.9	4.2.59	4.3-5.8	0.3	0.3	1
Homoserine + Threonine	119.0582	[M+H] ⁺ , [M-H] ⁻	4.8-5	4.8-5	4.7-5	0.04	bg	bg
Hydroxyglutaric acid	148.0372	[M-H] ⁻	2.6	2.7	3.5	0.04	bg	0.4
Inosine	268.0808	[M-H] ⁻ , [M+H] ⁺	2.8	2.7	2.7	0.01	0.3	0.03
Inosine 5'-monophosphate	348.0471	[M-H] ⁻ , [M+H] ⁺	3.8	4.1	4.8	0.03	0.3	0.4
Isoleucine + Leucine	131.0946	[M-H] ⁻ , [M+H] ⁺	2.8-3	2.6-2.7	2.8-2.9	0.04	bg	bg
Ketoisovalerate	116.0473	[M-H] ⁻	1.2	1.3	1.2	0.02	0.8	0.3
Kynurenine	208.0848	[M+H] ⁺ , [M-H] ⁻	3	3	2.9	0.004	0.2	0.03
Lactate	90.0317	[M-H] ⁻	1.7	1.7	1.7	0.5	0.6	2
L-Citrulline	175.0957	[M+H] ⁺ , [M-H] ⁻	5.2	5.2	5.2	0.4	bg	3
L-Cystathionine	222.0674	[M+H] ⁺ , [M-H] ⁻	6.3	6.3	6.3	0.04	0.04	0.004
L-Ornithine	132.0899	[M-H] ⁻ , [M+H] ⁺	5.2	5.2	5.2	0.007	0.36	bg
Lysine	146.1055	[M+H] ⁺ , [M-H] ⁻	12.6	12.6	12.1	1	bg	bg
Malate	134.0215	[M-H] ⁻	3.2	3.4	4.6	0.003	0.07	0.06
Mannitol	182.0790	[M-H] ⁻	4.1	4.1	4.1	0.4	bg	bg
Mannitol 1-phosphate	262.0454	[M-H] ⁻ , [M+H] ⁺	4.5	4.9	5.1	0.04	0.35	0.4
Melatonin	232.1212	[M+H] ⁺ , [M-H] ⁻	1.4	1.3	1.3	0.001	0.03	0.1
Methionine	149.0510	[M+H] ⁺ , [M-H] ⁻	3.3	3.3	3.3	0.006	0.14	bg
Methionine sulfone	181.0409	[M+H] ⁺ , [M-H] ⁻	4.2	4.3	4.2	0.01	bg	bg
Mevalonic acid	148.0736	[M-H] ⁻	1.3	1.3	1.3	0.01	1.00	0.3
N4-Acetylcytidine	285.0961	[M+H] ⁺ , [M-H] ⁻	2	1.9	1.9	0.004	0.04	0.5
N-Acetyl-Asp-Glu	304.0906	[M-H] ⁻ , [M+H] ⁺	4.7	4.7	5.2	0.04	1.00	bg
N-Acetyl-L-aspartic acid	175.0482	[M-H] ⁻ , [M+H] ⁺	2.5	2.6	2.8	0.004	bg	0.08
N-Acetyl-serine	147.0532	[M-H] ⁻ , [M+H] ⁺	1.9	1.9	2	0.003	0.3	0.05

Compound	Neutral exact mass [m/z]	Species	Retention time [min]			LOD [μ M]		
			Solvent	Urine	Plasma	Solvent	Urine	Plasma
NAD+	663.1091	[M+H] ⁺ , [M-H] ⁻	3.5	4	4.6	0.04	0.4	0.4
NADH	665.1248	[M+H] ⁺ , [M-H] ⁻	3.1	n.d.	n.d.	0.1	n.d.	n.d.
NADP+	743.0755	[M+H] ⁺ , [M-H] ⁻	6.3-6.9	6.3-6.9	6.7-7.2	0.1	1.00	1
NADPH	745.0911	[M+H] ⁺ , [M-H] ⁻	7-7.5	6.6-7.2	7.4	1	3.00	3
Nicotinamide	122.0480	[M+H] ⁺ , [M-H] ⁻	1.9	1.9	1.9	0.01	0.01	0.01
Octopamine	153.0790		Not detected					
Oxaloacetic acid	132.0059	[M-H] ⁻	5.9	n.d.	n.d.	3	n.d.	n.d.
Palmitic acid	256.2402	[M-H] ⁻ , [M+H] ⁺	1.1	1.1	1.1	n.d.	n.d.	n.d.
Phenylalanine	165.0790	[M-H] ⁻ , [M+H] ⁺	2.7	2.7	2.7	0.004	0.002	bg
Phosphocreatine	211.0358	[M+H] ⁺ , [M-H] ⁻	4.3	4.3	5.2	0.03	0.08	0.4
Proline	115.0633	[M+H] ⁺ , [M-H] ⁻	3.6	3.6	3.6	0.002	0.03	bg
Propionyl-L-carnitine	217.1314	[M+H] ⁺ , [M-H] ⁻	2.4	2.4	2.4	0.001	0.1	0.04
Pseudouridine	244.0695	[M-H] ⁻ , [M+H] ⁺	3.3	3.3	3.3	0.05	0.1	0.1
Pyruvate	88.01604	[M-H] ⁻	1.4	1.5	1.4	0.04	bg	
Ribose	150.0528	[M-H] ⁻	3.2	n.d.	n.d.	1	n.d.	n.d.
Ribose-5-phosphate + Ribulose-5-phosphate	230.0192	[M-H] ⁻ , [M+H] ⁺	3.9-4.1	4.1-4.2	4.9-5	0.04	0.06	0.4
S-(Adenosyl)-methionine	398.1372	[M+H] ⁺ , [M-H] ⁻	4.3	4.3	4.3	0.3	bg	0.4
Sarcosine	89.04768	[M+H] ⁺ , [M-H] ⁻	4.2	4.2	4.2	0.1	1	0.1
Sedoheptulose-7-phosphate	290.0403	[M-H] ⁻ , [M+H] ⁺	4.7	5	5.2	0.01	0.1	0.1
Seleno-methionine	196.9955	[M+H] ⁺ , [M-H] ⁻	3.3	3.3	3.2	0.004	0.2	0.4
Serine	105.0426	[M-H] ⁻ , [M+H] ⁺	5.3	5.2	5.3	0.2	bg	bg
Serotonine	176.0950	[M+H] ⁺ , [M-H] ⁻	1.4	1.3	1.4	0.007	0.04	0.04
Spermidine	145.1579		Not detected					
Spermine	202.2157		Not detected					
Succinate	118.0266	[M-H] ⁻	1.9	1.9	2.1	0.04	0.3	0.04
Thiamine hydrochloride	265.1123		Not detected					
Thymidine	242.0903	[M-H] ⁻ , [M+H] ⁺	1.5-1.9	1.5-1.9	1.5-1.9	0.01	0.1	0.03
Thymidine 5'-monophosphate	322.0566	[M-H] ⁻ , [M+H] ⁺	2	2.1	2.4	0.04	0.04	0.04
Thymine	126.0429	[M-H] ⁻ , [M+H] ⁺	1.9	1.9	1.9	0.003	0.06	0.04
Trehalose	342.1162	[M-H] ⁻ , [M+H] ⁺	5.1	5.1	5.1	0.04	0.2	0.05
Tryptophan	204.0899	[M-H] ⁻ , [M+H] ⁺	3.3	3.3	3.3	0.01	bg	bg
TTP (Thymidinetriphosphate)	481.9893	[M-H] ⁻ , [M+H] ⁺	8.8-9	8.7	n.d.	0.3	0.4	n.d.
Tyrosine	181.0739	[M-H] ⁻ , [M+H] ⁺	4.1	4.1	4.1	0.05	bg	bg

Compound	Neutral exact mass [m/z]	Species	Retention time [min]			LOD [μ M]		
			Solvent	Urine	Plasma	Solvent	Urine	Plasma
UMP	324.0359	[M-H] ⁻ , [M+H] ⁺	3.3	3.9	4.7	0.04	0.4	0.5
Uracil	112.0273	[M-H] ⁻ , [M+H] ⁺	2.2	2.2	2.2	0.1	bg	0.05
Uridine	244.0695	[M-H] ⁻ , [M+H] ⁺	2.4	2.4	2.4	0.05	bg	0.5
Uridine 5'-diphosphate	404.0022	[M-H] ⁻ , [M+H] ⁺	8.2-8.6	8-8.4	8.2-8.5	0.03	0.4	0.5
Uridine 5'-triphosphate	483.9685	[M-H] ⁻ , [M+H] ⁺	9	8.6- 8.8	n.d.	1	0.5	n.d.
Valine	117.078979	[M-H] ⁻ , [M+H] ⁺	3.6	3.6	3.6	0.04	bg	bg
Xanthine	152.033425	[M-H] ⁻ , [M+H] ⁺	2.6	2.7	2.7	0.5	bg	0.4
Xylose	150.052824	[M-H] ⁻	3.9	n.d.	n.d.	0.01	n.d.	n.d.

Table S7 Calibration parameter of analytes in all three matrices and used normalization method

Compound	Normalization Method	Slope	Solvent		R ²	Slope	Urine		R ²	Slope	Plasma		R ²
			Intercept	R ²			Intercept	R ²			Intercept	R ²	
Xenobiotics and endogenous estrogens													
1-OH-pyrene	Ratio to Zearalenone	1.61E-03	-9.18E-03	0.9586	3.25E-03	-3.21E-03	0.9519	0.001116	0.9519	0.001116	-1.85E-03	0.9298	
16-Epiestriol	Ratio to Ethylparaben	1.68E-02	-1.18E-03	0.9863	1.95E-02	-1.36E-02	0.8805	0.014192	0.8805	0.014192	-4.63E-03	0.9905	
16-Hydroxyestrone	Ratio to Ethylparaben	1.47E-02	1.30E-05	0.9926	1.46E-02	-4.86E-03	0.9893	0.012079	0.9893	0.012079	-2.85E-03	0.9828	
17-Epiestriol	Ratio to Ethylparaben	1.63E-02	-1.87E-03	0.9976	1.28E-02	-1.34E-02	0.993	0.013044	0.993	0.013044	-3.17E-03	0.9914	
2-Hydroxyestradiol	Ratio to PFOA	6.81E-03	-4.79E-03	0.9759	5.62E-03	-2.11E-02	0.9889	0.0002	0.9889	0.0002	-4.83E-03	0.9972	
2-Methoxyestrone	Ratio to Zearalenone	3.39E-03	-6.28E-04	0.9935	4.87E-03	-2.34E-03	0.9852	0.005489	0.9852	0.005489	-3.34E-03	0.9809	
2-Naphthol	Ratio to Propylparaben	2.19E-02	8.78E-04	0.9954	2.90E-02	-3.40E-04	0.9964	0.024809	0.9964	0.024809	4.74E-02	0.9699	
2-Methoxyestradiol	Ratio to Butylparaben	3.35E-03	-6.64E-05	0.9333	3.76E-03	4.84E-03	0.9541	0.005253	0.9541	0.005253	-6.31E-03	0.9719	
2-tert-Butylphenol	Ratio to Zearalenone	2.25E-02	7.43E-05	0.979	3.00E-02	-1.20E-02	0.9939	0.027336	0.9939	0.027336	4.27E-03	0.9975	
3-Benzylidencampher	Ratio to 4-tert-octylphenol	1.93E-02	-1.27E-04	0.8706	1.14E-02	1.37E-02	0.8856	0.011321	0.8856	0.011321	6.61E-02	0.8256	
4-Hydroxyestrone	Ratio to PFOA	3.57E-01	-3.82E-02	0.9426	3.72E-01	-4.09E-02	0.9821	0.004316	0.9821	0.004316	-8.85E-03	0.9628	
4-Methoxyestradiol	Ratio to Bisphenol A	4.19E-03	-2.86E-04	0.9947	4.35E-03	-1.14E-04	0.9912	0.006278	0.9912	0.006278	-3.96E-03	0.9956	
4-Methoxyestrone	Ratio to Zearalenone	1.56E-02	-2.67E-04	0.9874	2.06E-02	-3.84E-03	0.9948	0.026236	0.9948	0.026236	-2.46E-03	0.9816	
4-Methylbenzylidencampher	Ratio to 4-tert-octylphenol	5.00E-02	-5.72E-04	0.8719	2.23E-02	8.88E-03	0.9134	0.017001	0.9134	0.017001	8.94E-03	0.9474	
4-octylphenol	Ratio to 4-tert-octylphenol	2.65E-02	2.39E-02	0.9845	2.83E-02	1.29E-02	0.995	0.022614	0.995	0.022614	1.03E-02	0.9099	
4-tert-octylphenol	Ratio to Heavy	2.14E-02	1.06E-02	0.9982	2.41E-02	9.47E-03	0.9858	0.021099	0.9858	0.021099	3.78E-02	0.9993	
8-Prénylnaringenin	Ratio to Zearalenone	3.89E-02	-5.82E-04	0.9851	3.84E-02	-2.46E-03	0.9879	0.036337	0.9879	0.036337	-5.39E-04	0.989	
Aflatoxicol	Ratio to Methylparaben	5.50E-02	2.75E-04	0.9189	3.77E-02	-5.28E-02	0.9822	0.07386	0.9822	0.07386	-1.58E-02	0.9839	
Aflatoxin B1	Ratio to Aflatoxin M1	2.02E+00	2.91E-02	0.9187	1.30E+00	-2.46E+00	0.9051	2.1559	0.9051	2.1559	-2.10E-02	0.9343	
Aflatoxin B2	Ratio to Aflatoxin M1	2.26E+00	9.80E-03	0.9263	2.78E+00	2.81E-02	0.9737	2.175	0.9737	2.175	-6.83E-02	0.9443	
Aflatoxin G1	Ratio to Aflatoxin M1	2.00E+00	-8.54E-05	0.9402	2.43E+00	1.76E-02	0.9485	1.2168	0.9485	1.2168	-2.91E-02	0.923	
Aflatoxin G2	Ratio to Aflatoxin M1	1.94E+00	4.63E-03	0.9757	1.62E+00	-2.66E-02	0.9593	1.3938	0.9593	1.3938	-5.56E-02	0.9168	
Aflatoxin M1	Ratio to heavy	3.06E+00	-1.20E-02	0.9778	2.74E+00	-1.83E-01	0.9939	3.1011	0.9939	3.1011	-9.60E-02	0.9745	
Aflatoxin M2	Ratio to Aflatoxin M1	8.75E-01	-7.50E-03	0.8915	4.85E-01	-5.38E-02	0.9825	0.49819	0.9825	0.49819	-1.80E-02	0.9324	
Aflatoxin P1	Ratio to Methylparaben	2.25E-01	-7.78E-04	0.9923	2.81E-01	-1.26E-02	0.9446	0.08747	0.9446	0.08747	1.97E-01	0.9896	
Alpha-zearalenol	Ratio to Estradiol	9.08E-02	-1.84E-03	0.9711	7.30E-02	-2.31E-03	0.9915	0.049936	0.9915	0.049936	-1.02E-03	0.9818	
Alpha-zearalenol-14-glucuronide	Ratio to Methylparaben	8.93E-03	3.57E-03	0.8883	3.14E-03	-1.66E-03	0.9741	0.002296	0.8883	0.002296	-8.86E-03	0.9601	
Alpha-zearalenol	Ratio to Estradiol	1.08E-01	-4.39E-03	0.9629	9.28E-02	-1.66E-03	0.9916	0.082238	0.9916	0.082238	-1.08E-02	0.9177	

Alternariol	Ratio to PFOS	2.61E-01	-1.07E-03	0.9824	1.14E-01	-2.36E-03	0.9737	0.25361	-1.16E-02	0.9917
Alternariol monomethylether	Ratio to 4-tert-octylphenol	9.88E-02	-1.67E-03	0.9731	8.61E-02	-1.61E-03	0.9788	0.068212	-1.75E-03	0.9731
Anisodamine	Ratio to Methylparaben	2.55E-01	2.40E-03	0.9722	1.28E-01	-8.90E-02	0.9824	0.38523	-1.33E-02	0.8888
Aristolactam										
Calibration not possible										
Beavericin	Ratio to 4-tert-octylphenol	4.86E-02	-8.25E-03	0.9174	7.19E-02	-2.00E-01	0.98	0.032683	-8.32E-03	0.9538
Benzophenone 1	Ratio to PFOS	2.80E-01	5.32E-04	0.9872	2.67E-01	-8.19E-03	0.9772	0.28372	-2.43E-03	0.9611
Benzophenone 2	Ratio to Methylparaben	1.15E-01	-1.44E-03	0.9551	7.01E-02	-6.87E-03	0.9539	0.14632	-4.51E-02	0.9655
Benzylbutylphthalate	Ratio to 4-tert-octylphenol	3.32E-02	8.42E-03	0.9222	9.71E-03	5.39E-03	0.9617	0.008178	-4.19E-04	0.9475
Benzylparaben	Ratio to Butylparaben	6.59E-02	-3.34E-03	0.988	5.06E-02	-5.07E-03	0.9771	0.06375	-1.39E-03	0.9944
Beta-zearalanol	Ratio to Propylparaben	6.28E-02	1.17E-03	0.9024	3.42E-02	-3.48E-03	0.9906	0.051118	1.83E-03	0.9086
Beta-zearalanol-14-glucuronide	Ratio to Methylparaben	7.82E-03	-4.48E-03	0.9064	1.29E-03	1.14E-02	0.9102	0.005261	-1.67E-02	0.9513
Beta-zearalenol	Ratio to Propylparaben	5.99E-02	5.02E-04	0.8991	3.18E-02	-1.96E-03	0.9833	0.034194	-1.80E-04	0.9575
Bisphenol A	Ratio to Heavy	1.19E-02	-2.23E-05	0.9999	1.12E-02	-1.30E-03	0.9888	0.012178	4.00E-02	0.9993
Bisphenol AF	Ratio to Bisphenol A	2.80E-02	2.71E-04	0.9668	2.54E-02	-1.46E-03	0.9827	0.032505	-8.16E-04	0.9954
Bisphenol B	Ratio to PFOS	3.57E-02	-4.03E-03	0.9618	2.91E-02	-6.75E-03	0.9712	0.045717	-1.89E-03	0.9934
Bisphenol C	Ratio to Zearelonone	1.22E-02	-9.99E-04	0.9923	1.31E-02	-5.10E-03	0.9956	0.020067	-2.55E-03	0.9942
Bisphenol F	Ratio to Ethylparaben	3.88E-02	-9.08E-04	0.9974	2.28E-02	-2.88E-02	0.9821	0.031502	8.22E-04	0.9869
Bisphenol S	Ratio to Methylparaben	2.05E-01	3.24E-03	0.9775	1.75E-01	3.94E-02	0.9759	0.1763	9.02E-03	0.9721
Butylparaben	Ratio to Heavy	6.83E-02	2.36E-03	0.9969	7.09E-02	-3.09E-03	0.9899	0.064319	2.93E-03	0.9966
Citrinin	Ratio to Monobutyl phthalate	1.70E-01	-3.33E-04	0.8203	1.71E-02	8.18E-02	0.9	0.1489	-1.21E-01	0.9711
Cotinine	Ratio to Aflatoxin M1	2.82E+00	1.36E+00	0.9122	2.01E+00	-7.97E-01	0.9232	0.34778	7.65E+01	0.9799
Coumestrol	Ratio to Ethylparaben	1.28E-01	4.36E-04	0.9941	5.43E-02	-5.45E-04	0.9962	0.09237	-7.51E-03	0.9992
Daidzein	Ratio to Methylparaben	1.96E-01	-4.38E-04	0.9852	1.19E-01	2.41E-03	0.9676	0.16985	1.86E-03	0.94
Deoxyvalenol	Ratio to heavy	1.98E-02	-6.10E-03	0.9976	4.94E-02	-1.32E+00	0.9669	0.040926	-1.44E-01	0.9385
Dibutylphthalate	Ratio to 4-tert-octylphenol	2.81E-02	5.55E-01	0.9008	1.41E-02	2.14E-01	0.9747	0.01098	1.62E-01	0.9694
E2-17-GlCA	Ratio to Methylparaben	1.11E-02	-2.52E-03	0.8939	5.38E-03	2.73E-02	0.9569	0.004422	-9.96E-03	0.9526
Enterodiol	Ratio to Methylparaben	1.00E-01	-9.10E-04	0.9312	7.52E-02	7.87E-04	0.9773	0.033148	-4.59E-04	0.9893
Enterolactone	Ratio to PFOA	1.61E-01	2.50E-03	0.908	5.38E-02	1.89E-02	0.9609	0.10994	1.06E-03	0.9786
Equol	Ratio to Ethylparaben	4.79E-02	-2.89E-03	0.991	2.09E-02	-1.36E-02	0.9878	0.034082	-2.45E-03	0.9615
Estradiol-3-sulfate	Ratio to Methylparaben	1.45E-02	-1.89E-04	0.9938	1.63E-02	1.40E-03	0.9576	0.015993	3.34E-03	0.9926
Estradiol	Ratio to heavy	2.20E-02	-6.40E-04	0.9982	2.27E-02	-5.02E-03	0.9944	0.022114	-2.03E-03	0.9955
Estriol	Ratio to Methylparaben	1.47E-02	9.33E-04	0.9745	1.35E-02	-6.54E-03	0.9882	0.013999	-1.41E-03	0.9716

Estrone	Ratio to Butylparaben	1.85E-02	-7.76E-04	0.9658	1.74E-02	-8.67E-03	0.9808	0.021578	-4.28E-03	0.9933
Ethinylestradiol	Ratio to Butylparaben	8.89E-03	-1.50E-03	0.9397	7.67E-03	-6.77E-03	0.9944	0.010913	-1.32E-03	0.9781
Ethylparaben	Ratio to Heavy	1.10E-01	6.77E-03	0.9984	1.17E-01	3.69E-03	0.9891	0.10319	5.92E-02	0.9958
Fenarimol	Ratio to Zearelenone	2.14E-02	-1.83E-04	0.9866	8.28E-03	-2.05E-03	0.9846	0.003512	-2.98E-03	0.9787
Formnonetin	Ratio to Propylparaben	1.80E-01	-8.03E-04	0.9815	8.18E-02	-1.89E-02	0.9485	0.038494	-1.15E-02	0.9413
Fumonisin B1	Ratio to Aflatoxin M1	1.91E-01	-2.80E-02	0.8005	1.48E-01	4.04E-01	0.9337	No calibration possible		
Genistein	Ratio to Ethylparaben	1.54E-01	-6.08E-04	0.9859	5.72E-02	1.95E-02	0.9893	0.12658	-1.28E-02	0.9832
Glycitein	Ratio to Methylparaben	8.32E-02	-2.24E-03	0.9688	3.48E-02	-1.03E-02	0.9772	0.12332	-1.98E-01	0.9906
Isobutylparaben	Ratio to Butylparaben	1.22E-01	1.01E-03	0.9935	1.11E-01	-3.43E-04	0.9973	0.1271	-1.60E-03	0.9792
Isoxanthohumol	Ratio to Propylparaben	2.86E-02	-1.37E-03	0.9948	1.73E-02	-1.00E-02	0.9761	0.034054	-1.96E-02	0.8796
Jacobine-N-oxide	Ratio to Monobutylphthalate	8.49E-02	-1.77E-02	0.978	7.99E-02	-4.18E-01	0.9838	0.09504	-8.18E-02	0.9166
Jacobine	Ratio to Monobutylphthalate	2.75E-01	-1.35E-02	0.9297	2.44E-02	1.92E-01	1	0.33514	-1.88E-01	0.9975
Matairesinol	Ratio to PFOA	2.54E-02	-2.59E-03	0.9606	1.27E-02	-1.50E-02	0.988	0.022283	-1.25E-02	0.9585
MEHP	Ratio to Heavy	1.22E-02	3.32E-03	0.9983	1.20E-02	-1.10E-01	0.9921	No calibration possible		
Methiocarb	Ratio to Zearelenone	8.69E-03	-4.78E-04	0.9276	4.68E-03	4.12E-03	0.8552	0.008178	-1.37E-03	0.9892
Methylparaben	Ratio to Heavy	1.15E-01	5.44E-03	0.9982	1.22E-01	3.10E-02	0.996	0.11344	1.97E-01	0.9991
Monobutyl phthalate	Ratio to Heavy	1.45E-02	3.04E-04	0.9985	1.40E-02	-6.46E-03	0.9855	0.016108	8.49E-02	0.9731
n-Butylbenzolsulfonamid	Ratio to PFOs	3.03E-02	1.75E-02	0.9912	3.22E-02	1.95E-02	0.9914	0.048941	8.67E-02	0.9909
Nivalenol	Ratio to Methylparaben	7.89E-03	-1.18E-02	0.9924	No calibration possible			0.005436	-1.19E-01	0.9989
Nonylphenol	Ratio to 4-tert-octylphenol	2.20E-02	1.16E-01	0.9624	2.78E-02	1.07E-01	0.9973	0.023142	1.95E-01	0.9829
Ochratoxin A	Ratio to Methylparaben	7.66E-03	-8.02E-04	0.9761	8.01E-03	-4.28E-03	0.9834	0.007521	-3.63E-04	0.9895
Ochratoxin Alpha	Ratio to Methylparaben	5.57E-02	-5.61E-04	0.9135	6.36E-02	-6.35E-04	0.8304	0.016293	-1.08E-02	0.9777
Ochratoxin B	Ratio to Methylparaben	2.74E-02	-9.63E-04	0.9847	2.10E-02	-1.38E-04	0.9466	0.015959	-4.81E-03	0.9017
Ocylmethoxycinnamate	Ratio to Aflatoxin M1	3.38E-02	9.80E-02	0.8399	2.45E-02	8.46E-02	0.9442	0.032943	-2.67E+00	0.938
p-Hydrobenzoiacid	Ratio to Heavy	1.23E-03	6.69E-04	0.9962	1.16E-03	2.06E-01	0.9928	0.001174	4.25E-02	0.9969
PFOA	Ratio to Heavy	1.03E-01	1.64E-03	0.9814	1.13E-01	-1.96E-02	0.9957	0.10455	1.97E-01	0.9744
PFOs	Ratio to Heavy	5.08E-02	-1.73E-03	0.9974	4.81E-02	2.47E-03	0.9944	0.045655	5.01E-01	0.9958
PhIP	Ratio to Methylparaben	3.14E-01	1.01E-02	0.9805	2.83E-01	-6.58E-03	0.9878	0.093316	-1.57E-02	0.9552
Prochloraz	Ratio to Zearelenone	4.37E-02	-1.78E-03	0.9687	3.29E-02	-1.91E-03	0.9556	0.024809	-4.13E-03	0.9711
Propylparaben	Ratio to Heavy	1.17E-01	2.85E-03	0.9996	1.19E-01	7.19E-03	0.9985	0.11788	7.97E-03	0.9939
Resveratrol	Ratio to Methylparaben	2.05E-02	-1.38E-02	0.943	2.13E-02	-1.17E-02	0.9956	0.003321	-6.01E-03	0.9348

Riddelliin-N-oxide	Ratio to Monobutyl phthalate	6.15E-02	-1.90E-02	0.9759	3.24E-02	3.01E-02	0.9742	0.056873	-3.41E-02	0.942
Riddelliin	Ratio to Monobutyl phthalate	1.99E-01	6.96E-03	0.9161	3.52E-02	-1.44E-01	0.9772	0.19144	-6.45E-02	0.97
Scolopamine	Ratio to Monobutyl phthalate	1.62E-01	-4.27E-03	0.9476	2.62E-02	-7.62E-02	0.9437	0.21479	-3.92E-02	0.9534
Sterigmatocystein	Ratio to Zearalenone	5.89E-02	-1.30E-03	0.9365	2.78E-02	-2.34E-03	0.9969	0.010396	-2.67E-03	0.9931
Tentoxin	Ratio to Ethylparaben	5.22E-02	-3.63E-04	0.9587	3.74E-02	4.35E-03	0.9627	0.04868	-9.52E-03	0.9899
Tetrabromobisphenol A	Ratio to 4-tert-octylphenol	1.17E-03	-3.13E-04	0.9739	1.99E-03	1.06E-03	0.9954	0.001311	9.25E-03	0.9127
Toxin T2	Ratio to Butylparaben	1.93E-02	-6.80E-03	0.9552	6.96E-03	-4.90E-03	0.9872	0.003815	-4.54E-03	0.9499
trans-3-OH-cotinine	Ratio to Aflatoxin M1	9.87E-01	3.79E-01	0.968	8.89E-02	2.64E+01	0.9847	0.050591	4.82E+00	0.9462
Triclosan	Ratio to 4-tert-octylphenol	2.83E-02	1.10E-04	0.9927	2.29E-02	4.03E-04	0.9972	0.024914	3.03E-04	0.9883
Xanthohumol	Ratio to Zearalenone	4.44E-02	8.03E-04	0.928	4.91E-02	1.05E-03	0.9494	0.047208	-1.35E-03	0.9845
Zearalenone	Ratio to Zearalenone	4.36E-02	-5.21E-04	0.992	4.06E-02	-8.47E-04	0.9914	0.041506	-1.12E-03	0.9932
Zearalenone	Ratio to Heavy	3.93E-02	-6.69E-04	0.9993	3.99E-02	-5.56E-03	0.9986	0.039154	-2.78E-03	0.9988
Zearalenone-14-glucuronide	Ratio to Methylparaben	4.80E-03	-8.55E-04	0.9961	1.73E-03	-2.95E-03	0.9066	0.001513	-9.97E-03	0.9403
Zearalenone-14-sulfate	Ratio to Methylparaben	3.09E-02	-1.62E-03	0.9686	2.86E-02	-1.11E-02	0.998	3.39E-02	-1.66E-03	0.9921
Endogenous metabolites										
1-Methylhydantoin	Ratio to Heavy	3.96E-01	6.84E-02	0.9977	No calibration possible	No calibration possible	6.67E-01	1.30E+01	0.9337	
1-Methylnicotinamide	No calibration possible									
2-										
(Carbamoylamino)butanedioic acid	Ratio to surrogate Aspartic acid	3.45E-02	1.86E-03	0.9698	1.41E-02	7.45E-03	0.9172	No calibration possible		
2'-Deoxyadenosine 5'-monophosphate	Ratio to surrogate GMP	8.43E+00	-3.66E-03	0.99	1.30E+01	8.78E-01	0.9487	2.76E-01	-1.38E-02	0.9851
2'-Deoxycytidine	Ratio to surrogate Phenylalanine	6.78E-01	-1.30E-04	0.9976	1.25E-01	1.68E-01	0.9542	2.11E-01	1.60E-02	0.9639
2-Deoxycytidine 5'-Monophosphate	Ratio to surrogate UMP	9.07E-01	3.85E-03	0.9945	1.19E+00	9.72E-03	0.9446	4.24E-01	-7.73E-02	0.992
2-Deoxyuridine	Ratio to surrogate Succinic acid	5.18E-01	1.13E-03	0.9768	3.34E-01	1.39E-02	0.9745	1.40E-01	-2.55E-03	0.9761
2-Phosphoglyceric acid + 3-Phosphoglyceric acid	Ratio to surrogate ADP	6.05E-01	3.42E-02	0.9901	7.92E+00	2.18E+00	0.9769	1.10E+00	-9.19E-02	0.9777
3AMP	Ratio to surrogate 5'-AMP	1.49E-01	6.36E-05	0.9401	1.95E-01	2.89E-01	0.9035	2.09E-01	-1.11E-03	0.9673

3-Methyl-2-oxovaleric acid	Ratio to Heavy	6.15E+00	2.05E-01	0.994	1.03E+01	2.72E+01	0.968	No calibration possible
3-Methylcytidine	Ratio to surrogate Adenine	1.35E-03	-9.80E-04	0.9717	No calibration possible	No calibration possible	No calibration possible	No calibration possible
4-Hydroxy-proline	Ratio to surrogate Homoserin	6.94E-01	-2.97E-04	0.9423	3.76E+00	3.30E+00	0.9172	No calibration possible
5'AMP	Ratio to Heavy	2.37E-01	4.27E-04	0.9928	3.79E-01	1.04E-02	0.9682	2.30E-01
5'-Deoxy-5'-Methylthioadenosine	Ratio to Heavy	4.66E+00	2.65E-03	0.9976	5.21E+00	5.70E-01	0.9968	4.98E+00
5-Methyluridine	Ratio to surrogate Succinic acid	3.79E-01	3.42E-03	0.9967	1.75E+01	8.35E+00	0.9583	1.14E+01
6-Phosphogluconate	Ratio to surrogate ADP	1.14E-01	-8.96E-03	0.989	1.49E+00	-3.33E-01	0.9957	2.93E-01
Adenine	Ratio to Heavy	2.48E+01	6.06E-02	0.9964	2.60E+01	3.31E+00	0.9733	2.93E+01
Adenosine	Ratio to Heavy	1.52E+01	3.97E-02	0.9983	4.10E-01	1.25E-01	0.9526	2.11E-01
Adenosine 3',5'-cyclic monophosphate	Ratio to surrogate Succinic acid	2.19E-01	-6.20E-04	0.9858	2.44E-01	3.55E-01	0.927	1.46E-01
Adenosine 5'-triphosphate	Ratio to Heavy	6.64E-01	1.50E-01	0.9804	1.06E+00	-2.79E-01	0.9034	No calibration possible
Adenosine diphosphate	Ratio to Heavy	3.36E-01	9.98E-02	0.995	3.80E-01	-1.53E-02	0.9898	2.96E-01
Alanine	Ratio to Heavy	1.75E-02	2.56E-03	0.9939	No calibration possible	No calibration possible	No calibration possible	No calibration possible
alpha-Aminoadipic acid	Ratio to surrogate Proline	1.32E-02	2.81E-04	0.9256	No calibration possible	No calibration possible	No calibration possible	No calibration possible
alpha-Ketoglutarate	Ratio to Heavy	4.03E-01	-7.87E-04	0.994	No calibration possible	No calibration possible	No calibration possible	No calibration possible
Arginine	Ratio to Heavy	No calibration possible	No calibration possible	No calibration possible	No calibration possible	No calibration possible	No calibration possible	No calibration possible
Argininosuccinic acid	Ratio to Heavy	5.70E-01	-1.87E-03	0.9982	6.98E-01	3.12E+00	0.9657	5.85E-01
Asparagine	Ratio to Heavy	3.67E-01	-1.45E-03	0.9948	3.79E-01	9.05E+00	0.945	4.15E-01
Aspartate	Ratio to Heavy	4.63E-02	3.98E-04	0.9771	3.11E-02	6.26E-02	0.9629	4.70E-02
Betaine	Ratio to surrogate Phenylalanine	5.73E+01	6.33E-01	0.9859	No calibration possible	No calibration possible	No calibration possible	No calibration possible
Biotin	Ratio to surrogate Pyruvic acid	4.67E+00	6.26E-02	0.9714	2.92E+00	3.68E+00	0.9098	9.97E-01
Carnitine	Ratio to surrogate Glutamate	7.63E-01	2.90E-03	0.9949	No calibration possible	No calibration possible	No calibration possible	No calibration possible
Choline chloride	No calibration possible	No calibration possible	No calibration possible	No calibration possible	No calibration possible	No calibration possible	No calibration possible	No calibration possible
cis-Aconitate	Ratio to Heavy	5.04E+01	-1.14E+00	0.9976	No calibration possible	No calibration possible	3.70E+01	4.56E+00
Citrate + Isocitrate	Ratio to Heavy	1.27E+00	2.02E-01	0.998	No calibration possible	No calibration possible	1.74E+00	2.68E+00
CMP	Ratio to surrogate Aspartic acid	1.82E-02	-2.80E-04	0.9884	1.38E-02	-8.56E-04	0.9748	9.23E-03

Cysteic acid	Ratio to surrogate acid	Aspartic acid	3.34E-02	3.77E-05	0.9803	2.56E-02	1.21E-04	0.9683	1.38E-02	-6.62E-04	0.9864
Cysteine	Ratio to surrogate Cystathionine		2.27E-03	-5.34E-04	0.9788	No calibration possible	No calibration possible	No calibration possible	No calibration possible		
Cysteinyl-glycine	Ratio to surrogate	Serine	3.67E-03	-8.00E-03	0.906	No calibration possible	No calibration possible	No calibration possible	No calibration possible		
Cystine	Ratio to surrogate Cystathionine		3.97E-02	-1.95E-03	0.9958	No calibration possible	No calibration possible	No calibration possible	No calibration possible		
Cytidine	Ratio to surrogate	Proline	4.09E-02	1.99E-04	0.9725	3.30E-02	8.76E-04	0.9946	9.70E-02	9.72E-04	0.9927
Cytidine 5'-triphosphate	Ratio to surrogate	ATP	1.53E-01	-2.59E-02	0.9725	2.71E-01	-5.77E-01	0.9161	No calibration possible		
Cytosine	Ratio to surrogate	Glutamate_pos	3.60E-01	3.32E-03	0.9733	1.63E-01	-4.70E-03	0.99	8.96E-01	1.77E-02	0.9801
Deoxyguanosine triphosphate	Ratio to surrogate	ATP	6.64E-01	1.50E-01	0.9804	1.07E+00	-2.85E-01	0.9007	No calibration possible		
Dihydroxyacetonephosphate	Ratio to surrogate	Valine	2.87E-02	-1.18E-03	0.9882	1.23E-02	4.95E-03	0.9755	1.25E-02	-2.49E-02	0.9665
Dihydroxyisovalerate	Ratio to surrogate	3-Methyl-2-oxovaleric acid	9.37E+00	-1.44E-01	0.989	1.34E+01	1.03E+01	0.9679	2.06E+01	1.56E+01	0.9718
Erythritol	Ratio to surrogate	Valine	2.02E-01	6.66E-03	0.9928	No calibration possible	No calibration possible	No calibration possible	1.05E-01	1.01E+00	0.9255
Erythrose-4-phosphate	Ratio to surrogate	Aspartic acid	4.78E-03	-1.11E-03	0.9605	6.00E-04	-1.00E-05	0.913	9.10E-04	-8.30E-04	0.9366
Flavinadenin dinucleotide	Ratio to surrogate	Nicotinamide	3.76E-02	-9.45E-04	0.9269	1.34E-01	-3.53E-02	0.9293	1.27E-02	-9.59E-03	0.957
Hexose (Fructose, Galactose, Mannose, Glucose, Inositol)	Ratio to surrogate	Trehalose	9.7598E-1	2.4878E-2	0.9882	No calibration possible	No calibration possible	No calibration possible	No calibration possible		
Fructose-1,6-bisphosphate	Ratio to surrogate	ADP	7.08E-02	-3.17E-03	0.9852	1.03E-01	-1.46E-03	0.9335	No calibration possible		
Hexose-6-phosphate											
(Fructose-6-phosphate, Glucose-1-phosphate, Glucose-6-phosphate)	Ratio to surrogate	Trehalose	3.36E+00	-2.21E-02	0.9792	2.81E+00	9.51E-01	0.991	1.65E+00	1.12E-01	0.9736
Fumarate	Ratio to Heavy		2.56E-01	-7.82E-04	0.9987	3.05E-01	6.44E-01	0.9566	2.58E-01	3.63E-01	0.9957
Glucuronate	Ratio to surrogate	Valine	1.06E+00	5.90E-02	0.9709	No calibration possible	No calibration possible	4.52E+00	6.85E+00	0.9216	
Glutamate	Ratio to Heavy		7.53E-03	9.71E-05	0.9993	No calibration possible	No calibration possible	No calibration possible	No calibration possible		
Glutamine	Ratio to Heavy		3.18E-02	4.29E-04	0.9991	No calibration possible	No calibration possible	No calibration possible	No calibration possible		
Glutamyl-cysteine	Ratio to surrogate	Methionine	2.74E-01	-3.81E-03	0.9176	8.60E-02	-1.62E-02	0.8527	No calibration possible		
Glutathione, oxidized	Ratio to Heavy		1.84E-01	-1.12E-02	0.9939	2.33E-01	-1.35E-01	0.9786	1.64E-01	-1.40E-02	0.928

Glutathione, reduced	Ratio to surrogate Aspartic acid	1.09E-02	-4.97E-05	0.9233	6.31E-02	-3.31E-03	0.9361	6.64E-03	-2.67E-04	0.9824
Glycine	Ratio to Heavy	2.60E-01	1.21E-01	0.9925	No calibration possible	No calibration possible	No calibration possible	No calibration possible	No calibration possible	No calibration possible
Glyoxylic acid	No calibration possible									
GMP	Ratio to Heavy	1.85E+00	-2.60E-02	0.9952	2.62E+00	-3.96E-01	0.9521	1.77E+00	-7.84E-02	0.9768
Guanidineacetic acid	Ratio to surrogate Threonine	1.64E+00	1.05E-01	0.9794	No calibration possible	No calibration possible	No calibration possible	2.31E+00	6.36E+00	0.9207
Guanine	Ratio to surrogate Glutamate_pos	1.07E-01	2.10E-03	0.9804	4.56E-02	1.91E-02	0.9148	1.77E-01	-4.35E-03	0.9507
Guanosine + Isoguanosine	Ratio to surrogate Proline	1.59E-01	2.14E-04	0.9715	5.35E-02	9.11E-03	0.9552	1.92E+00	1.45E-03	0.9934
Guanosine 3',5'-cyclic monophosphate	Ratio to surrogate 5'-AMP	2.57E-01	-1.22E-04	0.9827	2.56E-01	8.42E-03	0.9374	1.19E-01	-7.78E-02	0.9686
Guanosine 5'-diphosphate	Ratio to surrogate ADP	1.37E-01	1.93E-02	0.992	1.80E-01	-2.62E-02	0.9533	2.82E-02	-7.39E-02	0.9785
Guanosine 5'-triphosphate	Ratio to surrogate ATP	9.17E-02	-1.99E-02	0.9662	1.65E-01	-4.33E-01	0.9071	No calibration possible	No calibration possible	No calibration possible
Histidine	Ratio to Heavy	1.81E-01	2.49E-02	0.9992	No calibration possible	No calibration possible	No calibration possible	No calibration possible	No calibration possible	No calibration possible
Homocysteine	Ratio to surrogate S-Adenosylhomocysteine	8.40E-02	1.52E-02	0.9094	1.83E-01	-1.38E-02	0.9687	7.84E-02	-2.89E-02	0.9713
Homoserine + Threonine	Ratio to Heavy	3.74E-01	3.33E-03	0.9987	No calibration possible	No calibration possible	No calibration possible	No calibration possible	No calibration possible	No calibration possible
Hydroxyglutaric acid	Ratio to Heavy	7.61E-01	9.21E-03	0.9937	9.37E-01	7.40E+00	0.9826	5.54E-01	3.73E-01	0.9462
Inosine	Ratio to surrogate Malic acid	9.05E-02	2.30E-05	0.9821	3.59E-02	3.31E-02	0.9088	5.46E-02	5.91E-04	0.987
Inosine 5'-monophosphate	Ratio to surrogate Aspartic acid	2.11E-02	-1.71E-04	0.9803	1.39E-02	-7.41E-04	0.9845	1.09E-02	-1.94E-03	0.9918
Isoleucine + Leucine	Ratio to Heavy	2.09E+00	4.24E-02	0.999	No calibration possible	No calibration possible	No calibration possible	No calibration possible	No calibration possible	No calibration possible
Ketoisovalerate	Ratio to surrogate Pyruvic acid	1.10E+00	1.80E-01	0.983	9.95E-01	6.12E+00	0.9563	4.16E+00	2.31E+01	0.9961
Kynurenine	Ratio to surrogate Methionine	1.66E+00	1.22E-02	0.9668	3.30E-01	-1.27E-02	0.9585	1.58E+00	1.04E+00	0.9829
Lactate	Ratio to surrogate Pyruvic acid	8.68E-01	2.45E+00	0.9586	9.37E-01	1.94E+01	0.9238	1.77E+02	5.29E+02	0.9938
L-Citrulline	Ratio to Heavy	1.32E-01	2.71E-03	0.9934	No calibration possible	No calibration possible	No calibration possible	1.50E-01	5.35E+00	0.9629
L-Cystathionine	Ratio to Heavy	2.42E-01	-1.71E-03	0.9927	3.43E-01	1.59E+00	0.9675	2.78E-01	5.21E-02	0.9985
L-Ornithine	Ratio to surrogate Serine	1.53E-01	4.37E-03	0.9976	8.94E-03	1.72E-02	0.9554	No calibration possible	No calibration possible	No calibration possible
Lysine	Ratio to Heavy	4.47E-02	1.98E-02	0.9797	No calibration possible	No calibration possible	No calibration possible	No calibration possible	No calibration possible	No calibration possible

Malate	Ratio to Heavy	1.84E-01	2.35E-03	0.9984	2.33E-01	9.07E-01	0.9837	2.36E-01	3.44E-01	0.9289
Mannitol	Ratio to surrogate Tyrosine	1.82E+00	6.62E-02	0.9853	No calibration possible	No calibration possible	No calibration possible	No calibration possible	No calibration possible	No calibration possible
Mannitol 1-phosphate	Ratio to surrogate Trehalose	1.02E+00	-2.27E-02	0.9731	1.00E+00	-2.16E-01	0.984	4.56E-01	-2.37E-02	0.9299
Melatonin	Ratio to surrogate Adenosine	2.02E+01	6.96E-03	0.948	2.12E+01	-2.63E-01	0.9221	3.38E+01	-1.44E+00	0.9317
Methionine	Ratio to Heavy	1.05E+00	7.05E-04	0.9937	1.14E+00	3.42E+00	0.9855	No calibration possible	No calibration possible	No calibration possible
Methionine sulfone	Ratio to surrogate Tyrosine	3.21E+00	4.75E-03	0.9517	2.42E+00	1.78E+00	0.9608	2.75E+00	3.77E+00	0.9755
Mevalonic acid	Ratio to surrogate 3-Methyl-2-oxovaleric acid	4.98E+00	9.78E-02	0.987	8.85E+00	2.63E+01	0.9765	6.86E+00	7.42E+00	0.9898
N4-Acetylcytidine	Ratio to surrogate Adenosine	2.92E+00	-6.08E-03	0.9796	4.12E+00	5.92E+00	0.948	1.37E+00	-1.39E-01	0.9256
N-Acetyl-Asp-Glu	Ratio to surrogate Aspartic acid	6.62E-02	-2.67E-04	0.9636	5.58E-01	1.55E+00	0.9822	No calibration possible	No calibration possible	No calibration possible
N-Acetyl-L-aspartic acid	Ratio to surrogate Hydroxyglutaric acid	5.51E-01	5.28E-03	0.9955	No calibration possible	No calibration possible	1.11E+00	2.23E-01	0.9898	0.9898
N-Acetyl-serine	Ratio to surrogate Succinic acid	3.52E-01	2.20E-03	0.9732	4.07E-01	2.07E+00	0.9893	1.72E-01	2.54E-01	0.9807
NAD+	Ratio to Heavy	8.04E-01	-3.43E-03	0.9473	1.14E+00	-2.09E-01	0.9675	1.39E+00	-3.41E-01	0.9226
NADH	Ratio to surrogate NAD+	9.70E-02	-3.49E-03	0.9771	No calibration possible	No calibration possible	No calibration possible	No calibration possible	No calibration possible	No calibration possible
NADP+	Ratio to surrogate ADP	1.28E-01	-1.19E-02	0.9885	8.98E-02	-5.78E-02	0.9261	8.38E-01	-5.83E-01	0.9703
NADPH	Ratio to surrogate ADP	1.62E-02	-8.42E-03	0.9752	1.03E-01	-2.51E-01	0.9653	2.03E-02	2.72E-02	0.9133
Nicotinamide	Ratio to Heavy	2.50E+00	5.26E-03	0.9961	2.47E+00	6.24E-01	0.9852	2.37E+00	1.40E-01	0.9811
Octopamine	No calibration possible	No calibration possible	No calibration possible	No calibration possible	No calibration possible	No calibration possible	No calibration possible	No calibration possible	No calibration possible	No calibration possible
Oxaloacetic acid	Ratio to surrogate Citric acid	4.18E-04	-2.78E-04	0.9573	No calibration possible	No calibration possible	No calibration possible	No calibration possible	No calibration possible	No calibration possible
Palmitic acid	No calibration possible	No calibration possible	No calibration possible	No calibration possible	No calibration possible	No calibration possible	No calibration possible	No calibration possible	No calibration possible	No calibration possible
Phenylalanine	Ratio to Heavy	1.49E+00	2.57E-02	0.98	No calibration possible	No calibration possible	No calibration possible	No calibration possible	No calibration possible	No calibration possible
Phosphocreatine	Ratio to surrogate Argininosuccinic acid	1.81E-01	-2.23E-03	0.9754	3.65E-01	4.61E-01	0.9598	2.23E-01	-1.25E-02	0.9948
Proline	Ratio to Heavy	6.05E-02	1.27E-03	0.9989	5.26E-02	8.98E-02	0.9781	-4.71E+00	1.29E+01	-447.114
Propionyl-L-carnitine	Ratio to surrogate Adenine	1.50E+01	5.44E-03	0.9835	7.64E+01	6.94E+01	0.9223	2.59E+01	2.35E+01	0.9623
Pseudouridine	Ratio to surrogate Valine	7.14E-01	4.75E-03	0.9814	6.55E-01	2.80E-01	0.9614	2.35E+00	3.35E+00	0.9829
Pyruvate	Ratio to Heavy	3.95E-01	1.46E-02	0.9921	4.93E-01	6.90E+00	0.9591	1.00E+00	2.28E+01	0.9375
Ribose	Ratio to surrogate Valine	5.46E-03	-3.72E-03	0.9633	No calibration possible	No calibration possible	No calibration possible	No calibration possible	No calibration possible	No calibration possible

Ribose-5-phosphate + Ribulose-5-phosphate	Ratio to surrogate acid	3.36E-02	-6.56E-04	0.9812	3.36E-02	3.06E-02	0.9814	1.44E-02	1.02E-02	0.9687
S-(Adenosyl)-methionine	Ratio to Heavy	8.56E-02	-6.27E-03	0.9987	No calibration possible			1.02E-01	4.11E-01	0.9751
Sarcosine	Ratio to surrogate S-Adenosylhomocysteine	1.68E+00	8.52E-02	0.9666	2.73E+00	3.50E+00	0.9443	2.54E+00	3.40E+00	0.9564
Sedoheptulose-7-phosphate	Ratio to surrogate ADP	2.05E-01	-1.53E-03	0.9428	4.29E-02	-8.91E-04	0.9687	4.26E-01	-2.04E-02	1
Seleno-methionine	Ratio to surrogate Methionine	7.36E-01	-1.86E-03	0.9542	7.54E-01	-5.83E-02	0.9911	8.36E-01	-1.87E-02	1
Serine	Ratio to Heavy	8.85E-02	8.53E-03	0.9978	No calibration possible			No calibration possible		
Serotonine	Ratio to surrogate Nicotinamide	3.51E-01	-2.43E-04	0.9812	6.75E-01	-1.34E-05	0.9631	6.64E-01	8.37E-01	1
Spermidine	No calibration possible									
Spermine	No calibration possible									
Succinate	Ratio to Heavy	3.46E-01	2.42E-02	0.9992	6.12E-01	3.19E+00	0.9906	7.01E-01	1.29E+00	1
Thiamine hydrochloride	No calibration possible									
Thymidine	Ratio to surrogate Pyruvic acid	3.31E+00	9.33E-03	0.9811	1.31E+00	1.98E-01	0.9282	2.01E+00	-1.79E-02	1
Thymidine 5'-monophosphate	Ratio to surrogate Hydroxyglutaric acid	1.24E-01	-3.00E-05	0.9963	1.16E-01	-8.02E-03	0.9196	6.19E-02	8.12E-04	1
Thymine	Ratio to surrogate Succinic acid	3.49E-01	-1.47E-03	0.9731	3.13E-01	1.05E-01	0.959	1.15E-01	1.27E-02	1
Trehalose	Ratio to Heavy	7.46E-01	-2.76E-03	0.9961	8.59E-01	1.06E+00	0.957	6.30E-01	2.66E-01	1
Tryptophan	Ratio to surrogate Valine	5.16E-01	-9.61E-06	0.9859	1.21E+00	1.10E+01	0.8534	No calibration possible		
TTP (Thymidinetriphosphate)	Ratio to surrogate ATP	5.48E-01	-1.62E-02	0.986	1.01E+00	-1.99E-01	0.9268	NaN	NaN	NaN
Tyrosine	Ratio to Heavy	1.78E+00	1.83E-02	0.9986	No calibration possible			No calibration possible		
UMP	Ratio to Heavy	1.01E+00	-1.61E-03	0.9974	1.17E+00	-2.56E-02	0.9887	1.18E+00	-1.66E-01	1
Uracil	Ratio to surrogate Hydroxyglutaric acid	1.96E-01	3.05E-03	0.9822	-9.54E+00	2.16E+00	-2193.68	1.40E-01	5.56E-03	1
Uridine	Ratio to surrogate Hydroxyglutaric acid	1.41E-01	8.86E-03	0.958	No calibration possible			7.01E-02	2.55E-01	1
Uridine 5'-diphosphate	Ratio to Heavy	1.65E+00	-8.23E-03	0.9927	2.64E+00	-4.62E-01	0.9815	2.55E+00	9.94E-01	1
Uridine 5'-triphosphate	Ratio to surrogate ATP	1.18E-01	-2.90E-02	0.98	2.07E-01	-8.44E-02	0.9264	No calibration possible		
Valine	Ratio to Heavy	3.08E-01	3.56E-03	0.9917	No calibration possible			No calibration possible		

Xanthine	Ratio to surrogate Hydroxyglutaric acid	4.78E-01	9.26E-03	0.9836	No calibration possible	2.58E-01	6.69E-01	1
Xylose	Ratio to surrogate Aspartic acid	1.03E-04	-8.02E-05	0.9633	No calibration possible	No calibration possible		

Table S19 Linear dynamic range of solvent standards and matrix-matched standards, recovery of solvent standards and extraction recovery of spiked matrix standards (urine and plasma) of the most abundant species for the xenobiotics and human estrogens measured on the reverse phase column. Not detected compounds are marked with n.d. (not detected) and bg indicates analytes where the background signal was too high to calculate analytical figures of merit

Compound	Species	Linear working range [ng/mL]			Recovery [%]		
		Urine	Plasma	Solvent	Solvent	Plasma	Urine
1-OH-pyrene	[M-H] ⁻ , [M+H] ⁺	3 - 100	3 - 30	3 - 100	103	104	104
16-Epiestriol	[M-H] ⁻	1.5 - 500	0.5 - 500	0.5 - 500	99	96	114
16-Hydroxyestrone	[M-H] ⁻	1 - 100	1 - 100	0.1 - 100	105	96	103
17-Epiestriol	[M-H] ⁻	5 - 500	0.5 - 500	0.5 - 500	106	102	106
2-Hydroxyestradiol	[M-H] ⁻	10 - 1000	100 - 1000	3 - 1000	112	99	n.d.
2-Methoxyestrone	[M-H] ⁻ , [M+H] ⁺	3 - 300	0.9 - 300	0.9 - 300	111	97	104
2-Naphtol	[M-H] ⁻	5 - 500	0.5 - 500	0.5 - 500	108	80	65
2-Methoxyestradiol	[M-H] ⁻	3 - 300	3 - 300	0.3 - 300	113	101	101
2-tert-Butylphenol	[M-H] ⁻	2 - 2000	0.2 - 2000	0.2 - 2000	110	n.d.	6
3-Benzylidencampher	[M+H] ⁺	5 - 5000	15 - 1500	0.5 - 1500	83	70	21
4-Hydroxyestrone	[M-H] ⁻	0.5 - 500	5 - 500	0.5 - 500	109	97	7
4-Methoxyestradiol	[M-H] ⁻	1.5 - 50	1.5 - 50	0.2 - 50	104	91	80
4-Methoxyestrone	[M-H] ⁻ , [M+H] ⁺	0.5 - 50	0.2 - 50	0.1 - 50	116	102	108
4-Methylbenzylidencampher	[M+H] ⁺	2 - 2000	2 - 2000	2 - 2000	88	93	58
4-octylphenol	[M-H] ⁻	1 - 1000	1 - 300	1 - 300	89	106	110
4-tert-octylphenol	[M-H] ⁻	1 - 1000	1 - 1000	1 - 1000	104	95	99
8-Prenylnaringenin	[M-H] ⁻ , [M+H] ⁺	1 - 10	0.1 - 10	0.03 - 10	98	93	98
Aflatoxicol	[M+H] ⁺	5 - 50	0.5 - 50	0.01 - 50	92	111	110
Aflatoxin B1	[M+H] ⁺ , [M-H] ⁻	0.1 - 100	0.1 - 30	0.01 - 100	95	102	113
Aflatoxin B2	[M+H] ⁺ , [M-H] ⁻	0.1 - 100	0.1 - 30	0.01 - 100	98	111	114
Aflatoxin G1	[M+H] ⁺ , [M-H] ⁻	0.1 - 100	0.1 - 30	0.01 - 100	99	93	102
Aflatoxin G2	[M+H] ⁺ , [M-H] ⁻	1 - 100	0.1 - 30	0.01 - 100	97	107	101
Aflatoxin M1	[M+H] ⁺ , [M-H] ⁻	1 - 100	0.1 - 100	0.01 - 100	98	99	96
Aflatoxin M2	[M+H] ⁺ , [M-H] ⁻	1 - 100	1 - 30	0.3 - 100	113	104	105
Aflatoxin P1	[M-H] ⁻ , [M+H] ⁺	0.1 - 100	10 - 100	0.01 - 100	107	95	91
Alpha-zearalanol	[M-H] ⁻ , [M+H] ⁺	0.1 - 100	1 - 100	0.1 - 100	98	97	105
Alpha-zearalenol-14-glucuronide	[M-H] ⁻ , [M+H] ⁺	10 - 100	0.1 - 100	3 - 100	120	85	n.d.
Alpha-zearalenol	[M-H] ⁻ , [M+H] ⁺	0.1 - 100	0.3 - 100	0.1 - 100	102	100	97
Alternariol	[M-H] ⁻ , [M+H] ⁺	1 - 100	0.1 - 100	0.01 - 100	117	99	101
Alternariol monomethylether	[M-H] ⁻ , [M+H] ⁺	0.1 - 100	0.1 - 100	0.1 - 100	93	99	102
Anisodamine	[M+H] ⁺	3 - 100	3 - 100	0.1 - 100	88	104	84
Beauvericin	[M+NH4] ⁺	5 - 50	0.5 - 50	0.5 - 50	87	118	104

Benzophenone 1	[M-H] ⁻ ; [M+H] ⁺	0.1 - 10	0.1 - 10	0.01 - 10	114	108	86
Benzophenone 2	[M-H] ⁻	0.5 - 50	0.5 - 50	0.1 - 50	99	97	101
Benzylbutylphthalate	[M+H] ⁺	1.5 - 150	1.5 - 150	0.5 - 150	95	92	113
Benzylparaben	[M-H] ⁻	0.2 - 5	0.1 - 5	0.1 - 5	104	100	99
Beta-zearalanol	[M-H] ⁻ ; [M+H] ⁺	0.3 - 100	0.1 - 100	0.1 - 100	122	96	78
Beta-zearalenol-14-glucuronide	[M-H] ⁻ ; [M+H] ⁺	30 - 100	10 - 100	3 - 100	113	n.d.	110
Beta-zearalenol	[M-H] ⁻ ; [M+H] ⁺	0.3 - 100	0.3 - 30	0.1 - 100	123	99	106
Bisphenol A	[M-H] ⁻	1 - 100	1 - 100	1 - 100	103	105	106
Bisphenol AF	[M-H] ⁻	0.2 - 50	0.1 - 50	0.1 - 50	107	91	86
Bisphenol B	[M-H] ⁻	1 - 100	1 - 100	0.3 - 100	111	86	101
Bisphenol C	[M-H] ⁻	2 - 200	0.2 - 200	0.2 - 200	108	101	104
Bisphenol F	[M-H] ⁻	20 - 200	0.2 - 200	0.2 - 200	106	96	103
Bisphenol S	[M-H] ⁻	0.3 - 10	0.1 - 10	0.03 - 10	103	97	104
Butylparaben	[M-H] ⁻	0.1 - 50	0.1 - 50	0.1 - 50	101	106	106
Citrinin	[M+H] ⁺ ; [M-H] ⁻	10 - 100	1 - 100	0.1 - 30	91	40	96
Cotinine	[M+H] ⁺	3 - 100	3 - 100	1 - 100	107	98	bg
Coumestrol	[M-H] ⁻ ; [M+H] ⁺	0.3 - 100	0.1 - 100	0.1 - 100	109	97	101
Daidzein	[M-H] ⁻ ; [M+H] ⁺	0.5 - 50	0.1 - 50	0.1 - 50	100	98	108
Deoxynivalenol	[M-H] ⁻ ; [M+H] ⁺	30 - 100	30 - 100	3 - 100	101	n.d.	n.d.
Dibutylphthalate	[M+H] ⁺	3 - 1000	3 - 1000	10 - 1000	100	105	55
E2-17-GlcA	[M-H] ⁻	15 - 150	15 - 150	1.5 - 150	103	97	77
Enterodiol	[M-H] ⁻	0.2 - 50	0.1 - 50	0.1 - 50	110	72	109
Enterolactone	[M-H] ⁻ ; [M+H] ⁺	0.3 - 100	0.3 - 100	0.1 - 100	117	106	100
Equol	[M-H] ⁻ ; [M+H] ⁺	3 - 100	0.3 - 100	0.1 - 100	117	102	110
Estradiol-3-sulfate	[M-H] ⁻	0.6 - 200	0.2 - 200	0.2 - 200	109	106	103
Estradiol	[M-H] ⁻	0.6 - 200	0.6 - 200	0.6 - 200	103	108	106
Estriol	[M-H] ⁻	2 - 200	2 - 200	0.2 - 200	114	95	104
Estrone	[M-H] ⁻	1 - 100	1 - 100	0.1 - 100	105	95	105
Ethinylestradiol	[M-H] ⁻	5 - 500	0.5 - 500	0.5 - 500	104	103	97
Ethylparaben	[M-H] ⁻	0.5 - 50	0.5 - 50	0.2 - 50	102	95	106
Fenarimol	[M+H] ⁺ ; [M-H] ⁻	0.5 - 5	0.5 - 5	0.02 - 5	102	n.d.	117
Formononetin	[M+H] ⁺ ; [M-H] ⁻	0.5 - 50	0.5 - 50	0.1 - 50	103	102	121
Fumonisin B1	[M+H] ⁺ ; [M-H] ⁻	3 - 100	3 - 100	1 - 100	94	85	79
Genistein	[M-H] ⁻ ; [M+H] ⁺	5 - 50	0.2 - 50	0.1 - 50	105	102	102
Glycitein	[M-H] ⁻ ; [M+H] ⁺	0.5 - 50	5 - 50	0.1 - 50	90	96	108
Isobutylparaben	[M-H] ⁻	0.5 - 50	0.1 - 50	0.1 - 50	106	96	104
Isoxanthohumol	[M-H] ⁻ ; [M+H] ⁺	0.5 - 5	0.5 - 5	0.1 - 5	98	99	104
Jacobine-N-oxide	[M+H] ⁺ ; [M-H] ⁻	10 - 100	3 - 100	0.3 - 100	104	85	106
Jacobine	[M+H] ⁺	30 - 100	1 - 100	0.1 - 100	101	90	97
Matairesinol	[M-H] ⁻ ; [M+H] ⁺	6 - 200	2 - 200	0.2 - 200	104	85	103
MEHP	[M-H] ⁻ ; [M+H] ⁺	20 - 200	bg	0.6 - 200	98	96	bg

Methiocarb	[M+H] ⁺	9 - 300	0.3 - 300	0.3 - 300	109	107	92
Methylparaben	[M-H] ⁻	0.1 - 100	1 - 100	0.3 - 100	104	107	112
Mono_buty_phthalate	[M-H] ⁻ , [M+H] ⁺	6 - 200	2 - 200	0.2 - 200	98	113	130
n-Butylbenzolsulfonamid	[M-H] ⁻ , [M+H] ⁺	2 - 200	0.6 - 200	0.2 - 200	112	97	103
Nivalenol	[M-H] ⁻ , [M+H] ⁺	-	30 - 100	3 - 100	105	n.d.	n.d.
Nonylphenol	[M-H] ⁻	0.5 - 500	1.5 - 500	0.5 - 500	102	103	104
Ochratoxin A	[M-H] ⁻ , [M+H] ⁺	1 - 100	10 - 100	1 - 100	111	86	n.d.
Ochratoxin Alpha	[M-H] ⁻ , [M+H] ⁺	3 - 100	1 - 30	1 - 100	107	18	47
Ochratoxin B	[M-H] ⁻ , [M+H] ⁺	1 - 100	1 - 100	1 - 100	102	90	80
Octylmethoxycinnamate	[M+H] ⁺	50 - 5000	50 - 5000	5 - 5000	99	94	111
p-Hydrobenzoic_acid	[M-H] ⁻	9 - 3000	300 - 3000	3 - 3000	98	120	113
PFOA	[M-H] ⁻	0.5 - 50	0.5 - 50	0.2 - 50	100	94	90
PFOS	[M-H] ⁻	0.3 - 30	0.3 - 30	0.9 - 30	103	94	90
PhIP	[M+H] ⁺ , [M-H] ⁻	0.1 - 100	0.3 - 30	0.01 - 100	109	97	98
Prochloraz	[M+H] ⁺	0.3 - 10	1 - 10	0.1 - 10	109	107	98
Propylparaben	[M-H] ⁻ , [M+H] ⁺	0.1 - 50	0.2 - 50	0.01 - 50	104	112	110
Resveratrol	[M-H] ⁻ , [M+H] ⁺	1.5 - 500	5 - 500	1.5 - 500	112	111	101
Riddeliin-N-oxide	[M+H] ⁺ , [M-H] ⁻	2.4 - 800	0.8 - 800	0.8 - 800	88	97	96
Riddeliin	[M+H] ⁺ , [M-H] ⁻	8 - 800	0.8 - 800	0.8 - 800	96	97	102
Scolpolamine	[M+H] ⁺ , [M-H] ⁻	5 - 50	0.5 - 50	0.1 - 50	105	90	103
Sterigmatocystein	[M+H] ⁺ , [M-H] ⁻	0.3 - 100	1 - 100	0.1 - 100	108	92	109
Tentoxin	[M+H] ⁺ , [M-H] ⁻	3 - 100	1 - 100	0.1 - 100	95	111	108
Tetrabrombisphenol A	[M-H] ⁻	0.6 - 200	6 - 200	2 - 200	94	53	15
Toxin T2	[M+H] ⁺	3 - 100	3 - 100	1 - 100	92	72	77
trans-3-OH-cotinine	[M+H] ⁺	24 - 800	24 - 800	0.8 - 800	114	96	bg
Triclosan	[M-H] ⁻	0.3 - 100	0.3 - 100	0.1 - 100	100	81	106
Xanthohumol	[M-H] ⁻ , [M+H] ⁺	0.1 - 15	0.1 - 50	0.1 - 15	112	88	102
Zearalanone	[M-H] ⁻ , [M+H] ⁺	0.1 - 100	0.1 - 100	0.1 - 100	106	102	105
Zearalenone-14-glucuronide	[M-H] ⁻	10 - 100	10 - 100	1 - 100	104	n.d.	106
Zearalenone-14-sulfate	[M-H] ⁻	1 - 100	0.1 - 100	0.3 - 100	109	83	91
Zearalenone	[M-H] ⁻ , [M+H] ⁺	0.3 - 100	0.3 - 100	0.1 - 100	101	110	103

Table S20 Linear dynamic range of solvent standards and matrix-matched standards, recovery of solvent standards and extraction recovery of spiked matrix standards (urine and plasma) of the most abundant species for endogenous metabolites on the HILIC column. Not detected compounds are marked with n.d. (not detected) and 'bg' indicates analytes where the background signal was too high to calculate analytical figures of merit

Compound	Species	Linear dynamic range [μM]			Recovery [%]		
		Solvent	Urine	Plasma	Solvent	Urine	Plasma
1-Methylhydantoin	[M-H] ⁻	1 - 10	bg	3 - 10	99	bg	bg
1-Methylnicotinamide		Not detected					
2-(Carbamoylamino)butanedioic acid	[M-H] ⁻ , [M+H] ⁺	0.1 - 10	1 - 10	0.1 - 3	98	94	33
2'-Deoxyadenosine 5'-monophosphate	[M+H] ⁺ , [M-H] ⁻	0.01 - 10	0.3 - 10	0.1 - 10	115	109	110
2'-Deoxycytidine	[M-H] ⁻ , [M+H] ⁺	0.01 - 3	0.3 - 10	0.3 - 10	91	42	107
2-Deoxycytidine 5'-Monophosphate	[M-H] ⁻ , [M+H] ⁺	0.01 - 10	0.1 - 10	0.3 - 10	104	57	n.d.
2'-Deoxyuridine	[M-H] ⁻ , [M+H] ⁺	0.001 - 10	0.03 - 10	0.03 - 10	108	50	38
2-Phosphoglyceric acid + 3-Phosphoglyceric acid	[M-H] ⁻ , [M+H] ⁺	0.06 - 20	0.2 - 20	0.6 - 20	118	92	n.d.
3'AMP	[M+H] ⁺ , [M-H] ⁻	0.01 - 10	3 - 10	0.03 - 10	98	n.d.	n.d.
3-Methyl-2-oxovaleric acid	[M-H] ⁻	0.03 - 10	0.3 - 10	bg	100	117	bg
3-Methylcytidine	[M-H] ⁻ , [M+H] ⁺	0.3 - 10	bg	0.3 - 10	89	bg	bg
4-Hydroxy-proline	[M-H] ⁻ , [M+H] ⁺	0.03 - 10	1 - 10	bg	98	bg	114
5'AMP	[M+H] ⁺ , [M-H] ⁻	0.01 - 10	0.3 - 10	0.03 - 10	95	102	112
5'-Deoxy-5'-Methylthioadenosine	[M+H] ⁺ , [M-H] ⁻	0.01 - 10	0.01 - 10	0.01 - 10	101	116	105
5-Methyluridine	[M-H] ⁻ , [M+H] ⁺	0.01 - 10	0.1 - 10	0.3 - 10	103	100	74
6-Phosphogluconate	[M-H] ⁻ , [M+H] ⁺	0.1 - 10	0.3 - 10	0.3 - 10	107	n.d.	n.d.
Adenine	[M+H] ⁺ , [M-H] ⁻	0.1 - 10	0.3 - 10	0.1 - 10	98	116	129
Adenosine	[M+H] ⁺ , [M-H] ⁻	0.01 - 10	0.1 - 10	0.01 - 10	101	92	92
Adenosine 3',5'-cyclic monophosphate	[M-H] ⁻ , [M+H] ⁺	0.01 - 10	0.3 - 10	0.1 - 10	103	100	70
Adenosine 5'-triphosphate	[M+H] ⁺ , [M-H] ⁻	0.3 - 10	0.3 - 10	n.d.	113	n.d.	n.d.
Adenosine diphosphate	[M-H] ⁻ , [M+H] ⁺	0.3 - 10	0.1 - 10	0.3 - 10	108	121	72
Alanine	[M+H] ⁺ , [M-H] ⁻	0.3 - 10	bg	bg	101	bg	bg
alpha-Aminoadipic acid	[M+H] ⁺ , [M-H] ⁻	0.03 - 10	bg	bg	107	bg	bg
alpha-Ketoglutarate	[M-H] ⁻	0.03 - 10	bg	bg	99	bg	bg
Arginine	[M-H] ⁻ , [M+H] ⁺	No calibration possible					

Compound	Species	Linear dynamic range [μM]			Recovery [%]		
		Solvent	Urine	Plasma	Solvent	Urine	Plasma
Argininosuccinic acid	$[\text{M}+\text{H}]^+$, $[\text{M}-\text{H}]^-$	0.01 - 10	0.3 - 10	0.03 - 10	102	107	105
Asparagine	$[\text{M}-\text{H}]^-$, $[\text{M}+\text{H}]^+$	0.03 - 10	3 - 10	0.3 - 10	101	bg	bg
Aspartate	$[\text{M}-\text{H}]^-$, $[\text{M}+\text{H}]^+$	0.03 - 10	1 - 10	0.3 - 10	97	92	114
Betaine	$[\text{M}+\text{H}]^+$, $[\text{M}-\text{H}]^-$	0.03 - 10	bg	bg	107	bg	bg
Biotin	$[\text{M}+\text{H}]^+$, $[\text{M}-\text{H}]^-$	0.01 - 10	0.3 - 10	0.1 - 10	88	97	21
Carnitine	$[\text{M}+\text{H}]^+$	0.03 - 10	bg	bg	95	bg	bg
Choline chloride		Not detected					
cis-Aconitate	$[\text{M}-\text{H}]^-$	0.1 - 10	bg	bg	95	bg	bg
Citrate + Isocitrate	$[\text{M}-\text{H}]^-$	0.6 - 20	bg	0.2 - 20	92	bg	bg
CMP	$[\text{M}-\text{H}]^-$, $[\text{M}+\text{H}]^+$	0.1 - 10	0.3 - 10	0.3 - 10	95	74	51
Cysteic acid	$[\text{M}-\text{H}]^-$, $[\text{M}+\text{H}]^+$	0.01 - 10	0.03 - 10	0.1 - 10	101	91	40
Cysteine	$[\text{M}-\text{H}]^-$, $[\text{M}+\text{H}]^+$	1 - 10	n.d.	n.d.	97	n.d.	n.d.
Cysteinyl-glycine	$[\text{M}-\text{H}]^-$, $[\text{M}+\text{H}]^+$	1 - 10	n.d.	n.d.	n.d.	n.d.	n.d.
Cystine	$[\text{M}+\text{H}]^+$, $[\text{M}-\text{H}]^-$	0.1 - 10	bg	bg	94	bg	bg
Cytidine	$[\text{M}+\text{H}]^+$, $[\text{M}-\text{H}]^-$	0.03 - 10	0.03 - 10	0.01 - 10	91	77	108
Cytidine 5'-triphosphate	$[\text{M}+\text{H}]^+$, $[\text{M}-\text{H}]^-$	1 - 10	3 - 10	n.d.	114	n.d.	n.d.
Cytosine	$[\text{M}+\text{H}]^+$, $[\text{M}-\text{H}]^-$	0.01 - 10	1 - 10	0.1 - 10	107	50	133
Deoxyguanosine triphosphate	$[\text{M}+\text{H}]^+$, $[\text{M}-\text{H}]^-$	0.3 - 10	1 - 10	n.d.	113	n.d.	n.d.
Dihydroxyacetonephosphate	$[\text{M}-\text{H}]^-$, $[\text{M}+\text{H}]^+$	1 - 10	3 - 10	3 - 10	91	n.d.	n.d.
Dihydroxyisovalerate	$[\text{M}-\text{H}]^-$	0.03 - 10	0.1 - 10	0.3 - 10	104	97	110
Erythritol	$[\text{M}-\text{H}]^-$	0.03 - 10	bg	1 - 10	95	bg	91
Erythrose-4-phosphate	$[\text{M}-\text{H}]^-$	0.3 - 10	3 - 10	3 - 10	95	n.d.	n.d.
Flavinadenin dinucleotide	$[\text{M}+\text{H}]^+$, $[\text{M}-\text{H}]^-$	0.1 - 10	1 - 10	1 - 10	102	66	14
Hexose (Fructose, Galactose, Mannose, Glucose, Inositol)	$[\text{M}-\text{H}]^-$	0.5 - 5	bg	bg	113	bg	bg
Fructose-1,6-bisphosphate	$[\text{M}-\text{H}]^-$, $[\text{M}+\text{H}]^+$	0.3 - 10	1 - 10	n.d.	108	105	n.d.
Hexose-6-phosphate (Fructose-6-phosphate, Glucose-1-phosphate, Glucose-6-phosphate)	$[\text{M}-\text{H}]^-$, $[\text{M}+\text{H}]^+$	0.03 - 30	0.09 - 30	0.3 - 30	95	n.d.	n.d.
Fumarate	$[\text{M}-\text{H}]^-$	0.1 - 10	3 - 10	0.3 - 10	98	93	134
Gluconate	$[\text{M}-\text{H}]^-$	0.1 - 10	bg	1 - 10	106	bg	93
Glutamate	$[\text{M}-\text{H}]^-$, $[\text{M}+\text{H}]^+$	0.01 - 10	0.3 - 10	bg	100	106	bg
Glutamine	$[\text{M}+\text{H}]^+$, $[\text{M}-\text{H}]^-$	0.03 - 10	bg	bg	98	bg	bg
Glutamyl-cysteine	$[\text{M}+\text{H}]^+$, $[\text{M}-\text{H}]^-$	0.1 - 3	n.d.	n.d.	112	n.d.	n.d.

Compound	Species	Linear dynamic range [μM]			Recovery [%]		
		Solvent	Urine	Plasma	Solvent	Urine	Plasma
Glutathione, oxidized	$[\text{M}+\text{H}]^+$, $[\text{M}-\text{H}]^-$	0.1 - 10	1 - 10	0.3 - 10	95	27	n.d.
Glutathione, reduced	$[\text{M}-\text{H}]^-$, $[\text{M}+\text{H}]^+$	0.1 - 10	0.1 - 10	1 - 10	n.d.	n.d.	n.d.
Glycine	$[\text{M}-\text{H}]^-$, $[\text{M}+\text{H}]^+$	0.3 - 10	bg	bg	102	bg	bg
Glyoxylic acid		Not detected					
GMP	$[\text{M}-\text{H}]^-$, $[\text{M}+\text{H}]^+$	0.01 - 10	0.3 - 10	0.1 - 10	102	123	119
Guanidineacetic acid	$[\text{M}+\text{H}]^+$, $[\text{M}-\text{H}]^-$	0.3 - 10	bg	1 - 10	104	bg	93
Guanine	$[\text{M}+\text{H}]^+$, $[\text{M}-\text{H}]^-$	0.01 - 10	0.03 - 10	0.03 - 10	93	108	51
Guanosine + Isoguanosine	$[\text{M}+\text{H}]^+$, $[\text{M}-\text{H}]^-$	0.2 - 6	0.6 - 20	0.02 - 6	99	32	101
Guanosine 3',5'-cyclic monophosphate	$[\text{M}+\text{H}]^+$, $[\text{M}-\text{H}]^-$	0.01 - 10	0.1 - 10	1 - 10	107	71	32
Guanosine 5'-diphosphate	$[\text{M}-\text{H}]^-$, $[\text{M}+\text{H}]^+$	0.3 - 10	0.3 - 10	3 - 10	107	71	n.d.
Guanosine 5'-triphosphate	$[\text{M}+\text{H}]^+$, $[\text{M}-\text{H}]^-$	0.3 - 10	3 - 10	n.d.	108	n.d.	n.d.
Histidine	$[\text{M}+\text{H}]^+$, $[\text{M}-\text{H}]^-$	0.3 - 10	bg	bg	98	bg	bg
Homocysteine	$[\text{M}+\text{H}]^+$, $[\text{M}-\text{H}]^-$	0.3 - 10	0.03 - 10	1 - 10	84	n.d.	n.d.
Homoserine + Threonine	$[\text{M}+\text{H}]^+$, $[\text{M}-\text{H}]^-$	0.03 - 10	bg	bg	102	bg	bg
Hydroxyglutaric acid	$[\text{M}-\text{H}]^-$	0.01 - 10	bg	1 - 10	103	bg	115
Inosine	$[\text{M}-\text{H}]^-$, $[\text{M}+\text{H}]^+$	0.01 - 10	0.3 - 10	0.03 - 10	101	74	115
Inosine 5'-monophosphate	$[\text{M}-\text{H}]^-$, $[\text{M}+\text{H}]^+$	0.1 - 10	0.1 - 10	0.3 - 10	47	70	47
Isoleucine + Leucine	$[\text{M}-\text{H}]^-$, $[\text{M}+\text{H}]^+$	0.06 - 20	bg	bg	bg	bg	bg
Ketoisovalerate	$[\text{M}-\text{H}]^-$	0.1 - 10	0.3 - 10	3 - 10	94	bg	94
Kynurenine	$[\text{M}+\text{H}]^+$, $[\text{M}-\text{H}]^-$	0.01 - 10	0.3 - 10	0.03 - 10	24	54	24
Lactate	$[\text{M}-\text{H}]^-$	0.3 - 10	1 - 10	1 - 10	bg	bg	bg
L-Citrulline	$[\text{M}+\text{H}]^+$, $[\text{M}-\text{H}]^-$	0.03 - 10	bg	3 - 10	bg	bg	bg
L-Cystathionine	$[\text{M}+\text{H}]^+$, $[\text{M}-\text{H}]^-$	0.03 - 10	1 - 10	0.03 - 10	94	107	94
L-Ornithine	$[\text{M}-\text{H}]^-$, $[\text{M}+\text{H}]^+$	0.1 - 10	0.3 - 10	bg	104	96	bg
Lysine	$[\text{M}+\text{H}]^+$, $[\text{M}-\text{H}]^-$	0.3 - 10	bg	bg	bg	bg	bg
Malate	$[\text{M}-\text{H}]^-$	0.01 - 10	0.1 - 10	0.03 - 10	111	115	111
Mannitol	$[\text{M}-\text{H}]^-$	0.03 - 10	bg	bg	bg	bg	bg
Mannitol 1-phosphate	$[\text{M}-\text{H}]^-$, $[\text{M}+\text{H}]^+$	0.1 - 10	1 - 10	0.3 - 10	68	n.d.	68
Melatonin	$[\text{M}+\text{H}]^+$, $[\text{M}-\text{H}]^-$	0.001 - 10	0.03 - 10	0.1 - 10	119	115	119
Methionine	$[\text{M}+\text{H}]^+$, $[\text{M}-\text{H}]^-$	0.03 - 10	0.3 - 10	0.1 - 10	110	bg	110
Methionine sulfone	$[\text{M}+\text{H}]^+$, $[\text{M}-\text{H}]^-$	0.01 - 10	bg	bg	100	bg	bg

Compound	Species	Linear dynamic range [μM]			Recovery [%]		
		Solvent	Urine	Plasma	Solvent	Urine	Plasma
Mevalonic acid	[M-H] ⁻	0.01 - 10	1 - 10	0.3 - 10	124	101	124
N4-Acetylcytidine	[M+H] ⁺ , [M-H] ⁻	0.01 - 10	0.3 - 10	1 - 10	100	95	100
N-Acetyl-Asp-Glu	[M-H] ⁻ , [M+H] ⁺	0.01 - 10	0.3 - 10	bg	93	61	bg
N-Acetyl-L-aspartic acid	[M-H] ⁻ , [M+H] ⁺	0.03 - 10	bg	0.1 - 10	96	bg	96
N-Acetyl-serine	[M-H] ⁻ , [M+H] ⁺	0.03 - 10	0.3 - 10	0.3 - 10	92	99	92
NAD ⁺	[M+H] ⁺ , [M-H] ⁻	0.01 - 10	0.3 - 10	0.3 - 10	111	97	111
NADH	[M+H] ⁺ , [M-H] ⁻	0.1 - 10	n.d.	n.d.	n.d.	n.d.	n.d.
NADP ⁺	[M+H] ⁺ , [M-H] ⁻	0.1 - 10	1 - 10	1 - 10	n.d.	n.d.	n.d.
NADPH	[M+H] ⁺ , [M-H] ⁻	1 - 10	3 - 10	3 - 10	n.d.	n.d.	n.d.
Nicotinamide	[M+H] ⁺ , [M-H] ⁻	0.01 - 10	0.01 - 10	0.01 - 10	105	90	105
Octopamine		Not detected					
Oxaloacetic acid	[M-H] ⁻	1 - 10	n.d.	n.d.	97	n.d.	n.d.
Palmitic acid	[M-H] ⁻ , [M+H] ⁺	n.d.	n.d.	n.d.	n.d.	n.d.	n.d.
Phenylalanine	[M-H] ⁻ , [M+H] ⁺	0.03 - 10	0.3 - 10	bg	99	103	bg
Phosphocreatine	[M+H] ⁺ , [M-H] ⁻	0.1 - 10	1 - 10	0.1 - 10	110	103	n.d.
Proline	[M+H] ⁺ , [M-H] ⁻	0.03 - 10	1 - 10	bg	102	115	bg
Propionyl-L-carnitine	[M+H] ⁺ , [M-H] ⁻	0.01 - 10	1 - 10	0.3 - 10	100	121	99
Pseudouridine	[M-H] ⁻ , [M+H] ⁺	0.01 - 10	0.1 - 10	0.1 - 10	102	100	111
Pyruvate	[M-H] ⁻	0.1 - 10	bg	1 - 10	101	bg	bg
Ribose	[M-H] ⁻	1 - 10	n.d.	n.d.	105	n.d.	n.d.
Ribose-5-phosphate + Ribulose-5-phosphate	[M-H] ⁻ , [M+H] ⁺	0.06 - 20	0.6 - 20	0.6 - 20	98	26	10
S-(Adenosyl)-methionine	[M+H] ⁺ , [M-H] ⁻	0.1 - 10	1 - 10	n.d.	119	n.d.	n.d.
Sarcosine	[M+H] ⁺ , [M-H] ⁻	0.1 - 10	1 - 10	0.1 - 10	102	96	102
Sedoheptulose-7-phosphate	[M-H] ⁻ , [M+H] ⁺	0.01 - 10	0.1 - 10	0.1 - 10	93	112	n.d.
Seleno-methionine	[M+H] ⁺ , [M-H] ⁻	0.03 - 10	0.3 - 10	0.1 - 10	102	107	114
Serine	[M-H] ⁻ , [M+H] ⁺	0.1 - 10	bg	bg	100	bg	bg
Serotonine	[M+H] ⁺ , [M-H] ⁻	0.03 - 10	0.03 - 10	0.03 - 10	98	114	99
Spermidine		Not detected					
Spermine		Not detected					
Succinate	[M-H] ⁻	0.1 - 10	1 - 10	0.1 - 10	98	115	151
Thiamine hydrochloride		Not detected					
Thymidine	[M-H] ⁻ , [M+H] ⁺	0.01 - 10	0.1 - 10	0.03 - 10	99	57	55

Compound	Species	Linear dynamic range [μM]			Recovery [%]		
		Solvent	Urine	Plasma	Solvent	Urine	Plasma
Thymidine 5'-monophosphate	[M-H] ⁻ , [M+H] ⁺	0.01 - 10	0.1 - 10	0.03 - 10	109	60	33
Thymine	[M-H] ⁻ , [M+H] ⁺	0.03 - 10	0.3 - 10	0.1 - 10	99	98	45
Trehalose	[M-H] ⁻ , [M+H] ⁺	0.01 - 10	0.3 - 10	0.1 - 10	98	95	94
Tryptophan	[M-H] ⁻ , [M+H] ⁺	0.01 - 10	bg	bg	93	bg	bg
TTP (Thymidinetriphosphate)	[M-H] ⁻ , [M+H] ⁺	0.3 - 10	0.3 - 10	n.d.	110	106	n.d.
Tyrosine	[M-H] ⁻ , [M+H] ⁺	0.03 - 10	bg	bg	98	bg	bg
UMP	[M-H] ⁻ , [M+H] ⁺	0.01 - 10	1 - 10	0.3 - 10	98	114	n.d.
Uracil	[M-H] ⁻ , [M+H] ⁺	0.1 - 10	bg	0.03 - 10	99	bg	68
Uridine	[M-H] ⁻ , [M+H] ⁺	0.01 - 10	bg	1 - 10	105	bg	111
Uridine 5'-diphosphate	[M-H] ⁻ , [M+H] ⁺	0.3 - 10	0.3 - 10	1 - 10	105	95	n.d.
Uridine 5'-triphosphate	[M-H] ⁻ , [M+H] ⁺	1 - 10	3 - 10	n.d.	109	n.d.	n.d.
Valine	[M-H] ⁻ , [M+H] ⁺	0.03 - 10	bg	bg	97	bg	bg
Xanthine	[M-H] ⁻ , [M+H] ⁺	0.01 - 10	bg	0.3 - 10	103	bg	90
Xylose	[M-H] ⁻	1 - 10	n.d.	n.d.	91	n.d.	n.d.

References

Pang, Z., J. Chong, G. Zhou, D.A. de Lima Morais, L. Chang, M. Barrette, C. Gauthier, P.-É. Jacques, S. Li, and J. Xia. 2021. 'MetaboAnalyst 5.0: narrowing the gap between raw spectra and functional insights', *Nucleic Acids Research*, 49: W388-W96.

Supporting Information

Integrated exposomics/metabolomics for rapid exposure and effect analyses

Mira Flasch^{1,2}, Veronika Fitz^{2,3}, Evelyn Rampler³, Chibundu N. Ezekiel⁴, Gunda Koellensperger^{3,5}, Benedikt Warth^{1,5*}

¹University of Vienna, Faculty of Chemistry, Department of Food Chemistry and Toxicology, Währinger Straße 38-40, 1090 Vienna, Austria

²University of Vienna, Vienna Doctoral School of Chemistry, Währinger Straße 42, 1090, Vienna, Austria

³University of Vienna, Faculty of Chemistry, Department of Analytical Chemistry, Währinger Straße 38-40, 1090 Vienna, Austria

⁴Department of Microbiology, Babcock University, Ilishan Remo, Ogun State, Nigeria

⁵Exposome Austria, Research Infrastructure and National EIRENE Hub, Austria

Contents

Table S9: Spot urine analysis of Nigerian women (n=23) at four different timepoints for xenobiotics and endogenous estrogens	
Table S10: Urine analysis (24h urine) of Austrian men (n=2) and women (n=2) for endogenous metabolites and xenobiotics	
Table S11: Spot urine analysis of Nigerian women (n=23) at four different timepoints for endogenous metabolites	
Table S12: Urine analysis (24h urine) of Austrian men (n=2) and women (n=2) for endogenous metabolites	
Table S13: SRM3672 analysis of certified analytes	
Table S14: SRM1950 analysis of certified analytes	
Table S15: Analysis of SRM3672 with additional analytes not present	
Table S16: Analysis of SRM1950 with additional analytes not present	
Table S17: Results of suspect screening in negative ionization mode	
Table S18: Results of suspect screening in positive ionization mode	

Table S9: Spot urine analysis of Nigerian women (n=23) at four different timepoints (morning and evening on two consecutive days) for xenobiotics and endogenous estrogens with limit of detection (LOD), limit of quantification (LOQ), number of positive samples per analytes, minimal and maximal concentration and number of detected analytes per sample

Analyte	LOD	LOQ	Number of positive samples	Concentration [ng/ml]											
				Min	Max	NIG2W	NIG1X	NIG2X	NIG1Y	NIG2Y	NIG1Z	NIG2Z	NIG3Z		
1-OH-pyrene	1.89	6.3	40 <LOQ	95.4	10.6 <LOQ	<LOQ	28.8 n.d.	<LOQ	<LOQ	<LOQ	<LOQ	<LOQ	<LOQ	<LOQ	
17-Epiestriol	3.4	11.3	2 <LOQ	<LOQ	n.d.	n.d.	n.d.	n.d.	n.d.	n.d.	n.d.	n.d.	n.d.	n.d.	
2-Hydroxyestradiol	12.8	42.6	6 <LOQ	97.5 n.d.	n.d.	n.d.	n.d.	n.d.	n.d.	n.d.	n.d.	n.d.	n.d.	n.d.	
2-Methoxyestrone	0.79	2.6	10 <LOQ	3.1 <LOQ	n.d.	n.d.	n.d.	n.d.	n.d.	n.d.	n.d.	n.d.	n.d.	n.d.	
2-Naphthol	5.42	18.1	28 <LOQ	129.6 n.d.	<LOQ	n.d.	n.d.	n.d.	n.d.	n.d.	n.d.	n.d.	n.d.	n.d.	
2-Methoxyestradiol	1.22	4.1	36 <LOQ	146.0	61.2 n.d.	94.4	15.7	52.2	9.3	30.0	4.1	<LOQ	<LOQ	<LOQ	
4-Methoxyestradiol	1.53	5.1	31 <LOQ	21.9 n.d.	6.3 n.d.	n.d.	<LOQ	n.d.	<LOQ	n.d.	<LOQ	<LOQ	<LOQ	<LOQ	
4-tert-octylphenol	0.5	1.7	33 <LOQ	12.4 n.d.	n.d.	<LOQ	1.8	2.5 <LOQ	n.d.	<LOQ	<LOQ	<LOQ	<LOQ	<LOQ	
Alternariol	0.45	1.5	4 <LOQ	2.6 n.d.	n.d.	n.d.	n.d.	n.d.	n.d.	n.d.	n.d.	n.d.	n.d.	n.d.	
Alternariolmonomethylether	0.06	0.2	31 <LOQ	38.1 n.d.	0.7 n.d.	0.7 n.d.	n.d.	n.d.	n.d.	0.4 <LOQ	2.0	<LOQ	<LOQ	<LOQ	
Benzophenone 1	0.04	0.1	65 <LOQ	17.1	0.9	0.5	0.3 <LOQ	n.d.	n.d.	0.4 <LOQ	<LOQ	<LOQ	<LOQ	<LOQ	
Benzylbutylphthalate	1.93	6.4	7 <LOQ	10.4 n.d.	n.d.	n.d.	n.d.	n.d.	n.d.	n.d.	n.d.	n.d.	n.d.	n.d.	
Benzylparaben	0.38	1.3	2 <LOQ	<LOQ	n.d.	n.d.	n.d.	n.d.	n.d.	n.d.	n.d.	n.d.	n.d.	n.d.	
Bisphenol A	0.05	0.2	74 <LOQ	55.1	5.2 n.d.	29.0	1.0	0.8	14.0	1.3	0.4	<LOQ	<LOQ	<LOQ	
Bisphenol S	0.24	0.8	12 <LOQ	6.9 n.d.	n.d.	n.d.	n.d.	n.d.	n.d.	n.d.	n.d.	n.d.	n.d.	n.d.	
Butylparaben	0.03	0.1	32 <LOQ	3.4 n.d.	0.2 <LOQ	n.d.	n.d.	n.d.	n.d.	n.d.	n.d.	<LOQ	<LOQ	<LOQ	
Cofthine	3.37	11.2	3 <LOQ	46.5 n.d.	n.d.	n.d.	n.d.	n.d.	n.d.	n.d.	n.d.	n.d.	n.d.	n.d.	
Coumestrol	0.42	1.4	31 <LOQ	24.1 n.d.	n.d.	n.d.	n.d.	n.d.	1.8 <LOQ	<LOQ	<LOQ	<LOQ	<LOQ	6.5	
Daidzein	0.57	1.9	67 <LOQ	4609.9	16.9	17.2	62.8	33.0	73.3	43.4	4609.9	19.4	19.4	19.4	
Dibutylphthalate	5.51	18.4	61 <LOQ	729.5	31.5	24.4 n.d.	51.4	36.7	48.8	57.7	76.8	76.8	76.8	76.8	
Enterodiol	0.19	0.6	56 <LOQ	363.0	16.9	1.3	3.5	4.8	4.0	8.6	261.0 <LOQ	<LOQ	<LOQ	<LOQ	
Enteractone	0.34	1.1	75 <LOQ	5159.7	96.7	39.7	119.7	37.1	254.7	260.7	9.0	37.2	37.2	37.2	
Equol	4	13.3	15 <LOQ	818.0 n.d.	n.d.	n.d.	n.d.	n.d.	n.d.	n.d.	n.d.	n.d.	n.d.	n.d.	
Estradiol	0.73	2.4	8 <LOQ	3.2 n.d.	n.d.	n.d.	n.d.	n.d.	n.d.	n.d.	n.d.	n.d.	n.d.	n.d.	
Estradiol-3-sulfate	0.63	2.1	2 <LOQ	0.0 n.d.	n.d.	n.d.	n.d.	n.d.	n.d.	n.d.	n.d.	n.d.	n.d.	n.d.	
Estrilol	0.88	2.9	33 <LOQ	613.0	7.7 n.d.	12.7	4.2 <LOQ	3.6	5.7	4.9	613.0 n.d.	<LOQ	<LOQ	1.4	
Estrone	0.41	1.4	61 <LOQ	165	3.6 <LOQ	4.2 <LOQ	0.6	0.4 n.d.	2.5 <LOQ	<LOQ	<LOQ	<LOQ	<LOQ	1.4	
Ethinylestradiol	2.5	8.3	2 <LOQ	<LOQ	n.d.	n.d.	n.d.	n.d.	n.d.	n.d.	n.d.	n.d.	n.d.	n.d.	
Ethylparaben	0.07	0.2	55 <LOQ	15.5	0.9 <LOQ	1.3	0.6	0.4 n.d.	0.6 <LOQ	<LOQ	<LOQ	<LOQ	<LOQ	<LOQ	
Formononetin	0.15	0.5	35 <LOQ	0.6 n.d.	n.d.	<LOQ	<LOQ	0.6	0.6 <LOQ	<LOQ	<LOQ	<LOQ	<LOQ	<LOQ	
Genistein	2.1	7.0	43 <LOQ	791.0 <LOQ	26.2 n.d.	<LOQ	<LOQ	8.1 n.d.	n.d.	<LOQ	<LOQ	<LOQ	<LOQ	<LOQ	
Glycitein	1.93	6.4	27 <LOQ	401.0 n.d.	<LOQ	33.6 n.d.	n.d.	n.d.	n.d.	n.d.	n.d.	n.d.	n.d.	n.d.	
Isobutylparaben	0.19	0.6	5 <LOQ	2.1 n.d.	n.d.	n.d.	n.d.	n.d.	n.d.	n.d.	n.d.	n.d.	n.d.	n.d.	
Isoxanthohumol	0.45	1.5	4 <LOQ	2.0 n.d.	n.d.	n.d.	n.d.	n.d.	n.d.	n.d.	n.d.	n.d.	n.d.	n.d.	
Jacobine	3.68	12.3	2 <LOQ	123.0 n.d.	n.d.	n.d.	n.d.	n.d.	n.d.	n.d.	n.d.	n.d.	n.d.	n.d.	
Matirastinol	6.69	22.3	16 <LOQ	42.4 <LOQ	n.d.	n.d.	n.d.	n.d.	n.d.	n.d.	n.d.	n.d.	n.d.	n.d.	
MEHP	11.8	39.2	41 <LOQ	39.7 <LOQ	n.d.	<LOQ	<LOQ	<LOQ	<LOQ	<LOQ	<LOQ	<LOQ	<LOQ	<LOQ	
Methylparaben	0.24	0.8	63 <LOQ	398.8	195.8	21.0	196.8	3.0	56.8	2.5	3.4	<LOQ	<LOQ	3.4	
Monobutylphthalate	0.59	2.0	63 <LOQ	473.0	59.2 n.d.	90.6	18.9	18.2	96.1 n.d.	314.0	314.0	<LOQ	<LOQ	314.0	
n-Butylbenzolsulfonamid	0.23	0.8	18 <LOQ	1.7 n.d.	n.d.	<LOQ	n.d.	<LOQ	n.d.	n.d.	n.d.	n.d.	n.d.	n.d.	
Nonylphenol	0.97	3.2	73 <LOQ	103.0	25.7	6.8	35.7	19.3	13.0	13.2	12.3	29.1	29.1	29.1	
p-Hydrobenzoicacid	0.15	0.5	70 <LOQ	4498.5	6595.3	345.3	5645.3	3815.3	3575.3	1625.3	2065.3	2645.3	2645.3	2645.3	
Propylparaben	0.02	0.1	71 <LOQ	102.0	19.9	0.7	7.0	0.4	0.5	0.1	0.2	0.3	0.3	0.3	
Resveratrol	0.55	1.8	7 <LOQ	4.0 n.d.	n.d.	n.d.	n.d.	n.d.	n.d.	n.d.	n.d.	n.d.	n.d.	n.d.	
Riddelliin	1.75	5.8	1 <LOQ	5.9 n.d.	n.d.	n.d.	n.d.	n.d.	n.d.	n.d.	n.d.	n.d.	n.d.	n.d.	
Triclosan	0.43	1.4	55 <LOQ	5010	700.0	652.0	968.0	2.7 n.d.	26.1	6.2	13.7	13.7	13.7	13.7	
Zearalenon	0.42	1.4	4 <LOQ	<LOQ	n.d.	n.d.	n.d.	n.d.	n.d.	n.d.	n.d.	n.d.	n.d.	n.d.	
Zearalenon-14-glucuronide	0.36	1.2	4 <LOQ	61.0 n.d.	n.d.	n.d.	n.d.	n.d.	n.d.	n.d.	n.d.	n.d.	n.d.	n.d.	
Number of detected analytes			31	25	24	27	26	27	28	28	32				

Table S11: Spot urine analysis of Nigerian women (n=23) at four different timepoints (morning and evening on two consecutive days) for endogenous metabolites with limit of detection (LOD). Limit of quantification (LOQ), number of positive samples per analyte, minimal and maximal concentration and number of detected analytes per sample

Analyte	Concentration [μM]		Max	Nunt/min		Max	Nunt/min		Max
	LOD	LOQ		Nunt	min		Nunt	min	
3-Methyl-2-oxovalerate	0.02	0.067	21	0.10					
3-Methylcrotonylate	1	3.333	45	<LOQ					
4-Hydroxyphenyllactate	0.05	0.167	51	<LOQ					
5-Methylthiohydron	0	0.013	24	<LOQ					
5-Methylvalerolactone	0	0.013	65	0.03					
Adenosine	0	0.013	60	<LOQ					
Alanine	0.4	1.333	77	<LOQ					
alpha-ketoglutarate	0.04	0.133	69	<LOQ					
Ammoniumlactate	0.04	0.133	70	<LOQ					
Argininosuccinate	0	0.013	62	0.02					
Aspartate	0.04	0.133	77	0.17					
Aspartic acid	0.04	0.133	76	<LOQ					
Betaine	0.04	0.133	64	0.01					
Brain	0	0.003	64	0.01					
CAMP	0.03	0.100	75	0.10					
Citrulline	0	0.013	76	<LOQ					
Cytidine	0.4	1.333	76	<LOQ					
DAHP	0.04	0.133	46	<LOQ					
Dihydroxyisovalerate	0.02	0.060	8	0.16					
Enthalpate	0.04	0.133	71	<LOQ					
Ferrocyanide	0.4	1.333	77	<LOQ					
Glutamate	0.04	0.133	77	<LOQ					
Glutamine	0.4	1.333	77	1.60					
Glycerate	0.04	0.133	75	<LOQ					
Glycine	0.4	1.333	75	<LOQ					
GMP	0.04	0.133	31	<LOQ					
Guanidinesulfate	0.4	1.333	76	<LOQ					
Guanine	0	0.013	76	0.02					
Heose	0.5	1.667	76	1.71					
Heose-phosphate	0.04	0.133	56	<LOQ					
Histidine	0.05	0.167	77	0.48					
Hydroxybutyrate	0.04	0.133	77	0.17					
Hydroxyphenyllactate	0.04	0.133	75	<LOQ					
Isoalloxanthine	0.04	0.133	77	0.14					
Ketoglutarate	0.02	0.067	67	0.45					
Lactic acid	0.5	1.667	48	8.25					
Malic acid	0	0.010	77	0.03					
Mannitol	0.4	1.333	64	<LOQ					
Mannitol-1-phospho	0.04	0.133	19	0.15					
Methionine	0.01	0.020	65	<LOQ					
N-Acetyl-Asp-Glu	0.04	0.133	64	0.27					
N-Acetyl-L-Aspartic	0	0.010	75	0.64					
N-Acetylserine	0	0.010	61	0.19					
N-Acetylvalerate	0	0.013	67	<LOQ					
Ornithine	0.01	0.023	71	0.05					
Penicillamine	0.04	0.133	70	<LOQ					
Phenylalanine	0	0.013	77	0.18					
Phosphocreatine	0.03	0.100	8	0.17					
Proline	0	0.007	77	0.11					
Propionylvalerate	0	0.003	47	<LOQ					
Pyruvic acid	0.05	0.167	67	<LOQ					
Succinic acid	0.2	0.7	77	<LOQ					
Serine	0.04	0.133	66	0.33					
Thymine	0	0.010	59	0.07					
TMP	0.04	0.133	6	<LOQ					
Trehalose	0.04	0.133	74	<LOQ					
Tryptophan	0.01	0.033	77	<LOQ					
Tyrosine	0.05	0.167	70	<LOQ					
UDP	0.03	0.100	5	<LOQ					
Uracil	0.1	0.333	74	0.52					
Valine	0.05	0.167	77	0.20					
Vinone	0.05	0.167	77	0.20					
Xanthine	0.01	0.033	76	<LOQ					

Table S16: Analysis of SRM1950 for analytes not reported in the certificate of analysis

Analyte	Category	Concentration [µM]	
		Average	Standard deviation
2-Naphtol	Industrial side product and pesticides	0.7	0.1
4-tert-octylphenol	Industrial side product and pesticides	7.6	0.2
Benzophenone 1	Personal care product ingredients and pharmaceuticals	0.02	0.0
Bisphenol A	Plasticizer	1.5	0.1
Bisphenol S	Plasticizer	0.4	0.2
Cotinine	Air pollutant	396	193
Daidzein	Phytoestrogen	0.2	0.0
Formononetin	Phytoestrogen	1.2	0.2
Genistein	Phytoestrogen	0.4	0.0
MEHP	Plasticizer	99.0	0.1
Methylparaben	Personal care product ingredients and pharmaceuticals	5.4	0.3
Nonylphenol	Industrial side product and pesticides	14.9	2.9
p-Hydrobenzoic acid	Personal care product ingredients and pharmaceuticals	1637	478
Propylparaben	Personal care product ingredients and pharmaceuticals	0.1	0.0
Scolpolamine	Phytotoxin	4.2	1.2
trans-3-OH-cotinine	Air pollutant	697	84
Analyte	Category	Concentration [ng/mL]	
3-Methyl-2-oxovaleric acid	Organic acids (Keto acids)	34.900	1.850
3-Methylcytidine	Nucleosides	82.294	17.371
4-Hydroxy-proline	Organic acids (Amino acids)	1.785	0.282
5'-Methylthioadenosine	Nucleosides	<LOQ	
5-Methyluridine	Nucleosides	0.157	0.013
Adenine	Nucleobases	0.011	0.001
alpha-Ketoglutaric acid	Organic acids (Keto acids)	10.295	0.366
Aminoadipic acid	Organic acids (Amino acids)	1.476	0.148
Argininosuccinic acid	Organic acids (Amino acids)	0.044	0.009
Asparagine	Organic acids (Amino acids)	23.029	0.252
Aspartic acid	Organic acids (Amino acids)	2.645	0.147
Betaine	Organic acids (Amino acids)	16.044	2.003
Biotin	Biotin and derivatives	0.030	0.006
Carnitine	Quaternary ammonium salts	16.145	1.935
Citric acid + Isocitric acid	Organic acids (Carboxylic acids)	26.959	2.862
Citrulline	Organic acids (Amino acids)	30.554	0.351
Cystathionine	Organic acids (Amino acids)	<LOQ	0.017
Cystine	Organic acids (Amino acids)	35.851	0.872
Dihydroxy-isovalerate	Fatty acyls	0.674	0.099
Erythritol	Carbohydrates and conjugates	7.510	1.066
Fumaric acid	Organic acids (Carboxylic acids)	1.914	0.145
Gluconate	Carbohydrates and conjugates	34.305	0.987
Glutamate	Organic acids (Amino acids)	66.213	0.608
Glutamine	Organic acids (Amino acids)	359.680	2.082
Guanidineacetic acid	Organic acids (Amino acids)	1.504	0.181
Hexose	Carbohydrates and conjugates	92.855	10.471
Homoserine+Threonine	Organic acids (Amino acids)	34.976	0.351
Hydroxyglutaric acid	Organic acids (Hydroxy acids)	0.392	0.032
Ketoisovaleric acid	Organic acids (Keto acids)	25.364	1.480
Lactic acid	Organic acids (Hydroxy acids)	1352.826	91.652
Malic acid	Organic acids (Hydroxy acids)	2.963	0.061
Mannitol	Carbohydrates and conjugates	3.080	1.087
N-Acetyl-Asp-Glu	Organic acids (Amino acids)	0.019	0.012
N-Acetyl-L-aspartic acid	Organic acids (Amino acids)	1.162	0.453
N-Acetylserine	Organic acids (Amino acids)	0.855	0.071
N-Methylhydantoin	Organoheterocyclic compounds	24.073	1.562
N4-Acetylcytidine	Nucleosides	<LOQ	0.053
Ornithine	Organic acids (Amino acids)	33.595	0.321
Pentose-phosphate	Organic acids (Amino acids)	0.197	0.042
Propionylcarnitine	Fatty acyls	0.512	0.036
Pseudouridine	Nucleosides	17.432	2.717
Pyruvic acid	Organic acids (Keto acids)	97.404	7.657
Serotonin	Indoles and derivatives	5.686	1.056
Succinic acid	Organic acids (Carboxylic acids)	3.650	0.240
Trehalose	Carbohydrates and conjugates	0.228	0.029
Uracil	Nucleobases	<LOQ	0.037
Uridine	Nucleosides	2.779	0.540
Xanthine	Nucleobases	1.242	0.535

Table S12: Urine analysis (24h urine) of Austrian men (n=2) and women (n=2) sampled on three consecutive days for endogenous metabolites with limit of detection (LOD), limit of quantification (LOQ), number of positive samples per analytes, minimal and maximal concentration and number of detected analytes per sample

Analyte	LOD	LOQ	Number of positive samples	Concentration [µM]		Replicate													
				Min	Max	24hU5W1	24hU5W1	24hU5W1	24hU5W2	24hU5W2	24hU5M1	24hU5M1	12hU6S1	24hU6S1	24hU5M2	24hU6S2			
3-Methyl-2-oxoglutaric acid	0.02	0.1	11	1.41	50.33	132.3	2960	3.45	50.33	4.67	1.41	25.23	15.33	6407	17734	4103	2313	7.79	40.93
3-Methylcytidine	1	3.3	11	1085	17734	n.d.	n.d.	2262	8843	1810	1085	15519	6407	17734	n.d.	8527	2313	1984	1993
4-Hydroxy-proline	0.05	0.2	11	0.16	0.48	0.27	0.18	0.37	0.32	0.32	0.20	0.44	0.16	0.40	0.31	0.40	0.31	0.18	0.48
5-Methylthioadenosine	0.004	0.01	11	0.42	2.25	0.85	0.49	1.69	0.54	0.42	2.25	0.87	1.95	1.20	0.51	0.88	0.51	0.88	0.88
5-Methyluridine	0.004	0.01	11	0.05	0.25	0.05	0.07	0.14	0.23	0.23	0.12	0.25	0.10	0.22	0.18	0.07	0.18	0.07	0.22
Adenosine	0.004	0.01	11	0.38	29.60	4.74	1.12	29.60	1.45	0.91	0.91	8.54	2.02	10.30	0.73	0.38	0.38	1.28	1.28
Alanine	0.04	1.3	11	51.05	37015	215	125	369	58.85	51.05	197.15	2.02	81.55	37015	154.15	93.15	245.15	245.15	245.15
alpha-Ketoglutaric acid	0.04	0.1	11	18.60	146.00	130.00	18.60	119.00	98.60	98.60	29.50	123.00	44.70	146.00	53.50	20.00	107.00	107.00	107.00
Aracetamidic acid	0.004	0.01	11	3.09	15.50	19.83	2.72	9.53	8.38	3.46	16.61	15.50	7.55	25.44	2.207	10.68	14.13	13.00	13.00
Aminoisuccinic acid	0.004	0.01	11	18.90	179.00	54.90	19.20	69.70	19.20	23.70	18.90	153.00	42.00	179.00	59.40	28.80	72.70	28.80	72.70
Asparagine	0.04	0.1	11	2.18	22.01	4.85	2.29	22.01	2.83	2.18	11.81	4.84	20.11	6.40	2.47	8.12	6.40	2.47	8.12
Aspartic acid	0.04	0.1	11	1.22	35.31	6.8	5.1	8.4	6.96	2.7	15.9	1.2	35.3	3.3	7.3	5.9	7.3	5.9	7.3
Betaine	0.002	0.01	11	1.63	62.51	2.02	1.64	62.51	1.64	62.51	6.96	1.83	2.87	9.84	2.26	1.63	2.48	1.63	2.48
Biotin	0.004	0.01	11	1.16	4.21	1.75	1.56	3.26	2.17	1.16	3.76	4.21	1.73	4.21	1.79	1.62	1.79	1.62	1.79
CAMP	0.004	0.01	9	9.00	180.00	10.30	9.00	180.00	20.90	n.d.	75.20	41.60	n.d.	99.50	96.70	110.00	99.50	96.70	110.00
Carnitine	0.03	0.1	11	1.16	4.21	1.75	1.56	3.26	2.17	1.16	3.76	4.21	1.73	4.21	1.79	1.62	1.79	1.62	1.79
Citric acid + Isocitric acid	1	3.3	11	238.2	2750.2	323.16	238.16	2750.16	399.16	299.16	1690.16	765.16	2610.16	485.16	299.16	819.16	299.16	819.16	819.16
Citrulline	0.4	1.3	11	2.67	9.78	5.59	3.16	9.78	4.54	4.54	7.42	2.67	9.55	6.76	9.78	4.61	9.78	4.61	9.78
Cystathionine	0.04	0.1	11	4.01	35.59	14.79	4.01	12.79	14.29	5.90	35.59	9.54	15.49	13.79	7.59	7.59	11.49	11.49	11.49
Cysteine	0.4	1.3	11	75.15	436.95	140.95	86.45	325.95	96.75	75.15	198.95	117.95	436.95	235.95	138.95	273.95	138.95	273.95	273.95
DAMP	0.003	0.01	1	0.12	0.12	n.d.	n.d.	n.d.	n.d.	n.d.	n.d.	0.12	n.d.	n.d.	n.d.	n.d.	n.d.	n.d.	n.d.
Dihydroxy-kovaleate	0.03	0.1	2	25.98	28.08	n.d.	n.d.	25.98	28.08	n.d.	28.08	n.d.	25.98	28.08	n.d.	25.98	28.08	n.d.	25.98
Erythritol	0.04	0.1	11	58.13	310.03	84.63	93.13	257.03	81.13	257.03	81.13	202.03	116.03	310.03	73.03	58.13	73.03	58.13	191.03
Fumaric acid	0.4	1.3	11	2.17	253.00	3.56	25.30	221.00	2.17	36.40	11.13	92.50	253.00	2.17	7.85	7.85	4.45	7.85	4.45
Glucuronate	0.04	0.1	11	173.37	1872.00	572.36	173.37	1277.10	490.89	547.57	1417.00	557.83	1872.00	822.35	211.01	106.00	106.00	106.00	106.00
Glutamate	0.4	1.3	11	5.42	57.61	12.01	5.42	57.61	14.21	9.79	45.91	12.61	56.41	8.66	31.21	8.66	31.21	8.66	31.21
Glutamine	0.04	0.1	11	78.61	808.01	150.01	78.61	808.01	105.01	82.11	624.01	273.01	808.01	269.01	165.01	368.01	165.01	368.01	368.01
Glycine	0.4	1.3	11	172.67	278.06	246.06	172.67	278.06	176.06	278.06	115.06	225.06	108.06	133.06	182.06	71.26	130.06	71.26	130.06
Guandiacetic acid	0.4	1.3	11	71.26	278.06	246.06	71.26	278.06	176.06	278.06	115.06	225.06	108.06	133.06	182.06	71.26	130.06	71.26	130.06
Guanine	0.004	0.01	11	0.24	2.10	0.24	2.10	0.84	0.90	0.31	0.46	0.61	2.10	1.20	0.67	1.20	0.67	1.20	0.67
Hexose	0.5	1.7	11	398	6989	584.20	511.70	3994.80	564.87	458.22	2237.10	747.13	6989.40	522.11	397.52	1414.60	522.11	397.52	1414.60
Hexose-phosphate	0.04	0.1	11	0.07	0.85	0.60	0.28	0.85	0.37	0.24	0.16	0.56	0.22	0.07	0.46	0.31	0.56	0.31	0.56
Histidine	0.05	0.2	11	183.14	1170.14	364.14	183.14	1140.14	283.14	221.14	1080	541.14	1170.14	867.14	561.14	1030.14	867.14	561.14	1030.14
Homoserine+Threonine	0.04	0.1	11	14.61	99.91	34.31	16.21	99.91	16.61	14.61	95.01	36.41	91.51	49.21	27.21	57.31	49.21	27.21	57.31
Hydroxyglutaric acid	0.04	0.1	11	3.21	14.49	7.33	4.61	12.61	10.61	7.25	4.79	3.53	10.61	7.50	3.21	14.49	7.50	3.21	14.49
Isoleucine+Leucine	0.04	0.1	11	16.12	130.02	52.62	16.12	35.12	40.82	31.62	43.52	130.02	43.42	21.22	4.22	16.62	4.22	16.62	4.22
Lactic acid	0.02	0.1	11	8.41	1770.16	15.46	12.06	1770.16	13.96	8.41	46.76	43.36	218.16	13.66	9.13	35.16	13.66	9.13	35.16
Ketovoleic acid	0.5	1.7	11	72	6298	7203	72	6298	8323	6298.00	112.83	151.83	167.83	1052.83	77.33	93.03	252.83	77.33	93.03
Malic acid	0.003	0.0	11	1.18	8.39	3.28	2.09	7.76	1.64	1.38	4.90	2.96	8.39	2.01	1.18	3.25	2.01	1.18	3.25
Mannitol	0.4	1.3	11	53	5925	124.31	68.52	5924.90	1734.00	157.64	1450.80	413.92	3541.20	96.03	52.59	430.47	96.03	52.59	430.47
Methionine	0.006	0.0	11	2.20	15.50	7.42	2.84	15.50	3.02	2.20	13.90	5.60	15.30	10.40	5.46	13.50	10.40	5.46	13.50
N-Acetyl-Asp-Glu	0.04	0.1	11	2.60	41.40	7.10	2.60	41.40	5.07	3.31	31.40	6.28	35.30	8.24	3.54	16.60	8.24	3.54	16.60
N-Acetyl-L-aspartic acid	0.004	0.01	11	26.21	124.01	34.71	35.61	26.21	124.01	34.01	43.71	41.01	29.01	89.61	36.11	35.31	89.61	36.11	35.31
N-Acetylserine	0.004	0.01	11	2.55	11.31	5.28	3.64	8.92	4.13	2.55	9.89	3.87	11.31	7.90	5.09	7.78	7.90	5.09	7.78
N4-Acetylcytidine	0.004	0.01	11	2.95	82.00	21.10	5.02	82.00	2.95	4.99	27.80	6.68	27.50	4.60	3.41	9.12	4.60	3.41	9.12
Ornithine	0.007	0.02	11	0.67	1.94	0.78	1.13	1.94	0.83	0.67	1.62	0.68	1.30	1.72	1.91	1.59	1.72	1.91	1.59
Pentose-phosphate	0.04	0.1	11	2.08	18.08	5.03	2.45	18.08	3.29	2.27	10.88	3.86	7.96	4.55	2.08	8.05	4.55	2.08	8.05
Phenylalanine	0.004	0.01	11	14.62	160.02	32.12	16.32	51.02	20.52	14.62	147.02	37.02	160.02	41.12	26.42	53.52	41.12	26.42	53.52
Phosphocreatine	0.03	0.1	8	0.58	10.19	1.93	0.58	10.19	3.11	n.d.	10.19	0.39	9.90	3.28	8.04	0.75	3.28	8.04	0.75
Proline	0.002	0.1	11	1.24	9.90	3.58	1.24	8.46	1.80	1.58	6.77	3.25	9.90	5.36	3.28	8.04	5.36	3.28	8.04
Propionylcarbamate	0.001	0.003	11	0.91	79.80	1.64	0.91	63.10	2.33	1.96	23.50	8.61	55.00	45.30	18.30	79.80	45.30	18.30	79.80
Pseudouridine	0.005	0.2	11	0.73	2.71	0.98	1.25	2.30	1.12	0.73	1.91	1.02	2.71	1.46	1.17	1.64	1.46	1.17	1.64
Pyruvic acid	0.04	0.1	9	19.54	107.04	53.74	36.14	n.d.	36.04	19.54	107.04	54.94	n.d.	61.04	35.44	72.74	61.04	35.44	72.74
Serine	0.2	0.7	11	74.40	808.10	192.10	108.10	65.10	30.10	74.40	808.10	199.10	108.10	260.10	150.10	313.10	260.10	150.10	313.10
Succinic acid	0.04	0.1	11	13.12	136.07	29.47	21.97	136.07	35.17	29.17	26.83	36.20	132.07	13.12	16.47	39.77	13.12	16.47	39.77
Thymine	0.003	0.0	11	0.49	1.44	0.56	0.62	1.42	0.73	0.54	1.07	0.77	1.44	0.70	0.49	0.61			

Table S13: SRM3672 analysis of certified analytes. Measurement was performed in triplicate (n=3)

	Concentration in SRM 3672 [$\mu\text{g}/\text{kg}$]					
	2-Naphtol	Methylparaben	Ethylparaben	Propylparaben	Butylparaben	Monobutylphthalate
Injection 1	9.98	106	9.22	14.8	9.05	11.3
Injection 2	8.23	102	9.03	14.6	9.11	10.0
Injection 3	10.6	101	9.21	13.8	8.90	15.3
Average	9.60	103	9.15	14.4	9.02	12.2
s	1.23	2.66	0.107	0.528	0.108	2.78

Table S14: SRM1950 analysis of certified analytes. Measurement was performed in triplicate (n=3)

	Concentration in SRM 1950														[ng/mL]		
	[µM]														PFOA	PFOs	
	Glycine	Alanine	Serine	Proline	Valine	(iso)leucine	Methionine	Histidine	Phenylalanine	Tyrosine							
Injection 1	183.82	243.61	83.81	158.53	166.70	113.52	22.36	63.94	50.02	50.02	3.41	13.31					
Injection 2	185.45	250.17	83.03	158.11	183.24	115.03	21.62	65.30	55.63	55.63	3.47	13.24					
Injection 3	183.96	246.99	83.88	156.12	183.63	115.33	21.65	64.98	51.81	51.81	3.41	13.17					
Average	184.41	246.92	83.58	157.59	177.86	114.63	21.88	64.74	52.43	58.94	3.43	13.24					
s	0.90	3.28	0.472	1.287	9.664	0.97	0.42	0.71	2.87	0.88	0.03	0.07					

Table S15: Analysis of SRM3672 for analytes not reported in the certificate of analysis

Analyte	Category	Concentration [ng/mL]	
		Average	Standard deviation
16-Hydroxyestrone	Endogenous estrogens	8.76	1.17
2-Naphtol	Industrial side product and pesticides	9.78	1.25
Benzophenone 1	Personal care product ingredients and pharmaceuticals	153.00	38.6
Butylparaben	Personal care product ingredients and pharmaceuticals	9.19	0.11
Cotinine	Air pollutant	1182	115.1
Daidzein	Phytoestrogen	86.73	24.31
Enterodiol	Phytoestrogen	3.95	1.60
Enterolactone	Phytoestrogen	388.00	148.4
Equol	Phytoestrogen	14.35	3.18
Estrone	Endogenous estrogens	2.78	0.26
Ethylparaben	Personal care product ingredients and pharmaceuticals	9.33	0.11
Genistein	Phytoestrogen	62.90	1.98
Glycitein	Phytoestrogen	25.13	8.17
Matairesinol	Phytoestrogen	122.93	69.4
Methylparaben	Plasticizer	104.65	2.71
Monobutylphthalate	Personal care product ingredients and pharmaceuticals	12.46	2.83
p-Hydrobenzoic acid	Personal care product ingredients and pharmaceuticals	1650.66	218.29
Propylparaben	Personal care product ingredients and pharmaceuticals	15	1
Resveratrol	Phytoestrogen	41.00	11.63
trans-3-OH-cotinine	Air pollutant	3683.86	409.06
Analyte	Category	Concentration [ng/mL]	
3-Methyl-2-oxovaleric acid	Organic acids (Keto acids)	13.67	6.06
3-Methylcytidine	Nucleosides	196.38	21.92
4-Hydroxy-proline	Organic acids (Amino acids)	58.63	8.21
5'-Methylthioadenosine	Nucleosides	0.27	0.03
5-Methyluridine	Nucleosides	0.55	0.06
Adenine	Nucleobases	0.22	0.07
Adenosine	Nucleosides	2.59	0.09
Alanine	Organic acids (Amino acids)	132.81	3.21
alpha-Ketoglutaric acid	Organic acids (Keto acids)	73.70	2.35
Aminoadipic acid	Organic acids (Amino acids)	16.71	8.89
Argininosuccinic acid	Organic acids (Amino acids)	7.47	0.55
Asparagine	Organic acids (Amino acids)	60.00	8.10
Aspartic acid	Organic acids (Amino acids)	8.45	1.92
Betaine	Organic acids (Amino acids)	5.39	0.96
Biotin	Biotin and derivatives	2.32	0.33
cAMP	Nucleotides	1.78	0.22
Carnitine	Quaternary ammonium salts	58.90	6.18
Citric acid + Isocitric acid	Organic acids (Carboxylic acids)	599.49	48.39
Citrulline	Organic acids (Amino acids)	2.18	0.24
Cystathionine	Organic acids (Amino acids)	6.78	0.22
Cystine	Organic acids (Amino acids)	161.95	5.29
Erythritol	Carbohydrates and conjugates	195.70	10.07
Fumaric acid	Organic acids (Carboxylic acids)	22.68	3.76
Gluconate	Carbohydrates and conjugates	804.72	129.77
Glutamate	Organic acids (Amino acids)	19.81	4.91
Glutamine	Organic acids (Amino acids)	204.68	4.04
Glycine	Organic acids (Amino acids)	789.80	47.52
Guanidineacetic acid	Organic acids (Amino acids)	106.06	44.33
Guanine	Carbohydrates and conjugates	0.60	0.33
Hexose	Carbohydrates and conjugates	586.60	27.91
Hexose-phosphate	Carbohydrates and conjugates	0.67	0.11
Histidine	Organic acids (Amino acids)	352.47	5.51
Homoserine+Threonine	Organic acids (Amino acids)	47.23	18.14
Hydroxyglutaric acid	Organic acids (Hydroxy acids)	21.85	1.00
Isoleucine+Leucine	Organic acids (Amino acids)	47.99	15.56
Ketoisovaleric acid	Organic acids (Keto acids)	36.93	1.10
Lactic acid	Organic acids (Hydroxy acids)	189.16	8.39
Malic acid	Organic acids (Hydroxy acids)	5.85	0.20
Mannitol	Carbohydrates and conjugates	557.47	201.78
Methionine	Organic acids (Amino acids)	6.28	0.53
N-Acetyl-Asp-Glu	Organic acids (Amino acids)	14.24	5.28
N-Acetyl-L-aspartic acid	Organic acids (Amino acids)	47.54	4.60
N-Acetyls erine	Organic acids (Amino acids)	7.98	0.43
N4-Acetylcytidine	Nucleosides	6.31	0.77
Ornithine	Organic acids (Amino acids)	0.47	0.30
Pentose-phosphate	Carbohydrates and conjugates	7.52	1.35
Phenylalanine	Organic acids (Amino acids)	25.75	1.21
Phosphocreatine	Organic acids (Amino acids)	1.11	0.28
Proline	Organic acids (Amino acids)	4.45	0.14
Propionylcarnitine	Fatty acyls	21.73	4.98
Pyruvic acid	Organic acids (Keto acids)	45.90	2.31
Serine	Organic acids (Amino acids)	154.43	3.79
Serotonin	Indoles and derivatives	58.87	6.71
Succinic acid	Organic acids (Carboxylic acids)	47.74	0.15
Trehalose	Carbohydrates and conjugates	7.38	0.65
Tryptophan	Organic acids (Amino acids)	20.30	1.39
Tyrosine	Organic acids (Amino acids)	129.98	52.86
Uracil	Nucleobases	7.37	1.22
Uridine	Nucleosides	94.13	17.59
Valine	Organic acids (Amino acids)	20.28	0.37
Xanthine	Nucleobases	5.11	0.81

6.3. Manuscript #2: Flasch et al. (2022c)

Status	Submitted for publishing
Title	Comparing the sensitivity of low- and high-resolution mass spectrometry for xenobiotic trace analysis: An exposome-type case study
Authors	Mira Flasch ^{1,2} , Gunda Koellensperger, Benedikt Warth ^{1,3*}
Affiliations	¹ University of Vienna, Faculty of Chemistry, Department of Food Chemistry and Toxicology, Währinger Straße 38-40, 1090 Vienna, Austria ² University of Vienna, Vienna Doctoral School of Chemistry, Währinger Straße 42, 1090, Vienna, Austria ³ Exposome Austria, Research Infrastructure and National EIRENE Hub, Austria *Corresponding author
Year	2022
Preprint server	ChemRxiv
DOI	10.26434/chemrxiv-2022-x4kk7
Contribution	Mira Flasch (MF) performed the sample preparation, conducted the LC-HRMS and LC-MS/MS measurements, evaluated and interpreted the results and wrote the manuscript.

Comparing the sensitivity of low- and high-resolution mass spectrometry for xenobiotic trace analysis: An exposome-type case study

Mira Flasch^{1,2}, Gunda Koellensperger^{3,4}, Benedikt Warth^{1,4*}

¹University of Vienna, Faculty of Chemistry, Department of Food Chemistry and Toxicology, Währinger Straße 38, 1090 Vienna, Austria

²University of Vienna, Vienna Doctoral School in Chemistry, Währinger Straße 42, 1090, Vienna, Austria

³University of Vienna, Faculty of Chemistry, Department of Analytical Chemistry, Währinger Straße 38, 1090 Vienna, Austria

⁴Exposome Austria, Research Infrastructure and National EIRENE Hub, Austria

ABSTRACT: The chemical exposome consists of all environmental exposures experienced throughout a lifetime. Liquid chromatography high-resolution mass spectrometry (HRMS) is common in untargeted exposome-wide analyses of xenobiotics in biological samples; however, human biomonitoring approaches usually utilize targeted low-resolution triple quadrupole (QQQ) mass spectrometry tailored to a small number of chemicals. HRMS can identify novel contaminants over a broad mass range but the detection of molecules from low-level exposure amidst a background of highly-abundant endogenous molecules has proven to be difficult. In this study, high- and low-resolution mass spectrometry with identical chromatography was utilized to determine the limits of quantitation (LOQ) of >100 xenobiotics and estrogenic hormones in pure solvent and human urine. For HRMS analyses, the median LOQ was 0.9 and 1.2 ng/mL in solvent and urine, respectively and for low-resolution QQQ measurements, the median LOQ was 0.1 and 0.2 ng/mL in solvent and urine, respectively. To evaluate the calculated LOQs in complex biological samples, spot urine samples from 24 Nigerian females were measured. The higher LOQ values for HRMS resulted in less quantified low-abundance analytes and decreased the number of compounds detected below the LOQ. Even at chronic low-dose exposure, such compounds might be relevant for human health because of a high individual toxicity or potential mixture effects. Nevertheless, HRMS enabled the additional screening for exposure to unexpected/unknown analytes, including emerging compounds and biotransformation products. Therefore, a synergy between high- and low-resolution mass spectrometry may currently be the best option to elucidate and quantify xenobiotics in exposome-wide association studies (ExWAS).

INTRODUCTION

Genetic and environmental factors, including exposure to toxic and bio-active chemicals play a pivotal role in the development of many diseases (Vermeulen et al. 2020). Despite the importance of non-genetic risk factors in disease etiology, the chemical exposome is still poorly understood. In addition, covering a wide and diverse chemical space in a highly-sensitive manner has several limitations. One bottleneck is often the lack of sensitivity in high-resolution mass spectrometry assays (HRMS) compared to the highly-specific targeted triple-quadrupole (QQQ) approaches (David et al. 2021). As only a limited number of chemicals/chemical groups are encompassed by such tailored, targeted approaches, a post-

analysis search for unknown analytes is not feasible. Thus, the application of low-resolution targeted methods is restricted in exposome-type research (Warth et al. 2017). With HRMS, however, the detection and quantification of low-abundance chemicals is impacted because the instrument's sensitivity often falls below that of low-resolution mass spectrometers. The problem is exacerbated by the presence of dominant high-abundance peaks that typically originate from endogenous metabolites and other interferences (Dennis et al. 2017).

As exogenous compounds are usually present at low concentrations in the human body, a reduced sensitivity hinders the detection of a certain portion of the chemical exposome. Additionally, poor ionization efficiency can further hamper the analysis. It is known that concentrations of endogenous and exogenous compounds in biological matrices (e.g., human plasma) can span eight to eleven orders of magnitude (David et al. 2021; Rappaport et al. 2014). Pharmaceuticals and many food constituents are present in concentrations similar to endogenous metabolites, however, chemicals such as pesticides and plasticizers and natural contaminants are approximately 400-700 times lower in mean concentration. Detection of such analytes requires therefore a high sensitivity and highlights the need for highly-sensitive LC-HRMS approaches (David et al. 2021).

Recently, HRMS was used in exposome-wide association studies (ExWAS) to decipher chemicals associated with disease aetiology, e.g., allergy-related outcomes (Granum et al. 2020), child cognitive function (Julvez et al. 2021), childhood obesity (Vrijheid et al. 2020), and semen quality (Chung et al. 2019). Nevertheless, targeted low-resolution methods are still widely used to capture specific areas of the chemical exposome (Preindl et al. 2019; Andra et al. 2016; Gao 2021; Vrijheid et al. 2020).

A systematic and thorough comparison between high-resolution instrumentation and triple quadrupole tandem mass spectrometry has only been described for individual analyte groups, e.g., polybrominated diphenyl ethers in fish (Mackintosh et al. 2012), clinically-relevant compounds in plasma (Grund et al. 2016), illicit drugs in wastewater (Fedorova et al. 2013), and cathinones in urine (Pascual-Caro et al. 2020). Uniformly, these studies indicated similar or better sensitivity of low-resolution instruments.

The aim of this study was to determine the disparity between the limit of quantitation (LOQ) of a high-resolution instrument and a triple quadrupole mass spectrometer. In this study, the LOQ was not only estimated in pure solvent but also in spiked urine samples. The evaluation included >100 xenobiotics and estrogens from

various sources. Following the Eurachem Guideline 2014 (Magnusson B. 2014), the LOQ was estimated by calculating the standard deviation of multiple injections of a low concentration standard. Moreover, the ability of both approaches to detect analytes at naturally occurring concentrations was demonstrated in urine samples.

MATERIALS AND METHODS

Chemicals

Highly-diverse compounds (n=105) were combined in a multi-analyte solution and diluted to seven concentration levels in ACN/H₂O (1:9 v/v). A mixture of labelled internal standards was used for sample preparation (Table S3). The complete list of analytes and the corresponding concentration levels are summarized in the Supporting Information (Table S2). Table S7 summarizes the ¹³C-labelled standards that were used. Solvents for extraction and eluents were LC-MS grade. Ammonium fluoride (NH₄F, EMSURE® ACS) was of high purity (> 98%).

Samples & sample preparation

To prepare the matrix-matched standards, urine from a female volunteer on a defined diet (where specific food-related exposures were minimized) was collected for three days and stored at -80°C. The sample preparation was performed according to Preindl et al. (2019). Briefly, 200 µL urine were combined with 10 µL internal standard mixture and 790 µL ACN/MeOH (1:1 v/v). After sonication for 10 min at 4°C, the samples were incubated for 2 h at -20°C and centrifuged at 18,000 x g for 10 min at 4°C. The supernatant was transferred to a CentriVap Vacuum concentrator (Labconco) and evaporated overnight at 4°C. The dried urine was then reconstituted with 200 µL of the respective solvent standard solution (seven concentrations). After a final centrifugation step, the samples were transferred to amber glass vials with a 200 µL insert. Several blank extractions (process blanks) where the 200 µL urine was replaced with 200 µL water were performed to consider potential contaminants throughout the sample preparation process. For the matrix-adjusted evaluation, a "blank urine" sample was prepared by extracting urine and reconstituting in 200 µL of 10% ACN. This was necessary to evaluate possible contaminations in the urine "blank" used to prepare the matrix-matched multi-analyte standard. To assess sensitivity differences in naturally-contaminated biological samples, spot urine (n=24), collected from female volunteers in Nigeria (Ezekiel et al. 2022) were prepared according to the procedure outlined above.

LC-(HR)MS(/MS) analysis

Low-resolution LC-MS/MS analysis

Measurements were performed using the method based on Jamnik et al. (2022). A 1290 Infinity II LC system (Agilent) was coupled to a QTrap 6500+ mass spectrometer equipped with an electrospray ionization (ESI) source (Sciex). Fast polarity switching in multiple reaction monitoring (MRM) mode was utilized. An established LC method (Preindl et al. 2019) was used for the chromatographic separation of the analytes. Briefly, an Acquity HSS T3 reversed-phase column (1.8 µm, 2.1 mm x 100 mm) (Waters) and a VanGuard pre-column (1.8 µm) (Waters) were used. Eluent A was 0.3 mM of

ammonium fluoride in LC-MS grade water and eluent B was 100% acetonitrile. A volume of 5 µL of sample was injected onto the system at a 0.4 mL/min flow rate. The column compartment and autosampler were maintained at constant temperatures of 40°C and 7°C, respectively. Elution of the analytes was achieved with the following gradient: 0-1 min, 5% B; 1-1.8 min, increased to 18% B; 1.8-4.2 min, increased to 35% B; 4.2-13 min, further increased to 48%; 13-15.8 min, constant to 90% B; 15.8-17.6 min, flushed with 98% B and 17.6-20 min re-equilibration with 5% B. Mycotoxins were additionally integrated as target molecules. MS/MS transitions were based on the method of Braum et al. (2020). Detailed information on the corresponding MRM transitions is provided in the Supporting Information (Table S4).

High-resolution LC-MS/MS analysis

A Q Exactive HF quadrupole-Orbitrap mass spectrometer coupled to a Vanquish UHPLC system (both Thermo Fisher Scientific) via heated electrospray ionization was used for the high-resolution measurements. To ensure maximal comparability, the column, eluents, gradient, injection volume and other LC parameters were identical to the low-resolution (QQQ) measurements. An MS full scan from 60-900 *m/z* was acquired, and, consistent with the QQQ measurements, polarity-switching mode was activated. Automatic gain control (AGC) was 1 x 10⁶ and the resolution was 60,000 (@ *m/z* 200). The maximum injection time was 100 ms. Each concentration in pure solvent and urine was injected at least twice within the sample sequence. Selected concentrations (n=4; levels 300/30/3/0.3 ng/mL; see Table S2) were injected 10 and 11 times for the solvent and urine, respectively. The identical sequence order was measured on both instruments to maximize the alignment of experiments.

Data Analysis

The targeted analysis of the high-resolution data was performed using Skyline (version 20.2.0.343). The LOQ calculation was based on the Eurachem Guide (2016). The standard deviation (*s*₀) of *n* replicate injections (n=min. 6) of a low concentration standard was determined and LOQ values were calculated with the following equation (Equation 1):

$$LOQ = 10 \cdot \frac{s_0}{\sqrt{n}}$$

For the calculated limit of quantitation, the ratio of standard deviation and the square root of the number of replicates was multiplied by three. This parameter was calculated separately for the solvent standards and the matrix-matched standards (urine). A linear calibration (1/x weighted) was applied for quantitation (Table S5/S6). A single-point calibration was applied if the analyte was only detected in one calibrant. This was primarily the case for the HRMS measurements, as the same concentrations were used as for the QQQ investigation. Some mycotoxins (deoxynivalenol, ochratoxin A, ochratoxin B), some endogenous estrogens (2-methoxyestradiol, 2-methoxyestrone, 4-methoxyestradiol), tetrabromobisphenol A, and methiocarb were detected only at the highest concentration in HRMS. The mycotoxins citrinin and deoxynivalenol, and the glucuronide conjugates of zearalenone and metabolites thereof were only observed in the highest concentrated standard on the

QQQ. An alternative approach to evaluate the LOQ is to estimate the concentration at which the signal to noise ratio (S/N) equals ten. However, this approach was not applied in this study. In the likelihood of background contamination in the urine "blank", the quantitation was achieved by standard addition. The contamination level in the process blank was subtracted from standards and samples. The suitability of a least square linear regression model for the calibration curves was assessed by the correlation coefficient (R²), a lack-of-fit analysis (F test, $\alpha = 0.05$) and a t-Student test to examine whether the slope is different from zero ($\alpha = 0.05$). The signal suppression/enhancement was calculated as the slope of the urine-matched calibration divided by the slope of the solvent calibration curve multiplied by 100. Simplified assessment of the expected urinary concentration of analytes, when exposed to the acceptable/tolerable daily intake (ADI, TDI), was based on 70 kg body weight (EFSA 2012), 2 L urine volume (Garde et al. 2004) and 100% urinary excretion rate. Bioavailability, biotransformation, and real urinary excretion rate were not considered as only a rough estimation was intended.

The following software was used for creating figures and performing statistics. Figures were created with ggplot2 (version 3.3.2) and the statistical tests of the linear regression model were carried out in RStudio (1.4.1717) using R (version 4.1.1). OriginPro 2021 was used to create correlation plots and to perform an ANOVA analysis to control if there was a significant difference between both measurements (confidence level = 95%). For the ANOVA analysis, only samples were considered where the analyte was present in both analyses within the calibration range above the LOQ. Moreover, the R package patRoan (Helmus et al. 2021) was utilized for suspect screening. Conversion to mzML files was performed using ProteoWizard (Chambers et al. 2012) and the files were split according to instrument polarity. Process blanks were selected as blank measurements and all 24 urine samples were used as samples. The "openms" algorithm was applied for peak picking and grouping. The parameters were as follows: noise threshold = 8E3, chromFWHM = 3, minFWHM = 1, maxFWHM = 30, chromSNR = 5, mzPPM = 3. In a subsequent filtering step, features with an intensity < 3E5 or a minimum feature intensity above blank < 5 that were present in < 25% of all samples were omitted. The candidate list was derived from the EPA's ToxCast library with > 4000 analytes used in the ENTACT trial (Sobus et al. 2019). An *m/z* window of 0.001 was defined for the suspect screening. To generate molecular formulae in genform, the adducts [M+H]⁺ and [M-H]⁻, and the elements C, H, N, O, P, S, Cl, and Br were utilized. The algorithm metfrag (Ruttkies et al. 2016) was used to generate compounds. Using annotateSuspects, the suspect screening output was complemented with the generated peak list, formula, and compound data. Depending on the rank and scores (isoScore, individualMoNAScore) of the formula and compound candidates, an identification level based on (Schymanski et al. 2014) was suggested. No MS² data was acquired, therefore, the highest assigned confidence level was 4b (good formula isotopic pattern match). This confidence level is assigned to a feature if it is: the top ranked formula candidate, the isoScore is > 0.9, and the score is at least 0.2 higher than the next best-ranked candidate. The

confidence level 5 was attributed to all other features as these did not match any criteria. The main focus of this study was to compare sensitivity in a targeted manner using reference standards and not to annotate analytes in a non-targeted fashion, therefore acquisition of fragmentation data was not performed.

RESULTS

Comparison of the limit of quantitation

The LOQ was calculated for 103 of the 105 analytes in pure solvent and urine for the high-resolution instrument (Table S1). Two molecules, nivalenol and ochratoxin A, were not detected even at the highest concentration level (30 ng/mL and 9 ng/mL, respectively). The median LOQs of the detected analytes were 0.9 ng/mL and 1.2 ng/mL in solvent and urine, respectively (Figure 1A). The calculated values ranged over five orders of magnitude from 0.006 ng/mL (formononetin) to 420 ng/mL (T2-toxin) in solvent and 0.016 ng/mL (benzophenone-2) to 4,800 ng/mL (octyl methoxycinnamate (OMC)) in urine, respectively. In the low-resolution QQQ experiments, the LOQ in urine of all 105 analytes was calculated with a median of 0.2 ng/mL. The median LOQ was slightly lower in solvent at 0.1 ng/mL (Table S1, Figure 1B). T2-Toxin had the worst performance with high LOQ values of 1,200 ng/mL and 890 ng/mL in solvent and urine, respectively. Excluding mycotoxins, the sunscreen ingredient octyl methoxycinnamate (OMC) (59 ng/mL) had the highest LOQ in solvent and in the matrix the barely retained acrylamide was challenging to detect at low levels (LOQ = 150 ng/mL). The lowest LOQs were obtained for benzyl paraben at 0.00031 ng/mL (solvent) and scopolamine at 0.00045 ng/mL (urine). The median LOQ was approximately eleven times lower in pure solvent compared to urine. The difference in the median LOQ between LC-MS configurations was a factor of 6 and the high-resolution measurements had higher LOQs than the QQQ configuration. When analyzing polar analytes such as acrylamide, the column material and chosen analytical instrumentation (LC-MS) were not ideal in this study. The broad structural spectrum of the analytes included in the multi-analyte method, however, clearly required a compromise. Independent of the instrumentation used and the sample analyzed, the substance classes with the highest median LOQ values in solvent were disinfection by-products, food-processing by-products, and certain mycotoxin categories (Figure 1C). In particular, the first two classes were not detected at low concentrations and a high background was apparent. All of the disinfection by-products included and one food processing by-product (acrylamide) were not retained on the reverse-phase column and eluted close to the dead volume. This lack in retention resulted in the interference of highly-abundant ions that subsequently explained the poor detection of the analytes and thus the low median LOQ for these classes. This was, however, not surprising given the fact that LC-MS is typically not the ideal instrument platform for these classes.

Personal care product ingredients and phytoestrogens were amongst the three categories with the lowest LOQ values for all sample/instrument combinations (<0.2 ng/mL and <0.05 ng/mL for HRMS and QQQ, respectively). In general, the median LOQs for the different categories were one order of magnitude higher in urine than in solvent; albeit, the overall order remained similar (Figure S1). For each category, the median LOQ was

largely decreased in the high-resolution measurements. Only disinfectant by-products and food processing by-products, that were too polar to be adequately retained on the selected C18-column, benefited from the higher mass resolution and had a lower median LOQ when analyzed by HRMS. Notably, the results per category were highly-dependent on the chosen representatives and must not be generalized.

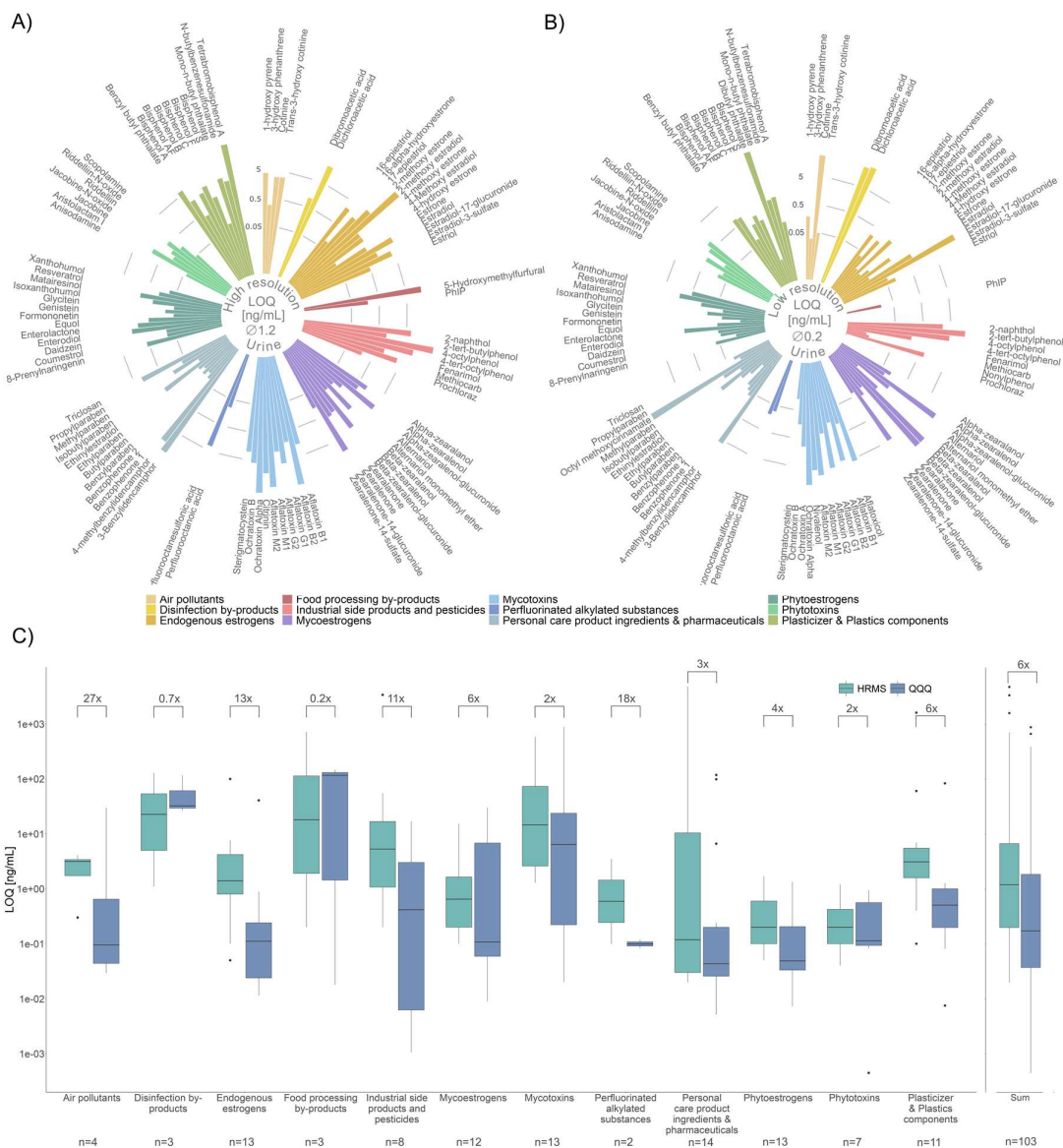


Figure 1 Comparison of the limit of quantitation (LOQ) between the low- (QQQ) and high-resolution mass spectrometric (HRMS) approaches in urine. Analytes with a LOQ value <100 ng/mL are illustrated. LOQs were estimated according to the Eurachem Guide (2016): (A) LOQs on the high-resolution instrument. (B) LOQ on the low-resolution instrument. (C) Comparison of the average LOQ for each class of toxicants between a high-resolution instrument (HRMS, green) and a low-resolution mass spectrometer (QQQ, blue) in urine.

Assessment of additional analytical figures of merit

On the low-resolution QQQ instrument, a median correlation coefficient (R2) of 0.99 in both solvent and urine and a minimum R2

of 0.95, supported by the lack-of-fit test (p < 0.05), indicated an excellent fit of the least square linear regression model in the calibration range. Moreover, the t-Student test proved the slopes

to be significantly different from zero. In HRMS, the analytes were detected at one to two concentration levels lower than on the QQQ because the LOQ of the high-resolution instrument was typically lower and the same concentration levels were used for both experimental data sets (Table S5). The orbitrap mass spectrometer had a slightly lower R2, although most compounds had a value >0.9, no significant lack of fit, and a slope different from zero suggesting a good fit of the linear regression model. In urine, the R2 was between 0.8 and 0.9 for several analytes (riddelliin-N-oxide, 3-benzylidene camphor, β -ZEL-14-glucuronide, isoxanthohumol, nonylphenol, prochloraz). The lack-of-fit test indicated a poor fit to the model for β -ZEL-14-glucuronide, prochloraz and 3-benzylidene camphor.

The retention time varied only slightly between the measurement on the high-resolution and low-resolution mass spectrometer. The difference in retention time was on average 11 s, which is very little given that two different LC systems with non-identical void volumes

were employed. The highest discrepancy was observed for PFOS with 37 s and isobutylparaben with 30 s. The signal suppression/enhancement (SSE) ranged between 27% - 208% with a median value of 89% for the QQQ method (Table S5). In the high-resolution analyses, the SSE varied more severely (8% - 264%), excluding analytes only detected in the standard with the highest concentration, the median was 97% (Table S5). Drastic signal suppression was particularly evident for PFOS (8%), nonylphenol (20%), 4-octylphenol (22%) and methiocarb (24%) in HRMS. Signal enhancement was pronounced for ZEN-14-glucuronide (231%), ZEN-14-sulfate (264%), and 2-tert-butylphenol (190%). In the low-resolution measurements, 2-tert-butylphenol (204%), citrinin (191%), ZEN-14-sulfate (160%), PFOS (27%), OMC (33%), and HMF (38%) experienced high signal suppression/enhancement. In the high-resolution measurements, the SSE was generally more pronounced, although the overall trends were similar with both approaches.

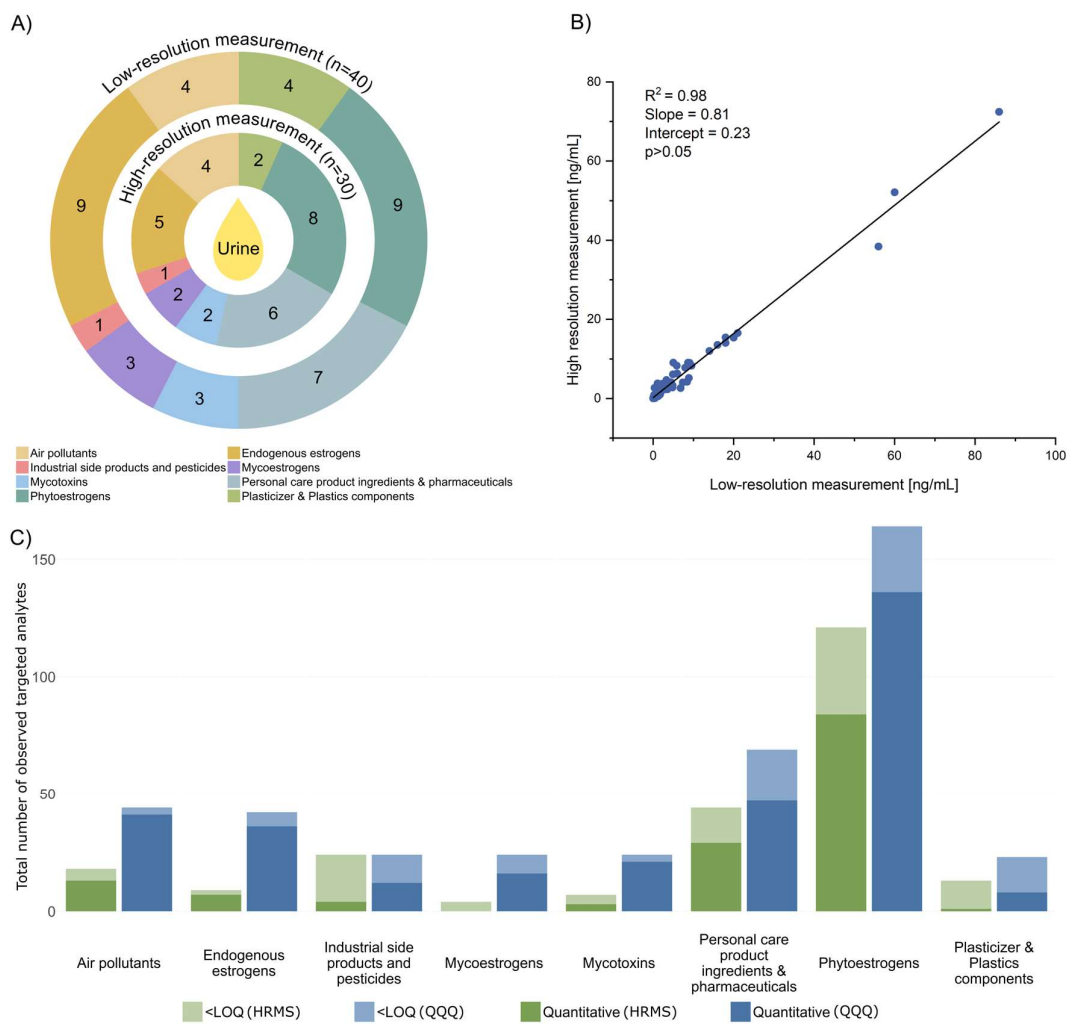


Figure 2 Screening for exposome-compounds in urine samples (n=24) from women living in Nigeria. (A) Comparison of individual analytes detected in at least one sample between low- and high-resolution mass spectrometry grouped by chemical category. (B) Plot of linear regression model between quantitative results obtained with both measurements demonstrates a good correlation. (C) Comparison of the total number of observed analytes across all samples with both low- (blue) and high-resolution mass spectrometry (green) separated by class. Analytes detected below the respective LOQ value (<LOQ) are marked in color.

Impact on the measurement of biological samples

Twenty-four urine samples collected from Nigerian women were analyzed with the same high- and low-resolution LC-MS configurations as the reference standards (Table S7, Table S8). Typically, approximately ten different analytes were detected in each sample with high-resolution mass spectrometry, whereas about 17 analytes were observed on the more sensitive QQQ instrument in each sample (Figure 2A). On average, each analyte was present in eight (HRMS) and ten samples (QQQ). In total, 40 different compounds were identified in the tailored, targeted approach. Ten compounds were exclusively detected with the low-resolution instrument, thus 30 individual contaminants were also identified by the HRMS assay. Excluding matairesinol (present in 7 samples), these analytes were usually only observed in a few samples (maximum 3). Nearly half of the analytes (40%) that were solely detected in the low-resolution measurements were from the category of endogenous estrogens. Other analytes not present in the HRMS analyses included the mycotoxins aflatoxin B1 and aflatoxicol, the plasticizer BPA, the plastic component tetrabromobisphenol A, isobutylparaben, and matairesinol.

For all the urine samples analyzed with the low-resolution assay, the targeted analytes were observed 415 times. Conversely, in the high-resolution analyses approximately 60% of the analytes were not detected ($n=240$) (Figure 2C). A quantitative result was achieved for approximately 60% and 75% of all detected analytes in high- and low-resolution mass spectrometry, respectively. Thus, the discrepancy between the number of analytes detected by high- and low-resolution mass spectrometry widened with approximately 55% less quantitative information obtained from the HRMS experiments.

For the analytes detected in a sample with both methods, at a concentration within the calibration range and a confidence level of 95% ($p > 0.05$), the concentrations in the high-resolution data were not significantly different from the low-resolution results (Figure 2B). When the QQQ values (x-axis) were plotted against the high-resolution results (y-axis), the correlation between both quantitative data sets was excellent with an R^2 of 0.98.

To highlight the versatility of high-resolution measurements in annotating additional toxicants beyond the pre-determined target list, additionally a preliminary suspect screening was performed. Only features detected in at least 6 of the 24 urine samples (25%) were considered. The search resulted in 57 and 418 features that matched 59 and 589 suspects in positive- and negative-ion mode, respectively (Table S9, Table S10). The number of candidates was higher than the number of features as several isomers with identical m/z values were included in the suspect list; thus, for one feature multiple candidates might be possible.

DISCUSSION

To the best of our knowledge, this is the first systematic LOQ comparison of a broad chemical space including xenobiotics from multiple exposure sources. Despite our efforts to ensure a high degree of comparison, inherent technical discrepancies remained because high- and low-resolution instruments are based on fundamentally different measurement principles. QQQ focuses on the reliable quantitation of a pre-defined target list, whereas HRMS specializes in the non-targeted discovery of molecules. Different acquisition modes were used (multiple reaction monitoring vs. full

MS scan) that imposed restrictions on the direct comparison of the generated data. Both instruments, however, were used in the measurement mode typically used in exposomic or metabolomic applications. The tailored LC-MS/MS assay was operated in multiple reaction monitoring and could even detect extremely low concentrations in the ppt range but was restricted to the pre-determined list of analytes. As showcased by the suspect screening of the urine samples, untargeted HRMS analyses within a specified mass range (full scan mode) enabled the detection of all chemicals in the chosen m/z window and the subsequent discovery of unexpected and unknown molecules. However, exposure to analytes at low levels is often not quantifiable in HRMS. In addition, the specific instruments and methods used in the comparison may impact the outcome. This study included two LC-MS configurations from leading vendors in the respective field. Therefore, e.g., the ESI source design was different and this aspect may influence instrument sensitivity. The LC systems' void volumes were also not identical; nevertheless, the remarkable similarity in retention time (average shift = 11 s) indicated that only minor variations originated from the chromatographic separation.

To thoroughly investigate the difference in the limit of quantitation on a larger scale, a broad variety of chemicals were included in the study. Comparisons between HRMS and QQQ measurements have been reported in the literature, but these targeted only a limited range of chemicals, e.g., flame retardants (polybrominated diphenyl ethers, PBDE) (Mackintosh et al. 2012), illicit drugs (Fedorova et al. 2013; Pascual-Caro et al. 2020), and small molecules used in the clinic (Grund et al. 2016). In our study, the LOQ of the QQQ was on average 6 and 9 times lower for urine and solvent, respectively, than HRMS. Most previous studies reported similar, or slightly lower, LOQs for QQQs (Grund et al. 2016; Fedorova et al. 2013; Pascual-Caro et al. 2020). Only Mackintosh et al. (2012) observed significantly lower LODs (10-100 fold) with QQQ for PBDEs with a maximum of four bromides in fish. The equipment used in all these studies differed from our selected configuration. In particular, instruments from an alternative vendor were used for the low-resolution measurements. The variation in instrumentation and investigated analytes may explain the observed higher discrepancy between QQQ and HRMS in our measurements.

For several analytes, the quantitation of the targeted analytes was successful on both instruments and the obtained results were comparable. The high correlation (>0.98) and no significant difference between both data sets for the measured analyte concentrations within the linear calibration range of the respective compound confirmed the potential of HRMS to produce accurate quantitative results. The agreement between data acquired with QQQ and HRMS has previously been demonstrated in several studies (Ponzetto et al. 2017; Herrero et al. 2014; Mackintosh et al. 2012).

The mean LOQ value determined from the high-resolution mass spectrometry measurements was approximately one order of magnitude higher than the LOQ determined from the low-resolution measurements. Thus, a certain proportion (about 40% of the detected analytes) of the extremely low-abundance analytes in the naturally contaminated urine samples were not quantified in the HRMS analyses. In addition, HRMS also detected fewer analytes

below the LOQ and above the limit of detection, which is about a third of the LOQ, compared to QQQ. However, the concentrations of the missed analytes were primarily low. Excluding compounds where the respective concentration was below the LOQ in the QQQ (approx. one third of the cases), the median concentration of analytes detected in QQQ but not in the high-resolution data was 0.15 ng/mL. The majority (90%) of the undetected chemicals were in the sub-ng/mL range or even lower. Most of the individual analytes were observed in at least one sample in the HRMS measurement (75%), and it was mainly the low-abundance contaminants below the LOQ in QQQ that were usually not detected in HRMS. The ultra-low LOQs of the QQQ approach might discover additional low-level contaminants and improves the extent of quantitative data and chronic background exposures. Nevertheless, screening for chemicals of interest and unknowns, the primary purpose of HRMS, is feasible for many chemicals. Human biomonitoring data for several chemicals supported sufficiently low LOQs/LODs in HRMS to observe and even quantify average contamination levels for most target analytes. From the HRMS data, the LOQ of the air pollutant 1-OH-pyrene was determined as 1.4 ng/mL (c.f., 0.06 ng/mL for the QQQ). The reference value from the German human biomonitoring commission is 0.5 ng/mL in urine for non-smoking adults and twice this value in smokers (Wilhelm et al. 2008). Thus, HRMS would only capture high-exposure levels above the reference value obtained from biomonitoring data and thus this analyte was only detected in one measured urine samples. The intermediate in dye production, 2-naphthol was detected in all urine sample with both approaches indicating an LOQ (1.2 ng/mL in HRMS) that is sufficiently low to detect this compound in biological samples. According to the Fourth National Report on Human Exposures to Environmental Chemicals (CDC 2021), this LOQ is more than three times below the geometric mean urinary level of the industrial side product (4.2 ng/mL) in the U.S. American population (n=2,641). Urinary phytoestrogen levels that primarily originate from food and are typically regarded as beneficial exposures, were frequent, high, and dependent on the diet of the individual. In the US-American population (n>3,000), mean levels in urine were 65, 32 and 6.6 ng/mL for daidzein, genistein and equol, respectively (Janulewicz et al. 2021). In our HRMS measurements, the LOQ value was 0.12 ng/mL (genistein, daidzein) to 0.41 ng/mL (equol), which are well below the mean levels obtained from large-scale biomonitoring data. In our urine samples, daidzein (24/24) and genistein (20/24) were detected in almost all samples with both instruments (HRMS/QQQ). At a lower concentration, equol was detected in only 50% of the samples by HRMS (n=9) compared to QQQ (n=18). Matairesinol was too low abundant to be detected in any urine samples with HRMS (LOQ: 0.85 ng/mL). The mean concentration value of this phytoestrogen was with 0.6 ng/mL in Mexican women below the LOQ in HRMS (Chávez-Suárez et al. 2017). The personal care product ingredients methylparaben, ethylparaben, and propylparaben were frequently investigated in human urine. The mean urinary concentrations in the US population (n>2,600) were 32 ng/mL (methylparaben), 4 ng/mL (propylparaben) and the 75th percentile is 5.1 ng/mL for ethylparaben (CDC 2021). A smaller Spanish study (n>200) reported slightly lower concentrations at 11.2 ng/mL (methylparaben), 1.1 ng/mL (ethylparaben), and 0.64

ng/mL (propylparaben) (Adoamnei et al. 2018). Mean concentration levels in human biomonitoring studies were more than 30-times higher than the LOQ values (0.01 to 0.07 ng/mL) in this study. Nevertheless, only 46% (ethylparaben) to 84% (methylparaben) of the analytes were observed with both assays. If a paraben in urine was solely detected with QQQ, the abundance was usually very low (< LOQ). Thus, the LOQ determined by HRMS was sufficient to measure exposure far below the average contamination for this chemical class. The antibacterial/antifungal triclosan was described at a mean concentration of 5.8 ng/mL in the USA (CDC 2021) and 2.7 ng/mL in the Belgian population (Pirard et al. 2012). The LOQ in HRMS was with 2.5 ng/mL (HRMS) slightly below the mean concentration in the biomonitoring studies, but this chemical was still only detected (below the LOQ) in three urine samples in HRMS. The mycoestrogens, alternariol monomethyl ether (AME) and alternariol (AOH) were observed in the urine of Chinese at a mean concentration of 0.19 ng/mL alternariol and 0.065 ng/mL AME (Qiao et al. 2022). The achieved LOQ in HRMS is below these mean urinary concentrations with 0.11 ng/mL (AME) and 0.20 ng/mL (AOH) and the analytes were also barely detected and not quantified in the urine samples. Despite a few analytes for which the LOQ and the LOD were not low enough to capture and quantify the analytes when present at mean concentrations reported in biomonitoring studies, HRMS detected exposures at, or even below, the population mean for most compounds. With the QQQ, however, even extremely low levels of exposure were detected. The comparison of the achieved LOQ in our study with human biomonitoring data revealed that the sensitivity required to measure chemical exposures in biospecimens strongly depends on the analyte of interest. The QQQ approach was superior in detecting and quantifying very low-abundance contaminants. The tolerable/acceptable daily intake (TDI, ADI) estimates the amount of an accidentally added compound or substance in general that can be daily consumed without health risk. These thresholds were available for thirteen target compounds, including bisphenol A, some phthalates, perfluorinated substances, several mycotoxins, parabens, methiocarb, and triclosan (Table S9). The approximate urinary concentrations of chemicals, when absorbed at the exposure limit for negative health implications such as the TDI or ADI, were in most cases significantly higher than the reported LOQs. Independent of the instrument, the estimated urinary concentration at the TDI/ADI was typically more than 1,000 times higher than the LOQ, indicating a sufficient sensitivity for detecting harmful concentrations of chemicals. The LOQ of dibutyl phthalate and PFOS was 160 ng/mL and 3.5 ng/mL, respectively, only about half of the estimated concentration in urine at the TDI/ADI. Thus, a critical exposure level might not be detected depending on the actual urinary excretion rate and bioavailability of these substances. The urinary elimination was estimated to be 16% for PFOS (Zhang et al. 2015) and dibutyl phthalate was reported to be primarily excreted as mono butyl phthalate (over 70%) (Frederiksen et al. 2011), consequently toxicological relevant concentrations might not be observed with the achieved LOQ/LOD. The LOQ of the mycotoxins deoxynivalenol and nivalenol and BPA was also not sufficiently low for detecting relevant exposure levels with HRMS. However, the slightly lower LOQ in the QQQ approach was (except for nivalenol), also not in the required range. The BPA

concentration estimation was based on the newly published EFSA draft opinion (Schiano et al. 2022) with a drastically lowered TDI of 0.01 ng/kg body weight per day. The LOQ was sufficiently low to observe concentrations at the previous TDI (0.4 µg/kg body weight per day) (EFSA 2015). In total, HRMS was suitable to detect and even quantify toxicologically relevant concentrations in urine for many analytes.

The sample pre-treatment, e.g. enzyme treatment, impacts the required LOQs for detecting toxicants as analytes might be masked from targeted analysis by biotransformation such as sulfation and glucuronidation. The urine samples were not pre-treated with glucuronidase or sulfatase; therefore, with the exception of a few analytes (zearalenone, zearalenol, estradiol), sulfated and glucuronidated metabolites of the target molecules were not captured in QQQ. Biotransformation products may be retrospectively discovered by HRMS, although these were not initially included in the target list. However, the search for biotransformation products was, although important (Flasch et al. 2022), not conducted in this study as the main focus was on the comparison between both instrument platforms. Nevertheless, some compounds are known to be primarily present as glucuronides in urine (Silva et al. 2003; Stein et al. 2015); therefore, with enzymatic pre-treatment, the concentration of the free analyte for the majority of toxicants should increase easing their detection and quantitation.

CONCLUSIONS

The high-resolution analysis was successful in detecting and quantifying medium to high concentration levels of xenobiotics in the ng/mL range, however, HRMS does capture fewer low-level exposures than targeted QQQ mass spectrometry. Nevertheless, the LOQ/LOD of HRMS was low enough to discover toxicologically relevant contamination levels for many toxicants. Individually, xenobiotics at low-levels may not pose a health risk. If mixture effects, longitudinal exposure, and exposure at certain sensitive time periods are considered, however, even minor levels may still play a central role in risk assessment and disease development. Therefore, the quantitative information obtained from low-level exposure in QQQ is highly valuable for risk assessments and exposomic investigations. Nevertheless, discovering emerging, unknown, and unexpected contaminants (including biotransformation products) where reference standards are frequently unavailable, is unique to HRMS and makes it essential to elucidate the exposome. However, broad, targeted QQQ methods are a crucial addition to HRMS for quantifying trace level exposures.

ACKNOWLEDGMENTS

The authors would like to thank the Mass Spectrometry Centre (MSC) at the Faculty of Chemistry for technical support, the Exposome Austria, and the University of Vienna for financing this study.

DATA AVAILABILITY

The raw data is available on the MetaboLights data repository (#MTBLS4646).

CONFLICT OF INTEREST

The authors declare that there are no conflicts of interest.

AUTHOR INFORMATION

Corresponding Author

*benedikt.warth@univie.ac.at; +43 664 60277 70806

REFERENCES

- Adoamnei, E., J. Mendiola, M. Moñino-García, F. Vela-Soria, L.M. Iribarne-Durán, M.F. Fernández, N. Olea, N. Jørgensen, S.H. Swan, and A.M. Torres-Cantero. 2018. 'Urinary concentrations of parabens and reproductive parameters in young men', *Science of the Total Environment*, 621: 201-09.
- Andra, S.S., C. Austin, and M. Arora. 2016. 'The tooth exposee in children's health research', *Current Opinion in Pediatrics*, 28: 221-27.
- Braun, D., C.N. Ezekiel, D. Marko, and B. Warth. 2020. 'Exposure to Mycotoxin-Mixtures via Breast Milk: An Ultra-Sensitive LC-MS/MS Biomonitoring Approach', *Front Chem*, 8: 423.
- CDC. 2021. 'Fourth National Report on Human Exposure to Environmental Chemicals', *Volume Two: NHANES 2011-2016*.
- Chambers, M.C., B. Maclean, R. Burke, D. Amodei, D.L. Ruderman, S. Neumann, L. Gatto, B. Fischer, B. Pratt, J. Egerton, K. Hoff, D. Kessner, N. Tasman, N. Schulman, B. Frewen, T.A. Baker, M.-Y. Brusniak, C. Paulse, D. Creasy, L. Flashner, K. Kani, C. Moulding, S.L. Seymour, L.M. Nuwaysir, B. Lefebvre, F. Kuhlmann, J. Roark, P. Rainer, S. Detlev, T. Hemenway, A. Huhmer, J. Langridge, B. Connolly, T. Chadick, K. Holly, J. Eckels, E.W. Deutsch, R.L. Moritz, J.E. Katz, D.B. Agus, M. MacCoss, D.L. Tabb, and P. Mallick. 2012. 'A cross-platform toolkit for mass spectrometry and proteomics', *Nature Biotechnology*, 30: 918-20.
- Chávez-Suárez, K.M., M.I. Ortega-Vélez, A.I. Valenzuela-Quintanar, M. Galván-Portillo, L. López-Carrillo, J. Esparza-Romero, M.S. Saucedo-Tamayo, M.R. Robles-Burgueño, S.A. Palma-Durán, M.L. Gutiérrez-Coronado, M.M. Campa-Siqueiros, P. Grajeda-Cota, and G. Caire-Juvera. 2017. 'Phytoestrogen Concentrations in Human Urine as Biomarkers for Dietary Phytoestrogen Intake in Mexican Women', *Nutrients*, 9: 1078.
- Chung, M.K., G.M. Buck Louis, K. Kannan, and C.J. Patel. 2019. 'Exposome-wide association study of semen quality: Systematic discovery of endocrine disrupting chemical biomarkers in fertility require large sample sizes', *Environment International*, 125: 505-14.
- David, A., J. Chaker, E.J. Price, V. Bessonneau, A.J. Chetwynd, C.M. Vitale, J. Klánová, D.I. Walker, J.-P. Antignac, R. Barouki, and G.W. Miller. 2021. 'Towards a comprehensive characterisation of the human internal chemical exposome: Challenges and perspectives', *Environment International*, 156: 106630.
- Dennis, K.K., E. Marder, D.M. Balshaw, Y. Cui, M.A. Lynes, G.J. Patti, S.M. Rappaport, D.T. Shaughnessy, M. Vrijheid, and D.B. Barr. 2017. 'Biomonitoring in the Era of the Exposome', *Environmental Health Perspectives*, 125: 502-10.
- EFSA. 2012. 'Guidance on selected default values to be used by the EFSA Scientific Committee, Scientific Panels and Units in the absence of actual measured data', *EFSA Journal*, 10: 2579.
- EFSA. 2015. 'Scientific Opinion on the risks to public health related to the presence of bisphenol A (BPA) in foodstuffs', *EFSA Journal*, 13: 3978.
- Ezekiel, C.N., W.A. Abia, D. Braun, B. Šarkanj, K.I. Ayeni, O.A. Oyedele, E.C. Michael-Chikezie, V.C. Ezekiel, B.N. Mark, C.P. Ahuchaogu, R. Krska, M. Sulyok, P.C. Turner, and B. Warth. 2022. 'Mycotoxin exposure biomonitoring in breastfed and non-exclusively breastfed Nigerian children', *Environment International*, 158: 106996.
- Fedorova, G., T. Randak, R.H. Lindberg, and R. Grabic. 2013. 'Comparison of the quantitative performance of a Q-Exactive high-resolution mass spectrometer with that of a triple quadrupole tandem mass spectrometer for the analysis of illicit drugs in wastewater', *Rapid Communications in Mass Spectrometry*, 27: 1751-62.
- Flasch, M., C. Bueschl, G. Del Favero, G. Adam, R. Schuhmacher, D. Marko, and B. Warth. 2022. 'Elucidation of xenoestrogen metabolism by non-targeted, stable isotope-assisted mass spectrometry in breast cancer cells', *Environment International*, 158: 106940.
- Frederiksen, H., L. Aksglaede, K. Sorensen, N.E. Skakkebaek, A. Juul, and A.-M.

- Andersson. 2011. 'Urinary excretion of phthalate metabolites in 129 healthy Danish children and adolescents: Estimation of daily phthalate intake', *Environmental Research*, 111: 656-63.
- Gao, P. 2021. 'The Exposome in the Era of One Health', *Environmental Science & Technology*, 55: 2790-99.
- Garde, A.H., Å.M. HANSEN, J. Kristiansen, and L.E. Knudsen. 2004. 'Comparison of uncertainties related to standardization of urine samples with volume and creatinine concentration', *Annals of Occupational Hygiene*, 48: 171-79.
- Granum, B., B. Oftedal, L. Agier, V. Siroux, P. Bird, M. Casas, C. Warembourg, J. Wright, L. Chatzi, M. de Castro, D. Donaire, R. Grazuleviciene, L. Småtuen Haug, L. Maitre, O. Robinson, I. Tamayo-Uria, J. Urquiza, M. Nieuwenhuijsen, R. Slama, C. Thomsen, and M. Vrijheid. 2020. 'Multiple environmental exposures in early-life and allergy-related outcomes in childhood', *Environment International*, 144: 106038.
- Grund, B., L. Marvin, and B. Rochat. 2016. 'Quantitative performance of a quadrupole-orbitrap-MS in targeted LC-MS determinations of small molecules', *Journal of Pharmaceutical and Biomedical Analysis*, 124: 48-56.
- Helmus, R., T.L. ter Laak, A.P. van Wezel, P. de Voogt, and E.L. Schymanski. 2021. 'patRoon: open source software platform for environmental mass spectrometry based non-target screening', *Journal of Cheminformatics*, 13: 1.
- Herrero, P., N. Cortés-Francisco, F. Borrull, J. Caixach, E. Pocurull, and R.M. Marcé. 2014. 'Comparison of triple quadrupole mass spectrometry and Orbitrap high-resolution mass spectrometry in ultrahigh performance liquid chromatography for the determination of veterinary drugs in sewage: benefits and drawbacks', *Journal of Mass Spectrometry*, 49: 585-96.
- Jamnik, T., M. Flasch, D. Braun, Y. Fareed, D. Wasinger, D. Seki, D. Berry, A. Berger, L. Wisgrill, and B. Warth. 2022. 'Next-generation biomonitoring of the early-life chemical exposome in neonatal and infant development', *Nature Communications*, 13: 2653.
- Janulewicz, P.A., J.M. Carlson, A.K. Wesselink, L.A. Wise, E.E. Hatch, L.M. Edwards, and J.L. Peters. 2021. 'Urinary Isoflavones Levels in Relation to Serum Thyroid Hormone Concentrations in Female and Male Adults in the U.S. General Population', *International Journal of Environmental Health Research*, 31: 389-400.
- Julvez, J., M. López-Vicente, C. Warembourg, L. Maitre, C. Philippat, K.B. Gützkow, M. Guxens, J. Evandt, S. Andrusaityte, M. Burgaleta, M. Casas, L. Chatzi, M. de Castro, D. Donaire-González, R. Gražulevičienė, C. Hernandez-Ferrer, B. Heude, R. McEachan, M. Mon-Williams, M. Nieuwenhuijsen, O. Robinson, A.K. Sakhi, N. Sebastian-Galles, R. Slama, J. Sunyer, I. Tamayo-Uria, C. Thomsen, J. Urquiza, M. Vafeiadi, J. Wright, X. Basagaña, and M. Vrijheid. 2021. 'Early life multiple exposures and child cognitive function: A multi-centric birth cohort study in six European countries', *Environmental Pollution*, 284: 117404.
- Mackintosh, S.A., A. Pérez-Fuentetaja, L.R. Zimmerman, G. Pacepavicius, M. Clapsadl, M. Alaei, and D.S. Aga. 2012. 'Analytical performance of a triple quadrupole mass spectrometer compared to a high resolution mass spectrometer for the analysis of polybrominated diphenyl ethers in fish', *Analytica Chimica Acta*, 747: 67-75.
- Magnusson B., Ö.U.e. 2014. 'EuraChem Guide: The Fitness for Purpose of Analytical Methods-A Laboratory Guide to Method Validation and Related Topics', Second Edition.
- Pascual-Caro, S., F. Borrull, C. Aguilar, and M. Calull. 2020. 'Determination of Synthetic Cathinones in Urine and Oral Fluid by Liquid Chromatography High-Resolution Mass Spectrometry and Low-Resolution Mass Spectrometry: A Method Comparison', *Separations*, 7.
- Pirard, C., C. Sagot, M. Deville, N. Dubois, and C. Charlier. 2012. 'Urinary levels of bisphenol A, triclosan and 4-nonylphenol in a general Belgian population', *Environment International*, 48: 78-83.
- Ponzetto, F., J. Boccard, N. Baume, T. Kouranne, S. Rudaz, M. Saugy, and R. Nicoli. 2017. 'High-resolution mass spectrometry as an alternative detection method to tandem mass spectrometry for the analysis of endogenous steroids in serum', *Journal of Chromatography B*, 1052: 34-42.
- Preindl, K., D. Braun, G. Aichinger, S. Sieri, M. Fang, D. Marko, and B. Warth. 2019. 'A Generic Liquid Chromatography-Tandem Mass Spectrometry Exposome Method for the Determination of Xenoestrogens in Biological Matrices', *Analytical Chemistry*, 91: 11334-42.
- Qiao, X., G. Li, J. Zhang, J. Du, Y. Yang, J. Yin, H. Li, J. Xie, Y. Jiang, X. Fang, X. Dai, and B. Shao. 2022. 'Urinary analysis reveals high Alternaria mycotoxins exposure in the general population from Beijing, China', *Journal of Environmental Sciences*, 118: 122-29.
- Rappaport, S.M., D.K. Barupal, D. Wishart, P. Vineis, and A. Scalbert. 2014. 'The blood exposome and its role in discovering causes of disease', *Environmental Health Perspectives*, 122: 769-74.
- Ruttkies, C., E.L. Schymanski, S. Wolf, J. Hollender, and S. Neumann. 2016. 'MetFrag relaunched: incorporating strategies beyond in silico fragmentation', *Journal of Cheminformatics*, 8: 3.
- Schiano, M.E., A. Abduvakhidov, M. Varra, and S. Albrizio. 2022. 'Aptamer-Based Biosensors for the Analytical Determination of Bisphenol A in Foodstuffs', *Applied Sciences*, 12: 3752.
- Schymanski, E.L., J. Jeon, R. Gulde, K. Fenner, M. Ruff, H.P. Singer, and J. Hollender. 2014. 'Identifying Small Molecules via High Resolution Mass Spectrometry: Communicating Confidence', *Environmental Science & Technology*, 48: 2097-98.
- Silva, M.J., D.B. Barr, J.A. Reidy, K. Kato, N.A. Malek, C.C. Hodge, D. Hurtz, A.M. Calafat, L.L. Needham, and J.W. Brock. 2003. 'Glucuronidation patterns of common urinary and serum monoester phthalate metabolites', *Archives of Toxicology*, 77: 561-67.
- Sobus, J.R., J.N. Grossman, A. Chao, R. Singh, A.J. Williams, C.M. Grulke, A.M. Richard, S.R. Newton, A.D. McEachan, and E.M. Ulrich. 2019. 'Using prepared mixtures of ToxCast chemicals to evaluate non-targeted analysis (NTA) method performance', *Analytical and Bioanalytical Chemistry*, 411: 835-51.
- Stein, T.P., M.D. Schluter, R.A. Steer, L. Guo, and X. Ming. 2015. 'Bisphenol A Exposure in Children With Autism Spectrum Disorders', *Autism Research*, 8: 272-83.
- Vermeulen, R., E.L. Schymanski, A.-L. Barabási, and G.W. Miller. 2020. 'The exposome and health: Where chemistry meets biology', *Science*, 367: 392-96.
- Vrijheid, M., S. Fossati, L. Maitre, S. Márquez, T. Roumeliotaki, L. Agier, S. Andrusaityte, S. Cadiou, M. Casas, M.d. Castro, A. Dedele, D. Donaire-Gonzalez, R. Grazuleviciene, L.S. Haug, R. McEachan, H.M. Meltzer, E. Papadopoulou, O. Robinson, A.K. Sakhi, V. Siroux, J. Sunyer, P.E. Schwarze, I. Tamayo-Uria, J. Urquiza, M. Vafeiadi, A. Valentin, C. Warembourg, J. Wright, M.J. Nieuwenhuijsen, C. Thomsen, X. Basagaña, R. Slama, and L. Chatzi. 2020. 'Early-Life Environmental Exposures and Childhood Obesity: An Exposome-Wide Approach', *Environmental Health Perspectives*, 128: 067009.
- Warth, B., S. Spangler, M. Fang, C.H. Johnson, E.M. Forsberg, A. Granados, R.L. Martin, X. Domingo-Almenara, T. Huan, D. Rinehart, J.R. Montenegro-Burke, B. Hilmer, A. Aisporna, L.T. Hoang, W. Uritboonthai, H.P. Benton, S.D. Richardson, A.J. Williams, and G. Siuzdak. 2017. 'Exposome-Scale Investigations Guided by Global Metabolomics, Pathway Analysis, and Cognitive Computing', *Analytical Chemistry*, 89: 11505-13.
- Wilhelm, M., J. Hardt, C. Schulz, and J. Angerer. 2008. 'New reference value and the background exposure for the PAH metabolites 1-hydroxypyrene and 1- and 2-naphthol in urine of the general population in Germany: Basis for validation of human biomonitoring data in environmental medicine', *International Journal of Hygiene and Environmental Health*, 211: 447-53.
- Zhang, T., H. Sun, X. Qin, Z. Gan, and K. Kannan. 2015. 'PFOS and PFOA in paired urine and blood from general adults and pregnant women: assessment of urinary elimination', *Environmental Science and Pollution Research International*, 22: 5572-9.

Supporting Information A

Comparing the sensitivity of low- and high-resolution mass spectrometry for xenobiotic trace analysis: An exposome-type case study

Mira Flasch^{1,2}, Gunda Koellensperger^{3,4}, Benedikt Warth^{1,4*}

¹University of Vienna, Faculty of Chemistry, Department of Food Chemistry and Toxicology, Währinger Straße 38, 1090 Vienna, Austria

²University of Vienna, Vienna Doctoral School in Chemistry, Währinger Straße 42, 1090, Vienna, Austria

³University of Vienna, Faculty of Chemistry, Department of Analytical Chemistry, Währinger Straße 38, 1090 Vienna, Austria

⁴Exposome Austria, Research Infrastructure and National EIRENE Hub, Austria

Contents

Table S1 LODs in urine for the high- and low-resolution instrument.....	2
Table S2 Concentrations of analytical standards at the different concentration levels.....	6
Table S3 Concentrations in internal standard mix.....	9
Table S4 LC-MS/MS parameters for the measurement of the analytes in low-resolution LC-MS/MS.....	10
Table S5 Calibration parameters and SSE in solvent and urine of the quantitation by LC-HRMS	14
Table S6 Calibration parameters in solvent and urine of the quantification by low resolution LC-MS/MS.....	18
Table S7 Concentrations of analytes in urine samples measured by high-resolution mass spectrometry.....	22
Table S8 Concentrations of analytes in urine samples measured by low-resolution mass spectrometry.....	23
Table S9 Estimation of urinary concentration at toxicological exposure limits.....	24
Figure S1 Comparison of LOQ values between the low- and high-resolution mass spectrometer in solvent.....	25

Table S1 LODs in urine for the high- and low-resolution instrument. For the low-resolution instrument two different approaches for LOD estimation were performed for most analytes.

Compound	Limit of Quantitation (LOQ) [ng/mL]					
	CAS	Q Exactive HF		QTrap 6500 ⁺		
		Solvent	Urine	Solvent	Urine	Urine (S/N)*
Plasticizers/Plastic Components						
Bisphenol A (BPA)	80-05-07	4.1	2.1	0.42	0.81	0.21
Bisphenol AF (BPAF)	1478-61-1	1.6	0.41	0.094	0.081	0.038
Bisphenol B (BPB)	77-40-7	4.6	2.5	0.043	0.28	0.022
Bisphenol C (BPC)	79-97-0	7.9	3.8	0.55	0.51	0.22
Bisphenol F (BPF)	620-92-8	2.3	1.2	0.24	0.29	0.064
Bisphenol S (BPS)	80-09-1	0.0073	0.13	0.0062	0.0075	0.036
Mono-n-butyl phthalate (MBP)	131-70-4	0.83	4.4	0.61	1.1	0.34
N-butylbenzenesulfonamide	3622-84-2	3.3	3.1	0.98	1.3	1.2
Benzyl butyl phthalate	85-68-7	0.69	6.9	0.64	0.90	0.18
Dibutyl phthalate	84-74-2	80	160	21	82	3.1
Tetrabromobisphenol A	79-94-7	43	60	0.17	0.14	0.021
Perfluorinated Alkylated Substances						
Perfluorooctanoic acid (PFOA)	335-67-1	0.36	0.13	0.067	0.083	0.22
Perfluorooctanesulfonic acid (PFOS)	1763-23-1	0.080	3.5	0.021	0.12	0.049
Industrial Side Products and Pesticides						
2-Naphthol	135-19-3	0.92	4.1	0.010	2.6	0.019
Methiocarb	2032-65-7	2.3	3.8	0.012	0.0067	0.017
Prochloraz	67747-09-5	0.16	0.17	0.00098	0.0011	0.0003
2-tert-Butylphenol (2-tert-BP)	88-18-6	6.1	1.0	6.9	16	34
4-Octylphenol (4-OP)	1806-26-4	124	55	6.7	4.8	1.4
4-tert-Octylphenol (4-tert-OP)	140-66-9	2.2	11	0.092	0.22	0.14
Fenarimol	60168-88-9	0.094	1.1	0.0068	0.0052	0.0028
Nonylphenol	84852-15-3	70	3394	0.15	0.80	3.2
Endogenous Estrogens						
Estrone (E1)	53-16-7	2.1	0.78	0.0069	0.017	0.0059
Estradiol (E2)	50-28-2	11	7.6	0.84	0.89	0.051
Estradiol-17-glucuronide (E2-17-GlcA)	15270-30-1	0.91	1.4	1.2	40	n.d.
Estradiol-3-sulfate (E2-3-sulfate)	4999-79-5	5.6	4.2	0.039	0.062	0.2
Estriol (E3)	50-27-1	0.60	0.49	0.094	0.11	0.12
16-Epiestriol (16EpiE3)	547-81-9	3.4	2.5	0.23	0.24	0.23
16- α -Hydroxyestrone (16OHE1)	566-76-7	0.26	0.13	0.054	0.035	0.096
17-Epiestriol (17EpiE3)	1228-72-4	3.1	1.9	0.28	0.23	0.12
2-Methoxy estrone (2MeOE1)	362-08-3	14	6.6	0.047	0.013	0.046
2-Methoxy estradiol(2MeOE2)	362-07-2	132	99	0.44	0.48	0.018
4-Methoxy estrone (4MeOE1)	58562-33-7	1.5	1.0	0.0064	0.011	0.016
4-Methoxy estradiol (4MeOE2)	26788-23-8	0.96	1.0	0.023	0.024	0.024

Compound	Limit of Quantitation (LOQ) [ng/mL]					
	CAS	Q Exactive HF		QTrap 6500 ⁺		
		Solvent	Urine	Solvent	Urine	Urine (S/N)*
4-Hydroxy estrone (4OHE1)	3131-23-5	0.027	0.052	0.035	0.17	0.013
Phytoestrogens and Metabolites						
8-Prenylnaringenin	53846-50-7	0.99	0.59	0.053	0.067	0.01
Coumestrol	479-13-0	0.14	0.11	0.013	0.011	0.01
Daidzein	486-66-8	0.18	0.12	0.013	0.040	0.025
Enterodiol	80226-00-2	0.10	1.7	0.017	0.047	0.18
Enterolactone	78473-71-9	0.62	1.0	0.082	0.76	1.1
Equol	94105-90-5	0.61	0.41	0.053	0.049	0.0076
Formononetin	485-72-3	0.0059	0.052	0.0078	0.0073	0.0028
Genistein (GEN)	446-72-0	0.149	0.12	0.016	0.033	0.011
Glycitein	40957-83-3	0.18	0.055	0.017	0.11	0.13
Isoxanthohumol	70872-29-6	0.015	0.29	0.0024	0.032	0.0072
Matairesinol	580-72-3	1.2	0.85	0.11	0.20	0.65
Resveratrol	501-36-0	0.19	0.21	0.22	1.3	2.2
Xanthohumol	569-83-5	0.12	0.086	0.024	0.52	0.052
Mycoestrogens and Metabolites						
Alternariol	641-38-3	0.26	0.20	0.24	0.20	0.16
Alternariol monomethyl ether	26894-49-5	0.10	0.11	0.011	0.0090	0.0077
α -zearalanol (α -ZAL)	26538-44-3	0.062	1.1	0.13	0.12	0.1
β -zearalanol (β -ZAL)	42422-68-4	1.8	1.2	0.15	0.098	0.13
α -zearalenol (α -ZEL)	36455-72-8	0.70	0.64	0.060	0.077	0.012
β -zearalenol (β -ZEL)	71030-11-0	0.18	0.13	0.27	30	0.4
α -zearalenol-14-glucuronide (α -ZEL-14-GlcA)	not given	7.3	4.6	0.041	17	n.d.
β -zearalenol-14-glucuronide (β -ZEL-14-GlcA)	not given	4.2	4.2	0.037	30	n.d.
Zearalanone (ZAN)	5975-78-0	1.1	0.63	0.093	0.038	0.08
Zearalenone (ZEN)	17924-92-4	0.95	0.65	0.068	0.068	0.025
Zearalenone-14-glucuronide (ZEN-14-GlcA)	1032558-19-2	34	15.2	0.17	5.0	n.d.
Zearalenone-14-sulfate (ZEN-14-sulfate)	not given	0.34	0.22	0.039	0.036	0.15
Personal Care Product Ingredients, Pharmaceuticals and Metabolites						
Benzophenone 1	131-56-6	0.045	0.033	0.049	0.051	0.0054
Benzophenone 2	131-55-5	0.031	0.016	0.0026	0.036	0.018
Benzylparaben	94-18-8	0.056	0.030	0.00031	0.0051	0.0006
Butylparaben	94-26-8	0.016	0.017	0.022	0.016	0.007
Ethylparaben	120-47-8	0.019	0.030	0.034	0.035	0.004
Isobutylparaben	4247-02-3	0.0091	0.018	0.026	0.026	0.008
Methylparaben	99-76-3	0.070	0.23	0.032	0.11	0.05
Propylparaben	94-13-3	0.054	0.067	0.012	0.016	0.01
Ethinylestradiol	57-63-6	1.9	0.83	0.22	0.24	0.04
3-Benzylidencamphor (3-BC)	15087-24-8	2.2	34	2.14	6.6	0.3

Compound	Limit of Quantitation (LOQ) [ng/mL]					
	CAS	Q Exactive HF		QTrap 6500 ⁺		
		Solvent	Urine	Solvent	Urine	Urine (S/N)*
4-methylbenzylidencamphor (4-MBC)	36861-47-9	0.98	16	0.082	0.075	0.43
Octyl methoxycinnamate (OMC)	5466-77-3	94	4800	59	98	160
p-Hydroxybenzoic acid (pOHBA)	99-96-7	2.7	112	7.7	117	n.d.
Triclosan	3380-34-5	0.14	2.5	0.012	0.026	0.035
Phytotoxins						
Anisodamine	55869-99-3	0.012	0.039	0.0028	0.11	0.066
Aristolactam I	13395-02-3	2.0	1.2	0.10	0.083	0.016
Jacobine	6870-67-3	0.077	0.24	0.083	0.50	0.4
Jacobine-N-oxide	38710-25-7	0.013	0.32	0.014	0.10	0.06
Riddelliin	23246-96-0	0.098	0.60	0.087	0.62	1.2
Riddelliin-N-oxide	75056-11-0	0.066	0.21	0.058	0.95	1
Scopolamine	114-49-8	0.055	0.050	0.00045	0.0005	0.0025
Disinfection By-Products						
Bromoacetic acid	79-08-3	5.0	127	1.2	115	n.d.
Dibromoacetic acid	631-64-1	5.0	1.1	6.2	26	32
Dichloroacetic acid	79-43-6	2.9	22	12	32	60
Food Processing By-Products						
Acrylamide	79-06-1	38	713	38	147	92
5-Hydroxymethylfurfural (HMF)	67-47-0	7.1	18	21	116	29
2-amino-1-methyl-6-phenylimidazo(4,5-b)pyridine (PhIP)	105650-23-5	0.027	0.24	0.0027	0.018	0.011
Air Pollutants						
Cotinine	486-56-6	0.70	3.1	0.084	30	0.89
Trans-3-hydroxy cotinine	159956-78-2	0.12	3.2	0.016	0.050	2.3
1-Hydroxy pyrene	5315-79-7	0.15	4.1	3.09	0.18	0.19
3-Hydroxy phenanthrene	605-87-8	0.38	0.29	0.036	0.030	0.021
Mycotoxins						
Aflatoxin B1	1162-65-8	0.15	1.9	0.31	0.22	-
Aflatoxin B2	7220-81-7	5.5	51.4	7.9	4.7	-
Aflatoxin G1	1165-39-5	3.1	1.3	0.28	0.17	-
Aflatoxin G2	7241-98-7	0.49	7.2	0.99	7.0	-
Aflatoxin M1	6795-23-9	0.19	2.6	0.30	0.37	-
Aflatoxin M2	6885-57-0	48	46.3	5.0	11	-
Aflatoxicol	29611-03-8	7.7	101	0.79	6.4	-
Sterigmatocystein	10048-13-2	0.13	2.6	0.026	0.020	-
Citrinin	518-75-2	3.3	14.6	7.8	672	-
Deoxynivalenol	51481-10-8	380	371	27	393	-
Nivalenol	23282-20-4	> 30	> 30	3.0	7.1	-
Toxin T2	21259-20-1	422	585	1203	886	-

Compound	Limit of Quantitation (LOQ) [ng/mL]					
	CAS	Q Exactive HF		QTrap 6500 ⁺		Urine (S/N)*
		Solvent	Urine	Solvent	Urine	
Ochratoxin A	303-47-9	> 9	> 9	0.71	0.99	-
Ochratoxin B	4825-86-9	13	6.3	0.068	0.16	-
Ochratoxin α	16281-39-3	5.0	73	7.0	23	-

* Limit of quantitation (LOQ) based on a signal/noise ratio of 3/1 estimated from original data of Jamnik et al. (2022)

Table S2 Concentrations of analytical standards at the different concentration levels

Compound	Concentration [ng/mL]						
	0.3	1	3	10	30	100	300
Plasticizer/Plastic Components							
Bisphenol A (BPA)	0.03	0.1	0.3	1	3	10	30
Bisphenol AF (BPAF)	0.0015	0.05	0.15	0.5	1.5	5	15
Bisphenol B (BPB)	0.015	0.01	0.03	0.1	0.3	1	3
Bisphenol C (BPC)	0.0075	0.2	0.6	2	6	20	60
Bisphenol F (BPF)	0.0015	0.05	0.15	0.5	1.5	5	15
Bisphenol S (BPS)	0.009	0.002	0.01	0.02	0.06	0.2	0.6
Mono-n-butyl phthalate (MBP)	0.006	0.5	1.5	5	15	50	150
N-butylbenzenesulfonamide	0.0005	1	3	10	30	100	300
Benzyl butyl phthalate	0.075	0.25	0.75	2.5	7.5	25	75
Dibutyl phthalate	1.5	5	15	50	150	500	1500
Tetrabromobisphenol A	0.03	0.1	0.3	1	3	10	30
Perfluorinated Alkylated Substances							
	2.25						
Perfluorooctanoic acid (PFOA)	0.0045	0.015	0.05	0.15	0.45	1.5	4.5
Perfluorooctanesulfonic acid (PFOS)	0.0045	0.015	0.05	0.15	0.45	1.5	4.5
Industrial Side Products and Pesticides							
2-Naphthol	0.009	0.03	0.09	0.3	0.9	3	9
Methiocarb	0.0015	0.005	0.02	0.05	0.15	0.5	1.5
Prochloraz	0.0001	0.0005	0	0.005	0.02	0.05	0.15
2-tert-Butylphenol (2-tert-BP)	15	50	150	500	1500	5000	15000
4-Octylphenol (4-OP)	3	10	30	100	300	1000	3000
4-tert-Octylphenol (4-tert-OP)	0.3	1	3	10	30	100	300
Fenarimol	0.0009	0.003	0.01	0.03	0.09	0.3	0.9
Nonylphenol	0.75	2.5	7.5	25	75	250	750
Endogenous Estrogens							
	0.9						
Estrone (E1)	0.0009	0.003	0.01	0.03	0.09	0.3	0.9
Estradiol (E2)	0.009	0.03	0.09	0.3	0.9	3	9
Estradiol-17-glucuronide (E2-17-GlcA)	0.09	0.05	0.15	0.5	1.5	5	15
Estradiol-3-sulfate (E2-3-sulfate)	0.015	0.015	0.05	0.15	0.45	1.5	4.5
Estriol (E3)	0.0045	0.03	0.09	0.3	0.9	3	9
16-Epiestriol (16EpiE3)	0.009	0.1	0.3	1	3	10	30
16- α -Hydroxyestrone (16OHE1)	0.03	0.015	0.05	0.15	0.45	1.5	4.5
17-Epiestriol (17EpiE3)	0.0045	0.1	0.3	1	3	10	30
2-Methoxy estrone (2MeOE1)	0.03	0.025	0.08	0.25	0.75	2.5	7.5
2-Methoxy estradiol(2MeOE2)	0.0075	0.2	0.6	2	6	20	60
4-Methoxy estrone (4MeOE1)	0.06	0.005	0.02	0.05	0.15	0.5	1.5
4-Methoxy estradiol (4MeOE2)	0.0015	0.01	0.03	0.1	0.3	1	3
4-Hydroxy estrone (4OHE1)	0.003	0.005	0.02	0.05	0.15	0.5	1.5
Phytoestrogens and Metabolites							
8-Prenylnaringenin	0.009	0.03	0.09	0.3	0.9	3	9

Compound	Concentration [ng/mL]						
	0.3	1	3	10	30	100	300
Coumestrol	0.0015	0.005	0.02	0.05	0.15	0.5	1.5
Daidzein	0.0015	0.005	0.02	0.05	0.15	0.5	1.5
Enterodiol	0.0015	0.005	0.02	0.05	0.15	0.5	1.5
Enterolactone	0.06	0.2	0.6	2	6	20	60
Equol	0.006	0.02	0.06	0.2	0.6	2	6
Formononetin	0.0008	0.0025	0.01	0.025	0.08	0.25	0.75
Genistein (GEN)	0.0015	0.005	0.02	0.05	0.15	0.5	1.5
Glycitein	0.0015	0.005	0.02	0.05	0.15	0.5	1.5
Isoxanthohumol	0.0003	0.001	0	0.01	0.03	0.1	0.3
Matairesinol	0.015	0.05	0.15	0.5	1.5	5	15
Resveratrol	0.45	1.5	4.5	15	45	150	450
Xanthohumol	0.03	0.1	0.3	1	3	10	30
Mycoestrogens and Metabolites							
Alternariol	0.03	0.1	0.3	1	3	10	30
Alternariol monomethyl ether	0.0015	0.005	0.02	0.05	0.15	0.5	1.5
α -zearalanol (α -ZAL)	0.015	0.05	0.15	0.5	1.5	5	15
β -zearalanol (β -ZAL)	0.015	0.05	0.15	0.5	1.5	5	15
α -zearalenol (α -ZEL)	0.0006	0.002	0.01	0.02	0.06	0.2	0.6
β -zearalenol (β -ZEL)	0.03	0.1	0.3	1	3	10	30
α -zearalenol-14-glucuronide (α -ZEL-14-GlcA)	0.0045	0.015	0.05	0.15	0.45	1.5	4.5
β -zearalenol-14-glucuronide (β -ZEL-14-GlcA)	0.0045	0.015	0.05	0.15	0.45	1.5	4.5
Zearalanone (ZAN)	0.009	0.03	0.09	0.3	0.9	3	9
Zearalenone (ZEN)	0.009	0.03	0.09	0.3	0.9	3	9
Zearalenone-14-glucuronide (ZEN-14-GlcA)	0.015	0.05	0.15	0.5	1.5	5	15
Zearalenone-14-sulfate (ZEN-14-sulfate)	0.0045	0.015	0.05	0.15	0.45	1.5	4.5
Personal Care Product Ingredients, Pharmaceuticals and Metabolites							
Benzophenone 1	0.006	0.02	0.06	0.2	0.6	2	6
Benzophenone 2	0.0045	0.015	0.05	0.15	0.45	1.5	4.5
Benzylparaben	0.0005	0.0015	0	0.015	0.05	0.15	0.45
Butylparaben	0.003	0.01	0.03	0.1	0.3	1	3
Ethylparaben	0.003	0.01	0.03	0.1	0.3	1	3
Isobutylparaben	0.003	0.01	0.03	0.1	0.3	1	3
Methylparaben	0.0075	0.025	0.08	0.25	0.75	2.5	7.5
Propylparaben	0.006	0.02	0.06	0.2	0.6	2	6
Ethinylestradiol	0.03	0.1	0.3	1	3	10	30
3-Benzylidencamphor (3-BC)	4.5	15	45	150	450	1500	4500
4-methylbenzylidencamphor (4-MBC)	0.45	1.5	4.5	15	45	150	450
Octyl methoxycinnamate (OMC)	6	20	60	200	600	2000	6000
p-Hydroxybenzoic acid (pOHBA)	1.5	5	15	50	150	500	1500
Triclosan	0.03	0.1	0.3	1	3	10	30

Compound	Concentration [ng/mL]						
	0.3	1	3	10	30	100	300
Phytotoxins							
Anisodamine	0.0015	0.005	0.015	0.05	0.15	0.5	1.5
Aristolactam I	0.015	0.05	0.15	0.5	1.5	5	15
Jacobine	0.0075	0.025	0.075	0.25	0.75	2.5	7.5
Jacobine-N-oxide	0.0015	0.005	0.015	0.05	0.15	0.5	1.5
Riddelliin	0.009	0.03	0.09	0.3	0.9	3	9
Riddelliin-N-oxide	0.006	0.02	0.06	0.2	0.6	2	6
Scopolamine	0.0005	0.0015	0.0045	0.015	0.045	0.15	0.45
Disinfection By-Products							
Bromoacetic acid	0.6	2	6	20	60	200	600
Dibromoacetic acid	0.45	1.5	4.5	15	45	150	450
Dichloroacetic acid	2.25	7.5	22.5	75	225	750	2250
Food Processing By-Products							
Acrylamide	3	10	30	100	300	1000	3000
5-Hydroxymethylfurfural (HMF)	1.05	3.5	10.5	35	105	350	1050
PhIP	0.003	0.01	0.03	0.1	0.3	1	3
Air Pollutants							
Cotinine	0.045	0.15	0.45	1.5	4.5	15	45
Trans-3-hydroxy cotinine	0.009	0.03	0.09	0.3	0.9	3	9
1-Hydroxy pyrene	0.06	0.2	0.6	2	6	20	60
3-Hydroxy phenantrene	0.0045	0.015	0.045	0.15	0.45	1.5	4.5
Mycotoxins							
Aflatoxin B1	0.03	0.1	0.3	1	3	10	30
Aflatoxin B2	0.9	3	9	30	90	300	900
Aflatoxin G1	0.03	0.1	0.3	1	3	10	30
Aflatoxin G2	0.09	0.3	0.9	3	9	30	90
Aflatoxin M1	0.03	0.1	0.3	1	3	10	30
Aflatoxin M2	0.6	2	6	20	60	200	600
Aflatoxicol	0.09	0.3	0.9	3	9	30	90
Sterigmatocystein	0.003	0.01	0.03	0.1	0.3	1	3
Citrinin	0.9	3	9	30	90	300	900
Deoxynivalenol	0.3	1	3	10	30	100	300
Nivalenol	0.03	0.1	0.3	1	3	10	30
Toxin T2	0.9	3	9	30	90	300	900
Ochratoxin A	0.009	0.03	0.09	0.3	0.9	3	9
Ochratoxin B	0.009	0.03	0.09	0.3	0.9	3	9
Ochratoxin Alpha	0.09	0.3	0.9	3	9	30	90

Table S3 Concentrations in the used multi-component internal standard mix

Internal Standard	Concentration in mixture [ng/mL]
¹³ C ₁₂ -Bisphenol A	20
¹³ C ₁₈ -Zearalenone	20
¹³ C ₂ -mono- <i>n</i> -butyl phthalate	40
¹³ C ₃ -Estradiol	20
¹³ C ₆ -4-tert-Octylphenol	200
¹³ C ₆ -Butylparaben	10
¹³ C ₆ -Ethylparaben	10
¹³ C ₆ -Methylparaben	10
¹³ C ₆ - <i>p</i> -Hydroxybenzoic acid	600
¹³ C ₆ -Propylparaben	10
¹³ C ₈ -Perfluorooctanesulfonic acid	20
¹³ C ₈ -Perfluorooctanoic acid	20
D ₄ -Genistein	10

Table S4 LC-MS/MS parameters for the measurement of the analytes in low-resolution LC-MS/MS including retention time (rt) and its deviation from the retention time in the high resolution measurement (dev).

Compound	Polarity	Q1 mass [Da]	DP [V]	Q3 mass [Da]	CE [V]	CXP [V]	rt [min]	dev [s]
Plasticizer/plastic components								
Bisphenol A (BPA)	neg	227.0	-140	133.0 116.9	-32 -56	-17 -21	8.3	21
Bisphenol AF (BPAF)	neg	335.0	-80	265.1 176.8	-32 -58	-19 -29	12.0	18
Bisphenol B (BPB)	neg	241.1	-45	212.1 210.9	-26 -40	-11 -15	10	20
Bisphenol C (BPC)	neg	255.0	-70	240.2 147.0	-26 -34	-29 -9	11.8	19
Bisphenol F (BPF)	neg	198.6	-120	105.0 106.0	-28 -28	-11 -11	6.3	13
Bisphenol S (BPS)	neg	249.1	-150	108.0 155.9	-36 -28	-13 -13	4.8	10
Mono-n-butyl phthalate (MBP)	neg	221.0	-5	77.2 71.1	-24 -20	-5 -11	4.8	2
N-butylbenzenesulfonamide	neg	211.9	-30	127.1 140.9	-20 -30	-11 -9	9.0	18
Benzyl butyl phthalate	pos	313.0	36	64.8 91.0	-24 45	-29 10	15.1	4
Dibutyl phthalate	pos	279.0	11	149.0 148.9	19 21	12 16	15.2	3
Tetrabromobisphenol A (TBPA)	neg	542.6	-110	204.8 445.8	11 -45	20 -28	15.0	4
				419.8 417.9	-53 -56	-23 -33		
Perfluorinated alkylated substances								
Perfluorooctanoic acid (PFOA)	neg	412.9	-20	368.9 168.9	-18 -22	-19 -13	6.8-7.1	-18
Perfluorooctanesulfonic acid (PFOS)	neg	498.8	-80	80.0 98.9	-126 -92	-37 -3	11-11.4	-37
Industrial side products and pesticides								
2-Naphthol	neg	143.0	-20	115.0 114.0	-34 -42	-13 -17	7.4	16
Methiocarb	pos	226.0	31	168.7 121.1	13 31	18 16	10.8	22
Prochloraz	pos	375.9	21	307.8 265.7	17 23	42 16	14.6	4
2-tert-Butylphenol (2-tert-BP)	neg	149.0	-85	132.9 93.0	-32 -30	-7 -11	13.3	24
4-Octylphenol (4-OP)	neg	205.1	-15	105.9 118.9	-28 -44	-19 -1	15.5	6
4-tert-Octylphenol (4-tert-OP)	neg	205.1	-15	134.0 133.0	-24 -36	-11 -19	15.1	3
Fenarimol	pos	330.9	121	267.9 189.1	31 59	18 12	11.9	18
Nonylphenol	neg	219.1	-20	133.0 134.0	-42 -24	-11 -9	15.4	5
Endogenous estrogens								
Estrone (E1)	neg	269.4	-140	144.8 143.0	-50 -50	-2 -2	10.5	23
Estradiol (E2)	neg	271.1	-50	144.9 183.0	-52 -52	-15 -2	8.9	14
Estradiol-17-glucuronide (E2-17-GlcA)	neg	447.1	-55	113.0 271.0	-30 -36	-9 -21	4.0	-1
Estradiol-3-sulfate sulfate)	(E2-3-sulfate) neg	351.1	-170	271.1 80.0	-44 -62	-17 -11	4.7	-4
Estriol (E3)	neg	287.0	-140	171.0 145.0	-48 -52	-27 -9	5.0	6

Compound	Polarity	Q1 mass [Da]	DP [V]	Q3 mass [Da]	CE [V]	CXP [V]	rt [min]	dev [s]
16-Epiestriol (16EpiE3)	neg	287.1	-95	145.0 171.1	-50 -52	-11 -11	6.0	7
16- α -Hydroxyestrone (16OHE1)	neg	285.1	-160	145.0 143.0	-46 -73	-11 -19	6.1	9
17-Epiestriol (17EpiE3)	neg	287.1	-125	145.0 143.1	-52 -64	-13 -9	6.3	8
2-Methoxy estrone (2MeOE1)	neg	299.1	-30	284.2 159.9	-32 -54	-21 -9	11.2	-12
2-Methoxy estradiol(2MeOE2)	neg	301.1	-45	286.1 285.2	-34 -48	-17 -21	10.0	15
4-Methoxy estrone (4MeOE1)	neg	299.1	-55	284.1 283.2	-28 -42	-23 -19	11.1	18
4-Methoxy estradiol (4MeOE2)	neg	301.1	-40	286.1 284.9	-28 -46	-17 -23	9.3	15
4-Hydroxy estrone (4OHE1)	neg	285.2	-130	161.1 159.1	-50 -66	-15 -9	8.4	-24
Phytoestrogens and metabolites								
8-Prenylnaringenin	neg	339.0	-15	219.0 119.0	-26 -38	-19 -15	11.6	19
Coumestrol	neg	267.0	-50	265.9 211.0	-38 -38	-15 -11	6.4	12
Daidzein	neg	253.0	-10	224.0 207.9	-36 -40	-17 -13	5.2	9
Enterodiol	neg	301.1	-90	253.1 271.1	-32 -32	-15 -19	5.2	4
Enterolactone	neg	297.1	-105	253.1 107.0	-28 -32	-43 -11	6.8	12
Equol	neg	241.1	-45	120.9 118.9	-18 -28	-13 -5	6.5	11
Formononetin	neg	267.0	-90	252.0 223.0	-28 -42	-17 -17	7.9	14
Genistein	neg	269.0	-5	133.1 132	-38 -54	-11 -21	6.4	15
Glycitein	pos	285.0	166	270.0 241.9	33 43	22 14	5.4	11
Isoxanthohumol	pos	355.1	31	179.0 298.9	35 21	12 18	8.4	12
Matairesinol	neg	269.0	-65	83.0 137.1	-26 -30	-11 -11	6.5	11
Resveratrol	neg	227.0	-45	185.0 142.9	-26 -30	-11 -17	5.0	8
Xanthohumol	pos	355.0	76	179.0 299.0	29 17	10 20	14.7	2
Mycostrogens and metabolites								
Alternariol	neg	257.0	-110	213 215	-32 -34	-13 -13	6.8	13
Alternariol monomethyl ether	neg	271.1	-95	256 228	-32 -39	-13 -20	11.4	24
α -Zearalanol (α -ZAL)	neg	321.1	-120	277.1 303.1	-30 -30	-18 -20	8.8	12
β -Zearalanol (β -ZAL)	neg	321.1	-120	277.1 303.1	-30 -30	-18 -20	7.5	11
α -Zearalenol (α -ZEL)	neg	319.1	-80	160 174	-44 -37	-13 -9	9.2	15
β -Zearalenol (β -ZEL)	neg	319.1	-115	275.2 160.0	-30 -44	-15 -13	7.7	12
α -Zearalenol-14-glucuronide (α -ZEL-14-GlcA)	neg	495.0	-20	319.2 113.0	-38 -26	-23 -13	4.1	-1
β -Zearalenol-14-glucuronide (β -ZEL-14-GlcA)	neg	495.1	-25	319.2 112.9	-38 -28	-23 -55	3.7	-2
Zearalanone (ZAN)	neg	319.2	-75	275.1 161.0	-35 -38	-20 -15	11.5	21

Compound	Polarity	Q1 mass [Da]	DP [V]	Q3 mass [Da]	CE [V]	CXP [V]	rt [min]	dev [s]
Zearalenone (ZEN)	neg	317.1	-75	175.0 131.0	-34 -40	-9 -9	11.7	21
Zearalenone-14-glucuronide (ZEN-14-GlcA)	neg	493.0	-35	317.0 112.9	-36 -26	-25 -13	4.4	-2
Zearalenone-14-sulfate (ZEN-14-sulfate)	neg	397.1	-80	316.9 175.0	-28 -46	-23 -15	5.3	-4
Personal care product ingredients, pharmaceuticals and metabolites								
Benzophenone 1	neg	213.0	-60	91 134.9	-34 -28	-11 -17	9.0	18
Benzophenone 2	neg	245.1	-40	135 109	-22 -30	-23 -15	5.5	9
Benzylparaben	neg	227.0	-20	92.1 136	-30 -20	-13 -13	10.5	17
Butylparaben	neg	193.1	-25	92 137	-32 -22	-7 -21	9.9	9
Ethylparaben	neg	164.9	-30	92.1 136.9	-30 -20	-9 -15	6.1	10
Isobutylparaben	neg	193.0	-55	92 135.9	-32 -24	-7 -11	10.2	30
Methylparaben	neg	151.0	-35	92.0 135.9	-26 -20	-13 -15	4.9	8
Propylparaben	neg	179.0	-55	92.0 93.0	-30 -26	-9 -11	7.8	18
Ethinylestradiol	neg	295.1	-155	145 159	-48 -48	-13 -17	10.2	19
3-Benzylidencamphor (3-BC)	pos	241.1	76	91.0 165.1	51 51	10 14	15.2	4
4-methylbenzylidencamphor (4-MBC)	pos	255.1	81	104.8 141.2	37 59	12 12	15.5	-6
Octyl methoxycinnamate (OMC)	pos	291.1	156	179.0 161.1	13 25	10 18	16.1	7
p-Hydroxybenzoic acid (pOHBA)	neg	136.9	-5	92.9 65.0	-18 -36	-17 -9	0.7-2.4	-6
Triclosan	neg	286.8	-5	35.0	-38	-15	14.9	2
Phytotoxins								
Anisodamine	pos	306.1	106	140.1 122.1 296	33 35 15	10 10 8	3.3-3.6	13
Aristolactam I	pos	293.9	191	279 250.9	37 47	18 22	10.5	18
Jacobine	pos	352.0	136	155 119.9	37 39	18 14	3.6	14
Jacobine-N-oxide	pos	368.0	116	296.0 120.1	33 43	18 8	3.1	6
Riddelliin	pos	350.0	86	120.0 138.0	37 39	14 16	3.2	12
Riddelliin-N-oxide	pos	366.0	126	120.0 118.0	41 39	14 12	3.1	5
Scopolamine	pos	304.0	41	156.2 138.1	23 25	10 16	3.5	15
Disinfection by-products								
Bromoacetic acid	neg	136.9	-10	78.9 81.0	-13 -13	-26 -26	0.8	3
Dibromoacetic acid	neg	216.8	-5	172.8 80.9	-14 -32	-27 -9	0.9	-1
Dichloroacetic acid	neg	126.9	-10	83.0 35.0	-32 -12	-5 -15	0.8	0
Food processing by-products								
Acrylamide	pos	72.0	26	44.0 55.0 45.0	49 41 13	14 10 12	0.9	11

Compound	Polarity	Q1 mass [Da]	DP [V]	Q3 mass [Da]	CE [V]	CXP [V]	rt [min]	dev [s]
5-Hydroxymethylfurfural (HMF)	pos	126.9	21	71.0	11	10	2.4	1
				109	15	14		
				81.0	23	10		
PhIP	pos	225.1	51	210.1	41	10	5.3	9
				140.1	69	14		
Air pollutants								
Cotinine	pos	176.9	86	80.0	31	10	3.1	4
				98.0	27	18		
Trans-3-hydroxy cotinine	pos	193.0	86	80.1	33	10	2.7	9
				134	27	14		
1-Hydroxypyrene	neg	217.0	-115	189.0	-46	-13	14.2	19
				188.0	-48	-25		
3-Hydroxyphenanthrene	neg	193.0	-135	165.0	-40	-13	11.4	22
				164.2	-46	-13		
Mycotoxins								
Aflatoxin B1	pos	313	106	241.0	49	14	6.3	10
				213.0	61	16		
Aflatoxin B2	pos	315	125	203.0	53	16	5.8	9
				243.0	49	12		
Aflatoxin G1	pos	329	86	243.0	59	14	5.8	13
				200.0	59	12		
Aflatoxin G2	pos	331	111	313.0	35	18	5.4	7
				245.2	43	14		
Aflatoxin M1	pos	329.1	91	273.2	35	16	5	5
				229.1	59	12		
Aflatoxin M2	pos	331.0	96	259.0	33	16	4.7	5
				241	57	14		
Aflatoxicol	pos	297.0	71	269.1	29	12	6.7	11
				115.0	83	14		
Sterigmatocystein	pos	325.1	96	281.1	51	16	12.6	22
				310.2	35	18		
Citrinin	pos	251.0	36	233.1	23	14	4.3	14
				205.0	37	18		
Deoxynivalenol	pos	296.9	21	249.3	15	16	3	4
				203.0	21	12		
Nivalenol	neg	311.1	20	281.1	20	19	2.6	4
				203	30	13		
Toxin T2	pos	467.3	56	215.2	29	18	10.3	14
				185.0	31	11		
Ochratoxin A	pos	404.0	91	239.0	37	16	6.3	9
				102.0	105	14		
Ochratoxin B	pos	370.1	86	205.0	33	12	5.3	3
				103.1	77	16		
Ochratoxin Alpha	neg	254.9	90	166.9	36	11	3.8	-1
				123.0	40	17		

Table S5 Calibration parameters in solvent and urine of the quantification by high resolution LC-HRMS. Signal suppression or enhancement (SSE) was assessed too.

Calibration parameters										
	Slope	Intercept	R ²	Concentration range [ng/mL]	Slope	Intercept	R ²	Concentration range [ng/mL]	SSE	
	Solvent				Urine					
Plasticizer/Plastic Components										
Bisphenol A (BPA)	2.9E+05	-1.3E+05	1.00	1-30	3.9E+05	-7.6E+04	0.98	1-30	135	
Bisphenol AF (BPAF)	1.1E+06	-1.2E+05	0.98	0.5-15	8.5E+05	5.3E+04	0.90	0.5-15	79	
Bisphenol B (BPB)	2.2E+05	-1.3E+05	1.00	1-3	3.1E+05	-1.7E+05	0.97	1-3	145	
Bisphenol C (BPC)	1.6E+05	-2.3E+05	1.00	2-60	2.2E+05	-1.1E+05	0.95	0.6-60	131	
Bisphenol F (BPF)	2.9E+05	-3.4E+04	0.96	0.5-15	5.2E+05	-4.5E+04	0.99	0.15-15	177	
Bisphenol S (BPS)	6.6E+06	-5.9E+03	0.99	0.02-0.6	7.9E+06	5.7E+05	0.97	0.06-0.6	120	
Mono-n-butyl phthalate (MBP)	3.3E+05	2.6E+05	1.00	0.15-150	4.9E+05	1.2E+06	0.95	1.5-150	149	
N-butylbenzenesulfonamide	9.6E+04	-3.2E+04	1.00	3-300	1.4E+05	1.0E+05	0.96	1-300	146	
Benzyl butyl phthalate	2.0E+05	5.9E+03	0.96	0.075-75	7.2E+04	-6.3E+04	0.91	7.5-75	35	
Dibutyl phthalate	6.8E+04	4.0E+06	0.94	15-1500	2.4E+04	7.6E+06	0.85	50-1500	36	
Tetrabromobisphenol A	2.9E+03*	-2.9E-13*	1.00*	30-30*	1.1E+03*	-1.1E-13*	0.99*	30-30*	38*	
Perfluorinated Alkylated Substances										
Perfluorooctanoic acid (PFOA)	6.7E+05	-1.8E+05	0.99	0.45-4.5	7.2E+05	-2.4E+04	0.93	0.45-4.5	108	
Perfluorooctanesulfonic acid (PFOS)	1.1E+06	-1.3E+06	1.00	1.5-4.5	9.2E+04	6.0E+04	0.96	0.45-4.5	8	
Industrial Side Products and Pesticides										
2-Naphthol	2.8E+05	-8.7E+04	1.00	0.9-9	2.7E+05	1.6E+06	0.92	0.9-9	94	
Methiocarb	1.2E+05	-2.6E+04	1.00	0.5-1.5	3.0E+04	-1.5E-13	1.00	1.5-1.5	24	
Prochloraz	3.6E+06	-9.4E+04	1.00	0.05-0.15	1.9E+06	-2.2E+04	0.87	0.05-0.15	51	
2-tert-Butylphenol (2-tert-BP)	1.3E+05	-1.4E+06	0.99	15-15000	2.4E+05	-1.5E+06	0.96	15-15000	190	
4-Octylphenol (4-OP)	2.0E+04	-2.4E+06	1.00	300-3000	4.4E+03	-1.6E+06	0.99	1000-3000	22	
4-tert-Octylphenol (4-tert-OP)	1.1E+05	-1.3E+05	0.98	3-300	8.5E+04	-1.4E+06	0.96	30-300	74	
Fenarimol	2.5E+06	-9.6E+04	1.00	0.09-0.9	1.5E+06	-1.1E+05	0.97	0.09-0.9	60	
Nonylphenol	3.0E+04	-1.8E+05	0.98	7.5-250	4.4E+03	6.6E+05	0.80	25-250	20	
Endogenous Estrogens										
Estrone (E1)	1.4E+05	-4.1E-13	1.00	0.9-0.9	3.3E+05	-7.0E+04	1.00	0.3-0.9	244	
Estradiol (E2)	8.8E+04	-2.4E+05	1.00	3-9	1.2E+05	-1.8E+05	0.94	3-9	136	

Calibration parameters									
	Slope	Intercept	R ²	Concentration range [ng/mL]	Slope	Intercept	R ²	Concentration range [ng/mL]	SSE
	Solvent				Urine				
Estradiol-17-glucuronide (E2-17-GlcA)	4.5E+04	-5.0E+04	1.00	1.5-15	3.7E+04	-1.9E+03	0.91	0.5-15	82
Estradiol-3-sulfate (E2-3-sulfate)	1.1E+05	-1.1E+05	1.00	1.5-4.5	1.4E+05	-1.0E+05	0.99	1.5-4.5	131
Estrinol (E3)	1.4E+05	-1.0E+05	1.00	0.9-9	1.5E+05	-5.4E+04	0.99	0.9-9	107
16-Epiestriol (16EpiE3)	1.2E+05	-6.2E+04	1.00	3-30	1.4E+05	-2.9E+04	0.99	0.3-30	112
16- α -Hydroxyestrone (16OHE1)	1.4E+05	-1.1E+05	1.00	1.5-4.5	1.9E+05	-5.2E+04	0.96	0.45-4.5	137
17-Epiestriol (17EpiE3)	1.3E+05	-2.8E+05	1.00	10-30	1.7E+05	-1.4E+05	0.99	1-30	131
2-Methoxy estrone (2MeOE1)	6.5E+03*	-1.6E-13*	1.00*	7.5-7.5*	1.1E+04*	-2.8E-13*	0.96*	7.5-7.5*	171*
2-Methoxy estradiol(2MeOE2)	2.5E+02*	-5.0E-14*	1.00*	60-60*	4.4E+02*	-8.9E-14*	0.63*	60-60*	176*
4-Methoxy estrone (4MeOE1)	1.1E+05	-5.6E-13	1.00	1.5-1.5	1.5E+05	-6.2E+04	0.98	0.5-1.5	136
4-Methoxy estradiol (4MeOE2)	6.8E+03*	-6.8E-14*	1.00*	3-3*	1.5E+04*	-1.5E-13*	1.00*	3-3*	223*
4-Hydroxy estrone (4OHE1)	1.8E+06	-2.0E+05	0.94	0.15-1.5	1.4E+06	-4.7E+03	0.97	0.05-1.5	73
Phytoestrogens and metabolites									
8-Prenylnaringenin	1.5E+06	-1.2E+05	0.97	0.09-9	1.2E+06	8.1E+04	0.97	0.3-9	79
Coumestrol	2.1E+06	-5.0E+04	1.00	0.05-1.5	2.2E+06	-5.3E+04	0.98	0.05-1.5	101
Daidzein	3.4E+06	-2.6E+04	0.97	0.02-1.5	4.2E+06	-2.9E+04	0.95	0.02-1.5	124
Enterodiol	3.8E+05	-2.0E+04	0.96	0.15-1.5	3.7E+05	-5.0E+03	0.95	0.15-1.5	95
Enterolactone	1.3E+06	-6.5E+04	0.99	0.06-60	1.6E+06	9.9E+05	0.98	0.06-60	121
Equol	1.0E+06	-1.5E+05	1.00	0.2-6	1.1E+06	-6.2E+04	0.95	0.2-6	108
Formononetin	2.0E+07	-5.8E+04	1.00	0.01-0.75	1.5E+07	-7.8E+04	0.98	0.025-0.75	75
Genistein (GEN)	3.1E+06	-1.3E+05	0.99	0.05-1.5	3.6E+06	-3.0E+04	0.98	0.02-1.5	116
Glycitein	1.3E+06	-4.8E+04	0.97	0.05-1.5	1.4E+06	-1.2E+05	0.93	0.15-1.5	111
Isoxanthohumol	1.8E+06	-3.6E+04	0.99	0.03-0.3	2.8E+06	-1.2E+05	0.82	0.1-0.3	152
Matairesinol	1.3E+05	-8.2E+04	0.96	1.5-15	1.4E+05	-6.1E+04	0.96	4.5-15	107
Resveratrol	8.0E+05	-2.3E+05	0.99	0.45-450	7.2E+05	-1.4E+05	0.96	0.45-450	90
Xanthohumol	1.8E+06	-4.1E+05	0.92	3-30	5.9E+05	-3.9E+06	0.99	10-30	32
Mycoestrogens and Metabolites									
Alternariol	2.8E+06	-1.4E+05	1.00	0.1-30	3.0E+06	-3.0E+05	0.99	0.3-30	109
Alternariol monomethyl ether	2.2E+06	-2.2E+05	0.98	0.15-1.5	1.4E+06	-3.3E+04	0.93	0.15-1.5	64
α -zearalanol (α -ZAL)	9.1E+05	-6.6E+04	0.99	0.5-15	1.0E+06	-1.2E+05	0.97	0.5-15	112
β -zearalanol (β -ZAL)	8.7E+05	-6.7E+04	1.00	0.15-15	9.9E+05	-1.0E+05	0.98	0.15-15	114
α -zearalenol (α -ZEL)	1.3E+06	-1.1E+05	1.00	0.2-0.6	1.2E+06	-4.4E+04	0.98	0.2-0.6	92
β -zearalenol (β -ZEL)	8.5E+05	-1.6E+05	1.00	0.3-30	8.6E+05	-4.7E+04	0.99	0.3-30	101
α -zearalenol-14-glucuronide (α -ZEL-14-GlcA)	1.9E+04	-2.9E-13	1.00	1.5-4.5	3.1E+04	-1.4E+04	0.99	1.5-4.5	163

Calibration parameters										
	Slope	Intercept	R ²	Concentration range [ng/mL]	Slope	Intercept	R ²	Concentration range [ng/mL]	SSE	
	Solvent				Urine					
β-zearalenol-14-glucuronide (β-ZEL-14-GlcA)	4.6E+04	-5.4E+04	1.00	1.5-4.5	4.4E+04	-4.0E+04	0.89	1.5-4.5	95	
Zearalanone (ZAN)	1.2E+06	-6.3E+04	0.99	0.09-9	1.4E+06	-1.0E+05	1.00	0.09-9	116	
Zearalenone (ZEN)	9.5E+05	-2.4E+05	1.00	0.9-9	9.2E+05	-4.8E+04	0.99	0.9-9	97	
Zearalenone-14-glucuronide (ZEN-14-GlcA)	5.5E+03	2.4E+03	1.00	5-15	1.3E+04	-2.7E+04	1.00	5-15	231	
Zearalenone-14-sulfate (ZEN-14-sulfate)	1.7E+05	-3.6E+04	0.96	0.45-4.5	4.5E+05	-1.2E+05	1.00	0.45-4.5	264	
Personal Care Product Ingredients, Pharmaceuticals and Metabolites										
Benzophenone 1	9.3E+06	-1.2E+05	1.00	0.02-6	9.3E+06	-8.8E+04	0.95	0.06-6	100	
Benzophenone 2	2.1E+06	-5.3E+04	0.99	0.05-4.5	2.2E+06	-6.8E+04	0.98	0.05-4.5	106	
Benzylparaben	1.9E+07	-1.3E+05	0.99	0.015-0.45	2.1E+07	-7.8E+04	0.97	0.005-0.45	111	
Butylparaben	4.0E+06	-5.7E+04	1.00	0.03-3	3.4E+06	-1.6E+04	0.99	0.03-3	84	
Ethylparaben	4.5E+06	-2.9E+04	1.00	0.03-3	6.1E+06	5.1E+04	0.98	0.03-3	138	
Isobutylparaben	3.7E+06	-1.8E+05	0.99	0.1-3	2.6E+06	-1.1E+02	0.98	0.1-3	70	
Methylparaben	6.2E+06	7.3E+04	1.00	0.25-7.5	8.4E+06	8.3E+05	0.99	0.25-7.5	135	
Propylparaben	5.3E+06	-4.0E+04	1.00	0.06-6	6.8E+06	7.3E+04	0.99	0.06-6	128	
Ethinylestradiol	6.8E+04	-2.5E+05	1.00	10-30	9.0E+04	-1.9E+05	0.98	3-30	131	
3-Benzylidencamphor (3-BC)	5.8E+04	-5.7E+04	0.94	4.5-4500	3.2E+04	5.3E+04	0.89	15-4500	56	
4-methylbenzyliden camphor (4-MBC)	1.9E+05	-7.8E+04	0.99	1.5-450	7.7E+04	1.2E+06	0.93	15-450	40	
Octyl methoxycinnamate (OMC)	3.5E+03	-1.4E+06	0.99	600-6000	1.0E+02*	-6.1E+02*	0.82*	6000-6000*	3*	
p-Hydroxybenzoic acid (pOHBA)	1.6E+06	1.5E+06	0.92	1.5-1500	5.1E+05	1.3E+06	0.92	150-1500	32	
Triclosan	4.2E+05	-5.4E+04	0.97	0.3-30	3.2E+05	2.8E+05	0.92	1-30	77	
Phytotoxins										
Anisodamine	6.2E+06	-1.4E+04	0.95	0.005-1.5	7.9E+06	-9.4E+05	0.93	0.15-1.5	129	
Aristolactam I	3.4E+05	-1.2E+05	1.00	0.5-15	1.7E+05	-1.2E+04	0.92	0.5-15	50	
Jacobine	3.2E+06	-4.7E+03	0.99	0.0075-7.5	1.7E+06	1.2E+05	0.94	0.075-7.5	51	
Jacobine-N-oxide	3.3E+06	-3.6E+03	1.00	0.015-1.5	3.2E+06	6.4E+05	0.95	0.015-1.5	96	
Riddelliin	3.2E+06	-2.7E+04	0.96	0.03-9	2.9E+06	-7.5E+05	0.94	0.3-9	92	
Riddelliin-N-oxide	3.0E+06	-8.5E+03	0.97	0.02-6	2.9E+06	-1.3E+06	0.89	0.6-6	98	
Scopolamine	3.9E+08	-7.2E+04	0.99	0.0005-0.45	1.7E+08	-1.6E+05	0.95	0.015-0.45	43	
Disinfection By-Products										
Bromoacetic acid	2.5E+04	-3.6E+04	0.96	2-600	1.8E+04	-3.3E+06	1.00	200-600	71	
Dibromoacetic acid	1.1E+05	-1.3E+05	1.00	0.45-450	1.3E+05	-5.5E+05	0.99	45-450	120	
Dichloroacetic acid	1.9E+05	1.6E+05	0.99	22.5-2250	1.3E+05	-9.4E+04	0.97	22.5-2250	70	
Food Processing By-Products										
Acrylamide	2.3E+04	1.5E+05	0.98	30-3000	1.3E+04	-1.2E+07	0.99	1000-3000	58	

Calibration parameters										
	Slope	Intercept	R ²	Concentration range [ng/mL]	Slope	Intercept	R ²	Concentration range [ng/mL]	SSE	
	Solvent				Urine					
5-Hydroxymethylfurfural (HMF)	5.0E+04	4.6E+04	1.00	3.5-1050	2.2E+04	-7.4E+05	0.96	105-1050	44	
PhIP	9.9E+06	-9.8E+04	0.97	0.03-3	1.1E+07	-2.5E+05	0.95	0.03-3	109	
Air Pollutants										
Cotinine	6.6E+06	5.3E+05	0.99	0.045-45	5.7E+06	-5.1E+06	0.94	1.5-45	87	
Trans-3-hydroxy cotinine	3.6E+06	-4.6E+04	1.00	0.03-9	3.3E+06	1.3E+06	0.95	3-9	91	
1-Hydroxy pyrene	8.6E+05	-3.9E+05	1.00	0.6-60	4.4E+05	-2.2E+05	0.99	0.6-60	51	
3-Hydroxy phenantrene	1.3E+06	-2.7E+05	1.00	0.45-4.5	1.2E+06	-8.3E+04	0.98	0.45-4.5	95	
Mycotoxins										
Aflatoxin B1	2.7E+05	-7.2E+04	1.00	0.3-30	2.5E+05	-1.8E+05	0.99	1-30	92	
Aflatoxin B2	8.1E+03	-4.2E+04	0.99	9-900	7.6E+03	-1.9E+05	0.99	30-900	93	
Aflatoxin G1	1.9E+05	-5.4E+04	0.99	1-30	1.9E+05	-3.2E+05	0.96	3-30	100	
Aflatoxin G2	6.3E+04	-2.1E+04	0.99	0.9-90	6.4E+04	-1.0E+05	0.96	3-90	101	
Aflatoxin M1	2.5E+05	-6.1E+04	0.96	0.3-30	2.2E+05	-1.7E+05	0.95	1-30	89	
Aflatoxin M2	2.9E+03	-9.1E+04	1.00	60-600	2.2E+03	1.7E+04	0.90	200-600	75	
Aflatoxicol	1.7E+04	-8.2E+03	0.99	0.9-90	7.0E+03	-3.9E+04	0.96	9-90	42	
Sterigmatocystein	3.3E+05	-5.1E+04	0.97	0.3-3	1.1E+05	-7.0E+04	1.00	0.3-3	35	
Citrinin	1.0E+04	-6.6E+04	0.98	9-900	1.5E+04	-3.5E+06	0.99	90-900	144	
Deoxynivalenol	1.8E+02*	-1.8E-13*	1.00*	300-300*	1.4E+02*	-1.4E-13*	1.00*	300-300*	80*	
Nivalenol		n.d.				n.d.				
Toxin T2	5.4E+02	-4.2E+04	0.99	90-900	3.7E+02	-8.4E+04	0.92	300-900	68	
Ochratoxin A	1.5E+03*	-4.6E-14*	1.00*	9-9*	1.4E+03*	-4.3E-14*	0.97*	9-9*	93*	
Ochratoxin B	1.5E+04*	-4.5E-13*	1.00*	9-9*	3.6E+04*	-7.7E+04*	1.00*	9-9*	239*	
Ochratoxin Alpha	7.7E+03	-1.5E+04	0.98	9-90	8.8E+03	-1.6E+05	0.98	9-90	115	

*One-point calibration as analyte was only detected at on concentration level

Table S6 Calibration parameters in solvent and urine of the quantification by low resolution LC-MS/MS

	Calibration parameters									
	Slope	Intercept	R ²	Concentration range [ng/mL]	Slope	Intercept	R ²	Concentration range [ng/mL]	SSE	
	Solvent					Urine				
Plasticizer/Plastic Components										
Bisphenol A (BPA)	1.2E+04	3.6E+03	0.99	0.1 -30	8.9E+03	5.6E+03	0.99	0.3 -30	76	
Bisphenol AF (BPAF)	5.2E+05	-1.0E+04	0.99	0.05 -15	3.4E+05	-1.6E+04	0.99	0.15 -15	64	
Bisphenol B (BPB)	8.6E+04	2.1E+03	0.99	0.01 -3	7.5E+04	-2.7E+02	0.99	0.1 -3	88	
Bisphenol C (BPC)	2.3E+04	1.8E+03	0.99	0.2 -60	2.0E+04	-1.6E+03	0.99	0.2 -60	88	
Bisphenol F (BPF)	8.5E+03	6.4E+02	0.99	0.015 -15	9.9E+03	1.6E+03	0.99	0.15 -15	116	
Bisphenol S (BPS)	5.9E+05	4.1E+04	0.99	0.02 -0.6	5.7E+05	2.3E+04	0.99	0.06 -0.6	97	
Mono-n-butyl phthalate (MBP)	9.0E+04	3.3E+04	1.00	0.15 -150	1.1E+05	7.7E+04	1.00	0.15 -150	120	
N-butylbenzene sulfonamide	3.2E+04	2.3E+04	0.99	0.3 -300	3.3E+04	1.8E+04	0.99	1 -300	103	
Benzyl butyl phthalate	9.8E+05	1.9E+05	0.99	0.25 -75	9.6E+05	2.7E+05	0.98	0.25 -75	98	
Dibutyl phthalate	1.2E+06	2.6E+07	0.99	15 -1500	8.2E+05	1.4E+08	0.97	50 -1500	67	
Tetrabromobisphenol A	3.5E+03	-1.8E+02	0.99	0.1 -30	3.7E+03	-1.9E+03	0.96	1 -30	107	
Perfluorinated Alkylated Substances										
Perfluorooctanoic acid (PFOA)	2.3E+05	1.4E+03	0.99	0.015 -4.5	3.1E+05	1.4E+04	0.99	0.15 -4.5	137	
Perfluorooctanesulfonic acid (PFOS)	7.1E+04	4.6E+02	1.00	0.015 -4.5	1.9E+04	5.2E+03	0.97	0.15 -4.5	27	
Industrial Side Products and Pesticides										
2-Naphthol	1.2E+05	9.8E+02	1.00	0.03 -9	8.4E+04	3.0E+05	0.98	0.9 -9	70	
Methiocarb	7.2E+05	-2.5E+03	0.99	0.02 -1.5	5.6E+05	-5.1E+03	0.99	0.02 -1.5	79	
Prochloraz	3.3E+06	-4.7E+01	1.00	0.0005 -0.15	4.2E+06	-2.5E+02	0.99	0.0005 -0.15	130	
2-tert-Butylphenol (2-tert-BP)	1.0E+03	-5.8E+03	0.99	15 -15000	2.1E+03	3.3E+03	1.00	15 -15000	204	
4-Octylphenol (4-OP)	1.2E+04	-9.8E+02	0.98	10 -3000	9.6E+03	-2.3E+06	0.98	300 -3000	80	
4-tert-Octylphenol (4-tert-OP)	5.1E+04	-7.9E+03	0.98	0.3 -300	7.6E+04	-4.9E+04	0.99	1 -300	148	
Fenarimol	9.8E+05	-8.4E+02	0.99	0.003 -0.9	1.1E+06	-1.7E+03	0.99	0.003 -0.9	109	
Nonylphenol	2.2E+04	-7.5E+01	0.98	2.5 -750	1.7E+04	-5.7E+04	0.98	7.5 -750	76	
Endogenous Estrogens										
Estrone (E1)	6.5E+04	-1.2E+02	0.99	0.03 -0.9	7.3E+04	4.4E+02	0.98	0.01 -0.9	113	
Estradiol (E2)	1.5E+04	-8.8E+02	0.99	0.3 -9	1.5E+04	-4.3E+02	0.99	0.3 -9	99	
Estradiol-17-glucuronide (E2-17-GlcA)	6.1E+03	-7.5E+02	0.99	0.5 -15	3.8E+03	1.1E+05	0.98	15 -15	63	
Estradiol-3-sulfate (E2-3-sulfate)	7.6E+04	1.7E+02	0.99	0.05 -4.5	8.8E+04	3.3E+03	1.00	0.15 -4.5	116	
Estriol (E3)	1.8E+04	1.6E+02	0.98	0.009 -9	2.3E+04	6.0E+02	1.00	0.09 -9	127	
16-Epiestriol (16EpiE3)	1.4E+04	-2.7E+02	0.99	0.1 -30	1.5E+04	-6.8E+01	1.00	0.3 -30	108	
16- α -Hydroxyestrone (16OHE1)	2.8E+04	2.8E+02	0.99	0.015 -4.5	3.5E+04	-2.3E+02	0.99	0.05 -4.5	124	

Calibration parameters									
	Slope	Intercept	R ²	Concentration range [ng/mL]	Slope	Intercept	R ²	Concentration range [ng/mL]	SSE
	Solvent				Urine				
17-Epiestriol (17EpiE3)	1.8E+04	-6.6E+02	0.99	0.1 -30	2.4E+04	1.1E+02	0.99	0.3 -30	131
2-Methoxy estrone (2MeOE1)	5.3E+04	-1.4E+03	0.99	0.08 -7.5	3.8E+04	-1.8E+03	0.99	0.25 -7.5	72
2-Methoxy estradiol(2MeOE2)	7.8E+03	1.9E+02	0.99	0.2 -60	6.4E+03	5.9E+02	1.00	0.2 -60	83
4-Methoxy estrone (4MeOE1)	3.3E+05	-4.8E+02	0.99	0.005 -1.5	3.4E+05	8.1E+02	0.99	0.005 -1.5	102
4-Methoxy estradiol (4MeOE2)	1.5E+05	1.4E+02	0.99	0.01 -3	1.5E+05	-6.6E+02	1.00	0.03 -3	101
4-Hydroxy estrone (4OHE1)	6.6E+04	-6.4E+03	1.00	0.15 -1.5	1.5E+05	7.0E+03	1.00	0.15-1.5	155
Phytoestrogens and Metabolites									
8-Prenylnaringenin	4.3E+05	-3.8E+03	0.99	0.009 -9	3.3E+05	-2.1E+03	0.99	0.03 -9	77
Coumestrol	2.2E+05	1.9E+02	0.99	0.005 -1.5	1.5E+05	6.7E+02	0.99	0.02 -1.5	69
Daidzein	1.2E+05	2.1E+02	1.00	0.005 -1.5	1.1E+05	2.7E+03	1.00	0.02 -1.5	90
Enterodiol	1.7E+05	3.6E+02	0.99	0.005 -1.5	2.0E+05	1.0E+04	1.00	0.02 -1.5	117
Enterolactone	1.3E+05	2.6E+03	0.99	0.06 -60	1.0E+05	6.2E+04	0.99	0.2 -60	79
Equol	2.9E+05	-6.1E+02	0.99	0.02 -6	2.1E+05	2.5E+02	0.99	0.02 -6	71
Formononetin	2.7E+06	1.4E+03	0.99	0.0008 -0.75	2.1E+06	1.5E+03	0.99	0.0025 -0.75	78
Genistein (GEN)	1.2E+05	6.1E+02	1.00	0.005 -1.5	7.9E+04	1.5E+03	1.00	0.02 -1.5	66
Glycitein	1.1E+06	5.1E+03	1.00	0.005 -1.5	6.2E+05	-1.8E+04	0.98	0.05 -1.5	55
Isoxanthohumol	1.0E+07	-3.3E+03	1.00	0.01 -0.3	6.0E+06	-1.7E+04	0.99	0.01 -0.3	58
Matairesinol	3.2E+04	-1.6E+02	0.99	0.05 -15	2.3E+04	1.9E+03	0.99	0.05 -15	73
Resveratrol	8.2E+04	-3.0E+04	1.00	0.45 -450	5.3E+04	1.8E+04	1.00	1.5 -450	64
Xanthohumol	3.4E+06	-8.9E+06	0.99	0.1 -30	5.4E+06	-1.7E+07	0.97	3 -30	158
Mycoestrogens and Metabolites									
Alternariol	1.7E+05	6.8E+02	1.00	0.03 -30	1.2E+05	-2.2E+03	1.00	0.1 -30	70
Alternariol monomethyl ether	7.9E+05	-1.2E+03	1.00	0.005 -1.5	7.2E+05	-8.5E+02	0.99	0.005 -1.5	91
α-zearalanol (α-ZAL)	1.5E+05	-1.0E+03	0.99	0.015 -15	1.2E+05	-3.5E+03	0.99	0.15 -15	79
β-zearalanol (β-ZAL)	1.9E+05	2.8E+03	1.00	0.015 -15	1.4E+05	-2.4E+03	0.99	0.15 -15	75
α-zearalenol (α-ZEL)	5.9E+04	1.5E+02	0.99	0.02 -0.6	4.5E+04	5.8E+02	0.99	0.02 -0.6	77
β-zearalenol (β-ZEL)	7.7E+04	7.5E+02	1.00	0.03 -30	6.4E+04	-2.6E+02	0.99	0.1 -30	83
α-zearalenol-14-glucuronide (α-ZEL-14-GlcA)	3.5E+04	-3.3E+02	0.99	0.05 -4.5	3.7E+04	2.8E+02	0.99	4.5 -4.5	106
β-zearalenol-14-glucuronide (β-ZEL-14-GlcA)	3.8E+04	-1.6E+02	0.99	0.015 -4.5	4.0E+04*	5.9E+03*	1.00*	4.5 -4.5*	106*
Zearalanone (ZAN)	9.0E+04	7.1E+02	0.99	0.03 -9	9.5E+04	-6.7E+03	1.00	0.3 -9	106
Zearalenone (ZEN)	1.2E+05	3.1E+02	0.99	0.009 -9	1.4E+05	-1.6E+03	0.99	0.03 -9	112
Zearalenone-14-glucuronide (ZEN-14-GlcA)	1.7E+04	2.9E+02	0.99	0.05 -15	1.6E+04	1.0E+04	1.00	15 -15	92

Calibration parameters									
	Slope	Intercept	R ²	Concentration range [ng/mL]	Slope	Intercept	R ²	Concentration range [ng/mL]	SSE
Solvent					Urine				
Zearalenone-14-sulfate (ZEN-14-sulfate)	3.2E+05	-5.6E+02	0.99	0.0045 -4.5	5.1E+05	9.6E+01	1.00	0.015 -4.5	160
Personal Care Product Ingredients, Pharmaceuticals and Metabolites									
Benzophenone 1	1.2E+06	-2.6E+03	1.00	0.006 -6	1.4E+06	-4.7E+03	1.00	0.02 -6	120
Benzophenone 2	5.5E+05	-5.1E+01	0.99	0.0045 -4.5	5.8E+05	-1.2E+03	1.00	0.015 -4.5	106
Benzylparaben	7.0E+06	-1.7E+03	1.00	0.0005 -0.45	5.6E+06	3.5E+03	1.00	0.0015 -0.45	79
Butylparaben	5.1E+05	2.5E+02	0.99	0.01 -3	5.1E+05	-2.9E+03	0.99	0.01 -3	99
Ethylparaben	6.8E+05	2.1E+03	1.00	0.01 -3	8.6E+05	6.4E+03	1.00	0.01 -3	127
Isobutylparaben	6.8E+05	1.5E+03	1.00	0.003 -3	7.9E+05	8.5E+02	0.99	0.01 -3	117
Methylparaben	1.2E+06	2.5E+04	1.00	0.0075 -7.5	1.8E+06	1.9E+05	0.99	0.025 -7.5	145
Propylparaben	9.4E+05	4.2E+03	1.00	0.006 -6	1.3E+06	2.6E+04	1.00	0.02 -6	133
Ethinylestradiol	1.0E+04	2.4E+02	0.99	0.1 -30	1.5E+04	-8.0E+02	1.00	0.1 -30	140
3-Benzylidencamphor (3-BC)	2.7E+05	-5.8E+05	0.99	4.5 -4500	1.5E+05	3.4E+06	0.97	15 -4500	56
4-methylbenzyliden camphor (4-MBC)	1.5E+05	-3.1E+04	0.98	0.45 -450	7.9E+04	-1.7E+04	0.99	1.5 -450	54
Octyl methoxycinnamate (OMC)	2.8E+02	-9.4E+02	0.96	200 -6000	9.3E+01	-3.7E+04	0.98	2000 -6000	33
p-Hydroxybenzoic acid (pOHBA)	1.7E+05	8.7E+05	0.99	1.5 -1500	1.1E+05	6.4E+06	0.98	150 -1500	64
Triclosan	1.5E+05	-2.2E+03	0.99	0.03 -30	1.4E+05	-3.1E+03	0.99	0.1 -30	91
Phytotoxins									
Anisodamine	2.8E+06	1.4E+03	1.00	0.0015 -1.5	2.4E+06	-5.5E+04	0.98	0.05 -1.5	84
Aristolactam I	3.5E+05	-3.1E+03	0.99	0.015 -15	1.9E+05	-3.3E+03	0.99	0.05 -15	54
Jacobine	2.0E+05	1.1E+03	1.00	0.025 -7.5	2.4E+05	-3.3E+04	0.99	0.25 -7.5	118
Jacobine-N-oxide	7.9E+05	-2.7E+02	1.00	0.0015 -1.5	5.2E+05	-1.8E+04	0.98	0.05 -1.5	65
Riddelliin	1.8E+05	1.1E+03	0.99	0.03 -9	2.2E+05	-3.2E+04	0.99	0.3 -9	126
Riddelliin-N-oxide	1.7E+05	4.5E+02	1.00	0.02 -6	1.4E+05	1.2E+04	0.99	0.6 -6	83
Scopolamine	8.6E+07	-7.0E+03	1.00	0.0005 -0.45	6.9E+07	-8.4E+04	0.98	0.0015 -0.45	80
Disinfection By-Products									
Bromoacetic acid	4.5E+03	5.4E+01	0.99	0.6 -600	4.0E+03	-1.9E+05	0.99	200 -600	90
Dibromoacetic acid	1.4E+04	5.9E+03	0.99	1.5 -450	1.8E+04	9.6E+04	0.98	15 -450	132
Dichloroacetic acid	9.2E+02	8.8E+03	0.99	2.25 -2250	9.0E+02	-2.0E+04	0.98	75 -2250	98
Food Processing By-Products									
Acrylamide	3.7E+02	7.4E+02	1.00	3 -3000	1.7E+02	-6.2E+03	0.97	100 -3000	46
5-Hydroxymethylfurfural (HMF)	7.0E+04	7.2E+04	0.99	1 -1050	2.6E+04	-2.3E+06	0.98	105 -1050	38
PhIP	2.7E+06	1.3E+03	1.00	0.003 -3	1.6E+06	-3.2E+03	0.99	0.01 -3	58

Calibration parameters									
	Slope	Intercept	R ²	Concentration range [ng/mL]	Slope	Intercept	R ²	Concentration range [ng/mL]	SSE
	Solvent				Urine				
Air Pollutants									
Cotinine	9.5E+05	2.8E+04	1.00	0.045 -45	7.7E+05	-1.1E+06	0.95	1.5 -45	81
Trans-3-hydroxy cotinine	4.3E+05	3.6E+03	0.98	0.009 -9	2.3E+05	-2.0E+05	0.95	0.9 -9	53
1-Hydroxy pyrene	6.1E+03	-3.2E+03	0.99	0.6 -60	3.3E+03	-1.7E+03	0.99	0.6 -60	54
3-Hydroxy phenantrene	1.6E+05	-4.0E+02	1.00	0.015 -4.5	1.2E+05	8.1E+01	1.00	0.015 -4.5	74
Mycotoxins									
Aflatoxin B1	5.5E+04	1.5E+03	1.00	0.03 -30	5.0E+04	-3.1E+03	0.99	0.1 -30	90
Aflatoxin B2	6.2E+02	-7.7E+02	0.99	9 -900	5.5E+02	-4.5E+03	0.98	30 -900	89
Aflatoxin G1	4.0E+04	-7.2E+02	0.99	0.1 -30	3.6E+04	-5.5E+03	0.99	0.3 -30	90
Aflatoxin G2	1.6E+04	3.5E+03	1.00	0.9 -90	1.4E+04	-1.3E+04	0.98	3 -90	84
Aflatoxin M1	6.3E+04	-4.3E+02	0.99	0.1 -30	4.5E+04	-7.3E+03	0.99	0.1 -30	71
Aflatoxin M2	9.9E+02	-1.7E+03	0.99	6 -600	7.3E+02	3.5E+03	0.99	20 -600	74
Aflatoxicol	4.9E+03	2.1E+02	1.00	0.3 -90	3.1E+03	9.7E+03	0.98	9 -90	64
Sterigmatocystein	6.8E+05	-5.2E+02	1.00	0.01 -3	3.9E+05	-9.5E+02	0.99	0.01 -3	56
Citrinin	6.5E+03	1.1E+04	1.00	9 -900	1.3E+04	-2.5E+06	0.99	900 -900	191
Deoxynivalenol	8.2E+01	2.3E+02	0.96	30 -300	5.2E+01	4.2E+03	0.99	300 -300	63
Nivalenol	6.8E+02	-1.2E+02	0.99	3 -30	9.6E+02	2.5E+03	0.99	3 -30	141
Toxin T2	5.5E+00	9.6E+02	1.00	300 -900	5.1E+00	8.9E+01	1.00	300 -900	93
Ochratoxin A	2.7E+04	-2.9E+02	0.99	0.3 -9	2.8E+04	4.8E+03	0.99	0.9 -9	104
Ochratoxin B	1.7E+05	-2.0E+02	1.00	0.03 -9	1.4E+05	8.0E+03	0.99	0.03 -9	85
Ochratoxin Alpha	1.1E+03	2.3E+02	1.00	3 -90	1.1E+03	2.6E+04	0.99	9 -90	96

Table S7 Concentrations of analytes in urine samples measured by high-resolution mass spectrometry (Q Exactive HF). Concentrations below the limit of quantification are marked as <LOQ and not detected analytes displayed as "n.d."

	Concentration [ng/ml]																									
	LOQ	S1	S2	S3	S4	S5	S6	S7	S8	S9	S10	S11	S12	S13	S14	S15	S16	S17	S18	S19	S20	S21	S22	S23	S24	
16-Hydroxystroton	0.13	4.7	n.d.	2.3	n.d.	n.d.	n.d.	n.d.	n.d.	n.d.	n.d.	n.d.	n.d.	n.d.	n.d.	n.d.	n.d.	n.d.	n.d.	n.d.	n.d.	n.d.	n.d.	n.d.	n.d.	n.d.
1-OH-pyrene	4.1	n.d.	n.d.	n.d.	n.d.	n.d.	n.d.	n.d.	n.d.	n.d.	n.d.	n.d.	n.d.	n.d.	n.d.	n.d.	n.d.	n.d.	n.d.	n.d.	n.d.	n.d.	n.d.	n.d.	n.d.	n.d.
2-Naphthol	4.1	6.1	<LOQ	<LOQ	<LOQ	<LOQ	<LOQ	8.1	<LOQ	<LOQ	<LOQ	<LOQ	6.3	<LOQ	<LOQ	<LOQ	<LOQ	<LOQ	<LOQ	<LOQ	<LOQ	<LOQ	<LOQ	<LOQ	4.2	<LOQ
3-Hydroxyphenanthrene	0.29	2.7	<LOQ	n.d.	<LOQ	0.47	n.d.	n.d.	n.d.	<LOQ	n.d.	n.d.	n.d.	n.d.	<LOQ	n.d.	n.d.	n.d.	n.d.	n.d.	0.37	n.d.	<LOQ	<LOQ	<LOQ	<LOQ
Aflatoxin G1	1.3	n.d.	9.03	n.d.	n.d.	n.d.	<LOQ	n.d.	n.d.	n.d.	n.d.	n.d.	n.d.	n.d.	n.d.	n.d.	n.d.	n.d.	n.d.	n.d.	n.d.	n.d.	n.d.	n.d.	n.d.	n.d.
Aflatoxin M1	2.6	n.d.	15	n.d.	n.d.	n.d.	<LOQ	n.d.	n.d.	n.d.	n.d.	4.1	n.d.	n.d.	n.d.	n.d.	n.d.	n.d.	n.d.	n.d.	n.d.	n.d.	<LOQ	n.d.	n.d.	n.d.
Alternariol	0.20	<LOQ	n.d.	n.d.	n.d.	n.d.	n.d.	n.d.	n.d.	n.d.	n.d.	n.d.	n.d.	n.d.	n.d.	n.d.	n.d.	n.d.	n.d.	n.d.	n.d.	n.d.	n.d.	n.d.	n.d.	n.d.
Alternariolmonomethyl ether	0.11	<LOQ	n.d.	n.d.	n.d.	n.d.	n.d.	n.d.	n.d.	n.d.	n.d.	n.d.	n.d.	n.d.	n.d.	n.d.	n.d.	n.d.	n.d.	n.d.	n.d.	n.d.	n.d.	n.d.	n.d.	n.d.
Benzylparaben	0.03	<LOQ	n.d.	n.d.	n.d.	n.d.	n.d.	n.d.	n.d.	n.d.	n.d.	n.d.	n.d.	n.d.	n.d.	n.d.	n.d.	n.d.	n.d.	n.d.	n.d.	n.d.	n.d.	n.d.	n.d.	n.d.
Butylparaben	0.017	n.d.	n.d.	n.d.	n.d.	n.d.	n.d.	n.d.	n.d.	n.d.	n.d.	n.d.	n.d.	n.d.	n.d.	n.d.	n.d.	n.d.	n.d.	n.d.	n.d.	n.d.	n.d.	n.d.	n.d.	n.d.
Colthine	3.1	n.d.	n.d.	n.d.	n.d.	3.20	n.d.	1.48	n.d.	n.d.	2.69	n.d.	n.d.	n.d.	n.d.	n.d.	n.d.	n.d.	n.d.	n.d.	n.d.	n.d.	n.d.	7.2	<LOQ	
Commestrol	0.11	1.7	0.14	n.d.	n.d.	0.44	n.d.	0.48	<LOQ	n.d.	n.d.	2.6	n.d.	n.d.	n.d.	n.d.	n.d.	n.d.	n.d.	n.d.	n.d.	n.d.	n.d.	<LOQ	<LOQ	
Daidzin	0.12	20	30	0.91	0.28	1.17	0.13	4.4	1.3	0.25	<LOQ	0.15	1.3	1.4	1.1	<LOQ	2.9	0.21	3.4	1.2	4.8	2.2	0.28	0.48	2.5	
Enterofol	1.7	<LOQ	n.d.	n.d.	n.d.	n.d.	n.d.	n.d.	<LOQ	<LOQ	n.d.	n.d.	<LOQ	n.d.	n.d.	n.d.	<LOQ	<LOQ	n.d.	9.2	n.d.	<LOQ	<LOQ	n.d.	n.d.	
Enteroflavanone	1.0	7.2	n.d.	2.3	<LOQ	<LOQ	8.3	n.d.	1.0	1.4	3.3	5.7	2.8	9.0	5.2	<LOQ	1.2	1.3	3.3	3.8	<LOQ	1.7	1.4	7.8	<LOQ	
Equlol	0.41	n.d.	n.d.	<LOQ	n.d.	n.d.	n.d.	<LOQ	0.54	n.d.	4.2	n.d.	7.1	2.3	n.d.	n.d.	n.d.	n.d.	n.d.	5.2	n.d.	n.d.	<LOQ	n.d.	n.d.	
Estradiol	7.6	<LOQ	n.d.	n.d.	n.d.	n.d.	n.d.	n.d.	n.d.	n.d.	n.d.	n.d.	n.d.	n.d.	n.d.	n.d.	n.d.	n.d.	n.d.	n.d.	n.d.	n.d.	n.d.	n.d.	n.d.	
Estradiol-3-sulfate	4.2	<LOQ	n.d.	n.d.	n.d.	n.d.	n.d.	n.d.	n.d.	n.d.	n.d.	n.d.	n.d.	n.d.	n.d.	n.d.	n.d.	n.d.	n.d.	n.d.	n.d.	n.d.	n.d.	n.d.	n.d.	
Estrifol	0.49	20	n.d.	3.3	n.d.	n.d.	n.d.	n.d.	n.d.	n.d.	n.d.	n.d.	n.d.	n.d.	n.d.	n.d.	n.d.	n.d.	n.d.	n.d.	n.d.	n.d.	n.d.	n.d.	n.d.	
Estrone	0.78	5.0	n.d.	1.2	n.d.	n.d.	n.d.	n.d.	n.d.	n.d.	n.d.	n.d.	n.d.	n.d.	n.d.	n.d.	n.d.	n.d.	n.d.	n.d.	n.d.	n.d.	n.d.	n.d.	n.d.	
Ethylparaben	0.03	n.d.	0.16	n.d.	0.14	n.d.	0.66	n.d.	n.d.	n.d.	n.d.	n.d.	n.d.	n.d.	n.d.	n.d.	n.d.	n.d.	n.d.	n.d.	n.d.	n.d.	n.d.	0.10	n.d.	
Formononetin	0.052	<LOQ	n.d.	<LOQ	n.d.	<LOQ	n.d.	<LOQ	n.d.	<LOQ	n.d.	n.d.	<LOQ	n.d.	n.d.	n.d.	<LOQ	n.d.	n.d.	n.d.	n.d.	n.d.	n.d.	n.d.	n.d.	
Genistein	0.12	2.1	0.28	0.26	<LOQ	5.8	0.56	1.6	0.90	n.d.	n.d.	<LOQ	7.8	1.4	2.8	n.d.	3.0	<LOQ	3.7	n.d.	<LOQ	3.1	0.58	0.21	<LOQ	
Glycetin	0.055	0.40	0.097	n.d.	0.10	1.5	n.d.	0.53	0.88	n.d.	n.d.	n.d.	7.4	3.8	0.17	n.d.	2.7	n.d.	0.27	1.4	0.20	0.18	n.d.	n.d.	1.6	
Methylparaben	0.23	0.23	3.6	1.0	2.5	n.d.	4.14	2.4	0.25	8.3	n.d.	n.d.	<LOQ	<LOQ	3.9	0.32	n.d.	n.d.	2.81	0.60	<LOQ	n.d.	<LOQ	<LOQ	<LOQ	
Monobutyl phthalate	4.4	n.d.	n.d.	n.d.	n.d.	n.d.	n.d.	n.d.	n.d.	n.d.	n.d.	n.d.	n.d.	n.d.	n.d.	n.d.	n.d.	n.d.	n.d.	n.d.	n.d.	n.d.	n.d.	n.d.	n.d.	
p-Butylbenzenesulfonamide	3.1	<LOQ	n.d.	<LOQ	n.d.	n.d.	<LOQ	n.d.	<LOQ	<LOQ	n.d.	n.d.	<LOQ	n.d.	n.d.	<LOQ	<LOQ	<LOQ	<LOQ	n.d.	n.d.	n.d.	n.d.	n.d.	<LOQ	
Propylparaben	0.067	0.098	9.0	<LOQ	n.d.	n.d.	1.95	0.18	0.11	<LOQ	<LOQ	n.d.	n.d.	0.11	0.51	<LOQ	n.d.	<LOQ	4.18	0.098	n.d.	n.d.	<LOQ	<LOQ	<LOQ	
trans-3-OH-colline	3.2	n.d.	n.d.	n.d.	n.d.	1.61	n.d.	5.2	n.d.	<LOQ	<LOQ	n.d.	n.d.	n.d.	n.d.	n.d.	n.d.	n.d.	n.d.	n.d.	4.51	n.d.	n.d.	6.2	n.d.	
Triloban	2.5	<LOQ	n.d.	n.d.	n.d.	n.d.	n.d.	n.d.	<LOQ	n.d.	n.d.	n.d.	n.d.	n.d.	n.d.	n.d.	n.d.	n.d.	n.d.	n.d.	n.d.	n.d.	n.d.	n.d.	n.d.	

Table S8 Concentrations of analytes in urine samples measured by low-resolution mass spectrometry (QTrap 6500⁺). Concentrations below the limit of quantification are marked as <LOQ and not detected analytes displayed as "n.d."

	LOQ	Concentration [ng/mL]																								
		S1	S2	S3	S4	S5	S6	S7	S8	S9	S10	S11	S12	S13	S14	S15	S16	S17	S18	S19	S20	S21	S22	S23	S24	
16-Epiestriol	0.24	2.6	n.d.	0.45	n.d.	n.d.	n.d.	n.d.	n.d.	n.d.	n.d.	n.d.	n.d.	n.d.	n.d.	n.d.	n.d.	n.d.	n.d.	n.d.	n.d.	n.d.	n.d.	n.d.	n.d.	
16-Hydroxyestron	0.035	3.3	n.d.	3.1	n.d.	n.d.	n.d.	n.d.	n.d.	n.d.	n.d.	n.d.	n.d.	n.d.	0.067	n.d.	n.d.	n.d.	n.d.	n.d.	n.d.	n.d.	n.d.	n.d.	n.d.	
17-Epiestriol	0.23	0.65	n.d.	n.d.	n.d.	n.d.	n.d.	n.d.	n.d.	n.d.	n.d.	n.d.	n.d.	n.d.	n.d.	n.d.	n.d.	n.d.	n.d.	n.d.	n.d.	n.d.	n.d.	n.d.	n.d.	
1-OH-pyrene	0.18	n.d.	n.d.	0.35	n.d.	n.d.	n.d.	n.d.	n.d.	<LOQ	0.41	0.56	0.59	0.46	n.d.	n.d.	0.75	n.d.	<LOQ	5.5	n.d.	n.d.	n.d.	n.d.	n.d.	
2-Methoxyestron	0.013	n.d.	n.d.	0.14	n.d.	n.d.	n.d.	n.d.	n.d.	n.d.	n.d.	n.d.	n.d.	n.d.	n.d.	n.d.	n.d.	n.d.	n.d.	n.d.	n.d.	n.d.	n.d.	n.d.	n.d.	
2-Naphthol	2.6	4.9	4.3	<LOQ	<LOQ	<LOQ	<LOQ	8.0	4.3	<LOQ	<LOQ	6.0	2.4	2.4	3.1	<LOQ	4.3	<LOQ	<LOQ	0.12	0.27	<LOQ	2.2	<LOQ	4.4	2.0
3-Hydroxyphenanthrene	0.03	3.0	0.30	0.15	0.45	0.6	0.27	0.18	0.26	0.23	0.64	0.24	0.15	0.17	0.10	n.d.	0.28	0.094	0.12	0.27	<LOQ	0.08	0.14	0.14	0.29	
4-Methoxyestron	0.011	n.d.	n.d.	n.d.	n.d.	n.d.	n.d.	n.d.	n.d.	n.d.	n.d.	n.d.	n.d.	n.d.	n.d.	n.d.	n.d.	n.d.	n.d.	n.d.	0.26	n.d.	n.d.	n.d.	n.d.	
Alfatoxin B1	4.7	0.24	0.42	n.d.	n.d.	n.d.	n.d.	n.d.	n.d.	n.d.	n.d.	<LOQ	n.d.	n.d.	n.d.	n.d.	n.d.	n.d.	n.d.	<LOQ	n.d.	n.d.	n.d.	n.d.	n.d.	
Alfatoxin G1	0.17	0.79	5.0	n.d.	n.d.	n.d.	n.d.	0.94	n.d.	n.d.	n.d.	0.38	n.d.	n.d.	0.29	n.d.	n.d.	n.d.	n.d.	0.71	n.d.	n.d.	n.d.	0.24	n.d.	
Alfatoxin M1	0.37	2.1	2.0	n.d.	n.d.	0.65	5.1	0.54	n.d.	n.d.	7.4	n.d.	1.1	1.2	n.d.	n.d.	0.88	<LOQ	3.2	n.d.	0.74	n.d.	2.7	n.d.	n.d.	
Aflatoxinol	11	n.d.	n.d.	n.d.	n.d.	n.d.	n.d.	n.d.	n.d.	n.d.	n.d.	n.d.	n.d.	n.d.	n.d.	n.d.	n.d.	n.d.	n.d.	n.d.	n.d.	n.d.	n.d.	n.d.	14	
Alternariol	0.20	0.45	n.d.	n.d.	n.d.	n.d.	n.d.	<LOQ	n.d.	n.d.	n.d.	n.d.	n.d.	<LOQ	n.d.	n.d.	<LOQ	n.d.	n.d.	n.d.	n.d.	n.d.	n.d.	<LOQ	n.d.	
Alternariol monomethyl ether	0.009	0.16	n.d.	0.010	0.016	0.011	0.010	0.062	0.017	n.d.	n.d.	0.022	<LOQ	<LOQ	0.048	n.d.	0.048	<LOQ	<LOQ	0.17	n.d.	n.d.	0.023	n.d.	0.060	
Benzyloparaben	0.005	0.027	n.d.	n.d.	n.d.	n.d.	n.d.	n.d.	n.d.	n.d.	n.d.	n.d.	n.d.	n.d.	n.d.	n.d.	n.d.	n.d.	n.d.	n.d.	n.d.	n.d.	n.d.	n.d.	n.d.	
Bisphenol A	0.81	n.d.	n.d.	n.d.	n.d.	n.d.	n.d.	n.d.	n.d.	n.d.	n.d.	n.d.	n.d.	n.d.	n.d.	n.d.	n.d.	n.d.	n.d.	n.d.	0.85	1.0	n.d.	n.d.	n.d.	
Butylparaben	0.016	n.d.	n.d.	n.d.	n.d.	n.d.	n.d.	n.d.	n.d.	n.d.	n.d.	n.d.	n.d.	n.d.	0.011	n.d.	n.d.	n.d.	n.d.	n.d.	n.d.	n.d.	n.d.	n.d.	n.d.	
Cofeine	30	n.d.	n.d.	n.d.	n.d.	282	n.d.	133	n.d.	n.d.	227	n.d.	n.d.	n.d.	0.011	n.d.	n.d.	n.d.	n.d.	0.31	n.d.	n.d.	n.d.	n.d.	n.d.	
Conestrol	0.011	3.4	0.29	n.d.	n.d.	0.55	0.025	0.27	0.77	n.d.	0.23	n.d.	6.8	0.10	0.11	0.013	2.5	0.13	0.15	0.14	n.d.	n.d.	0.23	n.d.	0.38	
Daidzein	0.040	19	10	0.56	0.26	93	0.27	5	15	0.58	1.1	0.21	12	12	1.1	0.14	25	0.29	3.6	11	4.5	2.3	0.38	0.88	24	
Enterofiol	0.047	0.49	n.d.	0.12	<LOQ	n.d.	n.d.	n.d.	0.79	0.34	0.094	n.d.	0.18	0.39	0.14	n.d.	0.34	n.d.	n.d.	12	n.d.	0.40	0.31	n.d.	n.d.	
Enterolactone	0.76	86	n.d.	n.d.	2.9	0.89	<LOQ	<LOQ	3.6	1.7	18	4.8	8.8	4.8	9.1	<LOQ	14	1.8	4.8	56	<LOQ	21	16	8.0	<LOQ	
Estrodiol	0.89	1.1	n.d.	<LOQ	n.d.	n.d.	n.d.	n.d.	n.d.	n.d.	n.d.	n.d.	n.d.	n.d.	n.d.	n.d.	n.d.	n.d.	n.d.	n.d.	n.d.	n.d.	n.d.	n.d.	n.d.	
Estrodiol-3-sulfate	0.062	45	n.d.	15	n.d.	20	3.7	n.d.	n.d.	n.d.	n.d.	16	n.d.	n.d.	n.d.	n.d.	n.d.	n.d.	n.d.	1.4	n.d.	n.d.	5.1	n.d.	n.d.	
Estriol	0.11	20	n.d.	2.1	n.d.	n.d.	n.d.	n.d.	n.d.	n.d.	n.d.	n.d.	n.d.	n.d.	n.d.	n.d.	n.d.	n.d.	n.d.	1.4	n.d.	n.d.	n.d.	n.d.	n.d.	
Equlol	0.049	<LOQ	n.d.	0.32	<LOQ	9.5	n.d.	0.45	1.2	n.d.	8.4	<LOQ	91	31	n.d.	<LOQ	<LOQ	<LOQ	n.d.	8.9	n.d.	0.19	0.42	n.d.	0.050	
Ethylparaben	0.035	<LOQ	0.13	0.040	0.078	n.d.	0.58	0.037	n.d.	0.52	n.d.	n.d.	n.d.	n.d.	0.061	n.d.	<LOQ	n.d.	<LOQ	0.16	n.d.	n.d.	<LOQ	n.d.	n.d.	
Formononetin	0.007	0.048	0.011	0.015	<LOQ	0.007	<LOQ	0.018	0.021	0.010	n.d.	0.021	5	<LOQ	<LOQ	0.028	<LOQ	<LOQ	4	0.022	<LOQ	0.024	<LOQ	n.d.	<LOQ	
Genistein	0.033	1.8	0.50	0.65	0.10	71	0.17	2.2	1.6	n.d.	n.d.	0.13	13	21	0.31	0.068	3.9	0.14	2.2	n.d.	4.2	0.91	0.26	0.27	5.8	
Glycetin	0.11	0.14	<LOQ	n.d.	0.11	9.6	<LOQ	0.45	0.24	n.d.	n.d.	<LOQ	6.2	2.7	<LOQ	n.d.	0.35	n.d.	0.16	2.4	0.27	<LOQ	<LOQ	<LOQ	1.5	
Isobutylparaben	0.026	n.d.	n.d.	n.d.	n.d.	n.d.	<LOQ	n.d.	n.d.	n.d.	n.d.	n.d.	n.d.	n.d.	<LOQ	n.d.	n.d.	n.d.	n.d.	0.82	n.d.	0.35	n.d.	n.d.	n.d.	
Metatresinol	0.20	n.d.	n.d.	n.d.	n.d.	n.d.	n.d.	0.32	<LOQ	<LOQ	0.49	n.d.	n.d.	n.d.	0.87	n.d.	n.d.	n.d.	n.d.	0.82	n.d.	n.d.	n.d.	n.d.	n.d.	
Methylparaben	0.11	0.19	25	0.51	2.2	n.d.	324	2.0	0.12	5.9	8.6	n.d.	0.18	<LOQ	3.2	0.22	n.d.	<LOQ	241	0.56	n.d.	<LOQ	<LOQ	<LOQ	0.17	
Monobutyl phthalate	1.1	n.d.	n.d.	20	1.5	n.d.	n.d.	3.9	n.d.	16	42	n.d.	n.d.	n.d.	n.d.	n.d.	n.d.	n.d.	n.d.	26	n.d.	n.d.	n.d.	n.d.	n.d.	
n-Butylbenzylsulfonamide	1.3	n.d.	n.d.	<LOQ	<LOQ	n.d.	<LOQ	<LOQ	0.93	0.044	<LOQ	<LOQ	<LOQ	<LOQ	<LOQ	<LOQ	<LOQ	<LOQ	359	0.12	<LOQ	<LOQ	<LOQ	<LOQ	<LOQ	
Propylparaben	0.016	0.10	8.7	0.039	0.021	<LOQ	174	0.13	0.93	0.044	<LOQ	<LOQ	<LOQ	<LOQ	0.55	0.053	<LOQ	0.091	359	0.12	0.029	<LOQ	0.046	<LOQ	0.029	
Tetrahydrobisphenol A	0.14	n.d.	n.d.	n.d.	n.d.	n.d.	n.d.	n.d.	n.d.	n.d.	0.31	n.d.	n.d.	n.d.	n.d.	n.d.	n.d.	n.d.	n.d.	n.d.	n.d.	n.d.	n.d.	n.d.	n.d.	
trans-3-OH-cocaine	0.050	n.d.	0.086	n.d.	n.d.	161	n.d.	52	n.d.	n.d.	121	n.d.	0.38	n.d.	n.d.	n.d.	n.d.	n.d.	n.d.	446	n.d.	n.d.	n.d.	80	0.31	
Triclosan	0.026	0.30	n.d.	n.d.	n.d.	n.d.	n.d.	n.d.	0.067	<LOQ	<LOQ	<LOQ	<LOQ	n.d.	n.d.	n.d.	0.074	n.d.	<LOQ	0.90	n.d.	n.d.	n.d.	n.d.	n.d.	

Table S9 Estimation of urinary concentration at toxicological exposure limits such as the acceptable daily intake (ADI) and the tolerable daily intake (TDI) compared to the limit of quantitation (LOQ) with high-resolution mass spectrometry (HRMS) and low-resolution mass spectrometry (QqQ). The estimation of the urinary concentration at the exposure limit assumed 70 kg body weight, 2 L urine volume and complete excretion (100%) via the urine. The feasibility to detect harmful exposure levels was classified as LOQ above the urinary concentration at TDI/ADI (*), LOQ more than tenfold the estimated urinary concentration at TDI/ADI (✓), and LOQ close to the estimated urinary concentration at TDI/ADI (?).

	Exposure limit [µg/kg body weight per day]	Estimated urinary concentration at TDI/ADI [ng/mL]	LOQ (HRMS) [ng/mL]	LOQ (QqQ) [ng/mL]	Feasible (HRMS)	Feasible (QqQ)
Bisphenol A (BPA)	0.00004 ^{a/4b}	0.0014	2.1	0.8	*	*
Benzyl butyl phthalate	500 ^c	17500	6.9	0.9	✓	✓
Dibutyl phthalate	10 ^c	350	160	82	?	?
Perfluorooctanoic acid (PFOA)	1.5 ^d	52.5	0.1	0.08	✓	✓
Perfluorooctanesulfonic acid (PFOS)	0.15 ^d	5.25	3.5	0.1	?	✓
Methiocarb	13 ^e	455	3.8	0.007	✓	✓
Prochloraz	100 ^f	3500	0.17	0.001	✓	✓
α-zearalenol (α-ZEL)*	15 ^g	525	0.6	0.08	✓	✓
Zearalenone (ZEN)	0.25 ^h	8.75	0.7	0.07	✓	✓
Ethylparaben	10000 ⁱ	350000	0.03	0.04	✓	✓
Methylparaben	10000 ⁱ	350000	0.2	0.11	✓	✓
Deoxynivalenol	1 ^j	35	370	390	✓	✓
Nivalenol	1.2 ^k	42	>30	7	?	✓

*TDI was based on the TDI of ZEN scaled by a relative potency factor of 60

^aTDI based on EFSA draft opinion (<https://www.efsa.europa.eu/en/news/bisphenol-efsa-draft-opinion-proposes-lowering-tolerable-daily-intake>) (Schiano et al. 2022); ^bTDI based on EFSA (2015); ^cTDI based on EFSA et al. (2019); ^dTDI based on EFSA et al. (2018); ^eADI based on EFSA (2006); ^fADI based on EFSA (2011); ^gTDI based on EFSA et al. (2017); ^hTDI based on EFSA (2004); ⁱADI based on (EFSA et al. 2004); ^jTDI based on (EFSA 2013a); ^kTDI based on (EFSA 2013b)

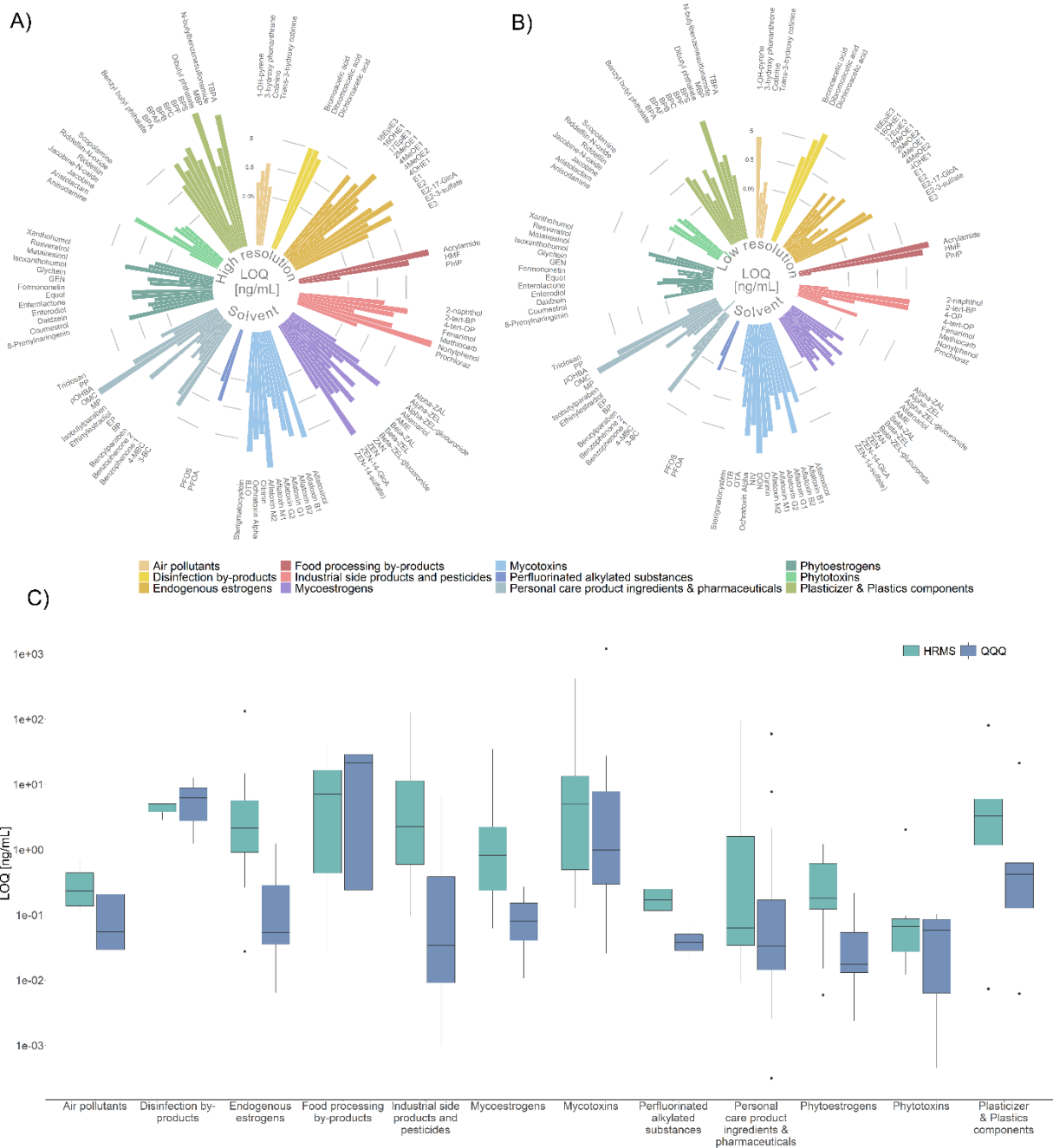


Figure S1 Comparison of LOQ values between the low- and high-resolution mass spectrometer in solvent (ACN/H₂O, 1:9). Analytes with a LOQ < 100 ng/mL are included. LOQ values were estimated according to the Eurachem Guide (2016) A) LOQs on the high-resolution instrument. B) LOD on the low-resolution instrument C) Comparison of the average LOD for each class of chemicals between the high-resolution instrument, Q Exactive (QE, green), and the low-resolution mass spectrometer QTrap 6500+ (QTrap, blue) in solvent.

References

- EFSA. 2004. 'Opinion of the scientific panel on contaminants in the food chain on a request from the commission related to zearalenone as undesirable substance in animal feed', *EFSA J*, 89: 1-35.
- EFSA. 2006. 'Conclusion regarding the peer review of the pesticide risk assessment of the active substance methiocarb', *EFSA Journal*, 4: 79r.
- EFSA. 2011. 'Conclusion on the peer review of the pesticide risk assessment of the active substance prochloraz', *EFSA Journal*, 9: 2323.
- EFSA. 2013a. 'Deoxynivalenol in food and feed: occurrence and exposure', *EFSA Journal*, 11: 3379.
- EFSA. 2013b. 'Scientific Opinion on risks for animal and public health related to the presence of nivalenol in food and feed', *EFSA Journal*, 11: 3262.
- EFSA. 2015. 'Scientific Opinion on the risks to public health related to the presence of bisphenol A (BPA) in foodstuffs', *EFSA J*, 13: 3978.
- EFSA, P. Aids, V. Silano, J.M. Barat Baviera, C. Bolognesi, A. Chesson, P.S. Cocconcelli, R. Crebelli, D.M. Gott, K. Grob, and E. Lampi. 2019. 'Update of the risk assessment of di-butylphthalate (DBP), butyl-benzyl-phthalate (BBP), bis (2-ethylhexyl) phthalate (DEHP), di-isononylphthalate (DINP) and di-isodecylphthalate (DIDP) for use in food contact materials', *EFSA Journal*, 17: e05838.
- EFSA, R. Anton, S. Barlow, and D. Boskou. 2004. 'Opinion of the scientific panel on food additives, flavourings, processing aids and materials in contact with food (AFC) related to para hydroxybenzoates (E 214-219)', *EFSA J*, 2: 83.
- EFSA, H.-K. Knutsen, J. Alexander, L. Barregård, M. Bignami, B. Brüschweiler, S. Ceccatelli, B. Cottrill, M. Dinovi, L. Edler, B. Grasl-Kraupp, C. Hogstrand, L. Hoogenboom, C.S. Nebbia, A. Petersen, M. Rose, A.-C. Roudot, T. Schwerdtle, C. Vleminckx, G. Vollmer, H. Wallace, C. Dall'Asta, S. Dänicke, G.-S. Eriksen, A. Altieri, R. Roldán-Torres, and I.P. Oswald. 2017. 'Risks for animal health related to the presence of zearalenone and its modified forms in feed', *EFSA Journal*, 15: e04851.
- EFSA, H.K. Knutsen, J. Alexander, L. Barregård, M. Bignami, B. Brüschweiler, S. Ceccatelli, B. Cottrill, M. Dinovi, and L. Edler. 2018. 'Risk to human health related to the presence of perfluorooctane sulfonic acid and perfluorooctanoic acid in food', *EFSA Journal*, 16: e05194.
- Jamnik, T., M. Flasch, D. Braun, Y. Fareed, D. Wasinger, D. Seki, D. Berry, A. Berger, L. Wisgrill, and B. Warth. 2022. 'Next-generation biomonitoring of the early-life chemical exposome in neonatal and infant development', *Nature Communications*, 13: 2653.
- Schiano, M.E., A. Abduvakhidov, M. Varra, and S. Albrizio. 2022. 'Aptamer-Based Biosensors for the Analytical Determination of Bisphenol A in Foodstuffs', *Applied Sciences*, 12: 3752.

Supporting Information B

Comparing the sensitivity of low- and high-resolution mass spectrometry for xenobiotic trace analysis: An exposome-type case study

Mira Flasch^{1,2}, Gunda Koellensperger^{3,4}, Benedikt Warth^{1,4*}

¹University of Vienna, Faculty of Chemistry, Department of Food Chemistry and Toxicology, Währinger Straße 38-40, 1090 Vienna, Austria

²University of Vienna, Vienna Doctoral School in Chemistry, Währinger Straße 42, 1090, Vienna, Austria

³University of Vienna, Faculty of Chemistry, Department of Analytical Chemistry, Währinger Straße 38-40, 1090 Vienna, Austria

⁴Exposome Austria, Research Infrastructure and National EIRENE Hub, Austria

Table S9: Results of suspect screening in negative ionization mode

Table S10: Results of suspect screening in positive ionization mode

Table S9. Results of suspect screening in negative ionization mode with peak group (orgroup), retention time in min (ret), m/z value (mz), intensity in each sample, name of suspect compound (suspp name), mz value of suspect compound (suspp mz), SMILES formula (suspp SMILES) and molecular formula of suspect compound (suspp formula), m/z difference between feature and suspect (suspp m/z diff), formula (suspp formula) and estimated identification level (suspp estIDLevel)																		
Peak group	ret (min)	m/z	SMILES formula	molecular formula	m/z difference	formula	formula	estIDLevel										
M141 R261 2903	4.4	141.1	2E+05	5E+06	3E+06	2E+06	4E+05	9E+05	8E+04	6E+03	6E+06	9E+05	Bufl methacrylate	141.0921	CCCCC(=O)OCC=C	C8H14O2	0.0002363	5
M141 R261 2903	4.4	141.1	2E+05	5E+06	3E+06	2E+06	4E+05	9E+05	8E+04	6E+03	6E+06	9E+05	delta-Octalactone	141.0921	CCCCC(=O)O=C1CCCCC1	C8H14O2	0.0002363	5
M141 R261 2903	4.4	141.1	2E+05	5E+06	3E+06	2E+06	4E+05	9E+05	8E+04	6E+03	6E+06	9E+05	4-Methylcyanoacetic acid	141.0921	CC(C)C#NCC(=O)O	C8H14O2	0.0002363	5
M141 R261 2903	4.4	141.1	2E+05	5E+06	3E+06	2E+06	4E+05	9E+05	8E+04	6E+03	6E+06	9E+05	isobutyl methacrylate	141.0921	CC(C)C#NCC(=O)OCC=C	C8H14O2	0.0002363	5
M141 R261 2903	4.4	141.1	2E+05	5E+06	3E+06	2E+06	4E+05	9E+05	8E+04	6E+03	6E+06	9E+05	Allyl isovaleate	141.0921	CCCCC(=O)OCC=C	C8H14O2	0.0002363	5
M141 R261 2903	4.4	141.1	2E+05	5E+06	3E+06	2E+06	4E+05	9E+05	8E+04	6E+03	6E+06	9E+05	2-Methylbutyl 2-enoate	141.0921	CC(C)C#NCC(=O)OCC=C	C8H14O2	0.0002363	5
M141 R210 2908	3.5	141.1	2E+05	5E+06	3E+06	2E+06	4E+05	9E+05	8E+04	6E+03	6E+06	9E+05	Bufl methacrylate	141.0921	CCCCC(=O)OCC=C	C8H14O2	0.0002363	5
M141 R210 2908	3.5	141.1	2E+05	5E+06	3E+06	2E+06	4E+05	9E+05	8E+04	6E+03	6E+06	9E+05	delta-Octalactone	141.0921	CCCCC(=O)O=C1CCCCC1	C8H14O2	0.0002363	5
M141 R210 2908	3.5	141.1	2E+05	5E+06	3E+06	2E+06	4E+05	9E+05	8E+04	6E+03	6E+06	9E+05	4-Methylcyanoacetic acid	141.0921	CC(C)C#NCC(=O)O	C8H14O2	0.0002363	5
M141 R210 2908	3.5	141.1	2E+05	5E+06	3E+06	2E+06	4E+05	9E+05	8E+04	6E+03	6E+06	9E+05	(Z)-3-Hexenyl acetate	141.0921	CC(=C/C)C(=O)OC	C8H14O2	0.0002363	5
M141 R210 2908	3.5	141.1	2E+05	5E+06	3E+06	2E+06	4E+05	9E+05	8E+04	6E+03	6E+06	9E+05	isobutyl methacrylate	141.0921	CC(C)C#NCC(=O)OCC=C	C8H14O2	0.0002363	5
M141 R210 2908	3.5	141.1	2E+05	5E+06	3E+06	2E+06	4E+05	9E+05	8E+04	6E+03	6E+06	9E+05	Allyl isovaleate	141.0921	CCCCC(=O)OCC=C	C8H14O2	0.0002363	5
M141 R210 2908	3.5	141.1	2E+05	5E+06	3E+06	2E+06	4E+05	9E+05	8E+04	6E+03	6E+06	9E+05	Cyclohexyl acetate	141.0921	CCCCC(=O)OC1CCCCC1	C8H14O2	0.0002363	5
M141 R210 2908	3.5	141.1	2E+05	5E+06	3E+06	2E+06	4E+05	9E+05	8E+04	6E+03	6E+06	9E+05	2-Methylpropyl but-2-enoate	141.0921	CC(C)C#NCC(=O)OCC=C	C8H14O2	0.0002363	5
M141 R215 2914	3.6	141.1	5E+06	4E+06	5E+05	5E+05	1E+07	3E+06	4E+05	6E+05	6E+05	6E+05	4-Octanone	141.0921	CCCCC(=O)O	C8H14O2	0.0002363	5
M141 R215 2914	3.6	141.1	5E+06	4E+06	5E+05	5E+05	1E+07	3E+06	4E+05	6E+05	6E+05	6E+05	delta-Octalactone	141.0921	CCCCC(=O)O=C1CCCCC1	C8H14O2	0.0002363	5
M141 R215 2914	3.6	141.1	5E+06	4E+06	5E+05	5E+05	1E+07	3E+06	4E+05	6E+05	6E+05	6E+05	4-Octanone	141.0921	CCCCC(=O)O	C8H14O2	0.0002363	5
M141 R215 2914	3.6	141.1	5E+06	4E+06	5E+05	5E+05	1E+07	3E+06	4E+05	6E+05	6E+05	6E+05	delta-Octalactone	141.0921	CCCCC(=O)O=C1CCCCC1	C8H14O2	0.0002363	5
M141 R215 2914	3.6	141.1	5E+06	4E+06	5E+05	5E+05	1E+07	3E+06	4E+05	6E+05	6E+05	6E+05	(Z)-3-Hexenyl acetate	141.0921	CC(=C/C)C(=O)OC	C8H14O2	0.0002363	5
M141 R215 2914	3.6	141.1	5E+06	4E+06	5E+05	5E+05	1E+07	3E+06	4E+05	6E+05	6E+05	6E+05	isobutyl methacrylate	141.0921	CC(C)C#NCC(=O)OCC=C	C8H14O2	0.0002363	5
M141 R215 2914	3.6	141.1	5E+06	4E+06	5E+05	5E+05	1E+07	3E+06	4E+05	6E+05	6E+05	6E+05	Allyl isovaleate	141.0921	CCCCC(=O)OCC=C	C8H14O2	0.0002363	5
M141 R215 2914	3.6	141.1	5E+06	4E+06	5E+05	5E+05	1E+07	3E+06	4E+05	6E+05	6E+05	6E+05	Cyclohexyl acetate	141.0921	CCCCC(=O)OC1CCCCC1	C8H14O2	0.0002363	5
M141 R293 2921	4.9	141.1	2E+05	7E+05	4E+06	3E+05	4E+05	4E+04	1E+03	3E+05	3E+05	3E+05	2-Methylpropyl but-2-enoate	141.1289	CC(C)C#NCC(=O)OCC=C	C8H14O2	0.0002363	5
M141 R293 2921	4.9	141.1	2E+05	7E+05	4E+06	3E+05	4E+05	4E+04	1E+03	3E+05	3E+05	3E+05	Nonanal	141.1289	CCCCCCCC	C8H14O2	0.0002363	5
M141 R293 2921	4.9	141.1	2E+05	7E+05	4E+06	3E+05	4E+05	4E+04	1E+03	3E+05	3E+05	3E+05	2-Nonanone	141.1289	CCCCC(=O)O	C8H14O2	0.0002363	5
M141 R293 2921	4.9	141.1	2E+05	7E+05	4E+06	3E+05	4E+05	4E+04	1E+03	3E+05	3E+05	3E+05	5-Methyl-2-octanone	141.1289	CCCCC(=O)O	C8H14O2	0.0002363	5
M141 R293 2921	4.9	141.1	2E+05	7E+05	4E+06	3E+05	4E+05	4E+04	1E+03	3E+05	3E+05	3E+05	(1R,5R)-3,5-trimethylcyclohexane	141.1289	CC1C(C)C(C)C(C)C1	C8H14O2	0.0002363	5
M141 R293 2921	4.9	141.1	2E+05	7E+05	4E+06	3E+05	4E+05	4E+04	1E+03	3E+05	3E+05	3E+05	3,5-Dimethylcyclohexane	141.1289	CC1C(C)C(C)C(C)C1	C8H14O2	0.0002363	5
M141 R293 2921	4.9	141.1	2E+05	7E+05	4E+06	3E+05	4E+05	4E+04	1E+03	3E+05	3E+05	3E+05	(6Z)-Non-6-ene-1-ol	141.1289	CCCCC=CO	C8H14O2	0.0002363	5
M141 R293 2921	4.9	141.1	2E+05	7E+05	4E+06	3E+05	4E+05	4E+04	1E+03	3E+05	3E+05	3E+05	3,5,5-Trimethylhexane	141.1289	CC(C)C(C)C(C)C(C)C	C8H14O2	0.0002363	5
M141 R293 2921	4.9	141.1	2E+05	7E+05	4E+06	3E+05	4E+05	4E+04	1E+03	3E+05	3E+05	3E+05	Diethylbutyl ether	141.1289	CCCCC(=O)O	C8H14O2	0.0002363	5
M141 R293 2921	4.9	141.1	2E+05	7E+05	4E+06	3E+05	4E+05	4E+04	1E+03	3E+05	3E+05	3E+05	4-Isopropylphenol	141.1289	CC(C)C1=CC=C(O)C=C1	C8H14O2	0.0002363	5
M141 R293 2921	4.9	141.1	2E+05	7E+05	4E+06	3E+05	4E+05	4E+04	1E+03	3E+05	3E+05	3E+05	1-Naphthylamine	142.0622	NC1=CC=C2C=CC=CC=C2C=C1	C10H9N	-6.34E-05	5
M141 R293 2921	4.9	141.1	2E+05	7E+05	4E+06	3E+05	4E+05	4E+04	1E+03	3E+05	3E+05	3E+05	Quinoline	142.0622	C1=NC2=C(N1)C=CC=C2	C10H9N	-6.34E-05	5
M141 R293 2921	4.9	141.1	2E+05	7E+05	4E+06	3E+05	4E+05	4E+04	1E+03	3E+05	3E+05	3E+05	6-Methylquinoline	142.0622	CC1=CC=C2C=CC=CC=C2N=C1	C10H9N	-6.34E-05	5
M141 R293 2921	4.9	141.1	2E+05	7E+05	4E+06	3E+05	4E+05	4E+04	1E+03	3E+05	3E+05	3E+05	Lapinone	142.0622	CC1=CC=C2C=CC=CC=C2C(=O)O1	C10H9N	-6.34E-05	5
M141 R293 2921	4.9	141.1	2E+05	7E+05	4E+06	3E+05	4E+05	4E+04	1E+03	3E+05	3E+05	3E+05	1-Naphthylamine	142.0622	NC1=CC=C2C=CC=CC=C2C=C1	C10H9N	-6.34E-05	5
M141 R293 2921	4.9	141.1	2E+05	7E+05	4E+06	3E+05	4E+05	4E+04	1E+03	3E+05	3E+05	3E+05	Quinoline	142.0622	C1=NC2=C(N1)C=CC=C2	C10H9N	-6.34E-05	5
M141 R293 2921	4.9	141.1	2E+05	7E+05	4E+06	3E+05	4E+05	4E+04	1E+03	3E+05	3E+05	3E+05	6-Methylquinoline	142.0622	CC1=CC=C2C=CC=CC=C2N=C1	C10H9N	-6.34E-05	5
M141 R293 2921	4.9	141.1	2E+05	7E+05	4E+06	3E+05	4E+05	4E+04	1E+03	3E+05	3E+05	3E+05	Lapinone	142.0622	CC1=CC=C2C=CC=CC=C2C(=O)O1	C10H9N	-6.34E-05	5
M141 R293 2921	4.9	141.1	2E+05	7E+05	4E+06	3E+05	4E+05	4E+04	1E+03	3E+05	3E+05	3E+05	1-Naphthylamine	142.0622	NC1=CC=C2C=CC=CC=C2C=C1	C10H9N	-6.34E-05	5
M141 R293 2921	4.9	141.1	2E+05	7E+05	4E+06	3E+05	4E+05	4E+04	1E+03	3E+05	3E+05	3E+05	Quinoline	142.0622	C1=NC2=C(N1)C=CC=C2	C10H9N	-6.34E-05	5
M141 R293 2921	4.9	141.1	2E+05	7E+05	4E+06	3E+05	4E+05	4E+04	1E+03	3E+05	3E+05	3E+05	6-Methylquinoline	142.0622	CC1=CC=C2C=CC=CC=C2N=C1	C10H9N	-6.34E-05	5
M141 R293 2921	4.9	141.1	2E+05	7E+05	4E+06	3E+05	4E+05	4E+04	1E+03	3E+05	3E+05	3E+05	Lapinone	142.0622	CC1=CC=C2C=CC=CC=C2C(=O)O1	C10H9N	-6.34E-05	5
M141 R293 2921	4.9	141.1	2E+05	7E+05	4E+06	3E+05	4E+05	4E+04	1E+03	3E+05	3E+05	3E+05	1-Naphthylamine	142.0622	NC1=CC=C2C=CC=CC=C2C=C1	C10H9N	-6.34E-05	5
M141 R293 2921	4.9	141.1	2E+05	7E+05	4E+06	3E+05	4E+05	4E+04	1E+03	3E+05	3E+05	3E+05	Quinoline	142.0622	C1=NC2=C(N1)C=CC=C2	C10H9N	-6.34E-05	5
M141 R293 2921	4.9	141.1	2E+05	7E+05	4E+06	3E+05	4E+05	4E+04	1E+03	3E+05	3E+05	3E+05	6-Methylquinoline	142.0622	CC1=CC=C2C=CC=CC=C2N=C1	C10H9N	-6.34E-05	5
M141 R293 2921	4.9	141.1	2E+05	7E+05	4E+06	3E+05	4E+05	4E+04	1E+03	3E+05	3E+05	3E+05	Lapinone	142.0622	CC1=CC=C2C=CC=CC=C2C(=O)O1	C10H9N	-6.34E-05	5
M141 R293 2921	4.9	141.1	2E+05	7E+05	4E+06	3E+05	4E+05	4E+04	1E+03	3E+05	3E+05	3E+05	1-Naphthylamine	142.0622	NC1=CC=C2C=CC=CC=C2C=C1	C10H9N	-6.34E-05	5
M141 R293 2921	4.9	141.1	2E+05	7E+05	4E+06	3E+05	4E+05	4E+04	1E+03	3E+05	3E+05	3E+05	Quinoline	142.0622	C1=NC2=C(N1)C=CC=C2	C10H9N	-6.34E-05	5
M141 R293 2921	4.9	141.1	2E+05	7E+05	4E+06	3E+05	4E+05	4E+04	1E+03	3E+05	3E+05	3E+05	6-Methylquinoline	142.0622	CC1=CC=C2C=CC=CC=C2N=C1	C10H9N	-6.34E-05	5
M141 R293 2921	4.9	141.1	2E+05	7E+05	4E+06	3E+05	4E+05	4E+04	1E+03	3E+05	3E+05	3E+05	Lapinone	142.0622	CC1=CC=C2C=CC=CC=C2C(=O)O1	C10H9N	-6.34E-05	5

Table S9: Results of suspect screening in negative ionization mode with peak group (group), retention time in min (ret), m/z-value (mz), intensity in each sample, name of suspect compound (suspp name), m/z-value of suspect compound (suspp mz), SMILES formula (suspp SMILES) and molecular formula of suspect compound (Suspp formula), m/z difference between feature and suspect (suspp mz), formula (suspp formula) and estimated identification level (suspp estIDlevel)

Peak group	ret	mz	SMILES	S1	S2	S3	S4	S5	S6	S7	S8	S9	S10	S11	S12	S13	S14	S15	S16	S17	S18	S19	S20	S21	S22	S23	S24	suspp name	suspp mz	suspp SMILES	suspp formula	suspp mz	suspp estIDlevel
M169 R204 48413	3.4	1691	1691																									14-Ethylhexan-1-ylbutanoate	169.1234	CCCCCCCCCCCCCCCC	C18H34O2	0.0001726	5
M169 R204 48413	3.4	1691	1691																									Hexyl methacrylate	169.1234	CCCCC=C(C)CCCC	C18H34O2	0.0001726	5
M169 R204 48413	3.4	1691	1691																									Allyl hexyl gamma-butyrolactone	169.1234	CCCCCCCCC1OCCCC	C18H34O2	0.0001726	5
M169 R204 48413	3.4	1691	1691																									gamma-Decalactone	169.1234	CCCCC=C(C)CCCC	C18H34O2	0.0001726	5
M169 R204 48413	3.4	1691	1691																									6-Nonamethylhept-3H-cyclo-2-ol	169.1234	CCCCCCCCC1CCCC1	C18H34O2	0.0001726	5
M169 R204 48413	3.4	1691	1691																									Methyl [2E]-non-2-enoate	169.1234	CCCCC=C(C)CCCC	C18H34O2	0.0001726	5
M169 R204 48413	3.4	1691	1691																									Methyl non-2-enoate	169.1234	CCCCC=C(C)CCCC	C18H34O2	0.0001726	5
M169 R204 48413	3.4	1691	1691																									Oct-1-en-1-yl acetate	169.1234	CCCCC=C(C)CCCC	C18H34O2	0.0001726	5
M169 R204 48413	3.4	1691	1691																									essillon Decalactone	169.1234	CCCCC=C(C)CCCC	C18H34O2	0.0001726	5
M169 R204 48413	3.4	1691	1691																									Methyl 3-nonenoate	169.1234	CCCCC=C(C)CCCC	C18H34O2	0.0001726	5
M169 R204 48413	3.4	1691	1691																									Et-3-hydroxybutanoate	169.1234	CCCCC=C(C)CCCC	C18H34O2	0.0001726	5
M169 R204 48413	3.4	1691	1691																									[3Z]-Hex-3-en-1-yl 2-methylpropanoate	169.1234	CCCCC=C(C)CCCC	C18H34O2	0.0001726	5
M169 R204 48413	3.4	1691	1691																									Citronellol	169.1234	CCCCC=C(C)CCCC	C18H34O2	0.0001726	5
M169 R204 48413	3.4	1691	1691																									2-Cyclohexylacetate	169.1234	CCCCC=C(C)CCCC	C18H34O2	0.0001726	5
M171 R170 49367	2.8	1711	1711																									1-Ethyl-4-cyclohexanecarboxylic acid	171.0628	CCCCC=C(C)CCCC	C18H34O2	2.306	5
M171 R170 49367	2.8	1711	1711																									Diethyl malonate	171.0628	CCCCC=C(C)CCCC	C18H34O2	2.306	5
M171 R63 49623	1.0	1711	1711																									Butyl 4-oxopentanoate	171.0267	CCCCC=C(C)CCCC	C18H34O2	0.0021197	5
M171 R246 49696	4.1	1711	1711																									Butyl 4-oxopentanoate	171.0267	CCCCC=C(C)CCCC	C18H34O2	0.0002287	5
M171 R246 49696	4.1	1711	1711																									Butyl 4-oxopentanoate	171.0267	CCCCC=C(C)CCCC	C18H34O2	0.0002414	4b
M171 R246 49696	4.1	1711	1711																									Butyl 4-oxopentanoate	171.0267	CCCCC=C(C)CCCC	C18H34O2	0.0002454	5
M173 R222 51013	3.7	1731	1731																									1-Phenyl-3-methyl-5-oxo-2-pyrrolidone	173.0726	CCCCC=C(C)CCCC	C18H34O2	4.176	5
M173 R222 51013	3.7	1731	1731																									1,4-Bis(2-hydroxyethyl)-2-butanol	173.0819	CCCCC=C(C)CCCC	C18H34O2	0.0011146	4b
M173 R222 51013	3.7	1731	1731																									Dimethyl adipate	173.0819	CCCCC=C(C)CCCC	C18H34O2	0.0011146	4b
M173 R222 51013	3.7	1731	1731																									Diethyl sebacate	173.0819	CCCCC=C(C)CCCC	C18H34O2	0.0011146	4b
M173 R222 51013	3.7	1731	1731																									Dimethyl sebacate	173.0819	CCCCC=C(C)CCCC	C18H34O2	0.0011146	4b
M173 R222 51013	3.7	1731	1731																									Ethylene diethyl diethyl ether	173.0819	CCCCC=C(C)CCCC	C18H34O2	0.0011146	4b
M173 R222 51013	3.7	1731	1731																									Indole-3-acetic acid	174.0565	CCCCC=C(C)CCCC	C18H34O2	0.0017322	4b
M174 R242 51615	4.0	1741	1741																									N-Ethylpyrrolidone	174.0565	CCCCC=C(C)CCCC	C18H34O2	0.0017322	4b
M174 R242 51615	4.0	1741	1741																									Indole-3-acetic acid	174.0565	CCCCC=C(C)CCCC	C18H34O2	0.001747	4b
M174 R242 51615	4.0	1741	1741																									N-Ethylpyrrolidone	174.0565	CCCCC=C(C)CCCC	C18H34O2	0.001747	4b
M174 R242 51615	4.0	1741	1741																									Indole-3-acetic acid	174.0565	CCCCC=C(C)CCCC	C18H34O2	0.001747	4b
M175 R155 52049	2.6	1751	1751																									1-L-ascorbic acid	175.02481	CCCCC=C(C)CCCC	C18H34O2	-5.638	5
M175 R155 52049	2.6	1751	1751																									Sodium erythorbate (1:1)	175.02481	CCCCC=C(C)CCCC	C18H34O2	-5.638	5
M175 R155 52049	2.6	1751	1751																									Sodium ascorbate	175.02481	CCCCC=C(C)CCCC	C18H34O2	-5.638	5
M175 R155 52049	2.6	1751	1751																									D-Glucuronolactone	175.02481	CCCCC=C(C)CCCC	C18H34O2	-5.638	5
M175 R155 52049	2.6	1751	1751																									L-Ascorbic acid	175.02481	CCCCC=C(C)CCCC	C18H34O2	-4.748	5
M175 R155 52049	2.6	1751	1751																									Sodium L-ascorbate (1:1)	175.02481	CCCCC=C(C)CCCC	C18H34O2	-4.748	5
M175 R155 52049	2.6	1751	1751																									Sodium L-ascorbate	175.02481	CCCCC=C(C)CCCC	C18H34O2	-4.748	5
M175 R155 52049	2.6	1751	1751																									L-Ascorbic acid	175.02481	CCCCC=C(C)CCCC	C18H34O2	-4.748	5
M175 R155 52049	2.6	1751	1751																									L-Ascorbic acid	175.02481	CCCCC=C(C)CCCC	C18H34O2	-4.748	5
M175 R155 52049	2.6	1751	1751																									Sodium erythorbate (1:1)	175.02481	CCCCC=C(C)CCCC	C18H34O2	-2.978	5
M175 R155 52049	2.6	1751	1751																									Sodium erythorbate (1:1)	175.02481	CCCCC=C(C)CCCC	C18H34O2	-2.978	5
M175 R155 52049	2.6	1751	1751																									Sodium L-ascorbate	175.02481	CCCCC=C(C)CCCC	C18H34O2	-2.978	5
M175 R155 52049	2.6	1751	1751																									D-Glucuronolactone	175.02481	CCCCC=C(C)CCCC	C18H34O2	-2.978	5
M175 R155 52049	2.6	1751	1751																									Ascorbic acid	175.02481	CCCCC=C(C)CCCC	C18H34O2	-2.978	5
M175 R155 52049	2.6	1751	1751																									Ascorbic acid	175.02481	CCCCC=C(C)CCCC	C18H34O2	-2.978	5
M175 R155 52049	2.6	1751	1751																									Ascorbic acid	175.02481	CCCCC=C(C)CCCC	C18H34O2	-2.978	5
M175 R155 52049	2.6	1751	1751																									Ascorbic acid	175.02481	CCCCC=C(C)CCCC	C18H34O2	-2.978	5

6.4. Publication #3: Flasch et al. (2020)

Status	Published
Title	Stable Isotope-Assisted Metabolomics for Deciphering Xenobiotic Metabolism in Mammalian Cell Culture
Authors	Mira Flasch ¹ , Christoph Bueschl ² , Lydia Woelflingseder ¹ , Heidi E Schwartz-Zimmermann ² , Gerhard Adam ³ , Rainer Schuhmacher ² , Doris Marko ¹ , Benedikt Warth ^{1,*}
Affiliations	¹ University of Vienna, Faculty of Chemistry, Department of Food Chemistry and Toxicology, Währinger Straße 38-40, 1090 Vienna, Austria ² University of Natural Resources and Life Sciences, Department of Agrobiotechnology, Vienna (BOKU), IFA-Tulln, Institute of Bioanalytics and Agro-Metabolomics, Konrad-Lorenz-Straße 20, 3430 Tulln, Austria ³ University of Natural Resources and Life Sciences, Department of Applied Genetics and Cell Biology, Vienna (BOKU), Konrad-Lorenz-Straße 20, 3430 Tulln, Austria *Corresponding author
Year	2020
Journal	ACS Chemical Biology , Volume 15, Issue 4, Pages 970-981
Accepted	March 13 th , 2020
DOI	https://doi.org/10.1021/acscchembio.9b01016
Contribution	Mira Flasch (MF) performed the LC-HRMS(/MS) measurements, interpreted the results from the MetExtract II analyses and wrote the manuscript.

Stable Isotope-Assisted Metabolomics for Deciphering Xenobiotic Metabolism in Mammalian Cell Culture

Mira Flasch,¹ Christoph Bueschl,¹ Lydia Woelflingseder, Heidi E. Schwartz-Zimmermann, Gerhard Adam, Rainer Schuhmacher, Doris Marko, and Benedikt Warth*



Cite This: *ACS Chem. Biol.* 2020, 15, 970–981



Read Online

ACCESS |



Metrics & More

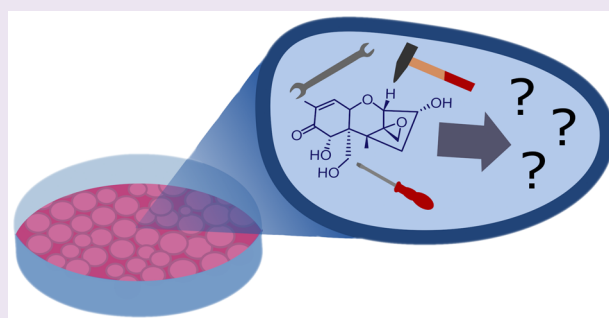


Article Recommendations



Supporting Information

ABSTRACT: Xenobiotics are ubiquitous in the environment and modified in the human body by phase I and II metabolism. Liquid chromatography coupled to high resolution mass spectrometry is a powerful tool to investigate these biotransformation products. We present a workflow based on stable isotope-assisted metabolomics and the bioinformatics tool MetExtract II for deciphering xenobiotic metabolites produced by human cells. Its potential was demonstrated by the investigation of the metabolism of deoxynivalenol (DON), an abundant food contaminant, in a liver carcinoma cell line (HepG2) and a model for colon carcinoma (HT29). Detected known metabolites included DON-3-sulfate, DON-10-sulfonate 2, and DON-10-glutathione as well as DON-cysteine. Conjugation with amino acids and an antibiotic was confirmed for the first time. The approach allows the untargeted elucidation of human xenobiotic products in tissue culture. It may be applied to other fields of research including drug metabolism, personalized medicine, exposome research, and systems biology to better understand the relevance of *in vitro* experiments.



INTRODUCTION

Humans and other organisms are exposed to a multitude of xenobiotics during their lifetime through food and environment.^{1–3} The human organism utilizes different metabolic mechanisms to activate, detoxify, and excrete them.⁴ Phase I reactions cause an increase in polarity and thereby enhance the reactivity of the parent molecule, and phase II reactions form conjugates that can be excreted via urine. Phase II reactions include sulfation, glucuronidation, glutathione-conjugation, and acylation.^{5,6} The metabolic fate of xenobiotics in human systems is frequently incompletely understood, although crucial for the assessment of toxicity.

Liquid chromatography high resolution mass spectrometry (LC-HRMS) is the premier technique for the sensitive and selective detection and characterization of unknown metabolites and allows for the elucidation of xenobiotic biotransformation. However, the evaluation of LC-HRMS data sets, originating from untargeted metabolite profiling, is time-consuming and challenging and requires advanced bioinformatics tools.⁷ A powerful tool for the elucidation of novel metabolic pathways and respective data analysis is the recently developed MetExtract II algorithm.⁸ Concurrent analysis of stable isotopically labeled and native sample material allows the automated and comprehensive extraction of metabolic features relevant for the metabolism of practically any investigated small molecule. The practicability and power of this approach

have already been proven in a number of plant-based experiments.^{8–12}

Deoxynivalenol (DON), a secondary metabolite produced by *Fusarium* fungi, is a mycotoxin frequently found as a contaminant in wheat, corn, oat, and other grains as well as in products thereof.¹³ The toxin inhibits protein synthesis and subsequently also RNA and DNA synthesis.¹⁴ Additionally, ribotoxic stress causes stimulation of the production of cytokines, and induction of apoptosis is triggered by high concentrations of the mycotoxin.¹⁵ Acutely, it induces emesis and abdominal pain.¹⁶ The effects of chronic exposure to DON include, besides growth retardation and immunotoxicity, also impairment of reproduction and development in animals. The impact of low dose chronic exposure to humans remains elusive.¹⁷ The prevalence of the DON producing fungi in cereal based crops and the thermal stability of the toxin itself make the mycotoxin an issue for global food safety.¹⁶ Multiple human biomonitoring studies suggested that the established tolerable daily intake of DON ($1 \mu\text{g kg}^{-1}$ body weight per day) is exceeded frequently in different populations, particularly by

Received: December 19, 2019

Accepted: March 13, 2020

Published: March 13, 2020



highly susceptible subgroups such as children and pregnant women.^{17–20} The metabolic fate of DON has been studied in humans *in vivo*,^{21,22} in animals,^{23–26} and also in the *Fusarium* host plant, wheat.^{9,27–29} DON-glucuronides (DON-GlcAs) were identified as the major urinary DON-metabolites in humans. While glucuronidation is the major detoxification pathway in humans, the formation of DON-GlcAs in human cell culture models has not been reported so far. The toxicological properties of DON biotransformation products significantly differ from the parent molecule. The ability of DON-sulfates to inhibit protein synthesis by inactivation of the ribosome was reduced,²⁹ and consequently cytotoxicity was decreased compared to DON. However, an increase of cellular proliferation and activation of autophagy were described.^{30,31} Incubation of human cells with DON-glucuronide resulted in decreased cytotoxicity when compared to the parent toxin.³² In addition, conjugates with thiol or sulfhydryl containing compounds including DON-GSH showed no toxicity in human monocytes and did not enhance proinflammatory cytokines.³³

In this study, an adapted workflow for the comprehensive elucidation of xenobiotic biotransformation through LC-HRMS, assisted by stable-isotope labeling and the bioinformatics tool MetExtract II, was established. Due to its potential for identifying known and unknown metabolic products, the *in vitro* metabolism of DON in human cell culture was studied with this technique. Two well-studied cell models of liver and colon, respectively, were tested and revealed unexpected insights into the *in vitro* metabolism of the model xenobiotic DON.

RESULTS

Optimization of Tissue Culture and the Analytical Workflow. The selection of the most appropriate cell lines was based on a number of preliminary experiments in five different cell models (HepG2, Caco-2, HT29, HEK293, and T24). The uptake rate of DON from the extracellular medium into the cells after 24 h was lower for cells from the urinary tract (HEK293 and T24; below 0.3%) than for the other cell lines (approximately 1.5%). When screening for biotransformation products, DON-3-sulfates and DONS2 were confirmed by the correct *m/z* value and retention time with an authentic reference standard and were present in the supernatant of all cell lines after a 24 h incubation. Besides, the accurate masses corresponded to two further sulfur containing derivatives of DON, namely DON-GSH ($\Delta\text{ppm} -0.7$) and DON-cysteine ($\Delta\text{ppm} -0.2$). They were detected in the lysate of HepG2, HT29, and Caco-2 cells. In cell lines originating from liver (HepG2) and colon tumors (HT29, Caco-2) the number and relative concentrations of biotransformation products were higher than in kidney and bladder-derived cell lines. As the uptake of DON was slightly higher in HT29 than in Caco-2, HT29 was selected as an intestinal cell model besides HepG2 which served as a model for liver metabolism.

Initially, six-well plates were chosen for growing cells since formats with a lower volume resulted in low cell numbers and the inability to detect any DON biotransformation product by LC-HRMS. However, during the course of these pre-experiments we encountered that even six-well plates allowed only for the detection of the most abundant known biotransformation products but failed to enable the identification of low-abundance metabolites of potentially high biological impact. Therefore, we further up-scaled the

approach to Petri dishes in order to maximize cell number and thus the concentrations of DON and its known and yet unknown metabolites in the cell lysate and in the extracellular medium. In addition, we increased the xenobiotic concentration from 1 μM to 10 μM (each 5 μM ¹²C-DON and ¹³C-DON). However, this required the incubation time to be reduced to 3 h since 10 μM DON induces cytotoxicity when cells are exposed to the mycotoxin for a longer period of time.^{16,30}

The chromatographic separation was optimized in order to allow for the separation of DON conjugate isomers. The retention of DON on C-18 RP columns is known to be typically very limited due to its high polarity. Phase II metabolites are even more polar, and the separation of isomers constitutes a well-known separation issue.^{20,25} The selected column-eluent combination exhibited sufficient retention of the highly polar conjugates when an optimized, very flat gradient (increase from 5% to 40% eluent B between minutes 2 and 7) was applied. Different mobile phases were evaluated, and water and methanol, both containing 0.1% acetic acid, were deemed the most suitable eluents due to enhanced retention of DON conjugates. Despite the flat gradient, the total run time was below 12 min.

Stable Isotope-Assisted Data Processing and Targeted Evaluation. In order to capture all detectable biotransformation products of DON, the TracExtract approach, a module of MetExtract II,⁸ was utilized. As the exogenous DON was applied as a mixture of both native and uniformly ¹³C₁₅-labeled toxin and similar metabolization of both forms can be assumed, all biotransformation products of DON formed in the cell cultures would also be present as a native and ¹³C-labeled form, while any other metabolite in the sample itself would only be present as a purely native form but not as a ¹³C-labeled form. Thus, this characteristic can be employed to automatically search for the native and ¹³C-labeled biotransformation products of DON with the MetExtract II software. The software tool is specifically designed to automatically search for coeluting ion pairs of native and ¹³C-labeled metabolite forms. In case of DON, which consists of 15 carbon atoms, a mass difference of 15.0503 *m/z* is expected if no carbon atom is cleaved. It only reports such metabolites but ignores any other chromatographic peaks in the LC-HRMS data thereby efficiently filtering out all other nontracer-derived metabolites from the data set. The reduction of peaks by the tool is visualized in Figure 2a. A detailed comparison was not conducted in this context.

For all masses of interest, agreement (retention time, accurate mass, MS₂) with the available reference standards was checked. Known metabolites included in the multi-component standard and other metabolites described in the literature like the plant metabolites DON-GSH, DON-cysteine, and DON-cysteinylglycine^{28,34,35} were annotated automatically by MetExtract II in case they were present. According to a study by Schwartz et al.,³⁶ other potential metabolites, namely the DON-sulfonates, were included in the analysis.

Annotation of Novel Detoxification Products. The next step was the annotation of unknown biotransformation products. For ion pairs with a mass difference of 15.0503 between the ¹³C-labeled and the unlabeled compound an intact carbon scaffold of the DON-molecule was assumed. This applies to nearly all feature pairs not identified by authentic

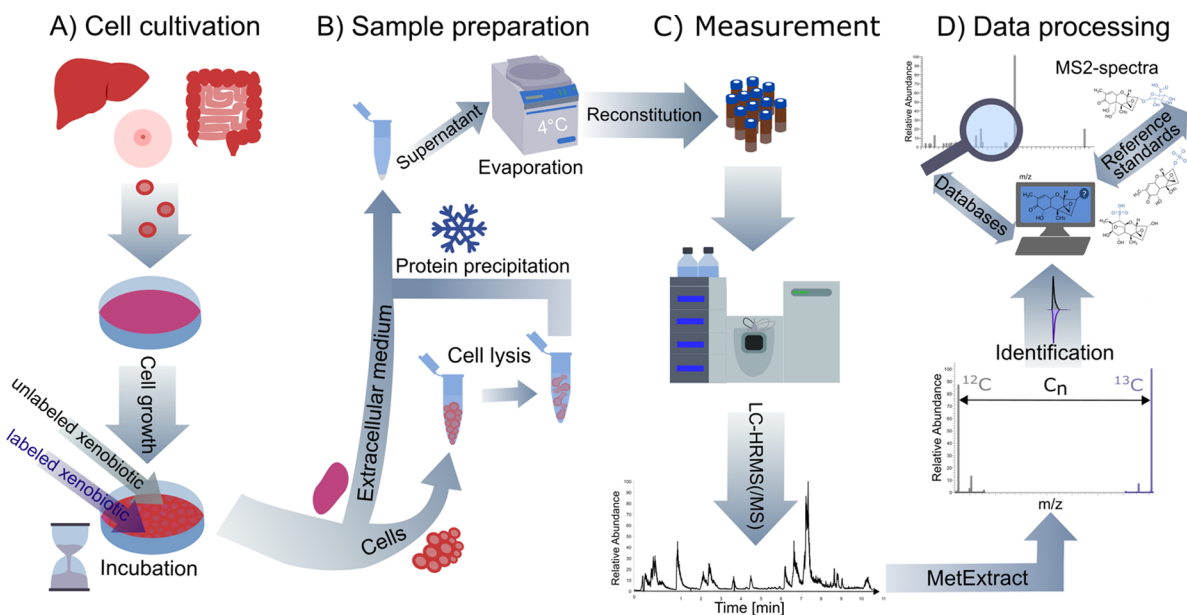


Figure 1. Schematic representation of the developed workflow for the stable isotope-assisted elucidation of xenobiotic metabolism in human cells including (A) cell cultivation, (B) sample preparation, (C) LC-HRMS (/MS)-measurement, and (D) data processing and annotation. Metabolism of the model xenobiotic DON was investigated in an intestine and liver cell model.

standards or reference MS2 spectra. Based on the known metabolites, thiols are conjugated to DON either via Michael addition at position C-10 or at position C-13, opening the epoxide moiety. Another possible reaction is the conjugation of DON at a hydroxy group, mainly at positions C-3 and C-15, by enzymatic reaction with activated cosubstrates (UDP-glucuronic acid, acetyl-CoA, or 3'-phosphoadenosine-5'-phosphosulfate) and elimination of water. The potential reaction sites of DON for glucuronidation (or glucosylation), acetylation, sulfation, and for reaction with thiol groups (like sulfonation) are highlighted in Figure 2b. With this knowledge the exact mass of molecules possibly conjugated to DON was calculated, and databases like the HMDB,³⁷ METLIN,³⁸ and MassBank³⁹ were explored to see if matching molecules potentially conjugated to DON could be found. In order to further characterize annotated conjugates, MS2 spectra were recorded and compared to reference spectra from mzCloud. As no reference spectra for the intact conjugates were available, reference spectra of the binding molecules were considered. The comprehensive workflow established is shown schematically in Figure 1.

In this study MetExtract II was applied to mammalian tissue culture, revealing ten ion pairs of interest. Authentic reference standards (commercially available or in-house synthesized), as well as MS2 reference spectra from the literature^{28,34,40} and the public databases HMDB,³⁷ METLIN,³⁸ and MassBank,³⁹ served to annotate eight of the ten ion pairs of interest. In addition, one biotransformation product, DON-glutamylcysteine, was detected only manually. The identity of two metabolites, DON-3-sulfate and DONS2, was confirmed at level 1 by authentic reference standards. Other metabolites present in the standard mix such as the DON-glucuronides, acetyl-DONs, and acetyl-DON-sulfates were not detected. Table 1 reports all annotated and identified metabolites of DON. Most metabolites were annotated exclusively in the positive ionization mode, while DON-3-sulfate and DONS2 were solely detected in the negative ionization mode. The parent compound DON was found in both modes as well as

DON-GSH and a putative DON-isoleucine/leucine conjugate. MS2 spectra were acquired for all compounds detected by MetExtract II, partly in additional experiments with inclusion lists and increased injection volume. DON-3-sulfate and DON-15-sulfate were distinguished by their fragmentation pattern. The fragment $[M - \text{CH}_2\text{O} - \text{H}]^-$ with m/z 345.3425, which is formed when the CH_2OH group at the C-6 position is cleaved off, is unique for DON-3-sulfate as for DON-15-sulfate the sulfate group is attached at this position.²⁹ The described fragment was present at the earlier eluting peak at 4.37 min (standard compound). In the sample a peak at retention time 4.37 min, matching DON-3-sulfate was detected. Due to the low abundance of DON-sulfates in the sample, the fragment at m/z 345.3425 was not present in the MS2 spectrum of the sample (Supplementary Figure 1). Based on the availability of both DON-sulfate standards and measured retention times, the candidate was annotated as DON-3-sulfate.

The extracted ion chromatograms (XIC) at m/z 377.0916 of the sample containing DON-sulfonate $[M - \text{H}]^-$ was compared to single standards of three different DON-sulfonate isomers (Supplementary Figure 2). DONS1 (around 1.51 min) elutes earlier than DONS2 (around 3.40 min) and DONS3 (around 3.91 min). The peak in the experimental sample (extracellular medium, HT29) appeared at 3.33 min, which agrees with the retention time of the DONS2 standard. In the acquired MS2 spectrum, besides the parent ion, two further matching fragments (m/z 265.11 and m/z 138.03) were present in both the single standard of DONS2 and in the cell-derived sample. DON-10-GSH (Supplementary Figure 3) and DON-10-cysteine (Supplementary Figure 4) were characterized at identification level 2a by a successful match with MS2 spectra from the literature.^{34,40} In addition, a comparison of the MS2 spectrum and the retention time with a wheat sample in which the presence of DON-10-GSH was confirmed before³⁵ further supported the identification. The remaining conjugates were annotated at level 2b (probable structure/diagnostic). The masses observed are consistent with the formation of adducts with different amino acids and an adduct

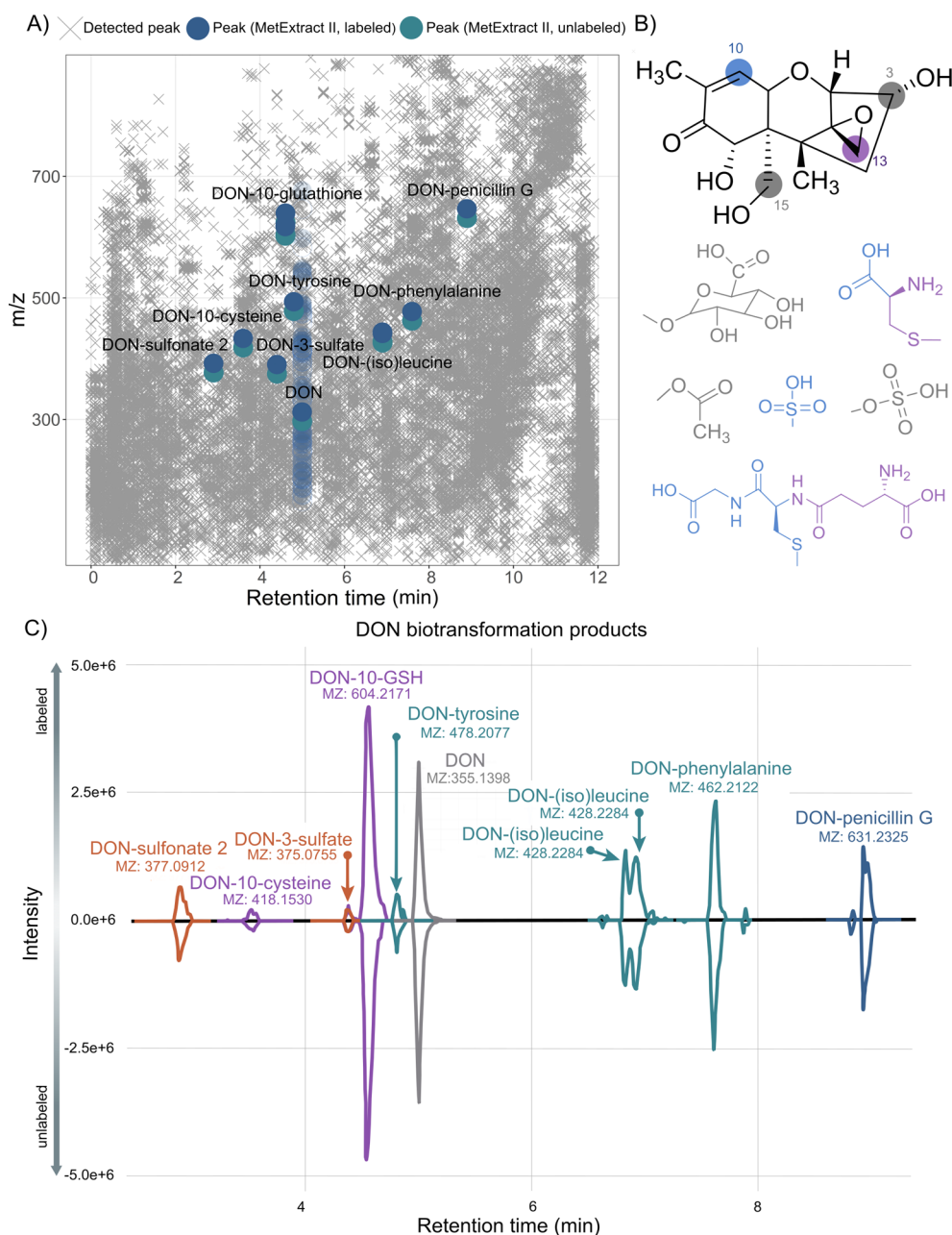


Figure 2. Overview of data reduction by MetExtract, chemical structure and potential reaction sites of the food toxin DON, and detected biotransformation products. (A) All detected features in the analyzed samples are illustrated by gray X's (X). Features of metabolic products of deoxynivalenol detected by the MetExtract II algorithm are highlighted in blue, and features related to the parent molecule DON (eluting at 5 min) are shown in faded blue symbols (except for the $[M + H]^+$ adduct) for better visibility. (B) Possible reaction sites for conjugation of DON. Positions C-3 and C-15 are targets for sulfate-, glucuronide-, and acetyl-conjugation. GSH as well as cysteine conjugates are formed at positions C-10 and C-13. DON-sulfonates are preferably formed by Michael addition at position C-10. (C) XIC chromatograms of annotated DON metabolites. The XICs of the native metabolite forms are shown with negative intensities, while the XICs of the ^{13}C -labeled metabolite forms are shown with positive intensity values. The XICs were extracted from different raw data files, and for each metabolite the dominant adduct/in-source fragment is shown.

with penicillin G. MS2 spectra were acquired and compared to available spectra of the amino acids and the antibiotic (penicillin G) in mzCloud (Figure 3). A good agreement of the obtained MS2 spectra and the ones from the literature was found despite the generally low abundance of these metabolites in our samples. For DON-(iso)leucine two peaks were present, originating from DON-leucine and its isomer DON-isoleucine. An assignment of the isomers was not conducted, and the peaks were not baseline separated. An

overlay of the XICs of all annotated metabolites is illustrated in Figure 2c. All ion traces of the labeled metabolite ions are presented on the positive axis, while the overlaid XICs of the monoisotopic unlabeled compound ions appear on the negative axis. Most of the annotated metabolites were found in positive ionization mode; only DON-3-sulfate and DON-10-GSH were present in negative mode. DON-(iso)leucine and DON-10-GSH were detected in both polarities. In addition to the automatically by MetExtract II derived DON derivatives,

Table 1. Metabolites of the Food Contaminant Deoxynivalenol Annotated by the Stable Isotope-Assisted Approach in HT29 and HepG2 Cells

DON metabolites	RT (min)	m/z^a	ion species ^b	mass accuracy (ppm)	polarity ^c	¹³ C-atoms ^d	sum formula ^e	level ^f	MS2
DON	4.99	355.1402	[M + Ac] ⁻	1.1	±	15	C ₁₅ H ₂₀ O ₆	1	yes
DON-sulfonate 2	3.33	377.0907	[M - H] ⁻	-1.3	-	15	C ₁₅ H ₂₂ O ₉ S	1	yes
DON-10-cysteine	3.50	418.1529	[M + H] ⁺	-0.2	+	15	C ₁₈ H ₂₇ NO ₈ S	2a	yes
DON-glutamylcysteine ^g	4.25	547.1955	[M + H] ⁺	-0.2	+	15	C ₂₃ H ₃₄ N ₂ O ₁₁ S	4	no
DON-3-sulfate	4.38	375.0748	[M - H] ⁻	-1.9	-	15	C ₁₅ H ₂₀ O ₉ S	1	yes
DON-10-glutathione	4.56	604.2167	[M + H] ⁺	-0.7	±	15	C ₂₅ H ₃₇ N ₃ O ₁₂ S	2a	yes
DON-tyrosine	4.81	478.2075	[M + H] ⁺	-0.5	+	15	C ₂₄ H ₃₁ O ₉ N	2b	yes
DON-(iso)leucine	6.91	428.2280	[M + H] ⁺	-1.0	±	15	C ₂₁ H ₃₃ O ₈ N	3	yes
DON-phenylalanine	7.59	462.2121	[M + H] ⁺	-0.2	+	15	C ₂₄ H ₃₁ O ₈ N	2b	yes
DON-penicillin G	8.96	631.2313	[M + H] ⁺	-1.9	+	15	C ₃₁ H ₃₈ N ₂ O ₁₀ S	2b	yes

^aAccurate mass of most abundant ion species of each metabolite based on MS2 spectra from the second run. ^bMost abundant ion species. ^cPolarity where metabolite could be detected. ^dNumber of ¹³C-atoms in the labeled conjugate. ^eSum formula of the neutral metabolite. ^fIdentification level based on Schymanski et al.⁴¹ ^gManually detected, not picked up by MetExtract.

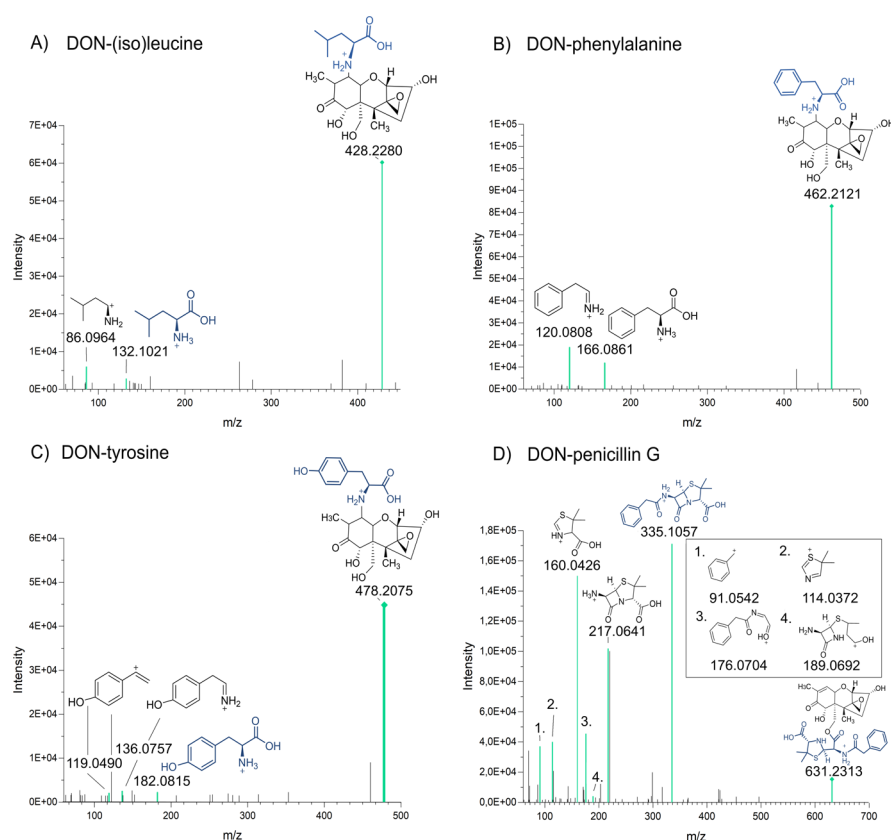


Figure 3. MS2 spectra illustrating conjugates of DON with amino acids and an antibiotic in positive mode [M + H]⁺, where fragments present in the spectra of the pure compound found in *mzCloud* too are colored in turquoise. All spectra were acquired with a stepped normalized collision energy at 20 and 50 eV. (A) MS2 spectrum of DON-isoleucine/leucine of m/z 428.2292 at 6.82 min, (B) MS2 spectrum of DON-phenylalanine of m/z 462.2120 at 7.61 min, (C) MS2 spectrum of DON-tyrosine of m/z 478.2074 at 4.81 min, and (D) MS2 spectrum of DON-penicillin G of m/z 631 at 8.06 min.

another conjugate, DON- γ -glutamylcysteine (m/z 547.1856, 4.25 min), was found manually at 4.25 min in the lysate of two out of three HepG2 samples. The retention time was, as expected, between those of DON-10-cysteine (3.56 min) and DON-10-GSH (4.57 min). However, the annotation of DON- γ -glutamylcysteine was somehow uncertain as the peak was of low abundance and no MS2 spectrum was triggered. The chemical structures of the newly annotated DON-metabolites remained ambiguous, and the reported conjugation sites can be regarded as preliminary as standards were lacking and the MS2 spectra did not contain enough information to determine their

precise structure. Based on theoretical mass calculation of DON conjugates (i.e., addition without loss of water), the only possible reaction sites for conjugation were at position C-10 or at position C-13 (Figure 2b).

Occurrence of Biotransformation Products. Not only the cell lysate samples but also the extracellular medium (supernatant) of the cells were screened for the presence of DON-metabolites excreted by the cells (Figure 4). In both cell lines, HT29 and HepG2, the abundance of the DON-metabolites was higher in the supernatant as compared to the lysate samples. Only DON-10-GSH and DON-10-cysteine

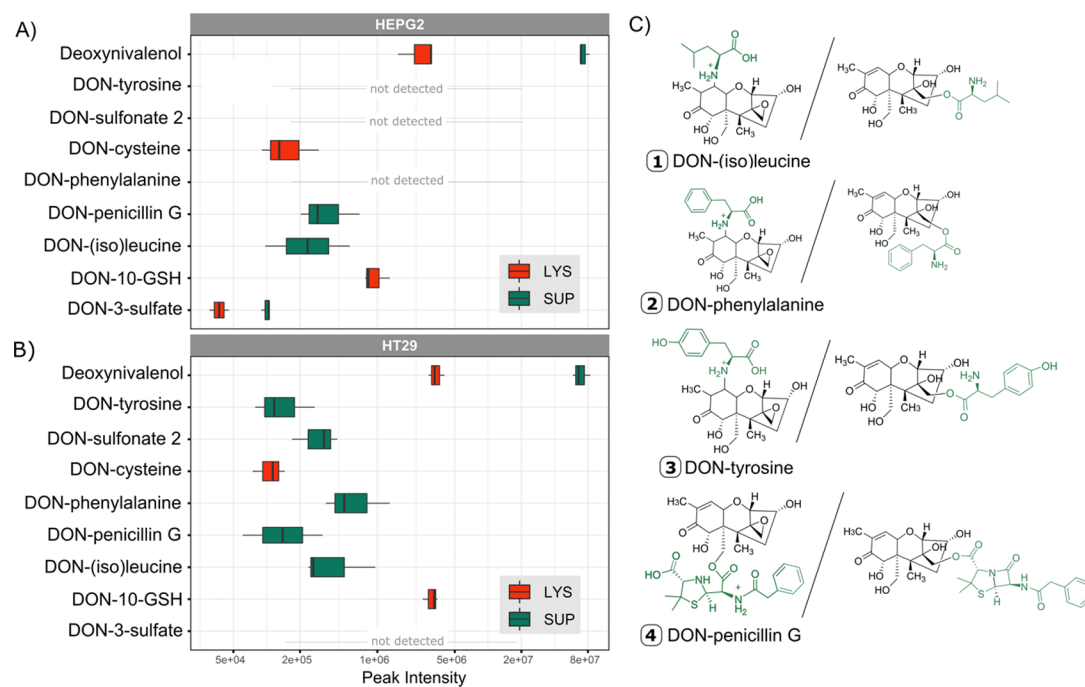


Figure 4. Peak intensities of annotated DON metabolites. (A) Peak intensities of unlabeled DON-metabolites in supernatant (SUP, green) and lysate (LYS, red) of HepG2 (top). Except for DON-3-sulfate and DONS2, measurements of the positive mode are shown. The average of all three biological replicates with a maximum $n = 3$ is plotted. The metabolite had to be present in at least two out of the three replicates. A logarithmic scale was used for the x -axis (abundance). (B) Abundance of unlabeled DON-metabolites in supernatant (green) and lysate (red) of HT29 (bottom). Except for DON-3-sulfate and DONS2 measurements of the positive mode are shown. The average of all three biological replicates with a maximum $n = 3$ was taken. The metabolite had to be present in at least two out of the three replicates. A logarithmic scale was used for the x -axis (abundance). (C) Putative structures of amino acids and xenobiotic conjugates of DON with both possible structures. For DON-penicillin G conjugation can occur either after epoxide opening at C-13 or at C-15-OH and C-3-OH (not shown) after lactam opening. For DON amino acid adducts the options include conjugation after epoxide opening at C-13 or at C-10 by Michael addition.

were present exclusively in the lysate. Very low amounts of DON-3-sulfate were present in the lysate of HepG2 cells although the concentration was about three times lower than in the supernatant. All amino acid conjugates except the sulfur-containing cysteine and the penicillin conjugate were solely present in the supernatant. Interestingly, the sulfo-conjugation pattern was different in the supernatant of both cell lines. DON-3-sulfate was produced only in HepG2 cells, while DONS2 was excreted by HT29 cells. Amino acids and penicillin G were present in the medium; thus, a direct chemical reaction could theoretically be responsible for the conjugation of DON to these molecules. Consequently, an additional control experiment (#2) without cells but identical incubation conditions was performed. None of the DON biotransformation products were detected in the cell-free incubations, strongly supporting a cell mediated and enzymatic formation of the observed metabolites. Absolute quantification of the produced metabolites was not possible as no standards for the newly described compounds were available. However, in additional spiking experiments an average recovery of >90% in the cell lysates and >50% in the supernatants for the parent toxin in both positive and negative ionization mode was observed. The discrepancy originated most likely from matrix effects. Looking at the relative abundance, DON-10-GSH was clearly the most prevalent metabolite in both cell lines reaching values of about 1×10^6 cps for HepG2 and 3×10^6 cps for HT29 in the lysate samples. The DON-10-GSH was even in the same order of magnitude as the parent compound DON in the lysate. All other metabolites were of low abundance with a maximum signal intensity of 5×10^5 cps for DON-

phenylalanine in HT29 and thereby close to the limit of detection.

DISCUSSION

The MetExtract II workflow⁸ was successfully adapted to cell culture experiments employing human cell models. The workflow provides an efficient way to detect novel biotransformation products of any xenobiotic with the only requirement that isotopically labeled substances need to be available. Our study revealed that various detoxification strategies were used by the tested cell models, and some metabolites were detected and further characterized for the first time. In humans, glucuronidation is normally by far the most prominent detoxification pathway *in vivo*.²⁰ Interestingly, the formation of DON glucuronides in human cell culture was not confirmed to date.^{19,42,43} In our tissue culture models DON-glucuronides were also absent despite the presence of uridine 5'-diphosphate (UDP)-glucuronosyltransferase transcripts involved in their formation.^{44–46} We assume that the concentrations of potentially formed DON glucuronides were most likely too low to be detected since the ionization efficiency of these conjugates was described as limited.³⁰

DON-GSH and Related Metabolites. A common phase II reaction is glutathione conjugation. In plants this tripeptide conjugate and its processing products DON-cysteinylglycine and DON-cysteine have been described.⁹ However, glutathione-conjugate formation of DON has not been recognized as a mammalian detoxification mechanism so far. We are only aware of one previous study indicating that this pathway seems to exist for DON.⁴⁷ In our experiment, we found two isomers

of DON-10-GSH and DON-10-cysteine. The fragmentation pattern indicates that both were conjugated at position C-10 via Michael addition. The two isomers of DON-10-GSH had different fragmentation patterns,³⁴ but both of them were likely to originate from DON-10-GSH as m/z 179.0482 (first peak, 4.36 min) and m/z 130.0499 (second peak, 4.54 min) were the most prominent peaks. Fragments like m/z 281.0836 and m/z 263.0733 characteristic for DON-13-GSH³⁴ were absent. A comparison to a wheat sample in which this metabolite was previously found confirmed this annotation. Thus, they were probably derived from 9,10-diastereoisomers of the Michael adduct described in Stanic et al.³⁴ which was formed in a nonenzymatic reaction with GSH after extended incubation at alkaline pH. The fragmentation pattern in the negative ionization mode supported this with a product ion at m/z 306.0772 being the base peak. To distinguish between a spontaneous reaction with glutathione and a glutathione-S-transferase (GST)-mediated conjugate formation, we performed incubations with the cell free medium. Neither DON-10-GSH nor other conjugates were detected in this control experiment (#2), indicating that the reaction was mediated by the cells. It is very unlikely that conditions exist in the cells that would allow for the nonenzymatic formation of Michael adducts. In the nonenzymatic synthesis of DON-10-GSH the reactants DON and GSH had to be incubated at pH 10.7 for 9 d.³⁴ Formation in most alkaline compartments in the cells, such as the mitochondrial matrix (reported pH 8.5, Abad et al.⁴⁸) or the peroxisomes (pH 8.2, Dansen et al.⁴⁹), seems unlikely considering the short incubation time of 3 h. On the other hand, so far no mammalian GST catalyzing the DON-GSH adduct formation is known, and trichothecenes are generally believed to be unreactive with GSTs.⁵⁰ However, plant GSTs catalyzing the formation of DON conjugates were recently identified.⁵¹ The level of glutathione S-transferases is lower in HepG2 compared to HT29 cells,⁵² which may explain the higher amount of formed DON-10-GSH in the colon carcinoma cell line compared to HepG2. DON-glutamylcysteine was detected in the lysate. During GSH-biosynthesis, γ -glutamylcysteine formation from glutamate and cysteine is the rate-limiting step catalyzed by the enzyme γ -glutamylcysteine ligase.⁵³ Again, a spontaneous reaction with the GSH precursor present in low amounts in the cell cannot be excluded, but the more likely explanation is that an enzymatically formed DON-GSH conjugate was processed by a peptidase cleaving glycine faster than the reaction occurred with γ -glutamyl-transpeptidase. Both activities are needed to generate DON-cysteine from DON-GSH. Cysteine might directly react nonenzymatically as well³⁵ in an alkaline cell compartment, but this seems unlikely. A subsequent step in the detoxification through the mercapturic pathway would be the formation of *N*-acetyl-cysteine-DON.⁵⁴ Neither our MetExtract II analysis nor a manual search of the LC-HRMS(/MS) raw data resulted in the detection of a metabolic feature corresponding to the m/z value of this structure, which might be explained by the short incubation time and the very low abundance already of the precursor DON-cysteine, which resulted in an MS2 spectrum with low intensity fragments. In one sample the fragment of the intact DON was present, indicating that the found substance was likely to be DON-S-10-cysteine. This was further supported by comparison with a literature spectrum.⁴⁰ The positive mode MS2 spectrum of the epoxide adduct included prominent fragments at m/z 388.1427, m/z 281.0846, and m/z 263.0739. Neither of them was present in our

spectrum. Moreover, product ions at m/z 122.0268 (Δ 4.9 ppm) and m/z 401.1268 (Δ 0.2 ppm) were detected in our study and were also reported in the published spectrum of DON-10-cysteine.⁴⁰

DON-Sulfate and Sulfonate. Two sulfur conjugates were identified by comparison with reference standards, namely DON-3-sulfate and DON-sulfonate 2. DON-3-sulfate was identified before as a minor metabolite in human urine.³⁰ However, DON-sulfonate was previously unknown to be produced by humans. It has only been described in rats and chickens so far.^{23,55} Several hypotheses have been formulated as to how DON-sulfonates are formed in animals by Wan et al.⁵⁵ One possible pathway is formation via the DON-GSH conjugate. After a breakdown to DON-cysteine, enzymatic cleavage of the conjugate by cysteine-S-conjugate β -lyase, the hypothetical DON-SH could be formed. It is known that in proteins the SH group of cysteine can be further oxidized⁵⁶ all the way to the sulfonate group. Yet, the oxidation of DON-SH would need high levels of H₂O₂ that are unlikely to exist in cells, potentially with the exception of peroxisomes. Another possibility would be the formation of sulfite from sulfate followed by nonenzymatic Michael addition to DON.^{23,55} The cell culture medium (DMEM) contains low amounts of magnesium sulfate but high levels of glutathione and cysteine as a sulfur source. We therefore propose as alternative, that cysteine is first converted by cysteine dioxygenase (KEGG R00893) to 3-sulfinyl-L-alanine. In the second step SO₂ could be released either enzymatically by 3-sulfinyl-L-alanine 4-carboxy-lyase (KEGG R00863) or by spontaneous decay of this compound into alanine and SO₂. The SO₂ released is in an equilibrium with sulfite,⁵⁷ which then might form non-enzymatically the Michael adduct.

Amino Acid and Penicillin Conjugates. The remaining ion pairs extracted by the MetExtract II algorithm were not identified by reference standards or respective literature spectra. When subtracting the mass of DON, the obtained masses were matching not only amino acids including phenylalanine, tyrosine, and (iso)leucine but also surprisingly the antibiotic penicillin G. As building blocks of proteins, amino acids are basal ingredients of cell culture, and higher concentrations can be found in DMEM (HT29) compared to RPMI 1640 (HepG2). In order to prevent bacterial contamination of the cell cultures, penicillin G was used as a supplement in both media. Conjugation with amino acids is a well-known metabolic reaction of xenobiotics in the human body. Typically, xenobiotics with a carboxyl group like salicylic acid or valproic acid are activated by the formation of CoA derivatives, which can react with the amino group of amino acids to build the corresponding *N*-substituted amides. A frequent reaction partner is glycine but also glutamine, glutamate, and taurine are involved. In most cases this is only a minor pathway in xenobiotic metabolism.⁵⁸ DON does not have a carboxy group to be activated for conjugation. The only primary alcohol that could be converted to a carboxy group is C15-OH, but the subsequent amide formation with an amino acid would not lead to a mass consistent with the observed reaction product. The formation of an adduct which fits the mass of the found novel DON-amino acid conjugates can either occur at the epoxide moiety or by addition at the double bond without water loss. The putative structures of both options are presented in Figure 4c. In the first scenario, the epoxide would be opened (by an epoxide hydrolase, +H₂O), and subsequently an ester with the carboxy group of

the amino acid would be formed ($-\text{H}_2\text{O}$). However, this is highly unlikely because so far no epoxide-hydrolase being able to act on the trichothecene's epoxide has ever been characterized,⁵⁹ and also the ester formation between the formed diol and the carboxy group is improbable to happen spontaneously. For the ester formation the amino acid would have to be activated to a thioester, which could occur by formation of an adenylate by tRNA synthetases or by a direct reaction with the charged tRNAs. Enzymes catalyzing ester formation with activated nonstandard amino acids have been described in secondary metabolite biosynthetic pathways (e.g., Lin et al.⁶⁰). Alternatively, direct epoxide ring opening involving the amino group with amino acid esters has been described to occur without a catalyst at harsh conditions.⁶¹ The adenylates of amino acids or charged tRNA could potentially also undergo this reaction.

The second more likely option to form a DON-amino acid conjugate which is in line with the mass of the measured molecules is a Michael adduct formation by addition of the amino group of the amino acid with the double bond of the α,β unsaturated ketone structure in DON.⁶² Potentially, such reactions could occur with N-terminal amino groups of proteins rather than with free amino acids (no reaction was observed in the cell free control). Specific proteins might catalyze such a protein-adduct formation with DON, followed by proteolytic degradation leading to release of the respective amino acid conjugate.

In the supernatant of HT29 more amino acid conjugates including DON-phenylalanine, DON-(iso)leucine, and DON-tyrosine were detected compared to the other cell line, while for HepG2 cells only DON-(iso)leucine was found. A possible reason for higher biotransformation product concentrations might be the medium as in the basal medium of the HT29 cells (DMEM) higher concentrations of amino acids are present. However, the different metabolic activity, based on the varying conjugation products of both cell lines, might be another explanation. For the formation of the DON-penicillin conjugate, again two possibilities exist (Figure 4). The carboxylic acid of penicillin G (presumably after activation to a CoA derivative) forms an ester with the opened epoxide of DON. Alternatively,—in order to arrive at the observed mass—the lactam ring of penicillin is opened ($+\text{H}_2\text{O}$) to benzylpenicilloic acid, and one of the hydroxyl groups of DON (C-3 or C-15) forms an ester with one of the two (again presumably CoA-activated) carboxyl groups.

The presented isotope-assisted approach enables the global untargeted screening of DON conjugation products in mammalian cell cultures, and application to HepG2 and HT29 cell lines resulted in several known and novel DON conjugates. The most abundant conjugate, DON-10-GSH, was known as a detoxification mechanism of DON in plants.²⁸ DON-sulfates and DON-sulfonates were also described to be less potent inhibitors of protein biosynthesis.^{30,63} The toxicity of the novel amino acid and penicillin conjugates is untested, but based on the structure of other known DON conjugates, an interaction with the ribosomal target site seems highly unlikely. However, as the majority of DON was not conjugated, the overall impact of metabolism on the toxicological potential is suspected to be minor in the specific case of DON. Only DON-10-GSH, formed in higher amounts, may have a significant effect. The pattern of metabolism for biotransformation products known in the past was clearly different from human *in vivo* experiments. Especially the lack of

glucuronidation in the cells implies a different toxicological profile compared to the human *in vivo* metabolism.

CONCLUSION

The presented comprehensive workflow demonstrated its vast potential for deciphering novel human biotransformation products of xenobiotics. It will be a highly versatile tool for the untargeted detection and structural annotation of so far unknown metabolic products of potentially any small molecule in cell culture. These metabolites are not only interesting in the context of toxicology and pharmacology but are also an important contributor to the exposome. Our results further highlight the abundant and fast metabolism of the food contaminant DON in tissue culture and demonstrate the need to investigate xenobiotic metabolism thoroughly to understand its full biological impact.

EXPERIMENTAL SECTION

Chemicals and Standards. Reference standards were purchased from RomerLabs and Sigma-Aldrich Chemie GmbH or synthesized in-house.^{64,65} The ^{13}C -DON was obtained from Romer Laboratories. A multistandard solution containing DON, de-epoxy-DON, DON-3-sulfate, DON-15-sulfate, DON-3-GlcA, DON-3,15-disulfate, 15-acetyl-DON-3-sulfate, 3,15-diacetyl-DON, 3-acetyl-DON, 3-acetyl-DON-15-sulfate, and 15-acetyl-DON was prepared in ACN/MeOH/ H_2O . In addition, individual standards of DON-sulfonate 1 (DONS1), DON-sulfonate 2 (DONS2), and DON-sulfonate 3 (DONS3), all conjugated at position C-10 and previously characterized by NMR,³⁶ were available and diluted in 10% MeOH before the measurements.

Cell Culture. Pre-experiments without the cost-intensive isotopically labeled xenobiotic were performed to identify the most suitable model cell lines with sufficient metabolic activity. Five human cell models, all purchased from ATCC, were evaluated: HT29 and Caco-2 (both colorectal adenocarcinoma cells), HepG2 (hepatocellular adenocarcinoma cells), HEK293 (embryonic kidney cells), and T24 (bladder carcinoma cells). Cells were grown in six-well plates and incubated with $1\ \mu\text{M}$ of unlabeled DON. Samples were harvested at two different time points (1 and 24 h).

For the main experiment employing native and uniformly ^{13}C labeled DON, HT29 and HepG2 were selected. HT29 cells were cultivated in Dulbecco's Modified Eagle Medium, and HepG2 cells were cultivated in RPMI 1640 Medium. Both basal media were supplemented with 10% heat inactivated fetal calf serum and 1% (v/v) of a solution containing penicillin G at $60\ \mu\text{g}\ \text{mL}^{-1}$ and streptomycin at $100\ \mu\text{g}\ \text{mL}^{-1}$ in the final medium. Cell culture media and supplements were purchased from GIBCO Invitrogen, Lonza Group Ltd., Sigma-Aldrich Chemie GmbH, and Sarstedt AG & Co. For cell cultivation and treatments humidified incubators at $37\ ^\circ\text{C}$ and 5% CO_2 were used. Cells were routinely tested for the absence of mycoplasma contamination and used for experiments at passages 10–14. Cells were seeded in 10 cm cell culture dishes ($1.500.000$ cells/Petri dish) from Sarstedt AG & Co with TC-treated surface, grown for 72 h, and incubated for 3 h after adding fresh medium containing $10\ \mu\text{M}$ of DON, consisting of $5\ \mu\text{M}$ of ^{12}C -DON and $5\ \mu\text{M}$ ^{13}C -DON. Three individual biological experiments were performed. In addition, two control experiments were executed under identical incubation conditions as during the main experiment. For this purpose, medium without DON was added to the cells (#1) and medium containing $5\ \mu\text{M}$ of ^{12}C -DON and $5\ \mu\text{M}$ ^{13}C -DON was added to Petri dishes without cells (#2) (both in triplicates).

Sample Preparation. Following incubation, 4 mL of the extracellular medium was transferred into reaction tubes and diluted 1:5 with ice-cold ACN/MeOH (1/1; v/v). The tubes were vortexed, incubated for 1 h at $-20\ ^\circ\text{C}$, and centrifuged for 15 min at $4\ ^\circ\text{C}$ to precipitate the proteins. A volume of 10 mL supernatant was transferred into 15 mL tubes and evaporated to dryness at $4\ ^\circ\text{C}$ using

a vacuum concentrator. Samples were reconstituted in 0.4 mL of dilution solvent (MeOH/water; 10/90; v/v), centrifuged, transferred to HPLC vials with microinserts, and stored at $-80\text{ }^{\circ}\text{C}$ until LC-HRMS analysis.

To evaluate intracellular metabolites, cell extracts were prepared. Cells were rinsed twice with 2.5 mL of prewarmed PBS. Subsequently, 0.7 mL of ice-cold quenching solution (ACN/MeOH/water; 40/40/20; v/v/v) was added. Cells were scraped off and transferred into reaction tubes, before three cycles of freeze–thaw cycles and sonication were performed for cell lysis and metabolite extraction as follows: a) vortex for 30 s, b) liquid nitrogen for 1 min, c) thawing, and d) ultrasonication in ice bath for 10 min. To aid protein precipitation, the samples were incubated at $-20\text{ }^{\circ}\text{C}$ for 1 h after extraction, followed by centrifugation at 15,000 rpm and $4\text{ }^{\circ}\text{C}$. Supernatants were transferred into a new reaction tube and evaporated to dryness. Thereafter, the dried extracts were reconstituted in 240 μL of dilution solvent (MeOH/water; 10/90; v/v), sonicated for 10 min, and centrifuged for 15 min at 15,000 rpm and $4\text{ }^{\circ}\text{C}$. Samples were transferred to HPLC vials with microinserts and stored at $-80\text{ }^{\circ}\text{C}$ until LC-MS/MS analysis.

To verify that conjugation with media components was mediated by the cells and not an artifact or a chemical reaction, a cell-free and a DON-free incubation was repeated exactly as described above. Moreover, a spiking experiment was performed to estimate matrix effects during electrospray ionization. For this purpose, cell lysate samples and extracellular medium from HepG2 and HT29 incubations in which no DON was added to the medium (control experiment #1) were fortified in triplicate with native DON only.

LC-HRMS (/MS) Analysis. The samples were measured using a Vanquish UHPLC system coupled to a QExactive HF quadrupole-Orbitrap mass spectrometer via an ESI interface. A volume of 5 μL was injected onto an Acquity HSS T3, column (1.8 μm , $150 \times 2.1\text{ mm}$) maintained at $40\text{ }^{\circ}\text{C}$. The flow rate was set to 0.5 mL min^{-1} . A gradient using water with 0.1% acetic acid (v/v) (eluent A) and methanol with 0.1% acetic acid (v/v) (eluent B) was applied. The gradient was optimized for separating highly polar DON conjugate isomers as follows: 0–2 min, 5% B; 2–7 min linear increase to 40% B; 7–9 min, linear increase to 100% B; 9–10.9 min, 100% B; 10.9–11 min, linearly decreased to 5% B; 11–11.9 min, equilibration at 5% B. The measurements were conducted consecutively in positive and negative mode. The settings of the ESI interface were as follows: sheath gas, 53 au; auxiliary gas, 14 au; capillary voltage, 3.5 kV (positive), 3.2 kV (negative); capillary temperature, $350\text{ }^{\circ}\text{C}$.

Full scan MS and data dependent MS2 spectra (ddMS2) for the ten most abundant ions in each full scan were acquired in a scan range of 60–900 m/z . The resolution (fwhm) was set to 60,000 (@ m/z 200) for full scan and 30,000 (@ m/z 200) for ddMS2 experiments. The automatic gain control (AGC) was set to 1×10^6 with a maximum injection time of 100 ms in full scan, whereas for the acquisition of ddMS2 2×10^5 with a maximum injection time of 60 ms was applied. The isolation window for the ddMS2 scans was 1 m/z . The ten most abundant ions (top 10) were selected for MS2 analysis. A stepped normalized collision energy (NCE) at 20 and 50 eV was applied. A minimum AGC of 1×10^3 and an intensity threshold of 1.7×10^4 were chosen. The apex trigger was set to 2–5 s. Dynamic exclusion was activated for 8 s. For generating MS2 spectra of suspected DON conjugates, the settings were adapted as follows: scan range, m/z 100–900; apex trigger, 3–8 s; dynamic exclusion, 10 s. Furthermore, an inclusion list consisting of all masses of interest was created (Supplementary Table 1). Specific m/z values for which MS2 spectra were already acquired in the initial run and the most abundant peaks in a solvent blank were suspended from MS2 triggering by an exclusion list. The injection volume was increased up to 20 μL in remeasurements in order to record spectra of higher quality for low abundance metabolites. The analysis of the samples obtained within the preliminary experiments was carried out according to Warth et al.³⁰

Data Processing. To find all detectable biotransformation products of DON—known as well as putative novel ones—the MetExtract II software (module TracExtract) was employed.⁸ Briefly

summarized, the software searched the LC-HRMS data for pairs of two chromatographic peaks from biotransformation products of DON that incorporated either the native or the uniformly ^{13}C -labeled DON tracer. Such pairs showed complete chromatographic coelution as well as an m/z difference corresponding to the number of carbon atoms from the ^{13}C -labeled DON. Any metabolite or chromatographic peak in the LC-HRMS data that was only present as a single form (i.e., native, non- ^{13}C -labeled form) was ignored by the software as it could be concluded that this peak was not derived from a biotransformation product of DON but rather an endogenous metabolite of the cells or any other unspecific compound (e.g., contamination, extraction artifact) present in the sample. Parameter settings for MetExtract II were as follows: module: TracExtract; intensity threshold (M and M'): 1.104 cps; ratio of native and ^{13}C -labeled tracer form: 0.75–1.25; number of carbon atoms searched for: 10–15 and 30 (for dimer ions); number of isotopologs checked: 2; maximum isotopolog deviation from expected relative abundance: 25%; XIC (ppm): 5; maximum mass deviation (ppm): 5; Pearson correlation threshold (minimum): 0.85. Thermo Xcalibur Qual Browser and TraceFinder (Thermo Scientific) were used for further data evaluation. The graphs of the MS2 spectra were drawn using OriginPro 2018 or directly exported from Xcalibur. The preparation of pictures and graphical illustrations were done with Inkscape. The data processing for Figure 2a is described in the Supporting Information. Metabolite identification levels reporting follow the scheme proposed by Schymanski et al.⁴¹ For Figure 2a the raw data files from all samples were transformed to a mzML file with ProteoWizard (version 3). The xcms R-package was used to perform peak picking with the CentWave algorithm using the following setting: peakwidth: 5–40 s; noise: 1000; ppm: 5. The detected features are represented by gray x's in the figure.

■ ASSOCIATED CONTENT

Supporting Information

The Supporting Information is available free of charge at <https://pubs.acs.org/doi/10.1021/acschembio.9b01016>.

Abbreviations, additional MS2 spectra and chromatograms of annotated metabolites, inclusion list for MS2 generation, and author contributions (PDF)

■ AUTHOR INFORMATION

Corresponding Author

Benedikt Warth – Department of Food Chemistry and Toxicology, Faculty of Chemistry, University of Vienna, 1090 Vienna, Austria; orcid.org/0000-0002-6104-0706; Phone: +43 664 60277 70806; Email: benedikt.warth@univie.ac.at

Authors

Mira Flasch – Department of Food Chemistry and Toxicology, Faculty of Chemistry, University of Vienna, 1090 Vienna, Austria; orcid.org/0000-0002-3518-3885

Christoph Bueschl – Department of Agrobiotechnology, IFA-Tulln, Institute of Bioanalytics and Agro-Metabolomics, University of Natural Resources and Life Sciences, Vienna (BOKU), 3430 Tulln, Austria; orcid.org/0000-0003-1729-9785

Lydia Woelflingseder – Department of Food Chemistry and Toxicology, Faculty of Chemistry, University of Vienna, 1090 Vienna, Austria

Heidi E. Schwartz-Zimmermann – Department of Agrobiotechnology, IFA-Tulln, Institute of Bioanalytics and Agro-Metabolomics, University of Natural Resources and Life Sciences, Vienna (BOKU), 3430 Tulln, Austria

Gerhard Adam – Department of Applied Genetics and Cell Biology, University of Natural Resources and Life Sciences, Vienna (BOKU), 3430 Tulln, Austria

Rainer Schuhmacher – Department of Agrobiotechnology, IFA-Tulln, Institute of Bioanalytics and Agro-Metabolomics, University of Natural Resources and Life Sciences, Vienna (BOKU), 3430 Tulln, Austria; orcid.org/0000-0002-7520-4943

Doris Marko – Department of Food Chemistry and Toxicology, Faculty of Chemistry, University of Vienna, 1090 Vienna, Austria; orcid.org/0000-0001-6568-2944

Complete contact information is available at:

<https://pubs.acs.org/10.1021/acscchembio.9b01016>

Author Contributions

[†]M.F. and C.B. contributed equally to this work.

Notes

The authors declare no competing financial interest.

ACKNOWLEDGMENTS

We would like to express our gratitude towards M. Doppler for providing wheat samples for comparison purposes and L. Niederstätter and H. Schoeny for support during the LC-HRMS measurements. The measurements were performed at the Mass Spectrometry Centre (MSC) of the Faculty of Chemistry at the University of Vienna. Furthermore, we would like to thank the Austrian Science Fund (SFB Fusarium #F3702, #F3715, and #F3718) as well as the Provincial Government of Lower Austria (projects NoBiTUM, OMICS 4.0) for financial support.

REFERENCES

- (1) Rappaport, S. M., and Smith, M. T. (2010) Environment and Disease Risks. *Science* 330, 460–461.
- (2) Niedzwiecki, M. M., Walker, D. I., Vermeulen, R., Chadeau-Hyam, M., Jones, D. P., and Miller, G. W. (2019) The Exposome: Molecules to Populations. *Annu. Rev. Pharmacol. Toxicol.* 59, 107–127.
- (3) Vermeulen, R., Schymanski, E. L., Barabási, A.-L., and Miller, G. W. (2020) The exposome and health: Where chemistry meets biology. *Science* 367, 392–396.
- (4) Ashrap, P., Zheng, G., Wan, Y., Li, T., Hu, W., Li, W., Zhang, H., Zhang, Z., and Hu, J. (2017) Discovery of a widespread metabolic pathway within and among phenolic xenobiotics. *Proc. Natl. Acad. Sci. U. S. A.* 114, 6062–6067.
- (5) Croom, E. (2012) Chapter Three - Metabolism of Xenobiotics of Human Environments, In *Prog. Mol. Biol. Transl. Sci.* (Hodgson, E., Ed.), pp 31–88, Academic Press, DOI: 10.1016/B978-0-12-415813-9.00003-9.
- (6) Nicholson, J. K., and Wilson, I. D. (2003) Understanding 'Global' Systems Biology: Metabonomics and the Continuum of Metabolism. *Nat. Rev. Drug Discovery* 2, 668–676.
- (7) Gertsman, I., and Barshop, B. A. (2018) Promises and pitfalls of untargeted metabolomics. *J. Inherited Metab. Dis.* 41, 355–366.
- (8) Bueschl, C., Kluger, B., Neumann, N. K. N., Doppler, M., Maschietto, V., Thallinger, G. G., Meng-Reiterer, J., Kraska, R., and Schuhmacher, R. (2017) MetExtract II: A Software Suite for Stable Isotope-Assisted Untargeted Metabolomics. *Anal. Chem.* 89, 9518–9526.
- (9) Kluger, B., Bueschl, C., Lemmens, M., Berthiller, F., Häubl, G., Jaunecker, G., Adam, G., Kraska, R., and Schuhmacher, R. (2013) Stable isotopic labelling-assisted untargeted metabolic profiling reveals novel conjugates of the mycotoxin deoxynivalenol in wheat. *Anal. Bioanal. Chem.* 405, 5031–5036.
- (10) Meng-Reiterer, J., Varga, E., Nathanail, A. V., Bueschl, C., Rechthaler, J., McCormick, S. P., Michlmayr, H., Malachová, A., Fruhmann, P., Adam, G., Berthiller, F., Lemmens, M., and Schuhmacher, R. (2015) Tracing the metabolism of HT-2 toxin and T-2 toxin in barley by isotope-assisted untargeted screening and quantitative LC-HRMS analysis. *Anal. Bioanal. Chem.* 407, 8019–8033.
- (11) Chassy, A. W., Bueschl, C., Lee, H., Lerno, L., Oberholster, A., Barile, D., Schuhmacher, R., and Waterhouse, A. L. (2015) Tracing flavonoid degradation in grapes by MS filtering with stable isotopes. *Food Chem.* 166, 448–455.
- (12) Nathanail, A. V., Varga, E., Meng-Reiterer, J., Bueschl, C., Michlmayr, H., Malachova, A., Fruhmann, P., Jestoi, M., Peltonen, K., Adam, G., Lemmens, M., Schuhmacher, R., and Berthiller, F. (2015) Metabolism of the Fusarium Mycotoxins T-2 Toxin and HT-2 Toxin in Wheat. *J. Agric. Food Chem.* 63, 7862–7872.
- (13) EFSA (2013) Deoxynivalenol in food and feed: occurrence and exposure. *EFSA Journal* 11, 3379.
- (14) Pestka, J. J. (2010) Deoxynivalenol: mechanisms of action, human exposure, and toxicological relevance. *Arch. Toxicol.* 84, 663–679.
- (15) Pestka, J. J., Uzarski, R. L., and Islam, Z. (2005) Induction of apoptosis and cytokine production in the Jurkat human T cells by deoxynivalenol: role of mitogen-activated protein kinases and comparison to other 8-ketotrichothecenes. *Toxicology* 206, 207–219.
- (16) Payros, D., Alassane-Kpembi, I., Pierron, A., Loiseau, N., Pinton, P., and Oswald, I. P. (2016) Toxicology of deoxynivalenol and its acetylated and modified forms. *Arch. Toxicol.* 90, 2931–2957.
- (17) Turner, P. C., Rothwell, J. A., White, K. L. M., Gong, Y., Cade, J. E., and Wild, C. P. (2008) Urinary deoxynivalenol is correlated with cereal intake in individuals from the United Kingdom. *Environ. Health Perspect.* 116, 21–25.
- (18) Deng, C., Li, C., Zhou, S., Wang, X., Xu, H., Wang, D., Gong, Y., Routledge, M. N., Zhao, Y., and Wu, Y. (2018) Risk assessment of deoxynivalenol in high-risk area of China by human biomonitoring using an improved high throughput UPLC-MS/MS method. *Sci. Rep.* 8, 3901.
- (19) Šarkanj, B., Warth, B., Uhlig, S., Abia, W. A., Sulyok, M., Klapek, T., Kraska, R., and Banjari, I. (2013) Urinary analysis reveals high deoxynivalenol exposure in pregnant women from Croatia. *Food Chem. Toxicol.* 62, 231–237.
- (20) Warth, B., Sulyok, M., Fruhmann, P., Berthiller, F., Schuhmacher, R., Hametner, C., Adam, G., Fröhlich, J., and Kraska, R. (2012) Assessment of human deoxynivalenol exposure using an LC-MS/MS based biomarker method. *Toxicol. Lett.* 211, 85–90.
- (21) Vidal, A., Claeys, L., Mengelers, M., Vanhoorne, V., Vervaeke, C., Huybrechts, B., De Saeger, S., and De Boevre, M. (2018) Humans significantly metabolize and excrete the mycotoxin deoxynivalenol and its modified form deoxynivalenol-3-glucoside within 24 h. *Sci. Rep.* 8, 5255.
- (22) Warth, B., Sulyok, M., Berthiller, F., Schuhmacher, R., and Kraska, R. (2013) New insights into the human metabolism of the Fusarium mycotoxins deoxynivalenol and zearalenone. *Toxicol. Lett.* 220, 88–94.
- (23) Schwartz-Zimmermann, H. E., Hametner, C., Nagl, V., Slavik, V., Moll, W.-D., and Berthiller, F. (2014) Deoxynivalenol (DON) sulfonates as major DON metabolites in rats: from identification to biomarker method development, validation and application. *Anal. Bioanal. Chem.* 406, 7911–7924.
- (24) Schwartz-Zimmermann, H. E., Fruhmann, P., Dänicke, S., Wiesenberger, G., Caha, S., Weber, J., and Berthiller, F. (2015) Metabolism of Deoxynivalenol and Deepoxy-Deoxynivalenol in Broiler Chickens, Pullets, Roosters and Turkeys. *Toxins* 7, 4706–4729.
- (25) Schwartz-Zimmermann, H. E., Hametner, C., Nagl, V., Fiby, I., Macheiner, L., Winkler, J., Dänicke, S., Clark, E., Pestka, J. J., and Berthiller, F. (2017) Glucuronidation of deoxynivalenol (DON) by different animal species: identification of iso-DON glucuronides and

iso-deepoxy-DON glucuronides as novel DON metabolites in pigs, rats, mice, and cows. *Arch. Toxicol.* 91, 3857–3872.

(26) Pestka, J., Clark, E., Schwartz-Zimmermann, H., and Berthiller, F. (2017) Sex Is a Determinant for Deoxynivalenol Metabolism and Elimination in the Mouse. *Toxins* 9, 240.

(27) Schmeitzl, C., Warth, B., Fruhmann, P., Michlmayr, H., Malachová, A., Berthiller, F., Schuhmacher, R., Krska, R., and Adam, G. (2015) The Metabolic Fate of Deoxynivalenol and Its Acetylated Derivatives in a Wheat Suspension Culture: Identification and Detection of DON-15-O-Glucoside, 15-Acetyl-DON-3-O-Glucoside and 15-Acetyl-DON-3-Sulfate. *Toxins* 7, 3112.

(28) Kluger, B., Bueschl, C., Lemmens, M., Michlmayr, H., Malachova, A., Koutnik, A., Maloku, I., Berthiller, F., Adam, G., Krska, R., and Schuhmacher, R. (2015) Biotransformation of the Mycotoxin Deoxynivalenol in Fusarium Resistant and Susceptible Near Isogenic Wheat Lines. *PLoS One* 10, No. e0119656.

(29) Warth, B., Fruhmann, P., Wiesenberger, G., Kluger, B., Sarkanj, B., Lemmens, M., Hametner, C., Fröhlich, J., Adam, G., Krska, R., and Schuhmacher, R. (2015) Deoxynivalenol-sulfates: identification and quantification of novel conjugated (masked) mycotoxins in wheat. *Anal. Bioanal. Chem.* 407, 1033–1039.

(30) Warth, B., Del Favero, G., Wiesenberger, G., Puntischer, H., Woelflingseder, L., Fruhmann, P., Sarkanj, B., Krska, R., Schuhmacher, R., Adam, G., and Marko, D. (2016) Identification of a novel human deoxynivalenol metabolite enhancing proliferation of intestinal and urinary bladder cells. *Sci. Rep.* 6, 33854.

(31) Del Favero, G., Woelflingseder, L., Braun, D., Puntischer, H., Kütt, M.-L., Dellafiora, L., Warth, B., Pahlke, G., Dall'Asta, C., Adam, G., and Marko, D. (2018) Response of intestinal HT-29 cells to the trichothecene mycotoxin deoxynivalenol and its sulfated conjugates. *Toxicol. Lett.* 295, 424–437.

(32) Wu, X., Murphy, P., Cunnick, J., and Hendrich, S. (2007) Synthesis and characterization of deoxynivalenol glucuronide: Its comparative immunotoxicity with deoxynivalenol. *Food Chem. Toxicol.* 45, 1846–1855.

(33) Stanic, A., Uhlig, S., Solhaug, A., Rise, F., Wilkins, A. L., and Miles, C. O. (2015) Nucleophilic Addition of Thiols to Deoxynivalenol. *J. Agric. Food Chem.* 63, 7556–7566.

(34) Stanic, A., Uhlig, S., Sandvik, M., Rise, F., Wilkins, A. L., and Miles, C. O. (2016) Characterization of Deoxynivalenol-Glutathione Conjugates Using Nuclear Magnetic Resonance Spectroscopy and Liquid Chromatography-High-Resolution Mass Spectrometry. *J. Agric. Food Chem.* 64, 6903–6910.

(35) Uhlig, S., Stanic, A., Hofgaard, I., Kluger, B., Schuhmacher, R., and Miles, C. (2016) Glutathione-Conjugates of Deoxynivalenol in Naturally Contaminated Grain Are Primarily Linked via the Epoxide Group. *Toxins* 8, 329.

(36) Schwartz, H. E., Hametner, C., Slavik, V., Greitbauer, O., Bichl, G., Kunz-Vekiru, E., Schatzmayr, D., and Berthiller, F. (2013) Characterization of Three Deoxynivalenol Sulfonates Formed by Reaction of Deoxynivalenol with Sulfur Reagents. *J. Agric. Food Chem.* 61, 8941–8948.

(37) Wishart, D. S., Feunang, Y. D., Marcu, A., Guo, A. C., Liang, K., Vázquez-Fresno, R., Sajed, T., Johnson, D., Li, C., Karu, N., Sayeeda, Z., Lo, E., Assempour, N., Berjanskii, M., Singhal, S., Arndt, D., Liang, Y., Badran, H., Grant, J., Serra-Cayuela, A., Liu, Y., Mandal, R., Neveu, V., Pon, A., Knox, C., Wilson, M., Manach, C., and Scalbert, A. (2018) HMDB 4.0: the human metabolome database for 2018. *Nucleic Acids Res.* 46, D608–D617.

(38) Guijas, C., Montenegro-Burke, J. R., Domingo-Almenara, X., Palermo, A., Warth, B., Hermann, G., Koellensperger, G., Huan, T., Uritboonthai, W., Aisporna, A. E., Wolan, D. W., Spilker, M. E., Benton, H. P., and Siuzdak, G. (2018) METLIN: A Technology Platform for Identifying Knowns and Unknowns. *Anal. Chem.* 90, 3156–3164.

(39) Horai, H., Arita, M., Kanaya, S., Nihei, Y., Ikeda, T., Suwa, K., Ojima, Y., Tanaka, K., Tanaka, S., Aoshima, K., Oda, Y., Kakazu, Y., Kusano, M., Tohge, T., Matsuda, F., Sawada, Y., Hirai, M. Y., Nakanishi, H., Ikeda, K., Akimoto, N., Maoka, T., Takahashi, H., Ara,

T., Sakurai, N., Suzuki, H., Shibata, D., Neumann, S., Iida, T., Tanaka, K., Funatsu, K., Matsuura, F., Soga, T., Taguchi, R., Saito, K., and Nishioka, T. (2010) MassBank: a public repository for sharing mass spectral data for life sciences. *J. Mass Spectrom.* 45, 703–714.

(40) Stanic, A., Uhlig, S., Solhaug, A., Rise, F., Wilkins, A. L., and Miles, C. O. (2016) Preparation and Characterization of Cysteine Adducts of Deoxynivalenol. *J. Agric. Food Chem.* 64, 4777–4785.

(41) Schymanski, E. L., Jeon, J., Gulde, R., Fenner, K., Ruff, M., Singer, H. P., and Hollender, J. (2014) Identifying Small Molecules via High Resolution Mass Spectrometry: Communicating Confidence. *Environ. Sci. Technol.* 48, 2097–2098.

(42) Gerding, J., Cramer, B., and Humpff, H.-U. (2014) Determination of mycotoxin exposure in Germany using an LC-MS/MS multibiomarker approach. *Mol. Nutr. Food Res.* 58, 2358–2368.

(43) Turner, P. C., Hopton, R. P., White, K. L. M., Fisher, J., Cade, J. E., and Wild, C. P. (2011) Assessment of deoxynivalenol metabolite profiles in UK adults. *Food Chem. Toxicol.* 49, 132–135.

(44) Komura, H., and Iwaki, M. (2011) In vitro and in vivo small intestinal metabolism of CYP3A and UGT substrates in preclinical animals species and humans: species differences. *Drug Metab. Rev.* 43, 476–498.

(45) Woelflingseder, L., Warth, B., Vierheilig, I., Schwartz-Zimmermann, H., Hametner, C., Nagl, V., Novak, B., Sarkanj, B., Berthiller, F., Adam, G., and Marko, D. (2019) The Fusarium metabolite culmorin suppresses the in vitro glucuronidation of deoxynivalenol. *Arch. Toxicol.* 93, 1729–1743.

(46) Yokoyama, Y., Sasaki, Y., Terasaki, N., Kawataki, T., Takekawa, K., Iwase, Y., Shimizu, T., Sanoh, S., and Ohta, S. (2018) Comparison of Drug Metabolism and Its Related Hepatotoxic Effects in HepaRG, Cryopreserved Human Hepatocytes, and HepG2 Cell Cultures. *Biol. Pharm. Bull.* 41, 722–732.

(47) Juan-García, A., Juan, C., König, S., and Ruiz, M.-J. (2015) Cytotoxic effects and degradation products of three mycotoxins: Alternariol, 3-acetyl-deoxynivalenol and 15-acetyl-deoxynivalenol in liver hepatocellular carcinoma cells. *Toxicol. Lett.* 235, 8–16.

(48) Abad, M. F., Di Benedetto, G., Magalhães, P. J., Filippin, L., and Pozzan, T. (2004) Mitochondrial pH monitored by a new engineered GFP mutant. *J. Biol. Chem.* 279, 11521–11529.

(49) Dansen, T. B., Wirtz, K. W. A., Wanders, R. J. A., and Pap, E. H. W. (2000) Peroxisomes in human fibroblasts have a basic pH. *Nat. Cell Biol.* 2, 51–53.

(50) Nakamura, Y., Ohta, M., and Ueno, Y. (1977) Reactivity of 12, 13-Epoxytrichothecenes with Epoxide Hydrolase, Glutathione-S-Transferase and Glutathione. *Chem. Pharm. Bull.* 25, 3410–3414.

(51) Adam, G. (2019) Method for biotransformation of trichothecenes, EP19181392.

(52) Lewis, A. D., Forrester, L. M., Hayes, J. D., Wareing, C. J., Carmichael, J., Harris, A. L., Mooghen, M., and Wolf, C. R. (1989) Glutathione S-transferase isoenzymes in human tumours and tumour derived cell lines. *Br. J. Cancer* 60, 327–331.

(53) Lu, S. C. (2013) Glutathione synthesis. *Biochim. Biophys. Acta, Gen. Subj.* 1830, 3143–3153.

(54) Lu, S. C. (2009) Regulation of glutathione synthesis. *Mol. Aspects Med.* 30, 42–59.

(55) Wan, D., Huang, L., Pan, Y., Wu, Q., Chen, D., Tao, Y., Wang, X., Liu, Z., Li, J., Wang, L., and Yuan, Z. (2014) Metabolism, Distribution, and Excretion of Deoxynivalenol with Combined Techniques of Radiotracing, High-Performance Liquid Chromatography Ion Trap Time-of-Flight Mass Spectrometry, and Online Radiometric Detection. *J. Agric. Food Chem.* 62, 288–296.

(56) Rudyk, O., and Eaton, P. (2014) Biochemical methods for monitoring protein thiol redox states in biological systems. *Redox Biol.* 2, 803–813.

(57) Grumbt, M., Monod, M., Yamada, T., Hertweck, C., Kunert, J., and Staib, P. (2013) Keratin Degradation by Dermatophytes Relies on Cysteine Dioxygenase and a Sulfite Efflux Pump. *J. Invest. Dermatol.* 133, 1550–1555.

- (58) Knights, K. M., Sykes, M. J., and Miners, J. O. (2007) Amino acid conjugation: contribution to the metabolism and toxicity of xenobiotic carboxylic acids. *Expert Opin. Drug Metab. Toxicol.* 3, 159–168.
- (59) Karlovsky, P. (2011) Biological detoxification of the mycotoxin deoxynivalenol and its use in genetically engineered crops and feed additives. *Appl. Microbiol. Biotechnol.* 91, 491–504.
- (60) Lin, S., Van Lanen, S. G., and Shen, B. (2009) A free-standing condensation enzyme catalyzing ester bond formation in C-1027 biosynthesis. *Proc. Natl. Acad. Sci. U. S. A.* 106, 4183–4188.
- (61) Philippe, C., Milcent, T., Crousse, B., and Bonnet-Delpon, D. (2009) Non Lewis acid catalysed epoxide ring opening with amino acid esters. *Org. Biomol. Chem.* 7, 2026–2028.
- (62) Calow, A. D. J., Carbó, J. J., Cid, J., Fernández, E., and Whiting, A. (2014) Understanding α,β -Unsaturated Imine Formation from Amine Additions to α,β -Unsaturated Aldehydes and Ketones: An Analytical and Theoretical Investigation. *J. Org. Chem.* 79, 5163–5172.
- (63) Schwartz-Zimmermann, H. E., Wiesenberger, G., Unbekannt, C., Hessenberger, S., Schatzmayr, G., and Berthiller, F. (2014) Reaction of (conjugated) deoxynivalenol with sulphur reagents - novel metabolites, toxicity and application. *World Mycotoxin J.* 7, 187–197.
- (64) Fruhmann, P., Skrinjar, P., Weber, J., Mikula, H., Warth, B., Sulyok, M., Krska, R., Adam, G., Rosenberg, E., Hametner, C., and Fröhlich, J. (2014) Sulfation of deoxynivalenol, its acetylated derivatives, and T2-toxin. *Tetrahedron* 70, 5260–5266.
- (65) Fruhmann, P., Warth, B., Hametner, C., Berthiller, F., Horkel, E., Adam, G., Sulyok, M., Krska, R., and Fröhlich, J. (2012) Synthesis of deoxynivalenol-3- β -D-O-glucuronide for its use as biomarker for dietary deoxynivalenol exposure. *World Mycotoxin J.* 5, 127–132.

Supporting Information

Stable isotope-assisted metabolomics for deciphering xenobiotic metabolism in mammalian cell culture

Mira Flasch ^{†,‡}, Christoph Bueschl^{‡,‡}, Lydia Woelflingseder[†], Heidi E. Schwartz-Zimmermann[‡], Gerhard Adam[§], Rainer Schuhmacher[‡], Doris Marko[†], Benedikt Warth^{†,*}

[†]University of Vienna, Faculty of Chemistry, Department of Food Chemistry and Toxicology, Währinger Straße 38, 1090 Vienna, Austria

[‡]University of Natural Resources and Life Sciences, Vienna (BOKU), Department of Agrobiotechnology, IFA-Tulln, Institute of Bioanalytics and Agro-Metabolomics, Konrad-Lorenz-Straße 20, 3430 Tulln, Austria

[§]University of Natural Resources and Life Sciences, Vienna (BOKU), Department of Applied Genetics and Cell Biology, Konrad-Lorenz-Straße 24, 3430 Tulln, Austria

[‡]The authors contributed equally to this work.

*Corresponding author

Table of Contents

1. General.....	2
2. Results and Discussion.....	2
2.1. Identification of DON-metabolites	2
Figure S1 Identification of DON-sulfates	3
Figure S2 Identification of DON-sulfonate	4
Figure S3 Annotation of DON-10-GSHa) Structure of DON-10-GSH	5
Figure S4 Identification of DON-10-cysteine	6
Table S1 Inclusion list for the additional MS2 measurement with the exact mass, the ion charge and species of the included ion, the polarity mode in which the ion is included, start and end time of the exclusion window and the corresponding compound.....	7
References.....	7
4. Author Contributions	7

1. General

Abbreviations: DON , Deoxynivalenol; AGC, Automatic Gain Control; GlcA, Glucuronide; LC-HRMS, Liquid Chromatography- High Resolution Mass Spectroscopy; DON-GSH, Deoxynivalenol-glutathione; DON-Cys, Deoxynivalenol-cysteine; DONS, Deoxynivalenol-sulfonate; DON-CysGly, Deoxynivalenol- cysteinyl glyline; DON-GlcA, Deoxynivalenol-glucuronide; GST, Glutathione-S-transferase; ddMS2, Data dependent MS2 spectra; FWHM, Full Width at Half Maximum; NCE, Stepped normalized collision energy; UGT, Uridine 5'-diphosphate –glucuronosyltransferase; UDP, Uridine 5'-diphosphate; XIC, Extracted Ion Chromatograms

2. Results and Discussion

2.1. Identification of DON-metabolites

Chromatograms and MS2 spectra of experimental samples and reference standards supporting the identification of DON-3-sulfate (Figure S1) and DON-sulfonate (Figure S2) are presented in the supporting information. The MS2 spectra used for the annotation of DON-10-glutathione (Figure S3) and DON-10-S-cysteine (Figure S4) are shown as well.

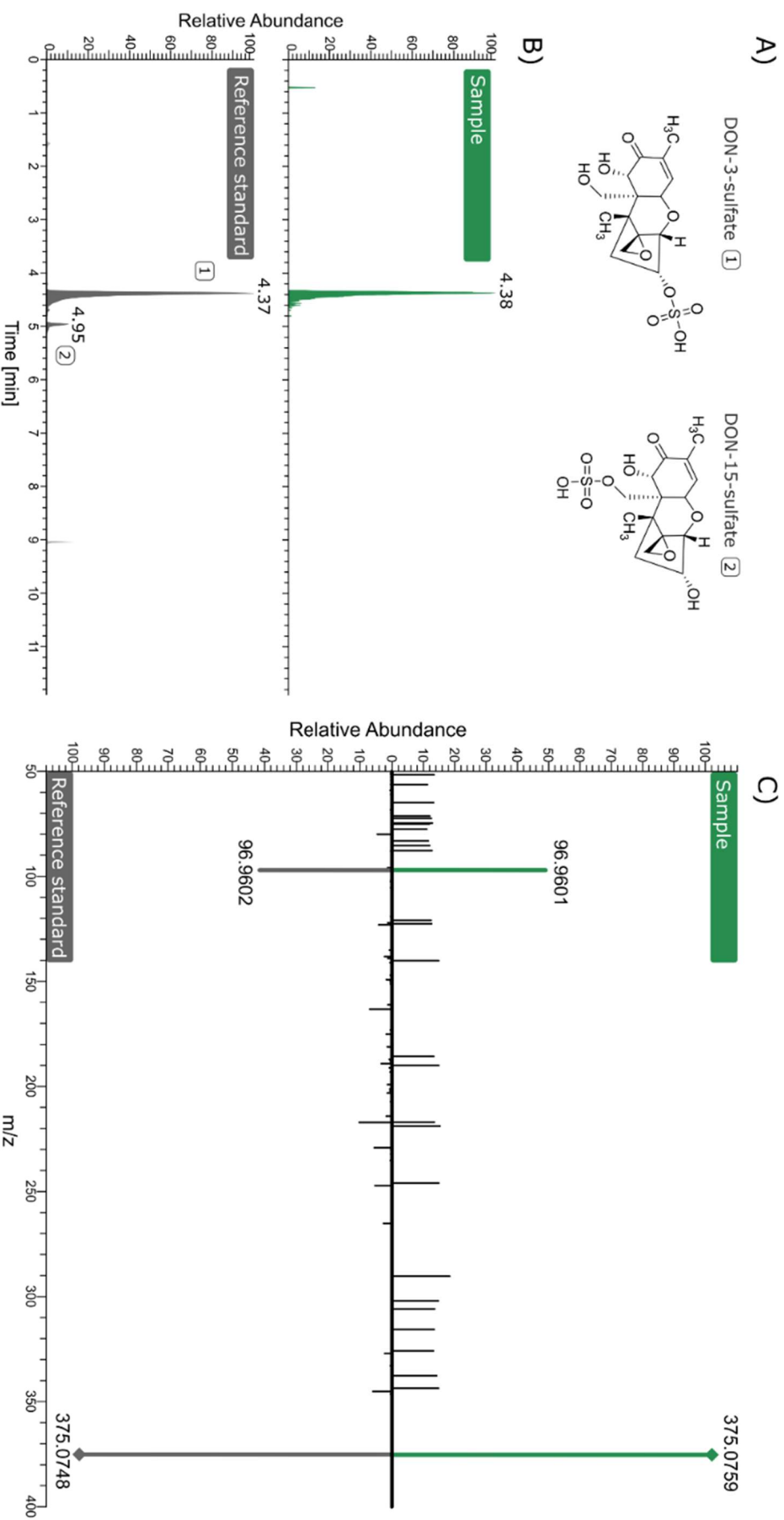


Figure S1 Identification of DON-sulfates

- Structures of DON-3-sulfate and DON-15-sulfate.
- Comparison of retention behaviour of sample (extracellular medium of HepG2 cells) in green and standards of both DON-sulfate isomers in grey. The earlier eluting peak in the standard is DON-3-sulfate. The extracted ion chromatogram (XIC) of the precursor ion at m/z 375.0748 (DON-sulfate, $[M-H]^-$) measured in negative mode with a mass tolerance of 5 ppm are shown.
- MS2 spectrum of the precursor ion (m/z 375.0748) at 4.37 min recorded with a stepped normalized collision energy at 20eV and 50eV of the sample. Fragments present in the sample and in the DON-15-sulfate standard are shown in bold.

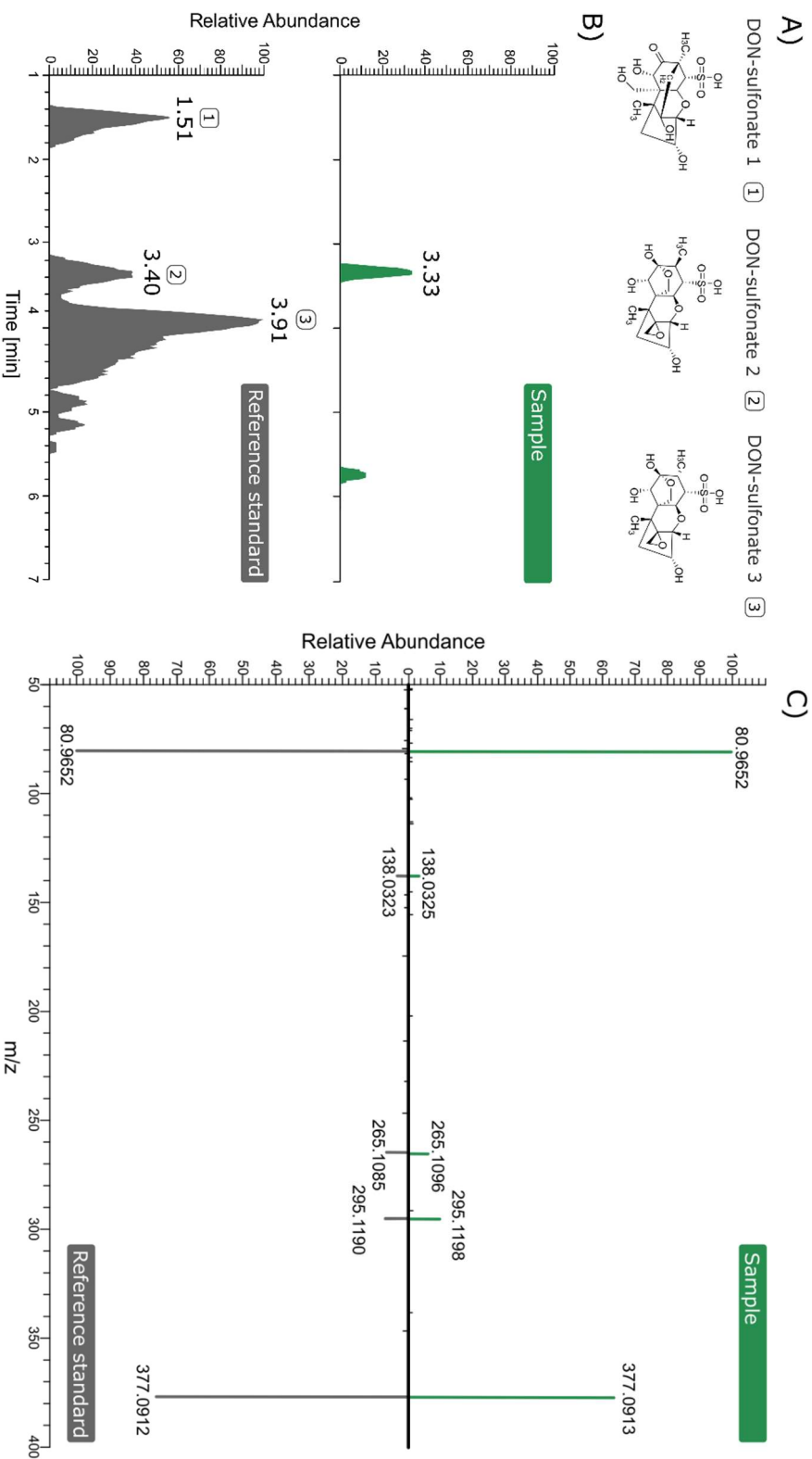


Figure S2 Identification of DON-sulfonate

a) Structures of the three isomers of DON-sulfonate.

b) Comparison of retention behaviour of the sample (extracellular medium of HT29 cells) in green and standards of the isomers DON-sulfonate 1, DON-sulfonate 2 and DON-sulfonate 3 in grey. The retention times slightly shifted between different runs since the eluents were not optimized for these specific metabolites. The XICs were extracted from a multi-standard solution containing all three sulfonates. For standards and sample the XIC of the precursor ion at m/z 377.0916 (DON-sulfonates, $[M-H]^-$) measured in negative mode with a mass tolerance of 5 ppm was used.

c) MS2 spectrum of the precursor ion (m/z 377.0916) at 3.33 min recorded with a stepped normalized collision energy at 20eV and 50eV of the sample. Fragments present in the sample and in the DON-sulfonate 2 standard are shown in bold.

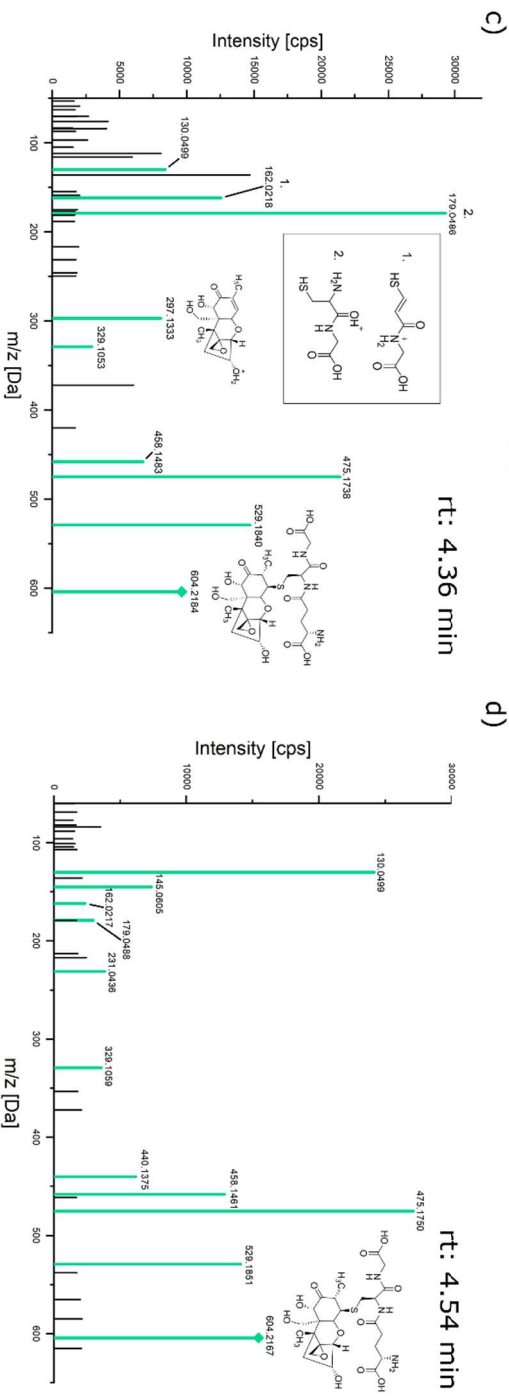
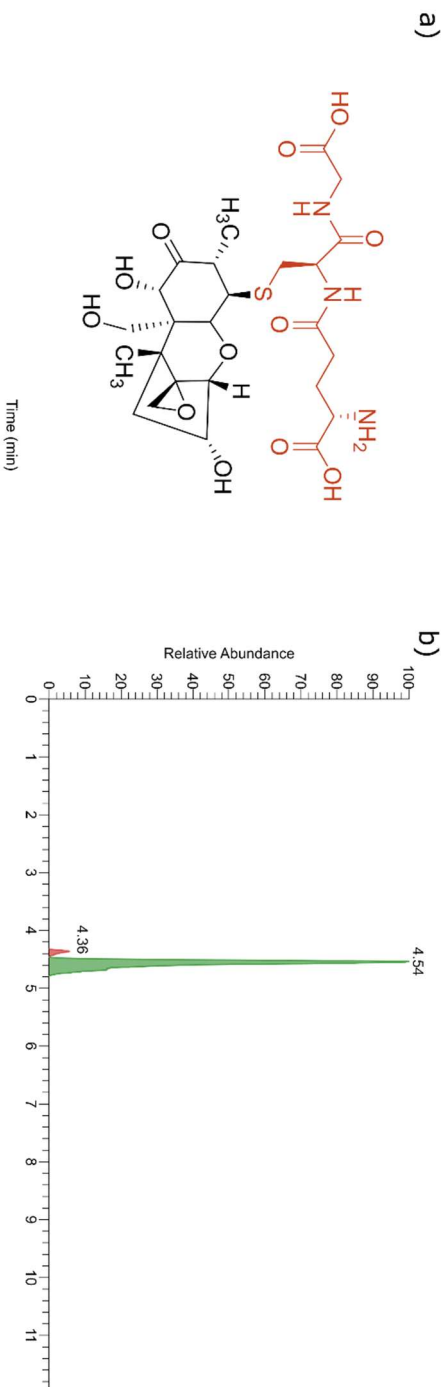


Figure S3 Annotation of DON-10-GSH

- a) Structure of DON-10-GSH
- b) XIC of the precursor ion at m/z 604.2167 (DON-GSH, $[M-H]^+$) with a mass tolerance of 5 ppm of a cell lysate sample.
- c) MS2 spectrum of the precursor ion (m/z 604.2167) at 4.36 min recorded with a stepped normalized collision energy at 20eV and 50eV whereby fragments also present in the literature spectrum^[1] are coloured in turquoise.
- d) MS2 spectrum of the precursor ion (m/z 604.2167) at 4.54 min recorded with a stepped normalized collision energy at 20eV and 50eV. Fragments present in a literature spectrum^[1] are coloured in turquoise.

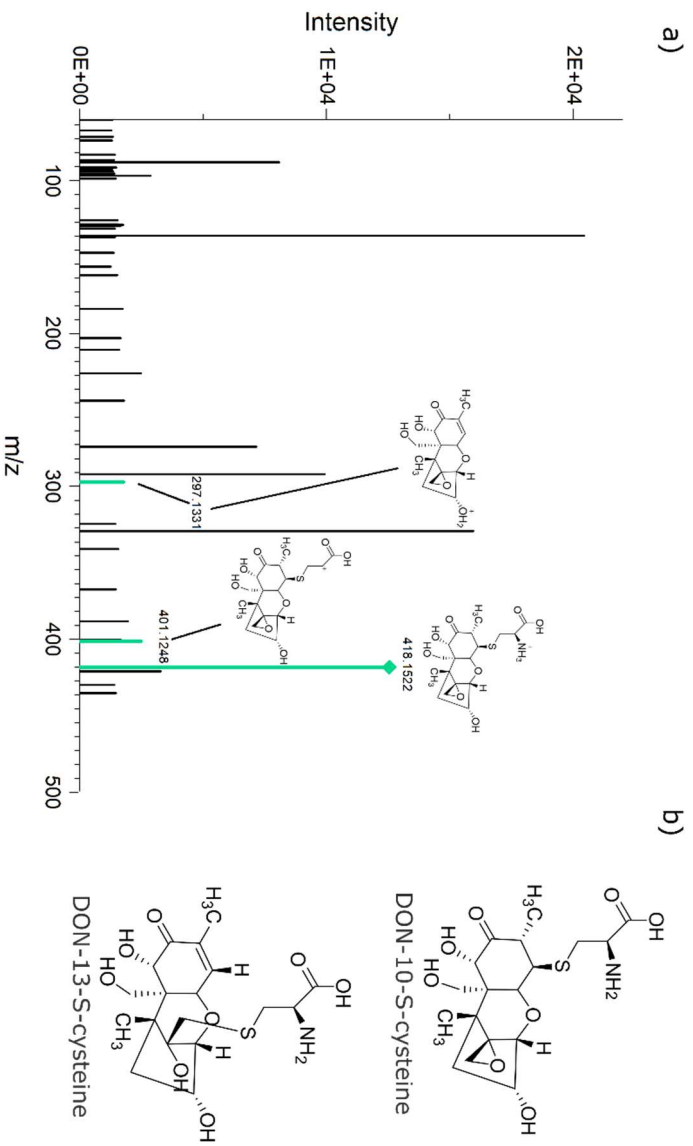


Figure S4 Identification of DON-10-cysteine

a) MS2 spectrum of the precursor ion at m/z 418:1525 (DON-Cys, $[M-H]^{-}$) of a DON-treated lysate sample of HepG2 cell at 3:56 min recorded with a stepped normalized collision energy at 20eV and 50eV whereby also in the literature spectrum (Stanic et al. 2016b) fragments are coloured in turquoise

b) Structures of DON-10-S-cysteine and DON-13-S-cysteine

Table S1 Inclusion list for the additional MS2 measurement with the exact mass, the ion charge and species of the included ion, the polarity mode in which the ion is included, start and end time of the exclusion window and the corresponding compound

Mass [m/z]	Charge [z]	Species	Polarity	Start [min]	End [min]	Compound
377.0916	1	[M-H] ⁻	Negative	1.2	4.4	DON-sulfonate
392.1419	1	[M-H] ⁻	Negative	1.2	4.4	¹³ C-DON-sulfonate
375.0759	1	[M-H] ⁻	Negative	3	5	DON-sulfate
390.1264	1	[M-H] ⁻	Negative	3	5	¹³ C-DON-sulfate
602.2036	1	[M-H] ⁻	Negative	3.5	6.5	DON-GSH
617.2541	1	[M-H] ⁻	Negative	3.5	6.5	¹³ C-DON-GSH
426.2137	1	[M-H] ⁻	Negative	5.3	8.3	DON-(Iso)Leucine
441.2640	1	[M-H] ⁻	Negative	5.3	8.3	¹³ C-DON-(Iso)Leucine
474.1773	1	[M-H] ⁻	Negative	4.3	5.7	Unknown
409.0597	1	[M-H] ⁻	Negative	4.3	5.7	Unknown
385.1507	1	[M-H] ⁻	Negative	4.3	5.7	Unknown
341.1245	1	[M-H] ⁻	Negative	4.3	5.7	Unknown
418.1519	1	[M+H] ⁺	Positive	3	5	DON-cysteine
433.2022	1	[M+H] ⁺	Positive	3	5	¹³ C-DON-cysteine
604.2171	1	[M+H] ⁺	Positive	3.5	6.5	DON-GSH
619.2657	1	[M+H] ⁺	Positive	3.5	6.5	¹³ C-DON-GSH
478.2060	1	[M+H] ⁺	Positive	3.3	6.3	DON-Tyr
493.2563	1	[M+H] ⁺	Positive	3.3	6.3	¹³ C-DON-Tyr
532.1100	1	[M+H] ⁺	Positive	3.5	6.5	Unknown
544.1517	1	[M+H] ⁺	Positive	3.5	6.5	Unknown
533.1084	1	[M+H] ⁺	Positive	3.5	6.5	Unknown
548.1582	1	[M+H] ⁺	Positive	3.5	6.5	Unknown
428.2267	1	[M+H] ⁺	Positive	5.3	8.3	DON-(iso)leucine
443.2770	1	[M+H] ⁺	Positive	5.3	8.3	¹³ C-DON-(iso)leucine
462.2111	1	[M+H] ⁺	Positive	6.1	9.1	DON-Phe
477.2613	1	[M+H] ⁺	Positive	6.1	9.1	¹³ C-DON-Phe
631.2325	1	[M+H] ⁺	Positive	6.5	10.5	DON-penicillin G
646.2804	1	[M+H] ⁺	Positive	6.5	10.5	¹³ C-DON-penicillin G

References

[1] A. Stanic, S. Uhlig, M. Sandvik, F. Rise, A. L. Wilkins, C. O. Miles, *J. Agric. Food Chem.* **2016**, *64*, 6903-6910.

Author Contributions

Conceptualization B.W., D.M and R.S.; Methodology L.W., M.F. and B.W.; Software C.B., M.F.; Investigation L.W., M.F., C.B. and B.W.; Writing-Original Draft M.F. ; Writing- Review &Editing M.F., C.B., L.W., H.S.Z., G.A., D.M., R.S. and B.W.; Funding Acquisition G.A., D.M. and B.W.; Resources H.S.Z., G.A.; Supervision, R.S, D.M. and B.W.;

6.5. Publication #4: Flasch et al. (2022a)

Status	Published
Title	Elucidation of xenoestrogen metabolism by non-targeted, stable isotope-assisted mass spectrometry in breast cancer cells
Authors	Mira Flasch ¹ , Christoph Bueschl ² , Giorgia Del Favero ¹ , Gerhard Adam ³ , Rainer Schuhmacher ² , Doris Marko ¹ , Benedikt Warth ^{1*}
Affiliations	<p>¹University of Vienna, Faculty of Chemistry, Department of Food Chemistry and Toxicology, Währinger Straße 38-40, 1090 Vienna, Austria</p> <p>²University of Natural Resources and Life Sciences, Department of Agrobiotechnology, IFA-Tulln, Institute of Bioanalytics and Agro-Metabolomics, Konrad-Lorenz-Straße 20, 3430 Tulln, Austria</p> <p>³University of Vienna, Faculty of Chemistry, Department of Analytical Chemistry, Währinger Straße 38, 1090 Vienna, Austria</p> <p>⁴University of Natural Resources and Life Sciences, Department of Applied Genetics and Cell Biology, Institute of Microbial Genetics, Konrad-Lorenz-Straße 20, 3430 Tulln, Austria</p> <p>*Corresponding author</p>
Year	2022
Journal	Environment International, Volume 158, Page 106940
Accepted	October 12 th , 2021
DOI	https://doi.org/10.1016/j.envint.2021.106940
Contribution	Mira Flasch performed additional LC-HRMS(/MS) measurements for MS/MS generation, interpreted the results from the MetExtract II analyses and wrote the manuscript.



Elucidation of xenoestrogen metabolism by non-targeted, stable isotope-assisted mass spectrometry in breast cancer cells

Mira Flasch^a, Christoph Bueschl^{b,c}, Giorgia Del Favero^a, Gerhard Adam^d,
Rainer Schuhmacher^b, Doris Marko^a, Benedikt Warth^{a,*}

^a University of Vienna, Faculty of Chemistry, Department of Food Chemistry and Toxicology, Währinger Str. 38, 1090 Vienna, Austria

^b University of Natural Resources and Life Sciences, Vienna (BOKU), Department of Agrobiotechnology, IFA-Tulln, Institute of Bioanalytics and Agro-Metabolomics, Konrad-Lorenz-Str. 20, 3430 Tulln, Austria

^c University of Vienna, Faculty of Chemistry, Department of Analytical Chemistry, Währinger Str. 38, 1090 Vienna, Austria

^d University of Natural Resources and Life Sciences, Vienna (BOKU), Department of Applied Genetics and Cell Biology, Institute of Microbial Genetics, Konrad-Lorenz-Str. 24, 3430 Tulln, Austria

ARTICLE INFO

Handling Editor: Da Chen

Keywords:

Endocrine disrupting chemicals (EDCs)

In vitro toxicology

Biotransformation

Metabolomics/exposomics

Isoflavones

Mycotoxins

Systems toxicology

ABSTRACT

Environmental exposure to xenoestrogens, *i.e.*, chemicals that imitate the hormone 17 β -estradiol, has the potential to influence hormone homeostasis and action. Detailed knowledge of xenobiotic biotransformation processes in cell models is key when transferring knowledge learned from *in vitro* models to *in vivo* relevance. This study elucidated the metabolism of two naturally-occurring phyto- and mycoestrogens; namely genistein and zearalenone, in an estrogen receptor positive breast cancer cell line (MCF-7) with the aid of stable isotope-assisted metabolomics and the bioinformatic tool MetExtract II. Metabolism was studied in a time course experiment after 2 h, 6 h and 24 h incubation. Twelve and six biotransformation products of zearalenone and genistein were detected, respectively, clearly demonstrating the abundant xenobiotic biotransformation capability of the cells. Zearalenone underwent extensive phase-I metabolism resulting in α -zearalenol (α -ZEL), a molecule known to possess a significantly higher estrogenicity, and several phase-II metabolites (sulfo- and glycoconjugates) of the native compound and the major phase I metabolite α -ZEL. Moreover, potential adducts of zearalenone with a vitamin and several hydroxylated metabolites were annotated. Genistein metabolism resulted in sulfation, combined sulfation and hydroxylation, acetylation, glucuronidation and unexpectedly adduct formation with pentose- and hexose sugars. Kinetics of metabolite formation and subsequent excretion into the extracellular medium revealed a time-dependent increase in most biotransformation products. The untargeted elucidation of biotransformation products formed during cell culture experiments enables an improved and more meaningful interpretation of toxicological assays and has the potential to identify unexpected or unknown metabolites.

1. Introduction

Biotransformation of xenobiotics frequently modifies the chemical properties and biological activity of the respective compound. Whereas phase I metabolism typically enhances functionality of a molecule, subsequent phase II metabolism is often regarded as a detoxification step. The type and extent of these reactions, however, are highly molecule specific and prone to inter-individual variation. Consequently, detailed knowledge of xenobiotic biotransformation in biological model systems, including cells used for *in vitro* testing, is a powerful tool for a comprehensive evaluation of possible toxicological effects and an

improved understanding of *in vitro* toxicology data (Moon et al., 2006; Pascussi et al., 2008; Kaur et al., 2020).

Xenoestrogens are a ubiquitous group of xenobiotics of synthetic or natural origin that mimic the female sex hormone 17 β -estradiol (Paterni et al., 2017). They belong to many different chemical classes and the interactions of these molecules with the endocrine system remain largely elusive (Preindl et al., 2019). Plant-derived phytoestrogens are divided into isoflavones, lignans, flavones, coumestans and stilbenes (Oesterle et al., 2021), and in addition to their natural presence in food commodities, they are increasingly marketed as fortified food or dietary supplements (Dhanjal et al., 2020). Among these is genistein (GEN), a

* Corresponding author.

E-mail address: benedikt.warth@univie.ac.at (B. Warth).

<https://doi.org/10.1016/j.envint.2021.106940>

Received 30 June 2021; Received in revised form 13 September 2021; Accepted 12 October 2021

Available online 18 October 2021

0160-4120/© 2021 The Authors. Published by Elsevier Ltd. This is an open access article under the CC BY license (<http://creativecommons.org/licenses/by/4.0/>).

prominent soy isoflavone. Additionally relevant for dietary exposure are mycoestrogens, secondary metabolites of fungi, which act as xenoestrogens. Representative molecules that are frequently monitored in humans are the non-steroidal estrogenic *Fusarium* mycotoxin zearalenone (ZEN) (Metzler et al., 2010) and the *Alternaria* toxins, alternariol (Lehmann et al., 2006) and alternariol monomethyl ether (Dellafiora et al., 2018).

Even at low concentrations, synthetic and natural xenoestrogens have the potential to interfere with the endocrine system (Xu et al., 2017; Sofie et al., 2014). This possible impact is a major concern for public health. While phytoestrogens such as the soy isoflavone genistein (GEN) are often associated with a lowered breast cancer risk (Basu and Maier, 2018; Verheus et al., 2007; Wu et al., 2008; Lecomte et al., 2017), synthetic xenoestrogens are reported to enhance the risk to develop hormone-dependent cancers such as breast cancer (Pastor-Barriuso et al., 2016; Yager and Davidson, 2006; Kumar et al., 2020). The period when exposure occurs in the lifetime of an individual is believed to be a critical factor in the manifestation of adverse or protective effects (Lee, 2018; Rice and Whitehead, 2006; Liu et al., 2019).

ZEN and metabolites thereof are also suspected to play a role in the promotion of hormone-dependent tumors arising, in particular, from breast tissue and endometrium because these interact with the estrogen receptor (ER) (Khosrokhavar et al., 2009; Pazaiti et al., 2012; Belhassen et al., 2015). The affinity of ZEN for ER- α and ER- β are similar, while phytoestrogens prefer the presumably-protective ER- β (Zhou and Liu, 2020; Metzler et al., 2010). Moreover, dietary GEN and ZEN influence the efficacy of various breast cancer treatments (Warth et al., 2018; Rigalli et al., 2016; Pristner and Warth, 2020) and consequently may impact therapy. The levels of the isoflavone GEN in urine that were measured during human biomonitoring studies are over one hundred times higher than the levels of the mycotoxin ZEN and metabolites thereof (Moors et al., 2007; Fleck et al., 2016; Berman et al., 2013; Tordjman et al., 2016; Ali and Degen, 2019); thus indicating a much higher exposure to the phytoestrogen. Despite its low concentration, zearalenone has also been detected in breast milk; potentially exposing breastfed infants to low levels (Braun et al., 2018).

Biotransformation may modify, enhance, or suppress the effects of the native compounds (e.g., estrogenicity). Similar to the parent compound, hydroxyl-derivates such as α - and β -zearalenol, and 4-hydroxy-alternariol also possess estrogenic potential (Dellafiora et al., 2018; Frizzell et al., 2011). For α -zearalenol, the estrogenic effect is far more pronounced than for ZEN (Metzler et al., 2010). In contrast, glucuronidation of ZEN and metabolites thereof reduces estrogenic activity (Frizzell et al., 2015).

To date, the metabolism of GEN and ZEN in exposed cell models has only been poorly investigated; and was primarily evaluated through HPLC with radioactively-labeled compounds or targeted LC-MS/MS. The fate of GEN was studied by Yuan et al. (2012), who reported extensive glucuronidation in MCF-7 cells, and abundant sulfate conjugates in T47D cells. An earlier study revealed GEN-7-sulfate as the exclusive metabolic product in MCF-7 cells, while both GEN-7-sulfate and GEN-4'-sulfate were detected in the HepG2 liver carcinoma cell line (Bursztyka et al., 2008a). In colorectal adenocarcinoma cells (Caco-2), both glucuronidation and sulfation occurred (Chen et al., 2005). The metabolism of ZEN has been mainly studied in microsomes (Yang et al., 2017; Pfeiffer et al., 2007; Pfeiffer et al., 2009; Hildebrand et al., 2012). To date, Caco-2 cells are the only cell model with published data. In the colorectal adenocarcinoma cells, ZEN was reduced to α -ZEL and β -ZEL and the formation of glucuronides and sulfates of the parent molecule and phase I metabolites thereof was observed (Appel et al., 2021; Pfeiffer et al., 2011). ZEN- and GEN glucuronides are the most prominent metabolites excreted via urine in humans (Soukup et al., 2016; Fleck et al., 2016; Warth et al., 2013).

Recent advances in LC-HRMS instrumentation and innovative bioinformatic algorithms have led to the advent of advanced workflows based on stable-isotope tracers to unravel the metabolism of endogenous

and exogenous substances (Kluger et al., 2014; Chokkathukalam et al., 2014; Balcerczyk et al., 2020; Baumeister et al., 2018). A tailored software suite to study the metabolism of isotopically-labeled tracer substances is MetExtract II. This program enables the detection of novel conjugates without the need for authentic reference standards to confirm identity and lineage from the parent compounds (Bueschl et al., 2017). This tool was recently optimized for the generic identification of xenobiotics in human tissue culture as exemplified by the food toxin deoxynivalenol (Flasch et al., 2020).

Here, the approach was used to investigate the metabolism of the abundant dietary xenoestrogens GEN and ZEN in a human breast cancer cell line (MCF-7), a cell model frequently applied for toxicological testing in the context of xenoestrogen research (Moche et al., 2021; Elfadul et al., 2021). The *in vitro* biotransformation reactions were studied at different time points to achieve time-resolved insights into the formation of metabolic products. Through the application of this workflow, known and unknown metabolic products of the two environmental xenobiotics were annotated. The use of partially-deuterated standards in MetExtract methodology was additionally demonstrated and will likely simplify its application.

2. Materials and methods

2.1. Chemicals and reagents

Acetonitrile (ACN), methanol and water (all LC-MS grade) were purchased from Sigma (Vienna, Austria) while dimethyl sulfoxide (DMSO) ($\geq 99.5\%$) was obtained from Carl Roth GmbH & Co. KG (Karlsruhe, Germany). Cell culture media and supplements were purchased from GIBCO Invitrogen (Karlsruhe, Germany), Carl Roth GmbH & Co. KG (Karlsruhe, Germany) and Sarstedt AG & Co (Nuembrecht, Germany). Non-labeled GEN was obtained from Extrasynthese (Genay, France) and $^2\text{H}_4$ -GEN from C.D.N isotopes (Augsburg, Germany). ZEN was purchased from Sigma-Aldrich (Vienna, Austria) while fully ^{13}C -zearalenone was a kind gift from Romer Labs (Tulln, Austria). Stocks of all compounds at a concentration of 10 mM were prepared in DMSO and diluted to each 5 μM of the labeled and non-labeled compound in the incubation media resulting in a final DMSO concentration of 0.1%.

Other reference compounds were obtained from Romer Labs (Tulln, Austria) and Sigma (Vienna, Austria) or synthesized internally (Mikula et al., 2013; Mikula et al., 2012). The standards included ZEN, α -ZEL, β -ZEL, ZEN-14-glucuronide, α -ZEL-14-glucuronide, β -ZEL-14-glucuronide, ZEN-14-sulfate, ZAN, α -ZAL and β -ZAL. The purity of commercially available standards was of the highest grade ($>98\%$) and those of custom synthesized ones were $>95\%$. Solid authentic reference standards were dissolved in ACN.

2.2. Cell culture experiments

The human breast adenocarcinoma cell line MCF-7 (ATCC HTB-22) was selected as the *in vitro* model and was purchased from LGC Standards (Wesel, Germany). The cells were cultivated in growth medium consisting of Dulbecco's Modified Eagle Medium F-12 Nutrient Mixture, 10% heat-inactivated calf serum and 1% penicillin/streptomycin (50 U/mL). Prior to the experiments, the cells were routinely split twice a week and maintained in T-175 flasks at a confluence between 75 and 85%. For sub-culturing, the cells were washed with PBS, detached with trypsin/EDTA, and re-suspended in fresh culture medium. The experiments were conducted on the cells during passages 7–9 and cells were routinely maintained at 37 °C, 5% CO_2 and 95% humidity.

For the experiments, 400,000 cells per well were seeded in 6-well plates. After 48 h, 66 h and 70 h of proliferation, the cells were incubated with 3 mL fresh incubation media containing equimolar amounts of the labeled and non-labeled compound (each 5 μM ZEN/ ^{13}C -ZEN or GEN/ $^2\text{H}_4$ -GEN) corresponding to incubation times of 24, 6, and 2 h, respectively. The procedure ensured identical cell harvest and extraction

after 72 h for all time points. In control experiments, the cells were incubated with fresh medium containing 0.1% DMSO without the xenobiotics and harvested after 72 h. In a second control experiment, cell culture medium was incubated without cells under the same conditions. All experiments were performed in triplicate.

2.3. Sample preparation

Both supernatants and cell extracts were prepared for LC-HRMS analysis to investigate excreted and intracellular metabolites of ZEN and GEN. To collect the supernatant, 0.5 mL of the medium were transferred into reaction tubes and 1 mL of chilled methanol was added. Subsequently, the tubes were vortexed and centrifuged for five minutes at 4 °C and 18,000 x g. A volume of 0.5 mL of the supernatant was transferred to LC-vials and mixed with 0.5 mL water to reach a final dilution of 1 + 5 (v/v).

Cell lysates were harvested after the remaining medium was removed using a vacuum pump. The cells were washed twice with 1 mL of ice-cold PBS and 0.7 mL quenching solution (ice-cold MeOH/water; 80/20, v/v) were added. The cells were detached using a cell scraper and the cell suspension was transferred to reaction tubes. Thereafter, the wells were washed with an additional 0.3 mL of quenching solution, which was combined with the cell suspension. Samples were vortexed followed by three cycles of shock freezing in liquid nitrogen and thawing at room temperature. Thereafter, the samples were again mixed thoroughly and centrifuged for 10 min (18,000 x g, 4 °C). The supernatants (0.8 mL) were transferred to reaction tubes, evaporated in a vacuum concentrator (Labconco), reconstituted in 0.1 mL dilution solvent (ACN/water; 10/90, v/v) and transferred to LC vials.

2.4. LC-HRMS (/MS) analysis

Samples were analyzed using an UHPLC Vanquish system coupled to a Q Exactive HF high-resolution mass spectrometer equipped with a heated electrospray ionization source (Thermo Fisher). A reversed-phase Acquity UPLC HSS T3 column (100 × 2.1 mm, 1.8 μm, Waters, Milford, USA) protected by a HSS T3 VanGuard pre-column at 40 °C was applied. A gradient with water containing 10 mM NH₄Ac as eluent A and ACN/water (96/4, v/v) with 10 mM NH₄Ac as eluent B was employed at a constant flow rate of 0.4 mL/min. After 2 min at 10% B, the gradient was linearly increased to 100% B until 15 min, maintained for a further 2 min, followed by a re-equilibration step for 2 min at 10% B. The injection volume was 5 μL. All samples were separately analyzed in positive and negative ionization mode. The following settings were applied: capillary temperature, 325 °C; vaporizer temperature, 400 °C; sheath gas, 40 arbitrary units (au); auxiliary gas, 15 au; sweep gas, 2 au; capillary voltage, 3 kV (negative mode)/3.5 kV (positive mode). The instrument was operated in profile mode (scan range, *m/z* 100–1000) with a resolving power (FWHM) of 120,000 (@*m/z* 200) and automatic gain control setting of 3 × 10⁶ with a maximum injection time of 100 ms. In addition to the full scan experiment, data dependent MS² spectra of the three most intense ions were recorded. These spectra were acquired at a resolving power (FWHM) of 30,000 (@*m/z* 200) with apex triggering (3 s) and dynamic exclusion (10 s). Additional LC-HRMS² measurements were performed with specific *m/z* values of interest via an inclusion list and applying the parameters described above for data dependent MS² measurements.

The instrument was calibrated with two calibration solutions (Pierce™ LTQ Velos ESI Positive and Pierce™ Negative Ion Calibration Solution) before the measurements. A quality control sample containing xenobiotics of different polarities was injected three times at the beginning and the end of the batch to assess the instrument's performance. Furthermore, a set of five multi-analyte reference standards was measured twice within the batch.

2.5. Data processing

2.5.1. MetExtract data evaluation

LC-HRMS data files were centroided (Thermo XCalibur, version 2.2) and converted to the mzXML data format using MSConvert from the Proteowizard package (Kessner et al., 2008, version 3.0.8789). With the purpose of detecting ion pairs of native and ²H- or ¹³C-labeled biotransformation products of (²H₄-) GEN and (¹³C₁₈-) ZEN, data processing was performed by MetExtract II (Bueschl et al., 2017). Briefly summarized, the algorithm searched for MS signal pairs of native and ²H- or ¹³C-labeled metabolites in each recorded MS scan ($\Delta m/z$ for ²H: 1.00627; $\Delta m/z$ for ¹³C: 1.00335; minimum abundance: 10,000 (ZEN)/5,000 (GEN); maximum *m/z* deviation: 3 ppm; ratio of monoisotopic and ¹³C-isotopologue MS signals: 0.5–2; ratio of monoisotopic and ²H-isotopologue MS signals: not assessed; searched ²H-isotopes: 2–4; searched ¹³C-isotopes: 12–18. Subsequently, detected ion pairs of all putative biotransformation products were binned using hierarchical clustering analysis (HCA; distance method: Euclidean distance; linkage method: average). For each bin (minimum number of MS signal pairs: 2; maximum allowed *m/z* deviation: 8 ppm), the EICs (extracted ion chromatogram) of the native and the ²H- or ¹³C-labeled ions were calculated (EIC window: ± 5 ppm) and separately inspected for presence/absence of the chromatographic peaks. Pairs of co-eluting chromatographic peaks that were apparent in both EICs at approximately the same retention time (maximum deviation: ± 10 scans) were retained. Furthermore, the profiles of co-eluting chromatographic peak pairs were compared using the Pearson correlation coefficient (minimum correlation coefficient for the native and ¹³C-labeled ions: 0.5; minimum correlation for the native and ²H-labeled ions: 0). All chromatographic peak pairs were further convoluted into feature groups by comparing the peak shape of the native, monoisotopic ions (maximum deviation: ± 10 scans; minimum correlation coefficient: 0.85). Subsequently, detected ions and convoluted metabolites were bracketed across all LC-HRMS data files (maximum *m/z* deviation: 6 ppm; maximum retention time deviation: 0.2 min). These automatically-processed results were manually inspected, verified, and putative false positives were discarded.

2.5.2. Annotation and quantitation of metabolites

To annotate biotransformation products, the masses of interest from the MetExtract II processing were initially compared to authentic reference standards of known biotransformation products including several ZEN metabolites. Furthermore, a literature search for additional conjugates was performed and matched with the potential masses of metabolic products. Based on known biotransformation reactions, the mass difference of the measured *m/z* value and the intact compound (ZEN or GEN) was then calculated and searched in databases including mzCloud and METLIN (Xue et al., 2020) to identify potential xenobiotic conjugates. Despite only one part of the structure of GEN, i.e., the phenyl-ring, containing heavy, deuterated atoms (*n* = 4); an intact molecule was assumed for calculations when the MetExtract II algorithm revealed a mass difference corresponding to all four deuterium atoms. For ZEN and GEN, the evaluation focused on feature pairs with a mass difference of 18 ¹³C ($\Delta m/z$ 18.0603) and 4 ²H ($\Delta m/z$ 4.0251), respectively, indicative of an intact structure. When successfully acquired, MS² spectra were evaluated and compared to databases and literature reports.

For many known ZEN metabolites, authentic standards were available. To differentiate isomers with the same exact mass, individual standards of α -ZEL, α -ZAL (α -zearalanol) and α -ZEL-glucuronide were measured in addition to the multi-analyte standard distinguishing them from their β -forms (Supporting Information, Fig. S2). These compounds were quantitated by Skyline (version 20.2.0.286) (MacLean et al., 2010). For each timepoint three biological replicates were measured, therefore the integrated peak areas of the individual measurements were averaged for each condition and the standard deviation was calculated. If a mass was not detected in at least two of the triplicate samples, the

peak area was omitted and considered zero. For quantification a multi-analyte standard containing ZEN and eight of its metabolites (ZEN-14-GlcA, α -ZEL, β -ZEL, α -ZEL-GlcA, β -ZEL-GlcA, ZAN, α -ZAL, ZEN-14-sulfate, ZEN) at five concentration levels (Table S4) was used to create linear calibration curves (1/x weighted).

The annotated biotransformation products were classified according to Schymanski et al. (2014) with level 1 being confirmed by reference standard including MS, MS/MS and retention time. Compounds at level 2 are defined as probable structures and annotated by a library spectrum match (2a) or diagnostic evidence (2b) allowing the proposal of an exact structure by MS and MS/MS. For tentative structures (level 3) evidence for a possible structure exists, but is insufficient to propose an exact structure (e.g. isomers).

Figures were plotted by OriginPro 2018 or exported from Skyline. MS² spectra were extracted from Xcalibur (version 4.1.31.9). The raw data is provided via the MetaboLights repository (MTBLS2716).

3. Results

3.1. Metabolism of ZEN in MCF-7 cells

For the potent mycoestrogen ZEN, fourteen ZEN metabolites were annotated (Table 1). Due to a very low abundance, two isomers of biotransformation products that were derived from automated MetExtract II evaluation were only detected after manual inspection of the EIC of the annotated metabolite. All were present in the cell lysate (Fig. 1a), but only ten were detected in the supernatant after 24 h (Fig. S1 a). All the highly-abundant metabolites (MS signal height > 100,000 ion counts) extracted by MetExtract II were successfully annotated. For ten of the less abundant feature groups of interest, no biologically-reasonable molecular structures were derived.

3.1.1. Annotation of known ZEN biotransformation products

Six of the 14 annotated biotransformation products including ZEN-14-glucuronide (ZEN-14-GlcA), α -zearalenol (α -ZEL), β -zearalenol (β -ZEL), zearalanone (ZAN), α -ZAL, ZEN-14-sulfate and native ZEN were identified by reference standards. A second, less-abundant glucuronide that eluted earlier than the dominant isomer (5.6 min) was detected in addition to ZEN-14-GlcA. Due to the low abundance of the peak, confirmation by MS² was not feasible. Mono- and di-hydroxylated ZEN (OH-ZEN, di-OH-ZEN) were also observed in the cell model. Manual inspection of the EIC chromatogram of OH-ZEN showed a potential

second peak at 7.9 min. This had not been automatically detected by MetExtract because the peak height was below the chosen abundance threshold. It was not possible to obtain MS² spectra of the tentatively-annotated OH-ZEN and di-OH-ZEN as the peaks were of very low intensity.

3.1.2. Annotation of novel ZEN biotransformation products

The difference of m/z 13.9795 between the native molecule and a potentially novel metabolite, referred to as O-ZEN in this study, indicates the addition of one oxygen atom (+15.995) and the removal of two hydrogen atoms (−1.008). The observed low-intensity peak, however, did not trigger an MS² spectrum to support the putative annotation.

A second unexpected finding was a peak with m/z 470.2159 ($[M+H]^+$). An MS² spectrum of the precursor ion mass was available revealing for pyridoxine, specific fragments at m/z 134.0600 and m/z 152.0705 (Fig. 2.), therefore the peak was putatively annotated as ZEN-pyridoxine. In addition, a second, manually-detected, low-intensity peak eluting at 7.0 min without an MS² spectrum was also detected. Taking into consideration the same exact mass, a conjugation of the reduced metabolite α -ZEL with pyridoxal (with an aldehyde group instead of a hydroxy moiety) may be a possible explanation for this second peak.

3.1.3. Quantitation with reference standards

Quantitation of seven compounds (ZEN-14-GlcA, α -ZEL, β -ZEL, ZAN, α -ZAL, ZEN-14-sulfate, ZEN) was performed since authentic reference standards were available (Table S2 and Table S1).

The breast cancer cells were incubated with 5 μ M ZEN. Consequently, if no uptake and metabolism occurs 833 nM ZEN would be expected in the supernatant samples (diluted 1 + 5 (v/v)). In the control experiments (i.e., no cells present during incubation), on average 775 nM ZEN (93%) was recovered. After 2 h incubation, 468 nM toxin (61%) remained. This value slightly decreased to 440 nM (57%) after 6 h and to 434 nM (56%) after 24 h. The recovery was calculated based on the measured concentration of ZEN in the control experiment. The precise cell volume is unknown, therefore the uptake into the cells could only be estimated by relating the intracellular concentration to the concentration of the toxin in the cell culture medium. Thus, less than 1% of ZEN was presumably incorporated into the cells.

When summing up all the ZEN-metabolites that could be quantitated, these accounted for about 160 nM in the 24 h incubated supernatant, i.e., approx. 40% of the present native ZEN (434 nM). The most abundant

Table 1

Summary of annotated ZEN biotransformation products detected by MetExtract II in MCF-7 breast cancer cells (average of three biological replicates).

ZEN metabolites	RT (min)	m/z^a	Ion species ^b	Mass accuracy(ppm)	Polarity ^c	¹³ C-atoms ^d	Sum formula ^e	Level ^f	MS2
ZEN-16-GlcA ^g	5.6	493.1717	[M−H] [−]	1.4	−	18	C ₂₄ H ₃₀ O ₁₁	2b	No
O-ZEN	5.7	331.1189	[M−H] [−]	2.1	−	18	C ₁₈ H ₂₀ O ₆	3	No
ZEN-14-GlcA	6.0	493.1718	[M−H] [−]	1.6	− (/+)	18	C ₂₄ H ₃₀ O ₁₁	1	Yes
α -ZEL-14-sulfate	6.9	399.1121	[M−H] [−]	1.7	− (/+)	18	C ₁₈ H ₂₄ O ₈ S	2b	Yes
ZEN-14-sulfate	7.4	397.0964	[M−H] [−]	1.7	−	18	C ₁₈ H ₂₂ O ₈ S	1	Yes
ZEN-pyridoxine	8.0	470.2169	[M+H] ⁺	2.2	+	18	C ₂₆ H ₃₁ NO ₇	3	Yes
ZEL-pyridoxal ^g	7.0	470.2169	[M+H] ⁺	2.1	+	18	C ₂₆ H ₃₁ NO ₇	3	No
OH-ZEN (peak 1)	7.9 ^g	333.1347	[M−H] [−]	1.8	−	18	C ₁₈ H ₂₂ O ₆	3	No
β -ZEL	8.4	319.1551	[M−H] [−]	1.5	−	18	C ₁₈ H ₂₄ O ₅	1	Yes
di-OH-ZEN	8.5	349.1294	[M−H] [−]	2.0	−	18	C ₁₈ H ₂₂ O ₇	3	No
α -ZAL	8.9	321.1707	[M−H] [−]	1.6	−	18	C ₁₈ H ₂₆ O ₅	1	Yes
α -ZEL	9.0	319.1551	[M−H] [−]	1.6	−	18	C ₁₈ H ₂₄ O ₅	1	Yes
OH-ZEN (peak 2)	9.2	333.1344	[M−H] [−]	1.8	−	18	C ₁₈ H ₂₂ O ₆	3	No
ZAN	9.9	319.1551	[M−H] [−]	1.6	−	18	C ₁₈ H ₂₄ O ₅	1	Yes
ZEN	10.0	317.1394	[M−H] [−]	1.6	− (/+)	18	C ₁₈ H ₂₂ O ₅	1	Yes

^a Accurate mass of ion species with highest intensity.

^b Primary ion species.

^c Polarity in which compounds were detected.

^d Number of ¹³C atoms in the observed labeled metabolite.

^e Sum formula of neutral compound.

^f Confidence of annotation according to Schymanski et al. (2014).

^g Manually detected.

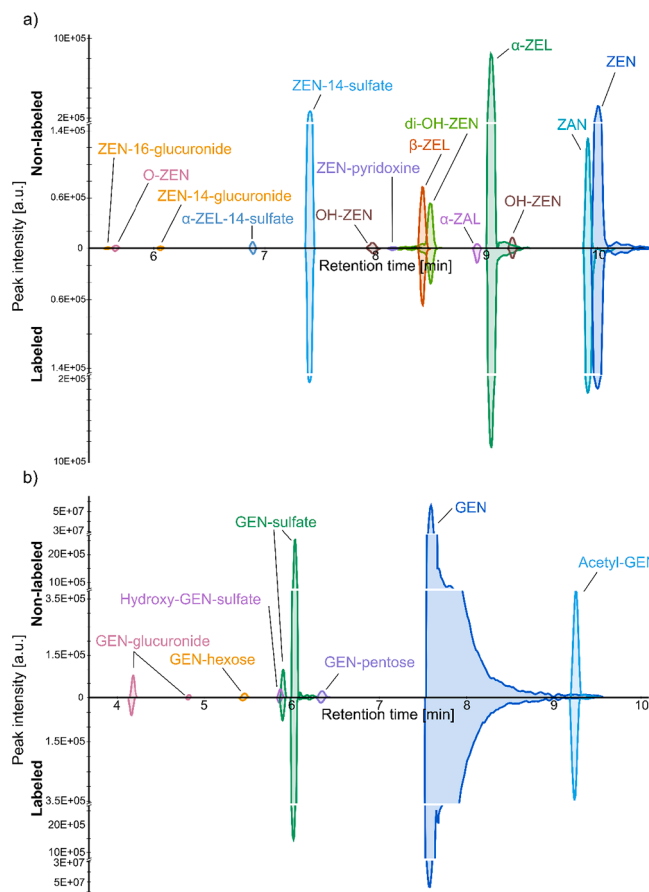


Fig. 1. Combined extracted LC-HRMS ion chromatograms (EICs) of the biotransformation products derived from ZEN (a) and GEN (b) with a mass tolerance of 5 ppm. Except for the native xenoestrogens the most abundant ion species ($[M+H]^+$ or $[M-H]^-$) is shown. The upper y-axis represents the absolute intensity of the non-labeled metabolite, while the lower y-axis shows the absolute intensity of the labeled metabolites. The chromatograms were extracted from a measurement in a cell lysate after incubation for 24 h.

metabolite was α -ZEL (99 nM), followed by ZEN-14-glucuronide (24 nM) and β -ZEL (18 nM). Inside the cells, metabolites that were quantitated (102 nM) accounted for about 29% of the available ZEN (363 nM). The metabolic pattern in the cell lysate was comparable to the supernatant.

Our sensitive method revealed that the incubation solution contained minor impurities of labeled and non-labeled ZAN (0.8 ng/mL), corresponding to approximately 0.3% of the ZEN concentration. Similar minor impurities (~1%) of a commercial ZEN standard (98.9%) with ZAN and β -ZEL have previously been reported and as such a correction factor is required (Warth et al., 2019). Moreover, minor impurities (<1%) of α -ZEL-14-sulfate were observed in the ZEN-14-sulfate standard.

3.2. Metabolism of GEN in MCF-7 cells

Eight different biotransformation products of GEN, namely GEN-glucuronide (two isomers), GEN-sulfate (two isomers), acetyl-GEN, GEN-hexose, GEN-pentose, hydroxy-GEN-sulfate, were annotated (Table 2). With the exception of GEN-glucuronide (second peak) and GEN-hexose, after 24 h, the biotransformation products were observed both in the cell lysate (Fig. 1b) and the cell culture medium (Fig. S1 b). For ten feature groups of interest that were revealed by MetExtract II, a meaningful biological annotation was not achieved. For GEN and metabolites thereof, no reference standards were included; and the peak

area was used to estimate the degree of metabolism. The initial concentration of GEN in the medium (5 μ M GEN) decreased from 4.80 μ M to 4.60 μ M after 2 h and 6 h, indicating as little as 4% and 8% conversion, respectively. After 24 h, a slight increase in metabolism to 13% (4.35 μ M GEN) was apparent. In comparison to ZEN, the metabolism of GEN in MCF-7 cells was less pronounced. The uptake into the cells as the intracellular concentration relative to the concentration of GEN in the medium was estimated to be approximately 2%.

3.2.1. Annotation of known GEN biotransformation products

For GEN-glucuronide, manual inspection of the EIC revealed a second, even less prominent peak at 4.8 min in addition to the low-abundance peak at 4.2 min (Supporting Information, Fig. S4 a). Due to the low intensity of the peaks, no MS² spectrum could be acquired. For GEN-sulfate, two isomers were annotated in the experiment (Supporting Information, Fig. S4 b). An MS² spectrum of both peaks was acquired. The spectrum of the dominant second peak (6.0 min) is represented in the Supporting Information (Fig. S5 b). A fragment ion (m/z 269) corresponding to the loss of sulfate confirmed the annotation. The less abundant isomers of both GEN-glucuronide and GEN-sulfate were only manually detected as the peak intensity was below the defined threshold for MetExtract processing.

3.2.2. Annotation of novel GEN biotransformation products

In addition, four further m/z values corresponded to unexpected biotransformation products. A MS² spectrum of the precursor ion (m/z 364.9972 $[M-H]^-$) contained a fragment ion at m/z 285 indicative of the loss of a sulfate group; thus supporting the tentative identification of the metabolite as hydroxy-GEN-sulfate (Supporting information, Fig. S5 c). The MS² spectrum for another precursor revealed a fragment ion at m/z 271 that corresponded to the loss of an acetyl group putatively revealing acetyl-GEN sulfate (Supporting information, Fig. S5 a). The peaks for m/z 403.108 and m/z 433.1120 were too low in intensity to successfully acquire MS² spectra, but their exact mass indicated adducts with a pentose- and hexose sugar, respectively.

3.3. Biotransformation kinetics of genistein and zearalenone

Across the three time points (2 h, 6 h, 24 h after application of xenoestrogen), the abundance of the xenoestrogens genistein and zearalenone (and biotransformation products thereof), was altered in both the lysate and supernatant (Fig. 3, Table S3). Metabolites that were only detected at the final 24 h time point included α -ZAL, ZEN-16-GlcA, ZEN-pyridoxine and GEN-GlcA 2 in the supernatant; and 3-OH-GEN-sulfate in both the lysate and extracellular medium.

Over the time course, ZEN increased in the lysate but decreased in the supernatant as expected. ZAN revealed a similar trend (Fig. S3 a/b). In general, the abundance of the metabolites steadily increased with time in both the lysate and the supernatant. In the supernatant, GEN behaved similar to ZEN and was reduced over the time course (Fig. 3.). Nonetheless, in the lysate, GEN was most abundant at 2 h, followed by 24 h, and least abundant at 6 h. With the exception of acetyl-GEN; the abundance levels of the xenoestrogens and the biotransformation products thereof in the lysate steadily increased during the time-course experiment.

4. Discussion

4.1. Reduction, glucuronidation and sulfation of ZEN

The results of our untargeted experiment with the detection of two ZEN-glucuronides, ZEN- and α -ZEL-14-sulfate and α -ZAL are in agreement with previous targeted *in vitro* studies on mammalian ZEN biotransformation (Huuskonen et al., 2015; Pfeiffer et al., 2011), *ex vivo* (Warth et al., 2019) and *in vivo* (Mirocha et al., 1981; Warth et al., 2013; Zinedine et al., 2007). The phase I reduction that forms the dominant

metabolites α -ZEL and β -ZEL, via the $3\alpha/3\beta$ -hydroxysteroid dehydrogenase enzyme or other alcohol dehydrogenases (HSD) (Malekinejad et al., 2006) was in accordance with our study the major pathway in humans (Warth et al., 2013; Bandera et al., 2011). Conjugation of ZEN and phase I metabolites thereof with glucuronic acid by UDP-glucuronosyltransferases (UGT) (Pfeiffer et al., 2010; Stevenson et al., 2008) and sulfate by sulfotransferases (SULTs) (Lorenz et al., 2019; Pfeiffer et al., 2011) was in line with literature as well. All three classes of enzyme, HSD (Poutanen et al., 1992), UGTs (Hanioka et al., 2012) and SULTs (Falany et al., 1993) have been found in MCF-7 cells. The reported isoforms include UGT1A1, which is involved in phenolic glucuronidation of ZEN (Pfeiffer et al., 2010). While SULT1E1 was stated to be absent in MCF-7 cells, SULT2A1 and SULT2B1 were described to be present (Hevir et al., 2011; Falany et al., 1993) indicating, in contrast to Schweiger et al. (2008), the involvement of another isoform than SULT1E1 in the sulfation of ZEN.

The most prevalent conjugation site of ZEN (and reduced metabolites thereof) is the sterically-unhindered C-14 position; however, the other hydroxy group at C-16 may also be a possible reaction site (Stevenson et al., 2008). The dominant isomer was annotated by an authentic standard as ZEN-14-GlcA and the less abundant peak was assumed to be ZEN-16-GlcA in accordance with results from Caco-2a cells (Pfeiffer et al., 2011). In agreement with the previously reported exclusive sulfation at C-14 in the Caco-2a cell line (Pfeiffer et al., 2011), no second isomeric form of ZEN-sulfate was observed in the present study.

The ZAN concentration in the incubation solution was higher than the concentration in the samples following 2 h incubation and decreased over time (0.43 ng/mL–0.6 ng/mL). We concluded that the observed ZAN was therefore most likely not a metabolite of ZEN but resulted from the impurity present in the purchased reference standard. The cells, however, were able to assimilate ZAN as the metabolite was also detected in the extracted lysates. Consequently, the origin of α -ZAL could not be determined. The metabolite was either derived from the ZAN impurity or from α -ZEL, a metabolite produced by the cells.

4.2. Oxidized ZEN-metabolites

Several oxidized ZEN-metabolites (mono- and di-hydroxylated ZEN and O-ZEN) were annotated by our workflow. Mono-hydroxylated ZEN has been demonstrated in liver microsomes from several animal species and humans (Pfeiffer et al., 2007; Pfeiffer et al., 2009; Bravin et al., 2009), and *in vivo* in rat previously (Bravin et al., 2009). In our study two peaks associated with OH-ZEN were described, but the hydroxylation sites remained ambiguous. Possible reaction sites were demonstrated by Pfeiffer et al. (2009), who confirmed 15-OH-ZEN, 13-OH-ZEN and a minor metabolite (6- or 8-OH-ZEN) created by aliphatic hydroxylation in microsomes (Fig. 4). In MCF-7 cells, the in hydroxylation involved isoforms of cytochrome P450 CYP1A1 (Piotrowska et al., 2013), CYP3A4 and CYP3A5 (Mitra et al., 2006) were detected. Di-hydroxylated-ZEN has not been previously reported in human cell models, however, Hagler et al. (1979) described these for a fungal culture. Two different isomers of OH-ZEN were discovered with our approach (Fig. 1) in the breast cancer cells supporting the availability of at least two hydroxylation sites. The formation of the metabolite O-ZEN is unclear. A likely reaction pathway is hydroxylation of ZEN in the aromatic system (C13-OH or C15-OH) by a CYP450 monooxygenase, followed by the spontaneous conversion of the catechol to a quinone, as described for chemically synthesized compounds (Hildebrand et al., 2010).

4.3. Conjugation of ZEN with pyridoxine

An unexpected finding was the putative formation of ZEN-pyridoxine and ZEL-pyridoxal. Two peaks with m/z -values consistent with these isomeric metabolites were observed. The surprising formation of xenobiotic conjugates with cell medium constituents (amino acids and antibiotics) has been described by our group before (Flasch et al., 2020). One of the three molecules that constitutes vitamin B6, pyridoxine, was present in the cell culture medium at 2 mg/L according to the manufacturers information. Conjugation with this essential supplements may decrease the amount available and could subsequently affect cell growth

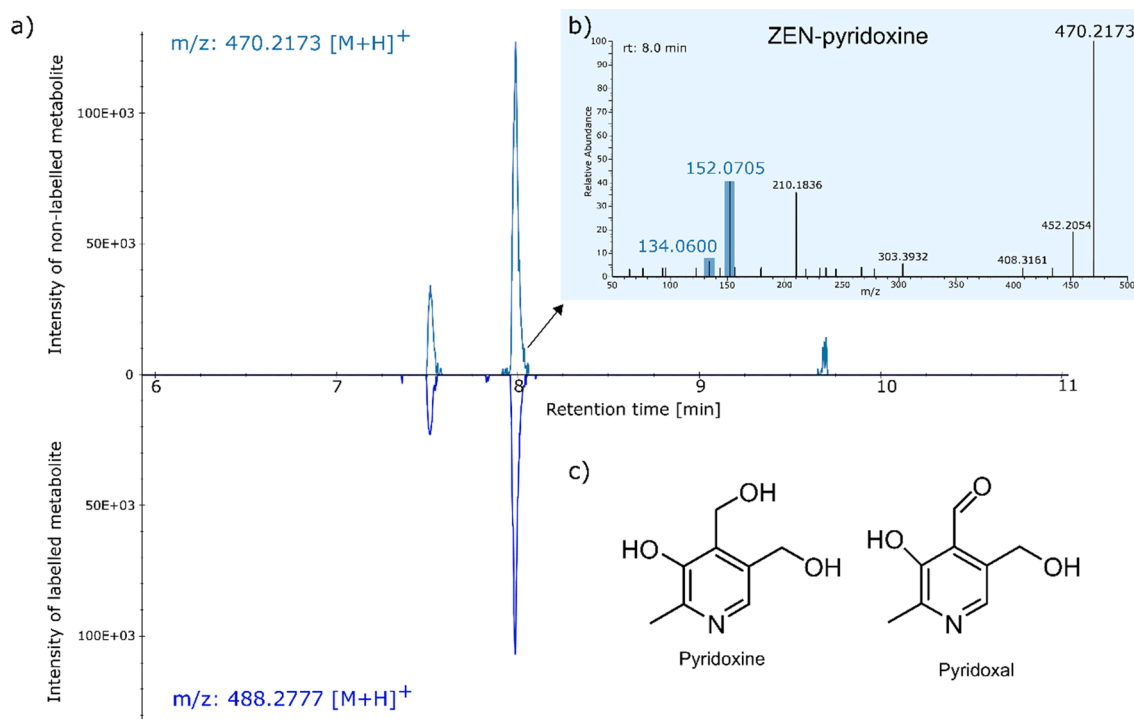


Fig. 2. Putative annotation of ZEN-pyridoxine a) Extracted ion chromatogram of the unlabeled (upper part) and labeled (lower part) metabolite b) MS2 spectrum of m/z 470.2159 at 8.0 min with a normalized collision energy of 30 eV. The shaded masses in the spectrum are present in a MS/MS spectrum of a pyridoxine standard in mzCloud. c) Structures of the potential adducts pyridoxine and pyridoxal.

Table 2Summary of annotated GEN biotransformation products detected by *MetExtract II* in MCF-7 breast cancer cells (average of three biological replicates).

GEN metabolites	RT (min)	m/z ^a	Ion species ^b	Mass accuracy(ppm)	Polarity ^c	² H-atoms ^d	Sum formula ^e	Level ^f	MS2
GEN-glucuronide (peak 1)	4.18	445.0778	[M-H] ⁻	1.80	- (/+)	4	C ₂₁ H ₁₈ O ₁₁	3	No
GEN-glucuronide (peak 2)	4.83 ^g	445.0778	[M-H] ⁻	1.80	- (/+)	4	C ₂₁ H ₁₈ O ₁₁	3	No
GEN-hexose	5.46	433.1120	[M+H] ⁺	-3.39	+	4	C ₂₁ H ₂₀ O ₁₀	3	No
Hydroxy-GEN-sulfate	5.88	364.9972	[M-H] ⁻	1.28	-	4	C ₁₅ H ₁₀ O ₉ S	2a	Yes
GEN-sulfate (peak 1)	5.93 ^g	349.0023	[M-H] ⁻	1.40	- (/+)	4	C ₁₅ H ₁₀ O ₈ S	2a	Yes
GEN-sulfate (peak 2)	6.04	349.0023	[M-H] ⁻	1.40	- (/+)	4	C ₁₅ H ₁₀ O ₈ S	2a	Yes
GEN-pentose	6.34	403.1018	[M+H] ⁺	-2.75	+	4	C ₂₀ H ₁₈ O ₉	3	No
GEN	7.59	269.0456	[M-H] ⁻	2.23	- (/+)	4	C ₁₅ H ₁₀ O ₅	1	Yes
Acetyl-GEN	9.25	313.0701	[M+H] ⁺	1.72	+(-)	4	C ₁₇ H ₁₂ O ₆	2a	Yes

^a Accurate mass of ion species with highest intensity.^b Primary ion species.^c Polarities in which compounds were detected.^d Number of ²H atoms in observed labeled metabolite.^e Sum formula of neutral compound.^f Confidence of identification according to Schymanski et al. (2014).^g Less abundant isomer, which was manually detected.

or endogenous cell metabolism. However, the formed amount seems to be relatively small, despite the high abundance of the vitamin in the medium. The mechanism behind the formation of ZEN-pyridoxine and ZEL-pyridoxal, respectively remains inconclusive. Cellular enzymes appear to be involved in the formation of these metabolites, as they were observed only in the cell lysate. One possible reaction pathway for ZEL-pyridoxal may be adduct formation via ring closure under water elimination of a phenolic hydroxy group like in ZEN and the acetal form of pyridoxal (Kibardina et al., 2018). Therefore, the *in vivo* conversion of pyridoxine to pyridoxal might be a requirement for its formation. However, the more abundant peak revealed a MS²-spectrum matching pyridoxine and not the more active pyridoxal.

4.4. Glucuronidation and sulfation of GEN and its metabolites

Two isomers of both GEN-glucuronide and GEN-sulfate were determined. Additionally, hydroxy-GEN-sulfate was annotated. Both glucuronidation and sulfation of GEN in MCF-7 cells and hepatocytes has been described previously. In good agreement with our findings, Yuan et al. (2012) investigated the metabolism of GEN in different breast cancer cell lines including MCF-7. In this study, two mono-glucuronides (GEN-7-GlcA and GEN-4'-GlcA) and two mono-sulfates (GEN-4'-sulfate and GEN-7-sulfate) were formed. Glucuronidation and sulfation have been described to preferably occur at position C-7 with minor formation at position C-4' (Yuan et al., 2012). Thus, the detected metabolites were tentatively annotated as GEN-7-O-GlcA and GEN-7-sulfate including GEN-4'-GlcA and GEN-4'-sulfate as minor biotransformation products.

The MCF-7 breast cancer cell line (Falany et al., 1993; Hevir et al., 2011; Hanioka et al., 2012) used in our experiments expressed the majority of UGTs and SULTs involved in metabolite formation (Doerge et al., 2000). To date, a hydroxy-GEN-sulfate has not been reported, but in human and murine liver microsomes, hydroxylated GEN (3'-OH-GEN and 8-OH-GEN) has been described in literature (Breinholt et al., 2003; Bursztyka et al., 2008b) and the isoform expressed in MCF-7-, CYP1A2, was supposed to be a major contributor to this hydroxylation. Consequently, the enzymatic capability of the cells to form hydroxy-GEN-sulfate are present. Despite the availability of an MS² spectrum for GEN-sulfate, the unambiguous allocation of the reaction site was not possible.

4.5. Acetylation, glucosylation, and other sugar modifications of GEN

To our knowledge, GEN-hexose and -pentose conjugates as well as acetylated GEN have only been reported in plants (Węgrzyn et al., 2010; Speroni Aguirre et al., 2007) or through chemical synthesis (Polkowski et al., 2004). Formation in human cells has not yet been described.

Nevertheless, a recent study reported GEN-glucoside in the stool and several gastrointestinal organs in germ-free and specific pathogen-free (SPF) mice (Quinn et al., 2020). The authors claimed that O-glucosylation was a minor pathway in phase II metabolism in human liver of certain xenobiotics with possible involvement of a UDP-glucose specific glucosyltransferase (Radomska et al., 1993; Shipkova et al., 2001). Moreover, it has been shown that UGT3A2, which is unreactive with UDP-glucuronic acid, utilizes both UDP-glucose and UDP-xylose as activated sugar donors (MacKenzie et al., 2011; Vergara et al., 2018). Detoxification via O-acetylation is not described in mammals, while this mechanism is prominent in microbes and plants. For instance, acetylated derivatives of ZEN have been described to be produced by *Fusarium*, yet only adducts with GEN have been detected in our study (Muñoz et al., 1989).

4.6. Impact of incubation time on metabolite formation

With increasing incubation time, ZEN is supposedly constantly assimilated by cells where the metabolite is exposed to cellular metabolism. The increasing trend of most metabolites is in accordance with metabolites accumulating in the cells and subsequent excretion. ZAN behaves similarly to ZEN; thus implying that the metabolite was introduced via the incubation solution and is not formed by cellular metabolism of ZEN. The decrease in OH-ZEN indicated that the metabolite may be unstable in the supernatant because of exposure to further chemical reactions. GEN and metabolites thereof revealed a similar time-dependent increase in metabolite formation. Compared to 2 h, the reduced abundance of GEN at the later time points even suggests that the uptake from the supernatant is lower than the rate of the metabolic reactions in the lysate at longer incubation times.

4.7. Impact of biotransformation on estrogenic potency

It is likely that the overall estrogenicity mediated by ZEN in the chosen cell model of ER+ breast cancer was increased by the formed metabolic products. ZEN-pyridoxine, OH-ZEN, di-ZEN, O-ZEN and ZEN-16-GlcA were excluded from the following estimate, as these could not be quantitated due to a lack of authentic reference standards (not commercially-available and not yet internally synthesized). Furthermore, their toxicological relevance is unknown, since their estrogenic potential is still to be explored once standards are available. Considering the abundance after 24 h, the non-quantified biotransformation products constituted approximately 3% of all metabolic products by peak area. However, the ionization efficiency may be different between the compounds, therefore even semi-quantitative conclusions need to be treated with caution.

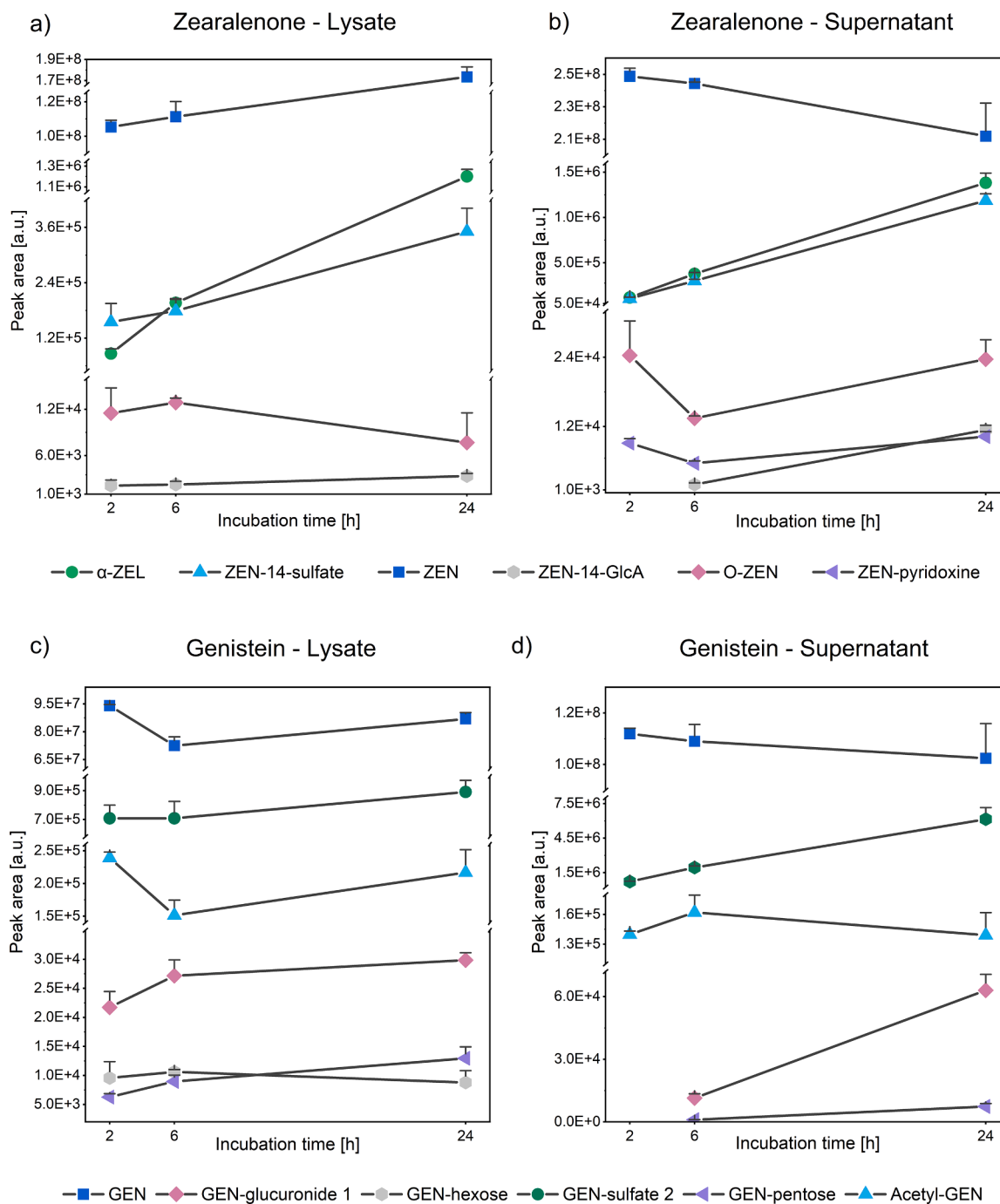


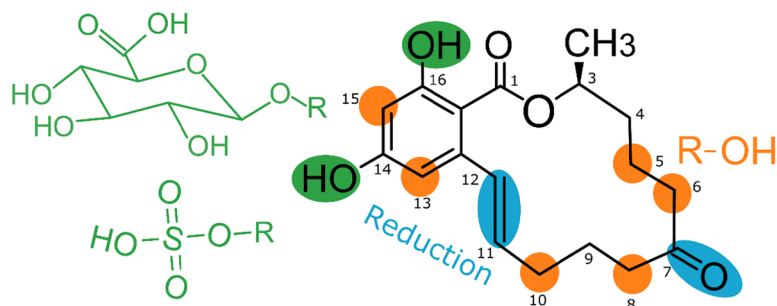
Fig. 3. Kinetics of metabolite formation. Averaged area ($n = 3$) including standard deviation (only positive error bars shown) of zearalenone (a, b) and genistein (c, d) and selected biotransformation products at three time points (2 h, 6 h, 24 h) in both compartments, lysate and supernatant, are shown. The metabolite's most abundant ion species ($[M+H]^+$ or $[M-H]^-$) are reported.

The major and more potent metabolite, α -ZEL, accounts for approximately half of the total metabolite concentration in the supernatant and 83% in the lysate. It is already well-known that this metabolite mediates increased estrogenicity compared to the parent xenoestrogen by up to a factor of 70 \times (Frizzell et al., 2011; Metzler et al., 2010; Tatay et al., 2018). β -ZEL (about 10% of the quantifiable metabolites) is only half as potent as native ZEN (Frizzell et al., 2011; Tatay et al., 2018), but compared to its α -isomer by far less abundantly formed. Detoxifying biotransformation products (Frizzell et al., 2015) that were comprised of phase II-metabolites and accurately quantitated via internally-developed reference standards, *i.e.*, ZEN-14-sulfates and ZEN-14-GlcA, were only minor metabolic products. These accounted for 9%

and 23% of the metabolites that could be quantitated in the lysate and supernatant, respectively. The simultaneous occurrence of the native compound and their metabolites might trigger mixture effects influencing their estrogenicity. In particular, the combination of ZEN with α -ZEL, β -ZEL or ZAN was recently demonstrated to show synergistic effects using a BLYES assay in *Saccharomyces cerevisiae* (Balázs et al., 2021).

The cellular metabolism of GEN is inclined towards a deactivating effect. The observed sulfated and glucuronidated metabolites were associated with reduced estrogenicity *in vitro* (Pugazhendhi et al., 2008; Zhang et al., 1999). The estrogenic potency of GEN-glucosides was reported to be lower than the native molecule (Kalita and Milligan, 2010).

a) Zearalenone



b) Genistein

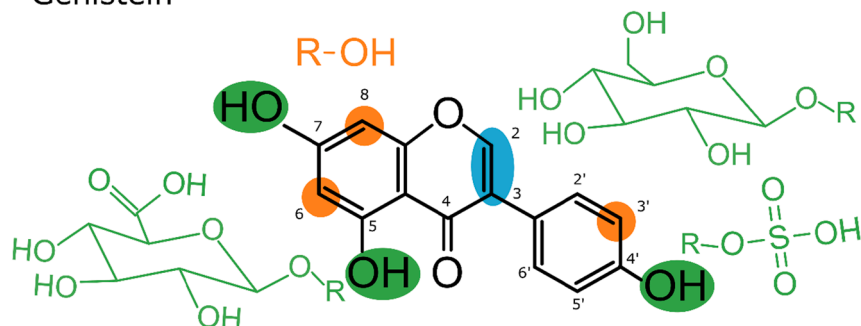


Fig. 4. Molecular structure and overview of sites, where biotransformation is expected to occur, for the two model xenoestrogens, (a) zearalenone and (b) genistein. Known positions of sulfation/glucuronidation/glucosylation (green), hydroxylation (orange) and reduction (blue) as described in the literature are highlighted. R represents the respective toxin. (For interpretation of the references to colour in this figure legend, the reader is referred to the web version of this article.)

Synthetic GEN-ribosides were described as non-cytostatic and non-cytotoxic in human breast cancer cells, but the estrogenicity was not assessed (Polkowski et al., 2004). Importantly, the transformation of GEN was less effective than that of ZEN and the non-conjugated GEN was by far the most prevalent form.

In toxicological assays, MCF-7 cells are regularly used as a model to test estrogenic compounds suspected to be involved in the etiology of breast cancer (Wang et al., 2021). Several metabolites with potential impact on the toxicological potential measured in these assays were observed. However, the formation of metabolites varies between cell models, and metabolic capabilities *in-vivo*, therefore the transfer of *in-vitro* results to real-life scenarios is not straight forward.

Despite differences in metabolic activities of various models, newly discovered metabolites in a specific cell line might be detected in different cells or *in vivo*. Since non-targeted measurements still tend to exhibit higher detection limits compared to specialized targeted methods with tailored sample preparation (Pouchet et al., 2020), the inclusion of novel, toxicologically relevant metabolites in highly-sensitive targeted assays might be a possibility to detect so-far unknown metabolic products in human biomonitoring samples. Most likely, they will occur at relatively low concentrations. Furthermore, suspect screening approaches can include newly discovered metabolites for examining samples from high exposure populations. This might lead to the detection of some of these biotransformation products in human specimen.

5. Conclusion

The generic, stable isotope-assisted workflow to elucidate the fate of xenobiotics in cell culture was implemented to successfully characterize the metabolism of two relevant xenoestrogens in a comprehensive manner. The use of genistein proved that not only fully labeled ^{13}C standards, but also partly deuterated compounds, can be applied in the established workflow. The capability to incorporate partly labeled ^2H

standards broadens the applicability of this approach since fully ^{13}C -labeled standards are frequently not available or very expensive. The fact that retention time shift between the native and isotope enriched compound was demonstrated to be no major issue in our example where the peaks overlapped partially. The less elaborate synthesis of deuterated standards and consequently often lower price are additional benefits of this type of labeled material. Thus, the approach is more amendable and cost-effective for large-scale applications in systems toxicology and pharmacology. Several known phase I- and phase II, but also unexpected metabolic products including ZEN-pyridoxine and GEN-hexose (assumingly GEN-glucose) and GEN-pentose (assumingly GEN-xylose), were found. The investigation of formation kinetics demonstrated the accumulation of most metabolites in the breast cancer cells despite constant excretion to the extracellular medium. Biotransformation products of virtually any xenobiotic will vastly influence the overall toxicological impact of a chemical. In particular, ZEN was significantly transformed to the reduced metabolite α -ZEL. The latter has a substantially higher estrogenic potential (Tatay et al., 2018). Furthermore, the co-occurrence of the native compound and its metabolites might trigger synergistic effects aggravating the toxin's effect. This highlights the importance of detailed investigations regarding biotransformation in *in vitro* models. Elucidation of these processes is also crucial in capturing potentially-harmful metabolic products during drug development, elucidating drug-exposome interactions ('pharmaco-exposomics') and gaining comprehensive insights into the chemical exposome. If newly-discovered metabolites with toxicological relevance are present in real-life samples, the inclusion in future targeted human biomonitoring studies and non-targeted screening approaches should be considered to investigate occurrence at the individual and population level within the exposome paradigm.

CRediT authorship contribution statement

Mira Flasch: Writing – original draft, Writing – review & editing.

Christoph Bueschl: Software, Writing – review & editing. **Giorgia Del Favero:** Writing – review & editing, Supervision. **Gerhard Adam:** Writing – review & editing, Funding acquisition. **Rainer Schuhmacher:** Conceptualization, Software, Writing – review & editing, Funding acquisition, Supervision. **Doris Marko:** Conceptualization, Writing – review & editing, Funding acquisition, Supervision. **Benedikt Warth:** Conceptualization, Writing – original draft, Writing – review & editing, Funding acquisition, Supervision.

Declaration of Competing Interest

The authors declare that they have no known competing financial interests or personal relationships that could have appeared to influence the work reported in this paper.

Acknowledgments

The authors would like to express their gratitude towards Verena Schmidt, Michaela Schwaiger and Christoph Gassner (all University of Vienna) for fruitful discussion and assistance in sample preparation, data acquisition and analysis. The Mikula laboratory (Technical University of Vienna) is greatly acknowledged for providing authentic reference standards for several ZEN-metabolites. Romer Labs (Tulln, Austria) kindly supplied the ¹³C-labeled ZEN. LC-HRMS measurements were performed at the Mass Spectrometry Center of the Faculty of Chemistry at the University of Vienna. The authors thank the Austrian Science Fund for the financial support through the project SFB Fusarium (#F3715 and #F3718 and #F3701), project P 33188-B and the Erwin-Schrödinger fellowship awarded to Benedikt Warth (#J-3808) as well as the Government of Lower Austria (project NovAlgo).

Data availability

The raw data is provided via the MetabLights repository (MTBLS2716).

References

- Ali, N., Degen, G.H., 2019. Biomonitoring of zearalenone and its main metabolites in urines of Bangladeshi adults. *Food Chem. Toxicol.* 130, 276–283.
- Appel, B.N., Gottmann, J., Schäfer, J., Bunzel, M., 2021. Absorption and metabolism of modified mycotoxins of alternariol, alternariol monomethyl ether, and zearalenone in Caco-2 cells. *Cereal Chem.* 98, 109–122.
- Balázs, A., Faisal, Z., Csepregi, R., Kőszegi, T., Kriszt, B., Szabó, I., Poór, M., 2021. In Vitro Evaluation of the Individual and Combined Cytotoxic and Estrogenic Effects of Zearalenone, Its Reduced Metabolites, Alternariol, and Genistein. *Int. J. Mol. Sci.* 22, 6281.
- Balcerczyk, A., Dambon, C., Elena-Herrmann, B., Panthu, B., Rautureau, G.J.P., 2020. Metabolomic Approaches to Study Chemical Exposure-Related Metabolism Alterations in Mammalian Cell Cultures. *Int. J. Mol. Sci.* 21, 6843.
- Bandera, E.V., Chandran, U., Buckley, B., Lin, Y., Isukapalli, S., Marshall, I., King, M., Zarbl, H., 2011. Urinary mycoestrogens, body size and breast development in New Jersey girls. *Sci. Total Environ.* 409, 5221–5227.
- Basu, P., Maier, C., 2018. Phytoestrogens and breast cancer: In vitro anticancer activities of isoflavones, lignans, coumestans, stilbenes and their analogs and derivatives. *Biomed. Pharmacother.* 107, 1648–1666.
- Baumeister, T.U.H., Ueberschaar, N., Schmidt-Heck, W., Mohr, J.F., Deicke, M., Wichard, T., Guthke, R., Pohnert, G., 2018. DeltaMS: a tool to track isotopologues in GC- and LC-MS data. *Metabolomics* 14, 41.
- Belhassen, H., Jiménez-Díaz, I., Arrebola, J.P., Ghali, R., Ghorbel, H., Olea, N., Hedili, A., 2015. Zearalenone and its metabolites in urine and breast cancer risk: A case-control study in Tunisia. *Chemosphere* 128, 1–6.
- Berman, T., Goldsmith, R., Göen, T., Spungen, J., Novack, L., Levine, H., Amitai, Y., Shohat, T., Grotto, I., 2013. Urinary concentrations of environmental contaminants and phytoestrogens in adults in Israel. *Environ. Int.* 59, 478–484.
- Braun, D., Ezekiel, C.N., Abia, W.A., Wisgrill, L., Degen, G.H., Turner, P.C., Marko, D., Warth, B., 2018. Monitoring Early Life Mycotoxin Exposures via LC-MS/MS Breast Milk Analysis. *Anal. Chem.* 90, 14569–14577.
- Bravin, F., Duca, R.C., Balaguer, P., Delaforge, M., 2009. In vitro cytochrome p450 formation of a mono-hydroxylated metabolite of zearalenone exhibiting estrogenic activities: possible occurrence of this metabolite in vivo. *Int. J. Mol. Sci.* 10, 1824–1837.
- Breinhold, V.M., Rasmussen, S.E., Brøsen, K., Friedberg, T.H., 2003. In vitro Metabolism of Genistein and Tangeretin by Human and Murine Cytochrome P450s. *Pharmacol. Toxicol.* 93, 14–22.
- Bueschl, C., Kluger, B., Neumann, N.K.N., Doppler, M., Maschietto, V., Thallinger, G.G., Meng-Reiterer, J., Krška, R., Schuhmacher, R., 2017. MetExtract II: A Software Suite for Stable Isotope-Assisted Untargeted Metabolomics. *Anal. Chem.* 89, 9518–9526.
- Bursztyka, J., Perdu, E., Pettersson, K., Pongratz, I., Fernández-Cabrera, M., Olea, N., Debrauwer, L., Zalko, D., Cravedi, J.P., 2008a. Biotransformation of genistein and bisphenol A in cell lines used for screening endocrine disruptors. *Toxicol. In Vitro* 22, 1595–1604.
- Bursztyka, J., Perdu, E., Tulliez, J., Debrauwer, L., Delous, G., Canlet, C., De Sousa, G., Rahmani, R., Benfenati, E., Cravedi, J.-P., 2008b. Comparison of genistein metabolism in rats and humans using liver microsomes and hepatocytes. *Food Chem. Toxicol.* 46, 939–948.
- Chen, J., Lin, H., Hu, M., 2005. Absorption and metabolism of genistein and its five isoflavone analogs in the human intestinal Caco-2 model. *Cancer Chemother. Pharmacol.* 55, 159–169.
- Chokkathukalam, A., Kim, D.-H., Barrett, M.P., Breiting, R., Creek, D.J., 2014. Stable isotope-labeling studies in metabolomics: New insights into structure and dynamics of metabolic networks. *Bioanalysis* 6 (4), 511–524.
- Dellafiora, L., Warth, B., Schmidt, V., Del Favero, G., Mikula, H., Fröhlich, J., Marko, D., 2018. An integrated in silico/in vitro approach to assess the xenoerogenic potential of Alternaria mycotoxins and metabolites. *Food Chem.* 248, 253–261.
- Dhanjal, D.S., Bhardwaj, S., Sharma, R., Bhardwaj, K., Kumar, D., Chopra, C., Nepovimova, E., Singh, R., Kuca, K., 2020. Plant Fortification of the Diet for Anti-Ageing Effects: A Review. *Nutrients* 12 (10), 3008.
- Doerge, D.R., Chang, H.C., Churchwell, M.I., Holder, C.L., 2000. Analysis of Soy Isoflavone Conjugation In Vitro and in Human Blood Using Liquid Chromatography-Mass Spectrometry. *Drug Metab. Dispos.* 28, 298.
- Elfadul, R., Jesien, R., Elnabawi, A., Chigbu, P., Ishaque, A., 2021. Analysis of Estrogenic Activity in Maryland Coastal Bays Using the MCF-7 Cell Proliferation Assay. *Int. J. Environ. Res. Public Health* 18, 6254.
- Falany, J.L., Lawing, L., Falany, C.N., 1993. Identification and characterization of cytosolic sulfotransferase activities in MCF-7 human breast carcinoma cells. *J. Steroid Biochem. Mol. Biol.* 46, 481–487.
- Flasch, M., Bueschl, C., Woelflingseder, L., Schwartz-Zimmermann, H.E., Adam, G., Schuhmacher, R., Marko, D., Warth, B., 2020. Stable Isotope-Assisted Metabolomics for Deciphering Xenobiotic Metabolism in Mammalian Cell Culture. *ACS Chem. Biol.* 15, 970–981.
- Fleck, S.C., Churchwell, M.I., Doerge, D.R., Teeguarden, J.G., 2016. Urine and serum biomonitoring of exposure to environmental estrogens II: Soy isoflavones and zearalenone in pregnant women. *Food Chem. Toxicol.* 95, 19–27.
- Frizzell, C., Ndossi, D., Verhaegen, S., Dahl, E., Eriksen, G., Sørli, M., Ropstad, E., Müller, M., Elliott, C.T., Connolly, L., 2011. Endocrine disrupting effects of zearalenone, alpha- and beta-zearalenol at the level of nuclear receptor binding and steroidogenesis. *Toxicol. Lett.* 206, 210–217.
- Frizzell, C., Uhlig, S., Miles, C.O., Verhaegen, S., Elliott, C.T., Eriksen, G.S., Sørli, M., Ropstad, E., Connolly, L., 2015. Biotransformation of zearalenone and zearalenols to their major glucuronide metabolites reduces estrogenic activity. *Toxicol. In Vitro* 29, 575–581.
- Hagler, W.M., Mirocha, C.J., Pathre, S.V., Behrens, J.C., 1979. Identification of the naturally occurring isomer of zearalenol produced by *Fusarium roseum* 'Gibbosum' in rice culture. *Appl. Environ. Microbiol.* 37 (5), 849–853.
- Hanioka, N., Iwabu, H., Hanafusa, H., Nakada, S., Narimatsu, S., 2012. Expression and Inducibility of UDP-glucuronosyltransferase 1As in MCF-7 Human Breast Carcinoma Cells. *Basic Clin. Pharmacol. Toxicol.* 110, 253–258.
- Hevir, N., Trost, N., Debeljak, N., Lanišnik Rižner, T., 2011. Expression of estrogen and progesterone receptors and estrogen metabolizing enzymes in different breast cancer cell lines. *Chem. Biol. Interact.* 191, 206–216.
- Hildebrand, A., Pfeiffer, E., Metzler, M., 2010. Aromatic hydroxylation and catechol formation: A novel metabolic pathway of the growth promotor zearanol. *Toxicol. Lett.* 192 (3), 379–386.
- Hildebrand, A.A., Pfeiffer, E., Rapp, A., Metzler, M., 2012. Hydroxylation of the mycotoxin zearalenone at aliphatic positions: novel mammalian metabolites. *Mycotoxin Res* 28 (1), 1–8.
- Huuskonen, P., Auriola, S., Pasanen, M., 2015. Zearalenone metabolism in human placental subcellular organelles, JEG-3 cells, and recombinant CYP19A1. *Placenta* 36, 1052–1055.
- Kalita, J., Milligan, S., 2010. In vitro Estrogenic Potency of Phytoestrogen-Glycosides and some Plant Flavanoids. *Ind. J. Sci. Technol.* 3, 1142–1147.
- Kaur, G., Gupta, S.K., Singh, P., Ali, V., Kumar, V., Verma, M., 2020. Drug-metabolizing enzymes: role in drug resistance in cancer. *Clin. Transl. Oncol.* 22, 1667–1680.
- Kessner, D., Chambers, M., Burke, R., Agusand, D., Mallick, P., 2008. ProteoWizard: open source software for rapid proteomics tools development. *Bioinformatics* 24, 2534–2536.
- Khosrokhavar, R., Rahimifard, N., Shoeibi, S., Hamedani, M.P., Hosseini, M.-J., 2009. Effects of zearalenone and α -Zearalenol in comparison with Raloxifene on T47D cells. *Toxicol. Mech. Methods* 19, 246–250.
- Kibardina, L.K., Trifonov, A.V., Burirov, A.R., Gazizov, A.S., Pudovik, M.A., 2018. Pyridoxal: A New Alkylating Agent in Reactions with Phenols and Polyphenols. *Russ. J. Gen. Chem.* 88, 1832–1837.
- Kluger, B., Bueschl, C., Neumann, N., Stuckler, R., Doppler, M., Chassy, A.W., Waterhouse, A.L., Rechthaler, J., Kamplleitner, N., Thallinger, G.G., Adam, G., Krška, R., Schuhmacher, R., 2014. Untargeted Profiling of Tracer-Derived Metabolites Using Stable Isotopic Labeling and Fast Polarity-Switching LC-ESI-HRMS. *Anal. Chem.* 86, 11533–11537.

- Kumar, M., Sarma, D.K., Shubham, S., Kumawat, M., Verma, V., Prakash, A., Tiwari, R., 2020. Environmental Endocrine-Disrupting Chemical Exposure: Role in Non-Communicable Diseases. *Front Public Health* 8, 553850.
- Lecomte, S., Demay, F., Ferrière, F., Pakdel, F., 2017. Phytochemicals Targeting Estrogen Receptors: Beneficial Rather Than Adverse Effects? *Int. J. Mol. Sci.* 18, 1381.
- Lee, D.H., 2018. Evidence of the Possible Harm of Endocrine-Disrupting Chemicals in Humans: Ongoing Debates and Key Issues. *Endocrinol Metab (Seoul)* 33, 44–52.
- Lehmann, L., Wagner, J., Metzler, M., 2006. Estrogenic and clastogenic potential of the mycotoxin alternariol in cultured mammalian cells. *Food Chem. Toxicol.* 44, 398–408.
- Liu, R., Yu, X., Chen, X., Zhong, H., Liang, C., Xu, X., Xu, W., Cheng, Y., Wang, W., Yu, L., Wu, Y., Yan, N., Hu, X., 2019. Individual factors define the overall effects of dietary genistein exposure on breast cancer patients. *Nutr. Res.* 67, 1–16.
- Lorenz, N., Dänicke, S., Edler, L., Gottschalk, C., Lassek, E., Marko, D., Rychlik, M., Mally, A., 2019. A critical evaluation of health risk assessment of modified mycotoxins with a special focus on zearalenone. *Mycotoxin Res* 35, 27–46.
- MacKenzie, P.I., Rogers, A., Elliot, D.J., Chau, N., Hulin, J.A., Miners, J.O., Meech, R., 2011. The novel UDP glycosyltransferase 3A2: cloning, catalytic properties, and tissue distribution. *Mol. Pharmacol.* 79, 472–478.
- MacLean, B., Tomazela, D.M., Shulman, N., Chambers, M., Finney, G.L., Frewen, B., Kern, R., Tabb, D.L., Liebler, D.C., MacCoss, M.J., 2010. Skyline: an open source document editor for creating and analyzing targeted proteomics experiments. *Bioinformatics (Oxford, England)* 26, 966–968.
- Malekinejad, H., Maas-Bakker, R., Fink-Gremmels, J., 2006. Species differences in the hepatic biotransformation of zearalenone. *Vet. J.* 172, 96–102.
- Metzler, M., Pfeiffer, E., Hildebrand, A., 2010. Zearalenone and its metabolites as endocrine disrupting chemicals. *World Mycot. J.* 3, 385–401.
- Mikula, H., Hametner, C., Berthiller, F., Warth, B., Krška, R., Adam, G., Fröhlich, J., 2012. Fast and reproducible chemical synthesis of zearalenone-14- β -D-glucuronide. *World Mycot. J.* 5, 289–296.
- Mikula, H., Weber, J., Lexmüller, S., Bichl, G., Schwartz, H., Varga, E., Berthiller, F., Hametner, C., Krška, R., Fröhlich, J., 2013. Simultaneous preparation of α/β -zearalenol glucosides and glucuronides. *Carbohydr. Res.* 373, 59–63.
- Mirocha, C.J., Pathre, S.V., Robison, T.S., 1981. Comparative metabolism of zearalenone and transmission into bovine milk. *Food Cosmet. Toxicol.* 19, 25–30.
- Mitra, R., Srirangam, A., Capdevila, J., Potter, D.A., 2006. Cytochrome P450 promotes breast cancer cell proliferation. *Cancer Res.* 66, 1220.
- Moche, H., Chentouf, A., Neves, S., Corpant, J.-M., Nesslany, F., 2021. Comparison of in vitro endocrine activity of phthalates and alternative plasticizers. *J. Toxicol.* 2021, 8815202.
- Moon, Y.J., Wang, X., Morris, M.E., 2006. Dietary flavonoids: Effects on xenobiotic and carcinogen metabolism. *Toxicol. In Vitro* 20, 187–210.
- Moors, S., Blaszkewicz, M., Bolt, H.M., Degen, G.H., 2007. Simultaneous determination of daidzein, equol, genistein and bisphenol A in human urine by a fast and simple method using SPE and GC-MS. *Mol. Nutr. Food Res.* 51, 787–798.
- Muñoz, L., Castro, J.L., Cardelle, M., Castedo, L., Riguera, R., 1989. Acetylated mycotoxins from *Fusarium graminearum*. *Phytochemistry* 28, 83–85.
- Oesterle, I., Braun, D., Berry, D., Wisgrill, L., Rompel, A., Warth, B., 2021. Polyphenol exposure, metabolism, and analysis: a global exposomics perspective. *Ann. Rev. Food Sci. Technol.* 12, 461–484.
- Pascucci, J.-M., Gerbal-Chaloin, S., Duret, C., Daujat-Chavanieu, M., Vilarem, M.-J., Maurel, P., 2008. The Tangle of Nuclear Receptors that Controls Xenobiotic Metabolism and Transport: Crosstalk and Consequences. *Annu. Rev. Pharmacol. Toxicol.* 48, 1–32.
- Pastor-Barriuso, R., Fernández, M.F., Castaño-Vinyals, G., Whelan, D., Pérez-Gómez, B., Llorca, J., Villanueva, C.M., Guevara, M., Molina-Molina, J.-M., Artacho-Córdón, F., Barriuso-Lapresa, L., Tusquets, I., Diessen-Sotos, T., Aragonés, N., Olea, N., Kogevinas, M., Pollán, M., 2016. Total Effective Xenoestrogen Burden in Serum Samples and Risk for Breast Cancer in a Population-Based Multicase Control Study in Spain. *Environ. Health Perspect.* 124, 1575–1582.
- Paterni, I., Granchi, C., Minutolo, F., 2017. Risks and benefits related to alimentary exposure to xenoestrogens. *Crit. Rev. Food Sci. Nutr.* 57, 3384–3404.
- Pazaiti, A., Kontos, M., Fentiman, I.S., 2012. ZEN and the art of breast health maintenance. *Int. J. Clin. Pract.* 66, 28–36.
- Pfeiffer, E., Heyting, A., Metzler, M., 2007. Novel oxidative metabolites of the mycoestrogen zearalenone in vitro. *Mol. Nutr. Food Res.* 51, 867–871.
- Pfeiffer, E., Hildebrand, A., Damm, G., Rapp, A., Cramer, B., Humpf, H.U., Metzler, M., 2009. Aromatic hydroxylation is a major metabolic pathway of the mycotoxin zearalenone in vitro. *Mol. Nutr. Food Res.* 53, 1123–1133.
- Pfeiffer, E., Hildebrand, A., Mikula, H., Metzler, M., 2010. Glucuronidation of zearalenone, zearanol and four metabolites in vitro: Formation of glucuronides by various microsomes and human UDP-glucuronosyltransferase isoforms. *Mol. Nutr. Food Res.* 54, 1468–1476.
- Pfeiffer, E., Kommer, A., Dempe, J.S., Hildebrand, A.A., Metzler, M., 2011. Absorption and metabolism of the mycotoxin zearalenone and the growth promoter zearanol in Caco-2 cells in vitro. *Mol. Nutr. Food Res.* 55, 560–567.
- Piotrowska, H., Kucinska, M., Murias, M., 2013. Expression of CYP1A1, CYP1B1 and MnSOD in a panel of human cancer cell lines. *Mol. Cell. Biochem.* 383, 95–102.
- Polkowski, K., Popiolkiewicz, J., Krzeczynski, P., Ramza, J., Pucko, W., Zegrocka-Stendel, O., Boryski, J., Skierski, J.S., Mazurek, A.P., Gryniewicz, G., 2004. Cytostatic and cytotoxic activity of synthetic genistein glucosides against human cancer cell lines. *Cancer Lett.* 203, 59–69.
- Pourchet, M., Debrauwer, L., Klanova, J., Price, E.J., Covaci, A., Caballero-Casero, N., Oberacher, H., Lamoree, M., Damont, A., Fenaillé, F., Vlaanderen, J., Meijer, J., Krauss, M., Sarigiannis, D., Barouki, R., Le Bizec, B., Antignac, J.-P., 2020. Suspect and non-targeted screening of chemicals of emerging concern for human biomonitoring, environmental health studies and support to risk assessment: From promises to challenges and harmonisation issues. *Environ. Int.* 139, 105545.
- Poutanen, M., Isomaa, V., Lehto, V.-P., Vihko, R., 1992. Immunological analysis of 17 β -hydroxysteroid dehydrogenase in benign and malignant human breast tissue. *Int. J. Cancer* 50, 386–390.
- Preindl, K., Braun, D., Aichinger, G., Sieri, S., Fang, M., Marko, D., Warth, B., 2019. A Generic Liquid Chromatography–Tandem Mass Spectrometry Exposome Method for the Determination of Xenoestrogens in Biological Matrices. *Anal. Chem.* 91, 11334–11342.
- Pristner, M., Warth, B., 2020. Drug-exposome interactions: the next Frontier in precision medicine. *Trends Pharmacol. Sci.* 41, 994–1005.
- Pugazhendhi, D., Watson, K.A., Mills, S., Botting, N., Pope, G.S., Darbre, P.D., 2008. Effect of sulphation on the oestrogen agonist activity of the phytoestrogens genistein and daidzein in MCF-7 human breast cancer cells. *J. Endocrinol.* 197, 503.
- Quinn, R.A., Melnik, A.V., Vrbanac, A., Fu, T., Patras, K.A., Christy, M.P., Bodai, Z., Belda-Ferre, P., Tripathi, A., Chung, L.K., Downes, M., Welch, R.D., Quinn, M., Humphrey, G., Panitchpakdi, M., Weldon, K.C., Aksenov, A., da Silva, R., Avila-Pacheco, J., Clish, C., Bae, S., Mallick, H., Franzosa, E.A., Lloyd-Price, J., Bussell, R., Thron, T., Nelson, A.T., Wang, M., Leszczynski, E., Vargas, F., Gauglitz, J.M., Meehan, M.J., Gentry, E., Arthur, T.D., Komor, A.C., Poulsen, O., Boland, B.S., Chang, J.T., Sandborn, W.J., Lim, M., Rhee, N., Lumeng, J.C., Xavier, R.J., Kazmierczak, B.I., Jain, R., Egan, M., Garg, M., Gao, D., Raffatellu, M., Vlamakis, H., Haddad, G.G., Siegel, D., Huttenhower, C., Mazmanian, S.K., Evans, R. M., Nizet, V., Knight, R., Dorrestein, P.C., 2020. Global chemical effects of the microbiome include new bile-acid conjugations. *Nature* 579, 123–129.
- Radomska, A., Little, J., Pyrek, J.S., Drake, R.R., Igari, Y., Fournel-Gigleux, S., Magdalou, J., Burchell, B., Elbein, A.D., Siest, G., et al., 1993. A novel UDP-Glc-specific glucosyltransferase catalyzing the biosynthesis of 6-O-glucosides of bile acids in human liver microsomes. *J. Biol. Chem.* 268, 15127–15135.
- Rice, S., Whitehead, S.A., 2006. Phytoestrogens and breast cancer –promoters or protectors? *13*, 1995.
- Rigalli, J.P., Tocchetti, G.N., Arana, M.R., Villanueva, S.S.M., Catania, V.A., Theile, D., Ruiz, M.L., Weiss, J., 2016. The phytoestrogen genistein enhances multidrug resistance in breast cancer cell lines by translational regulation of ABC transporters. *Cancer Lett.* 376, 165–172.
- Schweiger, W., Berthiller, F., Fischer, A., Erhart, C., Bicker, W., Shams, M., Schuhmacher, R., Krška, R., Wiesenberger, G., Mitterbauer, R., Glatt, H., Adam, G., 2008. Formation of zearalenone-4-sulfate by yeast cells expressing sulfotransferase genes. *Cereal Res. Commun.* 36, 385–387.
- Schymanski, E.L., Jeon, J., Gulde, R., Fenner, K., Ruff, M., Singer, H.P., Hollender, J., 2014. Identifying Small Molecules via High Resolution Mass Spectrometry: Communicating Confidence. *Environ. Sci. Technol.* 48, 2097–2098.
- Shipkova, M., Strassburg, C.P., Braun, F., Streit, F., Gröne, H.J., Armstrong, V.W., Tukey, R.H., Oellerich, M., Wieland, E., 2001. Glucuronide and glucoside conjugation of mycophenolic acid by human liver, kidney and intestinal microsomes. *Br. J. Pharmacol.* 132, 1027–1034.
- Sofie, C., Marta, A., Julie, B., Anne Marie, V., Gitte Alsing, P., Ulla, H., 2014. Low-dose effects of bisphenol A on early sexual development in male and female rats. *Reproduction* 147, 477–487.
- Soukup, S.T., Helppi, J., Müller, D.R., Zierau, O., Watzl, B., Vollmer, G., Diel, P., Bub, A., Kulling, S.E., 2016. Phase II metabolism of the soy isoflavones genistein and daidzein in humans, rats and mice: a cross-species and sex comparison. *Arch. Toxicol.* 90 (6), 1335–1347.
- Speroni Aguirre, F.J., Milesi, V., Añón, M.C., 2007. Effect of Extraction and Precipitation Conditions During Soybean Protein Isolate Production on the Genistein Series Content. *J. Am. Oil Chem. Soc.* 84, 305–314.
- Stevenson, D.E., Hansen, R.P., Loader, J.I., Jensen, D.J., Cooney, J.M., Wilkins, A.L., Miles, C.O., 2008. Preparative enzymatic synthesis of glucuronides of zearalenone and five of its metabolites. *J. Agric Food Chem* 56, 4032–4038.
- Tatay, E., Espín, S., García-Fernández, A.-J., Ruiz, M.-J., 2018. Estrogenic activity of zearalenone, α -zearalenol and β -zearalenol assessed using the E-screen assay in MCF-7 cells. *Toxicol. Mech. Methods* 28, 239–242.
- Tordjiman, K., Grinshpan, L., Novack, L., Göen, T., Segev, D., Beacher, L., Stern, N., Berman, T., 2016. Exposure to endocrine disrupting chemicals among residents of a rural vegetarian/vegan community. *Environ. Int.* 97, 68–75.
- Vergara, A.G., Watson, C.J.W., Chen, G., Lazarus, P., 2018. Detoxification of Polycyclic Aromatic Hydrocarbons (PAHs) by UDP-glycosyltransferase 3A2 (UGT3A2) Variants using Alternative Sugars. *FASEB J.* 32, 564.15–64.15.
- Verheus, M., Gils, C.H.V., Keinan-Boker, L., Grace, P.B., Bingham, S.A., Peeters, P.H.M., 2007. Plasma Phytoestrogens and Subsequent Breast Cancer Risk. *J. Clin. Oncol.* 25, 648–655.
- Wang, X., Ha, D., Yoshitake, R., Chan, Y.S., Sadava, D., Chen, S., 2021. Exploring the Biological Activity and Mechanism of Xenoestrogens and Phytoestrogens in Cancers: Emerging Methods and Concepts. *Int. J. Mol. Sci.* 22, 8798.
- Warth, B., Preindl, K., Manser, P., Wick, P., Marko, D., Buerki-Thurnherr, T., 2019. Transfer and Metabolism of the Xenoestrogen Zearalenone in Human Perfused Placenta. *Environ. Health Perspect.* 127, 107004–107104.
- Warth, B., Raffener, P., Granados, A., Huan, T., Fang, M., Forsberg, E.M., Benton, H.P., Goetz, L., Johnson, C.H., Siuzdak, G., 2018. Metabolomics Reveals that Dietary Xenoestrogens Alter Cellular Metabolism Induced by Palbociclib/Letrozole Combination Cancer Therapy. *Cell Chem. Biol.* 25, 291–300.e3.
- Warth, B., Sulyok, M., Berthiller, F., Schuhmacher, R., Krška, R., 2013. New insights into the human metabolism of the *Fusarium* mycotoxins deoxynivalenol and zearalenone. *Toxicol. Lett.* 220, 88–94.
- Węgrzyn, G., Jakóbkiewicz-Banecka, J., Gabig-Cimińska, M., Piotrowska, E., Narajczyk, M., Kloska, A., Malinowska, M., Dziedzic, D., Gołębska, I., Moskot, M.,

- Węgrzyn, A., 2010. Genistein: a natural isoflavone with a potential for treatment of genetic diseases. *Biochem. Soc. Trans.* 38, 695–701.
- Wu, A.H., Yu, M.C., Tseng, C.C., Pike, M.C., 2008. Epidemiology of soy exposures and breast cancer risk. *Br. J. Cancer* 98, 9–14.
- Xu, Z., Liu, J., Wu, X., Huang, B., Pan, X., 2017. Nonmonotonic responses to low doses of xenoestrogens: A review. *Environ. Res.* 155, 199–207.
- Xue, J., Guijas, C., Benton, H.P., Warth, B., Siuzdak, G., 2020. METLIN MS² molecular standards database: a broad chemical and biological resource. *Nat. Methods* 17, 953–954.
- Yager, J.D., Davidson, N.E., 2006. Estrogen Carcinogenesis in Breast Cancer. *N. Engl. J. Med.* 354, 270–282.
- Yang, Shupeng, Zhang, Huiyan, Sun, Feifei, De Ruyck, Karl, Zhang, Jinzhen, Jin, Yue, Li, Yanshen, Wang, Zhanhui, Zhang, Suxia, De Saeger, Sarah, Zhou, Jinhui, Li, Yi, De Boevre, Marthe, 2017. Metabolic Profile of Zearalenone in Liver Microsomes from Different Species and Its in Vivo Metabolism in Rats and Chickens Using Ultra High-Pressure Liquid Chromatography-Quadrupole/Time-of-Flight Mass Spectrometry. *J. Agric. Food. Chem.* 65 (51), 11292–11303.
- Yuan, Bo, Wang, Linglan, Jin, Yi, Zhen, Huijuan, Xu, Pingwei, Xu, Youjun, Li, Chibing, Xu, Haiyan, 2012. Role of Metabolism in the Effects of Genistein and Its Phase II Conjugates on the Growth of Human Breast Cell Lines. *AAPS J.* 14 (2), 329–344.
- Zhang, Y., Song, T.T., Cunnick, J.E., Murphy, P.A., Hendrich, S., 1999. Daidzein and Genistein Glucuronides In Vitro Are Weakly Estrogenic and Activate Human Natural Killer Cells at Nutritionally Relevant Concentrations. *J. Nutr.* 129, 399–405.
- Zhou, Y., Liu, X., 2020. The role of estrogen receptor beta in breast cancer. *Biomarker Res.* 8, 39.
- Zinedine, A., Soriano, J.M., Moltó, J.C., Mañes, J., 2007. Review on the toxicity, occurrence, metabolism, detoxification, regulations and intake of zearalenone: An oestrogenic mycotoxin. *Food Chem. Toxicol.* 45, 1–18.

Supplementary Information

Elucidation of xenoestrogen metabolism by non-targeted, stable isotope-assisted mass spectrometry in breast cancer cells

Mira Flasch¹, Christoph Bueschl^{2,3}, Giorgia Del Favero¹, Gerhard Adam⁴,
Rainer Schuhmacher², Doris Marko¹, Benedikt Warth^{1,*}

¹University of Vienna, Faculty of Chemistry, Department of Food Chemistry and Toxicology, Währinger Str. 38, 1090 Vienna, Austria

²University of Natural Resources and Life Sciences, Vienna (BOKU), Department of Agrobiotechnology, IFA-Tulln, Institute of Bioanalytics and Agro-Metabolomics, Konrad-Lorenz-Str. 20, 3430 Tulln, Austria

³University of Vienna, Faculty of Chemistry, Department of Analytical Chemistry, Währinger Str. 38, 1090 Vienna, Austria

⁴University of Natural Resources and Life Sciences, Vienna (BOKU), Department of Applied Genetics and Cell Biology, Institute of Microbial Genetics, Konrad-Lorenz-Str. 24, 3430 Tulln, Austria

*Correspondence: benedikt.warth@univie.ac.at

This file contains:

Supplementary Figures 1 to 5

Supplementary Tables 1 to 4

Figures Supplement

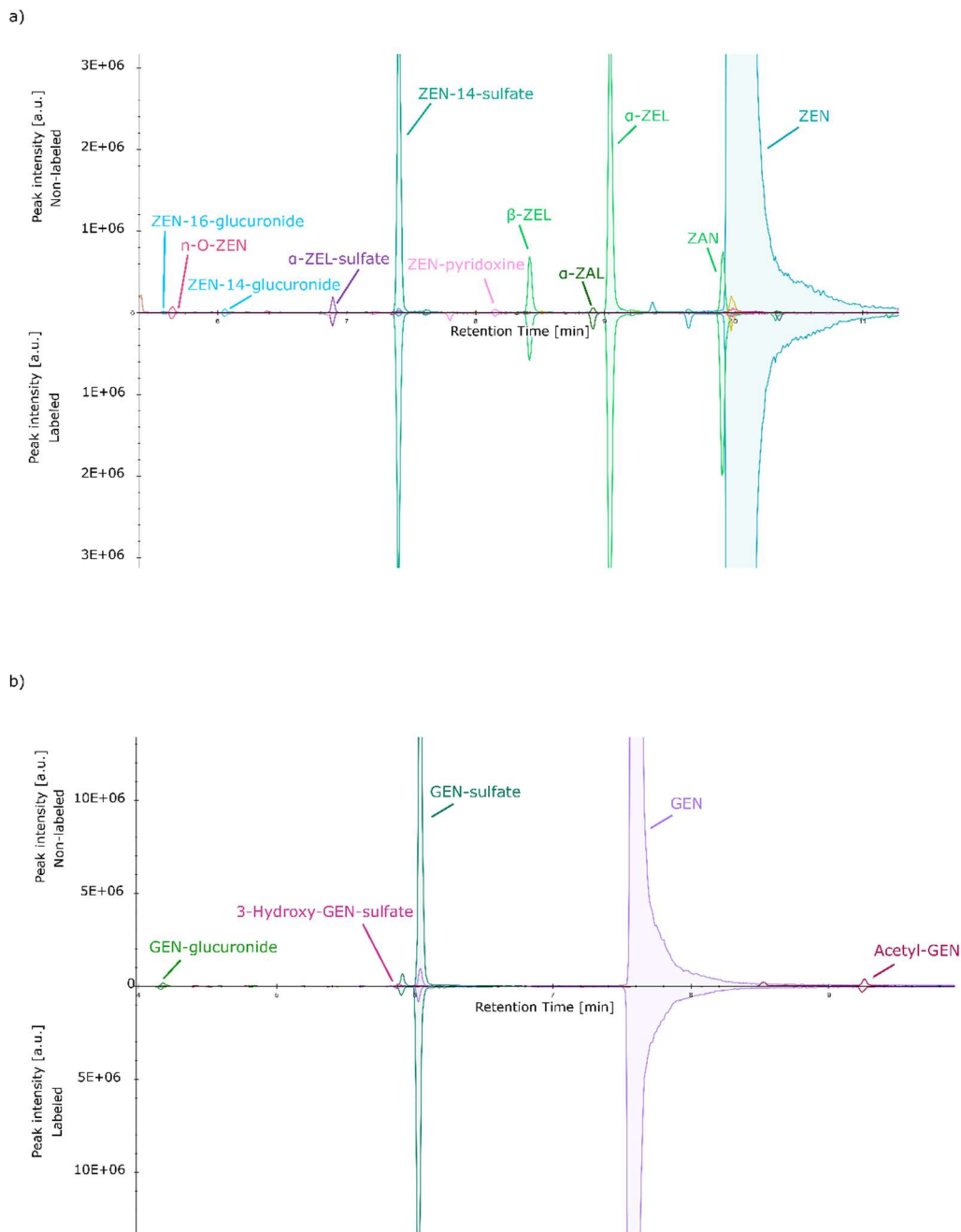


Figure S 1. Combined extracted ion chromatograms (EIC) of the masses (mass tolerance = 5 ppm) of the most abundant species in either positive or negative ionization mode of the annotated biotransformation products of (a) ZEN and (b) GEN. The x-axis represents the retention time in minutes and the upper y-axis the absolute intensity of the non-labeled metabolite while the lower y-axis shows the absolute intensity of the labeled metabolites. The chromatograms are taken from a single measurement in the supernatant after a 24 h incubation.

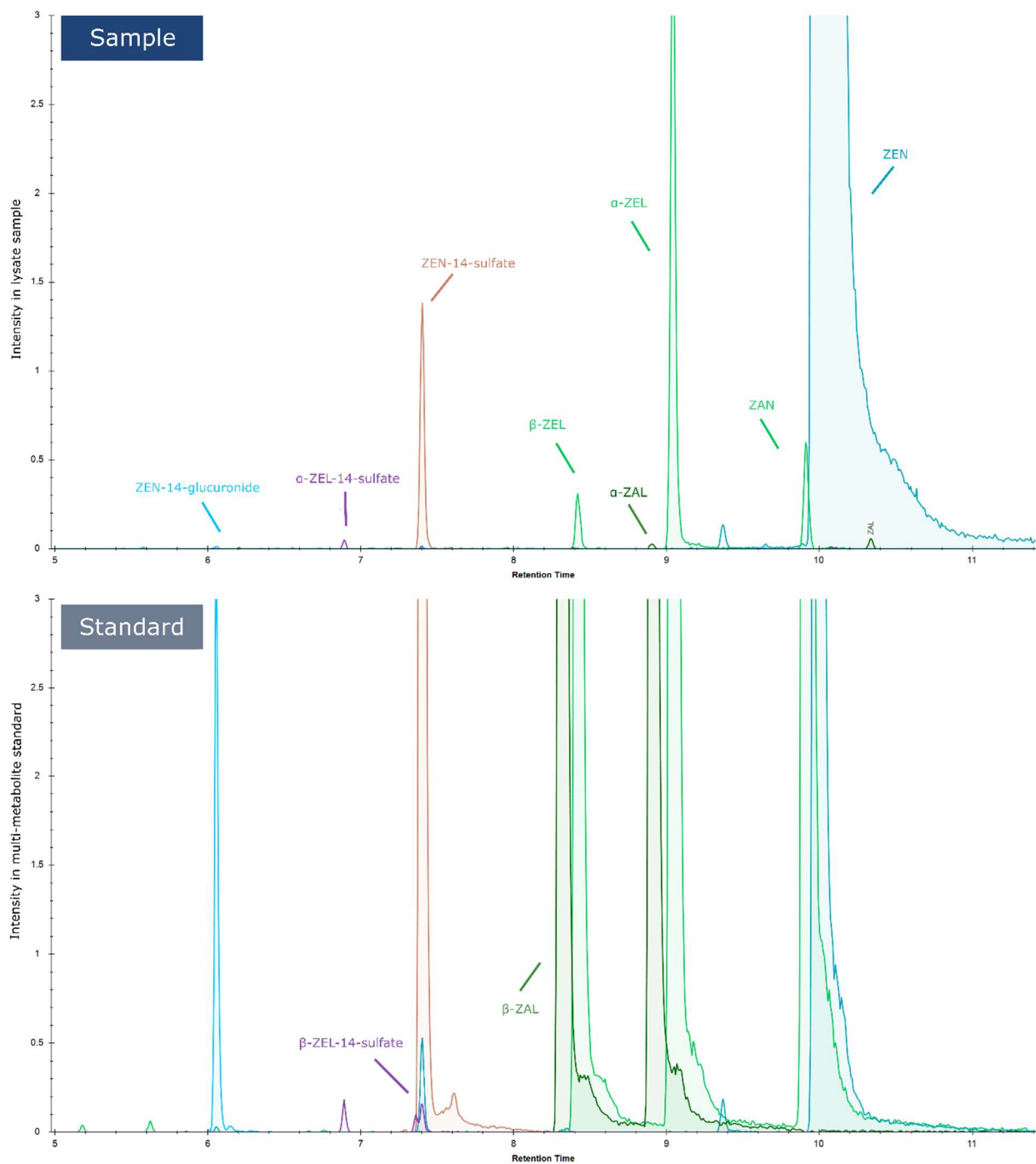


Figure S 2. Comparison of a multi-analyte standard and a lysate sample. A combined extracted ion chromatogram of the multi-metabolite standard (5-50 ng/mL depending on analyte) in the lower half and an extracted ion chromatogram of a single lysate sample after 24 h incubation in the upper half is shown.

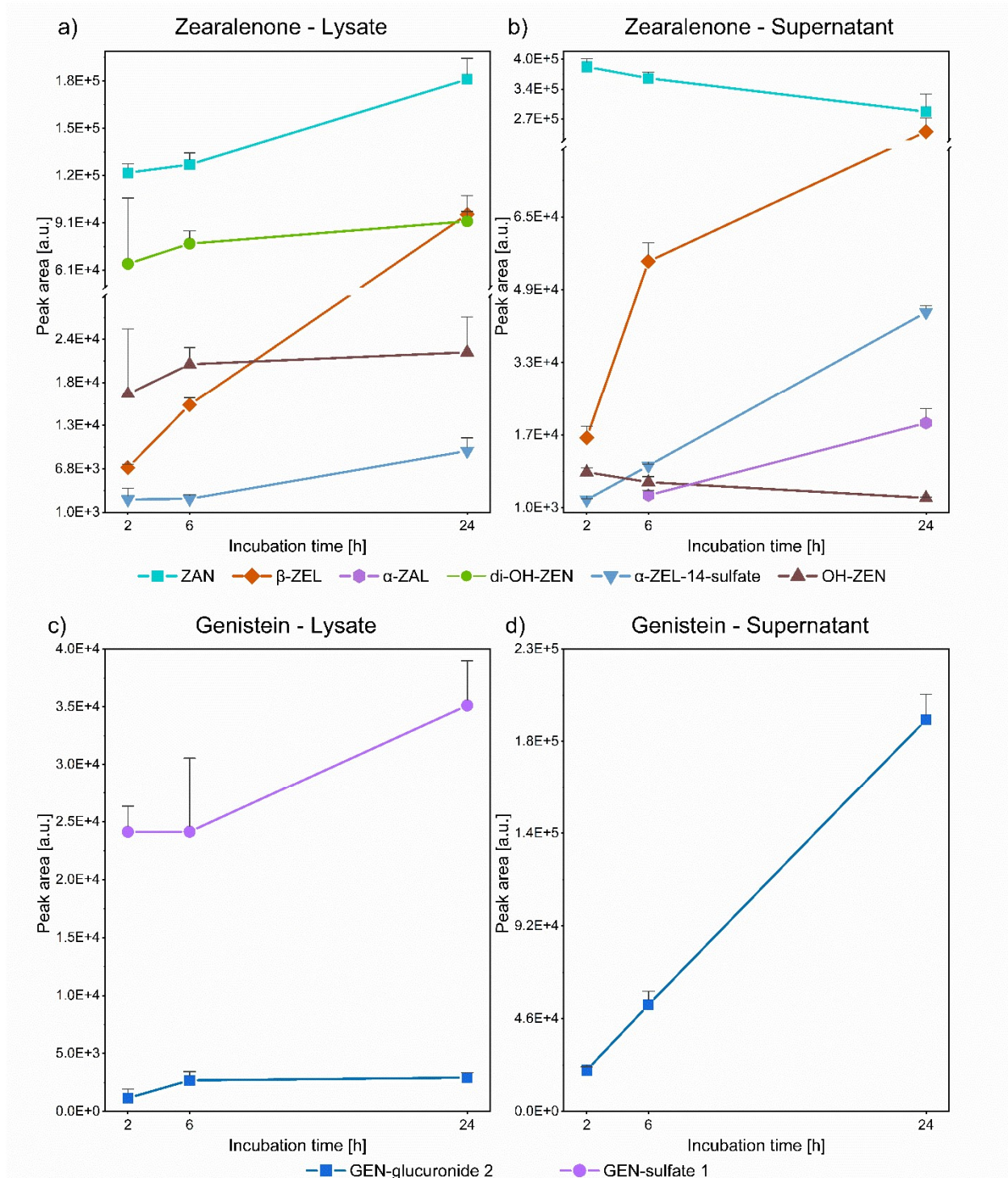


Figure S 3. Time-dependence of metabolite formation. Averaged area (n=3) of low abundant zearalenone (a, b) and genistein (c, d) metabolites at three time points (2h, 6h, 24h) in both compartments, lysate and supernatant, are presented. The metabolite's most abundant ion species ($[M-H]^-$ or $[M+H]^+$) are reported.

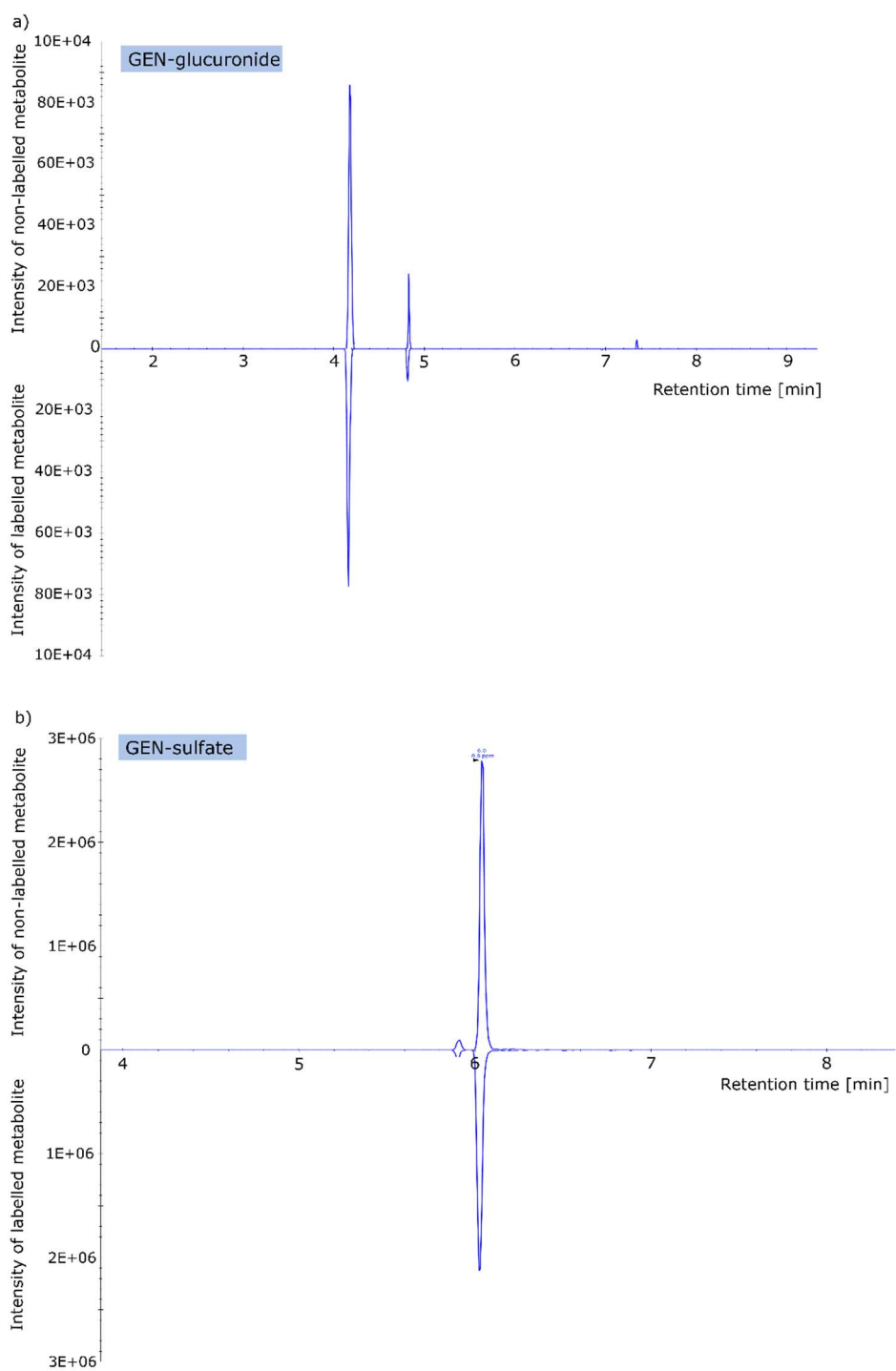


Figure S 4. Extracted ion chromatograms (EIC) of labeled and unlabeled Genistein (GEN) metabolites. a) EIC of GEN-glucuronide at m/z 445.0776 and m/z 449.1027 in positive ionization mode with two peaks at 4.2 min and 4.8 min. b) EIC of GEN-sulfate at m/z 349.0024 and m/z 353.0275 in positive ionization mode with two peaks at 5.9 min and 6.0 min.

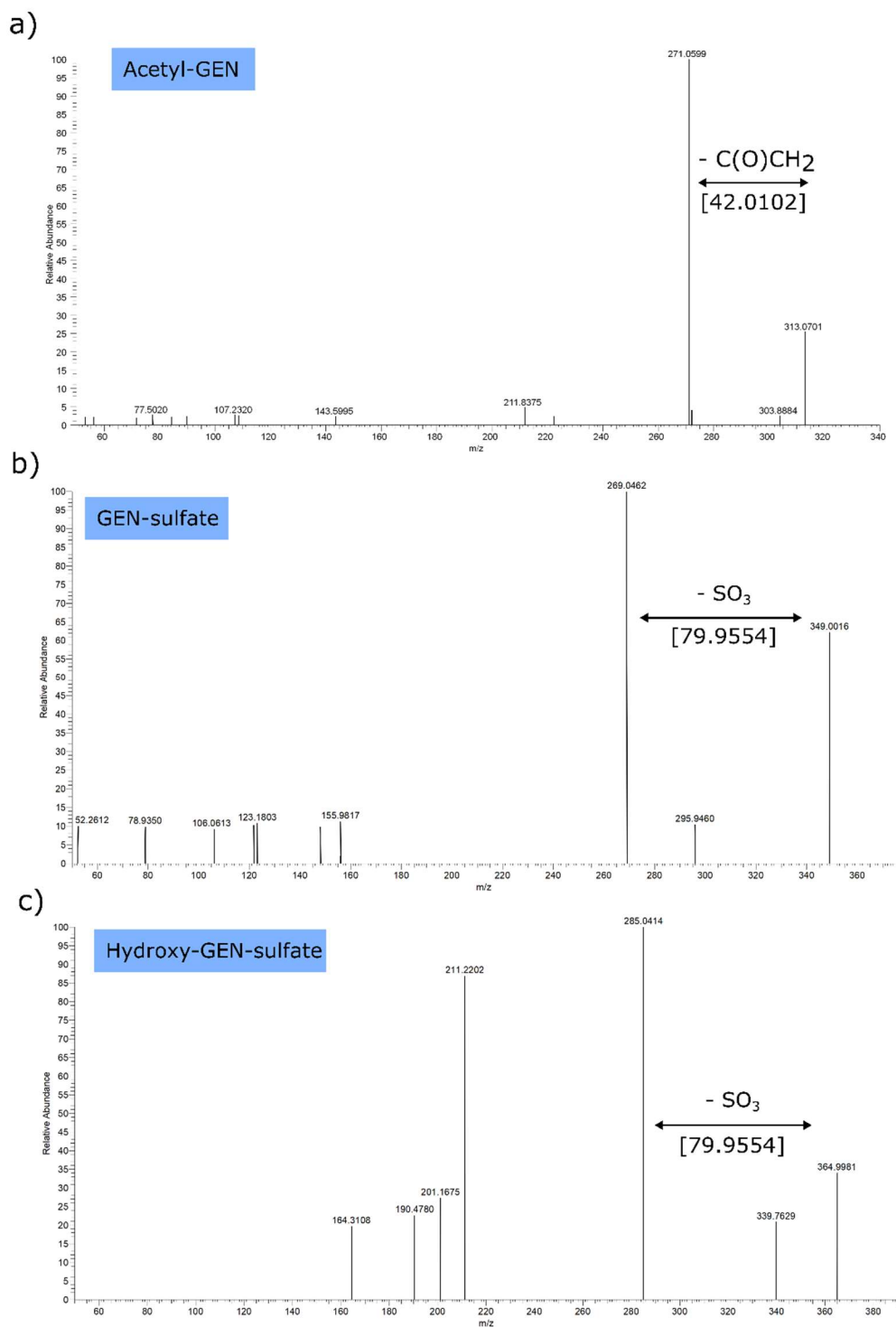


Figure S 5. MS²-spectra of Genistein (GEN)-metabolites at a normalized collision energy of 30. a) MS² spectrum of precursor *m/z* 313.0700 (Acetyl-GEN) at 9.3 min. b) MS² spectrum of precursor *m/z* 349.0025 (GEN-sulfate) at 5.9 min. c) MS² spectrum of precursor *m/z* 364.9975 (Hydroxy-GEN-sulfate) at 6.0 min.

Tables Supplement

Table S 1. Quantitative results for ZEN and its metabolites, where authentic standards were available. Each replicate was presented separately and for ZEN the concentration in the medium with the added toxin before incubation was included.

		Incubation time [h]						
		2	6	24	2	6	24	Medium+5 μ ZEN
		Lysate			Supernatant			
		Concentration [ng/mL]						
ZEN	Replicate 1	74.29	76.08	109.3	169.2	169.7	124.1	267.0
	Replicate 2	73.71	81.01	116.9	172.5	166.	149.4	246.0
	Replicate 3	71.26	70.90	120.3	175.6	167.6	141.1	225.0
ZAN	Replicate 1	0.180	0.198	0.264	0.571	0.57	0.364	0.904
	Replicate 2	0.196	0.204	0.295	0.597	0.533	0.475	0.869
	Replicate 3	0.191	0.185	0.274	0.622	0.532	0.454	0.807
α -ZAL	Replicate 1	n.d.	n.d.	0.208	n.d.	0.193	0.536	n.d.
	Replicate 2	n.d.	n.d.	0.325	n.d.	0.250	0.715	n.d.
	Replicate 3	n.d.	n.d.	0.335	n.d.	0.233	0.663	n.d.
α -ZEL	Replicate 1	1.78	4.60	24.8	2.54	9.01	28.7	n.d.
	Replicate 2	2.25	4.74	27.6	2.66	8.86	33.4	n.d.
	Replicate 3	2.02	4.34	26.8	3.07	8.27	32.7	n.d.
β -ZEL	Replicate 1	0.261	0.482	2.90	0.505	1.86	6.27	n.d.
	Replicate 2	0.297	0.525	2.81	0.528	1.60	7.36	n.d.
	Replicate 3	0.266	0.479	2.95	0.645	1.68	7.88	n.d.
ZEN-14-sulfate	Replicate 1	0.481	0.659	1.25	0.456	1.32	5.00	n.d.
	Replicate 2	0.805	0.850	1.64	0.412	1.43	5.59	n.d.
	Replicate 3	0.702	0.793	1.58	0.556	1.29	4.92	n.d.
ZEN-14-GlcA	Replicate 1	1.96	1.84	2.74	n.d.	1.88	7.92	n.d.
	Replicate 2	2.38	2.19	2.47	n.d.	1.94	7.93	n.d.
	Replicate 3	1.59	1.98	2.81	n.d.	2.13	7.29	n.d.

Table S 2. Additional information on the calibration curves for the quantification of ZEN and its metabolites

Metabolite	Slope	Intercept	R²
ZEN	9.52E+06	-9.01E+05	0.992
α-ZEL	3.04E+05	-3.78E+04	1.000
β-ZEL	2.44E+05	-2.18E+04	0.998
ZEN-14-GlcA	1.14E+04	-1.04E+04	0.998
ZEN-14-sulfate	1.60E+06	-3.43E+04	0.997
ZAN	4.54E+06	-3.21E+04	0.999
α-ZAL	2.57E+05	-3.21E+04	0.999
β-ZAL	2.60E+05	-1.62E+04	0.999

Table S 3. Averaged areas (n= 3) of all detected metabolites at the three timepoints in lysate and supernatant including standard deviation. Only the most abundant ion species (considering positive and negative mode together) was reported.

	Incubation time [h]					
	2			6		
	Lysate			Supernatant		
	Area					
	2	6	24	2	6	24
ZEN	1.06E+08± 2.76E+06	1.10E+08± 6.18E+06	1.76E+08± 7.56E+06	2.49E+08± 4.94E+06	2.44E+08± 8.82E+05	2.12E+08± 2.03E+07
ZAN	1.23E+05± 5.67E+03	1.28E+05± 7.38E+03	1.82E+05± 1.33E+04	3.85E+05± 1.86E+04	3.59E+05± 1.36E+04	2.84E+05± 3.95E+04
OH-ZEN	1.68E+04± 8.73E+03	2.08E+04± 2.25E+03	2.24E+04± 4.73E+03	8.81E+03± 9.22E+02	6.61E+03± 1.22E+03	3.13E+03± 1.88E+02
α-ZEL	8.64E+04± 1.02E+04	1.96E+05± 9.15E+03	1.15E+06± 6.78E+04	1.16E+05± 1.11E+04	3.78E+05± 1.53E+04	1.38E+06± 1.06E+05
α-ZAL	-	-	6.72E+03± 2.71E+03	-	3.71E+03± 1.05E+03	1.96E+04± 3.15E+03
β-ZEL	6.95E+03± 4.49E+02	1.54E+04± 9.42E+02	9.64E+04± 1.94E+03	1.64E+04± 2.57E+03	5.52E+04± 4.12E+03	2.40E+05± 3.11E+04
di-OH-ZEN	6.51E+04± 4.17E+04	7.79E+04± 8.21E+03	9.21E+04± 1.62E+04	-	-	-
ZEN-pyridoxine	-	-	4.39E+03± 1.55E+03	9.11E+03± 7.78E+02	5.61E+03± 4.17E+02	1.03E+04± 8.65E+02
α-ZEL-14-sulfate	2.72E+03± 1.48E+03	2.79E+03± 5.84E+02	9.18E+03± 1.76E+03	2.73E+03± 2.72E+02	1.02E+04± 3.29E+02	4.41E+04± 1.51E+03
ZEN-14-sulfate	1.55E+05± 4.00E+04	1.79E+05± 2.47E+04	3.51E+05± 5.03E+04	1.04E+05± 1.61E+04	3.00E+05± 1.78E+04	1.19E+06± 7.40E+04
ZEN-14-GlcA	2.10E+03± 7.24E+02	2.25E+03± 4.11E+02	3.35E+03± 3.27E+02	-	1.92E+03± 2.90E+02	1.14E+04± 7.87E+02
O-ZEN	1.15E+04± 3.27E+03	1.29E+04± 5.78E+02	7.69E+03± 3.86E+03	2.43E+04± 5.97E+03	1.34E+04± 3.98E+02	2.37E+04± 3.36E+03
ZEN-16-GlcA	-	9.57E+02± 3.55E+02	1.45E+03± 3.80E+02	-	-	1.97E+03± 8.10E+02
GEN-GlcA 1	2.17E+04± 2.74E+03	2.72E+04± 2.75E+03	2.98E+04± 1.28E+03	-	1.14E+04± 2.02E+03	6.30E+04± 7.62E+03
GEN-GlcA 2	1.16E+03± 7.77E+02	2.69E+03± 7.42E+02	2.92E+03± 4.35E+02	-	-	5.90E+03± 1.10E+03
GEN	9.40E+07± 5.66E+05	7.24E+07± 4.81E+06	8.69E+07± 3.41E+06	1.12E+08± 2.19E+06	1.09E+08± 6.58E+06	1.02E+08± 1.35E+07
3-Hydroxy-GEN-sulfate	-	-	1.17E+04± 5.76E+02	-	-	3.18E+04± 5.38E+03
GEN-sulfate 1	2.41E+04± 2.22E+03	2.41E+04± 6.41E+03	3.51E+04± 3.88E+03	2.05E+04± 1.67E+03	5.29E+04± 6.72E+03	1.95E+05± 1.27E+04
GEN-sulfate 2	7.07E+05± 9.23E+04	7.07E+05± 1.18E+05	8.91E+05± 8.08E+04	7.18E+05± 3.46E+04	1.94E+06± 1.34E+05	6.14E+06± 1.01E+06
GEN-pentose	6.26E+03± 5.84E+02	8.95E+03± 1.09E+03	1.29E+04± 1.97E+03	-	1.02E+03± 5.49E+01	7.36E+03± 1.40E+03
Acetyl-GEN	2.39E+05± 9.03E+03	1.51E+05± 2.34E+04	2.17E+05± 3.49E+04	1.40E+05± 3.39E+03	1.62E+05± 1.75E+04	1.39E+05± 2.29E+04
GEN-O-glucoside	9.56E+03± 2.83E+03	1.06E+04± 3.99E+02	8.78E+03± 2.05E+03	-	-	-

Table S 4. Concentration levels of ZEN and its metabolites in the multi-analyte standards.

Metabolite	Concentration [ng/mL]				
	Standard 0.05	Standard 0.5	Standard 5	Standard 50	Standard 500
ZEN	0.05	0.5	5	50	500
α -ZEL	0.5	5	50	500	5000
β -ZEL	0.5	5	50	500	5000
ZEN-14-GlcA	0.5	5	50	500	5000
ZEN-14-sulfate	0.05	0.5	5	50	500
ZAN	0.05	0.5	5	50	500
α -ZAL	0.5	5	50	500	5000
β -ZAL	0.5	5	50	500	5000
α -ZEL-GlcA	0.5	5	50	500	5000
β -ZEL-GlcA	0.5	5	50	500	5000

7. Conclusion and Outlook

The complexity of environmental exposures requires the combination of several analytical approaches for monitoring them properly in human samples. The established dual-column configuration addresses the need for a broad chemical coverage by applying two columns, an RP column for the measurement of apolar xenobiotics and a HILIC for detecting polar metabolites, enabling simultaneous exposure and effect analyses at the metabolome level in human matrices. This combined method exhausts the limits of xenobiotic detection with LC-HRMS as two complementary column chemistries and both ionisation modes are combined in a short, united run. The simplicity and rapidness of the dual-column approach might be ideal for exposome-wide association studies that require a high sample throughput to achieve sufficient sample sizes for identifying the effect of xenobiotics on human health and disease development.

The novel dual-column setup emphasised that HRMS can obtain quantitative results. However, the detection and, in particular, quantitation of very low concentrated chemicals might be limited. The direct comparison of model xenobiotics determined with high- and low-resolution mass spectrometry with identical LC parameters reveals a discrepancy between both approaches and indicates a higher limit of quantitation for HRMS. Thus, trace level exposures might be incompletely covered with HRMS. Nevertheless, the strength of this approach is to discover various molecules without prior knowledge on top of gaining quantitative results. Therefore, tailored, low-resolution mass spectrometric methods should only be regarded as a complementary technique in exposomic research. Nevertheless, triple quadrupole approaches are essential for collecting comprehensive exposure data for target molecules, especially at extremely low levels, to support, e.g. risk assessment.

The internal chemical exposome is not restricted to the native xenobiotics introduced into the human body. Biotransformation processes transform these chemicals, creating molecules with different chemical and toxicological properties. Moreover, metabolic transformations vary between individuals and organisms. Toxicological tests are frequently performed in cells derived from human material. These models mimic the human body, but their enzymatic properties might be different, hampering the interpretation of *in vitro* data and drawing conclusions for humans *in vivo*. The introduced workflow combining stable isotope labelling, HRMS, and a unique bioinformatics tool (MetExtractII) for investigating the fate of exogenous chemicals in cell culture at a large scale reveals diverse biotransformation for deoxynivalenol, zearalenone and genistein, altering the toxicological impact of these chemicals on the cells. In addition, this approach discovered several unusual metabolic products, e.g. conjugates to vitamins, penicillin, and amino acids. Biotransformation products are an integral part of the chemical exposome. Therefore, detailed knowledge of formed metabolites is essential for deciphering the exposome.

The elucidation of the chemical exposome depends on advanced mass spectrometric approaches. The developed workflows are unique in reducing analysis time by combining two columns or adapting stable isotope-assisted mass spectrometry to cell culture samples. Both features are essential to get a more detailed insight into the human exposome. Thus, the established approaches will serve to unravel environmental exposures and their role in disease development.

8. References

- Abdel-Aziz, M.I., A.H. Neerincx, S.J. Vijverberg, A.D. Kraneveld, and A.H. Maitland-van der Zee. 2020. 'Omics for the future in asthma', *Seminars in Immunopathology*, 42: 111-26.
- Abdelsalam, N.A., A.T. Ramadan, M.T. ElRakaiby, and R.K. Aziz. 2020. 'Toxicomicromicrobiomics: The Human Microbiome vs. Pharmaceutical, Dietary, and Environmental Xenobiotics', *Frontiers in Pharmacology*, 11.
- Al-Jaal, B.A., M. Jaganjac, A. Barcaru, P. Horvatovich, and A. Latiff. 2019. 'Aflatoxin, fumonisin, ochratoxin, zearalenone and deoxynivalenol biomarkers in human biological fluids: A systematic literature review, 2001–2018', *Food and Chemical Toxicology*, 129: 211-28.
- Angerer, J., L.L. Aylward, S.M. Hays, B. Heinzow, and M. Wilhelm. 2011. 'Human biomonitoring assessment values: Approaches and data requirements', *International Journal of Hygiene and Environmental Health*, 214: 348-60.
- Antignac, J.-P., K. de Wasch, F. Monteau, H. De Brabander, F. Andre, and B. Le Bizec. 2005. 'The ion suppression phenomenon in liquid chromatography–mass spectrometry and its consequences in the field of residue analysis', *Analytica Chimica Acta*, 529: 129-36.
- Avula, B., S. Sagi, Y.-H. Wang, J. Zweigenbaum, M. Wang, and I.A. Khan. 2015. 'Characterization and screening of pyrrolizidine alkaloids and N-oxides from botanicals and dietary supplements using UHPLC-high resolution mass spectrometry', *Food Chemistry*, 178: 136-48.
- Barupal, K., and O. Fiehn. 2019. 'Generating the Blood Exposome Database Using a Comprehensive Text Mining and Database Fusion Approach', *Environmental Health Perspectives*, 127: 097008.
- Bedia, C. 2022. 'Metabolomics in environmental toxicology: Applications and challenges', *Trends in Environmental Analytical Chemistry*, 34: e00161.
- Beyerle, J., E. Frei, M. Stiborova, N. Habermann, and C.M. Ulrich. 2015. 'Biotransformation of xenobiotics in the human colon and rectum and its association with colorectal cancer', *Drug Metabolism Reviews*, 47: 199-221.
- Bhat, S.S., S.K. Prasad, C. Shivamallu, K.S. Prasad, A. Syed, P. Reddy, C.A. Cull, and R.G. Amachawadi. 2021. 'Genistein: A Potent Anti-Breast Cancer Agent', *Current Issues in Molecular Biology*, 43: 1502-17.
- Blaženović, I., T. Kind, J. Ji, and O. Fiehn. 2018. 'Software Tools and Approaches for Compound Identification of LC-MS/MS Data in Metabolomics', *Metabolites*, 8: 31.
- Bocato, M.Z., J.P. Bianchi Ximenez, C. Hoffmann, and F. Barbosa. 2019. 'An overview of the current progress, challenges, and prospects of human biomonitoring and exposome studies', *Journal of Toxicology and Environmental Health, Part B*: 1-26.
- Bouatra, S., F. Aziat, R. Mandal, A.C. Guo, M.R. Wilson, C. Knox, T.C. Bjorn Dahl, R. Krishnamurthy, F. Saleem, P. Liu, Z.T. Dame, J. Poelzer, J. Huynh, F.S. Yallou, N. Psychogios, E. Dong, R. Bogumil, C. Roehring, and D.S. Wishart. 2013. 'The Human Urine Metabolome', *PLoS One*, 8: e73076.
- Bousoumah, R., V. Leso, I. Iavicoli, P. Huuskonen, S. Viegas, S.P. Porras, T. Santonen, N. Frery, A. Robert, and S. Ndaw. 2021. 'Biomonitoring of occupational exposure to bisphenol A, bisphenol S and bisphenol F: A systematic review', *Science of the Total Environment*, 783: 146905.
- Buszewski, B., and S. Noga. 2012. 'Hydrophilic interaction liquid chromatography (HILIC)--a powerful separation technique', *Analytical and bioanalytical chemistry*, 402: 231-47.
- Caballero-Casero, N., L. Belova, P. Vervliet, J.-P. Antignac, A. Castaño, L. Debrauwer, M.E. López, C. Huber, J. Klanova, M. Krauss, A. Lommen, H.G.J. Mol, H. Oberacher, O. Pardo, E.J. Price, V. Reinstadler, C.M. Vitale, A.L.N. van Nuijs, and A. Covaci. 2021. 'Towards harmonised criteria in quality assurance and quality control of suspect and non-target LC-HRMS analytical workflows for screening of emerging contaminants in human biomonitoring', *TRAC Trends in Analytical Chemistry*, 136: 116201.
- Cajka, T., and O. Fiehn. 2016. 'Toward Merging Untargeted and Targeted Methods in Mass Spectrometry-Based Metabolomics and Lipidomics', *Analytical Chemistry*, 88: 524-45.
- Caldwell, J., I. Gardner, and N. Swales. 1995. 'An introduction to drug disposition: the basic principles of absorption, distribution, metabolism, and excretion', *Toxicologic Pathology*, 23: 102-14.
- Chen, James C., Mariano J. Alvarez, F. Talos, H. Dhruv, Gabrielle E. Rieckhof, A. Iyer, Kristin L. Diefes, K. Aldape, M. Berens, Michael M. Shen, and A. Califano. 2014. 'Identification of Causal Genetic Drivers of Human Disease through Systems-Level Analysis of Regulatory Networks', *Cell*, 159: 402-14.

- Chen, L., M. Yu, Q. Wu, Z. Peng, D. Wang, K. Kuča, P. Yao, H. Yan, A.K. Nüssler, and L. Liu. 2017. 'Gender and geographical variability in the exposure pattern and metabolism of deoxynivalenol in humans: a review', *Journal of Applied Toxicology*, 37: 60-70.
- Cimmino, I., F. Fiory, G. Perruolo, C. Miele, F. Beguinot, P. Formisano, and F. Oriente. 2020. 'Potential mechanisms of bisphenol A (BPA) contributing to human disease', *International Journal of Molecular Sciences*, 21: 5761.
- Coughlin, S.S. 2014. 'Toward a Road Map for Global -Omics: A Primer on -Omic Technologies', *American Journal of Epidemiology*, 180: 1188-95.
- Croom, E. 2012. 'Chapter Three - Metabolism of Xenobiotics of Human Environments.' in Ernest Hodgson (ed.), *Progress in Molecular Biology and Translational Science* (Academic Press).
- David, A., J. Chaker, E.J. Price, V. Bessonneau, A.J. Chetwynd, C.M. Vitale, J. Klánová, D.I. Walker, J.-P. Antignac, R. Barouki, and G.W. Miller. 2021. 'Towards a comprehensive characterisation of the human internal chemical exposome: Challenges and perspectives', *Environment International*, 156: 106630.
- de Groot, P.M., C.C. Wu, B.W. Carter, and R.F. Munden. 2018. 'The epidemiology of lung cancer', *Translational lung cancer research*, 7: 220-33.
- De Santis, B., F. Debegnach, B. Miano, G. Moretti, E. Sonogo, A. Chiaretti, D. Buonsenso, and C. Brera. 2019. 'Determination of deoxynivalenol biomarkers in Italian urine samples', *Toxins*, 11: 441.
- Dennis, K.K., E. Marder, D.M. Balshaw, Y. Cui, M.A. Lynes, G.J. Patti, S.M. Rappaport, D.T. Shaughnessy, M. Vrijheid, and D.B. Barr. 2017. 'Biomonitoring in the Era of the Exposome', *Environmental Health Perspectives*, 125: 502-10.
- Easton, D.F., and R.A. Eeles. 2008. 'Genome-wide association studies in cancer', *Human Molecular Genetics*, 17: R109-R15.
- EFSA. 2011. 'Scientific Opinion on the risks for public health related to the presence of zearalenone in food', *EFSA Journal*, 9: 2197.
- Elbaz, A., and C. Tranchant. 2007. 'Epidemiologic studies of environmental exposures in Parkinson's disease', *Journal of the Neurological Sciences*, 262: 37-44.
- Eriksen, G.S., H.K. Knutsen, M. Sandvik, and A.-L. Brantsæter. 2021. 'Urinary deoxynivalenol as a biomarker of exposure in different age, life stage and dietary practice population groups', *Environment International*, 157: 106804.
- Ezekiel, C.N., W.A. Abia, D. Braun, B. Šarkanj, K.I. Ayeni, O.A. Oyedele, E.C. Michael-Chikezie, V.C. Ezekiel, B.N. Mark, C.P. Ahuchaogu, R. Krska, M. Sulyok, P.C. Turner, and B. Warth. 2022. 'Mycotoxin exposure biomonitoring in breastfed and non-exclusively breastfed Nigerian children', *Environment International*, 158: 106996.
- Fiehn, O. 2002. 'Metabolomics—the link between genotypes and phenotypes', *Functional genomics*: 155-71.
- Föllmann, W., N. Ali, M. Blaszkewicz, and G.H. Degen. 2016. 'Biomonitoring of Mycotoxins in Urine: Pilot Study in Mill Workers', *Journal of Toxicology and Environmental Health, Part A*, 79: 1015-25.
- Gálvez-Ontiveros, Y., I. Moscoso-Ruiz, L. Rodrigo, M. Aguilera, A. Rivas, and A. Zafra-Gómez. 2021. 'Presence of Parabens and Bisphenols in Food Commonly Consumed in Spain', *Foods*, 10.
- Ganesan, A.R., K. Mohan, D. Karthick Rajan, A.A. Pillay, T. Palanisami, P. Sathishkumar, and L. Conterno. 2022. 'Distribution, toxicity, interactive effects, and detection of ochratoxin and deoxynivalenol in food: A review', *Food Chemistry*, 378: 131978.
- Gao, C.-J., and K. Kannan. 2020. 'Phthalates, bisphenols, parabens, and triclocarban in feminine hygiene products from the United States and their implications for human exposure', *Environment International*, 136: 105465.
- GBD. 2017. 'Global, regional, and national comparative risk assessment of 84 behavioural, environmental and occupational, and metabolic risks or clusters of risks, 1990-2016: a systematic analysis for the Global Burden of Disease Study 2016', *Lancet*, 390: 1345-422.
- Geer Wallace, M.A., and J.P. McCord. 2020. 'Chapter 16 - High-resolution mass spectrometry.' in Jonathan Beauchamp, Cristina Davis and Joachim Pleil (eds.), *Breathborne Biomarkers and the Human Volatilome (Second Edition)* (Elsevier: Boston).
- Giuliani, A., M. Zuccarini, A. Cichelli, H. Khan, and M. Reale. 2020. 'Critical Review on the Presence of Phthalates in Food and Evidence of Their Biological Impact', *International Journal of Environmental Research and Public Health*, 17: 5655.
- Gonzaga-Jauregui, C., J.R. Lupski, and R.A. Gibbs. 2012. 'Human Genome Sequencing in Health and Disease', *Annual Review of Medicine*, 63: 35-61.

- González-Domínguez, R., O. Jáuregui, M.I. Queipo-Ortuño, and C. Andrés-Lacueva. 2020. 'Characterization of the Human Exposome by a Comprehensive and Quantitative Large-Scale Multianalyte Metabolomics Platform', *Analytical Chemistry*, 92: 13767-75.
- Gooderham, N.J., H. Zhu, S. Lauber, A. Boyce, and S. Creton. 2002. 'Molecular and genetic toxicology of 2-amino-1-methyl-6-phenylimidazo [4, 5-b] pyridine (PhIP)', *Mutation Research/Fundamental and Molecular Mechanisms of Mutagenesis*, 506: 91-99.
- Gore, A.C., V.A. Chappell, S.E. Fenton, J.A. Flaws, A. Nadal, G.S. Prins, J. Toppari, and R.T. Zoeller. 2015. 'EDC-2: the Endocrine Society's second scientific statement on endocrine-disrupting chemicals', *Endocrine Reviews*, 36: E1-E150.
- Gujas, C., J.R. Montenegro-Burke, X. Domingo-Almenara, A. Palermo, B. Warth, G. Hermann, G. Koellensperger, T. Huan, W. Uritboonthai, A.E. Aisporna, D.W. Wolan, M.E. Spilker, H.P. Benton, and G. Siuzdak. 2018. 'METLIN: A Technology Platform for Identifying Knowns and Unknowns', *Analytical Chemistry*, 90: 3156-64.
- Hansen, Å.M., L. Mathiesen, M. Pedersen, and L.E. Knudsen. 2008. 'Urinary 1-hydroxypyrene (1-HP) in environmental and occupational studies—A review', *International Journal of Hygiene and Environmental Health*, 211: 471-503.
- Hermann, G., M. Schwaiger, P. Volejnik, and G. Koellensperger. 2018. '¹³C-labelled yeast as internal standard for LC-MS/MS and LC high resolution MS based amino acid quantification in human plasma', *Journal of Pharmaceutical and Biomedical Analysis*, 155: 329-34.
- Hirschhorn, J.N., and M.J. Daly. 2005. 'Genome-wide association studies for common diseases and complex traits', *Nature Reviews Genetics*, 6: 95-108.
- Honda, M., M. Robinson, and K. Kannan. 2018. 'Parabens in human urine from several Asian countries, Greece, and the United States', *Chemosphere*, 201: 13-19.
- Jagne, J., D. White, and F. Jefferson. 2016. 'Endocrine-Disrupting Chemicals: Adverse Effects of Bisphenol A and Parabens to Women's Health', *Water, Air, & Soil Pollution*, 227: 182.
- Jiang, C., X. Wang, X. Li, J. Inlora, T. Wang, Q. Liu, and M. Snyder. 2018. 'Dynamic Human Environmental Exposome Revealed by Longitudinal Personal Monitoring', *Cell*, 175: 277-91.
- Jones, D.P. 2015. 'Sequencing the exposome: A call to action', *Toxicology reports*, 3: 29-45.
- Judson, R., A. Richard, J. Dix David, K. Houck, M. Martin, R. Kavlock, V. Dellarco, T. Henry, T. Holderman, P. Sayre, S. Tan, T. Carpenter, and E. Smith. 2009. 'The Toxicity Data Landscape for Environmental Chemicals', *Environmental Health Perspectives*, 117: 685-95.
- Kabir, E.R., M.S. Rahman, and I. Rahman. 2015. 'A review on endocrine disruptors and their possible impacts on human health', *Environmental Toxicology and Pharmacology*, 40: 241-58.
- Karpuzoglu, E., S.D. Holladay, and R.M. Gogal. 2013. 'Parabens: Potential impact of Low-Affinity Estrogen receptor Binding chemicals on Human health', *Journal of Toxicology and Environmental Health, Part B*, 16: 321-35.
- Kim, S., J. Chen, T. Cheng, A. Gindulyte, J. He, S. He, Q. Li, B.A. Shoemaker, P.A. Thiessen, B. Yu, L. Zaslavsky, J. Zhang, and E.E. Bolton. 2021. 'PubChem in 2021: new data content and improved web interfaces', *Nucleic Acids Research*, 49: D1388-D95.
- Kowalska, K., D.E. Habrowska-Górczyńska, and A.W. Piastowska-Ciesielska. 2016. 'Zearalenone as an endocrine disruptor in humans', *Environmental Toxicology and Pharmacology*, 48: 141-49.
- Kruve, A. 2020. 'Strategies for Drawing Quantitative Conclusions from Nontargeted Liquid Chromatography-High-Resolution Mass Spectrometry Analysis', *Analytical Chemistry*, 92: 4691-99.
- Kucuk, O. 2017. 'Soy foods, isoflavones, and breast cancer', *Cancer*, 123: 1901-03.
- Landrigan, P.J., R. Fuller, N.J.R. Acosta, O. Adeyi, R. Arnold, N.N. Basu, A.B. Baldé, R. Bertollini, S. Bose-O'Reilly, J.I. Boufford, P.N. Breyse, T. Chiles, C. Mahidol, A.M. Coll-Seck, M.L. Cropper, J. Fobil, V. Fuster, M. Greenstone, A. Haines, D. Hanrahan, D. Hunter, M. Khare, A. Krupnick, B. Lanphear, B. Lohani, K. Martin, K.V. Mathiasen, M.A. McTeer, C.J.L. Murray, J.D. Ndahimananjara, F. Perera, J. Potočník, A.S. Preker, J. Ramesh, J. Rockström, C. Salinas, L.D. Samson, K. Sandilya, P.D. Sly, K.R. Smith, A. Steiner, R.B. Stewart, W.A. Suk, O.C.P. van Schayck, G.N. Yadama, K. Yumkella, and M. Zhong. 2018. 'The Lancet Commission on pollution and health', *Lancet*, 391: 462-512.
- Lawal, A.T. 2017. 'Polycyclic aromatic hydrocarbons. A review', *Cogent Environmental Science*, 3: 1339841.
- Lebedev, A.T., and S.D. Richardson. 2022. 'Planet Contamination with Chemical Compounds', *Molecules*, 27: 1621.
- LeBlanc, G.A. 2008. 'Phase II—Conjugation of toxicants', *Molecular and biochemical toxicology*: 219-37.

- Lehmler, H.-J., B. Liu, M. Gadogbe, and W. Bao. 2018. 'Exposure to Bisphenol A, Bisphenol F, and Bisphenol S in U.S. Adults and Children: The National Health and Nutrition Examination Survey 2013–2014', *ACS Omega*, 3: 6523-32.
- Li, X.-F., and W.A. Mitch. 2018. 'Drinking Water Disinfection Byproducts (DBPs) and Human Health Effects: Multidisciplinary Challenges and Opportunities', *Environmental Science & Technology*, 52: 1681-89.
- Lv, W., L. Guo, F. Zheng, Q. Wang, W. Wang, L. Cui, Y. Ouyang, X. Liu, E. Li, X. Shi, and G. Xu. 2020. 'Alternate reversed-phase and hydrophilic interaction liquid chromatography coupled with mass spectrometry for broad coverage in metabolomics analysis', *Journal of Chromatography B*, 1152: 122266.
- Mally, A., M. Solfrizzo, and G.H. Degen. 2016. 'Biomonitoring of the mycotoxin Zearalenone: current state-of-the art and application to human exposure assessment', *Archives of Toxicology*, 90: 1281-92.
- Mankidy, R., S. Wiseman, H. Ma, and J.P. Giesy. 2013. 'Biological impact of phthalates', *Toxicology Letters*, 217: 50-58.
- Meijer, J., M. Lamoree, T. Hamers, J.-P. Antignac, S. Hutinet, L. Debrauwer, A. Covaci, C. Huber, M. Krauss, D.I. Walker, E.L. Schymanski, R. Vermeulen, and J. Vlaanderen. 2021. 'An annotation database for chemicals of emerging concern in exposome research', *Environment International*, 152: 106511.
- Michel, T., M. Halabalaki, and A.-L. Skaltsounis. 2013. 'New concepts, experimental approaches, and dereplication strategies for the discovery of novel phytoestrogens from natural sources', *Planta Medica*, 79: 514-32.
- Miller, G.W., and D.P. Jones. 2014. 'The Nature of Nurture: Refining the Definition of the Exposome', *Toxicological Sciences*, 137: 1-2.
- Miranda-Galvis, M., R. Loveless, L.P. Kowalski, and Y. Teng. 2021. 'Impacts of Environmental Factors on Head and Neck Cancer Pathogenesis and Progression', *Cells*, 10: 389.
- Mishra, S., S. Srivastava, J. Dewangan, A. Divakar, and S. Kumar Rath. 2020. 'Global occurrence of deoxynivalenol in food commodities and exposure risk assessment in humans in the last decade: a survey', *Critical Reviews in Food Science and Nutrition*, 60: 1346-74.
- Misra, B.B. 2021. 'Advances in high resolution GC-MS technology: a focus on the application of GC-Orbitrap-MS in metabolomics and exposomics for FAIR practices', *Analytical Methods*, 13: 2265-82.
- Moldoveanu, S.C., and V. David. 2013. 'Chapter 5 - Retention Mechanisms in Different HPLC Types.' in Serban C. Moldoveanu and Victor David (eds.), *Essentials in Modern HPLC Separations* (Elsevier).
- Montes-Grajales, D., E. Martínez-Romero, and J. Olivero-Verbel. 2018. 'Phytoestrogens and mycoestrogens interacting with breast cancer proteins', *Steroids*, 134: 9-15.
- Murphy, N., V. Moreno, D.J. Hughes, L. Vodicka, P. Vodicka, E.K. Aglago, M.J. Gunter, and M. Jenab. 2019. 'Lifestyle and dietary environmental factors in colorectal cancer susceptibility', *Molecular Aspects of Medicine*, 69: 2-9.
- Niedzwiecki, M.M., D.I. Walker, R. Vermeulen, M. Chadeau-Hyam, D.P. Jones, and G.W. Miller. 2019. 'The Exposome: Molecules to Populations', *Annual Review of Pharmacology and Toxicology*, 59: 107-27.
- Nilsen, F.M., and N.S. Tulve. 2020. 'A systematic review and meta-analysis examining the interrelationships between chemical and non-chemical stressors and inherent characteristics in children with ADHD', *Environmental Research*, 180: 108884.
- Nowak, K., E. Jabłońska, and W. Ratajczak-Wrona. 2021. 'Controversy around parabens: Alternative strategies for preservative use in cosmetics and personal care products', *Environmental Research*, 198: 110488.
- Oberacher, H., M. Sasse, J.-P. Antignac, Y. Guitton, L. Debrauwer, E.L. Jamin, T. Schulze, M. Krauss, A. Covaci, N. Caballero-Casero, K. Rousseau, A. Damont, F. Fenaille, M. Lamoree, and E.L. Schymanski. 2020. 'A European proposal for quality control and quality assurance of tandem mass spectral libraries', *Environmental Sciences Europe*, 32: 43.
- Omicinski, C.J., J.P. Vanden Heuvel, G.H. Perdew, and J.M. Peters. 2011. 'Xenobiotic metabolism, disposition, and regulation by receptors: from biochemical phenomenon to predictors of major toxicities', *Toxicological Sciences*, 120: 49-75.
- Orešič, M., A. McGlinchey, C.E. Wheelock, and T. Hyötyläinen. 2020. 'Metabolic Signatures of the Exposome—Quantifying the Impact of Exposure to Environmental Chemicals on Human Health', *Metabolites*, 10: 454.
- Ostry, V., F. Malir, J. Toman, and Y. Grosse. 2017. 'Mycotoxins as human carcinogens—the IARC Monographs classification', *Mycotoxin Research*, 33: 65-73.

- Page, J.S., R.T. Kelly, K. Tang, and R.D. Smith. 2007. 'Ionization and transmission efficiency in an electrospray ionization—mass spectrometry interface', *Journal of the American Society for Mass Spectrometry*, 18: 1582-90.
- Patel, C.J. 2017. 'Analytic Complexity and Challenges in Identifying Mixtures of Exposures Associated with Phenotypes in the Exposome Era', *Current Epidemiology Reports*, 4: 22-30.
- Patel, C.J., J. Bhattacharya, and A.J. Butte. 2010. 'An Environment-Wide Association Study (EWAS) on type 2 diabetes mellitus', *PLoS One*, 5: e10746.
- Paterni, I., C. Granchi, J.A. Katzenellenbogen, and F. Minutolo. 2014. 'Estrogen receptors alpha (ER α) and beta (ER β): Subtype-selective ligands and clinical potential', *Steroids*, 90: 13-29.
- Paterni, I., C. Granchi, and F. Minutolo. 2017. 'Risks and benefits related to alimentary exposure to xenoestrogens', *Critical reviews in food science and nutrition*, 57: 3384-404.
- Place, B.J., E.M. Ulrich, J.K. Challis, A. Chao, B. Du, K. Favela, Y.-L. Feng, C.M. Fisher, P. Gardinali, A. Hood, A.M. Knolhoff, A.D. McEachran, S.L. Nason, S.R. Newton, B. Ng, J. Nuñez, K.T. Peter, A.L. Phillips, N. Quinete, R. Renslow, J.R. Sobus, E.M. Sussman, B. Warth, S. Wickramasekara, and A.J. Williams. 2021. 'An Introduction to the Benchmarking and Publications for Non-Targeted Analysis Working Group', *Analytical Chemistry*, 93: 16289-96.
- Poupko, J.M., S.I. Baskin, and E. Moore. 2007. 'The pharmacological properties of anisodamine', *Journal of Applied Toxicology*, 27: 116-21.
- Pourchet, M., L. Debrauwer, J. Klanova, E.J. Price, A. Covaci, N. Caballero-Casero, H. Oberacher, M. Lamoree, A. Damont, F. Fenaille, J. Vlaanderen, J. Meijer, M. Krauss, D. Sarigiannis, R. Barouki, B. Le Bizec, and J.-P. Antignac. 2020. 'Suspect and non-targeted screening of chemicals of emerging concern for human biomonitoring, environmental health studies and support to risk assessment: From promises to challenges and harmonisation issues', *Environment International*, 139: 105545.
- Preindl, K., D. Braun, G. Aichinger, S. Sieri, M. Fang, D. Marko, and B. Warth. 2019. 'A Generic Liquid Chromatography–Tandem Mass Spectrometry Exposome Method for the Determination of Xenoestrogens in Biological Matrices', *Analytical Chemistry*, 91: 11334-42.
- Price, E.J., C.M. Vitale, G.W. Miller, A. David, R. Barouki, K. Audouze, D.I. Walker, J.-P. Antignac, X. Coumoul, V. Bessonneau, and J. Klánová. 2022. 'Merging the exposome into an integrated framework for “omics” sciences', *iScience*, 25: 103976.
- Psychogios, N., D.D. Hau, J. Peng, A.C. Guo, R. Mandal, S. Bouatra, I. Sinelnikov, R. Krishnamurthy, R. Eisner, B. Gautam, N. Young, J. Xia, C. Knox, E. Dong, P. Huang, Z. Hollander, T.L. Pedersen, S.R. Smith, F. Bamforth, R. Greiner, B. McManus, J.W. Newman, T. Goodfriend, and D.S. Wishart. 2011. 'The Human Serum Metabolome', *PLoS One*, 6: e16957.
- Rai, A., M. Das, and A. Tripathi. 2020. 'Occurrence and toxicity of a fusarium mycotoxin, zearalenone', *Critical Reviews in Food Science and Nutrition*, 60: 2710-29.
- Rappaport, S.M. 2016. 'Genetic Factors Are Not the Major Causes of Chronic Diseases', *PLoS One*, 11: e0154387.
- Rappaport, S.M., D.K. Barupal, D. Wishart, P. Vineis, and A. Scalbert. 2014. 'The blood exposome and its role in discovering causes of disease', *Environmental Health Perspectives*, 122: 769-74.
- Rappaport, S.M., and M.T. Smith. 2010. 'Environment and Disease Risks', *Science* 330: 460-61.
- Regulation, C. 2014. "Commission Regulation (EU) no. 1004/2014 of 18 September 2014 amending Annex V to Regulation (EC) No 1223/2009 of the European Parliament and of the Council on cosmetic products." In *Off. J. Eur. Union* 282/5, edited by Commission Regulation (EU). <https://eur-lex.europa.eu/legal-content/EN/TXT/PDF/?uri=CELEX:32014R1004&from=EN>.
- Rietjens, I.M.C.M., A.M. Sotoca, J. Vervoort, and J. Lousse. 2013. 'Mechanisms underlying the dualistic mode of action of major soy isoflavones in relation to cell proliferation and cancer risks', *Molecular Nutrition & Food Research*, 57: 100-13.
- Ropejko, K., and M. Twarużek. 2021. 'Zearalenone and Its Metabolites—General Overview, Occurrence, and Toxicity', *Toxins*, 13: 35.
- Ruiz, D., M. Becerra, J.S. Jagai, K. Ard, and R.M. Sargis. 2017. 'Disparities in Environmental Exposures to Endocrine-Disrupting Chemicals and Diabetes Risk in Vulnerable Populations', *Diabetes Care*, 41: 193-205.
- Ruttkies, C., E.L. Schymanski, S. Wolf, J. Hollender, and S. Neumann. 2016. 'MetFrag relaunched: incorporating strategies beyond in silico fragmentation', *Journal of Cheminformatics*, 8: 3.

- Saha, S., and P.A. Kroon. 2020. 'A simple and rapid LC-MS/MS Method for quantification of total daidzein, genistein, and equol in human urine', *Journal of Analytical Methods in Chemistry*, 2020.
- Schulze, B., Y. Jeon, S. Kaserzon, A.L. Heffernan, P. Dewapriya, J. O'Brien, M.J. Gomez Ramos, S. Ghorbani Gorji, J.F. Mueller, K.V. Thomas, and S. Samanipour. 2020. 'An assessment of quality assurance/quality control efforts in high resolution mass spectrometry non-target workflows for analysis of environmental samples', *TRAC Trends in Analytical Chemistry*, 133: 116063.
- Schwaiger, M., H. Schoeny, Y. El Abiead, G. Hermann, E. Rampler, and G. Koellensperger. 2019. 'Merging metabolomics and lipidomics into one analytical run', *Analyst*, 144: 220-29.
- Schymanski, E.L., J. Jeon, R. Gulde, K. Fenner, M. Ruff, H.P. Singer, and J. Hollender. 2014a. 'Identifying Small Molecules via High Resolution Mass Spectrometry: Communicating Confidence', *Environmental Science & Technology*, 48: 2097-98.
- Schymanski, E.L., H.P. Singer, P. Longrée, M. Loos, M. Ruff, M.A. Stravs, C. Ripollés Vidal, and J. Hollender. 2014b. 'Strategies to Characterize Polar Organic Contamination in Wastewater: Exploring the Capability of High Resolution Mass Spectrometry', *Environmental Science & Technology*, 48: 1811-18.
- Selevan, S.G., C.A. Kimmel, and P. Mendola. 2000. 'Identifying critical windows of exposure for children's health', *Environmental Health Perspectives*, 108: 451-55.
- Sévin, D.C., A. Kuehne, N. Zamboni, and U. Sauer. 2015. 'Biological insights through nontargeted metabolomics', *Current Opinion in Biotechnology*, 34: 1-8.
- Sharifi-Rad, J., C. Quispe, M. Imran, A. Rauf, M. Nadeem, T.A. Gondal, B. Ahmad, M. Atif, M.S. Mubarak, and O. Sytar. 2021. 'Genistein: an integrative overview of its mode of action, pharmacological properties, and health benefits', *Oxidative Medicine and Cellular Longevity*, 2021.
- Sirotkin, A.V., and A.H. Harrath. 2014. 'Phytoestrogens and their effects', *European Journal of Pharmacology*, 741: 230-36.
- Smith, C.J., and T.A. Perfetti. 2020. 'Exposure to chemicals formed from natural processes is ubiquitous', *Toxicology Research and Application*, 4: 2397847320922940.
- Smoluch, M., G. Grasso, P. Suder, and J. Silberring. 2019. *Mass Spectrometry* (John Wiley & Sons).
- Snyder, L.R., J.J. Kirkland, and J.W. Dolan. 2010. *Introduction to Modern Liquid Chromatography* (A John Wiley & Sons, Inc., Publication).
- Sobus, J.R., J.N. Grossman, A. Chao, R. Singh, A.J. Williams, C.M. Grulke, A.M. Richard, S.R. Newton, A.D. McEachran, and E.M. Ulrich. 2019. 'Using prepared mixtures of ToxCast chemicals to evaluate non-targeted analysis (NTA) method performance', *Analytical and Bioanalytical Chemistry*, 411: 835-51.
- Sobus, J.R., J.F. Wambaugh, K.K. Isaacs, A.J. Williams, A.D. McEachran, A.M. Richard, C.M. Grulke, E.M. Ulrich, J.E. Rager, M.J. Strynar, and S.R. Newton. 2018. 'Integrating tools for non-targeted analysis research and chemical safety evaluations at the US EPA', *Journal of Exposure Science & Environmental Epidemiology*, 28: 411-26.
- Soltow, Q.A., F.H. Strobel, K.G. Mansfield, L. Wachtman, Y. Park, and D.P. Jones. 2013. 'High-performance metabolic profiling with dual chromatography-Fourier-transform mass spectrometry (DC-FTMS) for study of the exposome', *Metabolomics*, 9: 132-43.
- Sosvorova, L.K., T. Chlupacova, J. Vitku, M. Vlč, J. Heracek, L. Starka, D. Saman, M. Simkova, and R. Hampl. 2017. 'Determination of selected bisphenols, parabens and estrogens in human plasma using LC-MS/MS', *Talanta*, 174: 21-28.
- Stiborová, M., L. Bořek-Dohalská, P. Hodek, J. Mráz, and E. Frei. 2002. 'New selective inhibitors of cytochromes P450 2B and their application to antimutagenesis of tamoxifen', *Archives of Biochemistry and Biophysics*, 403: 41-49.
- Tamayo-Uria, I., L. Maitre, C. Thomsen, M.J. Nieuwenhuijsen, L. Chatzi, V. Siroux, G.M. Aasvang, L. Agier, S. Andrusaityte, M. Casas, M. de Castro, A. Dedele, L.S. Haug, B. Heude, R. Grazuleviciene, K.B. Gutzkow, N.H. Krog, D. Mason, R.R.C. McEachan, H.M. Meltzer, I. Petraviciene, O. Robinson, T. Roumeliotaki, A.K. Sakhi, J. Urquiza, M. Vafeiadi, D. Waiblinger, C. Warembourg, J. Wright, R. Slama, M. Vrijheid, and X. Basagaña. 2019. 'The early-life exposome: Description and patterns in six European countries', *Environment International*, 123: 189-200.
- Thoene, M., E. Dzika, S. Gonkowski, and J. Wojtkiewicz. 2020. 'Bisphenol S in food causes hormonal and obesogenic effects comparable to or worse than bisphenol A: a literature review', *Nutrients*, 12: 532.

- Topliss, J.G., A.M. Clark, E. Ernst, C.D. Hufford, G.A.R. Johnston, J.M. Rimoldi, and B.J. Weimann. 2002. 'Natural and synthetic substances related to human health (IUPAC Technical Report)', *Pure and Applied Chemistry*, 74: 1957-85.
- Trufelli, H., P. Palma, G. Famigliani, and A. Cappiello. 2011. 'An overview of matrix effects in liquid chromatography–mass spectrometry', *Mass Spectrometry Reviews*, 30: 491-509.
- Tshala-Katumbay, D., J.-C. Mwanza, D.S. Rohlman, G. Maestre, and R.B. Oriá. 2015. 'A global perspective on the influence of environmental exposures on the nervous system', *Nature*, 527: S187-S92.
- Vailaya, A., and C. Horváth. 1998. 'Retention in reversed-phase chromatography: partition or adsorption?', *Journal of Chromatography A*, 829: 1-27.
- van der Schyff, V., L. Suchánková, K. Kademoglou, L. Melymuk, and J. Klánová. 2022. 'Parabens and antimicrobial compounds in conventional and “green” personal care products', *Chemosphere*, 297: 134019.
- Vejdovszky, K., K. Hahn, D. Braun, B. Warth, and D. Marko. 2017. 'Synergistic estrogenic effects of Fusarium and Alternaria mycotoxins in vitro', *Archives of Toxicology*, 91: 1447-60.
- Vermeulen, R., E.L. Schymanski, A.-L. Barabási, and G.W. Miller. 2020. 'The exposome and health: Where chemistry meets biology', *Science*, 367: 392-96.
- Vilcins, D., J. Cortes-Ramirez, D. Currie, and P. Preston. 2021. 'Early environmental exposures and life-long risk of chronic non-respiratory disease', *Paediatric Respiratory Reviews*, 40: 33-38.
- Vineis, P., O. Robinson, M. Chadeau-Hyam, A. Dehghan, I. Mudway, and S. Dagnino. 2020. 'What is new in the exposome?', *Environment International*, 143: 105887.
- Vorkamp, K., A. Castaño, J.-P. Antignac, L.D. Boada, E. Cequier, A. Covaci, M. Esteban López, L.S. Haug, M. Kasper-Sonnenberg, H.M. Koch, O. Pérez Luzardo, A. Osíte, L. Rambaud, M.-T. Pinorini, G. Sabbioni, and C. Thomsen. 2021. 'Biomarkers, matrices and analytical methods targeting human exposure to chemicals selected for a European human biomonitoring initiative', *Environment International*, 146: 106082.
- Walker, D.I., D. Valvi, N. Rothman, Q. Lan, G.W. Miller, and D.P. Jones. 2019. 'The Metabolome: a Key Measure for Exposome Research in Epidemiology', *Current Epidemiology Reports*, 6: 93-103.
- Wang, L.-Q. 2002. 'Mammalian phytoestrogens: enterodiol and enterolactone', *Journal of Chromatography B*, 777: 289-309.
- Waring, S.C., and R.N. Rosenberg. 2008. 'Genome-Wide Association Studies in Alzheimer Disease', *Archives of Neurology*, 65: 329-34.
- Warth, B., S. Spangler, M. Fang, C.H. Johnson, E.M. Forsberg, A. Granados, R.L. Martin, X. Domingo-Almenara, T. Huan, D. Rinehart, J.R. Montenegro-Burke, B. Hilmers, A. Aisporna, L.T. Hoang, W. Uritboonthai, H.P. Benton, S.D. Richardson, A.J. Williams, and G. Siuzdak. 2017. 'Exposome-Scale Investigations Guided by Global Metabolomics, Pathway Analysis, and Cognitive Computing', *Analytical Chemistry*, 89: 11505-13.
- Wasito, H., G. Hermann, V. Fitz, C. Troyer, S. Hann, and G. Koellensperger. 2021. 'Yeast-based reference materials for quantitative metabolomics', *Analytical and Bioanalytical Chemistry*.
- Watson, C.S., N.N. Bulayeva, A.L. Wozniak, and R.A. Alyea. 2007. 'Xenoestrogens are potent activators of nongenomic estrogenic responses', *Steroids*, 72: 124-34.
- Wigle, D.T., T.E. Arbuckle, M.C. Turner, A. Bérubé, Q. Yang, S. Liu, and D. Krewski. 2008. 'Epidemiologic evidence of relationships between reproductive and child health outcomes and environmental chemical contaminants', *Journal of Toxicology and Environmental Health. Part B: Critical Reviews*, 11: 373-517.
- Wild, C.P. 2005. 'Complementing the Genome with an “Exposome”': The Outstanding Challenge of Environmental Exposure Measurement in Molecular Epidemiology', *Cancer Epidemiology Biomarkers & Prevention*, 14: 1847.
- Wild, C.P., and Y.Y. Gong. 2009. 'Mycotoxins and human disease: a largely ignored global health issue', *Carcinogenesis*, 31: 71-82.
- Williams, A.J., C.M. Grulke, J. Edwards, A.D. McEachran, K. Mansouri, N.C. Baker, G. Patlewicz, I. Shah, J.F. Wambaugh, R.S. Judson, and A.M. Richard. 2017. 'The CompTox Chemistry Dashboard: a community data resource for environmental chemistry', *Journal of Cheminformatics*, 9: 61-61.
- Wishart, D.S., Y.D. Feunang, A. Marcu, A.C. Guo, K. Liang, R. Vázquez-Fresno, T. Sajed, D. Johnson, C. Li, N. Karu, Z. Sayeeda, E. Lo, N. Assempour, M. Berjanskii, S. Singhal, D. Arndt, Y. Liang, H. Badran, J. Grant, A. Serra-Cayuela, Y. Liu, R. Mandal, V. Neveu, A. Pon, C. Knox, M. Wilson, C. Manach, and A. Scalbert. 2018. 'HMDB 4.0: the human metabolome database for 2018', *Nucleic Acids Research*, 46: 608-17.

- Wishart, D.S., A. Guo, E. Oler, F. Wang, A. Anjum, H. Peters, R. Dizon, Z. Sayeeda, S. Tian, B.L. Lee, M. Berjanskii, R. Mah, M. Yamamoto, J. Jovel, C. Torres-Calzada, M. Hiebert-Giesbrecht, V.W. Lui, D. Varshavi, D. Varshavi, D. Allen, D. Arndt, N. Khetarpal, A. Sivakumaran, K. Harford, S. Sanford, K. Yee, X. Cao, Z. Budinski, J. Liigand, L. Zhang, J. Zheng, R. Mandal, N. Karu, M. Dambrova, H.B. Schiöth, R. Greiner, and V. Gautam. 2022. 'HMDB 5.0: the Human Metabolome Database for 2022', *Nucleic Acids Research*, 50: 622-31.
- Witte, J.S. 2010. 'Genome-Wide Association Studies and Beyond', *Annual Review of Public Health*, 31: 9-20.
- Yu, L., E. Rios, L. Castro, J. Liu, Y. Yan, and D. Dixon. 2021. 'Genistein: Dual Role in Women's Health', *Nutrients*, 13: 3048.
- Zanger, U.M., and M. Schwab. 2013. 'Cytochrome P450 enzymes in drug metabolism: regulation of gene expression, enzyme activities, and impact of genetic variation', *Pharmacology & Therapeutics*, 138: 103-41.
- Zhang, P., C. Carlsten, R. Chaleckis, K. Hanhineva, M. Huang, T. Isobe, V.M. Koistinen, I. Meister, S. Papazian, K. Sdougkou, H. Xie, J.W. Martin, S.M. Rappaport, H. Tsugawa, D.I. Walker, T.J. Woodruff, R.O. Wright, and C.E. Wheelock. 2021a. 'Defining the Scope of Exposome Studies and Research Needs from a Multidisciplinary Perspective', *Environmental Science & Technology Letters*, 8: 839-52.
- Zhang, W., and R. Ramautar. 2021b. 'CE-MS for metabolomics: Developments and applications in the period 2018–2020', *Electrophoresis*, 42: 381-401.
- Zheng Kang, H., G. Wang, W. Yao, and W.-y. Zhu. 2006. 'Isoflavonic phytoestrogens-new prebiotics for farm animals: a review on research in China', *Current issues in intestinal microbiology*, 7: 53-60.
- Zinedine, A., J.M. Soriano, J.C. Moltó, and J. Mañes. 2007. 'Review on the toxicity, occurrence, metabolism, detoxification, regulations and intake of zearalenone: An oestrogenic mycotoxin', *Food and Chemical Toxicology*, 45: 1-18.
- Žuvela, P., M. Skoczylas, J. Jay Liu, T. Bączek, R. Kaliszan, M.W. Wong, and B. Buszewski. 2019. 'Column Characterization and Selection Systems in Reversed-Phase High-Performance Liquid Chromatography', *Chemical Reviews*, 119: 3674-729.

9. Appendix

9.1. List of additional contributions to peer-reviewed publications

- 03/2022 Christoph Bueschl, Maria Doppler, Elisabeth Varga, Bernhard Seidl, **Mira Flasch**, Benedikt Warth, and Juergen Zanghellini. 'PeakBot: Machine learning based chromatographic peak picking'. *BioRxiv*, 2022, DOI: 10.1101/2021.10.11.463887
- 05/2022 Thomas Jamnik, **Mira Flasch**, Dominik Braun, Yasmin Fareed, Daniel Wasinger, David Seki, David Berry, Angelika Berger, Lukas Wisgrill and Benedikt Warth, 'Next-generation biomonitoring of the early-life chemical exposome in neonatal and infant development'. *Nature Communications*, 2022, DOI: 10.1038/s41467-022-30204-y

9.2. List of oral presentations

- 06/2021 **JunganalytikerInnen Forum 2021**, Online
Flasch Mira, Fitz Veronika, Rampler Evelyn, Koellensperger Gunda, Warth Benedikt, *Non-targeted mass spectrometry for elucidating the exposome and its impact on the endogenous metabolome*
- 01/2021 **USA-European Exposome Symposium** - Exposomics, COVID-19 and Health Disparities, Online
Flasch Mira, Jamnik Thomas, Braun Dominik, Warth Benedikt, *Comparing sensitivity of low- and high-resolution mass spectrometry for xenobiotic trace analysis*
- 02/2020 **31st MassSpec Forum Vienna**, Vienna, Austria
Flasch Mira, Bueschl Christoph, Woelflingseder Lydia, Adam Gerhard, Schumacher Rainer, Marko Doris, Warth Benedikt, *Unravelling the fate of xenobiotics in human cell culture by stable-isotope assisted metabolomics*

9.3. List of poster presentations

- 09/2021 **DoSChem Internatioanl Student Symposium**, Vienna
Flasch Mira, Fitz Veronika, Rampler Evelyn, Koellensperger Gunda, Warth Benedikt, *Simultaneously covering the chemical exposome and endogenous metabolites by untargeted mass spectrometry*
- 03/2020 **Exposome Symposium 2020**, New York City, USA
Flasch Mira, Bueschl Christoph, Woelflingseder Lydia, Adam Gerhard, Schumacher Rainer, Marko Doris, Warth Benedikt, *Holistic identification of xenobiotoc biotransformation products by stable-isotope assisted LC-HRMS*
- 06/2019 **ASMS Conference on Mass Spectrometry and Allied Topics**, Atlanta, Georgia
Flasch Mira, Woelflingseder Lydia, Bueschl Christoph, Schuhmacher Rainer, Marko Doris, Warth Benedikt, *Untargeted metabolomics and 13C-labeling in tissue culture for identifying unknown human biotransformation products of xenobiotics*
- 04/2019 **ASTOX Symposium**, Vienna, Austria
Flasch Mira, Bueschl Christoph, Woelflingseder Lydia, Schuhmacher Rainer, Marko Doris, Warth Benedikt, *Untargeted metabolomics assisted by 13C-labeling in tissue culture for identifying human biotransformation products of xenobiotics*

9.4. List of abbreviations

BP4NTA, Benchmarking and Publications for Non-Targeted Analysis Working Group; BPA, bisphenol A; BPF, bisphenol F; BPS, bisphenol S; CE, capillary electrophoresis; CoA, Coenzyme A; COMT, catechol-O-methyl transferase; CYS, cysteine; CYP, cytochrome P450; DC, direct current; DON, deoxynivalenol; EDTA, ethylenediaminetetraacetic acid; EDC, endocrine disrupting chemicals; ENTACT, non-Targeted Analysis Collaborative Trial; EPA, environmental Protection Agency; ESI, electrospray ionisation; EU, European Union; ExWAS, exposome-wide association studies; FMO, flavin-containing monooxygenase; GC, gas chromatography; GEN, genistein; GSH, glutathione; GST, glutathione-S-transferase; HBM4EU, European Human Biomonitoring Initiative; HCD, Higher-energy collision-induced dissociation chamber; HILIC, hydrophilic interaction liquid chromatography; HRMS, high-resolution mass spectrometry; HSD, hydroxysteroid dihydrogen, IC, ion-exchange chromatography, LC, liquid chromatography; LD, lethal dose; LOD, limit of detection; LOQ, limit of quantitation; MS, mass spectrometry; m/z, mass to charge ratio; MRM, multiple reaction monitoring; NAT, N-acetyltransferase; NP, normal phase chromatography; NTA, non-targeted screening; PAH, polycyclic aromatic hydrocarbons; PAPS, 3-phosphoadenosine-5' phosphosulfate; QA, quality assurance; QC, quality control; QqQ, triple quadrupole mass spectrometry; RF, radio frequency; RP, reverse phase; SRM, selected reaction monitoring; SULT, sulfotransferase; TDI, tolerable daily intake; UGT, UDP-glucuronyltransferase; UPLC, ultra-performance liquid chromatography; ZEN, zearalenone

9.5. List of figures

Figure 1. Schematic overview of the internal chemical exposome.....	10
Figure 2. Chemical structures of selected xenoestrogens from natural and synthetic sources.....	16
Figure 3. Biotransformation processes in the human body.....	18
Figure 4. Scheme of the processes during electrospray ionisation (ESI).....	24
Figure 5. Schematic setup mass spectrometers.....	26

9.6. Glossary

Term	Definition
Biotransformation	Process transforming an exogenous substance in the body
Exposome	Totality of environmental exposures, including lifestyle factors from conception onwards
Exposomics	Systematic investigation of environmental exposures
Internal chemical exposome	Totality of internal contact of an organism with environmental chemicals, including their biotransformation products
Metabolism	Sum of all chemical reactions that take place in a cell to sustain life
Metabolite	Compound involved in metabolism
Metabolome	Totality of endogenous metabolites
Metabolomics	Systematic investigation of endogenous metabolites
Xenobiotics	Chemical foreign to an organism

9.7. Overview of measured LC-(HR)MS(/MS) sequences acquired and corresponding data storage location

Batch name	Purpose of experiment	Methods	Data storage	Instrument
180507_QE_5	Method optimisation for DON metabolites Measurement DON-metabolites in HepG2/HT29	180507_QE_neg_ddMS2 180508_QE_neg_ddMS2_ACN 180509_QE_neg_ddMS2_12min 180509_QE_pos_ddMS2_12min	Imch (\\share.univie.ac.at)\40 MSC raw file \\Q_Exactive_HF\2018\QE_KW-19	Q Exactive HF
180625_QE_Xeno	Test xenoestrogens in breast milk	180625_QE_neg_Pos_Xeno	\\Q_Exactive_HF\2018\QE_KW-26	Q Exactive HF
180813_DON_mf	MS2 Spectra for DON-metabolites in HepG2/HT29 Measurement DON-sulfonate standards	180813_QE_neg_ddMS2_12min 180509_QE_pos_ddMS2_12min 180813_QE_neg_oe_ddMS2_12min 180813_QE_pos_oe_ddMS2_12min	\\Q_Exactive_HF\2018\QE_KW-33 \\TSQ Vantage\2018\KW-43\181024_DONS	Q Exactive HF TSQ Vantage
181107_RatoxMet_Plasma	Rat plasma metabolomics	20181107_pHILLC_neg	\\Q_Exactive_HF\2018\QE_KW-45	Q Exactive HF
181110_ZENC13	Remeasurement ZEN-metabolites	181110_HF_ZENM_neg 181110_HF_ZENM_pos	\\Q_Exactive_HF\2018\QE_KW-45	Q Exactive HF
190125_HBM4EU_BPs_Urine	HBM4EU BPA	181123_Xeno_20_v3_newPC	\\TSQ Vantage\2019\KW-04\190125_HBM4EU_BPs_Urin	TSQ Vantage
190129_13GDDON_HEPA_ms2_spike	MS2 Spectra for DON-metabolites in HepG2/HT29 DON-metabolites in HepARG	190129_QE_neg_ddMS2_12min 190129_QE_pos_ddMS2_12min 190129_QE_pos_ddMS2_exin_CE50_12min 190131_QE_pos_ddMS2_exin_CE45_12min_PheTyr 190131_QE_pos_ddMS2_exin_CE45_12min_Cys 190129_QE_neg_ddMS2_12min_4de	\\Q_Exactive_HF\2019\QE_KW-5 \\Q_Exactive_HF\2019\QE_KW-5 \\Q_Exactive_HF\2019\QE_KW-5 \\Q_Exactive_HF\2019\QE_KW-5	Q Exactive HF Q Exactive HF Q Exactive HF Q Exactive HF
190131_CCK_2	Cell culture samples of CCK	20190130_pHILLC_15min_ddMS2_pos_neg	\\Q_Exactive_HF\2019\QE_KW-5	Q Exactive HF
190131_RATOX_plasma_Hilic	Rat plasma metabolites	20190130_pHILLC_15min_ddMS2_pos_neg	\\Q_Exactive_HF\2019\QE_KW-5	Q Exactive HF
190201_RATOX_plasma_Hilic	Rat plasma metabolites	20190130_pHILLC_15min_ddMS2_pos_neg	\\Q_Exactive_HF\2019\QE_KW-5	Q Exactive HF
20190313_Spiking DON	Spiking of DON samples	190129_QE_neg_ddMS2_12min	\\Q_Exactive_HF\2019\QE_KW-11	Q Exactive HF

Batch name	Purpose of experiment	Methods	Data storage	Instrument
190315_RatTox_Hilic	Rat plasma metabolomics	190129_QE_pos_ddMS2_12min 20190315_pHILIC_15min_neg 20190315_pHILIC_15min_ddMS2_neg 20190315_pHILIC_15min_pos 20190314_pHILIC_15min_ddMS2_pos		Q Exactive HF
20190318_CCK3_MCF7	Cell culture samples of CCK	20190315_pHILIC_15min_neg 20190315_pHILIC_15min_pos		Q Exactive HF
20190318_CCK4_Ishikawa	Cell culture samples of CCK	20190315_pHILIC_15min_neg 20190315_pHILIC_15min_pos	\\Q_Exactive_HF\2019\QE_KW_12	Q Exactive HF
20190432_ENTACT	ENTACT Trial	190423_QE_25min_TOP4_pos 190423_QE_25min_TOP4_neg 190425_QE_25min_TOP6_pos 190425_QE_25min_TOP6_neg	\\Q_Exactive_HF\2019\QE_KW_17	Q Exactive HF
20190432_ENTACT	ENTACT Trial	190425_QE_25min_TOP6_pos 190425_QE_25min_TOP6_neg	\\Q_Exactive_HF\2019\QE_KW_17	Q Exactive HF
190627_HBM4EU_Urine	HBM4EU BPA	181123_Xeno_20_v3_newPFC	\\TSQ_Vantage\2019\KW-25\190626_HBM4EU	TSQ Vantage
190703_HBM4EU_3	HBM4EU BPA	190703_HBM4EU_BPs_V1	\\QTrap6500+\\Analyst_Data\Pro-jects\2019\HBM4EU_BPs\Data\Round 3	QTrap6500+
190703_HBM4EU_Seq2	HBM4EU BPA	190703_HBM4EU_BPs_V2	\\QTrap6500+\\Analyst_Data\Pro-jects\2019\HBM4EU_BPs\Data\Round 3	QTrap6500+
190717_RatTox_Hilic	Rat plasma metabolomics	20190717_luna_HILIC_30min_neg	\\Q_Exactive_HF\2019\QE_KW_29	Q Exactive HF
190722_DONSulfonates	DON sulfonates	190722_DONSulfonates	\\Q_Exactive_HF\2019\QE_KW_30	Q Exactive HF
191015_HILIC_Hep2_Exp01	Measurement virus infected cells Urine spikes with xenobiotics/metabolites	20191015_pHILIC_15min_pos 20191015_pHILIC_15min_neg 20191015_pHILIC_15min_ddMS2_neg 20191015_pHILIC_15min_pos_neg 20191015_pHILIC_15min_pos_neg 20191015_pHILIC_15min_ddMS2_pos	\\Q_Exactive_HF\2019\QE_KW_42	Q Exactive HF
191017_RP_Hep2_Exp01	Measurement virus infected cells Urine spikes with xenobiotics/metabolites	20191016_RP_15min_pos 20191015_RP_15min_ddMS2_pos 20191016_RP_15min_pos_neg 20191015_RP_15min_ddMS2_pos_neg 20191016_RP_15min_neg	\\Q_Exactive_HF\2019\QE_KW_42	Q Exactive HF

Batch name	Purpose of experiment	Methods	Data storage	Instrument
191212_HBM4EU_Round4_2	HBM4EU BPA	20191015_RP_15min_ddMS2_neg	\\QTrap6500+\\Analyst Data\\Projects\\2019\\HBM4EU_BPs\\Data\\191212_HBM4EU_Round4_2	QTrap6500+
191216_HBM4EU_Round4_3	HBM4EU BPA	191212_HBM4EU_BPs_V3	\\QTrap6500+\\Analyst Data\\Projects\\2019\\HBM4EU_BPs\\Data\\191212_HBM4EU_Round4_3	QTrap6500+
200113_HBM4EU_Round4_4	HBM4EU BPA	191212_HBM4EU_BPs_V4	\\QTrap6500+\\Analyst Data\\Projects\\2019\\HBM4EU_BPs\\Data\\191212_HBM4EU_Round4_4	QTrap6500+
200228_Exp02_HILIC	Pre-experiment dual column setup	20200224_luna_HILIC_15min_neg 20200224_luna_HILIC_15min_pos 20200224_luna_HILIC_15min_negpos 20200224_luna_HILIC_15min_negpos_dd	\\Q_Exactive_HF\\2020\\KW-09\\Exp02	Q Exactive HF
200301_Exp02_RP	Pre-experiment dual column setup	200301_RP_15min_pos_neg 200301_RP_15min_pos_neg_dd 200301_RP_15min_neg 200301_RP_15min_pos	\\Q_Exactive_HF\\2020\\KW-09\\Exp02	Q Exactive HF
200720_OpHILIC_RP_v1	Optimisation LC setup for dual column	200720_luna_HILIC_15min_negpos_B_b1_03 200720_luna_HILIC_15min_negpos_B_b1_01 200720_XBridge_HILIC_15min_negpos_A_a2_03 200720_XBridge_HILIC_15min_negpos_B_a2_03 200720_XBridge_HILIC_15min_negpos_A_a1_03 200720_XBridge_HILIC_15min_negpos_B_a1_03 200720_XBridge_HILIC_15min_negpos_A_b2_03 200720_XBridge_HILIC_15min_negpos_B_b2_03 200722_ZICrHILIC_HILIC_15min_negpos_B_b3_03_cIII 200722_ZICrHILIC_HILIC_15min_negpos_B_b3_03_cIV 200722_ZICrHILIC_HILIC_15min_negpos_B_b1_03_cIV 200723_HSSTS_20min_NH4F_posneg 200723_HSSTS_20min_NH4F_neg 200723_HSSTS_15min_NH4F_v1 200723_HSSTS_15min_NH4F_v2	\\Q_Exactive_HF\\2020\\KW-30\\Exp02	Q Exactive HF

Batch name	Purpose of experiment	Methods	Data storage	Instrument
200908_OpHILIC_v2	Optimisation LC setup for dual column	200723_HSSTS_20min_NH4F_posneg 230723_HSSTS_20min_FA 200722_ZICpHILIC_HILIC_15min_neg- pos_B_b3_03_cIII 200722_BEH_HILIC_15min_negpos_B_b3_03_cIII 200720_BEH_HILIC_15min_negpos_A_b2_03 200909_BEH_HILIC_15min_negpos_A_a1_03 200909_BEH_HILIC_15min_negpos_A_a2_03	\\Q_Exactive_HF\2020\KW-37	Q Exactive HF
200909_OpRP_v2	Optimisation LC setup for dual column	200909_HSST3_15min_NH4F_v1 200909_HSST3_15min_NH4F_v2	\\Q_Exactive_HF\2020\KW-37	Q Exactive HF
20201214_ExpODUO	Dual column measurement	20201214_ExpODUO_500uL 20201214_ExpODUO_500uL_ddMS2_neg 20201214_ExpODUO_500uL_ddMS2_pos	\\QE_Duo\202012\Mira\20201214_ExpODUO	Q Exactive (Dual)
210224_Test_MEP	Test MEP	2102234_XenoQTrap_MEP_v11 2102234_XenoQTrap_MEP_only	\\QE_Duo\202012\Mira\210224_Test_MEP	QTrap6500+
210225_XenoQTrap_Urine_Umweltbundesamt_deconjugated_diluted	Diluted, deconjugated Umweltbundesamtsamples	2102234_XenoQTrap_MEP_v11	\\QTrap6500+\\Analyst_Data\Projects\2021\XenoQTrap\Data\210225_XenoQTrap_Urine_Umweltbundesamt_deconjugated_diluted	QTrap6500+
210312_XenoQTrap_Urine_Umweltbundesamt_deconjugated_diluted_2		2102234_XenoQTrap_MEP_v11	\\2021\XenoQTrap\Data\210312_XenoQTrap_Urine_Umweltbundesamt_deconjugated_diluted_2	QTrap6500+
20201005_ExpODUO2	Optimisation LC setup for dual column	2020510_ExpODUO_500uL_V1_pZIC 2020510_ExpODUO_500uL_V2_pZIC 2020510_ExpODUO_500uL_V3_pZIC 2020510_ExpODUO_500uL_V5_BEH	\\QE_Duo\202105\ExpODuo_2	Q Exactive (Dual)
210622_ExpODUO3_Seq	Main experiment dual column setup	210622_ExpODUO_500uL_HILIC-only 210622_ExpODUO_500uL_RP-only 2120622_ExpODUO_500uL_V2_pZIC_v2	\\QE_Duo\20210629	Q Exactive (Dual)
211029_LODDComp	LOD comparison	200623_XenoQTrap_v10	\\QTrap6500+\\Analyst_Data\Projects\2021\XenoQTrap\Data\211029_LODDComp	QTrap6500+
211115_LODDComp	LOD comparison	211115_HSST3_20min_NH4F_v2	\\Q_Exactive_HF\2021\KW-46	Q Exactive HF